



# LUND UNIVERSITY

## Design and Simulation of a Coordinated Drum Boiler-Turbine Controller

Lindahl, Sture

1976

*Document Version:*

Publisher's PDF, also known as Version of record

[Link to publication](#)

*Citation for published version (APA):*

Lindahl, S. (1976). *Design and Simulation of a Coordinated Drum Boiler-Turbine Controller*. [Licentiate Thesis, Department of Automatic Control]. Department of Automatic Control, Lund Institute of Technology (LTH).

*Total number of authors:*

1

### General rights

Unless other specific re-use rights are stated the following general rights apply:

Copyright and moral rights for the publications made accessible in the public portal are retained by the authors and/or other copyright owners and it is a condition of accessing publications that users recognise and abide by the legal requirements associated with these rights.

- Users may download and print one copy of any publication from the public portal for the purpose of private study or research.
- You may not further distribute the material or use it for any profit-making activity or commercial gain
- You may freely distribute the URL identifying the publication in the public portal

Read more about Creative commons licenses: <https://creativecommons.org/licenses/>

### Take down policy

If you believe that this document breaches copyright please contact us providing details, and we will remove access to the work immediately and investigate your claim.

LUND UNIVERSITY

PO Box 117  
221 00 Lund  
+46 46-222 00 00





DESIGN AND SIMULATION OF A COORDINATED  
DRUM BOILER-TURBINE CONTROLLER

STURE LINDAHL

Department of Automatic Control  
Lund Institute of Technology  
December 1976

DESIGN AND SIMULATION  
OF A  
COORDINATED DRUM BOILER-TURBINE CONTROLLER

Sture Lindahl

Dokumentutgivare  
Lund Institute of Technology  
Handläggare Dept of Automatic Control  
Författare  
Sture Lindahl

Dokumentnamn  
REPORT  
Utgivningsdatum  
Dec. 1976

Dokumentbeteckning  
LUTFD2/(TFRT-3134)/1-339/(1976)  
Ärendebeteckning  
733607

10T4

Dokumenttitel och undertitel

Design and simulation of a coordinated drum boiler-turbine controller

Referat (sammandrag)

The control of a drum boiler-turbine unit during disturbances and during normal operation is investigated. The task of a control system for a boiler-turbine unit is reviewed with respect to the changing structure of the Swedish power system. A control system is designed loop-by-loop using approximate decoupling, feedforward, and PI-feedback. The performance of the control system is investigated by simulation of a nonlinear drum boiler-turbine model. The simulated responses are promising in spite of the limited capacity of the actuators. The control system can be tuned so that unacceptable stresses can be avoided.

Referat skrivet av

Author

Förslag till ytterligare nyckelord

Klassifikationssystem och -klass(er)

Indextermer (ange källa)

Omfång

339 pages

Övriga bibliografiska uppgifter

Språk

English

Sekretessuppgifter

ISSN

ISBN

Dokumentet kan erhållas från

Department of Automatic Control  
Lund Institute of Technology  
P O Box 725, S-220 07 LUND 7, Sweden

Mottagarens uppgifter

Pris

100:- Sw Kr

SIS-  
DB 1

DOKUMENTATABLAD enligt SIS 62 10 12

Blankett LU 11:25 1976-07

DESIGN AND SIMULATION OF A COORDINATED DRUM BOILER-TURBINE  
CONTROLLER

Sture Lindahl

ABSTRACT

The control of a drum boiler-turbine unit during disturbances and during normal operation is investigated. The task of a control system for a boiler-turbine unit is reviewed with respect to the changing structure of the Swedish power system. A control system is designed loop-by-loop using approximate decoupling, feedforward, and PI-feedback. The performance of the control system is investigated by simulation of a nonlinear drum boiler-turbine model. The simulated responses are promising in spite of the limited capacity of the actuators. The control system can be tuned so that unacceptable stresses can be avoided.

# TABLE OF CONTENTS

|   | <u>Page</u> |
|---|-------------|
| 1. Introduction                             | 1           |
| 2. Control Objectives                       | 4           |
| 3. Design Method                            | 10          |
| 4. Structure of the Control System          | 16          |
| 5. Power Demand Setter                      | 22          |
| 6. Drum Pressure Reference Setter           | 29          |
| 7. Drum Pressure Loop                       | 33          |
| 8. Drum Level Loop                          | 37          |
| 9. Steam Temperature Loop                   | 42          |
| 10. Output Power Loop                       | 51          |
| 11. Simulations                             | 61          |
| 12. Decrease of Output Power in Normal Mode | 66          |
| 13. Transfer from Normal to Alert Mode      | 102         |
| 14. Increase of Output Power in Alert Mode  | 137         |
| 15. Decrease of Output Power in Alert Mode  | 172         |
| 16. Transfer from Alert to Normal Mode      | 208         |
| 17. Increase of Output Power in Normal Mode | 242         |
| 18. Conclusions                             | 278         |
| 19. Acknowledgements                        | 318         |
| 20. References                              | 319         |

APPENDIX: Computer Program

## 1. INTRODUCTION

The interest in the dynamics of thermal power plants for electric energy production has grown considerably in Sweden during the last years [5, 14, 15]. The reason is the changing structure of the production system. The electric energy consumption was 80 TWh during 1975. The hydro energy production was 60 TWh and the thermal energy production was 19 TWh. The future demand for increased electric energy production will be covered by nuclear power units. New hydro power units will be installed to cover the load peaks.

### The changing structure of the Swedish energy production system.

The new nuclear power units will be larger (800-1000 MW) than both the hydro power units (<250 MW) and the fossile power units (<340 MW) in service today. Due to their complexity the nuclear power units will be disconnected from the network more frequently than the units in service today. Network short-circuits will sometimes disconnect a whole power plant (1600-3400 MW). The size and allocation of spinning reserve will be more critical during such circumstances. The spinning reserve is for the present mostly allocated to hydro power units in the northern part of Sweden. The utilization of the production system and the transmission system will require that more spinning reserve will be allocated to the southern part of Sweden. Most of the units in the southern part of Sweden are fossile or nuclear units.

### Nordic cooperation

The Swedish power system is connected to the power systems in Denmark (Sjælland), Finland, and Norway with AC-transmission lines. This cooperation between the Nordic countries has been beneficial from economic point of view. The interconnection

lines have made it possible to exploit the different structure of the production systems. Denmark has merely thermal power units, Finland and Sweden have both hydro and thermal power units, and Norway has merely hydro power units. If the amount of available water is large the inexpensive hydro power may be transmitted to the thermal areas of the Nordic countries. If the amount of available water is small the collected thermal resources may be used to produce the energy demand.

The interconnection lines have also reduced the demand for peaking power because the peak of the sum is less than the sum of the individual peaks. The interconnection lines have also made it possible to exploit composition effects of the total load. The variation of the total load is less than the sum of the individual load variations. The interconnection lines have finally reduced the demand for spinning reserve. The spinning reserve must be capable of replacing the largest unit of the interconnected system but not the sum of the largest units in the subsystems.

#### Utilization of the production system.

The power demand must be allocated among the units so that the total operating costs are reduced as much as possible. This allocation may lead to situations, when most of the hydro power units are disconnected. The amount of installed hydro power units will be so large that the exploitation of the available amount of water during high-load periods gives the best economic result. Energy production with e.g. gas turbines may be reduced. The consequences are that during low-load periods merely nuclear power units and fossile power units are in service. There is limited experience of the long-term effects on the fuel-rods of nuclear units, which have been used in automatic generation control. Until such experience has been collected the fossile power units have to contribute to the automatic generation control.

### Types of boiler-turbine units.

The amount of installed power of fossile units in Sweden is about 6 GW. The amount of installed power of drum boiler units is more than 90%. The new fossile units are usually equipped with once-through boilers. The reason is that they allow higher pressures, which contributes to a reduction of specific fuel consumption. The economic operation of the production system requires that the most economic units are loaded to their maximum capacity. The less economic units are part-loaded and have to change their production to meet the power demand. These units are often older and equipped with drum boilers.

### Conclusions.

The changing structure of the Swedish power system gives rise to more complicated control tasks both during disturbances and during normal operation. The number and the magnitude of the losses of production will increase due to the introduction of new and large nuclear power units. More spinning reserve will be allocated to fossile power units. There are a number of fairly weak interconnection lines between the Nordic countries. Such tie-lines are sensitive to power oscillations. Fossile power units have to contribute to the automatic generation control. Investigations of drum boiler-turbine control systems are motivated.



## 2. CONTROL OBJECTIVES.

The changing structure of the Swedish power system gives rise to more complicated control tasks both during disturbances and during normal operation. Some background material will be summarized and the objectives of the control system will be formulated in this section.

There are only limited means of storing energy in an AC power system. Most of the energy is stored in rotating masses. The stored energy is proportional to the second power of the rotational speed, which is proportional to the network frequency. The stored energy is proportional to the difference between the production and the consumption of energy. The amount of stored energy is usually less than the energy, which is consumed during ten seconds. This means that the energy production must be adjusted carefully to the continuously varying energy consumption. The most rapid adjustments are accomplished by the speed governors. They adjust the output power of the units in proportion to the frequency deviation. Only hydro power units participate in the automatic frequency control in Sweden for the present. A large number of hydro power units are equipped with modern electro-hydraulic turbine governors. The response rate of the hydro power units are high, more than 50%/minute. In general the power response rate of thermal power units are lower. The power setpoints of the governors are adjusted automatically or manually. During power system disturbances accompanied by losses of production the speed governors have to compensate for a large difference between production and consumption. This compensation has to be rapid in order to avoid large frequency deviations. During normal operation the output power variations have to be as small and slow as possible.

Control requirements due to a sudden loss of production.

The most severe disturbance of the energy production system is a sudden loss of a large production unit. Such a loss of production can be caused by a network short-circuit, by some incident within the unit, or by some other reason. The number and the magnitude of the losses of production will increase due to the introduction of new and large nuclear power units. The first 20 seconds after a sudden loss of production are very dramatic. The rest of the power system must remain synchronized. The power oscillations must be damped out. The power deficit must be reduced without exceeding the capacity of the transmission network. The network frequency drops rapidly during the first seconds after a loss of production. There is a risk that other units have to be disconnected from the network if the frequency decreases below 47.5 Hz. Such disconnections increase the loss of production and make the disturbance more severe. The output power of the remaining units have to be increased in order to avoid large frequency deviations. The task of instantaneous compensation of power deficit is at the present assigned to hydro power units in the Nordic system. In the future it may be desirable to assign this task to thermal power units too. One situation occurs during summer nights, when the demand is low and only run-the-river hydro power units are operating. The conclusion is that one task of the control system is to increase the output power as fast as possible during disturbances accompanied by losses of production.

Control requirements due to tie-line oscillations.

If the power system remains synchronized after a power system disturbance severe tie-line oscillations may have been excited. Tie-line oscillations may also be excited during normal operation. The tie-line oscillations in the Nordic power system have periods between one and four seconds. If the amplitude of the tie-line oscillations are increasing or if their amplitude decreases too slowly there is a risk that some tie-lines may be

tripped and a disturbance is enlarged or introduced. Therefore there is a need for means of increasing the damping of tie-line oscillations. The damping can be increased by feeding the automatic voltage regulators with supplementary signals proportional to the speed error and the speed error derivative. The damping of the oscillations can also be increased if the mechanical power could be changed in proportion to the speed error. The non-minimum phase character of water turbines makes it difficult to utilize them. The steam turbines on the other hand may contribute to the damping of tie-line oscillations. The conclusion is that one task of the control system is to increase the damping of tie-line oscillations.

#### Control requirements due to normal load variations.

The random load variations disturb the power system during normal operation. The task of following these random load variations in the Nordic power system has been assigned to the hydro power units. When the demand is low and mainly supplied by nuclear power plants and run-the-river hydro power plants it will be necessary to let the thermal power plants follow the random load variations. The conclusion is that one task of the control system is to adjust the output power to the total demand.

#### Control requirements due to transmission network limitations.

The load centres are located in the southern part of Sweden but most of the hydro power plants are located in the northern part. The capacity of the transmission network has been increased rapidly during the last 25 years. The capacity will increase more slowly in the future. When the demand is high the maximum capacity of the transmission network will be reached. The marginal production cost will be lower in the northern part of Sweden due to this constraint. The total production cost will be reduced if the transmission from the north to the south is as high as pos-

sible during such periods. This can be achieved by adjusting the output power of the thermal power units in the southern part of Sweden according to the load there. The conclusion is that one task of the control system is to adjust the output power of the unit according to the load in one area.

#### Control requirements due to power system control.

One task of the power system is to supply the demand at a minimum cost. The different units have different operating costs. The production must be allocated correctly among the units in order to reduce the total cost. This allocation is often computed in a dispatch centre and the result has to be transmitted to the different units. The conclusion is that one task of the control system is to receive a set-point signal from a control centre.

#### Control requirement due to risk of process damage.

The output power of the units must not be changed so rapidly that the units are damaged. There are many ways of damaging a thermal power unit; Feedwater may reach the turbine. Heat exchanger tubes may be overheated. Thermal stresses may reduce the life-time of the unit. The acceptable magnitude of thermal stresses depend on the frequency of their occurrence. The maximum power response rate must be used during severe and infrequent disturbances. A lower power response rate must be used during normal load-following. The conclusion is that there shall be two different power response rates, one to be used during disturbances and another to be used during normal operation. The selection of the higher response rate shall be done manually from the unit's control room, automatically based on the network frequency, or from a control centre.

Summary.

Following conclusions may be drawn from the previous discussion: There is a need for a unit control system for drum boilers. The primary task of the control system is to:

- 1) increase the output power during disturbances,
- 2) increase the damping of tie-line oscillations,
- 3) adjust the output power according to the load,
- 4) receive a set-point signal from the unit's control room or from a remote dispatch centre,
- 5) modify the set-point with respect to the network frequency in order to form the reference value of the output power,
- 6) limit the power response rate to adjustable values, one set to be used during normal operation, and another set to be used during disturbances, and
- 7) use the power response rate selected manually from the units control room, automatically based on network frequency, or from a dispatch centre.

The secondary task of the control system is to control

- 1) the drum pressure,
- 2) the drum level, and
- 3) the steam temperature.

The four variables shall be controlled by manipulating

- 1) the control valve position,
- 2) the fuel flow,
- 3) the feedwater valve position,
- 4) the position of the first attemperator spray flow valve, and
- 5) the position of the second attemperator spray flow valve.

The possibilities of improving the performance of the boiler-turbine unit by manipulating the extraction flows shall also be investigated.

### 3. DESIGN METHOD.

The problem is to design a control system for a drum boiler-turbine unit. Four important variables are to be controlled by manipulating seven variables. One model [12] of the boiler-turbine unit has 20 state variables. There are several nonlinearities in the process, e.g. the opening of the valves are limited, the speed of the servos are limited, and the thermodynamic state of water is described by nonlinear equations.

#### 3.1. Review of Earlier Work.

There are many papers on application of modern control theory to boiler-turbine control [1, 6, 13]. It has been proposed to apply deterministic optimal control theory to the problem of large load changes. Much of the interest has focused on the multivariable and stochastic character of the problem. Linear stochastic control theory has been used to find a control law valid for small perturbations around one operating point. The separation theorem, which states that the optimal control of a linear stochastic system can be separated into one estimation problem and one deterministic control problem has been used. The estimation problem has usually been solved by a Kalman-Bucy filter, which provides the best estimate of the state vector, given the observations. The solution of the control problem is a linear feedback from the best estimate of the state vector [3].

To implement the control law the following problems must be solved:

- 1) nonlinearities,
- 2) reference values,
- 3) restrictions,
- 4) start-up and shut-down,
- 5) on-line tuning.

### Nonlinearities.

A linear model is valid only in the vicinity of an operating point but the boiler-turbine unit has to be controlled over the full power range. Some of the parameters will change by a factor of two when the output power changes from minimum to maximum. This means that the control law will change and that the Kalman filter will change. In spite of these variations in process dynamics boilers are traditionally controlled by regulators having fixed gains. The controllers have usually been tuned for operation with high output power. To cope with the problem of nonlinearities the feedback and the Kalman filter have to be recomputed or precomputed and stored. This means that a number of control laws and a number of switching surfaces have to be introduced.

Thus the linear control system has been converted to a nonlinear control system, the stability of which has to be investigated carefully by simulation of the nonlinear model and the control system.

### Reference values.

A control law, obtained by applying linear theory, is based on a model

$$d(\Delta x)/dt = A\Delta x + B\Delta u$$

$$\Delta y = C\Delta x + D\Delta u$$

where  $\Delta x = x - x_{ref}$ ,  $\Delta u = u - u_{ref}$  and  $\Delta y = y - y_{ref}$ . The Kalman filter is given by:

$$d(\hat{\Delta x})/dt = A\hat{\Delta x} + B\Delta u + K(\Delta y - C\hat{\Delta x})$$

and the control law by:



$$\Delta u = -L\Delta\hat{x}$$

where  $\Delta\hat{x} = \hat{x} - x_{ref}$  and  $\hat{x}$  is the estimate of  $x$ . There is a problem how to compute consistent values of  $x_{ref}$ ,  $u_{ref}$  and  $y_{ref}$ . There are, however, several attempts to solve this problem [2, 4].

### Start-up and shut-down.

During start-up and shut-down the boiler-turbine unit is usually controlled manually. As the starting procedure advances it is desirable to switch over to automatic control successively. This means that a set of control laws has to be computed or precomputed and stored. During start-up and shut-down there is not one system but in fact a number of systems to be controlled.

### On-line tuning.

During comissioning the control system has to be tuned. Differences between the dynamic properties of the boiler-turbine unit and the dynamic properties of the model as well as late changes of components of the boiler-turbine unit may be the reason. The problem of on-line tuning of a controller designed using linear stochastic control theory is not straightforward.

### 3.2. Design Procedure.

The problems mentioned above may not be impossible to solve but even if they were solved it is questionable how much can be gained from the application of sophisticated control schemes. There are indications that the performance of boiler-turbine units are not limited by the interaction between control loops. On the contrary the performance of the boiler-turbine unit is

knowingly limited by measures taken to avoid unacceptable stresses of the boiler-turbine unit. It was decided to use a loop-by-loop approach and simulation for the design.

Two different models have been used in order to design the control system; One simplified model, describing the steady state and the most important dynamics, has been used in order to find the structure of the control system. Another model, described in [12] has been used in order to simulate the control system.

The design procedure can be described as approximative decoupling, feedforward and PI-feedback. The procedure used to obtain the decoupling and feedforward is illustrated using a simple linear system. Assume that the most important dynamics can be described by the linear model

$$dx/dt = Ax + Bu$$

$$y = Cx$$

where  $x$  are the state variables,  $u$  are the manipulated variables,  $y$  are the variables to be controlled, and  $A$ ,  $B$ , and  $C$  are matrices of appropriate dimensions. The derivative of the controlled variables are given by

$$dy/dt = CAx + CBu \tag{3.1}$$

Assuming that  $CB$  is invertible and applying the control law

$$u = - (CB)^{-1} (CAx - w)$$

gives

$$dy/dt = w$$

Using this procedure the system is transformed into a system, consisting of a number of decoupled integrators.

Only a limited class of systems can be controlled using such a procedure. If it works, the procedure is easy to apply. The crucial step is to solve  $u$  from (3.1), which required CB regular. It is well-known from linear system theory e.g. [4] how to handle the general case. The general solution is not known for nonlinear systems. Specific results for the nonlinear boiler-turbine model are given in the following.

The procedure used to obtain the feedforward is also illustrated in Fig. 3.1.

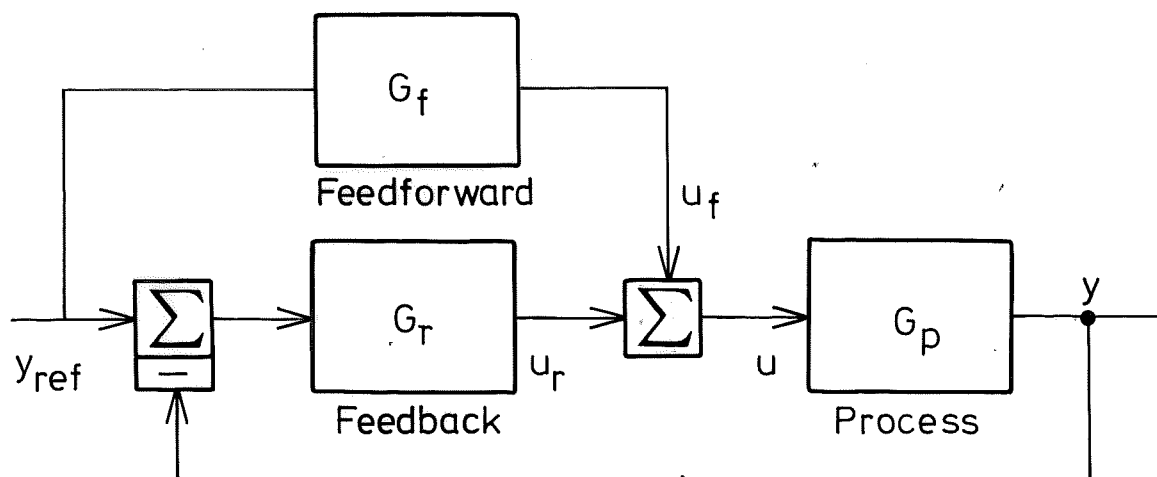


Fig. 3.1 - The basic control loop.

From Fig. 3.1 it follows that the manipulated variables,  $u$  consist of two components; the feedforward,  $u_f$  and the feedback,  $u_r$ . If possible  $G_f$  is chosen so that  $G_f G_p = 1$  and, in such cases  $u_r$  is zero when  $y_{ref}$  changes. This means that  $y$  follows  $y_{ref}$  perfectly. In many cases  $G_f$  is chosen so that  $G_f G_p \approx 1$  or even  $G_f(0)G_p(0) = 1$ . In such cases  $u_r$  is not zero and  $y$  does not follow  $y_{ref}$  perfectly. The task of the feedback is easier after the introduction of the feedforward.

The following elementary rules are helpful when designing a control system by this procedure:

- 1) Feedforward counteracts the creation of a control error.
- 2) Feedforward does not affect the stability.
- 3) Feedback reduces an existing error.
- 4) Feedback does affect the stability.

#### 4. STRUCTURE OF THE CONTROL SYSTEM.

The ideas underlying the design of the control system were described in the previous section. A detailed structure of the control system will be given in this section. The following procedure was used to arrive at the structure: The model described in [12] was simplified. The simplified model was used in order to find the inputs used to control a particular output. The simplified model was also used in order to find the variables used to close minor control loops. The simplified model was finally used to achieve decoupling and feedforward in analogy to the treatment of the linear case in the example in the last section. The procedure is not unique because there is arbitrariness in choosing the inputs used to control a particular output. This choice was guided by previous practice in boiler control as well as physical insight. Apart from this the procedure is unique once the simplified model is given. To arrive at the structure the different control loops will now be discussed starting with the most important variables.

##### Control loops.

There are four important variables to be controlled:

- output power,
- drum pressure,
- drum level, and
- steam temperature.

The most important variable is the output power. The output power is approximately proportional to the steam flow. The steam flow depends on the opening of the steam control valve and the drum pressure. The drum pressure depends on the fuel flow and the steam flow. These circumstances motivate that drum pressure is considered more important than drum level and steam temperature. The drum level is considered more important

than steam temperature because drum level deviations will lead to process damage.

#### Reference value of the output power.

The reference value of the output power is generated by the power demand setter (PDS) in Fig. 4.1. The reference value is based on the set-point of the output power and the actual network frequency. The set-point of the output power may be generated in the control room of the unit or in a remote control centre. The set-point can be specified by a final value and a gradient. The set-point of the output power is modified in two steps before it becomes the reference value of the output power. The desired output power is reduced if the network frequency is high. The desired output power is increased if the network frequency is low. There are adjustable limits of the desired output power. The variations of the output power is limited by a jump-and-rate circuit.

#### Reference value of drum pressure.

The steam flow depends on both the opening of the control valve and the drum pressure as mentioned before. The desired steady-state relation between steam flow and drum pressure is not given a priori. Constant pressure control or sliding pressure control is often used.

If constant pressure control is used the drum pressure or the steam pressure before the control valve is kept constant near its maximum allowable value. The opening of the steam control valve is used to control the steam flow. Hydraulic servos for the control valve permit very short (0.3 - 5.0 s) positioning times. The steam flow can be changed very rapidly if constant pressure control is used.

If sliding pressure control is used the steam control valve is

kept in a fully open position. The drum pressure is changed in order to change the steam flow. The fuel flow and the stored energy has to be changed before the steam flow is changed. This means that the steam flow cannot be changed rapidly if sliding pressure control is used.

The specific fuel consumption is lower if sliding pressure control is used than if constant pressure control is used. The choice between constant pressure control and sliding pressure control is a trade off between economy and dynamic properties.

It is desirable to design a control system with better dynamic properties than can be achieved by sliding pressure control. Therefore it was decided to use modified sliding pressure control. The sliding pressure control is modified in two ways. Firstly the reference of the drum pressure is determined from the reference value of the output power in such a way that the output power can be increased approximately 15% by opening of the steam control valve. Secondly the extraction flows are temporarily reduced when the output power is to be increased and vice versa.

The reference value of the drum pressure is generated by the drum pressure reference setter (DPRS) in Fig. 4.1. The reference value of the drum pressure cannot be changed faster than an adjustable value in order to avoid unacceptable stresses.

#### The output power loop.

The output power is controlled by the turbine power controller (TPC), the high-pressure preheater controller (HPPC), and the low-pressure preheater controller (LPPC). The TPC compares the output power with its reference value and computes the reference value of the stroke of the steam control valve. The control valve servo (CVS) changes the opening of the steam control valve by changing the stroke of the control valve.

The reference value of the output power is high-pass filtered in the HPPC in order to compute the reference value of the stroke of the high-pressure preheater extraction valves. The high-pressure preheater servo (HPPS) changes the opening of the high-pressure preheater valves by changing the stroke of the valves.

The reference value of the output power is high-pass filtered in the LPPC in order to compute the reference value of the stroke of the low-pressure preheater extraction valves. The deaerator pressure and its reference value is also used in order to compute the reference value. The low-pressure preheater servo (LPPS) changes the opening of the low-pressure preheater valves by changing the strokes of the valves.

#### The drum pressure loop.

The drum pressure controller (DPC) computes the reference value of the fuel flow. The inputs to the DPC are the steam flow, the derivative of the reference value of the drum pressure, the drum pressure and its reference value. The fuel flow servo (FFS) controls the fuel flow by manipulating the fuel flow valve and the number of burners.

#### The drum level loop.

The drum level controller (DLC) computes the reference value of the feedwater flow. The inputs to the DLC are the steam flow, the drum level, and its reference value. The feedwater servo (FWS) controls the feedwater flow by manipulating the feedwater valve.



The steam temperature loop.

The steam temperature before the control valve is controlled by the secondary superheater steam temperature controller (SSSTC) and by the tertiary superheater steam temperature controller (TSSTC). The SSSTC computes the reference value of the steam temperature before the secondary superheater. The inputs to the SSSTC are the fuel flow, the steam flow, the steam temperature after the secondary superheater, and its reference value. The TSSTC computes the reference value of the steam temperature before the tertiary superheater. The inputs to the TSSTC are the fuel flow, the steam flow, the steam temperature after the tertiary superheater, and its reference value. The secondary superheater steam temperature servo (SSSTS) controls the steam temperature before the secondary superheater by manipulating the first attemperator spray flow valve. The tertiary superheater steam temperature servo (TSSTS) controls the steam temperature before the tertiary superheater by manipulating the second attemperator spray flow valve.



## 5. POWER DEMAND SETTER.

The task of the power demand setter (PDS) is to generate the reference value of the output power. The PDS is comprised of three parts; PDS1, PDS2, and PDS3.

The task of the PDS1 is to receive the set-point of the output power and its derivative from a control centre and to select the set-point of the output power and its derivative from the control room of the unit or from a control centre. The block diagram of the PDS1 is given in Fig. 5.1. The PDS1 contains a switch, which selects the set-point of the output power from the control room of the unit or from a control centre. The preliminary reference value of the output power is the output of an integrator,  $s_{nsl}$  (SNS1) as shown in Fig. 5.1. There is a feedback around the integrator and the output of the integrator is compared with the selected set-point of the output power. The difference is limited to  $\pm 1$  and multiplied by the selected gradient of the set-point of the output power,  $u_{nslr}$  in order to form the input to the integrator. If the difference between the selected set-point of the output power,  $s_{nslr}$  and the preliminary reference value of the output power,  $s_{nsl}$  is larger than  $1/g_{nsl_i}$  ( $= 2.0$  kW) the input to the integrator is equal to the selected gradient of the set-point of the output power,  $u_{nslr}$ . If the difference is smaller than  $1/g_{nsl_i}$  ( $= 2.0$  kW) the difference decays exponentially with a time constant given by the slope of the nonlinear block. The maximum rate of change of the preliminary reference value of the output power is equal to the selected gradient of the set-point of the output power.

The task of the PDS2 is to modify the preliminary reference value of the output power with respect to the measured network frequency and to limit the modified reference value with respect to the allowable operating range of the boiler-turbine unit. The preliminary reference value of the output power,  $s_{nsl}$  is modified with respect to measured network frequency as shown in Fig. 5.2. The frequency error is here defined as the difference

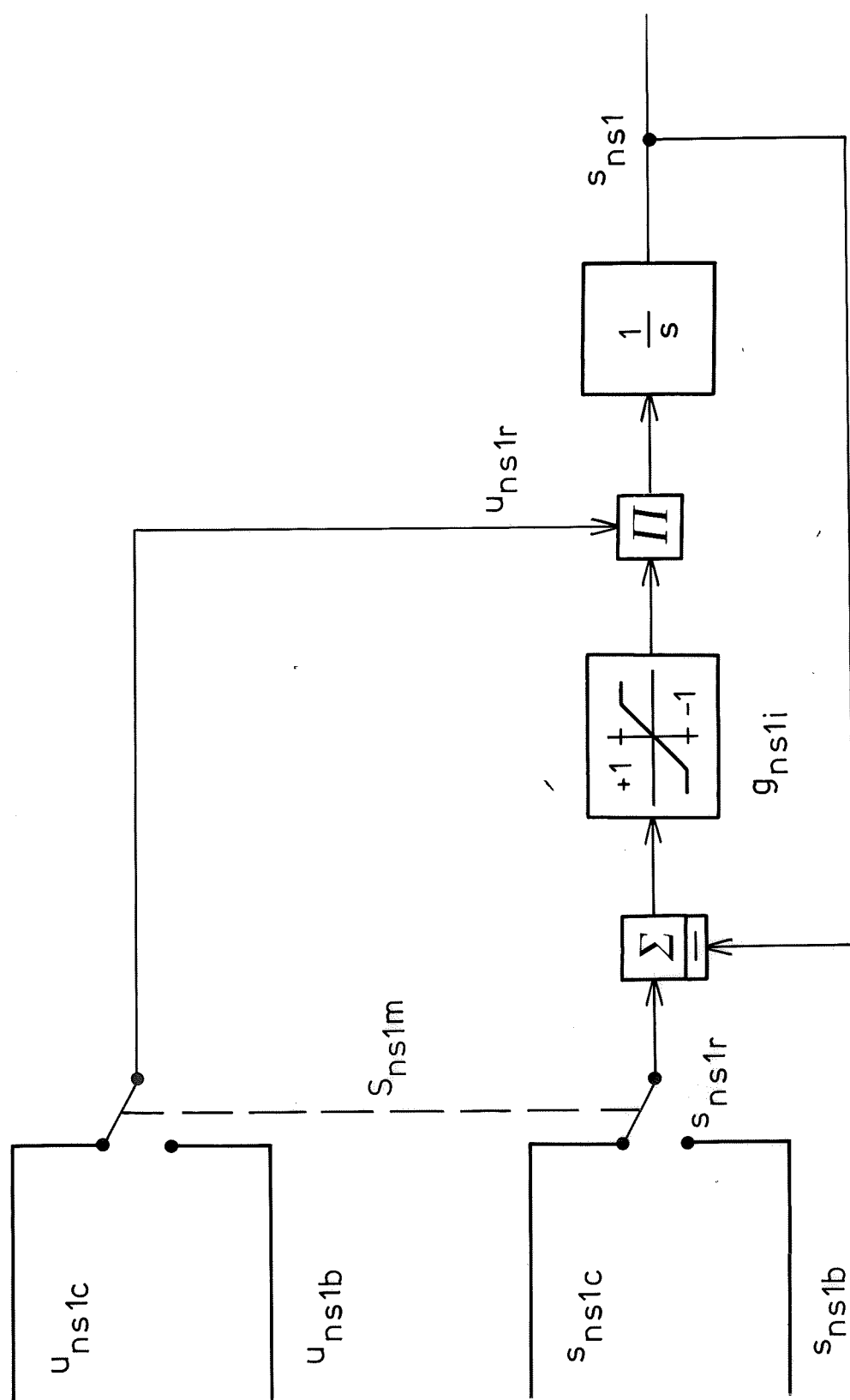


Fig. 5.1 - Block diagram of the first part of the power demand setter (PDS1).

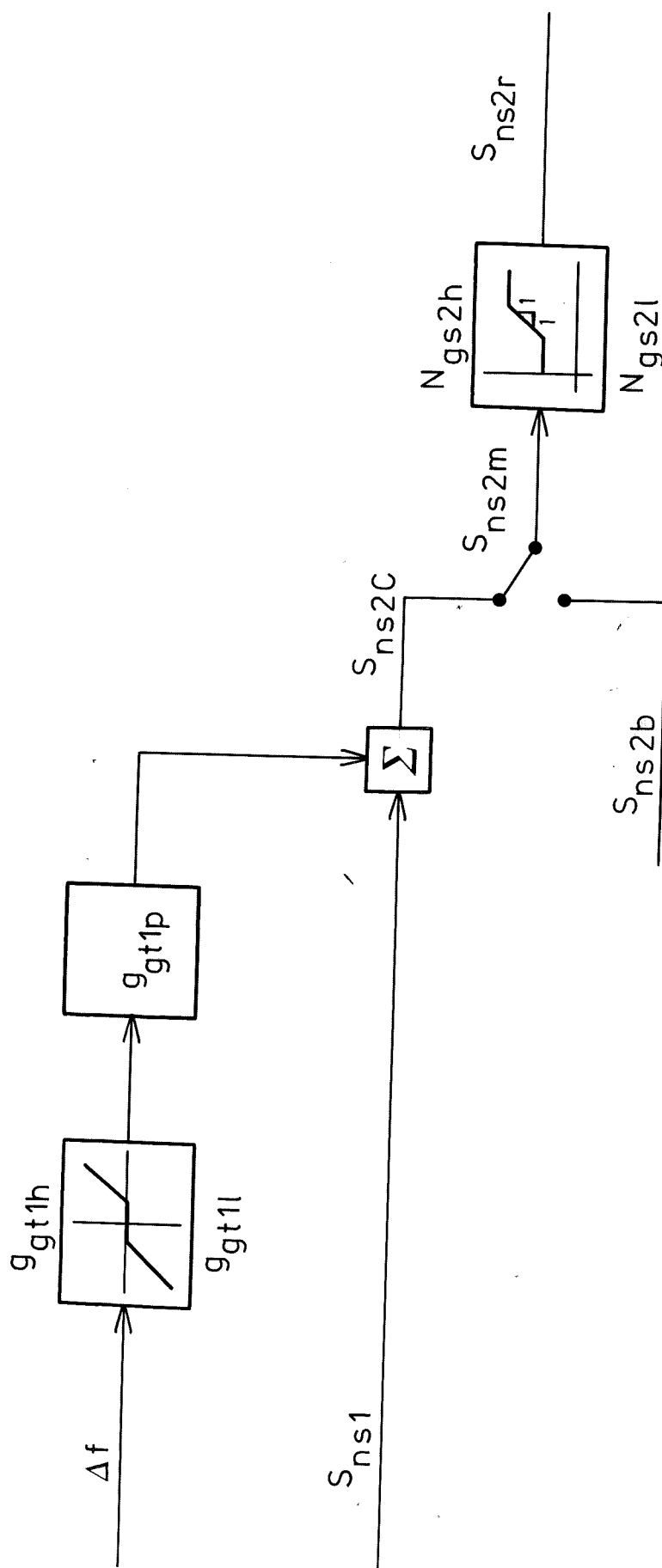


Fig. 5.2 - Block diagram of the second part of the power demand setter (PDS2).

between the reference value of the network frequency and the measured value of the network frequency. This error is positive if the energy demand is larger than the energy production. This means that a positive frequency error has to modify the reference value of the output power in positive direction. This modification is mainly intended to be used during disturbances, i.e. large frequency errors. During normal operation the necessary changes of the energy production is transmitted from the control centre. The frequency error input is therefore furnished with a dead-zone, with adjustable limits. The positive limit,  $g_{gtlh}$  and the negative limit,  $g_{gtll}$  are individually adjustable. If it is desirable the size of the dead-zone can be reduced to zero. The ratio between the change of the output power and the change of the network frequency can be changed with the adjustable gain,  $g_{ntlp}$ . This corresponds to the droop of speed governors commonly used. To prevent unacceptable values of the reference value of the output power the modified value is limited between a minimum,  $N_{gs2l}$  and a maximum,  $N_{gs2h}$  value. The maximum value  $N_{gs2h}$  is determined by the smallest value of the maximum output power of the turbine and the maximum output power of the generator. This value can be reduced if all burners are not used, if all feedwater pumps are not in operation, or if all fans are not in operation. The maximum output power,  $N_{gs2h}$  has been fixed ( $= 160 \cdot \text{MW}$ ) during the simulations.

The task of the PDS3 is to limit the variations of the reference value of the output power with respect to the allowable stresses of the boiler-turbine unit. The variation of the reference value of the output power is limited in a jump-and-rate circuit as shown in Fig. 5.3. The negative jump ( $-\text{JUMP1}$ ) and the positive jump ( $\text{JUMP2}$ ) used during normal operation are individually adjustable. The negative rate-of-change ( $-\text{RATE1}$ ) and the positive rate-of-change ( $\text{RATE2}$ ) used during normal operation are also individually adjustable. During disturbances larger values of the negative jump ( $-(\text{JUMP1} + \text{JUMP3})$ ) and the positive jump ( $\text{JUMP2} + \text{JUMP4}$ ) are used. The additions ( $-\text{JUMP3}$ ) and ( $\text{JUMP4}$ ) are also individually adjustable. During disturbances larger values of the negative

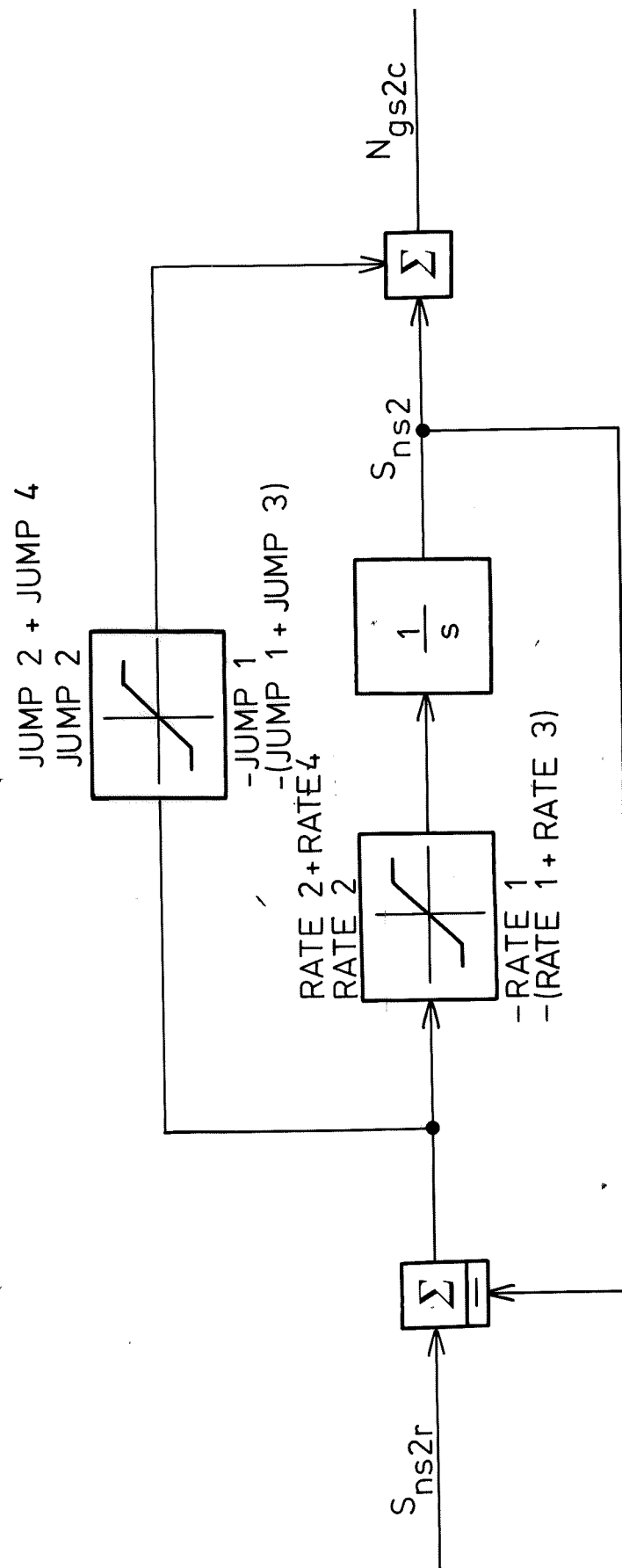


Fig. 5.3 - Block diagram of the third part of the power demand setter (PDS3).

rate  $\{-(\text{RATE1}+\text{RATE3})\}$  and the positive rate  $(\text{RATE2}+\text{RATE4})$  are used. The additions are also individually adjustable.

The power response rates to be used during normal operation must be chosen so that they can be used arbitrarily often. The power response rates to be used during disturbances must be chosen so that they can be used a limited number of times. The values of the power response rates used during the simulations are given in Table 5.1. The power response rates have to be chosen in cooperation with the manufacturer of the boiler turbine unit.

| Mode   | Jump |    | Rate  |    |
|--------|------|----|-------|----|
|        | %    |    | %/min |    |
|        | -    | +  | -     | +  |
| Normal | 5    | 5  | 9     | 6  |
| Alert  | 10   | 10 | 15    | 12 |

Table 5.1 - Power response rates used during the simulations.

The final reference value of the output power,  $N_{gs2r}$  is a central variable of the control system for the boiler-turbine unit. It is fed forward to the drum pressure reference setter (DPRS), to the turbine power controller (TPC), to the low pressure preheater controller (LPPC), and to the high-pressure preheater controller (HPPC). Typical responses of the PDS at nominal network frequency is shown in Fig. 5.4.



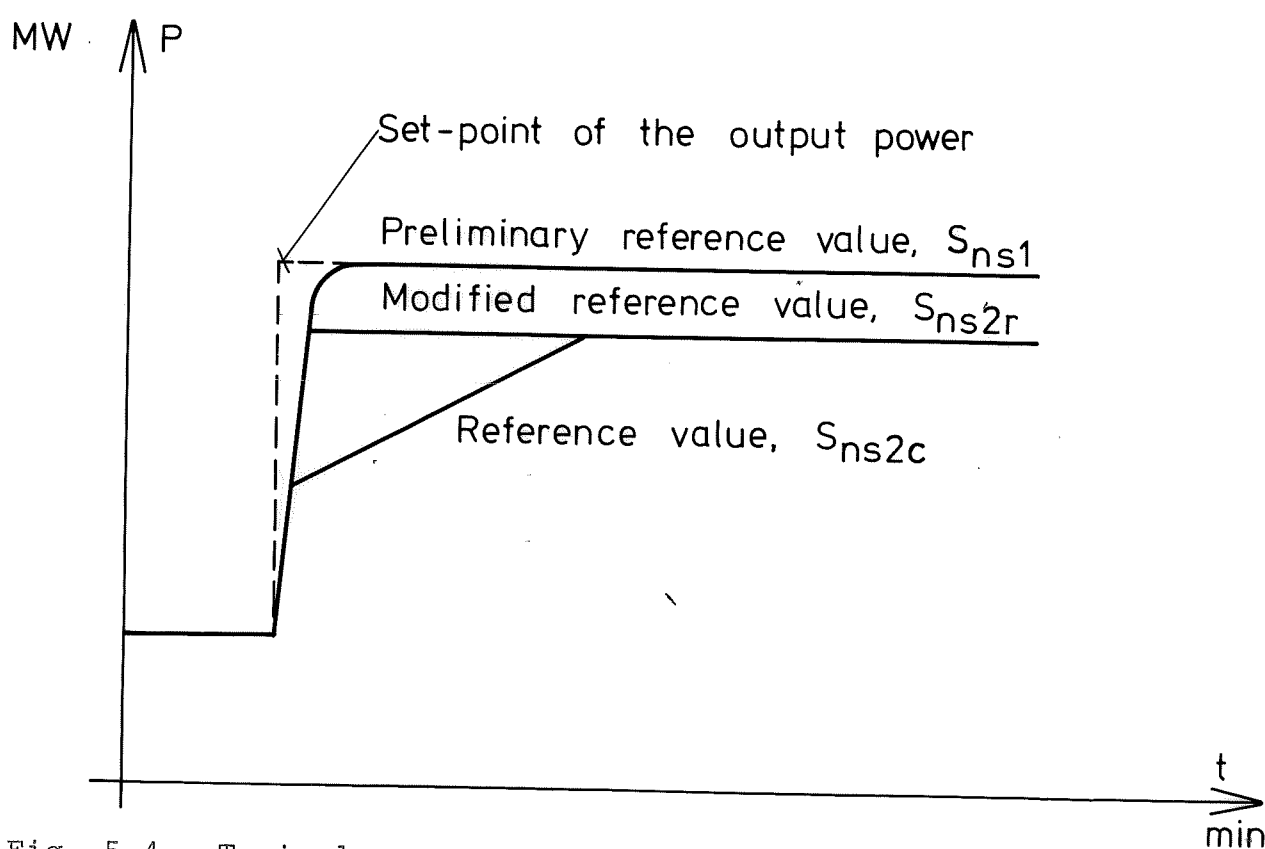


Fig. 5.4 - Typical responses of the power demand setter (PDS).

## 6. DRUM PRESSURE REFERENCE SETTER.

The reference value of the drum pressure is computed by the drum pressure reference setter (DPRS). The task of the DPRS is to compute the reference value of the drum pressure based on the reference value of the output power, to limit the reference value of the drum pressure with respect to the stresses of the boiler, and to limit the variations of the reference value of the drum pressure with respect to the thermal stresses of the boiler.

Modified sliding pressure control is used during normal operation but constant pressure control is used during disturbances. The reference value of the drum pressure is given in Fig. 6.1 as a function of the reference value of the output power. The output power is approximately proportional to the drum pressure if sliding pressure control is used. The reference value of the drum pressure is linearly related to the reference value of the output power if modified sliding pressure control is used. If possible the reference value of the drum pressure is 10-20% higher than the pressure necessary to produce the same power using sliding pressure control. The computed reference value of the drum pressure is given by

$$p_{ds2r} = g_{bol f}^{N_{gs2r}} p_{ds2h}^{/N_{gs2h}}$$

where  $g_{bol f}$  ( $= 1.25$ ) is an adjustable parameter. The reference value of the drum pressure is limited from below by  $p_{ds2l}$  ( $= 70 \cdot 10^5$  Pa) and from above by  $p_{ds2h}$  ( $= 145 \cdot 10^5$  Pa). The derivative of the reference value of the drum pressure is limited from below ( $-RATE5$ ) and from above ( $RATE6$ ) during normal operation. The two parameters are individually adjustable. The derivative is limited from below ( $-RATE5-RATE7$ ) and from above ( $RATE6+RATE8$ ) during disturbances. Both additions are individually adjustable. The values of the rate-of-change are shown in Table 6.1.

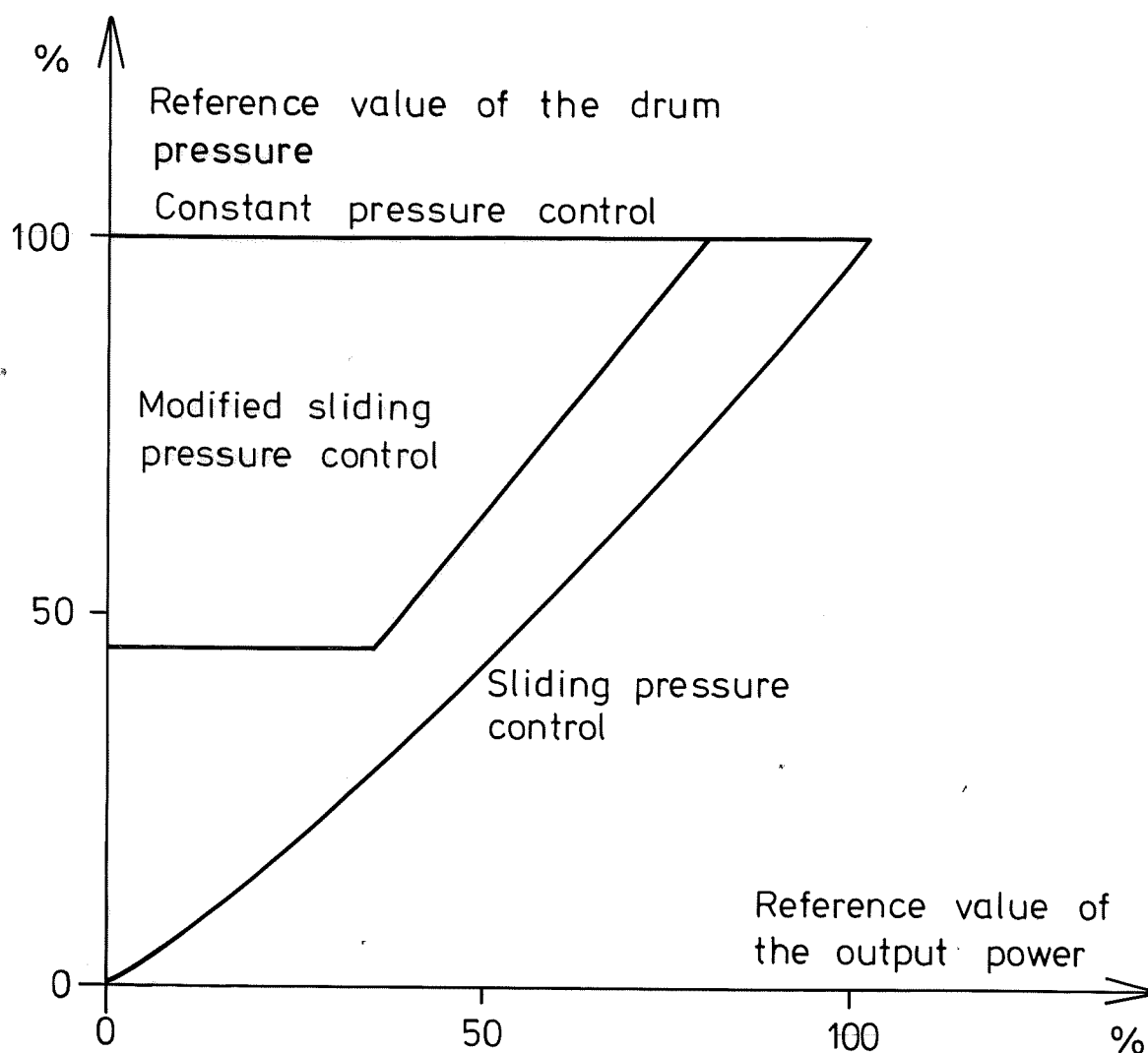


Fig. 6.1 - Reference value of the drum pressure as a function of the reference value of the output power.

| Mode   | Rate-of-change        |      |
|--------|-----------------------|------|
|        | $10^5 \text{ Pa/min}$ |      |
|        | -                     | +    |
| Normal | 4.5                   | 9.0  |
| Alert  | 9.0                   | 18.0 |

Table 6.1 - Values of the rate-of-change of the reference value of the drum pressure.

The drum pressure reference setter consists of an integrator with limited input and output as shown in Fig. 6.2. The input to the integrator is the derivative of the reference value of the drum pressure, which is used in the drum pressure controller (DPC).

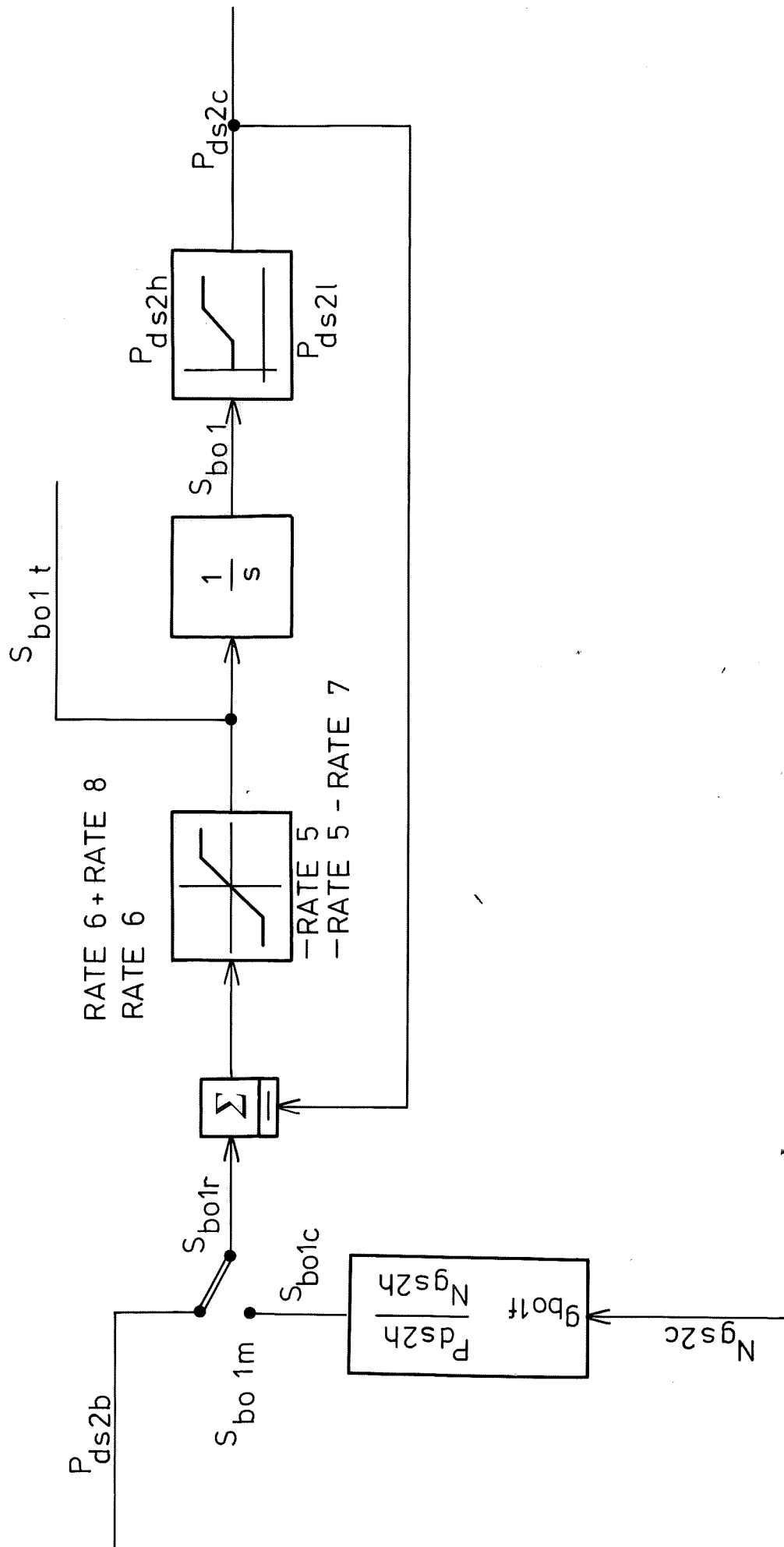


Fig. 6.2 - Block diagram of the drum pressure reference setter (DPRS).

## 7. DRUM PRESSURE LOOP.

The task of the drum pressure loop is to control the drum pressure by manipulating the fuel flow. The drum pressure loop is comprised of the drum pressure controller (DPC) and the fuel flow servo (FFS). The task of the DPC is to compute the reference value of the fuel flow. The task of the FFS is to control the fuel flow.

The following simplified model of the energy storage is used in order to determine the structure of the drum pressure controller:

$$\frac{dH(p_{ds2})}{dt} = kw_{bol} + h_{dwl}w_{dwl} - h_{ds2}w_{ds2}$$

Introducing  $\Delta p = p_{ds2r} - p_{ds2}$  and assuming that  $w_{dwl} = w_{ds2}$  we get

$$\frac{\partial H}{\partial p} \frac{d\Delta p}{dt} = \frac{\partial H}{\partial p} \frac{dp_{ds2r}}{dt} - kw_{bol} + (h_{ds2} - h_{dwl})w_{ds2}$$

The derivative of the drum pressure error is equal to zero if

$$w_{bol} = \left| \frac{\partial H}{\partial p} \frac{dp_{ds2r}}{dt} + (h_{ds2} - h_{dwl})w_{ds2} \right| / k$$

The feedforward part of the DPC becomes:

$$g_{bo3c}w_{tsl} + g_{bo3d}dp_{ds2r}/dt$$

The control law of the DPC becomes:

$$w_{bolr} = g_{bo3c}w_{tsl} + g_{bo3d}dp_{ds2r}/dt + \\ + g_{bo2p}\Delta p_{ds2} + g_{bo2i} \int_{-\infty}^t \Delta p_{ds2} dt$$

The term  $g_{bo3c} \bar{w}_{tsl}$  is the fuel flow which is needed to keep the drum pressure in steady state. The parameter  $g_{bo3c}$  (GB03C = 0.00703) was determined from a steady-state simulation:

$$g_{bo3c} = \bar{w}_{bo1} / \bar{w}_{tsl}$$

where  $\bar{w}_{tsl}$  is the steam flow (113.8 kg/s) and  $\bar{w}_{bo1}$  is the fuel flow (7.78 kg/s). The term  $g_{bo3d} dp_{ds2r}/dt$  represents the extra fuel flow, which is needed to change the drum pressure with  $dp_{ds2r}/dt$  Pa/s.

The parameter  $g_{bo3d}$  (GB03D =  $4 \cdot 10^{-5}$ ) was determined by simulation.

It has been assumed that the fuel flow is governed by a fuel flow servo during the simulations. From [7] it was known that the actuator needed 25 s to shut or open completely. From [9] it was further known that a typical start up time for an oil-burner is 80 s. This means that there is a considerable delay from the command signal to the fuel flow. In order not to underestimate this effect the delay was replaced by a minimal ( $WB01S = 0.1$  kg/s) and a maximal ( $WB01O = 0.1$  kg/s) rate-of-change. This means that the FFS is four times slower than the real process. The fuel flow is limited from below ( $WB01L = 0.0$  kg/s) and from above ( $WB01H = 11.0$  kg/s).

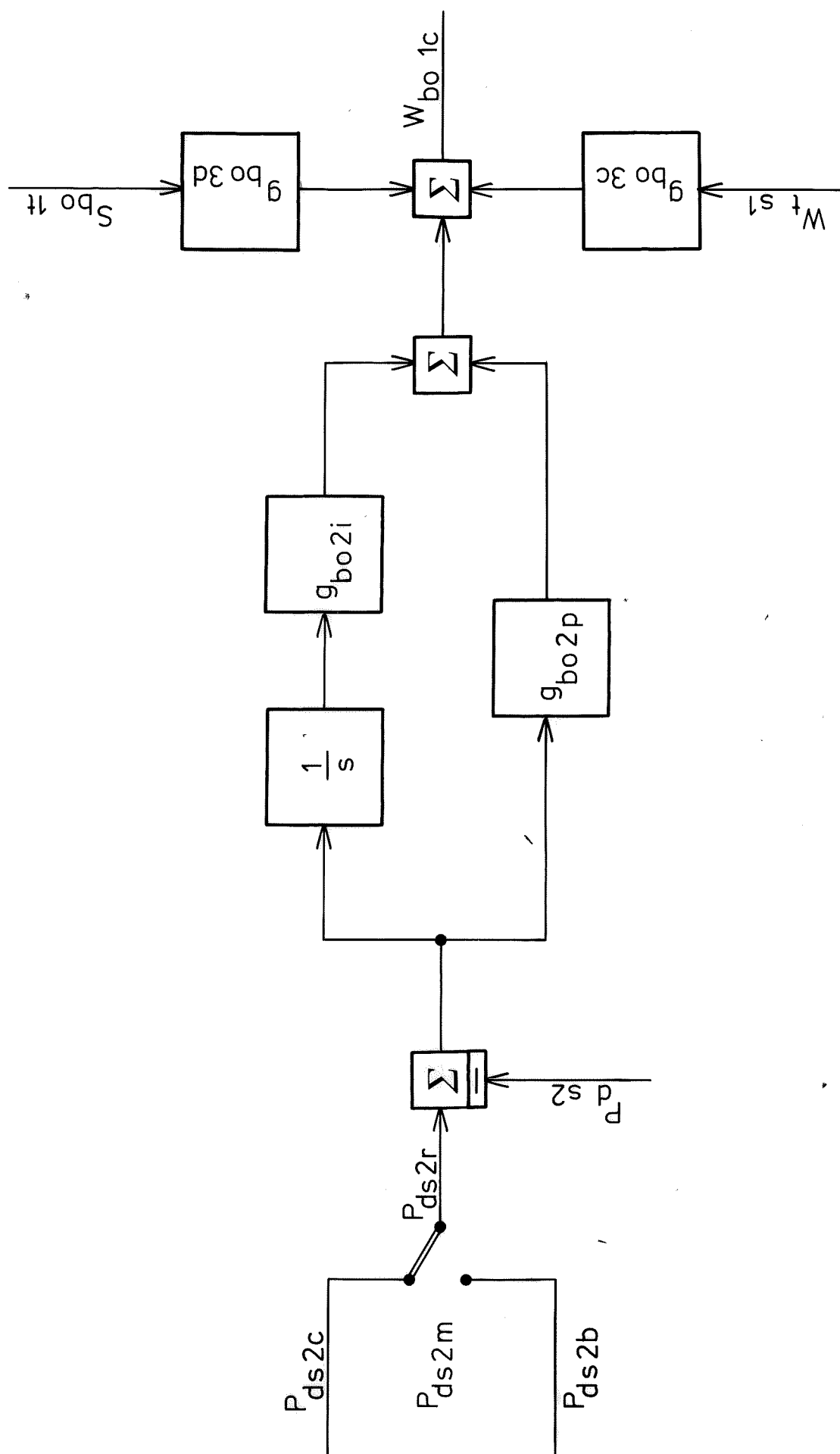


Fig. 7.1 - Block diagram of the drum pressure controller (DPC).



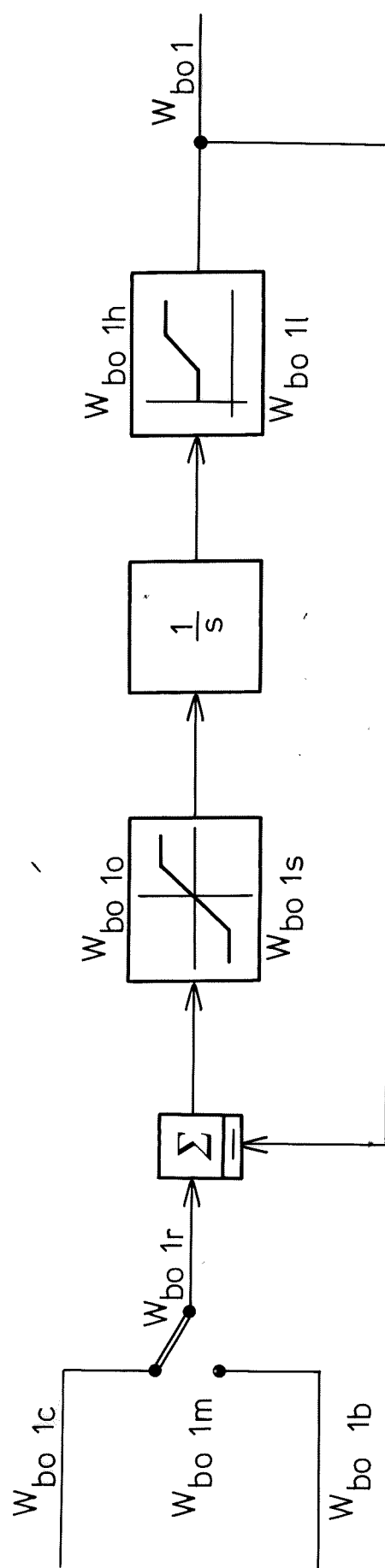


Fig. 7.2 - Block diagram of the fuel flow servo (FFS).

## 8. DRUM LEVEL LOOP.

The task of the drum level loop is to control the drum level by manipulating the feedwater valve. The drum level loop is comprised of the drum level controller (DLC) and the feedwater servo (FWS). The task of the DLC is to compute the reference value of the feedwater flow. The task of the FWS is to control the feedwater flow by manipulating the feedwater valve.

The control of the drum level is difficult due to the shrink and swell phenomenon. This causes the non-minimum phase character of the transfer function from the steam flow to the drum level. The phenomenon is pronounced when the drum pressure changes. In such cases the mean density of the steam-water mixture in the riser tubes is affected. If e.g. the steam flow increases rapidly the drum pressure begins to decrease. The reduced pressure forces some water in the riser tubes at the initial saturation temperature to evaporate. This steam is not available in the drum immediately, but forces water and steam from the uppermost part of the riser tubes into the drum. This means that the drum level starts to increase. After a while (20-40 s) the level will decrease due to the increased steam flow.

If we rely upon feedback only it is necessary to increase the gain in order to prevent too large excursions of the drum level. The situation is more difficult if the servo of the feedwater valve has a limited rate of change. The feedwater valve starts to close during the initial swell. Then the drum level decreases and the feedwater valve has to be opened. Unfortunately the servo has to start from an almost closed position due to the initial swell. This means that the drum level will reach low values before the feedwater valve has reached a position corresponding to the steam flow.

The limits of the drum level are determined by a compromise between the risks of insufficient cooling of the riser tubes and of water carrying over into the high-pressure turbine.

The following simplified model of the mass storage is used in order to determine the structure of the drum level controller:

$$\frac{d(V\rho)}{dt} = w_{dwl} - w_{tsl}$$

where  $V$  is the volume of the steam water mixture in the drum system,  $\rho$  is the mean density and it has been assumed that there is no mass storage in the steam volume. Introducing  $\Delta z_{dl4} = z_{dl4r} - z_{dl4}$  and assuming that  $d(z_{dl4r})/dt = 0$  we obtain:

$$V \frac{d\Delta z_{dl4}}{dt} = V \frac{d\rho}{dt} + w_{tsl} - w_{dwl}$$

The derivative of the drum level is equal to zero if

$$w_{dwl} = w_{tsl} + V \frac{d\rho}{dt}$$

The term  $Vd\rho/dt$  is neglected because it causes the shrink and swell phenomenon. The feedforward part of the DLC simply becomes:

$$w_{tsl}$$

The control law of the DLC becomes

$$w_{dwlr} = w_{tsl} + g_{wwlp} \Delta z_{dl4} + g_{wwli} \int_{-\infty}^t \Delta z_{dl4} dt$$

The proportional gain,  $g_{wwlp}$  ( $GWWLP = 500$ ) and the integral gain,  $g_{wwli}$  ( $GWWLI = 1$ ) have been determined by simulation. The block diagram of the DLC is shown in Fig. 8.1.

The feedwater flow is determined by the speed and the characteristics of the feedwater pump, the opening of the feedwater valve, the drum pressure and the friction losses in the high-

pressure preheater and the economizer. The details about the feedwater pump were not available and it has been assumed that the pump can be represented by a constant pressure behind a quadratic flow resistance. The influence of drum pressure, feedwater valve opening and friction losses have been taken into consideration. According to [7] the speed of the feedwater pump can be changed from 0 to 100% in 70 s, but the actuating times for the feedwater valve were not given. The feedwater valve servo has been modelled by an integrator with minimal,  $s_{ww2s}$  ( $-S_{WW2S} = -0.05 \text{ s}^{-1}$ ) and maximal,  $s_{ww2o}$  ( $S_{WW2O} = 0.05 \text{ s}^{-1}$ ) rate of change. The stroke of the valve has been limited from below, by  $s_{ww2l}$  ( $S_{WW2L} = 0.0$ ) and from above, by  $s_{ww2h}$  ( $S_{WW2H} = 1.0$ ). It has been assumed that the opening of the feedwater valve is a quadratic function of the stroke. The block diagram of the FWS is shown in Fig. 8.2.

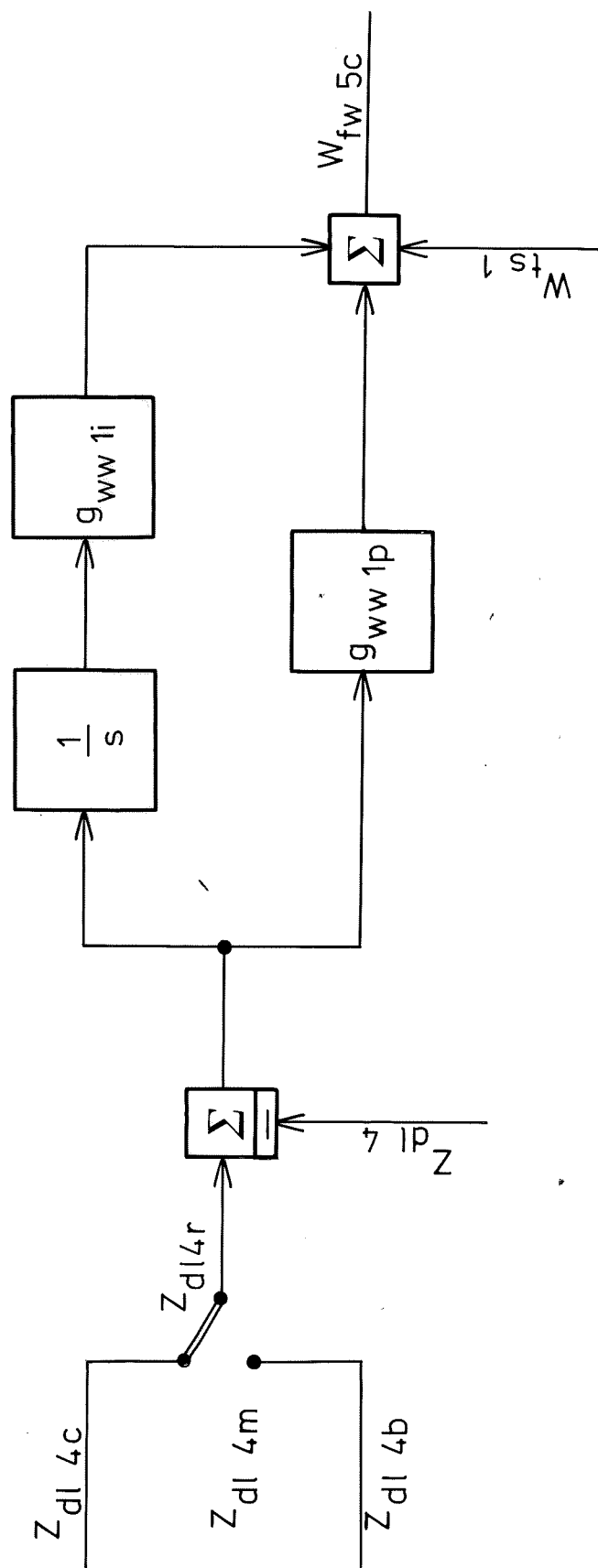


Fig. 8.1 - Block diagram of the drum level controller (DLC).

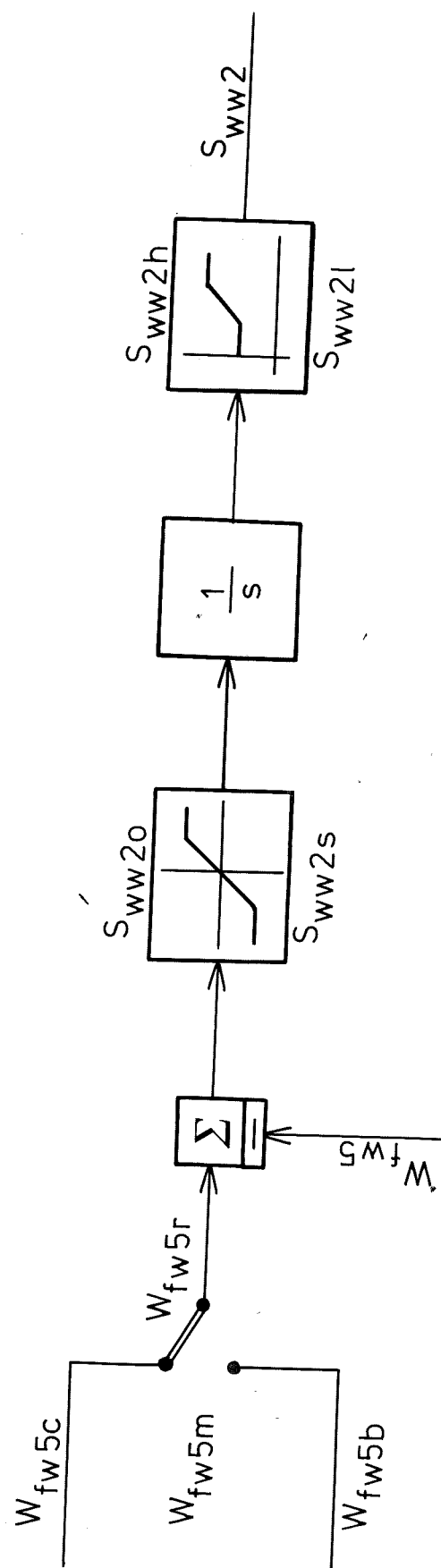


Fig. 8.2 - Block diagram of the feedwater servo (FWS).

## 9. STEAM TEMPERATURE LOOP.

The task of the steam temperature loop is to control the steam temperature by manipulating the attemperator spray flow valves. There are two valves to be manipulated; one before the tertiary superheater and another before the secondary superheater. The steam temperature loop is comprised of the tertiary superheater steam temperature controller (TSSTC), the secondary superheater steam temperature controller (SSSTC), the tertiary superheater steam temperature servo (TSSTS), and the secondary superheater steam temperature servo (SSSTS).

The task of the TSSTC is to compute the reference value of the steam temperature before the tertiary superheater in order to keep its outlet temperature at the reference value. The task of the SSSTC is to compute the reference value of the steam temperature before the secondary superheater. The task of the TSSTS is to control the steam temperature before the tertiary superheater by manipulating the second attemperator spray flow valve. The task of the SSSTS is to control the steam temperature before the secondary superheater by manipulating the first attemperator spray flow valve.

The performance of the steam temperature loop is important from economic point of view. The specific fuel consumption is reduced by a high steam temperature but the superheater material limits the temperature. If it is possible to design a steam temperature loop, which reduces the steam temperature variations it is possible to choose a higher reference value of the steam temperature. This means that a good performance of the steam temperature loop can reduce the specific fuel consumption.

The control of the steam temperature is difficult due to the disturbances from the output power loop and the drum pressure loop. These control loops change the steam flow through the superheaters, the heat flow to the superheaters, and the steam temperature after the primary superheater. Especially the steam flow variations are rapid.

Each superheater is modelled by a first order system. In [7] it was shown that higher order systems do not give an essentially better fit to the measurements. The first order model does overestimate the phase margin of the steam temperature control loop. This means that the gain of the steam temperature controllers must be low in order to attain stability. This implies that we cannot rely on feedback only. The use of feedforward is thus appropriate.

The following simplified model of a superheater is used in order to determine the structure of the steam temperature controllers:

$$\tau \frac{dh_2}{dt} = q - w(h_2 - h_1)$$

The derivative of the outlet enthalpy is equal to zero if

$$h_2 - h_1 = h_T(T_2 - T_1) = q/w$$

The feedforward part of a steam temperature controller becomes:

$$T_{1r} = T_{2r} - k_f q/w$$

The control law of a steam temperature controller becomes:

$$T_{1r} = T_{2r} - k_f q/w + k_p \Delta T_2 + k_i \int_{-\infty}^t \Delta T_2 dt$$

The TSSTC now becomes:

$$\begin{aligned} T_{ts1r} = & T_{ts2r} - g_{twlf} w_{bol} / w_{ts1} \\ & + g_{twlp} \Delta T_{ts2} + g_{twli} \int_{-\infty}^t \Delta T_{ts2} dt \end{aligned}$$



and the SSSTC becomes

$$T_{sslr} = T_{ss2r} - g_{swlf} w_{bol} / w_{tsl} \\ + g_{swlp} \Delta T_{ss2} + g_{swli} \int_{-\infty}^t \Delta T_{ss2} dt$$

This equation will now be used in order to examine the function of the feedforward part of the control law. If the reference value of the outlet steam temperature is changed by  $\delta T$  the reference value of the inlet steam temperature will be changed by  $\delta T$  too. If the heat flow and the steam flow remain unchanged this is the only action which is necessary. If the fuel flow is increased the reference value will be decreased. Notice that the gain depends on the steam flow and decreases with increasing load. If the steam flow is increased the reference value will be increased. Notice that the gain depends on the fuel flow and the steam flow and decreases with increasing load. The control law thus automatically changes the gain of the feedforward term. In all cases the inlet steam temperature is changed as fast as the steam temperature servo allows. The proportional feedback makes the closed loop system faster and the integral feedback eliminates steady state errors.

The block diagrams of the TSSTC and the SSSTC are given in Fig. 9.1 and Fig. 9.2 respectively. The gains of the TSSTC and the SSSTC have been determined by simple stability considerations and by simulation. The feedforward gains,  $g_{twlf}$  ( $GTWLF = 849.0$ ) and  $g_{swif}$  ( $GSWIF = 853.0$ ) have been found from simulation in steady state at 150 MW. The proportional gains,  $g_{twlp}$  ( $GTWLP = 1.0$ ) and  $g_{swlp}$  ( $GSWLP = 1.0$ ) have been chosen to guarantee stability of the closed loop system in absence of integral feedback for any phase shift of the superheater. The integral gains,  $g_{twli}$  ( $GTWLI = 0.04$ ) and  $g_{swli}$  ( $GSWLI = 0.03$ ) have been chosen by simulation.

The inlet steam temperatures of the secondary and the tertiary superheaters are controlled by the first and the second attem-

perators respectively. The temperatures are controlled by manipulating the spray flow valves. The disturbances of the steam temperature servos are the steam temperatures before the attenuators, the driving pressures of the spray flow valves, and last but not least the steam flow. The steam flow will vary from 20% to 100%. This means that the steady state gain of the transfer function from spray flow to steam temperature will vary from 1.0 to 0.2. The driving pressure of the spray flow valves depend on the position where the spray flow is taken from the feedwater line (before or after the feedwater valve), and on the feedwater flow as well as on the steam flow. From control point of view it is most suitable to connect the spray flow line after the feedwater valve. This means that the driving pressures of the spray flow valves are proportional to the steam flow:

$$\Delta p = \frac{w_s^2}{2A_{ekv}^2 \rho_s}$$

The attenuator spray flow is given by:

$$w_w = \frac{A_w}{A_{ekv}} \sqrt{\frac{\rho_w}{\rho_s}} w_s$$

The enthalpy of the steam after the attenuator is given by:

$$h_{s2} = h_{s1} - \frac{w_w}{w_s} (h_{s1} - h_w)$$

Introducing the spray flow gives:

$$h_{s2} = h_{s1} - \frac{A_w}{A_{ekv}} \sqrt{\frac{\rho_w}{\rho_s}} (h_{s1} - h_w)$$

It follows from this equation that the enthalpy of the steam after the attenuator ( $h_{s2}$ ) does not change with the steam flow. This would not be the case if the attenuator flows were

extracted before the feedwater valve [10].

Each attemperator servo is modelled by an integrator. The outputs of the integrators are limited from below,  $s_{tw2l}$  (STW2L = 0.0) and  $s_{sw2l}$  (SSW2L = 0.0) and from above,  $s_{tw2h}$  (STW2H = 1.0) and  $s_{sw2h}$  (SSW2H = 1.0). The rates of change are also limited from below,  $-s_{tw2s}$  (STW2S = 0.04) and  $-s_{sw2s}$  (SSW2S = 0.04) and from above,  $s_{tw2o}$  (STW2O = 0.04) and  $s_{sw2o}$  (SSW2O = 0.04). The openings of the spray flow valves have been assumed to be quadratic functions of the strokes of the valves. The block diagrams of the TSSTS and the SSSTS are given in Fig. 9.3 and Fig. 9.4 respectively. The differences between the reference values and the measured values of the inlet steam temperatures are multiplied by the gains,  $g_{tw2i}$  (GTW2I = 0.005) and  $g_{sw2i}$  (GSW2I = 0.005) in order to obtain the rates of change of the strokes.

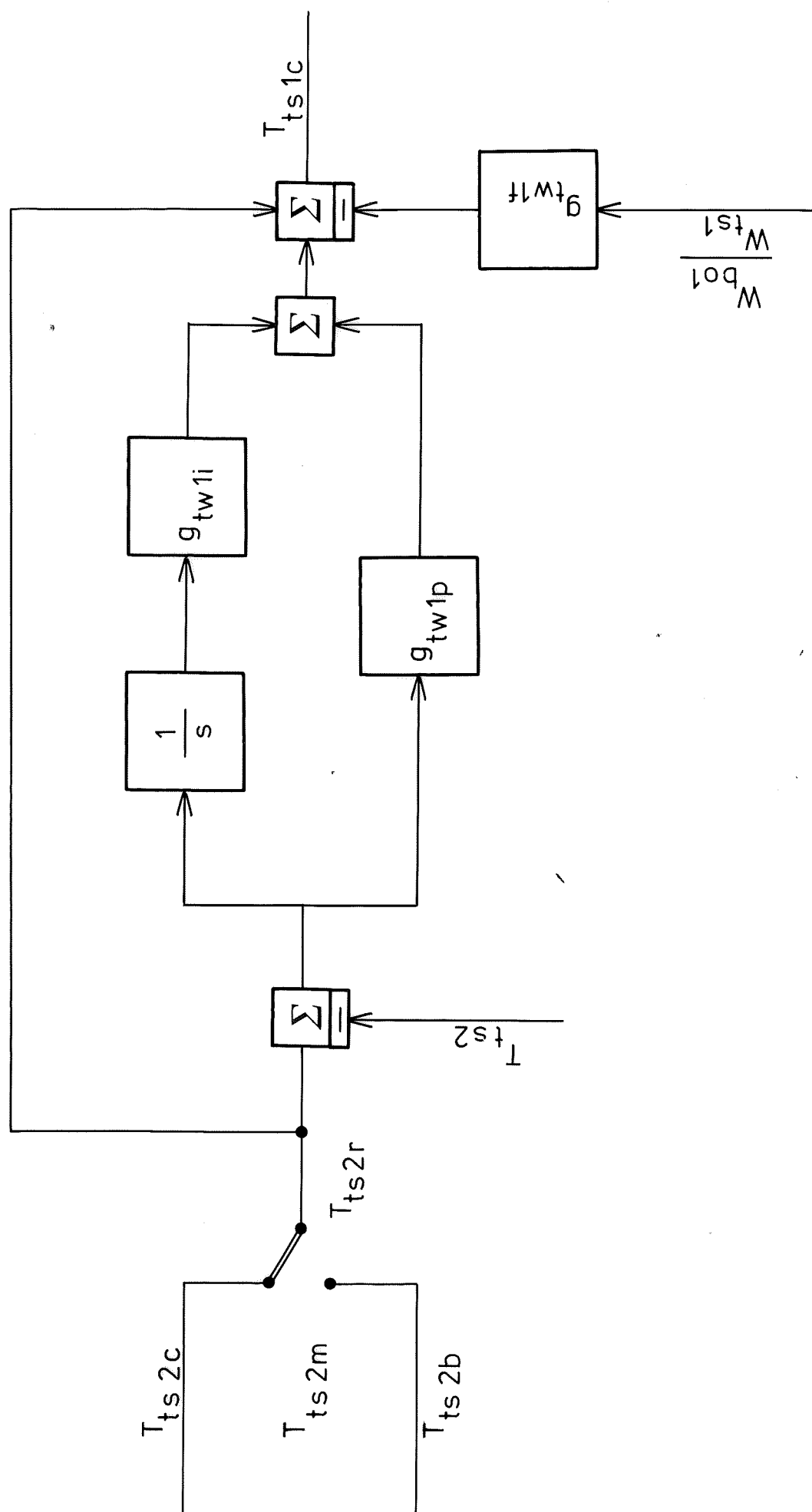


Fig. 9.1 - Block diagram of the tertiary superheater steam temperature controller (TSSSTC).

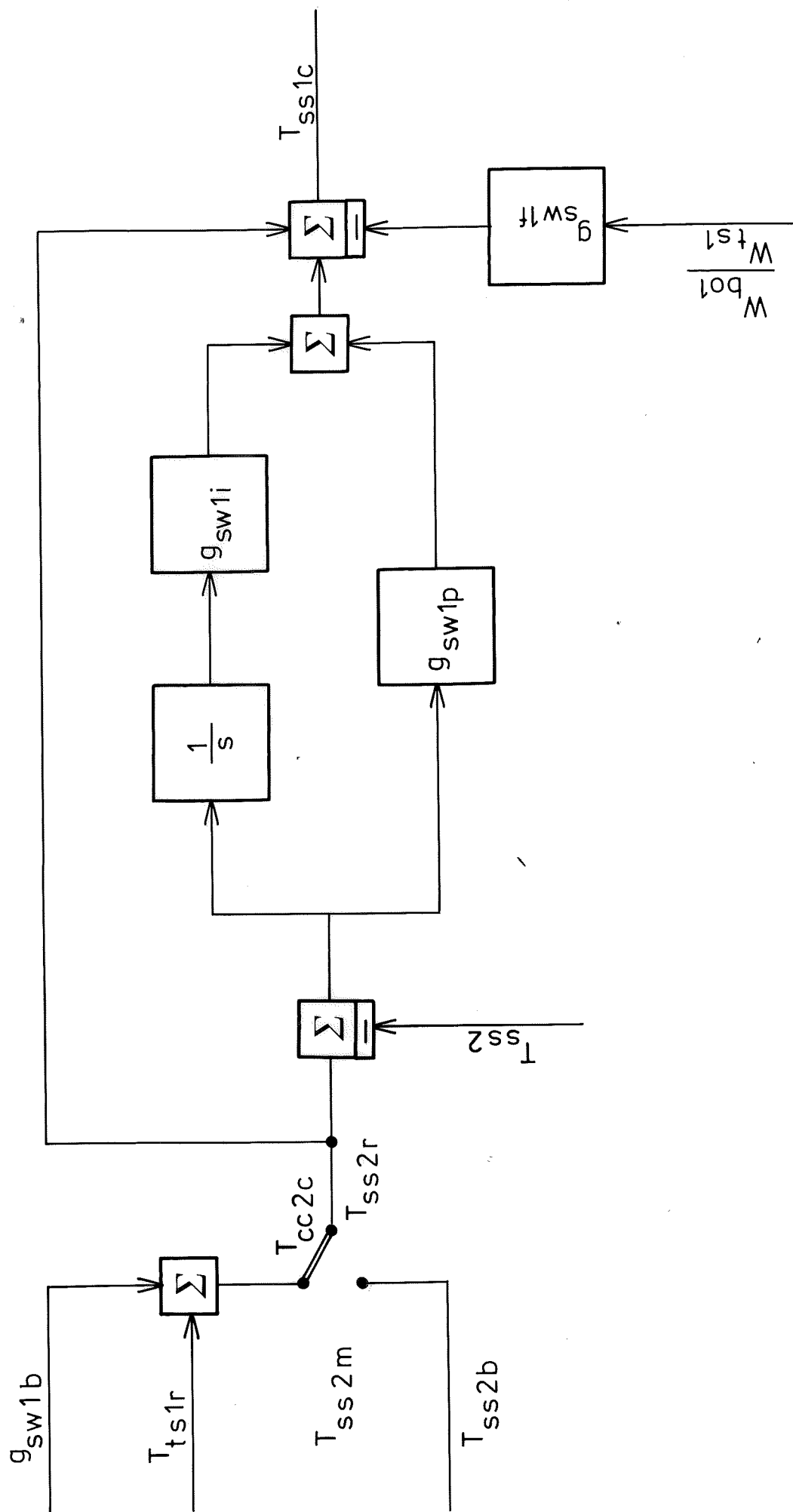


Fig. 9.2 - Block diagram of the secondary superheater steam temperature controller (SSSTC).

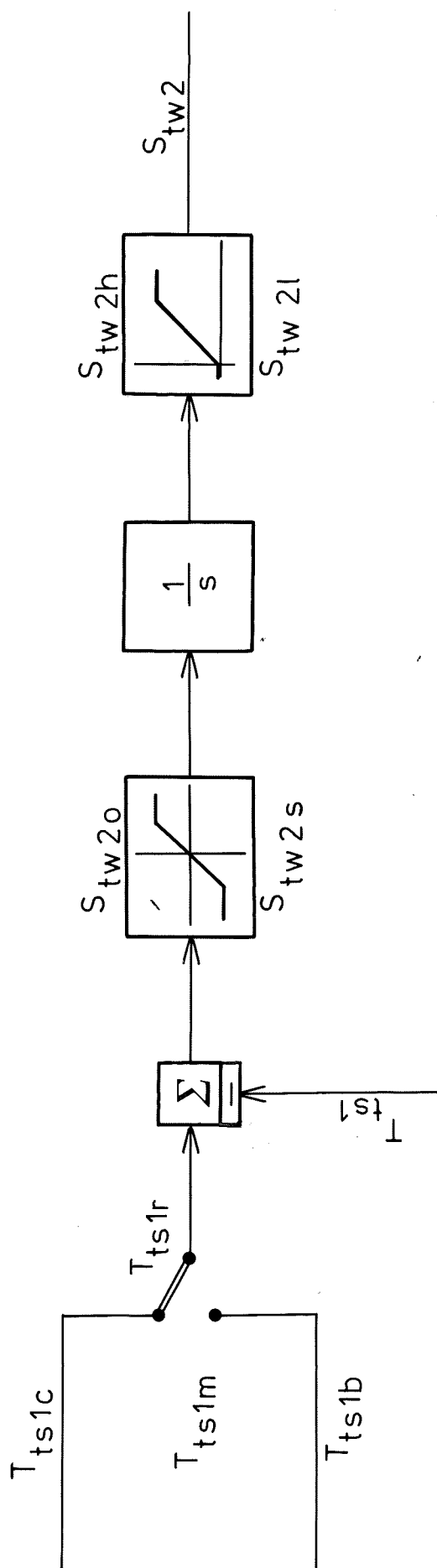


Fig. 9.3 - Block diagram of the tertiary superheater steam temperature servo (TSSTS).

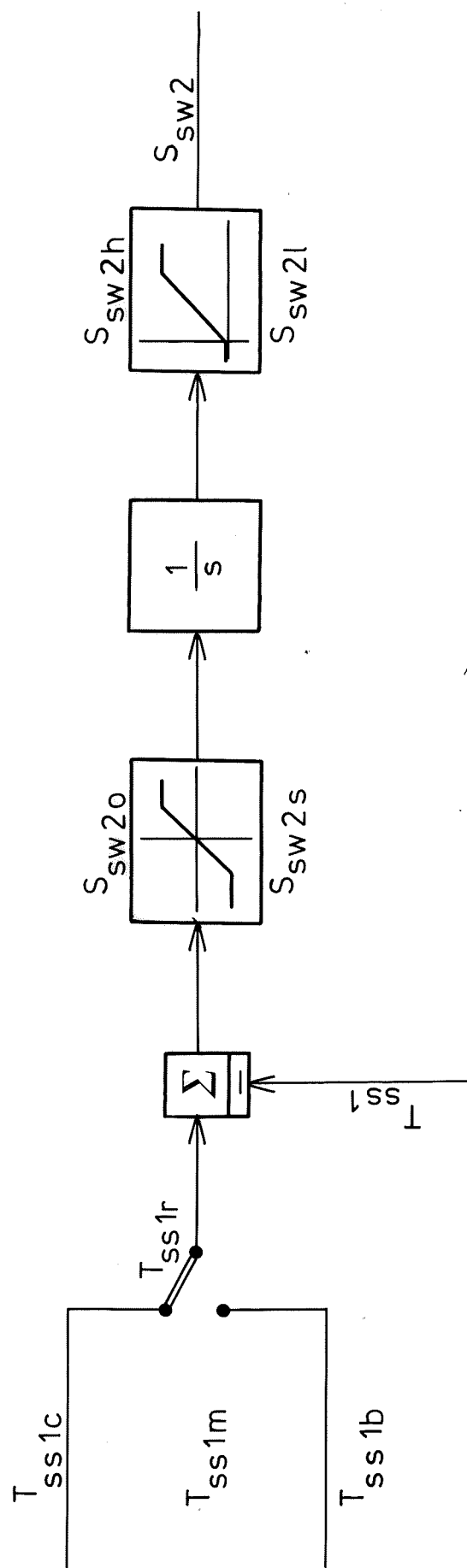


Fig. 9.4 - Block diagram of the secondary superheater steam temperature servo (SSSTS).

## 10. OUTPUT POWER LOOP

The task of the output power loop is to control the output power by manipulating the steam control valve and the extraction steam valves. There are seven extractions. The output power loop is comprised of the turbine power controller (TPC), the control valve servo (CVS), the high-pressure preheater controller (HPPC), the low-pressure preheater controller (LPPC), the high-pressure preheater servo (HPPS), and the low-pressure preheater servo (LPPS).

The task of the TPC is to compute the reference value of the stroke of the control valve in order to keep the output power at its reference value. The task of the CVS is to control the stroke of the control valve. The tasks of the HPPC and the LPPC are to compute the reference values of the strokes of the extraction valves. The tasks of the HPPS and the LPPS are to control the strokes of the extraction valves.

The output power of the turbine is given by:

$$N = \sum_{i=1}^7 \left( w_{ts1} - \sum_{j=1}^{i-1} w_{esj} \right) (h_{i-1} - h_i) \eta_i$$

which is valid in steady state, but not during transients due to the mass storage in the reheater. In order to increase the output power the stroke of the control valve may be increased. There is an almost linear relationship between the steam flow through the high-pressure turbine and the steam pressure before the turbine. The increased opening of the control valve is accompanied by an increased steam flow through the high-pressure turbine. The steam pressure in the reheater remains unchanged, but the increased steam flow causes a pressure gradient. There is an almost linear relationship between the steam flow through the intermediate-pressure turbine and the steam pressure before the turbine. When the steam pressure in the reheater increases the steam flow through the intermediate-pres-



sure turbine will increase too. The time constant of this transient is 5-15 s. The extraction flows can be decreased in order to increase the output power rapidly. The response of the output power is not delayed by the mass storage in the reheater. The limited rates of change of the extraction valve servos may delay the response of the output power. The mass storages in the intermediate-pressure turbine and the low-pressure turbine are associated with small time constants (0.1-0.3 s).

The block diagram of the TPC is given in Fig. 10.1. The reference value of the output power is selected by a switch,  $N_{gs2m}$  (NGS2M). One reference value,  $N_{gs2c}$  is computed by the PDS and another,  $N_{gs2b}$  (NGS2B) is manually adjustable. The TPC is a PI-controller with an adjustable dead-zone in the P-channel. The output of the TPC is the reference value of the stroke of the steam control valve. The proportional gain,  $g_{vs1p}$  ( $GVS1P = 5.0 \cdot 10^{-5}$ ) and the integrating gain,  $g_{vs1i}$  ( $GVS1I = 1.0 \cdot 10^{-5}$ ) have been found by simulation. The size of the dead-zone,  $[-g_{vs1l}, g_{vs1h}]$  ( $[-GVS1L, GVS1H]$ ) was zero.

The stroke of the steam control valve is controlled by the CVS. It was known from [7] that the opening time is 5.0 s and the closing time is 0.4 s. The servo has been modelled by an integrator. The output of the integrator has been limited from below,  $s_{vs2l}$  ( $SVS2L = 0.0$ ) and from above,  $s_{vs2h}$  ( $SVS2H = 1.0$ ). The rate of change has also been limited from below,  $-s_{vs2s}$  ( $SVS2 = 2.0 \text{ s}^{-1}$ ) and from above,  $s_{vs2o}$  ( $SVS2O = 0.2 \text{ s}^{-1}$ ). The opening of the steam control valve is a piecewise linear function of the stroke of the control valve [11].

The block diagram of the CVS is shown in Fig. 10.2. The reference value of the stroke of the control valve is selected by a switch,  $s_{vs2m}$  (SVS2M). One reference value,  $s_{vs2c}$  (SVS2C) is computed by the TPC and another,  $s_{vs2b}$  (SVS2B) is manually adjustable. The integral gain,  $g_{vs2i}$  ( $GVS2I = 0.2 \text{ s}^{-1}$ ) is chosen in order to avoid stiff equations in the simulation.

The extraction flows are changed in order to increase the power response rate of the unit. The contribution from the extraction flow changes is limited (10-15%) but is added to the responses due to changes of the steam control valve. This improves the responses of the output power considerably during the first (10) seconds. There is no contribution from the extraction flow changes to the output power in steady state. The low-pressure preheater extraction flows are also adjusted in order to control the steam pressure in the deaerator.

The block diagram of the HPPC is given in Fig. 10.3. The HPPC consists of a first order high-pass filter. The bandwidth of the filter is determined by the gain,  $g_{fs1i}$  ( $GFS1I = 0.03$ ). This choice implies that the bandwidth is 0.03 rad/s. The steady state value of the extraction valve servo,  $s_{fs2b}$  ( $SFS2B = 0.5$ ) is a parameter to be chosen.

The block diagram of the LPPC is given in Fig. 10.4. The LPPC also consists of a first order high-pass filter with a bandwidth of 0.03 rad/s. The bandwidth is determined by the gain,  $g_{fs6i}$  ( $GFS6I = 0.03$ ). The reference value of the steam pressure in the deaerator is selected by a switch,  $p_{as2m}$  ( $PAS2M$ ). One reference value,  $p_{as2c}$  ( $PAS2C$ ) is computed and another  $p_{as2m}$  is manually adjustable. The parameters of the deaerator pressure controller  $g_{fs5p}$  ( $GFS5P = 1.0$ ) and  $g_{fs2i}$  ( $GFS2I = 0.0$ ) was chosen by simulation.

The extraction valves are moved into their positions by the preheater servos. During the simulations it was assumed that the four valves of the high-pressure preheater are controlled by one servo and that the three valves of the low-pressure preheater are controlled by another servo. Each preheater servo is modelled by an integrator. The outputs of the integrators are limited from below,  $s_{fs7l}$  ( $SFS7L = 0.0$ ) and  $s_{fs2l}$  ( $SFS2L = 0.0$ ) and from above,  $s_{fs7h}$  ( $SFS7H = 1.0$ ) and  $s_{fs2h}$  ( $SFS2H = 1.0$ ). The rates of change are also limited from below,  $-s_{fs7s}$  ( $SFS7S = 1.0 \text{ s}^{-1}$ ) and  $-s_{fs2s}$  ( $SFS2S = 1.0 \text{ s}^{-1}$ ) and from above,  $s_{fs7o}$  ( $SFS7O = 1.0 \text{ s}^{-1}$ ) and  $s_{fs2o}$  ( $SFS2O = 1.0 \text{ s}^{-1}$ ). The openings of the extraction valves are assumed to be quadratic functions of the strokes of the valves.

The extraction valve openings have been adjusted to agree with measurements [11].

The block diagram of the HPPS is shown in Fig. 10.5. The reference value of the stroke of the high-pressure preheater extraction valve is selected by a switch,  $s_{fs2m}$  (SFS2M). One reference value,  $s_{fs2c}$  (SFS2C) is computed by the HPPC and the other  $s_{fs2b}$  (SFS2B) is manually adjustable. The integral gain,  $g_{fs2i}$  (GFS2I = 0.5) is chosen in order to avoid stiff differential equations in the simulation.

The block diagram of the LPPS is shown in Fig. 10.6. The reference value of the strokes of the low-pressure preheater extraction valves is selected by a switch,  $s_{fs7m}$  (SFS7M). One reference value,  $s_{fs7c}$  (SFS7C) is computed by the LPPC and the other  $s_{fs7b}$  (SFS7B) is manually adjustable. The integral gain,  $g_{fs7i}$  (GFS7I = 0.5) is chosen in order to avoid stiff differential equations in the simulation.

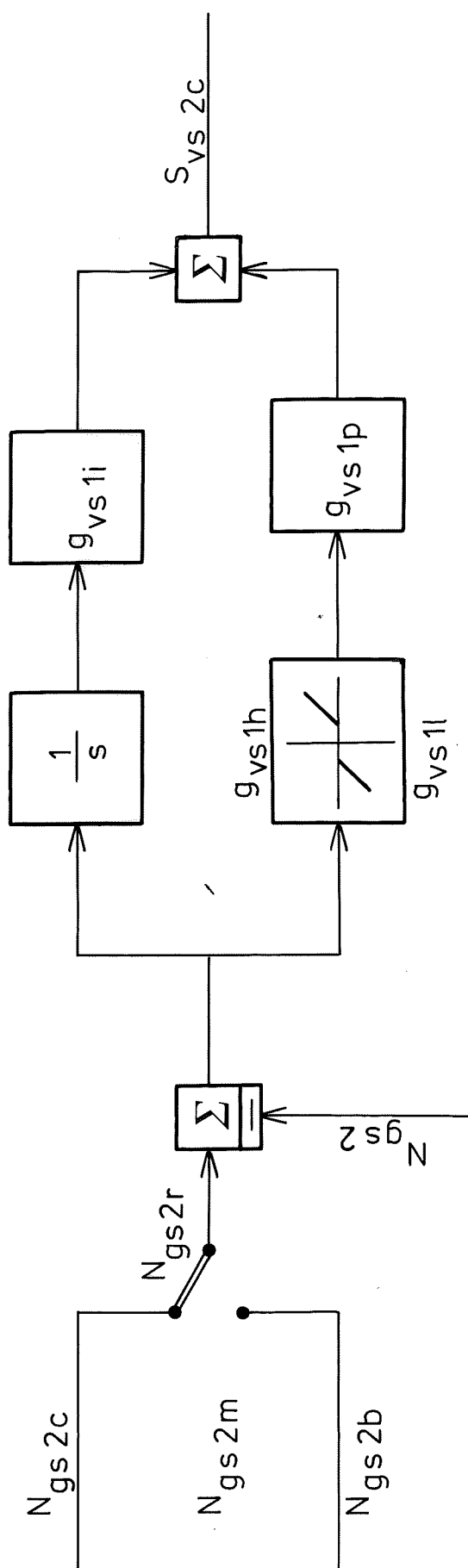


Fig. 10.1 - Block diagram of the turbine power controller (TPC).

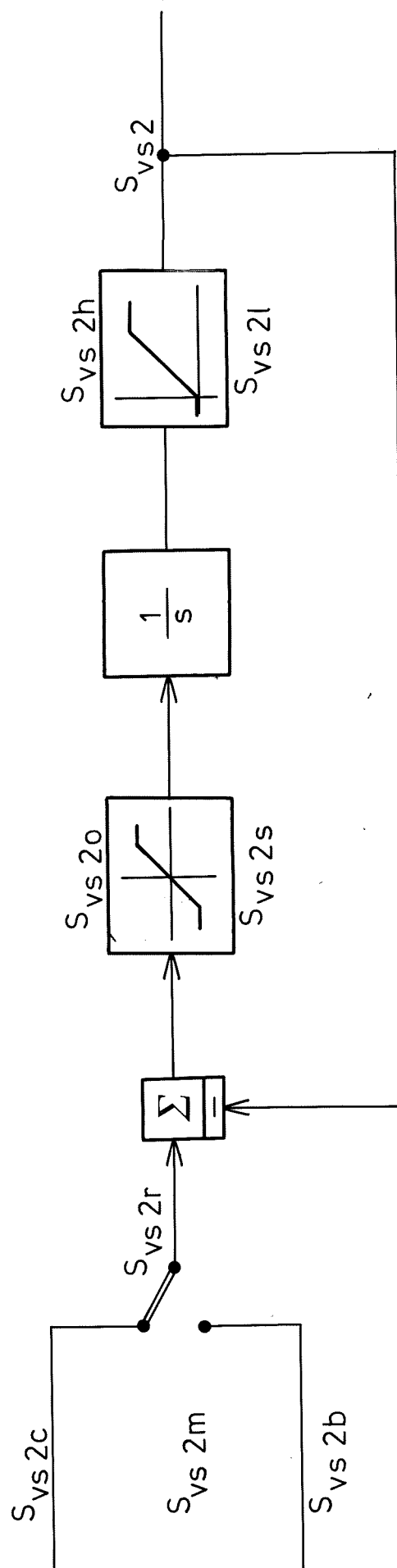


Fig. 10.2 - Block diagram of the control valve servo (CVS).

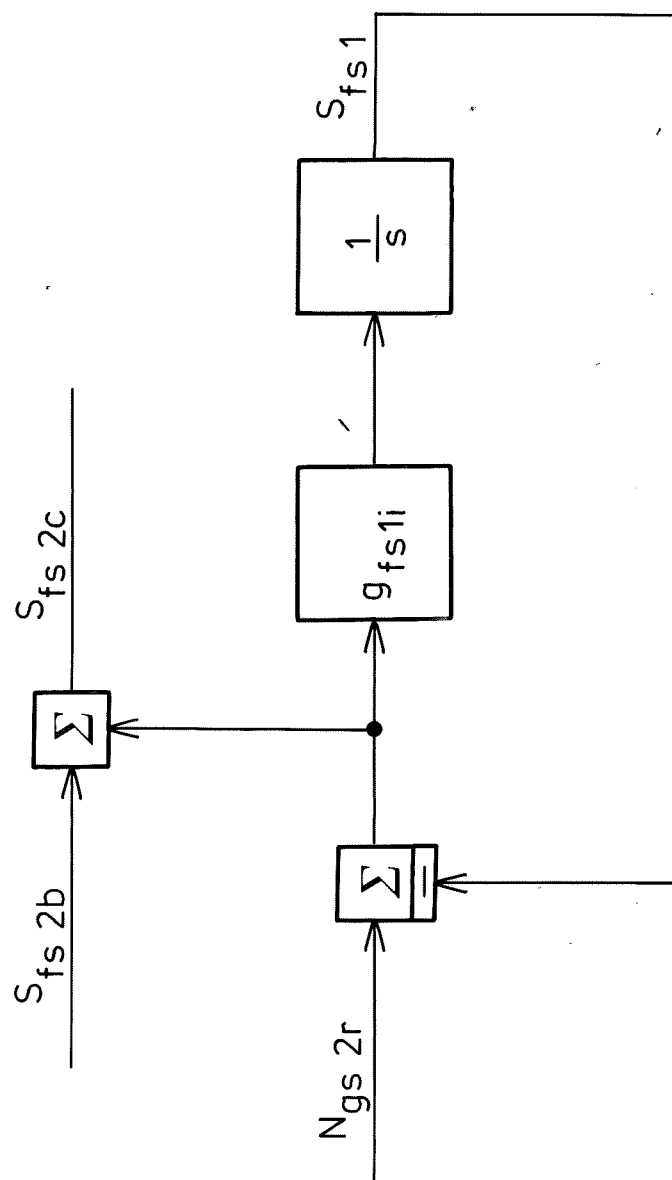


Fig. 10.3 - Block diagram of the high-pressure preheater controller (HPPC).

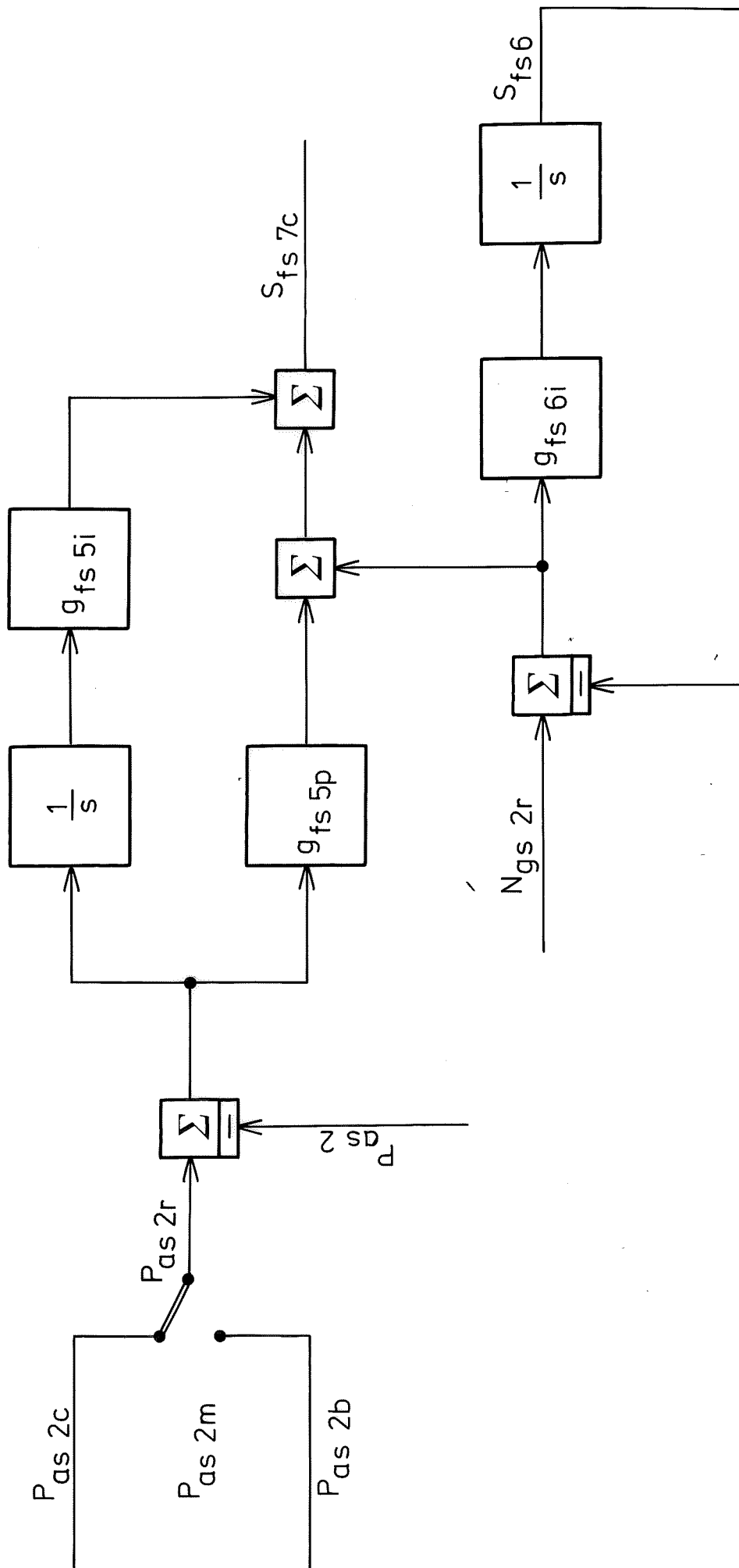


Fig. 10.4 - Block diagram of the low-pressure preheater controller (LPPC).

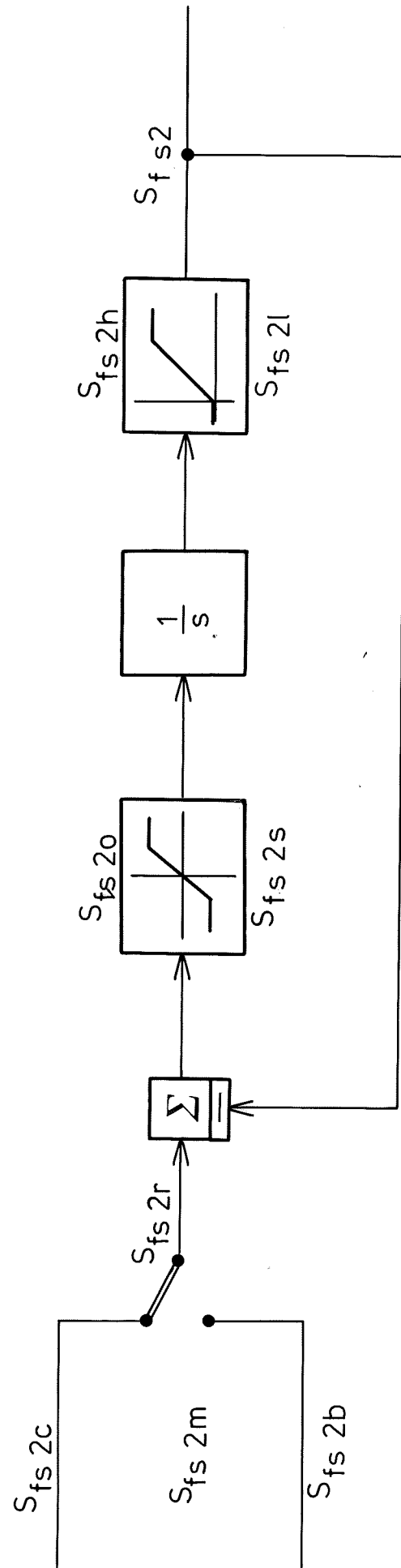


Fig. 10.5 - Block diagram of the high-pressure preheater servo (HPPS).



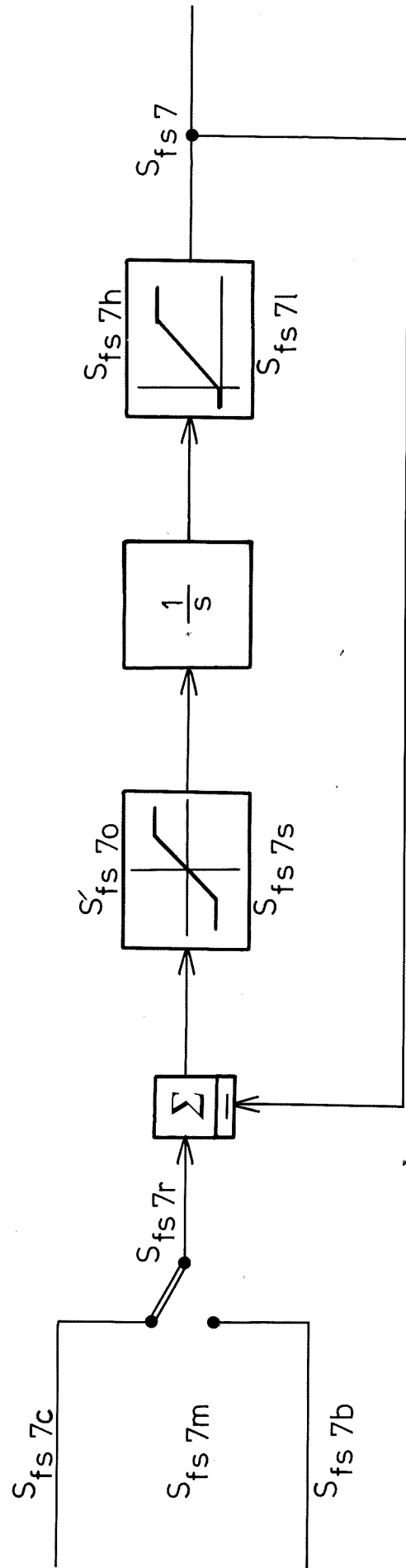


Fig. 10.6 - Block diagram of the low-pressure preheater servo (LPPS).

## 11. SIMULATIONS.

There are well-established methods of describing the performance of control systems for single-input single-output linear systems. The model of the drum boiler-turbine is neither linear nor single-input single-output. The control system does also contain several nonlinearities, designed in order to utilize the process. It was decided to investigate the performance of the control system by simulation instead of trying to express the performance by some performance index. There are both advantages and disadvantages with this approach. One disadvantage is that it is necessary to investigate a large number of cases. Another disadvantage is that it is difficult to make sure that every solution is stable and not only that the investigated solutions are stable. One advantage is that it is possible to communicate the results of the investigation to persons, who are not familiar with control theory.

### 11.1. Simulation Method.

The boiler-turbine and the control system are simulated completely digitally using a mathematical model. One reason is the availability of a very flexible interactive simulation program. The program is developed at the Institute of Automatic Control, LTH, by H. Elmqvist [8]. The program is capable of integrating nonlinear differential equations of the form:

$$\frac{dx}{dt} = f(x, u, p, t) \quad (1a)$$

$$y = g(x, u, p, t) \quad (1b)$$

where

x is a vector of states,  
 u is a vector of inputs,  
 y is a vector of outputs,  
 p is a vector of parameters, and  
 t is time.

The right hand side of (1) can be defined by statements written in an ALGOL-like high-level language or by subroutines written in FORTRAN. It was decided to define the model and the control systems by subroutines written in FORTRAN. This choice was discussed in [12], where the subroutines defining the drum boiler-turbine are given. The subroutines defining the control system are given in Appendix.

### 11.2. Investigated Cases.

The following six cases were investigated by simulation:

- A) decrease of output power in normal mode,
- B) transfer from normal to alert mode,
- C) increase of output power in alert mode,
- D) decrease of output power in alert mode,
- E) transfer from alert to normal mode, and
- F) increase of output power in normal mode.

The relation between output power and drum pressure is determined by the mode (normal or alert) of the control system. The variations of the output power and the drum pressure are illustrated in Fig. 11.1.

#### Decrease of output power in normal mode (Section 12).

A decrease of the energy consumption or a new agreement between partners in a power pool may result in a desire to decrease the output power. The time needed for the decrease is not critical in such cases and it was assumed that the control system was in normal mode. The power response rate and the pressure response rate must be chosen so that the thermal stresses and the risk of process damage are sufficiently low. The total operating cost may be reduced slightly by increasing the power response rate

and only during the decrease of the output power. This decrease of cost does not, however, motivate very high response rates.

Transfer from normal to alert mode (Section 13).

A high probability that a rapid increase of output power will be required may lead to a desire to initiate a transfer from normal to alert mode. The main reason is that there is an increased probability of loss of production, e.g. load rejection tests or routine checks of control and stop valves on thermal power units in operation. Another reason is that the transmission network is weakened or a high probability that it will be disturbed. The transmission network will be weakened if one crucial transmission line is out of service. The risk of transmission network disturbances is high e.g. during thunderstorms, snowstorms, or saltstorms.

Increase of output power in alert mode (Section 14).

A loss of production, a weakening of the transmission network, or a separation of the power system may lead to a desire to increase the output power as fast as possible. It is reasonable to assume that the control system is in alert mode if the power demand could be anticipated.

Decrease of output power in alert mode (Section 15).

A separation of the power system may lead to a desire to decrease the output power as fast as possible. It is reasonable to assume that the control system is in alert mode if the power system disturbance could be anticipated.

### Transfer from alert to normal mode (Section 16).

A reduction of the probability that a rapid increase of output power will be required may lead to a desire to initiate a transfer from alert to normal mode. One reason is the completion of load rejection tests or routine tests of valves. Another reason is that a transmission line is taken into service again. The ceasing of thunderstorms, snowstorms, or saltstorms will also reduce the probability of power network disturbances.

### Increase of output power in normal mode (Section 17).

An increase of the energy consumption or a new agreement concerning power exchange may result in a desire to increase the output power. The time needed for the increase may not be critical and it was assumed that the control system was and remained in normal mode. The power response rate and the pressure response rate must be chosen so that thermal stresses and the risk of process damage are sufficiently low. The total operating cost may be reduced slightly by increasing the power response rate and only during the increase of the output power. This decrease of cost does not, however, motivate very high response rates.

### 11.3. Details of Computation.

Every case starts from steady state. The steady state values were found by integration of the differential equation until the steady state was reached. The disturbance occurs at  $t = 10$  s. Every case lasted from  $0 < t < 500$  s. The simulation time on a PDP 15 with floating point hardware was about 40 min. per case.

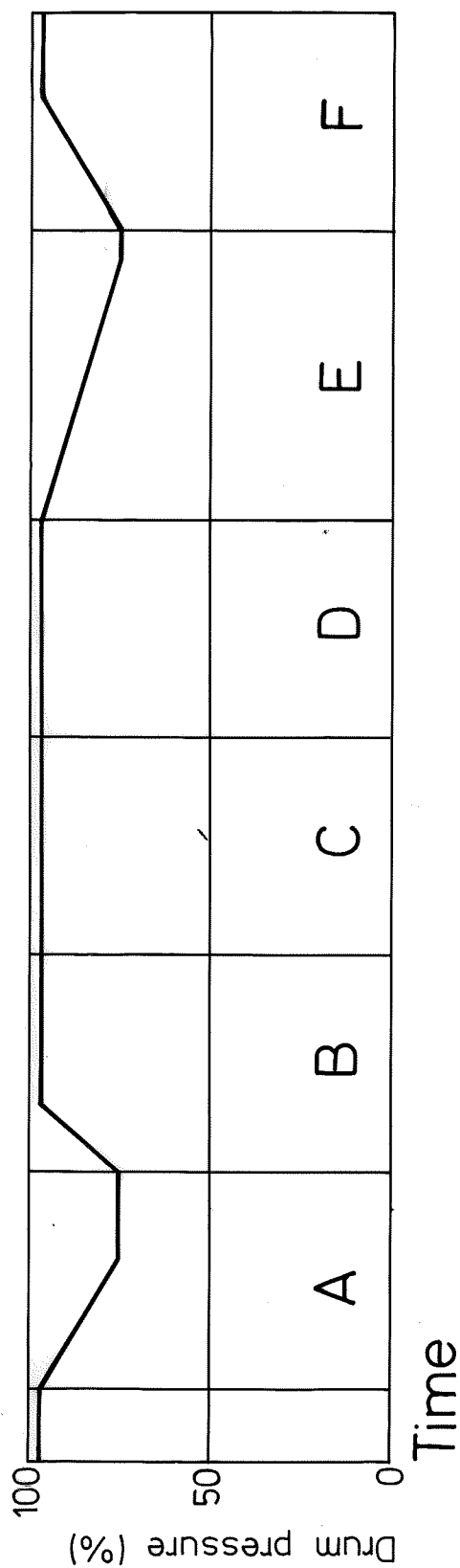
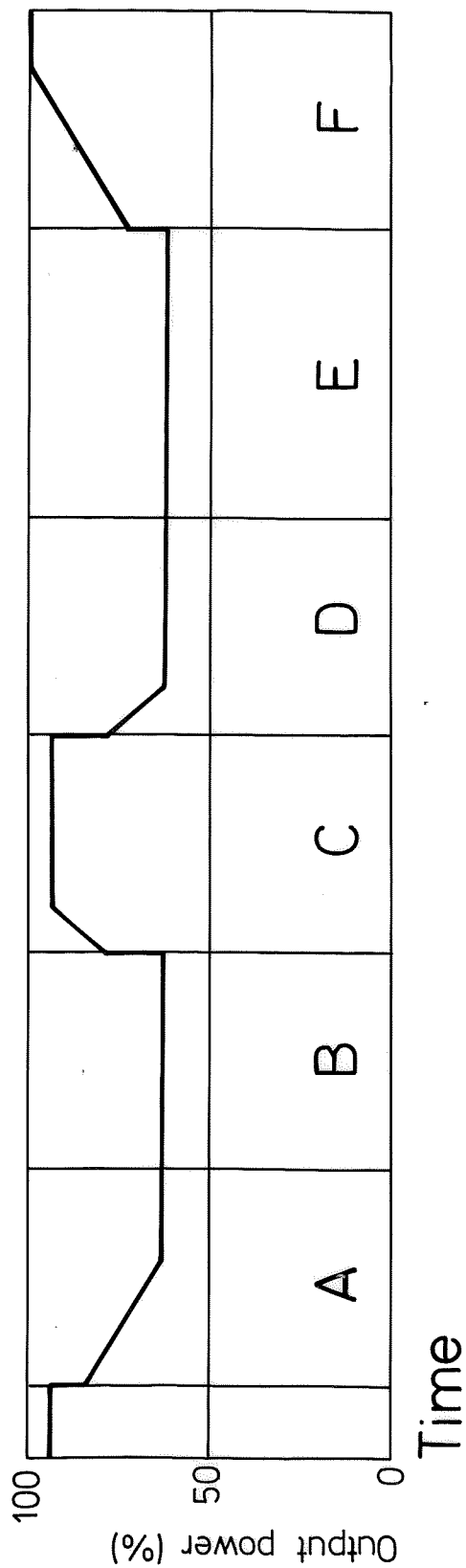


Fig. 11.1 - Investigated cases: A) Decrease of output power in normal mode, B) Transfer from normal to alert mode, C) Increase of output power in alert mode, D) Decrease of output power in alert mode, E) Transfer from alert to normal mode, and F) Increase of output power in normal mode.

## 12. DECREASE OF OUTPUT POWER IN NORMAL MODE.

The performance of the control system when the output power is decreased in normal mode will be examined in this section. The output power was changed by changing the power demand signal from 150 MW (94%) to 100 MW (63%) at  $t = 10$  s. The power demand signal,  $s_{nslr}$  is input to the power demand setter (PDS), which generates the reference value of the output power. The reference value of the output power,  $N_{gs2r}$  is limited by the jump-and-rate circuit (PDS3) in Fig. 5.3. The numerical value of the jump of  $N_{gs2r}$  is 16 MW (10%) and the numerical value of the rate of  $N_{gs2r}$  is 9.6 MW/min (6%/min) in normal mode. The performance of the drum pressure loop, the drum level loop, the steam temperature loop, and the output power loop will now be examined.

### The drum pressure loop.

The task of the drum pressure loop is to control the drum pressure by manipulating the fuel flow. The reference value of the drum pressure,  $p_{ds2r}$ , is generated by the drum pressure reference setter (DPRS), which was described in Section 6. The reference value of the drum pressure is determined by the reference value of the output power,  $N_{gs2r}$  and by the mode (normal or alert) of the control system. In this case  $p_{ds2r}$  is decreased from  $145 \cdot 10^5$  Pa (97%) to  $113 \cdot 10^5$  Pa (75%) with a limited,  $4.5 \cdot 10^5$  Pa/min (3%/min) rate-of-change. The steam flow (Fig. 12.22), the feedwater flow (Fig. 12.6), and the feedwater temperature after the high-pressure preheater (Fig. 12.19) disturb the drum pressure loop. The mean density of the steam-water mixture in the riser tubes, the steam temperature after the primary superheater, the heat flows to the superheaters, to the reheater, and to the economizer are disturbed by the fuel flow variations. The fuel flow,  $w_{bol}$  is the output of the fuel flow servo (FFS), which was described in Section 7. The reference value of the fuel flow,  $w_{bolr}$  is determined by the drum pressure controller (DPC), which was described in Section 7. The inputs to the DPC are  $p_{ds2r}$  and its derivative,  $s_{bolt}$ , the drum pressure,  $p_{ds2}$ , and the steam

flow,  $w_{tsl}$ . The block diagram of the DPC is given in Fig. 7.1. The rate-of-change of the fuel flow is limited in the FFS. The limits are parameters,  $w_{bolo}$  and  $w_{bols}$  of the first nonlinear block in Fig. 7.2. The numerical value of  $w_{bolo}$  and  $w_{bols}$  are both  $0.1 \text{ kg/s}^2$  (60%/min).

The response of the fuel flow is shown in Fig. 12.1. The fuel flow decreases linearly for  $10 < t < 30 \text{ s}$ , due to the limited rate-of-change of the fuel flow. The effect of the feedforward from the steam flow can be observed at  $t = 225 \text{ s}$ . The effect of the feedforward from the derivative of the reference value of the drum pressure can be observed at  $t = 470 \text{ s}$ .

The response of the drum pressure is shown in Fig. 12.2. The drum pressure increases for  $10 < t < 40 \text{ s}$  due to the rapid decrease of the steam flow (Fig. 12.22). The fuel flow is decreased as fast as possible during the increase of the drum pressure. The maximum drum pressure error is  $4 \cdot 10^5 \text{ Pa}$  (3%). The maximum rate-of-change of the drum pressure is  $4.5 \cdot 10^5 \text{ Pa/min}$  (3%/min).

The response of the steam pressure before the control valve is shown in Fig. 12.3. The steam pressure increases at  $t = 10 \text{ s}$  due to the decreased steam flow (Fig. 12.22). The decreased steam flow decreases the pressure drop in the superheaters due to friction losses. The increase and the decrease of the drum pressure can be observed in the response of the steam pressure before the control valve too.

The response of the steam temperature after the primary superheater is shown in Fig. 12.4. The total variation of the temperature is about  $20^\circ\text{C}$ . The temperature increases for  $10 < t < 50 \text{ s}$  due to the decreased steam flow (Fig. 12.22) and the increased steam temperature before the primary superheater with no corresponding decrease of the heat flow to the primary superheater. The steam temperature before the primary superheater is determined by the drum pressure (Fig. 12.2). The heat flow to the primary superheater is approximately proportional to the fuel flow (Fig. 12.1).



Properties: The steam flow is the most severe disturbance of the drum pressure loop. The steam flow and the derivative of the reference value of the drum pressure influences the fuel flow through the feedforward. The effects of the other disturbances are reduced by feedback. The limited rate-of-change of the fuel flow deteriorates the performance of the drum pressure loop for  $10 < t < 40$  s. This must, however, be accepted because of the restrictions of the burner equipment. The maximum drum pressure error is  $4 \cdot 10^5$  Pa (3%).

#### The drum level loop.

The task of the drum level loop is to control the drum level,  $z_{dl4}$  by manipulating the feedwater control valve. The reference value of the drum level,  $z_{dl4r}$  is constant. The steam flow (Fig. 12.22) and the fuel flow (Fig. 12.1) disturb the drum level loop. The feedwater temperature is disturbed by the variations of the feedwater flow. If the drum level is too high there is a danger that water will reach the turbine. If the drum level is too low there is a danger that the riser tubes will be damaged due to insufficient cooling. The feedwater flow,  $w_{fw5}$  is the output of the feedwater servo (FWS), which was described in Section 8. The reference value of the feedwater flow,  $w_{fw5r}$  is determined by the drum level controller (DLC), which was described in Section 8.

The inputs to the DLC are  $z_{dl4r}$ ,  $z_{dl4}$ , and the steam flow,  $w_{ts1}$ . The block diagram of the DLC is given in Fig. 8.1. The rate-of-change of the stroke of the feedwater valve is limited in the feedwater servo (FWS). The limits are parameters,  $s_{ww2o}$  and  $s_{ww2s}$  of the first nonlinear block in Fig. 8.2. The numerical values of  $s_{ww2o}$  and  $s_{ww2s}$  are both 5%/s.

The response of the stroke of the feedwater valve is shown in Fig. 12.5. The valve opening has to be decreased in order to decrease the feedwater flow and to compensate for the decreasing drum pressure. The valve is closing for  $10 < t < 20$  s due to the feedfor-

ward from the steam flow (Fig. 12.22). The valve is opening for  $20 < t < 40$  s due to the feedback from the drum level (Fig. 12.7). The valve is closing for  $t > 40$  s due to the feedforward from the steam flow and the feedback from the drum level.

The response of the feedwater flow is shown in Fig. 12.6. The response of the feedwater flow is similar to the response of the stroke of the feedwater valve. The response of the feedwater flow is also similar to the response of the steam flow (Fig. 12.22). The effect of the changing mean density of the steam-water mixture in the drum system is visible. The feedwater flow is at most 15 kg/s (11%) higher than the steam flow for  $10 < t < 60$  s. The drum level is, however, decreasing for  $10 < t < 30$  s. The feedwater flow is about 5 kg/s (4%) lower than the steam flow for  $t > 220$  s. The drum level is, however, fairly constant but the drum pressure is decreasing.

The response of the drum level is shown in Fig. 12.7. The shrink phenomenon decreases the drum level 4 cm at  $t = 30$  s. The drum level is about 1 cm high during the decrease of the drum pressure.

The response of the drum water temperature is shown in Fig. 12.8. The rate-of-change of drum water temperature determines the thermal stresses of the drum material. The rate-of-change is less than  $3^{\circ}\text{C}/\text{min}$ .

Properties: The steam flow is the most severe disturbance of the drum level loop. The control of the drum level is difficult due to the shrink-and-swell phenomenon. The steam flow influences the feedwater through the feedforward. The effects of the other disturbances are reduced by feedback. The maximum drum level error is about 4 cm.

### The steam temperature loop.

The task of the steam temperature loop is to control the steam temperature after the tertiary superheater,  $T_{ts2}$  by manipulating the first and the second attemperator spray flow valves. The reference value of the steam temperature after the tertiary superheater,  $T_{ts2r}$  is constant. The steam flow (Fig. 12.22), the heat flows to the secondary and tertiary superheaters, and the steam temperature after the primary superheater (Fig. 12.4) disturb the steam temperature loop. The heat flows to the secondary and tertiary superheaters are both approximately proportional to the fuel flow (Fig. 12.1). The specific fuel consumption is reduced if the steam temperature after the tertiary superheater is increased. The steam temperature is limited by the properties of the superheater material. The steam temperature before the secondary superheater,  $T_{ss1}$  is the output of the secondary superheater steam temperature servo (SSSTS), which was described in Section 9. The steam temperature before the tertiary superheater,  $T_{ts1}$  is the output of the tertiary superheater steam temperature servo (TSSTS), which was described in Section 9. The reference value of the steam temperature before the tertiary superheater,  $T_{ts1r}$  is determined by the tertiary superheater steam temperature controller (TSSTC), which was described in Section 9. The inputs to the TSSTC are  $T_{ts2r}$ ,  $T_{ts2}$ , the steam flow,  $w_{ts1}$ , and the fuel flow,  $w_{bol}$ . The block diagram of the TSSTC is given in Fig. 9.1. The reference value of the steam temperature before the secondary superheater,  $T_{ss1r}$  is determined by the secondary superheater steam temperature controller (SSSTC), which was described in Section 9. The inputs to the SSSTC are  $T_{ss2r}$ ,  $T_{ss2}$ ,  $w_{ts1}$ , and  $w_{bol}$ . The rate-of-change of the stroke of the second attemperator spray flow valve is limited in the TSSTS. The limits are parameters,  $s_{tw2o}$  and  $s_{tw2s}$  of the first nonlinear block in Fig. 9.3. The numerical values of  $s_{tw2o}$  and  $s_{tw2s}$  are both 4%/s. The rate-of-change of the stroke of the first attemperator spray flow valve is limited in the SSSTS. The limits are parameters,  $s_{sw2o}$  and  $s_{sw2s}$  of the first nonlinear block in Fig. 9.4. The numerical values of  $s_{sw2o}$  and  $s_{sw2s}$  are both 4%/s. The difference between  $T_{ss2r}$  and  $T_{ts1r}$  is a parameter,  $g_{sw2b}$  of the SSSTC. The numerical value of  $g_{sw2b}$  is 30°C and is

chosen so that the second attemperator spray flow valve is approximately halfopen. This means that the steam temperature before the tertiary superheater can be changed rapidly in both directions.

The response of the stroke of the first attemperator spray flow valve is shown in Fig. 12.9. The valve is opening for  $10 < t < 25$  s due to the decreasing steam flow through the secondary superheater with no corresponding decrease of the heat flow. The valve is then closing for  $25 < t < 90$  s due to the decreasing heat flow. The valve is completely closed for  $t > 90$  s and is thus incapable of controlling the steam temperature before the secondary superheater.

The response of the spray flow of the first attemperator is shown in Fig. 12.10. The spray flow follows the stroke of the valve fairly well. The decreasing steam flow gives, however, a more rapidly decreasing spray flow for  $25 < t < 90$  s.

The response of the steam temperature before the secondary superheater is shown in Fig. 12.11. The steam temperature is reduced for  $10 < t < 25$  s in order to compensate for the decreased steam flow. The steam temperature is then increased for  $25 < t < 90$  s in order to compensate for the decreasing heat flow. The steam temperature is continuously decreasing for  $t > 90$  s due to the decreasing steam temperature after the primary superheater (Fig. 12.4) and the limited capacity of the first attemperator.

The response of the steam temperature after the secondary superheater is shown in Fig. 12.12. The difference between the steam temperature after the secondary superheater and the steam temperature before the tertiary superheater (Fig. 12.15) shall be  $30^{\circ}\text{C}$ . This is, however, not the case due to the limited capacity of the first attemperator.

The response of the stroke of the second attemperator spray flow valve is shown in Fig. 12.13. The valve is opening for  $10 < t <$

$< 15$  s in order to compensate for the decreasing steam flow. The valve is then closing for  $15 < t < 460$  s in order to compensate for the decreasing heat flow to the tertiary superheater and for the decreasing steam temperature after the secondary superheater. The valve is finally opening for  $t > 460$  s in order to compensate for the increased heat flow to the tertiary superheater.

The response of the spray flow of the second attemperator is shown in Fig. 12.14. The spray flow follows the stroke of the valve fairly well.

The response of the steam temperature before the tertiary superheater is shown in Fig. 12.15. The steam temperature is decreased for  $10 < t < 25$  s in order to compensate for the decreasing steam flow. The steam temperature is then increased for  $25 < t < 130$  s in order to compensate for the decreasing heat flow to the tertiary superheater. The steam temperature is decreased for  $t > 460$  s in order to compensate for the increasing heat flow.

The response of the steam temperature after the tertiary superheater is shown in Fig. 12.16. The maximum steam temperature error is  $2^{\circ}\text{C}$ .

Properties: The steam flow and the fuel flow are the most severe disturbances of the steam temperature loop. The steam flow and the fuel flow influence the spray flows by feedforward. The effects of the other disturbances are reduced by feedback. The maximum steam temperature error is  $2^{\circ}\text{C}$ . The limited capacity of the first attemperator does not increase the error of the steam temperature after the tertiary superheater.

### The output power loop.

The task of the output power loop is to control the output power,  $N_{gs2}$  by manipulating the steam control valve and the extraction steam valves. The reference value of the output power,  $N_{gs2r}$  is generated by the power demand setter (PDS), which was described in Section 5. A preliminary reference value of the output power,  $s_{nsl}$  is determined from the set-point of the output power,  $s_{nslr}$  in the first part of the power demand setter (PDS1). The block diagram of the PDS1 is given in Fig. 5.1. The  $s_{nslr}$  is modified with respect to the network-frequency in the second part of the power demand setter (PDS2). The block diagram of the PDS2 is given in Fig. 5.2. The  $N_{gs2r}$  is obtained from the third part of the power demand setter (PDS3), which limits the jump and the rate-of-change of  $N_{gs2r}$ . The block diagram of the PDS3 is given in Fig. 5.3. The steam pressure before the control valve,  $p_{ts2}$  (Fig. 12.3) and the steam temperature before the steam control valve,  $T_{ts2}$  (Fig. 12.16) disturb the output power loop. The superheated steam flow,  $w_{ts1}$  (Fig. 12.22), the reheated steam flow,  $w_{rs2}$  and the extraction steam flows,  $w_{hs2}$ ,  $w_{is2}$ ,  $w_{is4}$ ,  $w_{is6}$ ,  $w_{is8}$ ,  $w_{ls2}$ , and  $w_{ls4}$  are disturbed by the output power loop. The stroke of the steam control valve is the output of the control valve servo (CVS), which was described in Section 10. The reference value of the stroke of the control valve,  $s_{vs2r}$  is determined by the turbine power controller (TPC), which was described in Section 10. The inputs to the TPC are  $N_{gs2r}$  and  $N_{gs2}$ . The block diagram of the TPC is given in Fig. 10.1. The rate-of-change of the stroke of the control valve is limited in the CVS. The limits are parameters,  $s_{vs2o}$  and  $s_{vs2s}$  of the first nonlinear block in Fig. 10.2. The numerical values of  $s_{vs2o}$  and  $s_{vs2s}$  of the first nonlinear block in Fig. 10.2. The numerical values of  $s_{vs2o}$  and  $s_{vs2s}$  are 20%/s and 200%/s respectively. The strokes of the preheater extraction valves are the outputs of the high-pressure preheater servo (HPPS), which was described in Section 10. The reference value of the strokes of the high-pressure preheater valves,  $s_{fs2r}$  are determined by the high-pressure preheater controller (HPPC), which was described in Section 10. The input to the HPPC is  $N_{gs2r}$ . The block diagram of the HPPC is given in

Fig. 10.3. The strokes of the low-pressure preheater extraction valves are the outputs of the low-pressure preheater servo (LPPS) which was described in Section 10. The reference value of the strokes of the low-pressure preheater extraction valves,  $s_{fs7r}$  is determined by the low-pressure preheater controller (LPPC), which was described in Section 10. The inputs to the LPPC are  $N_{gs2r}$ , the reference value of the deaerator steam pressure,  $p_{as2r}$ , and the deaerator steam pressure,  $p_{as2}$ . The block diagram of the LPPC is given in Fig. 10.4. The rates-of-change of the strokes of the high-pressure preheater extraction valves are limited in the HPPS. The limits are parameters of the first nonlinear block in Fig. 10.5. The numerical values of  $s_{fs2o}$  and  $s_{fs2s}$  are both 100%/s. The rates-of-change of the strokes of the low-pressure preheater extraction valves are limited in the LPPS. The limits are parameters,  $s_{fs7o}$  and  $s_{fs7s}$  of the first nonlinear block in Fig. 10.6. The numerical values of  $s_{fs7o}$  and  $s_{fs7s}$  are both 100%/s.

The responses of the strokes of the low-pressure preheater extraction valves are shown in Fig. 12.17. The strokes of the valves are then decreasing with a time constant of about 30 s. The reference value of the output power reaches its final value at  $t = 220$  s which is visible in the responses of the strokes.

The responses of the strokes of the high-pressure preheater extraction valves are shown in Fig. 12.18. The strokes of the valves are increased for  $10 < t < 15$  s due to the feedforward from the decreasing reference value of the output power. The strokes of the valves are then decreasing with a time constant of about 30 s. The target value is higher than 0.5 and is determined by the derivative of the reference value of the output power. The reference value of the output power reaches its final value at  $t = 220$  s, which is clearly visible in the responses of the strokes.

The response of the feedwater temperature after the high-pressure preheater is shown in Fig. 12.19. The temperature decreases about  $25^{\circ}\text{C}$  due to the final decrease of extraction steam flows. The tem-

porary opening of the extraction valves do not affect the feedwater temperature seriously. The low-pass filtering effect of the seven preheater stages are pronounced. The feedwater temperature starts to decrease when the pressures before the extraction valves decrease.

The response of the feedwater temperature after the economizer is shown in Fig. 12.20. The temperature decreases about  $40^{\circ}\text{C}$  due to the decreasing feedwater temperature before the economizer and the decreasing heat flow to the economizer.

The response of the stroke of the control valve is shown in Fig. 12.21. The valve opening is decreased with maximum rate-of-change for  $10 < t < 13 \text{ s}$  in order to decrease the output power rapidly. The valve opening is then decreased with a lower rate-of-change in order to decrease the output power like a ramp. The reference value of the output power is constant for  $t > 220 \text{ s}$  but the drum pressure is still decreasing. This means that the opening of the valve has to be increased. The output power loop has been tuned for fast responses. This explains the peak in the response of the stroke of the control valve at  $t = 13 \text{ s}$ . This type of response may lead to unacceptable wear of the control valve and its servo. The wear can, however, be reduced by reducing the response rate of the output power loop. The high response rate was chosen in order to demonstrate that it does not lead to severe interaction between the control loops.

The response of the steam flow is shown in Fig. 12.22. The response of the steam flow is similar to the response of the stroke of the control valve for  $10 < t < 40 \text{ s}$ . The effect of the decreasing steam pressure is easily recognized for  $t > 220 \text{ s}$ . The stroke of the control valve is increasing but the steam flow is fairly constant.

The response of the reheater steam pressure is shown in Fig. 12.23. The pressure is approximately proportional to the steam flow. The pressure responds, however, more slowly due to the mass



storage in the reheater.

The response of the output power is shown in Fig. 12.24. The output power shows a jump-and-rate response. The settling-time is about 3 s. The output power has reached its final value within 250 s. The output power error is less than 1 MW for  $t > 15$  s.

Properties: The steam pressure before the control valve is the only important disturbance of the output power loop. The variations of the steam pressure before the control valve do not, however, cause any difficulties. The effects of the disturbances are reduced by feedback. The output power error is less than 1 MW for  $t > 15$  s. The response of the stroke of the control valve may lead to unacceptable wear of the control valve and its servo. The wear can, however, be reduced by reducing the response rate of the output power loop. The high response rate was chosen in order to demonstrate the performance of the control system.

### Conclusions.

The performance of the control system when the output power is decreased from 150 MW (94%) to 100 MW (63%) in normal mode has been investigated by simulation. In order to decrease the output power it is necessary to decrease both the steam flow and the fuel flow. The steam flow is the most severe disturbance of the drum pressure loop, the drum level loop, and the steam temperature loop. The fuel flow is a severe disturbance of the steam temperature loop. The influences of the variations of the steam flow and the fuel flow have been reduced by feedforward. The limited rate-of-change of the fuel flow deteriorates the performance of the drum pressure loop. The maximum drum pressure error is  $4 \cdot 10^5$  Pa (3%). The control of the drum level is difficult due to the shrink-and-swell phenomenon. The maximum drum level error is 4 cm. The limited capacity of the first attemperator does not deteriorate the performance of the steam temperature loop. The maximum steam temperature error is  $2^\circ\text{C}$ . The steam pressure before the control valve

is the only important disturbance of the output power loop. The output power error is less than 1 MW for  $t > 15$  s. The output power loop has been tuned for fast responses, which may cause unacceptable wear of the control valve and its servo. The simulations show that even with such a tight loop there are no difficulties due to interaction with other loops.

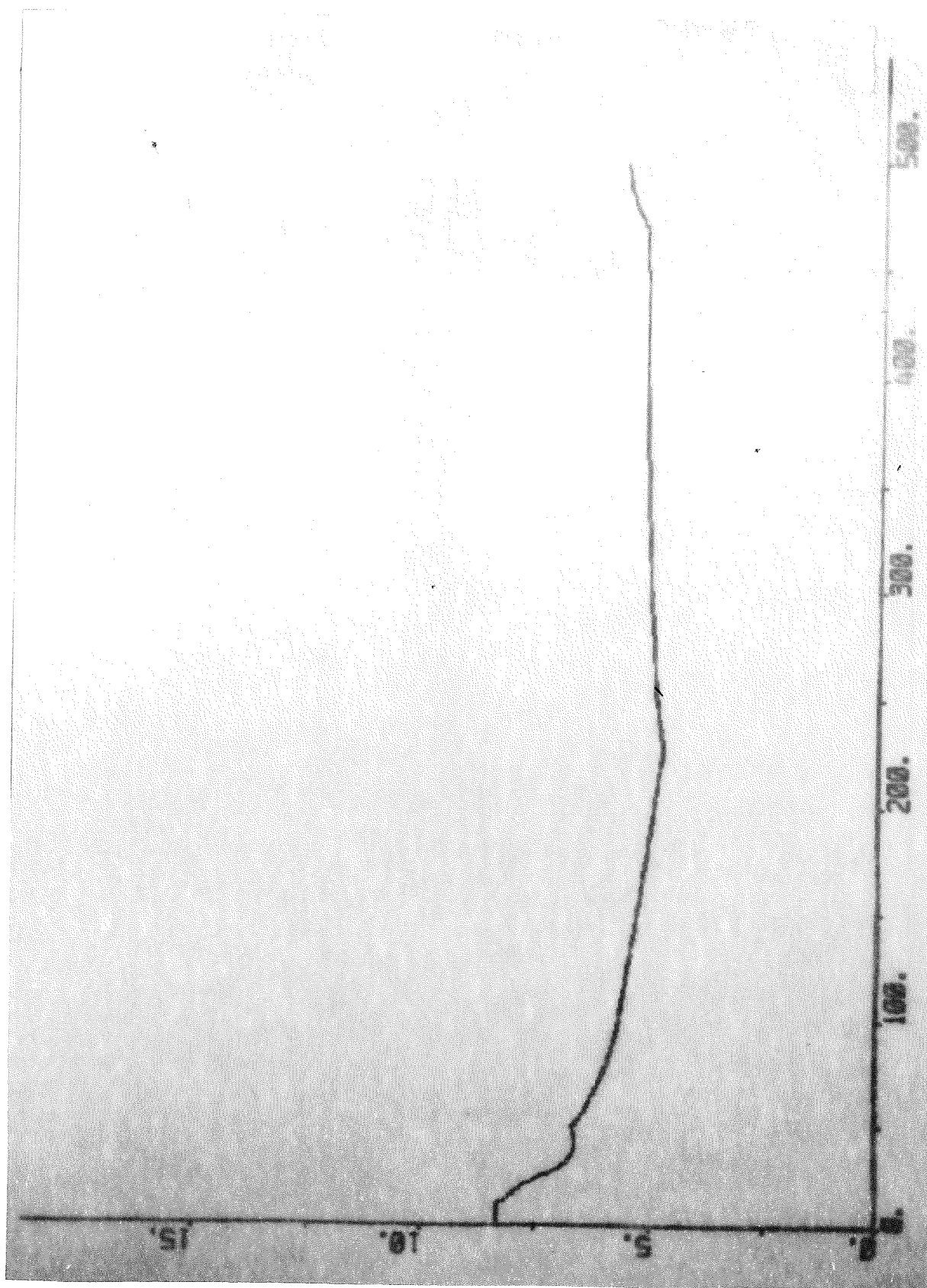


Fig. 12.1 - Response of the fuel flow due to decrease of output power in normal mode.

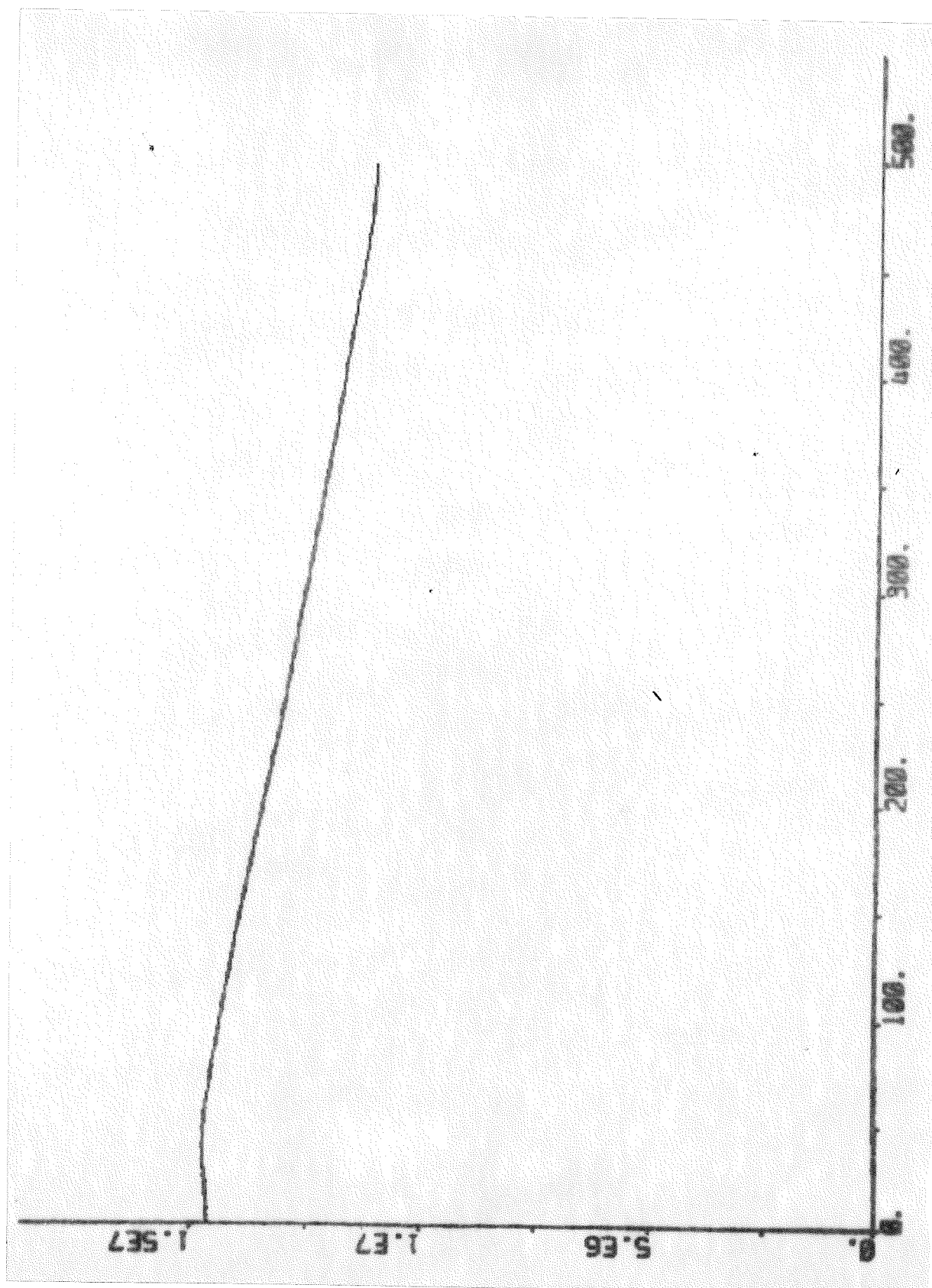


Fig. 12.2 - Response of the drum pressure due to decrease of output power in normal mode.

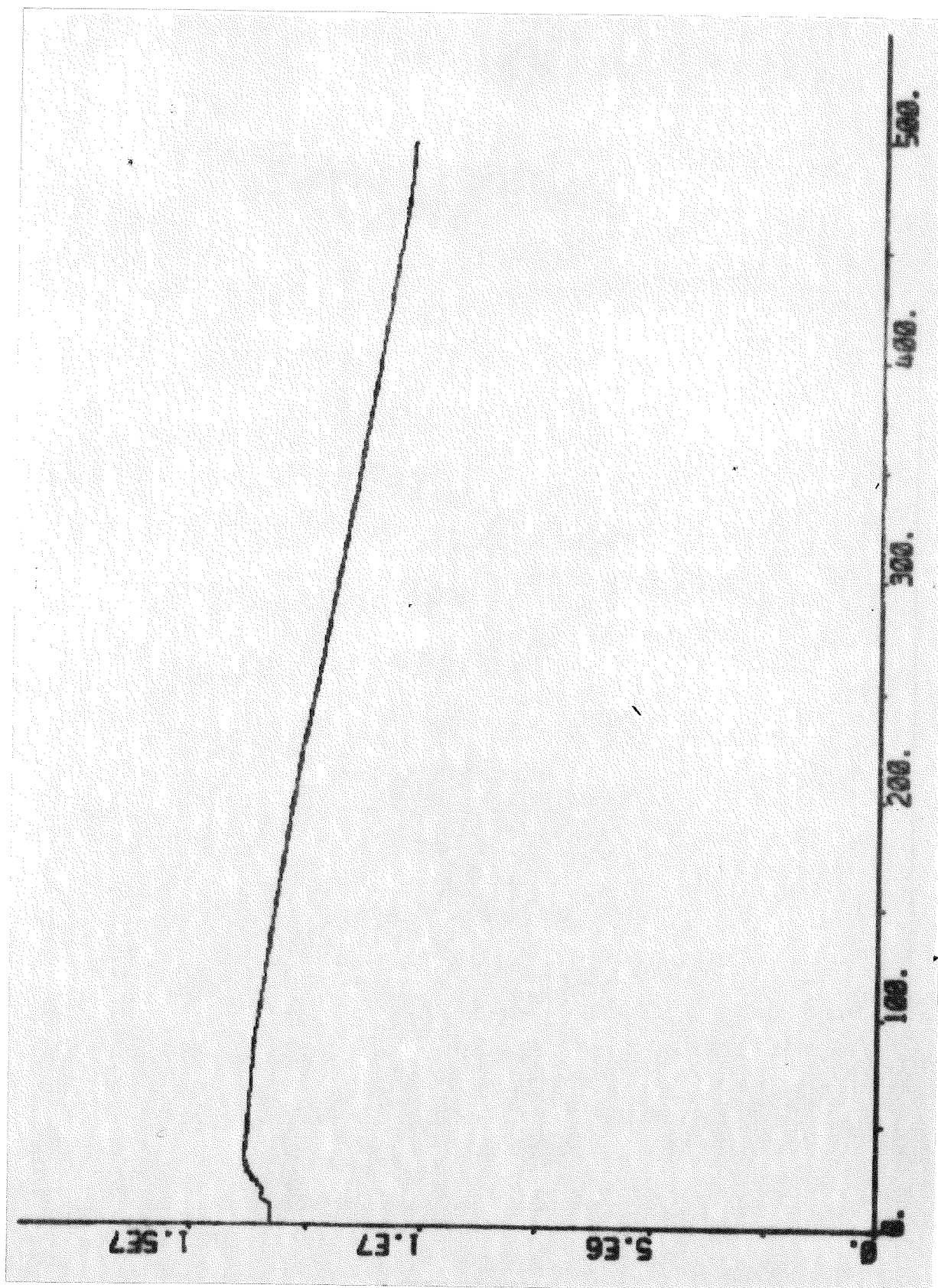


Fig. 12.3 - Response of the steam pressure before the control valve due to decrease of output power in normal mode.

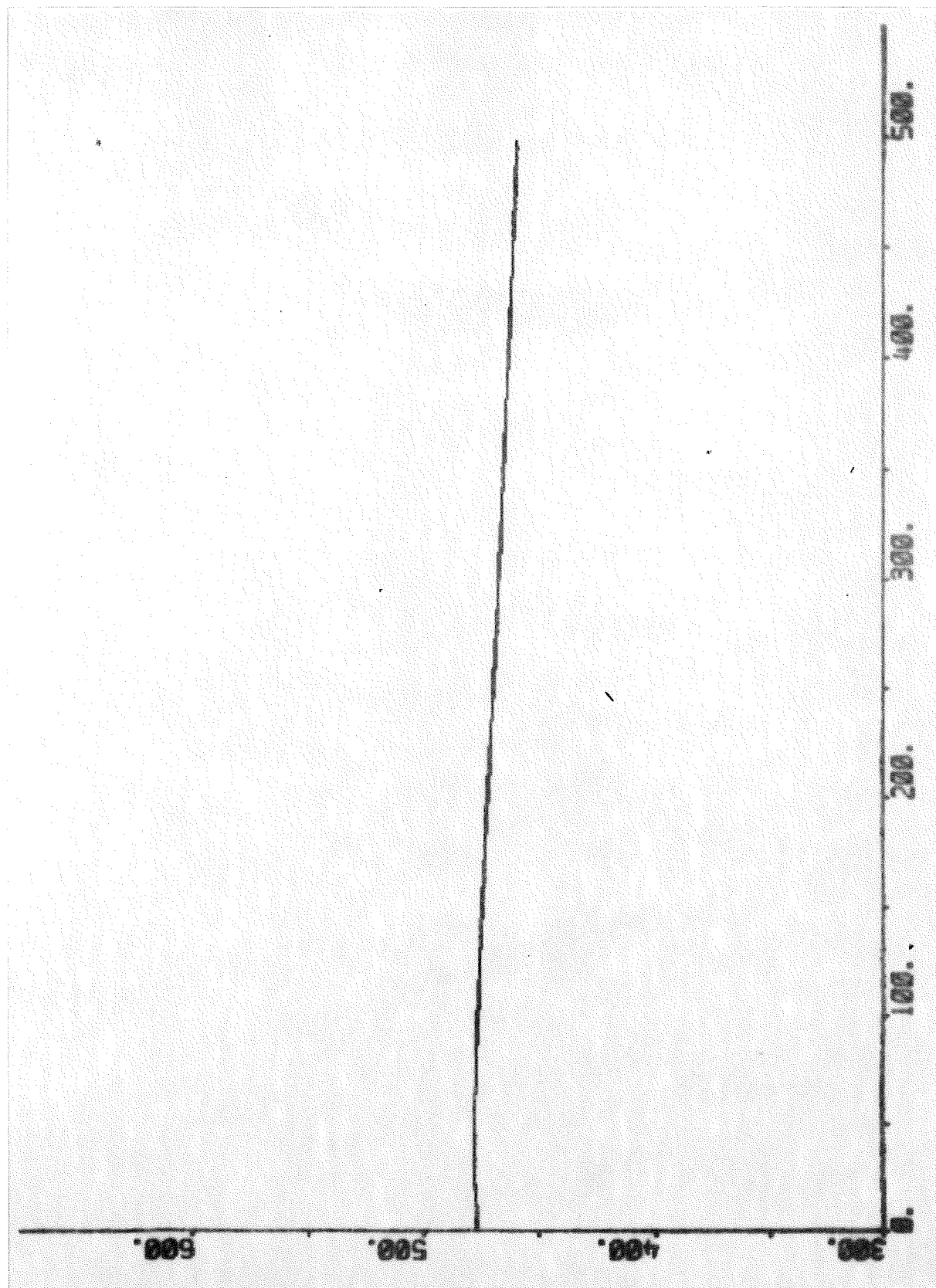


Fig. 12.4 - Response of the steam temperature after the primary superheater due to decrease of output power in normal mode.

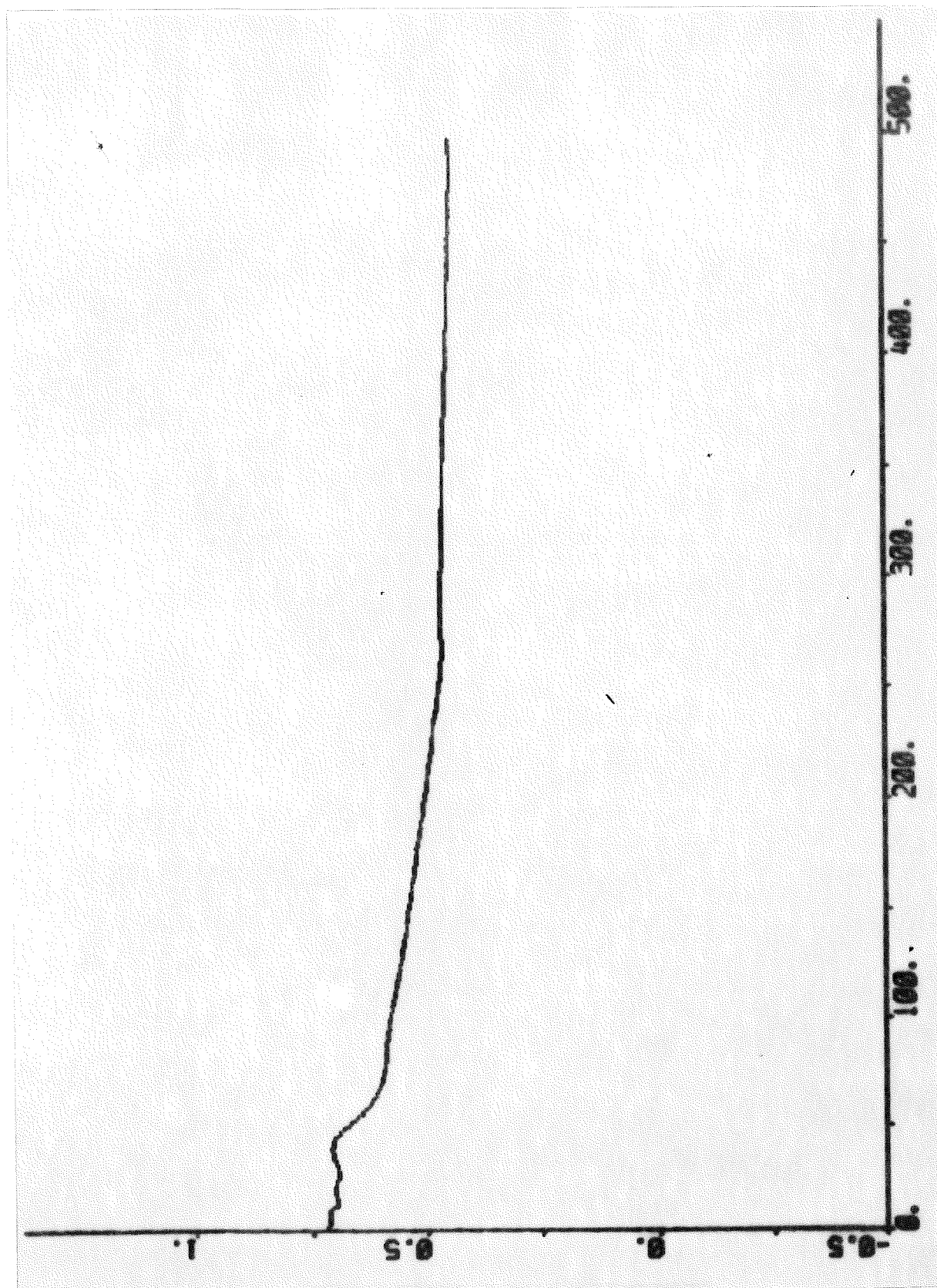


Fig. 12.5 - Response of the stroke of the feedwater valve due to decrease of output power in normal mode.

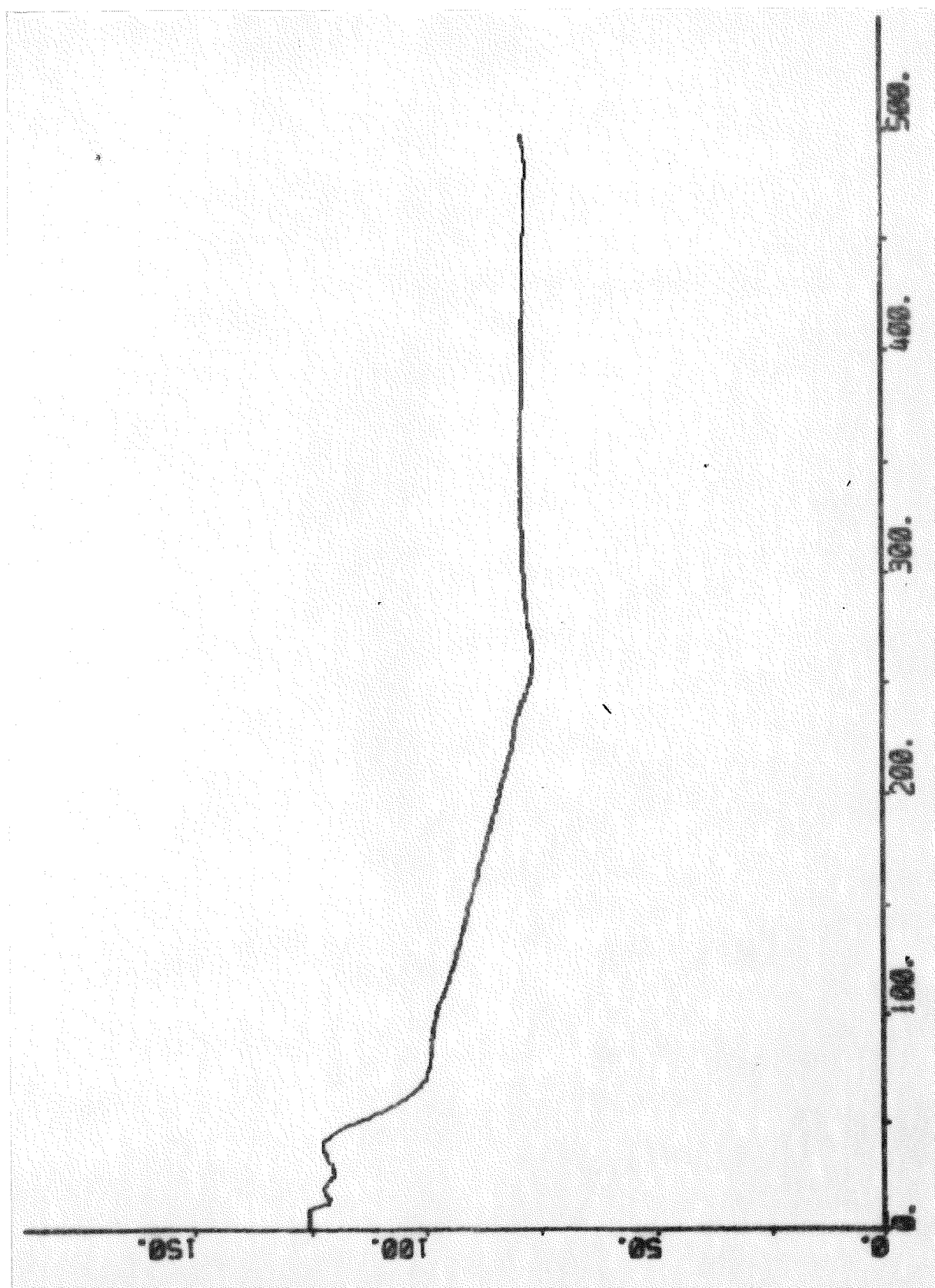


Fig. 12.6 - Response of the feedwater flow due to decrease of output power in normal mode.



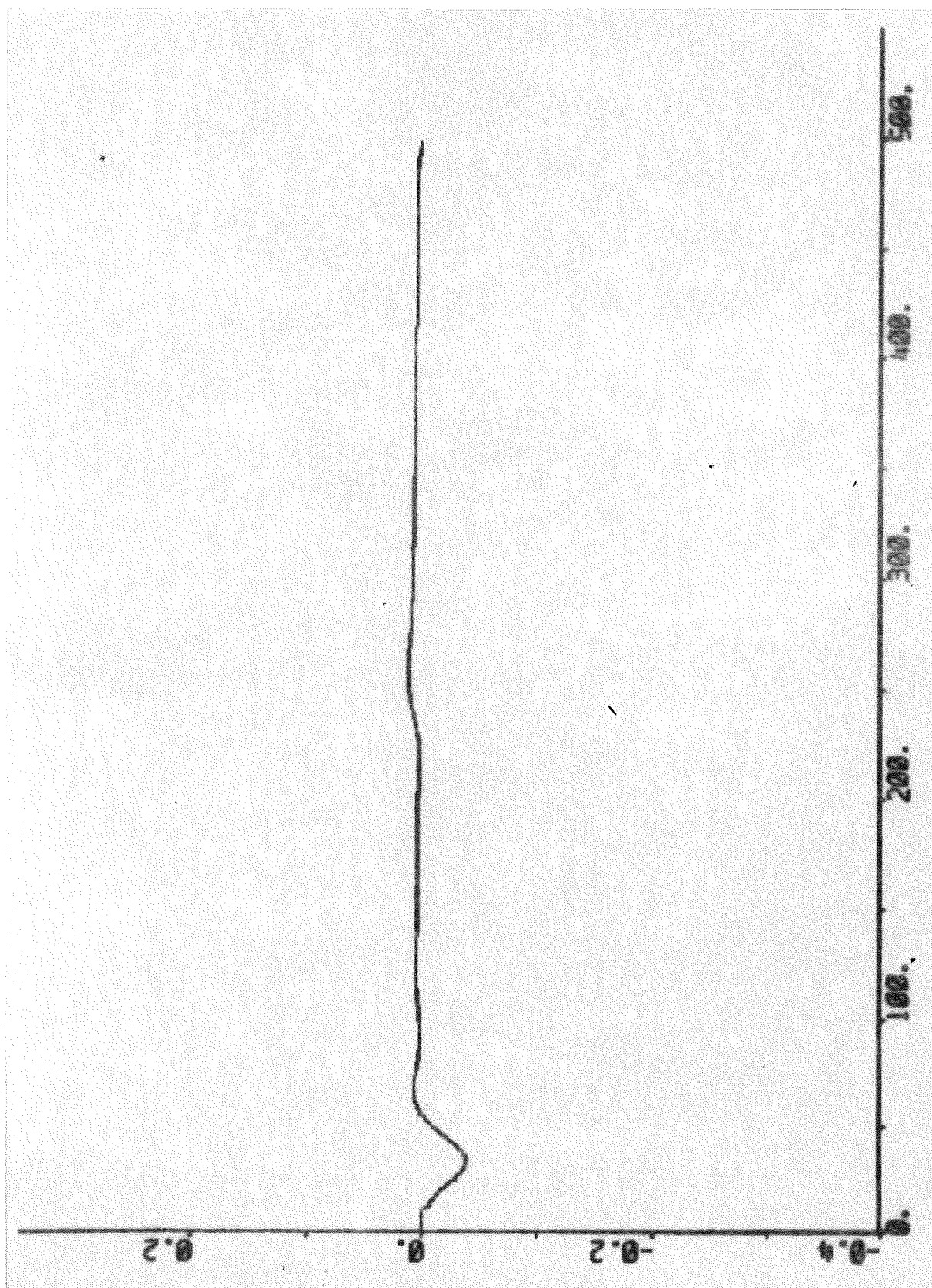


Fig. 12.7 - Response of the drum level due to decrease of output power in normal mode.

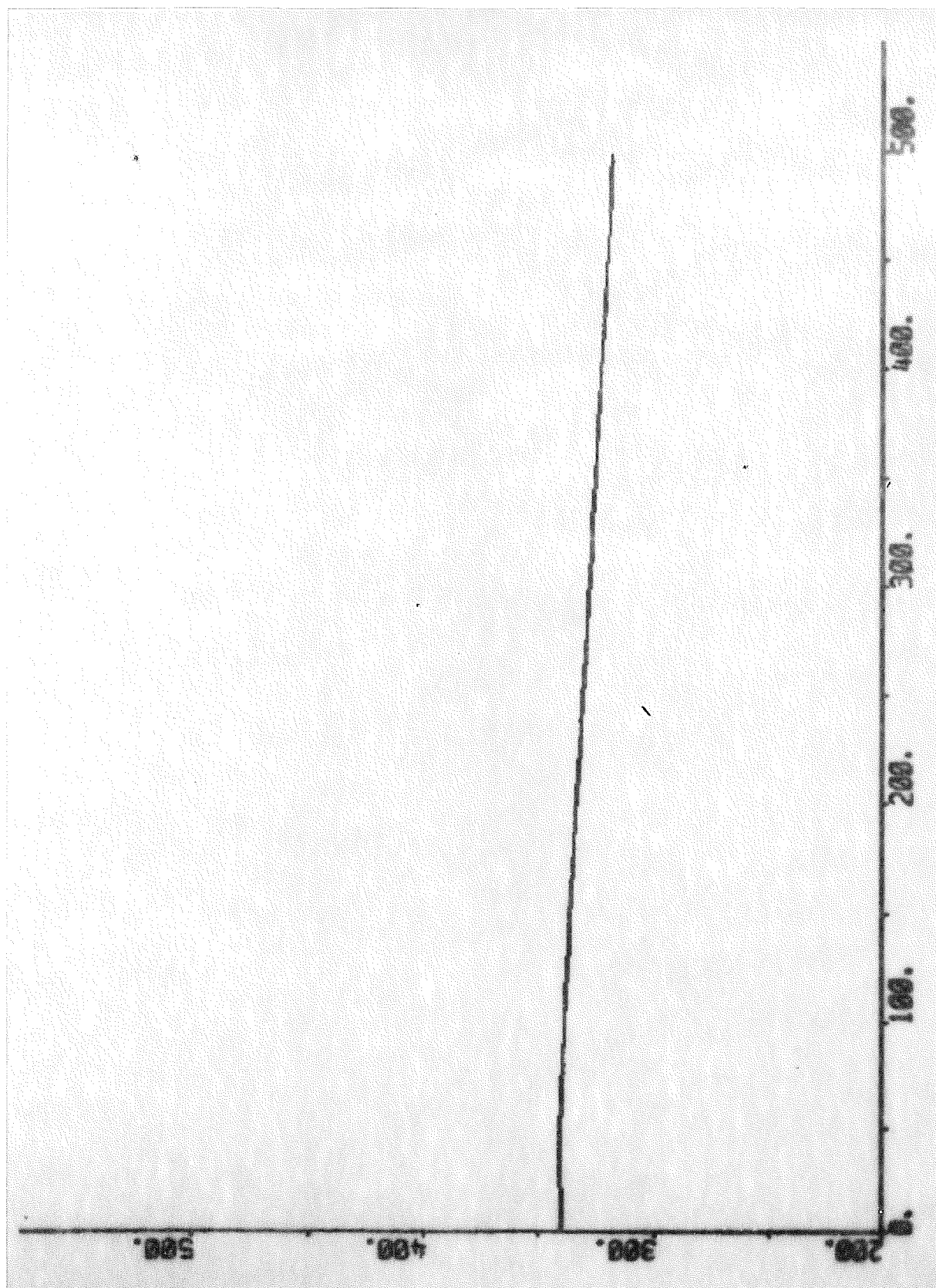


Fig. 12.8 - Response of the drum water temperature due to decrease of output power in normal mode.

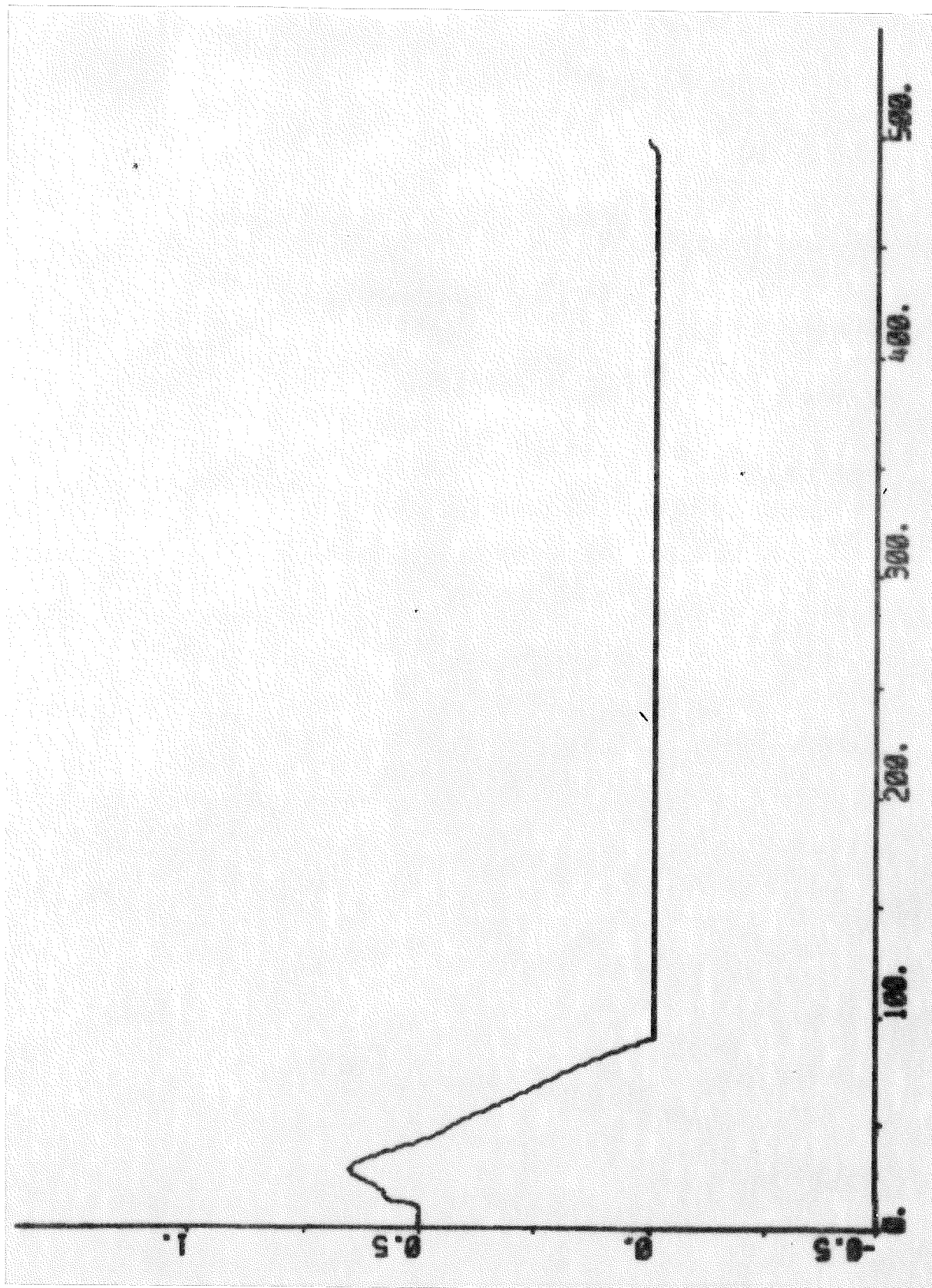


Fig. 12.9 - Response of the stroke of the first attenuator spray flow value due to decrease of output power in normal mode.

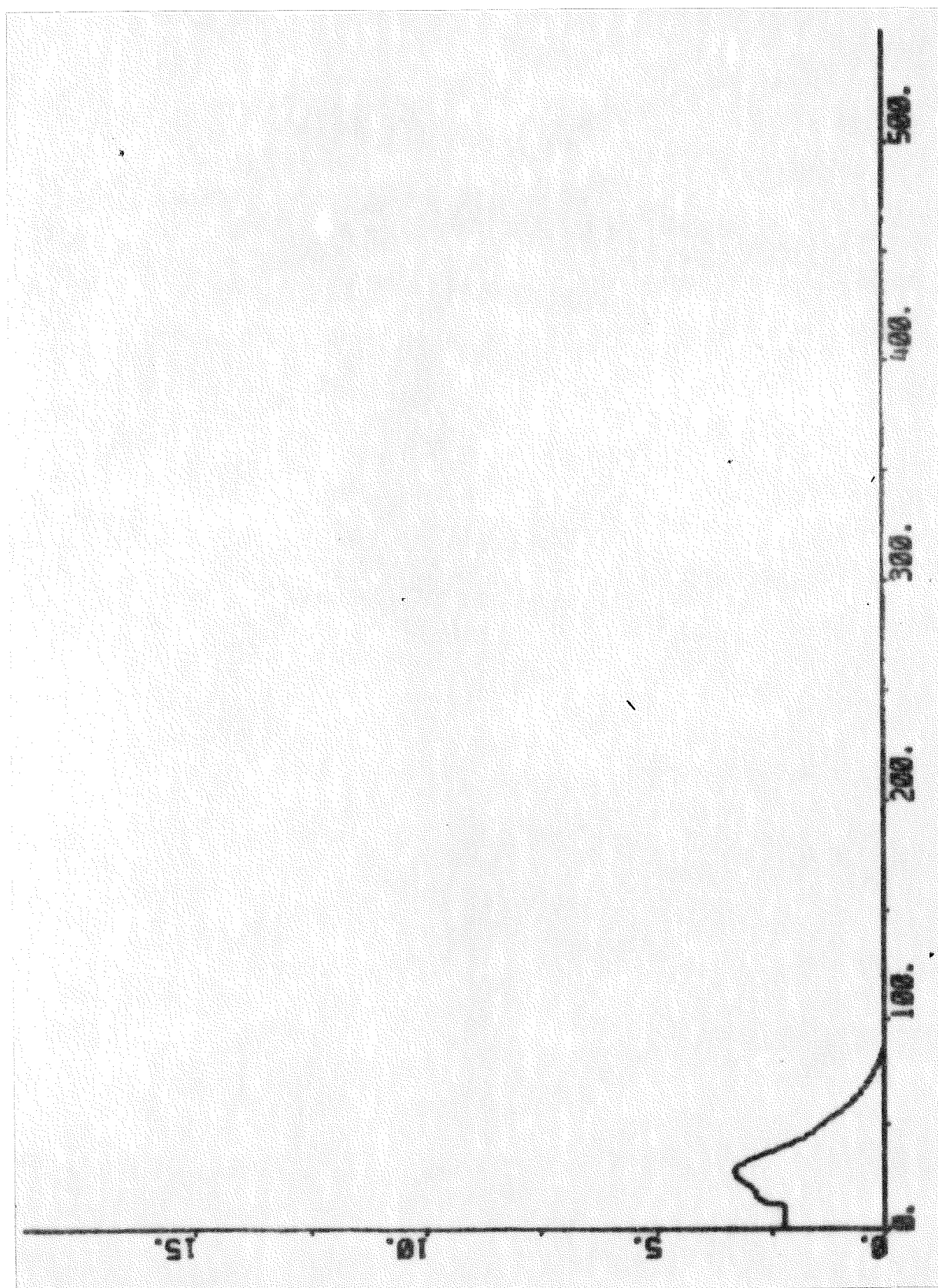


Fig. 12.10 - Response of the spray flow of the first attenuator due to decrease of output power in normal mode.

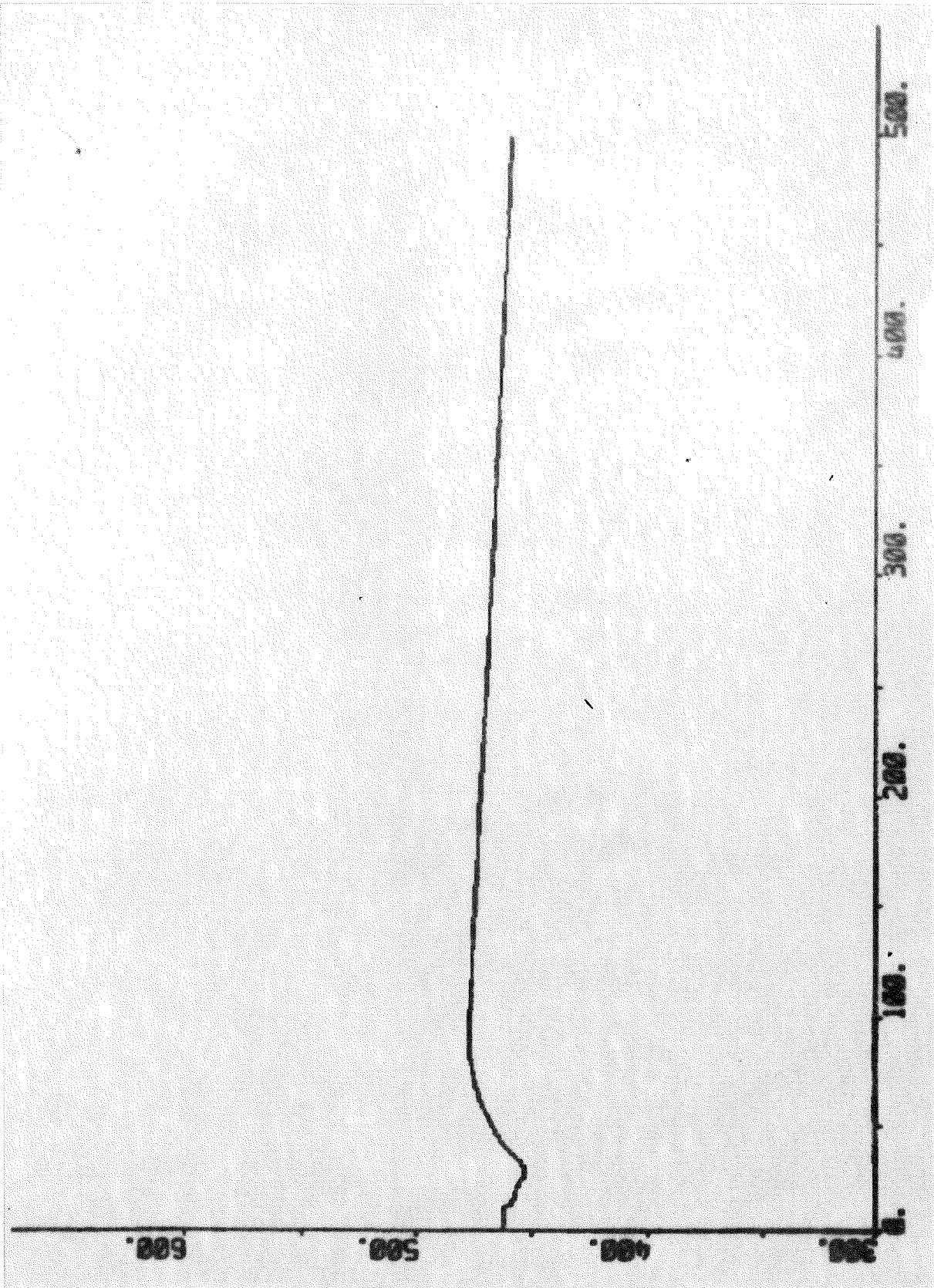


Fig. 12.11 - Response of the steam temperature before the secondary superheater due to decrease of output power in normal mode.

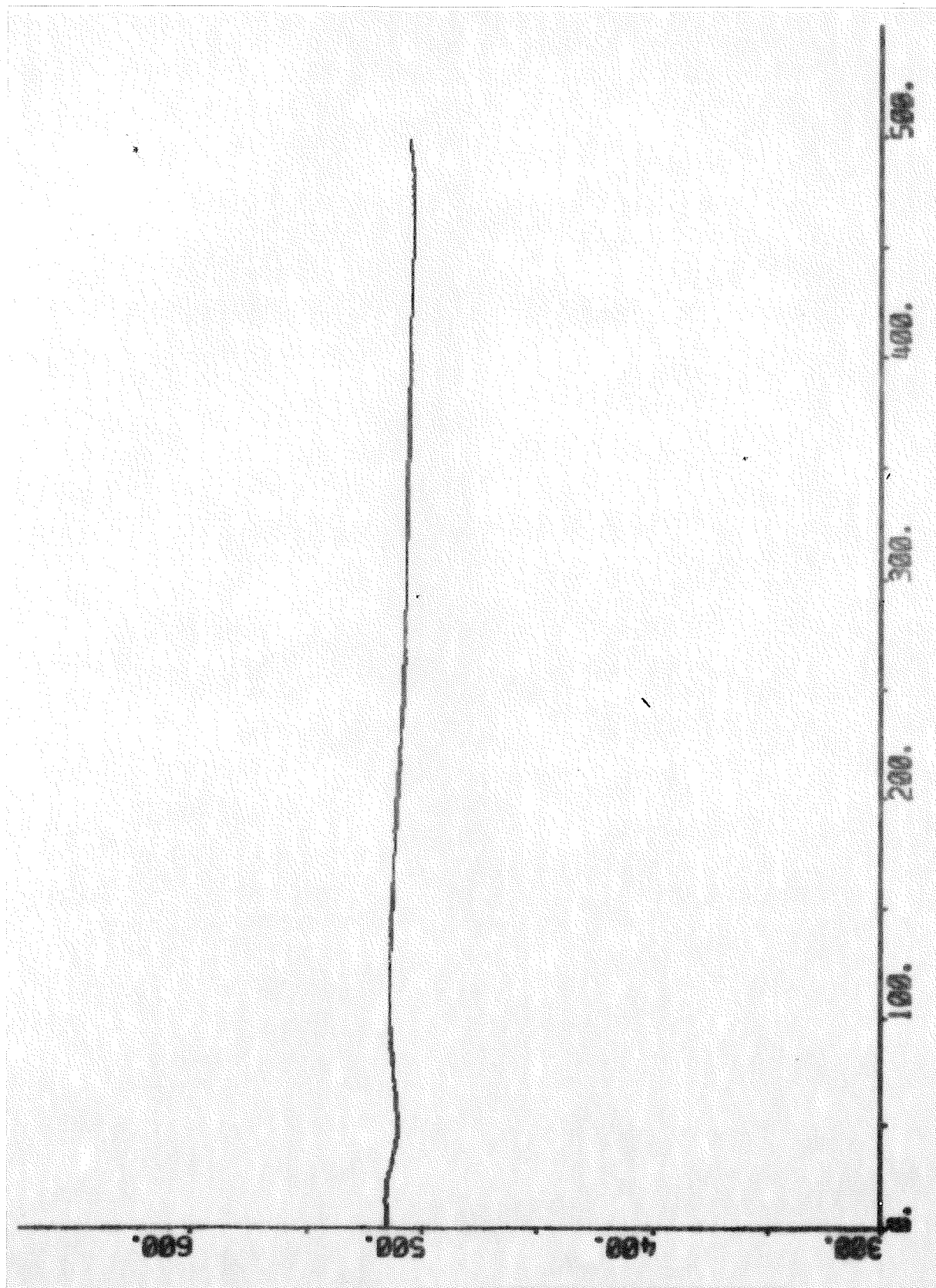


Fig. 12.12 - Response of the steam temperature after the secondary superheater due to decrease of output power in normal mode.



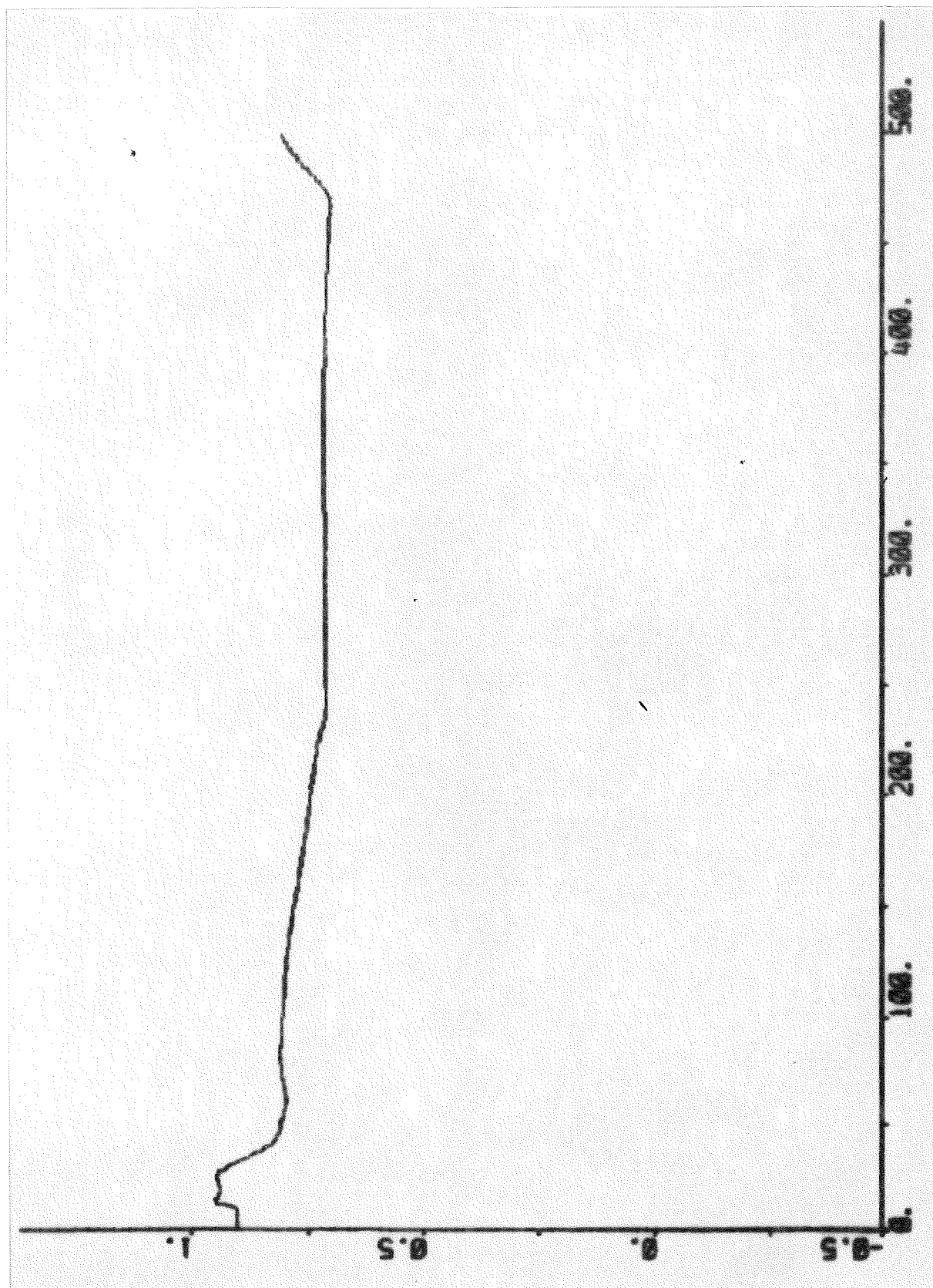


Fig. 12.13 - Response of the stroke of the second attenuator spray flow valve due to de-crease of output power in normal mode.

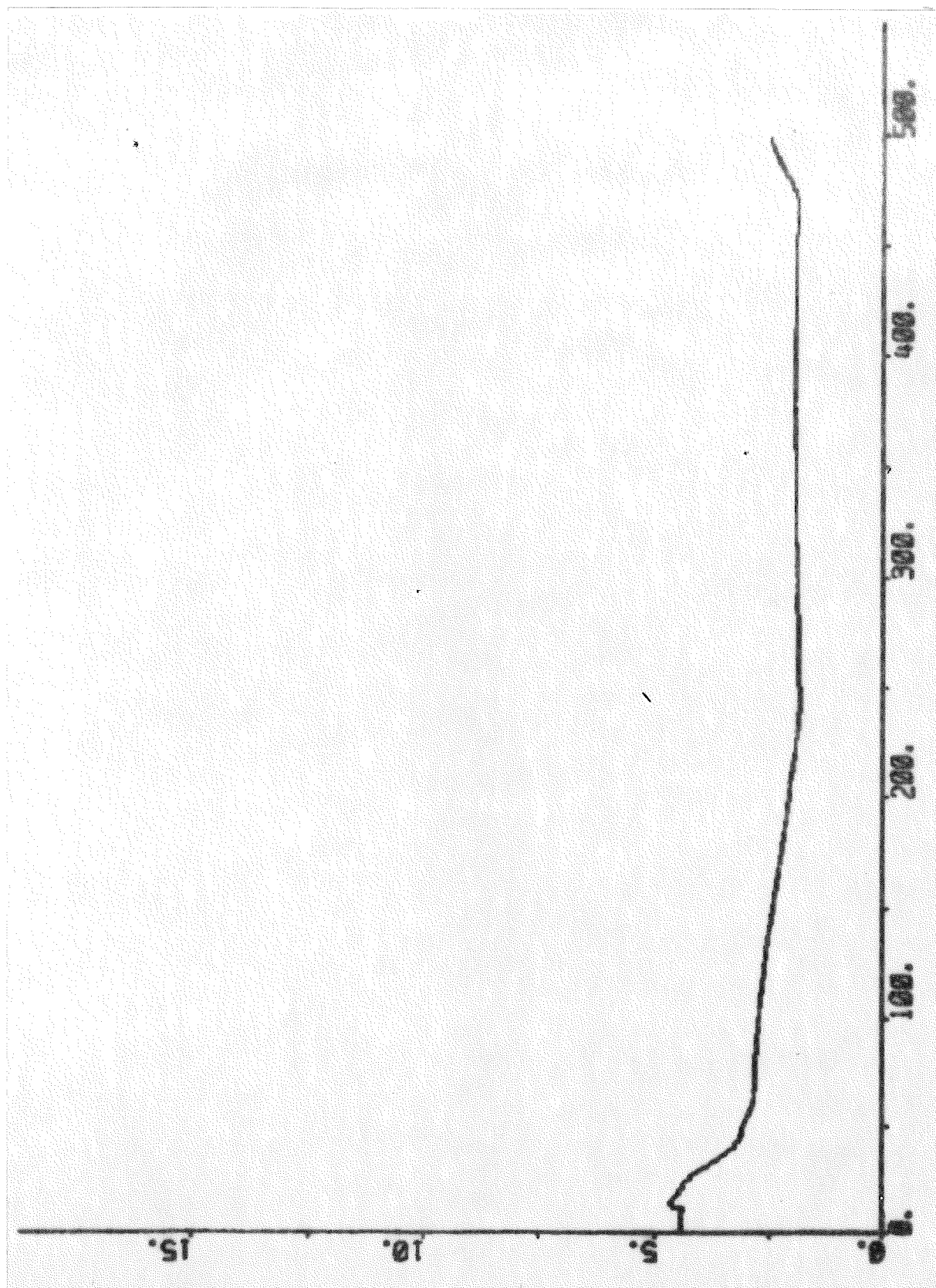


Fig. 12.14 - Response of the spray flow of the second attenuator due to decrease of output power in normal mode.



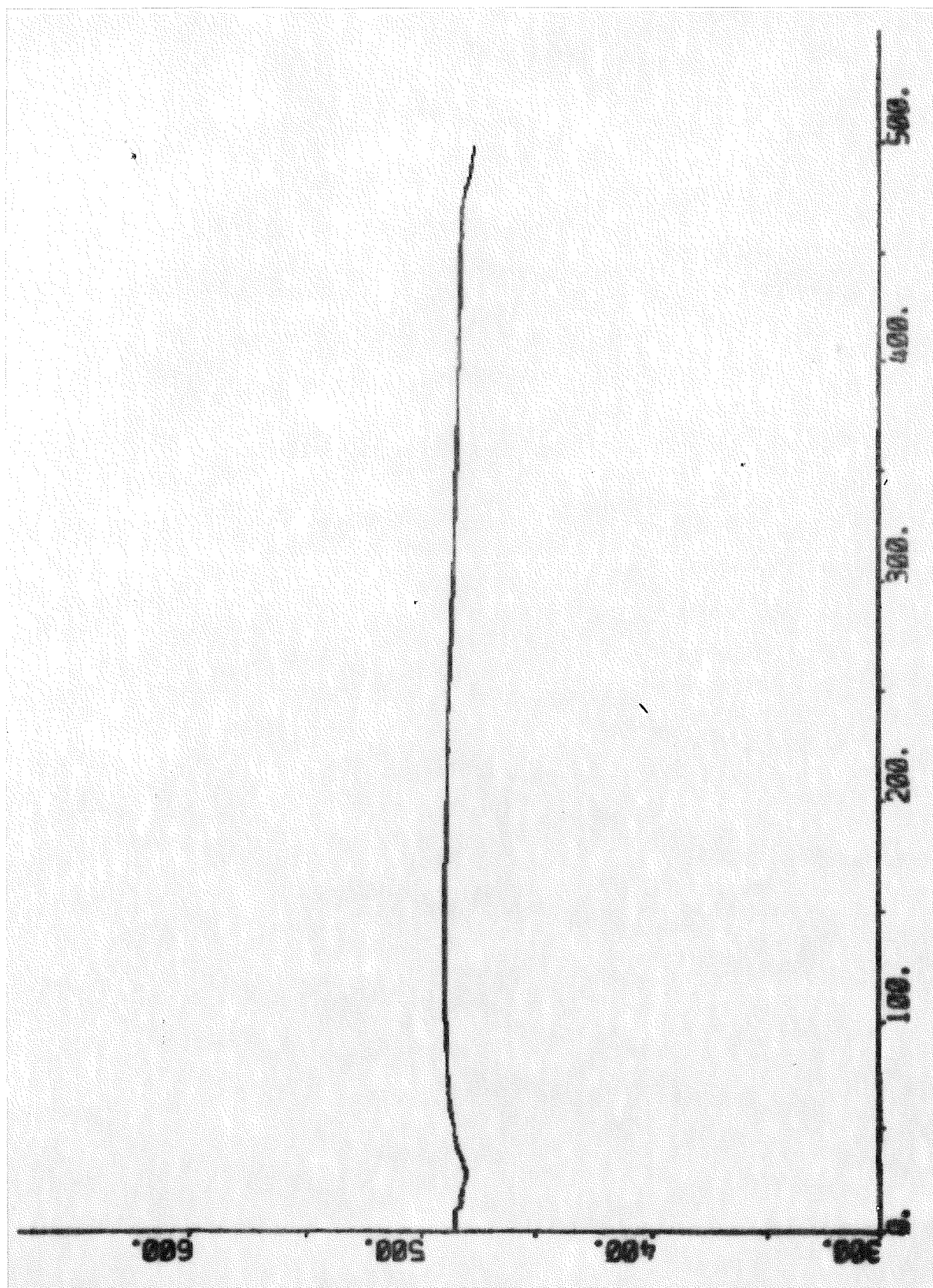


Fig. 12.15 - Response of the steam temperature before the tertiary superheater due to decrease of output power in normal mode.

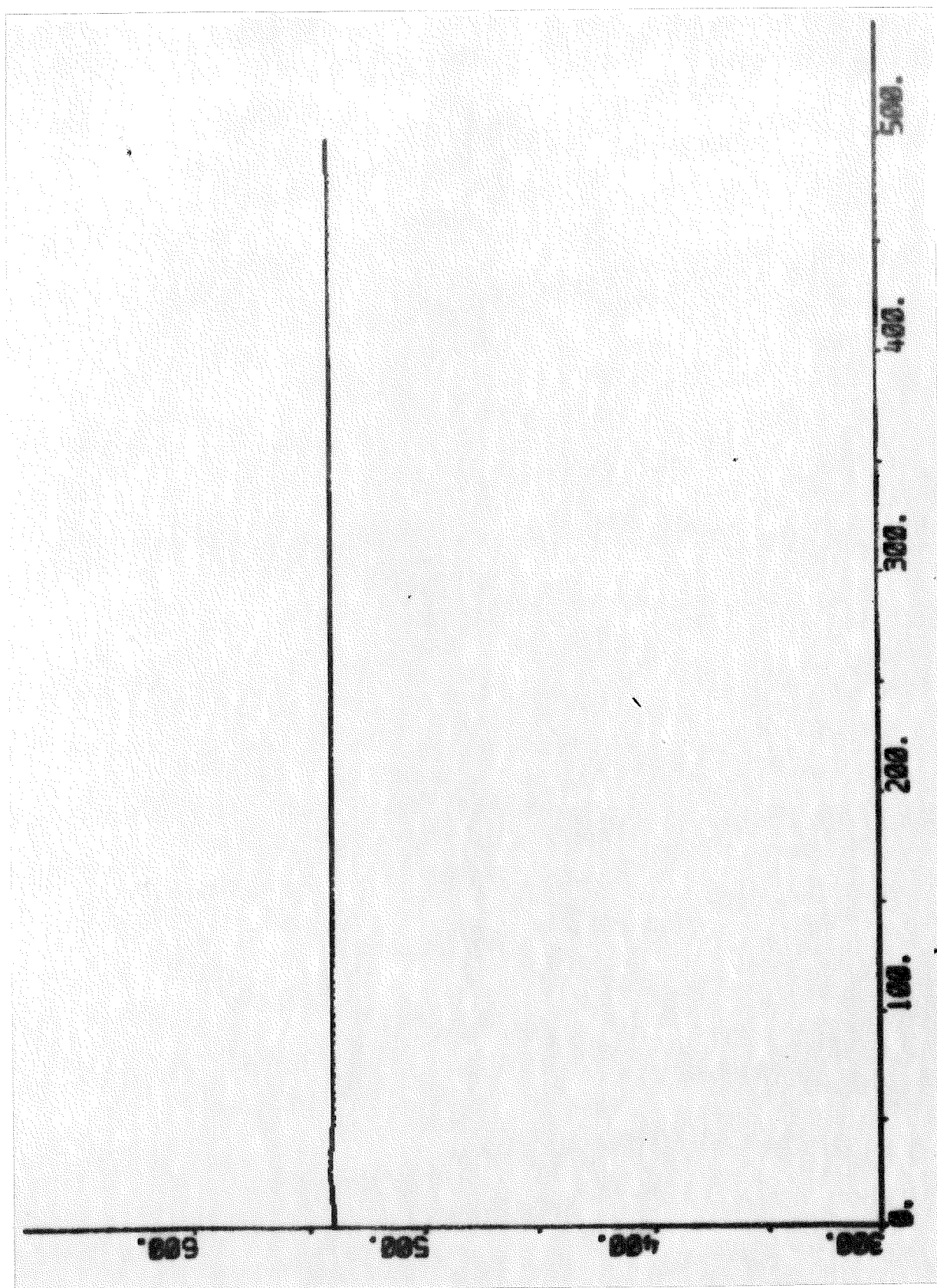


Fig. 12.16 - Response of the steam temperature after the tertiary superheater due to decrease of output power in normal mode.

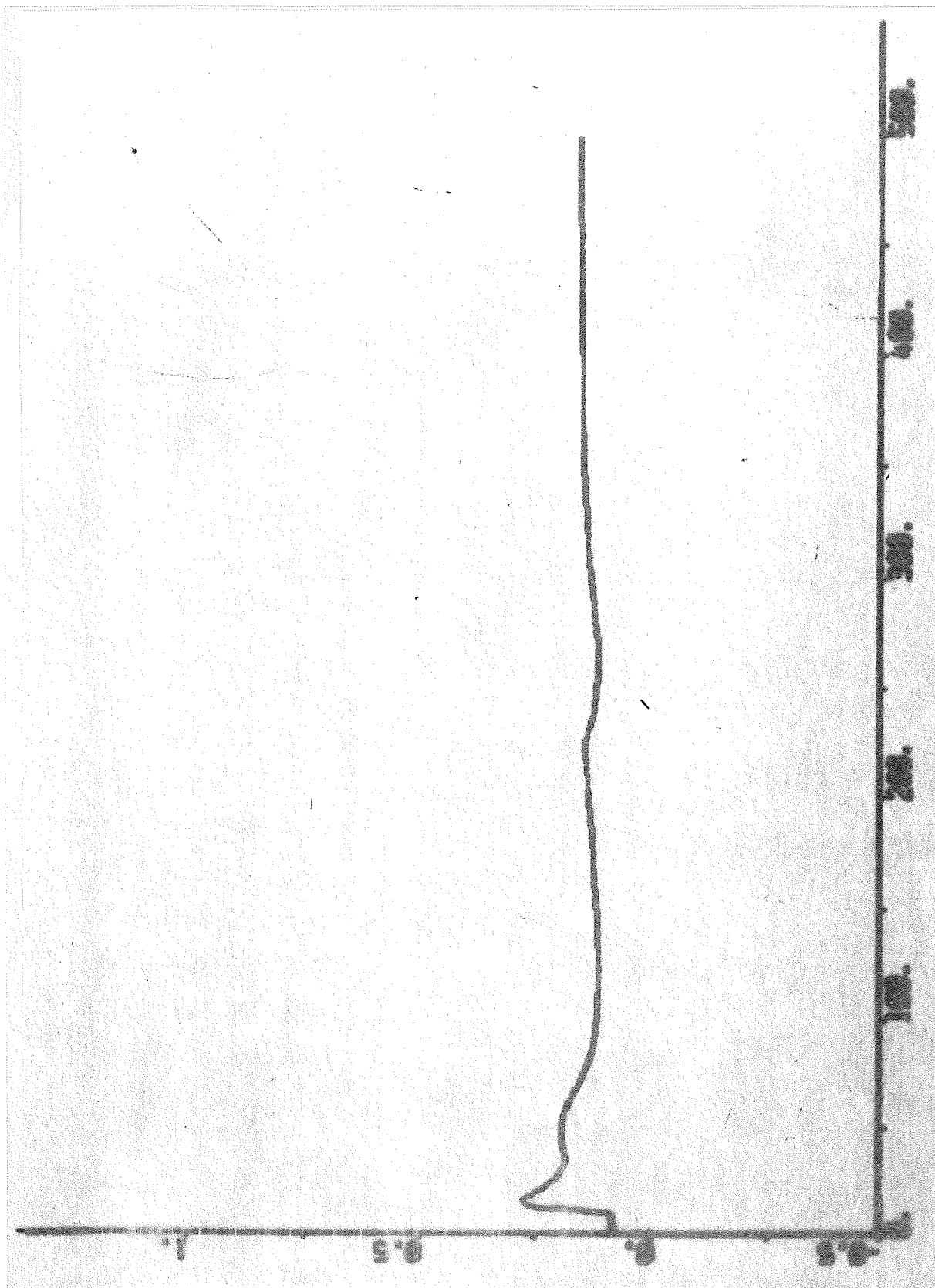


Fig. 12.17 - Response of the strokes of the low-pressure preheater extraction valves due to decrease of output power in normal mode.

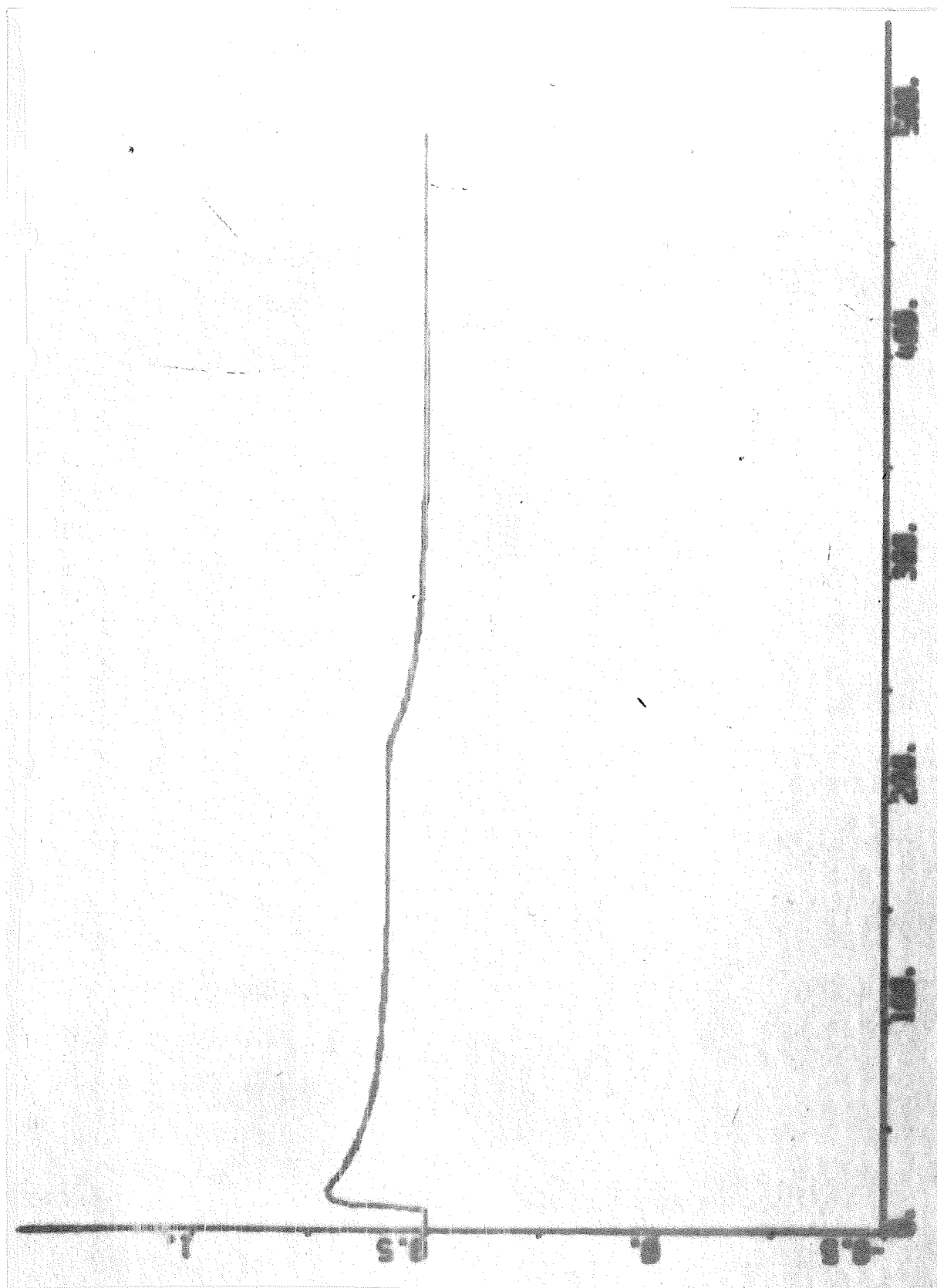


Fig. 12.18 - Response of the strokes of the high-pressure preheater extraction valves due to decrease of output power in normal mode.

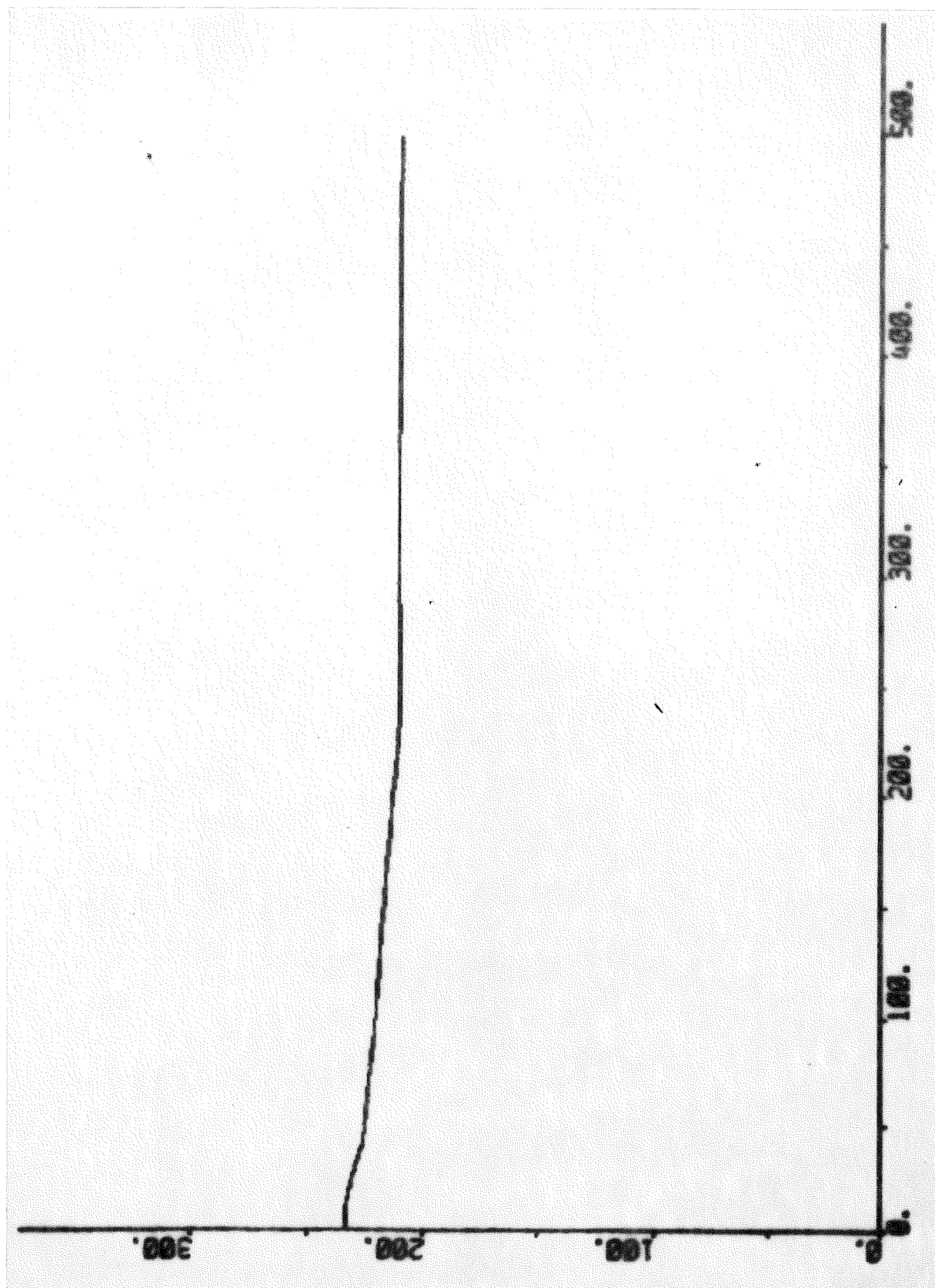


Fig. 12.19 - Response of the feedwater temperature after the high-pressure preheater due to decrease of output power in normal mode.

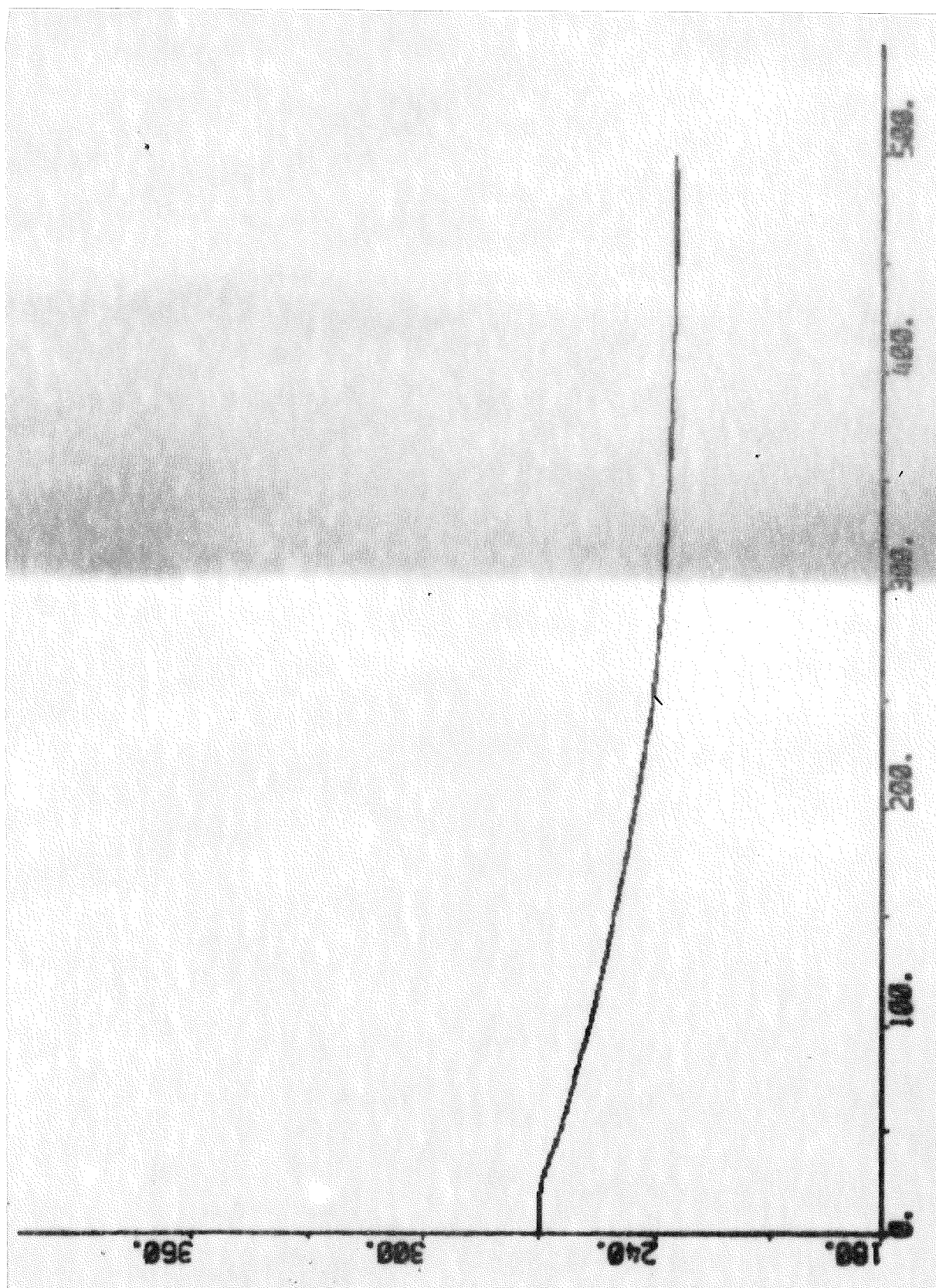


Fig. 12.20 - Response of the feedwater temperature after the economizer due to decrease of output power in normal mode.

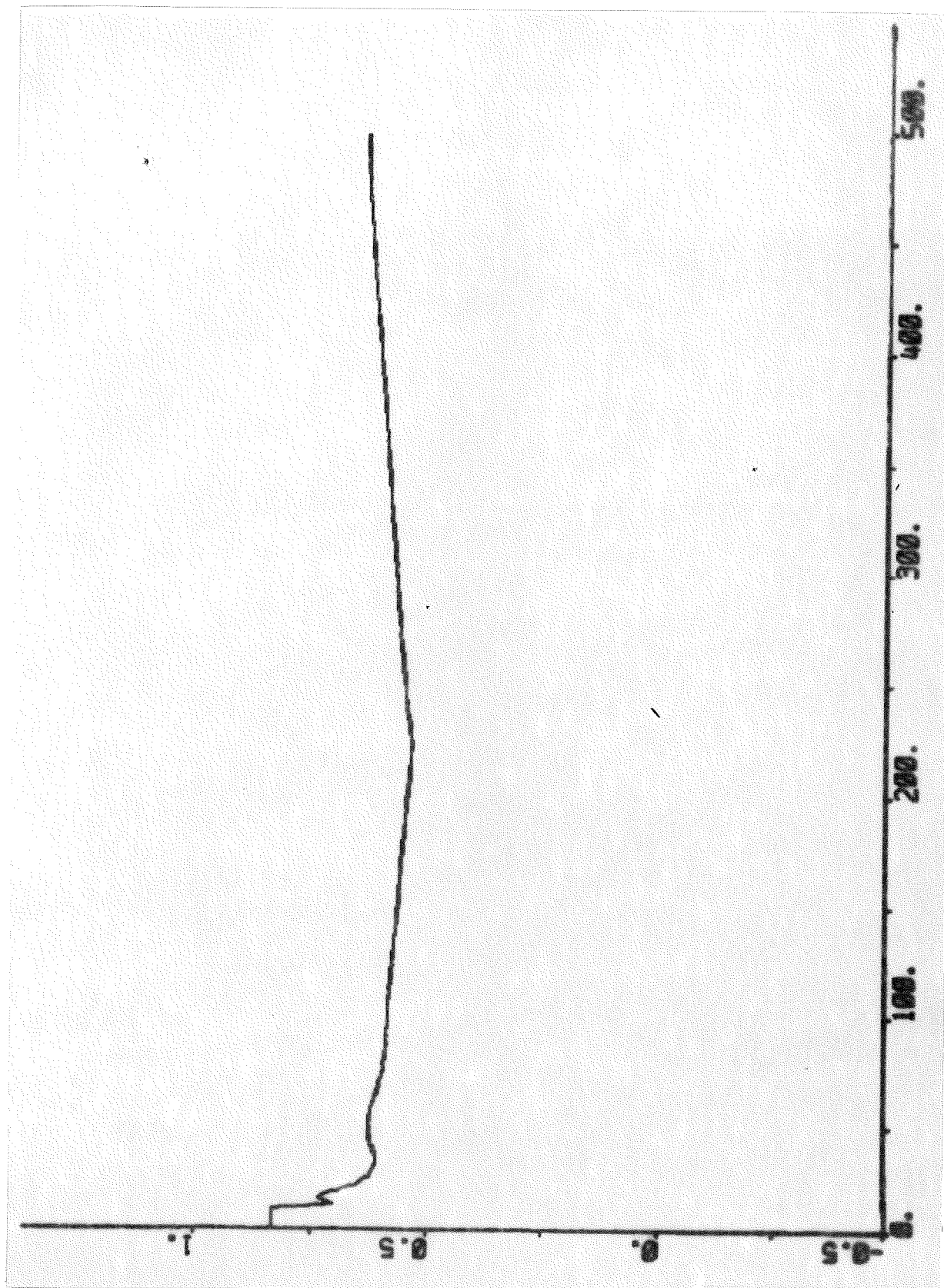


Fig. 12.21 - Response of the stroke of the control valve due to decrease of output power in normal mode.



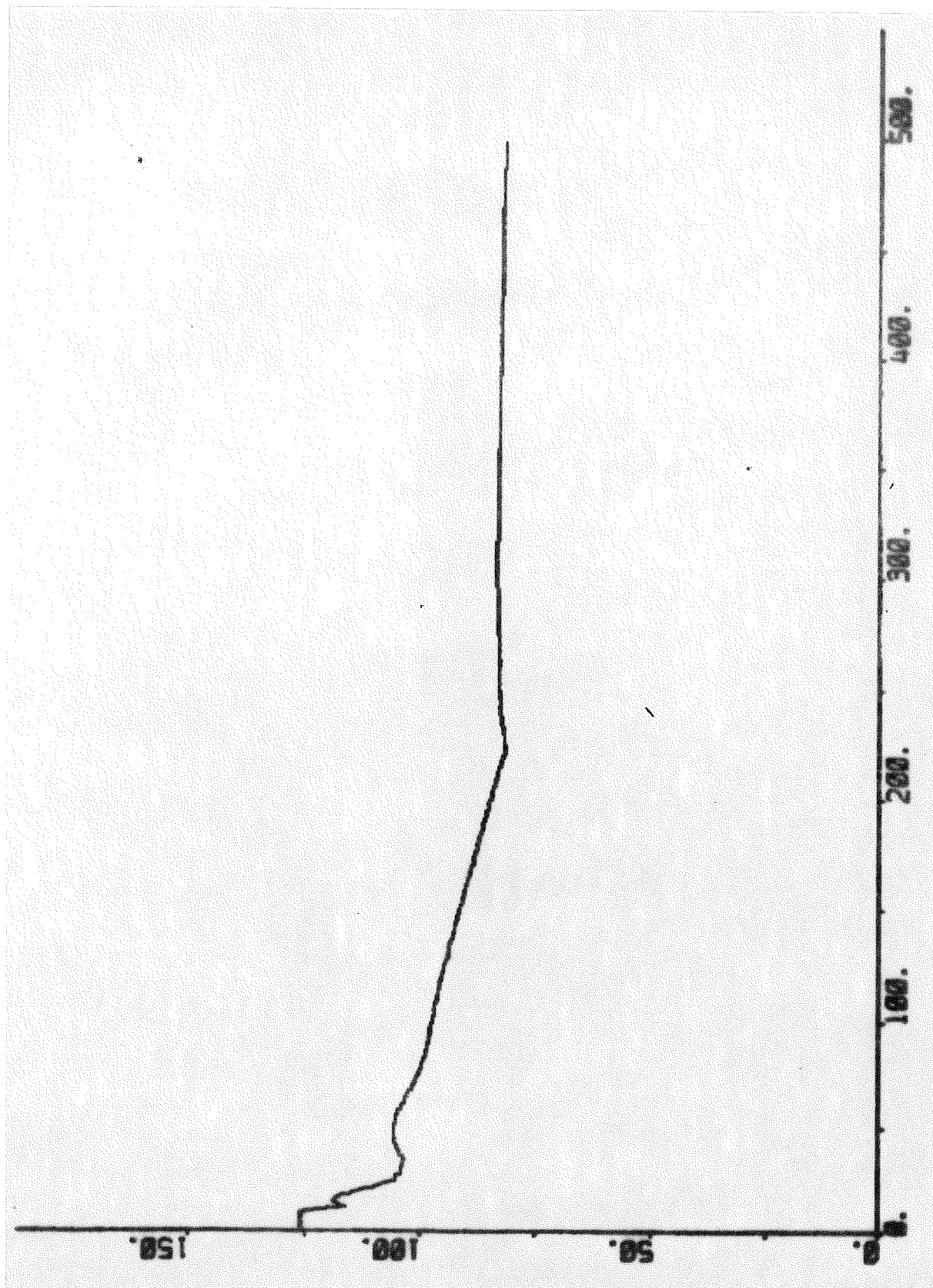


Fig. 12.22 - Response of the steam flow due to decrease of output power in normal mode.



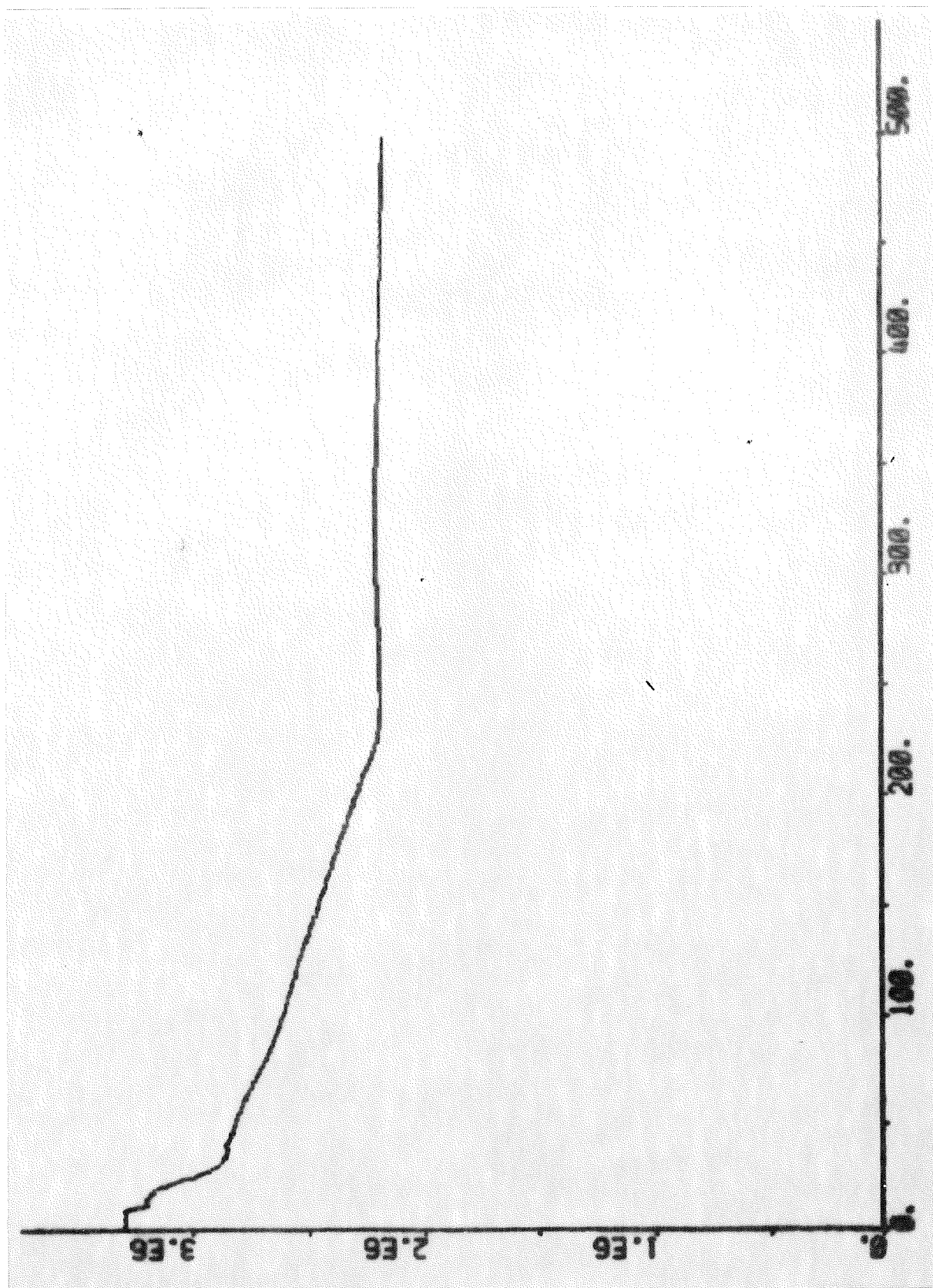


Fig. 12.23 - Response of the reheat steam pressure due to decrease of output power in normal mode.

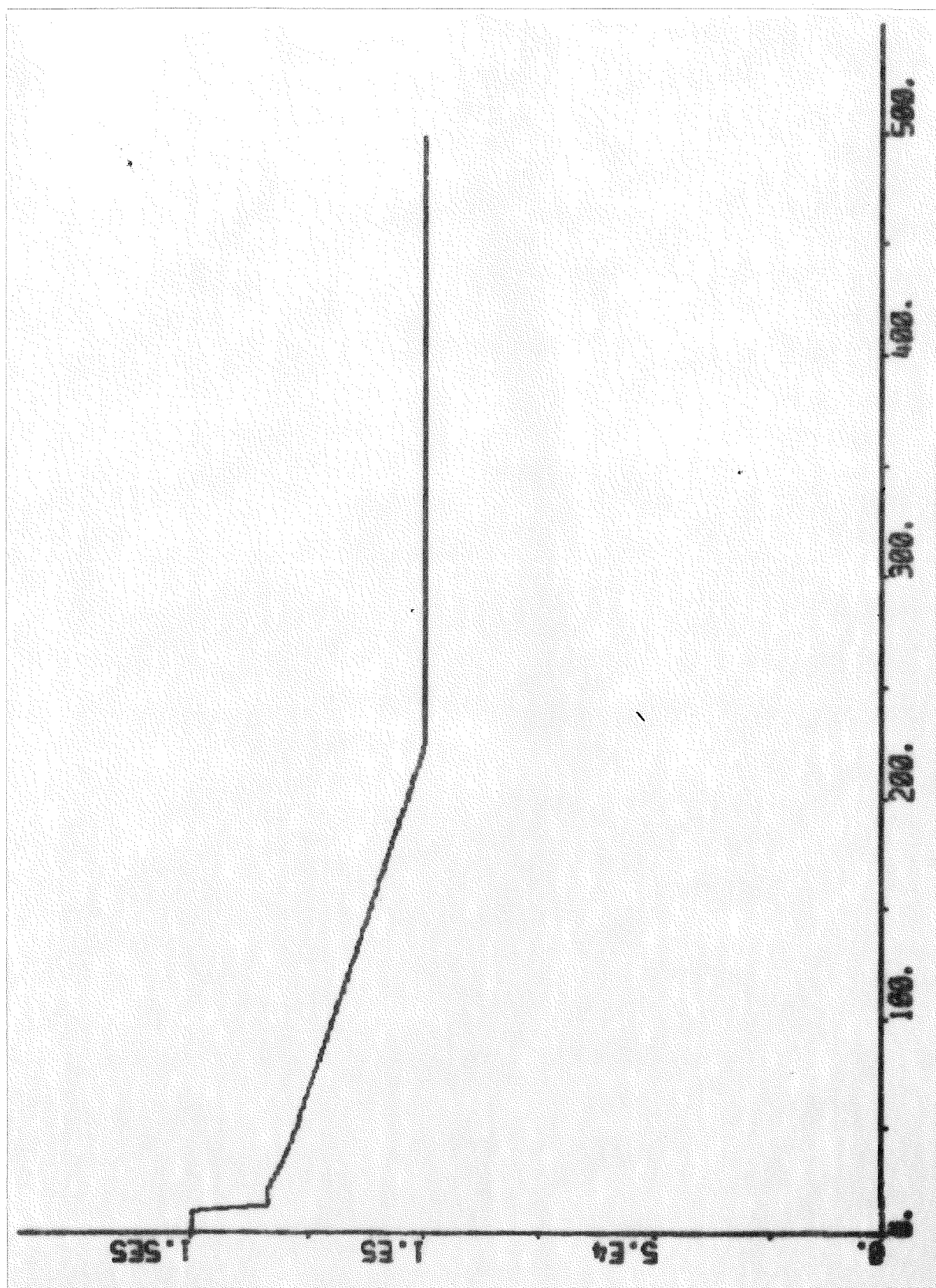


Fig. 12.24 - Response of the output power in normal mode.

### 13. TRANSFER FROM NORMAL TO ALERT MODE.

The performance of the control system during transfer from normal to alert mode will be examined in this section. The reference value of the output power,  $N_{gs2r}$  is constant and equal to 100 MW (63%) during the transfer from normal to alert mode. The mode was changed by changing the parameter ALERT from 0 to 1 at  $t = 10$  s. The parameter ALERT determines the magnitude of the jump and the rate of  $N_{gs2r}$ . The parameter ALERT also determines the relation between the reference value of the drum pressure,  $p_{ds2r}$  and  $N_{gs2r}$ . In this case  $p_{ds2r}$  is increased from  $113 \cdot 10^5$  Pa (75%) to  $145 \cdot 10^5$  Pa (97%) with a limited,  $18 \cdot 10^5$  Pa/min (12%/min), rate of change. The performance of the drum pressure loop, the drum level loop, the steam temperature loop, and the output power loop will now be examined.

#### The drum pressure loop.

The reference value of the drum pressure,  $p_{ds2r}$  is generated by the drum pressure reference setter (DPRS), which was described in Section 6. The reference value of the drum pressure is determined by the reference value of the output power,  $N_{gs2r}$  and by the mode of the control system (normal or alert). In this case  $p_{ds2r}$  is increased from  $113 \cdot 10^5$  Pa (75%) to  $145 \cdot 10^5$  Pa (97%) with a limited,  $18 \cdot 10^5$  Pa/min (12%/min), rate of change. The fuel flow,  $w_{bol}$  is the control variable of the drum pressure loop. The steam flow (Fig. 13.22), the feedwater flow (Fig. 13.6), and the feedwater temperature after the economizer (Fig. 13.20) disturb the drum pressure loop. The mean density of the steam-water mixture in the riser tubes, the steam temperature after the primary superheater, the heat flows to the superheaters, to the reheater, and to the economizer are disturbed by the fuel flow variations. The fuel flow,  $w_{bol}$  is the output of the fuel flow servo (FFS), which was described in Section 7. The reference value of the fuel flow,  $w_{bolr}$  is determined by the drum pressure controller (DPC), which was described in Section 7. The inputs to the DPC are  $p_{ds2r}$  and

its derivative,  $s_{bolt}$ , the drum pressure,  $p_{ds2}$ , and the steam flow,  $w_{ts1}$ . The block diagram of the DPC is given in Fig. 7.1. The rate of change of the fuel flow is limited in the FFS. The limits are parameters,  $w_{bolo}$  and  $w_{bols}$  of the first nonlinear block in Fig. 7.2. The numerical value of  $w_{bolo}$  and  $w_{bols}$  are 0.1 kg/s (60%/min).

The response of the fuel flow is shown in Fig. 13.1. The fuel flow increases linearly for  $10 < t < 25$  s, due to the limited rate of change. The fuel flow is about 3 kg/s (30%) higher than normally during the pressure increase. The effect of the feed-forward term from the derivative of the reference value of the drum pressure can be observed at  $t = 110$  s.

The response of the drum pressure is shown in Fig. 13.2. The gradient of the drum pressure is not greater than the gradient of the reference value of the drum pressure. There is an overshoot of  $3 \cdot 10^5$  Pa (2%), which lasts more than 300 s.

The response of the steam pressure before the control valve is shown in Fig. 13.3. The steam pressure before the control valve follows the drum pressure closely. The decreased pressure drop due to higher density is visible.

The response of the steam temperature after the primary superheater is shown in Fig. 13.4. The steam temperature variation is about  $20^\circ\text{C}$ . The steam temperature increases for  $10 < t < 180$  s due to the increased heat flow to the primary superheater and the increased steam temperature before the primary superheater without corresponding increase of the steam flow (Fig. 13.22). The steam temperature before the primary superheater is determined by the drum pressure (Fig. 13.2). The heat flow to the primary superheater is roughly proportional to the fuel flow (Fig. 13.1).

Properties: The reference value of the drum pressure increases rapidly in this case. The derivative of the reference value of the drum pressure and the steam flow influence the fuel flow

through the feedforward terms. The effects of the other disturbances are reduced by feedback. The limited rate of change of the fuel flow deteriorates the performance of the drum pressure loop for  $10 < t < 30$  s. This must, however, be accepted because of the restrictions of the burner equipment. The maximum drum pressure error is  $7 \cdot 10^5$  Pa (5%).

#### The drum level loop.

The task of the drum level loop is to control the drum level,  $z_{dl4}$  by manipulating the feedwater control valve. The reference value of the drum level,  $z_{dl4r}$  is constant. The fuel flow (Fig. 13.1) and the steam flow (Fig. 13.22) disturb the drum level loop. The drum level loop disturbs the feedwater temperature. If the drum level is too high there is a danger that water will reach the turbine. If the drum level is too low there is a danger that the riser tubes will be damaged due to insufficient cooling. The reference value of the feedwater flow,  $w_{fw5r}$  is determined by the drum level controller (DLC), which was described in Section 8. The inputs to the DLC are  $z_{dl4r}$ ,  $z_{dl4}$  and the steam flow,  $w_{ts1}$ . The block diagram of the DLC is given in Fig. 8.1. The rate of change of the stroke of the feedwater valve is limited in the feedwater servo (FWS). The limits are parameters,  $s_{ww2o}$  and  $s_{ww2s}$  of the first nonlinear block in Fig. 8.2. The numerical values of  $s_{ww2o}$  and  $s_{ww2s}$  are both 5%/s.

The response of the stroke of the feedwater valve is shown in Fig. 13.5. There are two reasons for changing the valve opening. The first is that the pressure drop over the feedwater valve has to be decreased due to the increasing drum pressure. The second is that the feedwater flow has to be increased due to the increasing mean density of the steam-water mixture in the riser tubes.

The response of the feedwater flow is shown in Fig. 13.6. The feedwater flow is about 10 kg/s higher than in steady-state during the increase of the drum pressure. The increase of the feedwater flow compensates for the increasing mean density of the

steam-water mixture in the riser tubes.

The response of the drum level is shown in Fig. 13.7. The drum level error is about  $3 \cdot 10^{-2}$  m during the increase of the drum pressure. The settling time of the drum level is about 50 s.

The response of the drum water temperature is shown in Fig. 13.8. The rate of change of the drum water temperature determines the thermal stresses of the drum material. The temperature variation is about  $20^{\circ}\text{C}$ . The rate of change of the temperature is less than  $12^{\circ}\text{C}/\text{min}$ .

Properties: The heat flow to the riser tubes is the most severe disturbance of the drum level loop in this case. The steam flow influences the feedwater flow through the feedforward term. The effects of the other disturbances are reduced by feedback. The maximum drum level error is 3 cm.

#### The steam temperature loop.

The task of the steam temperature loop is to control the steam temperature after the tertiary superheater,  $T_{ts2}$  by manipulating the first and the second attemperators spray flow valves. The reference value of the steam temperature after the tertiary superheater,  $T_{ts2r}$  is constant. The heat flows to the secondary and tertiary superheaters, the steam temperature after the primary superheater (Fig. 13.4), and the steam flow (Fig. 13.22), disturb the steam temperature loop. The heat flows to the secondary and tertiary superheaters are both approximately proportional to the fuel flow (Fig. 13.1). The specific fuel consumption is reduced if the steam temperature after the tertiary superheater is increased. The steam temperature is limited by the properties of the superheater material. The steam temperature before the secondary superheater,  $T_{ss1}$  is the output of the secondary superheater steam temperature servo (SSSTS), which was described in Section 9. The steam temperature before the tertiary superheater,  $T_{ts1}$  is the output of the tertiary superheater steam temperature servo (TSSTS),

which was described in Section 9. The reference value of the steam temperature before the tertiary superheater,  $T_{tslr}$  is determined by the tertiary superheater steam temperature controller (TSSTC), which was described in Section 9. The inputs to the TSSTC are  $T_{ts2r}$ ,  $T_{ts2}$ , the steam flow,  $w_{ts1}$ , and the fuel flow,  $w_{bol}$ . The block diagram of the TSSTC is given in Fig. 9.1. The reference value of the steam temperature before the secondary superheater,  $T_{sslr}$  is determined by the secondary superheater steam temperature controller (SSSTC), which was described in Section 9. The inputs to the SSSTC are  $T_{ss2r}$ ,  $T_{ss2}$ ,  $w_{ts1}$ , and  $w_{bol}$ . The rate of change of the stroke of the second attemperator spray flow valve is limited in the TSSTS. The limits are parameters,  $s_{tw2o}$  and  $s_{tw2s}$  of the first nonlinear block in Fig. 9.3. The numerical values of  $s_{tw2o}$  and  $s_{tw2s}$  are both 4%/s. The rate of change of the stroke of the first attemperator spray flow valve is limited in the SSSTS. The limits are parameters,  $s_{sw2o}$  and  $s_{sw2s}$  of the first nonlinear block in Fig. 9.4. The numerical values of  $s_{sw2o}$  and  $s_{sw2s}$  are both 4%/s. The difference between  $T_{ss2r}$  and  $T_{tslr}$  is a parameter,  $g_{sw2b}$  of the SSSTC. The numerical value of  $g_{sw2b}$  is 30°C and is chosen so that the second attemperator spray flow valve is approximately half-open. This means that the steam temperature before the tertiary superheater can be changed rapidly in both directions.

The response of the stroke of the first attemperator spray flow valve is shown in Fig. 13.9. The stroke of the valve is changed in order to maintain the steam temperature before the secondary superheater at its reference value. The valve opens for  $10 < t < 30$  s due to the increasing heat flow to the secondary superheater. The valve is fully open for  $30 < t < 140$  s. This means that the performance of the steam temperature loop is deteriorated by the limited capacity of the first attemperator.

The response of the spray flow of the first attemperator is shown in Fig. 13.10. The spray flow follows the stroke of the valve quite well. The maximum spray flow is 6 kg/s (8% of the steam flow).

The response of the steam temperature before the secondary super-

heater is shown in Fig. 13.11. The steam temperature is reduced about  $50^{\circ}\text{C}$  for  $10 < t < 30$  s. The consequences of the limited capacity of the first attemperator is clearly visible for  $30 < t < 140$  s.

The response of the steam temperature after the secondary superheater is shown in Fig. 13.12. The difference between the steam temperature after the secondary superheater and the steam temperature before the tertiary superheater (Fig. 13.15) shall be about  $30^{\circ}\text{C}$ . This is, however, not the case due to the limited capacity of the attemperator. The steam temperature after the secondary superheater starts to increase due to the increased heat flow to the superheater. The temperature then decreases for  $20 < t < 70$  s due to the decreased steam temperature before the secondary superheater. For  $70 < t < 120$  s the steam temperature after the secondary superheater increases due to the limited capacity of the first attemperator. The temperature then decreases for  $120 < t < 160$  s due to the decreased heat flow to the secondary superheater.

The response of the stroke of the second attemperator spray flow valve is shown in Fig. 13.13. The valve opens for  $10 < t < 25$  s due to the increasing heat flow to the tertiary superheater. The valve is completely open for  $25 < t < 130$  s. This means that the performance of the steam temperature loop is also deteriorated by the limited capacity of the second attemperator.

The response of the spray flow of second attemperator is shown in Fig. 13.14. The spray flow follows the stroke of the valve quite well. The maximum spray flow is about 4 kg/s (5% of the steam flow).

The response of the steam temperature before the tertiary superheater is shown in Fig. 13.15. The steam temperature decreases for  $10 < t < 25$  s due to the increasing spray flow. The steam temperature before the tertiary superheater starts to increase for  $25 < t < 30$  due to the limited capacity of the second attemperator. The temperature is then determined by the steam tempera-



ture after the secondary superheater for  $30 < t < 130$  s. For  $t > 130$  s the steam temperature before the tertiary superheater is increasing due to the reduced spray flow to the tertiary superheater.

The response of the steam temperature after the tertiary superheater is shown in Fig. 13.16. The steam temperature increases for  $10 < t < 30$  s due to the increased heat flow to the tertiary superheater. The steam temperature controllers can cope with the situation for  $30 < t < 60$  s and the steam temperature error is less than  $3^{\circ}\text{C}$ . The steam temperature error increases for  $60 < t < 130$  s due to the limited capacity of the attemperators. The maximum error is about  $8^{\circ}\text{C}$ . The steam temperature after the tertiary superheater has reached its final value at  $t = 350$  s.

Properties: The heat flows to the secondary and the tertiary superheater and the steam temperature after the primary superheater are the most severe disturbances in this case. The fuel flow and the steam flow influence the steam temperature controllers by feedforward terms. The effects of the other disturbances are reduced by feedback. The maximum steam temperature error is about  $8^{\circ}\text{C}$ . The performance of the steam temperature loop is deteriorated by the limited capacity of the attemperators but not by the multivariable nature of the problem. In this case the fuel flow is increased about 30% in order to increase the drum pressure very rapidly. The control system cannot handle more severe disturbances.

#### The output power loop.

The task of the output power loop is to control the output power,  $N_{gs2}$  by manipulating the steam control valve and the extraction steam valves. The reference value of the output power,  $N_{gs2r}$  is generated by the power demand setter (PDS), which was described in Section 5. A preliminary reference value of the output power,  $s_{nsl}$  is determined from the setpoint of the output power,  $s_{nslr}$  in the first part of the power demand setter (PDS1). The block diagram of the PDS1 is given in Fig. 5.1. The  $s_{nslr}$  is modified with respect to the network-frequency in the second part of the

power demand setter (PDS2). The block diagram of the PDS2 is given in Fig. 5.2. The  $N_{gs2r}$  is obtained from the third part of the power demand setter (PDS3), which limits the jump and the rate of  $N_{gs2r}$ . The block diagram of the PDS3 is given in Fig. 5.3. The steam pressure before the control valve,  $p_{ts2}$  (Fig. 13.3) and the steam temperature before the control valve,  $T_{ts2}$  (Fig. 13.16) disturb the output power loop. The superheated steam flow,  $w_{ts1}$  (Fig. 13.22), the reheated steam flow,  $w_{rs2}$  and the extraction steam flows,  $w_{hs2}$ ,  $w_{is2}$ ,  $w_{is4}$ ,  $w_{is6}$ ,  $w_{is8}$ ,  $w_{ls2}$  and  $w_{ls4}$  are disturbed by the output power loop. The stroke of the control valve is the output of the control valve servo (CVS), which was described in Section 10. The strokes of the high-pressure preheater extraction valves are the outputs of the high-pressure preheater servo (HPPS), which was described in Section 10. The strokes of the low-pressure preheater extraction valves are the outputs of the low-pressure preheater servo (LPPS), which was described in Section 10. The reference value of the stroke of the control valve,  $s_{vs2r}$  is determined by the turbine power controller (TPC), which was described in Section 10. The inputs to the TPC are  $N_{gs2r}$  and  $N_{gs2}$ . The block diagram of the TPC is given in Fig. 10.1. The reference values of the strokes of the high-pressure preheater extraction valves,  $s_{fs2r}$  are determined by the high-pressure preheater controller (HPPC), which was described in Section 10. The input to the HPPC is  $N_{gs2r}$ . The block diagram of the HPPC is given in Fig. 10.3. The reference value of the strokes of the low-pressure extraction valves,  $s_{fs7r}$  are determined by the low-pressure preheater controller (LPPC), which was described in Section 10. The inputs of the LPPC are  $N_{gs2r}$ , the reference value of the deaerator steam pressure,  $p_{as2r}$  and the deaerator steam pressure,  $p_{as2}$ . The rate of change of the stroke of the control valve is limited in the CVS. The limits are parameters,  $s_{vs2o}$  and  $s_{vs2s}$  of the first nonlinear block in Fig. 10.2. The numerical values of  $s_{vs2o}$  and  $s_{vs2s}$  are 20%/s and 200%/s respectively. The rates of change of the strokes of the high-pressure extraction steam flow valves are limited in the HPPS. The limits are parameters,  $s_{fs2o}$  and  $s_{fs2s}$  of the first nonlinear block in Fig. 10.4. The numerical values of  $s_{fs2o}$  and  $s_{fs2s}$  are both 100%/s. The rates of change of the strokes of the low-pressure extraction steam flow valves are limited in the LPPS. The limits

are parameters,  $s_{fs7o}$  and  $s_{fs7s}$  of the first nonlinear block in Fig. 10.6. The numerical values of  $s_{fs7o}$  and  $s_{fs7s}$  are both 100%/s.

The response of the strokes of the LP-preheater extraction valves are shown in Fig. 13.17. The reference value of the output power is constant and the reference value of the strokes of the LP-preheater extraction valves are only influenced by the deaerator pressure controller. The increase of the strokes are due to the increased feedwater flow without corresponding increase of the steam flow.

The response of the strokes of the HP-preheater extraction valves are shown in Fig. 13.18. The reference value of the output power is constant and the strokes of the HP-preheater extraction valves are constant too.

The response of the feedwater temperature after the HP-preheater is shown in Fig. 13.19. The temperature decreases about 5°C due to the increased feedwater flow.

The response of the feedwater temperature after the economizer is shown in Fig. 13.20. The feedwater temperature increases for  $10 < t < 130$  s due to the increased heat flow. The feedwater temperature decreases for  $130 < t$  due to the decreased heat flow. The temperature increase is about 15°C.

The response of the stroke of the control valve is shown in Fig. 13.21. The control valve opening decreases for  $10 < t < 120$  s due to the increasing drum pressure.

The response of the steam flow is shown in Fig. 13.22. The steam flow decreases for  $10 < t < 120$  s due to the increasing steam temperature. The steam flow then increases for  $120 < t$  due to the decreasing steam temperature. The maximum steam flow deviation is about 5 kg/s (4%).

The response of the reheater steam pressure is shown in Fig. 13.23.

The pressure follows the steam flow quite well.

The response of the output power is shown in Fig. 13.24. The reference value of the output power is constant. The output power error is barely visible.

Properties: The steam temperature and the steam pressure before the control valve disturb the output power loop in this case. The effects of the disturbances are reduced by feedback. The output power error is barely noticable.

### Conclusions.

The performance of the control system during transfer from normal to alert mode has been investigated by simulation. In this case the reference value of the drum pressure was increased from  $113 \cdot 10^5$  Pa (75%) to  $145 \cdot 10^5$  Pa (97%) with a limited,  $18 \cdot 10^5$  Pa/min (12%/min), rate of change. The reference value of the output power is constant and equal to 100 MW (63%) during the transfer from normal to alert mode. The fuel flow has to be increased temporarily in order to increase the drum pressure. The fuel flow is about 3 kg/s (30%) higher than normally during the increase of the drum pressure. The limited rate of change of the fuel flow deteriorates the performance of the drum pressure loop for  $10 < t < 30$  s. The maximum drum pressure error is  $7 \cdot 10^5$  Pa (5%). The heat flow to the riser tubes is the most severe disturbance of the drum level loop in this case. The maximum drum level error is about 4 cm. The heat flows to the superheaters are the most severe disturbances of the steam temperature loop in this case. The performance of the steam temperature loop is deteriorated by the limited capacity of the attemperators but not by the multi-variable nature of the problem. In this case the fuel flow is increased about 3 kg/s (30%) in order to increase the drum pressure very rapidly. The control system cannot cope with a more severe disturbance. The maximum steam temperature error is about  $8^\circ\text{C}$ . The steam temperature and the steam pressure before the control

valve disturb the output power loop in this case. The output power error is, however, barely noticable.

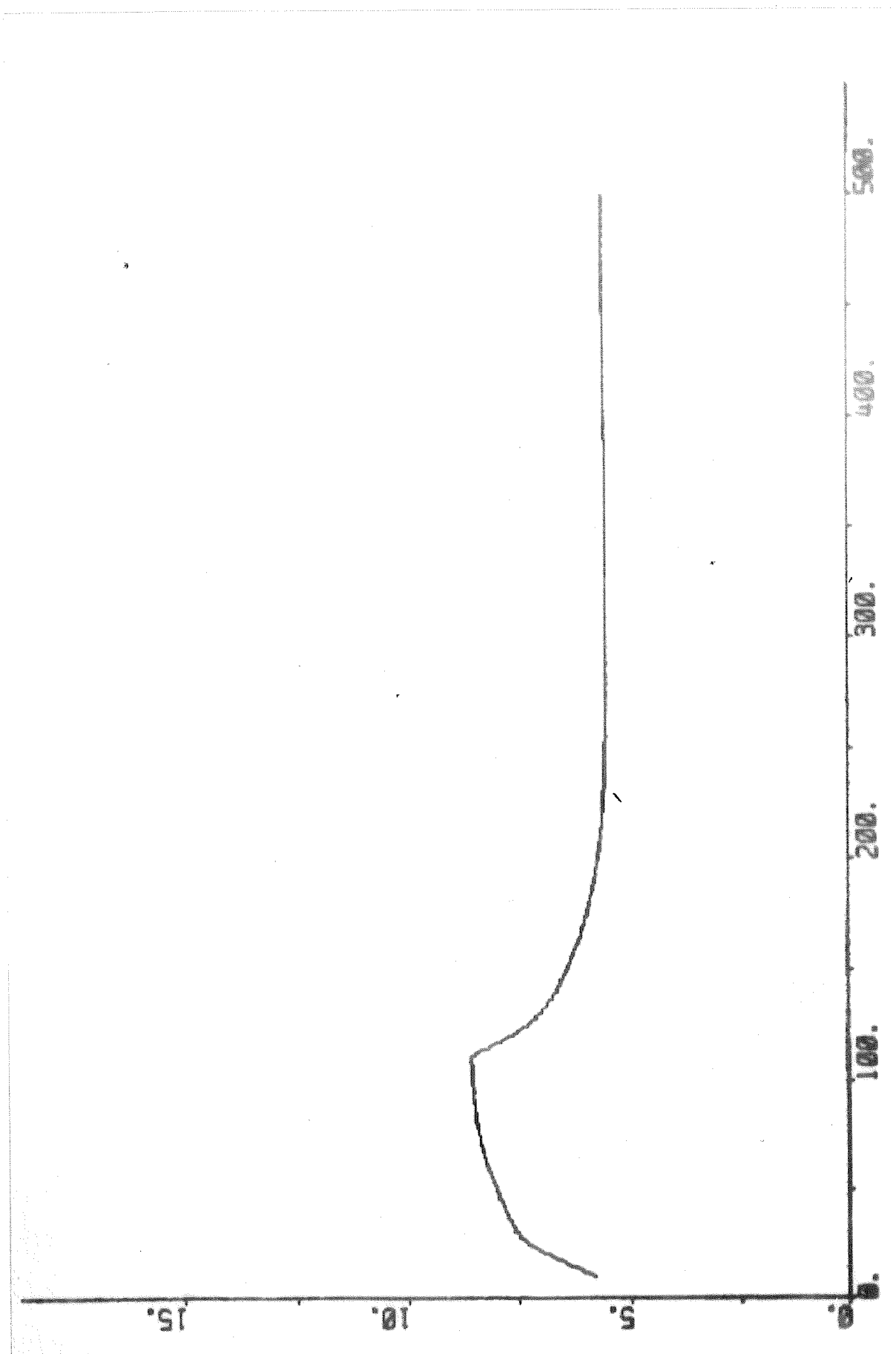


Fig. 13.1 - Response of the fuel flow during transfer from normal to alert mode.

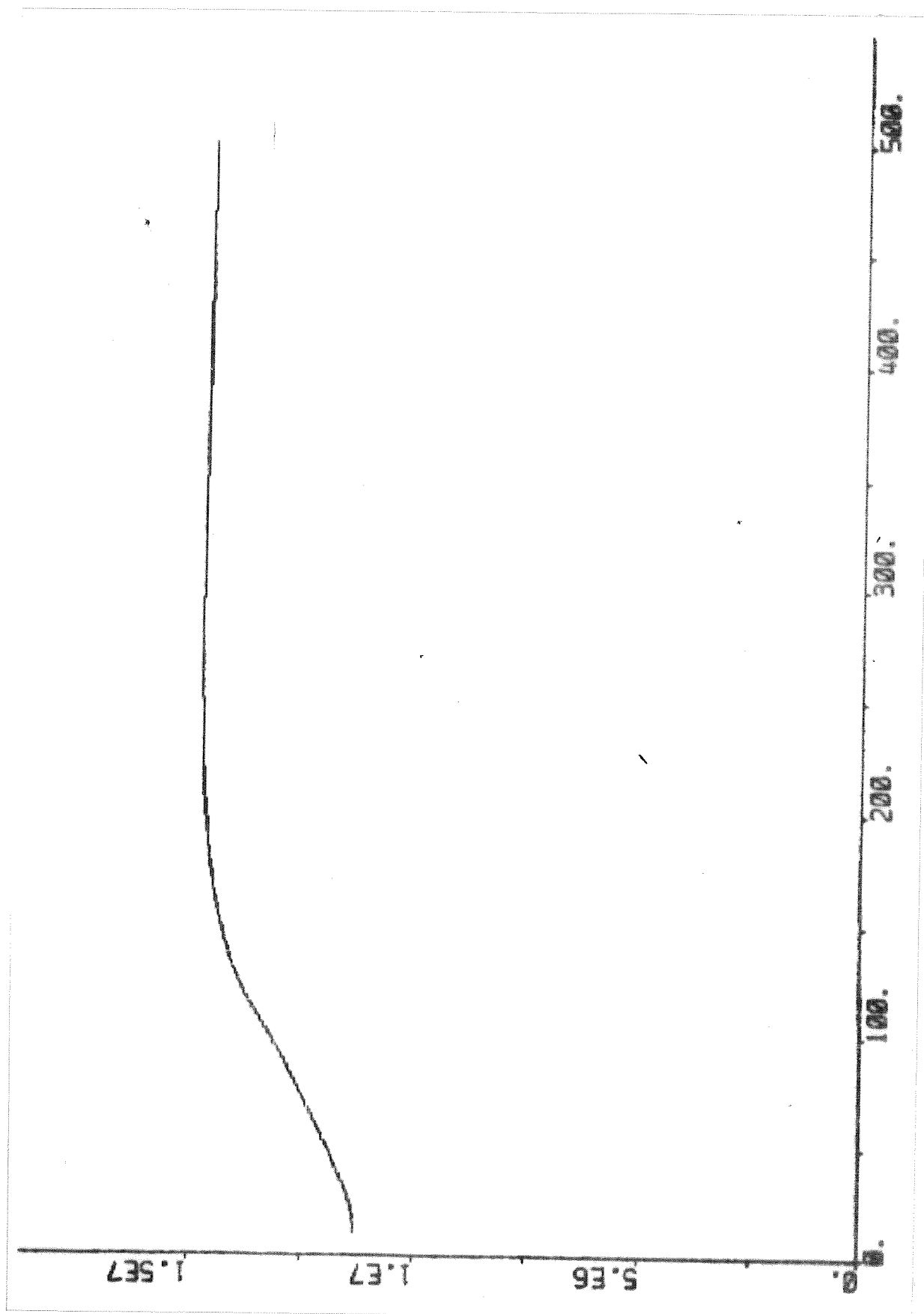


Fig. 13.2 - Response of the drum pressure during transfer from normal to alert mode.

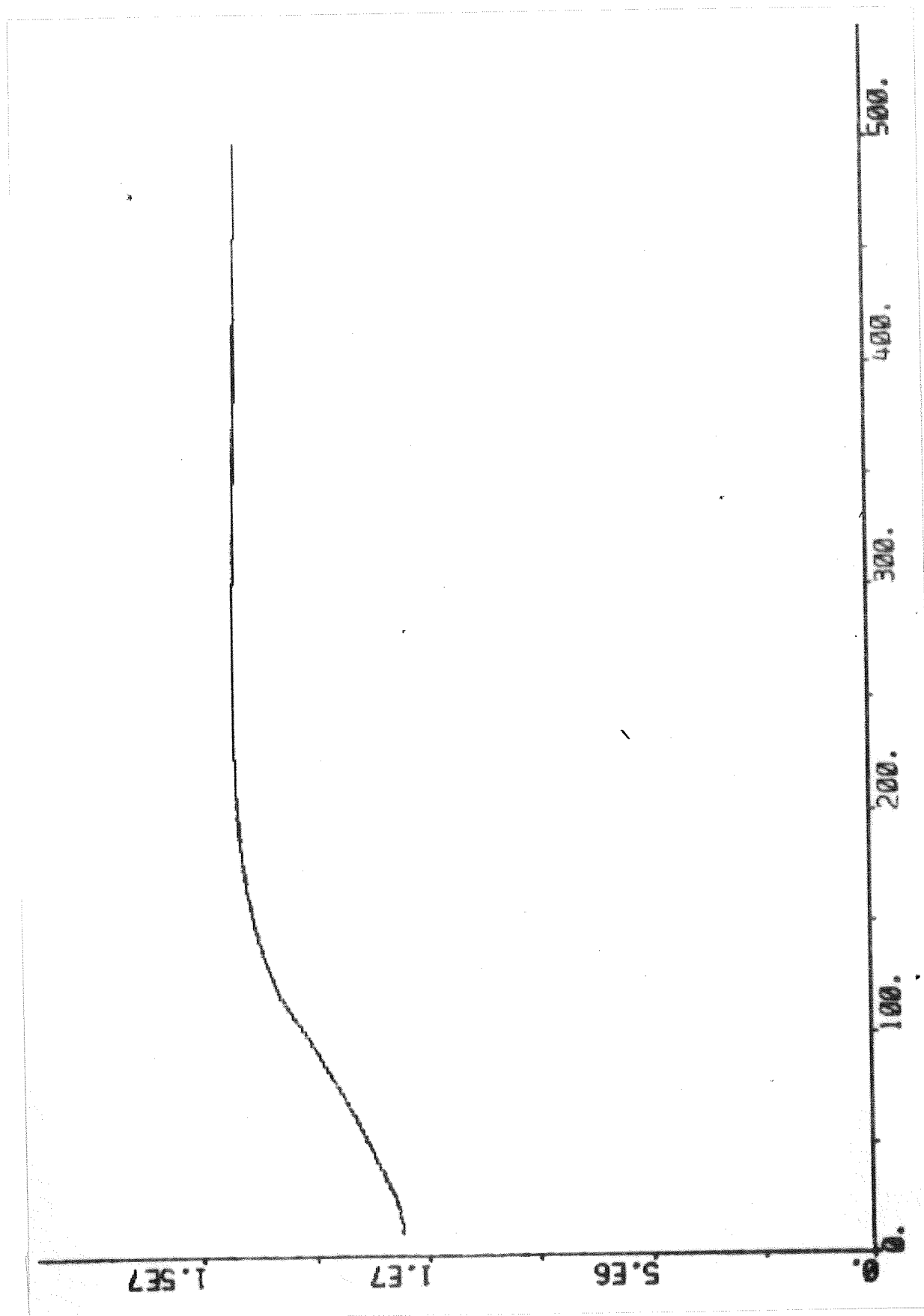


Fig. 13.3 - Response of the steam pressure before the control valve during transfer from normal to alert mode.



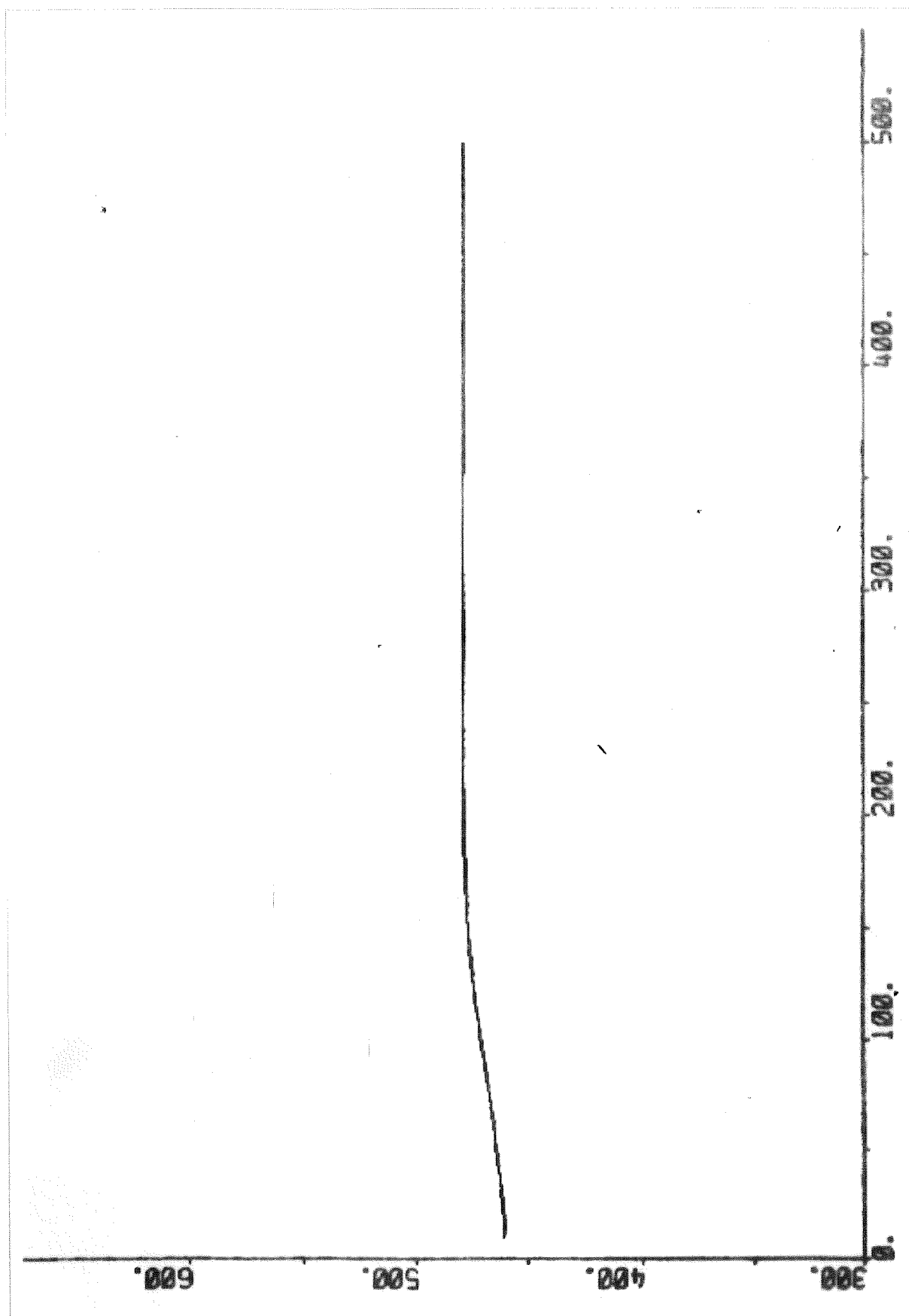


Fig. 13.4 - Response of the steam temperature after the primary superheater during transfer from normal to alert mode.

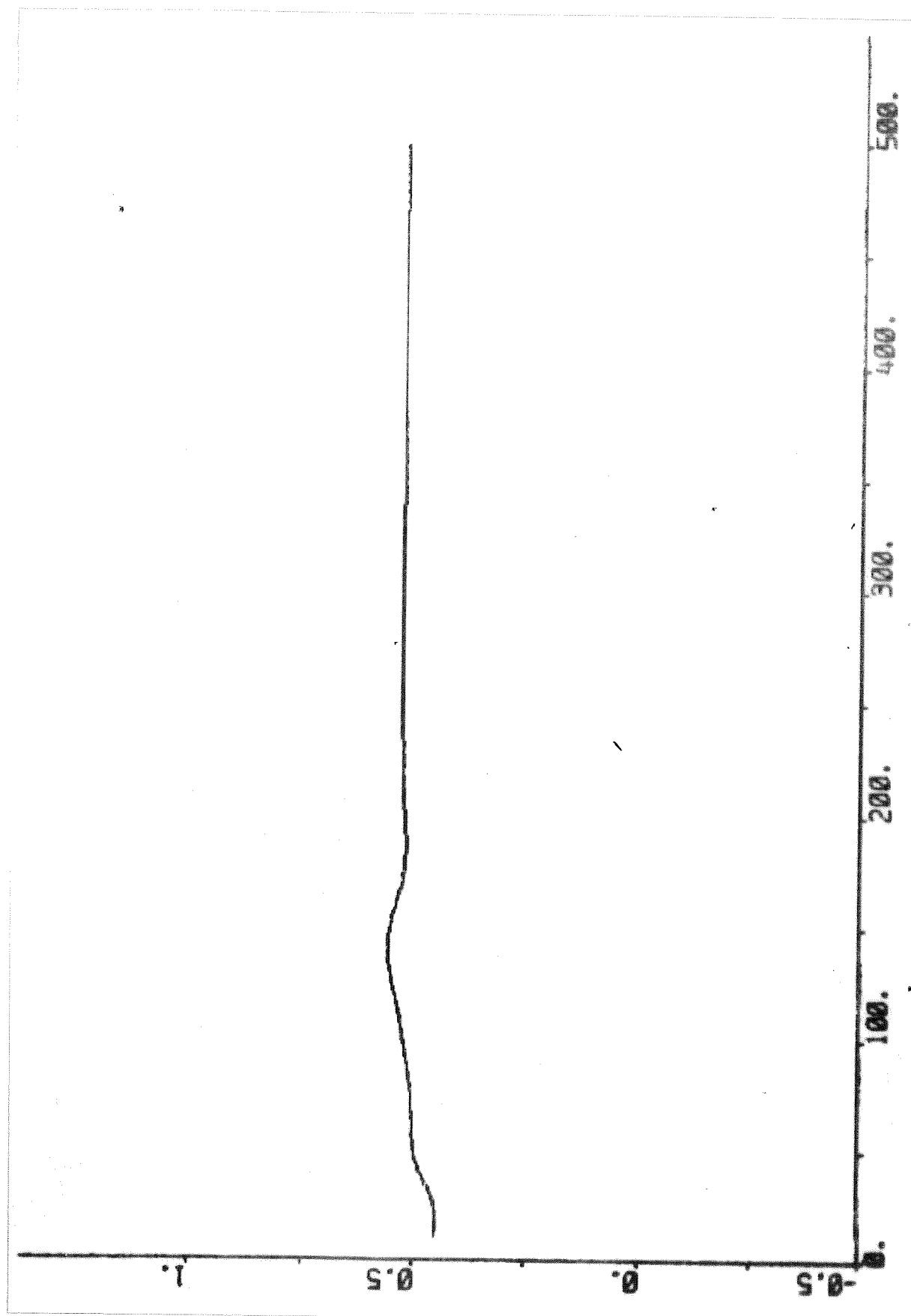


Fig. 13.5 - Response of the stroke of the feedwater valve during transfer from normal to alert mode.

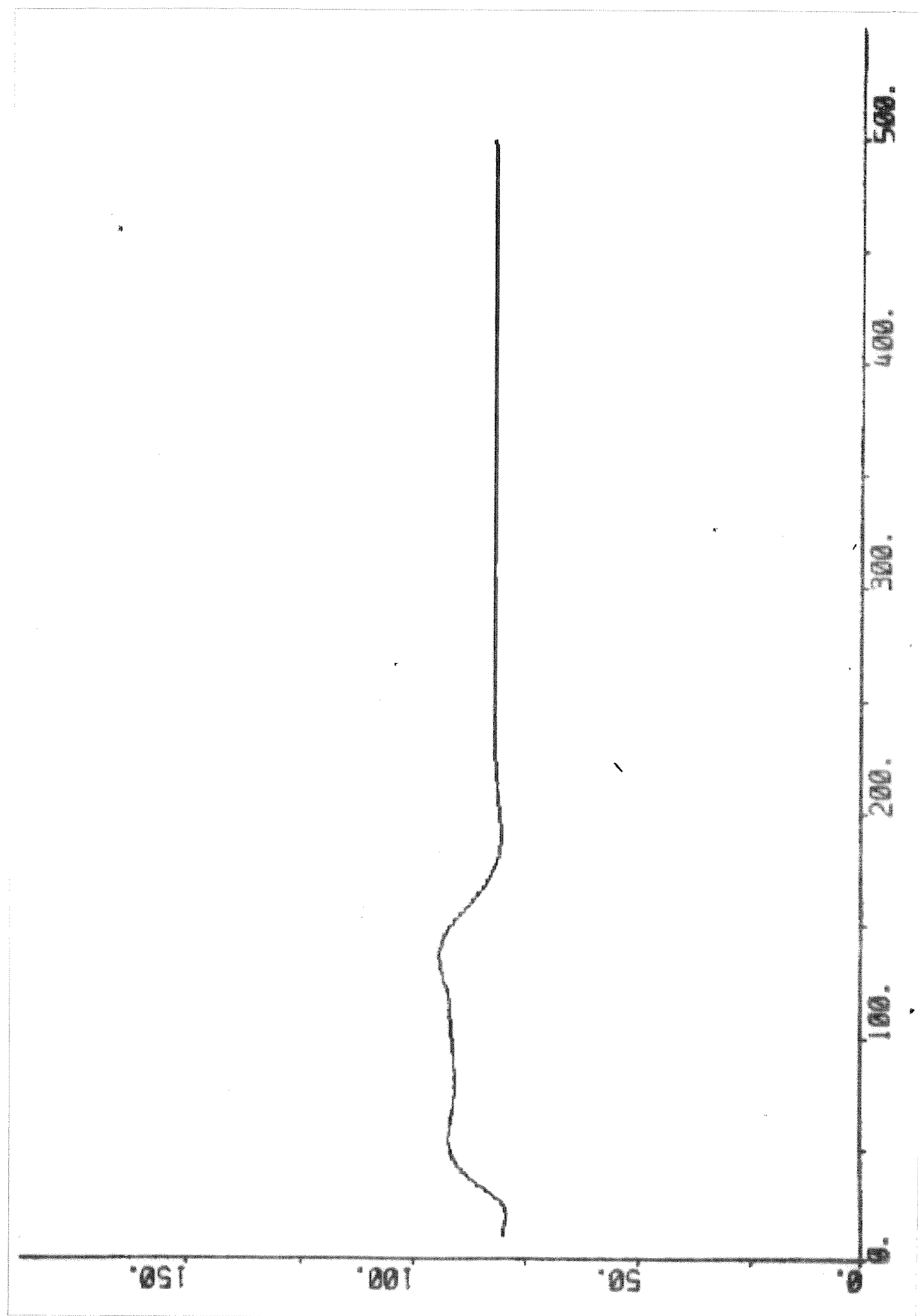


Fig. 13.6 - Response of the feedwater flow during transfer from normal to alert mode.

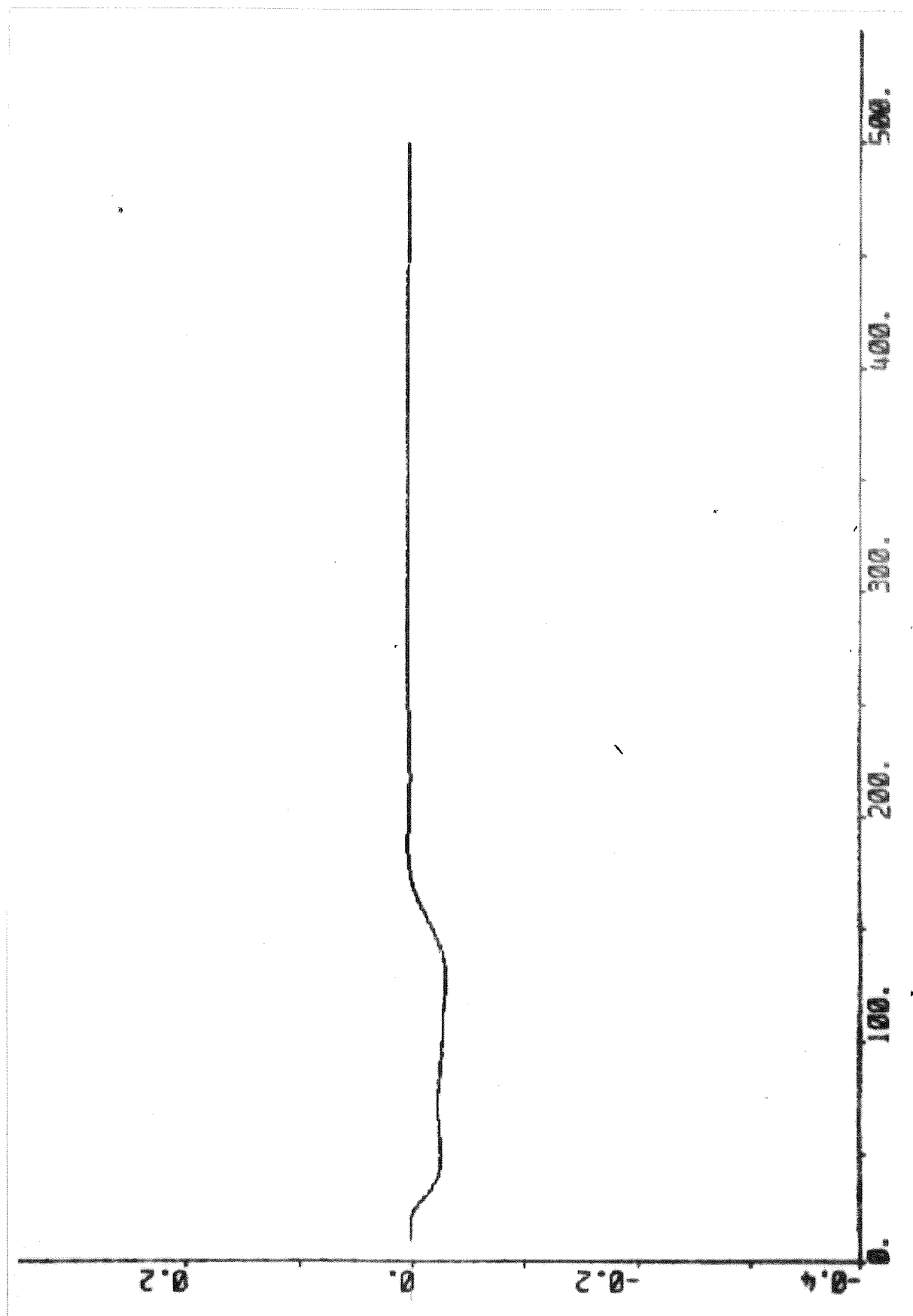


Fig. 13.7 - Response of the drum level during transfer from normal to alert mode.

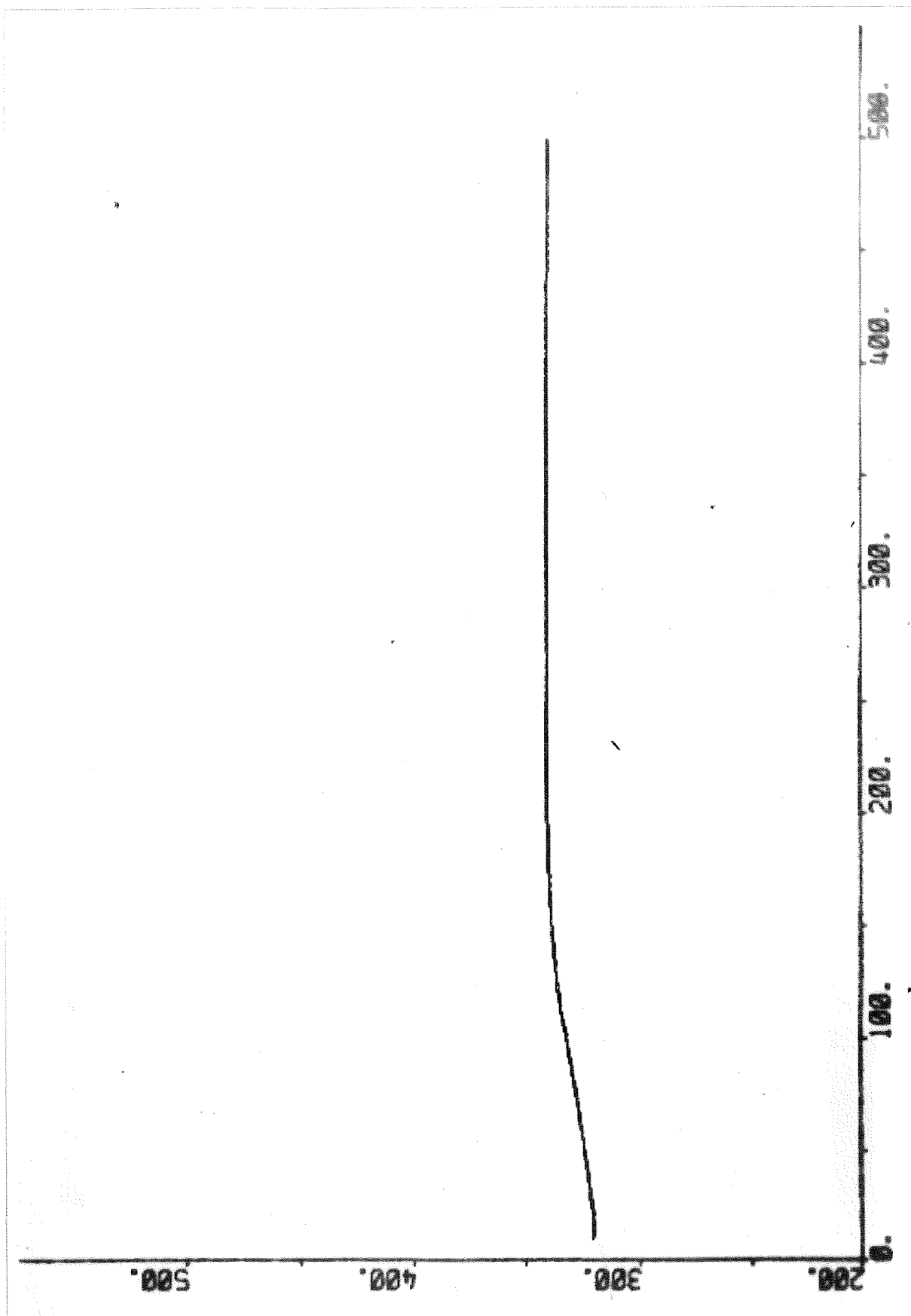


Fig. 13.8 - Response of drum water temperature during transfer from normal to alert mode.

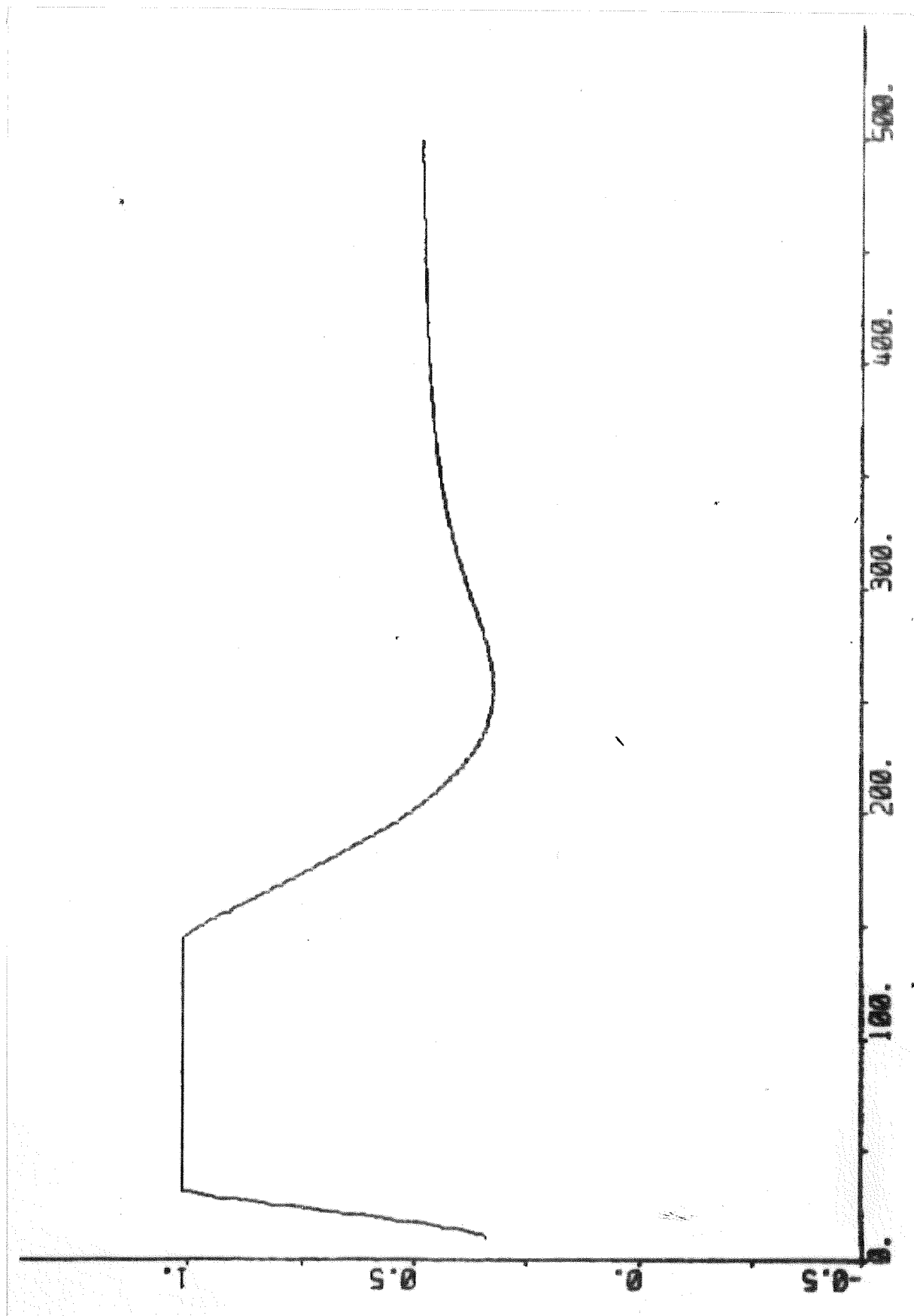


Fig. 13.9 - Response of the stroke of the first attenuator spray flow valve during transfer from normal to alert mode.

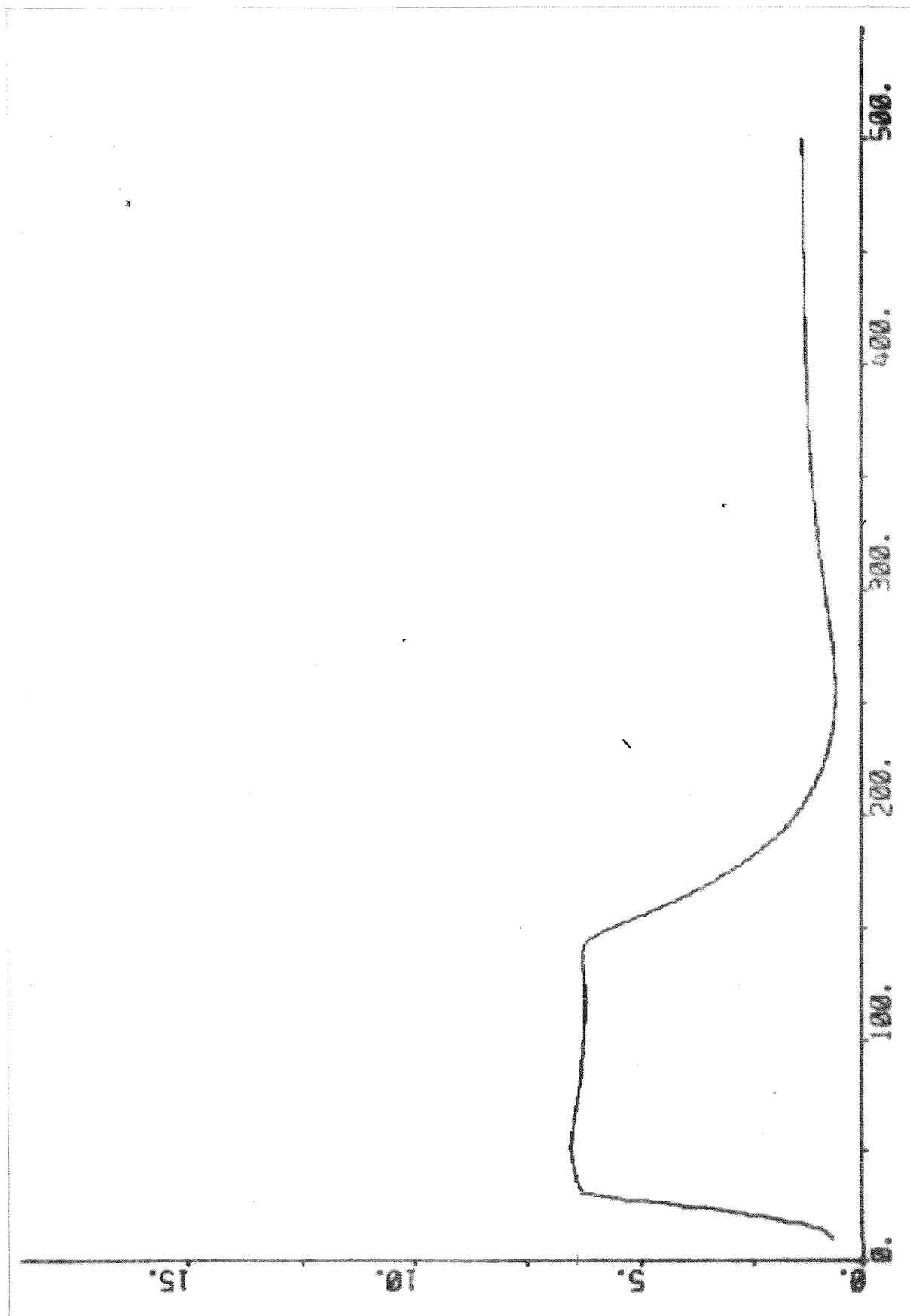


Fig. 13.10 - Response of the spray flow of the first attenuator during transfer from normal to alert mode.

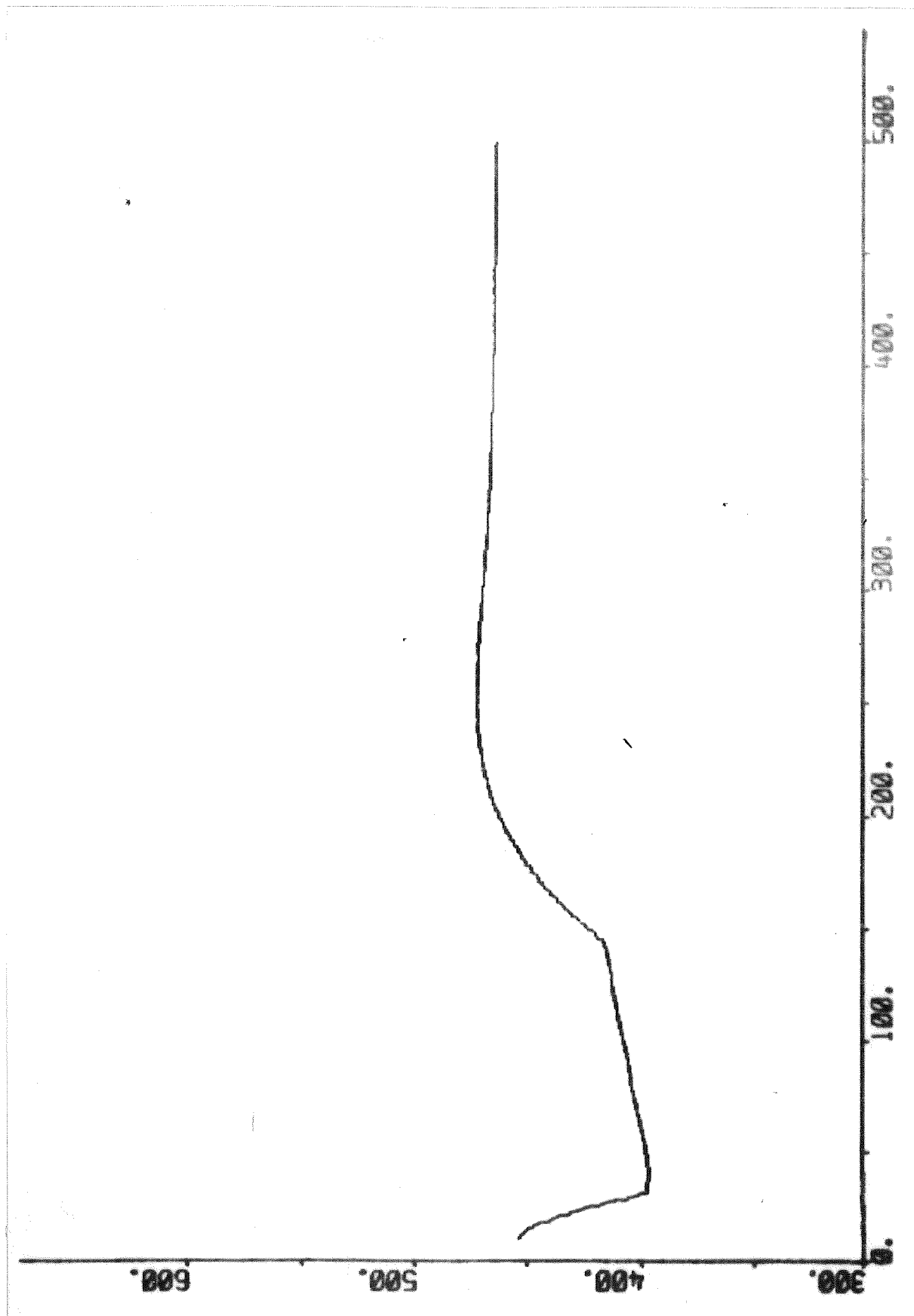


Fig. 13.11 - Response of the steam temperature before the secondary superheater during transfer from normal to alert mode.



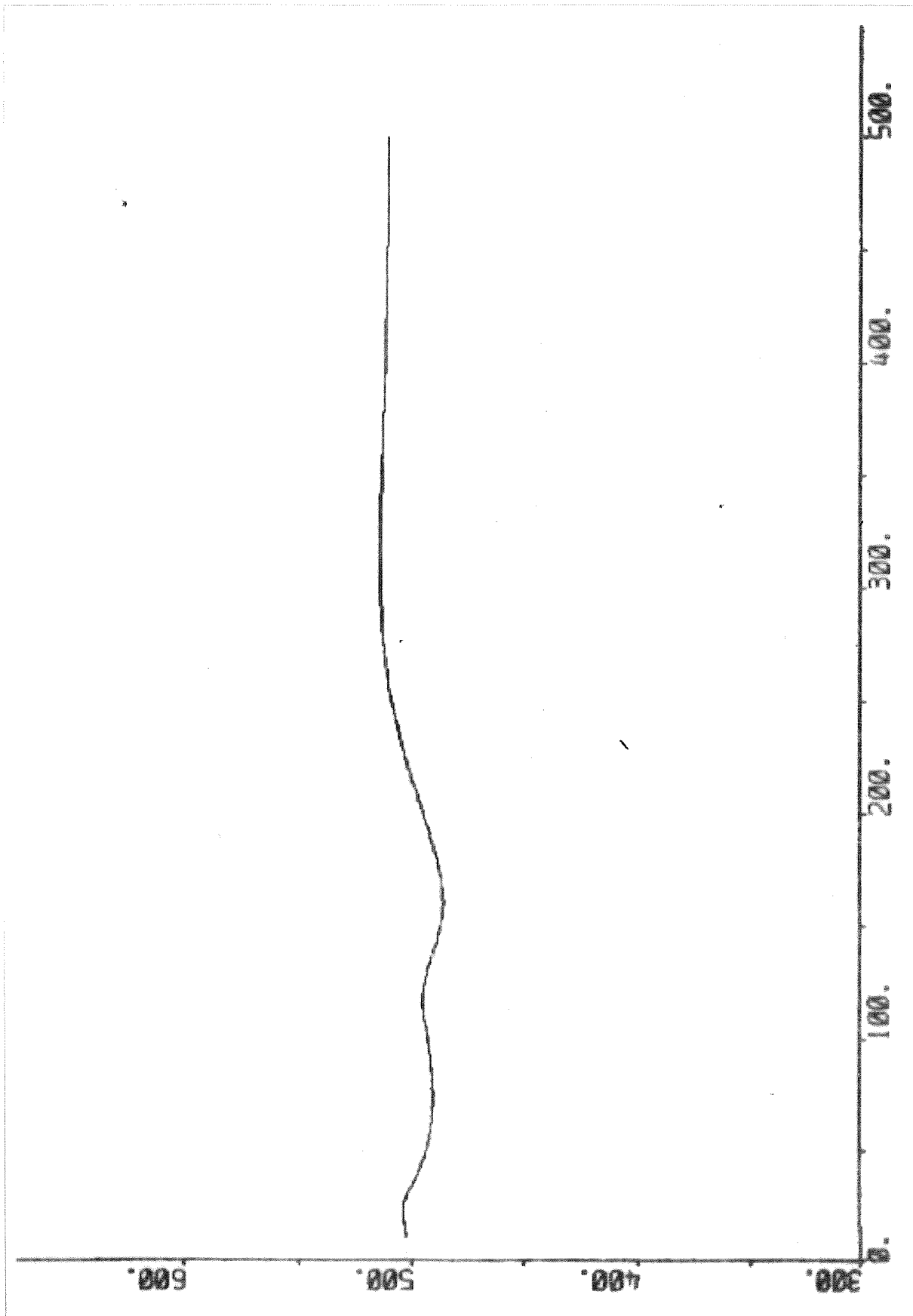


Fig. 13.12 - Response of the steam temperature after the secondary superheater during transfer from normal to alert mode.

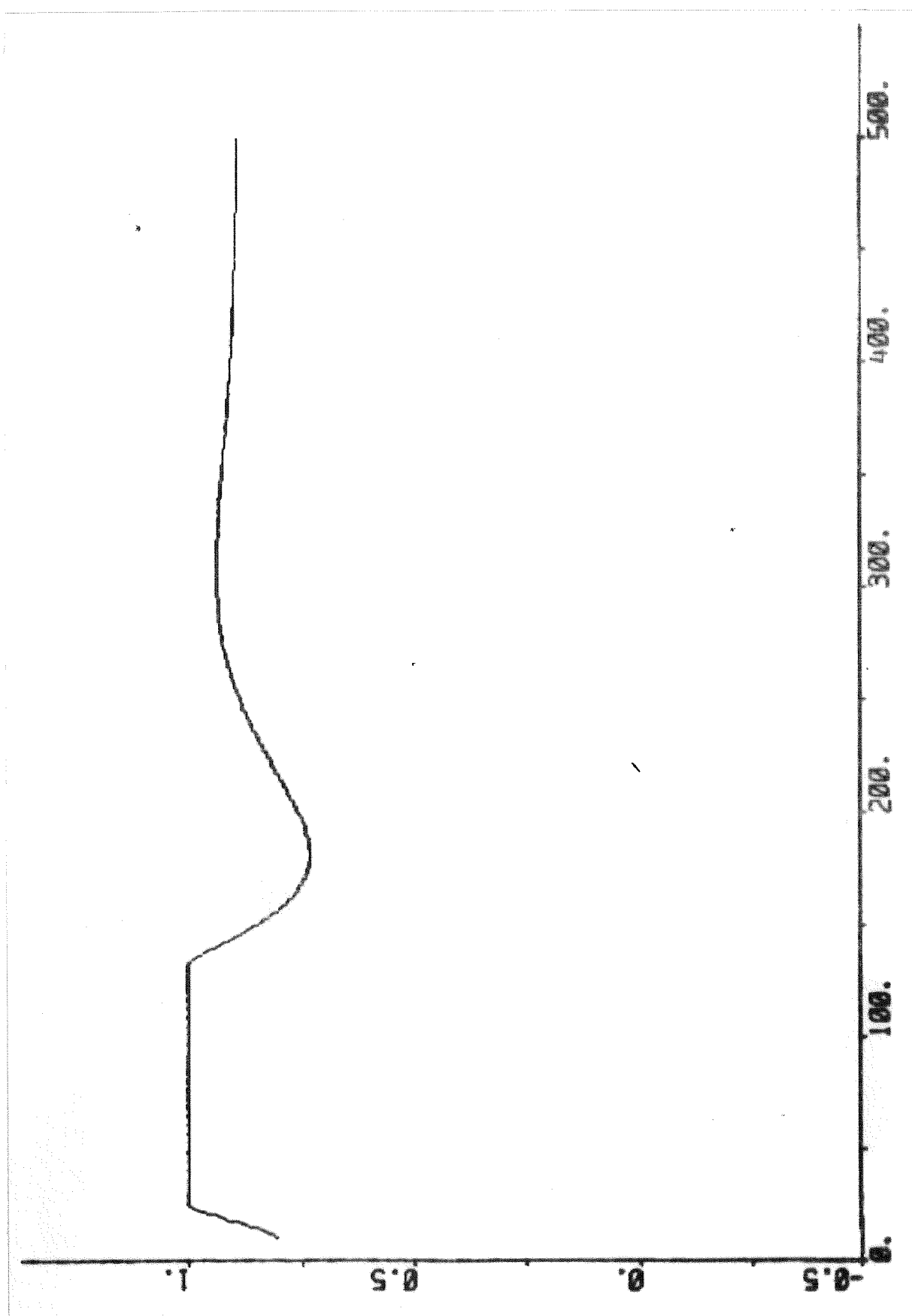


Fig. 13.13 - Response of the stroke of the second attenuator spray flow valve during transfer from normal to alert mode.

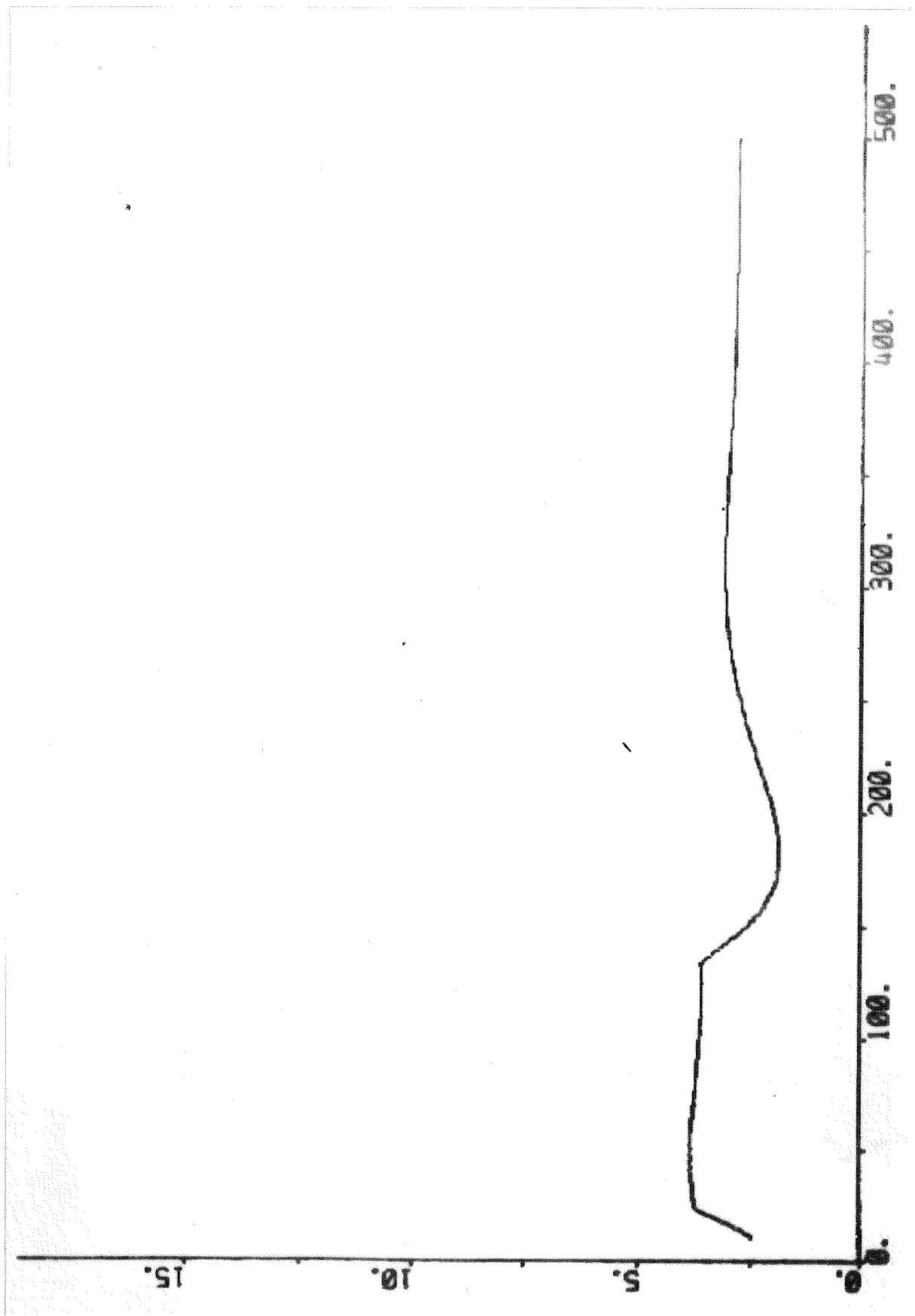


Fig. 13.14 - Response of the spray flow of the second attenuator during transfer from normal to alert mode.

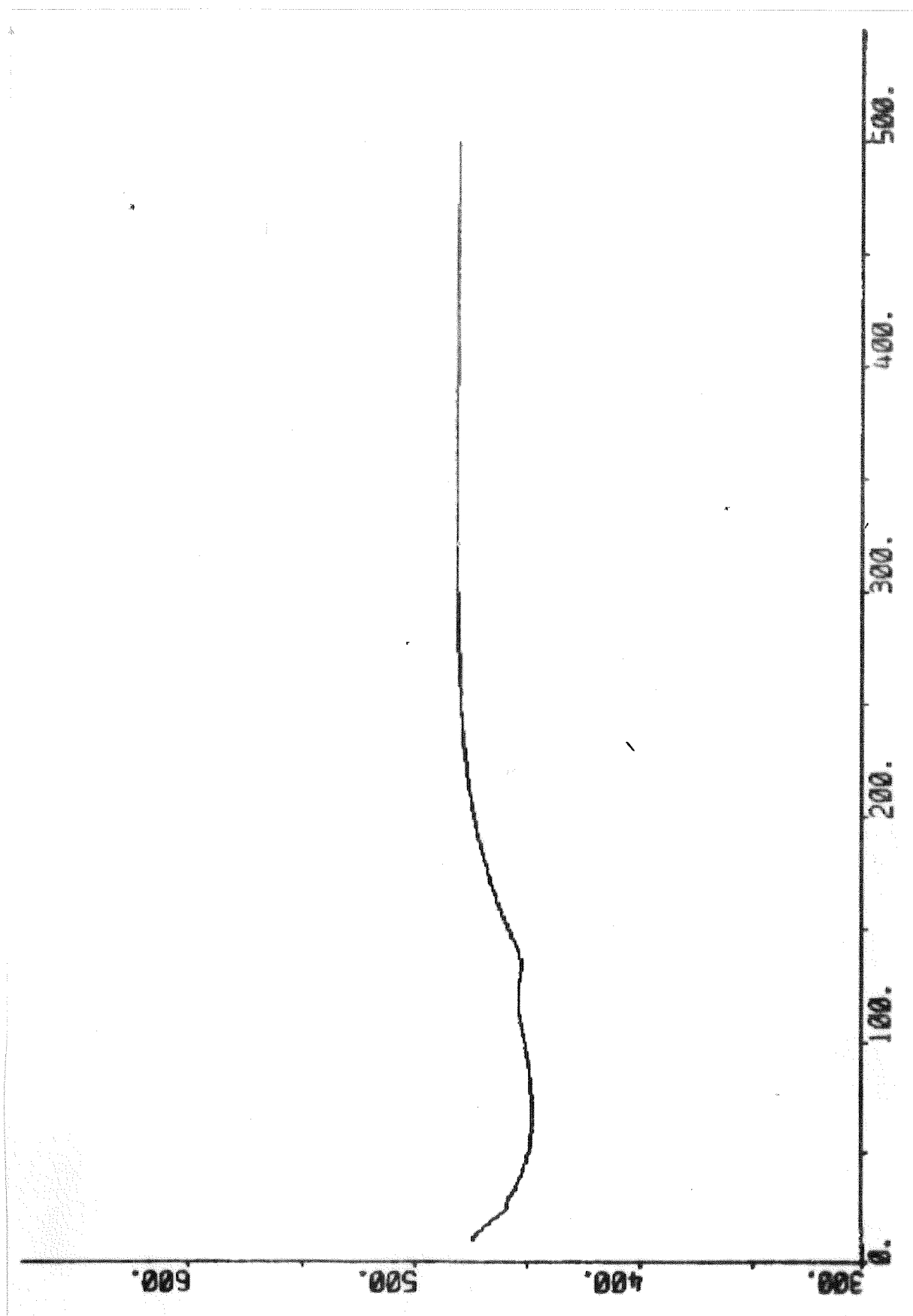


Fig. 13.15 - Response of the steam temperature before the tertiary superheater during transfer from normal to alert mode.

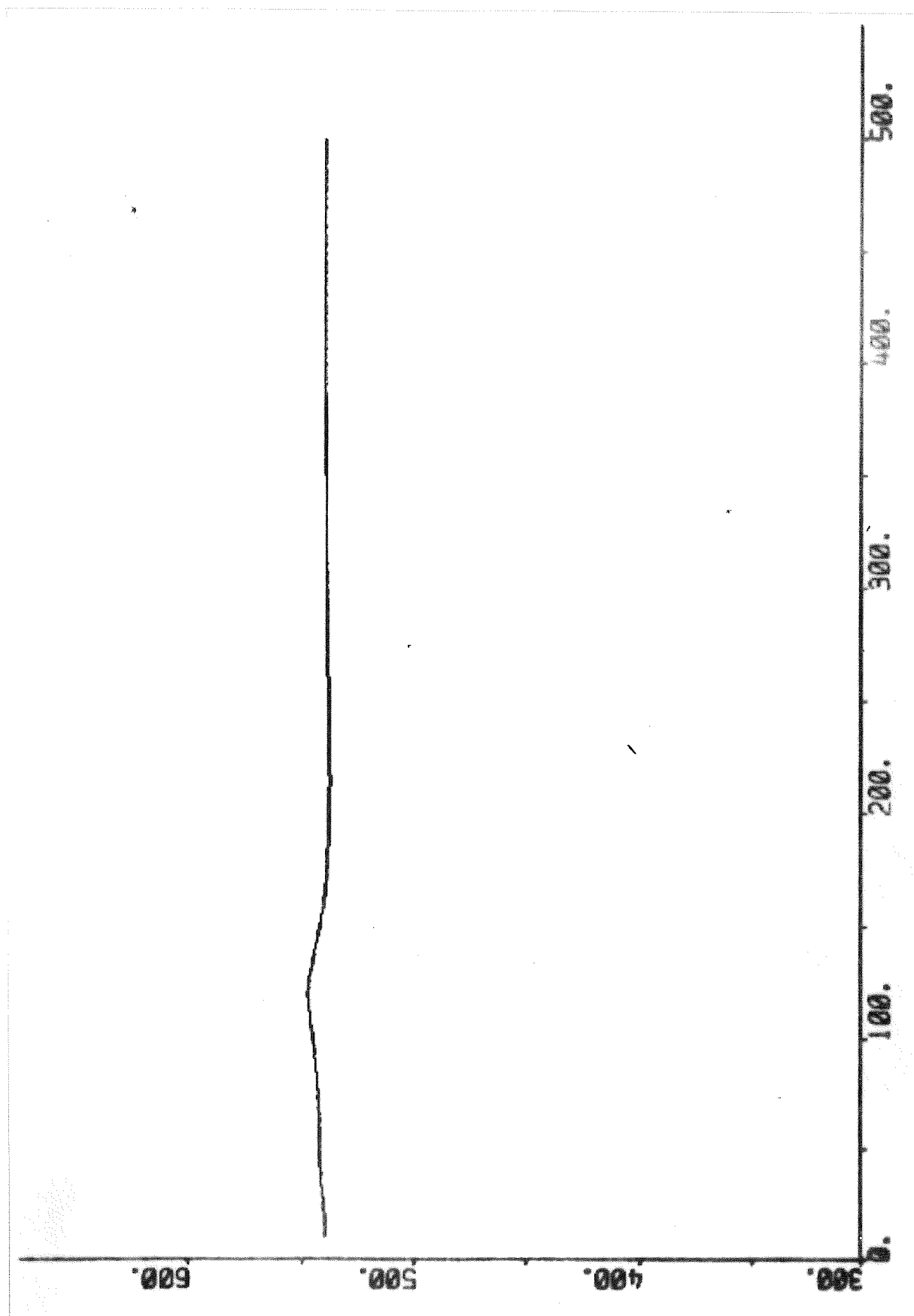


Fig. 13.16 - Response of the steam temperature after the tertiary superheater during transfer from normal to alert mode.

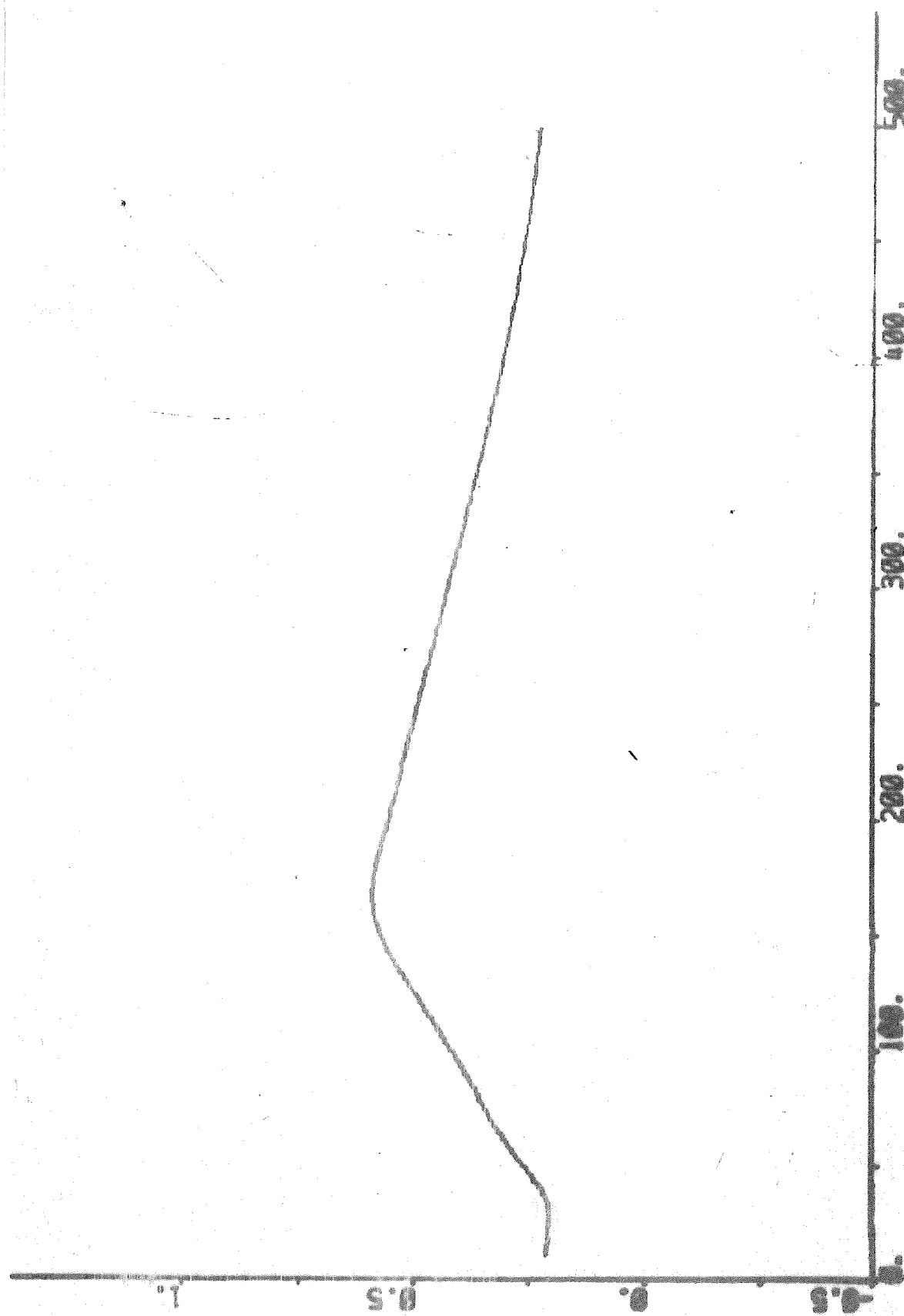


Fig. 13.17 - Response of the stroke of the LP-preheater extraction valve during transfer from normal to alert mode.

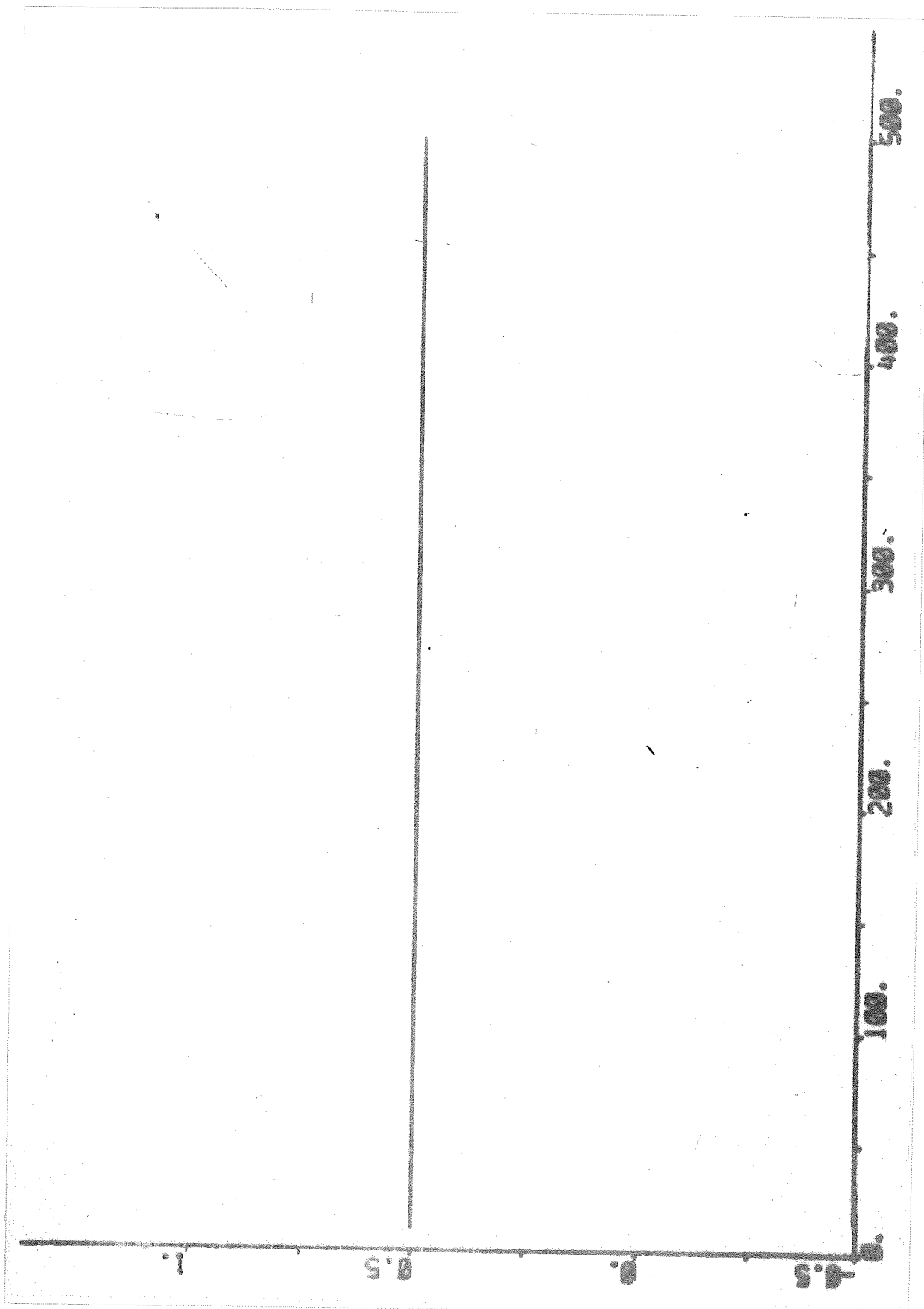


Fig. 13.18 - Response of the stroke of the HP-preheater extraction valve during transfer from normal to alert mode.

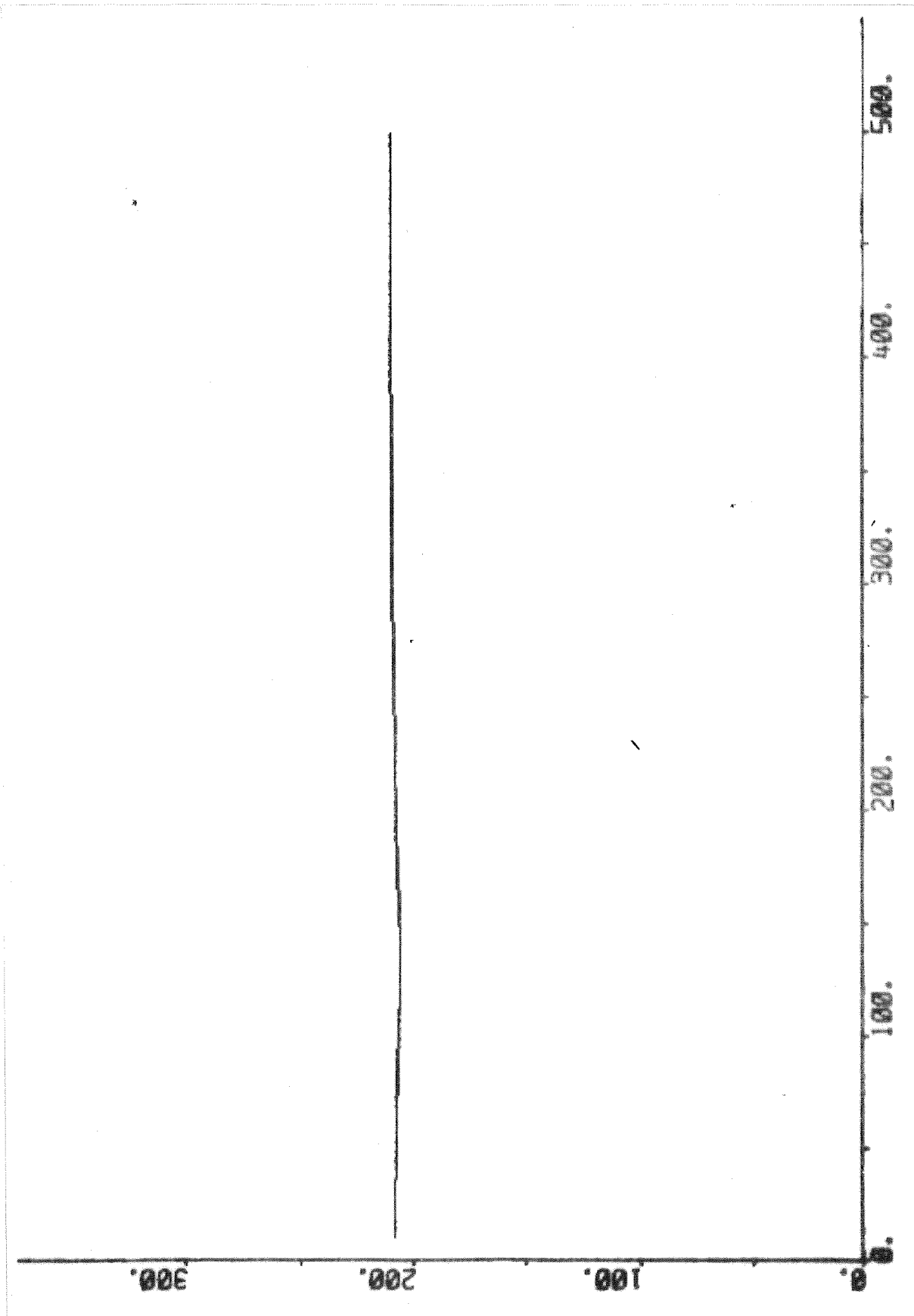


Fig. 13.19 - Response of the feedwater temperature after the HP-preheater during transfer from normal to alert mode.



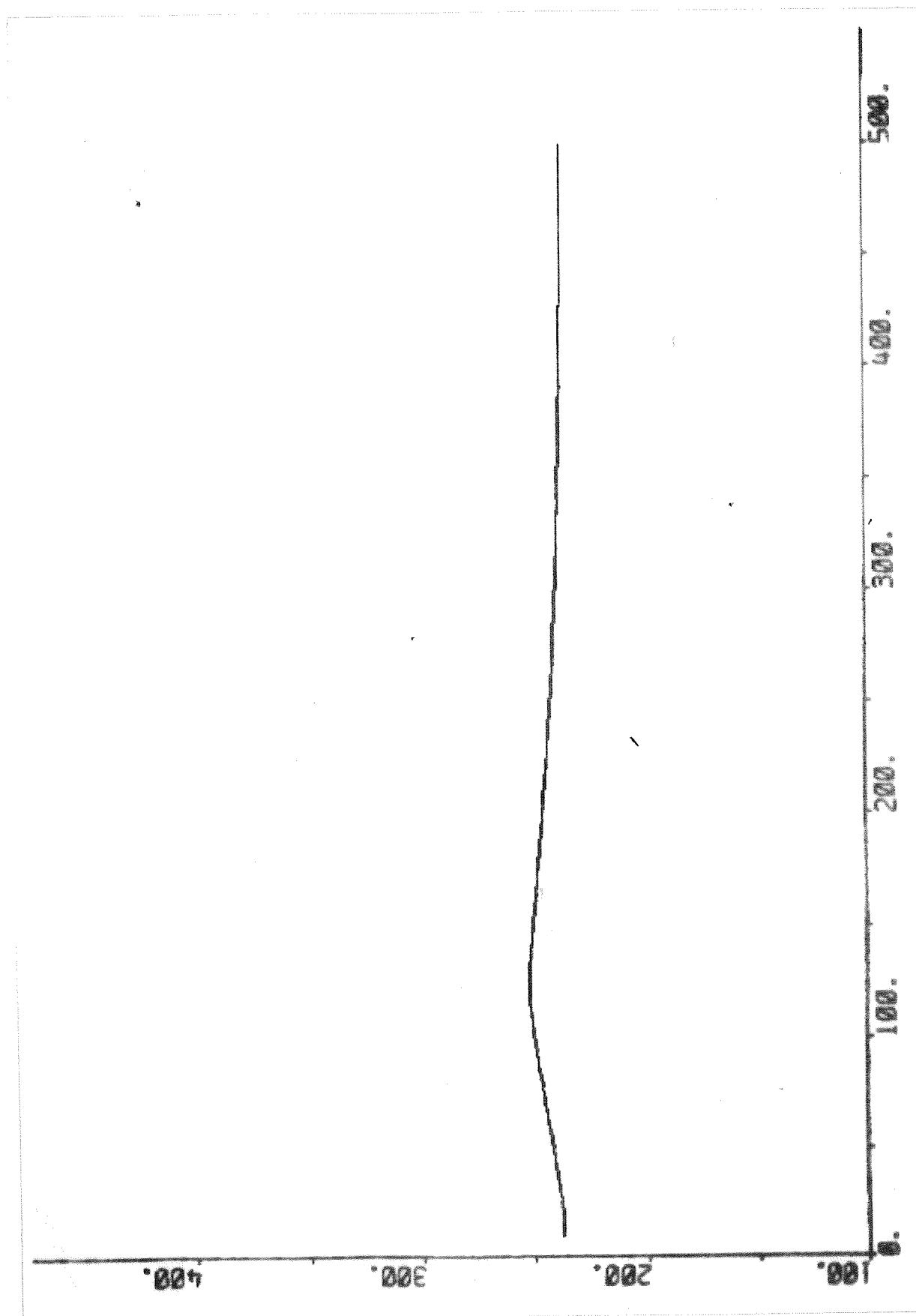


Fig. 13.20 - Response of the feedwater temperature after the economizer during transfer from normal to alert mode.

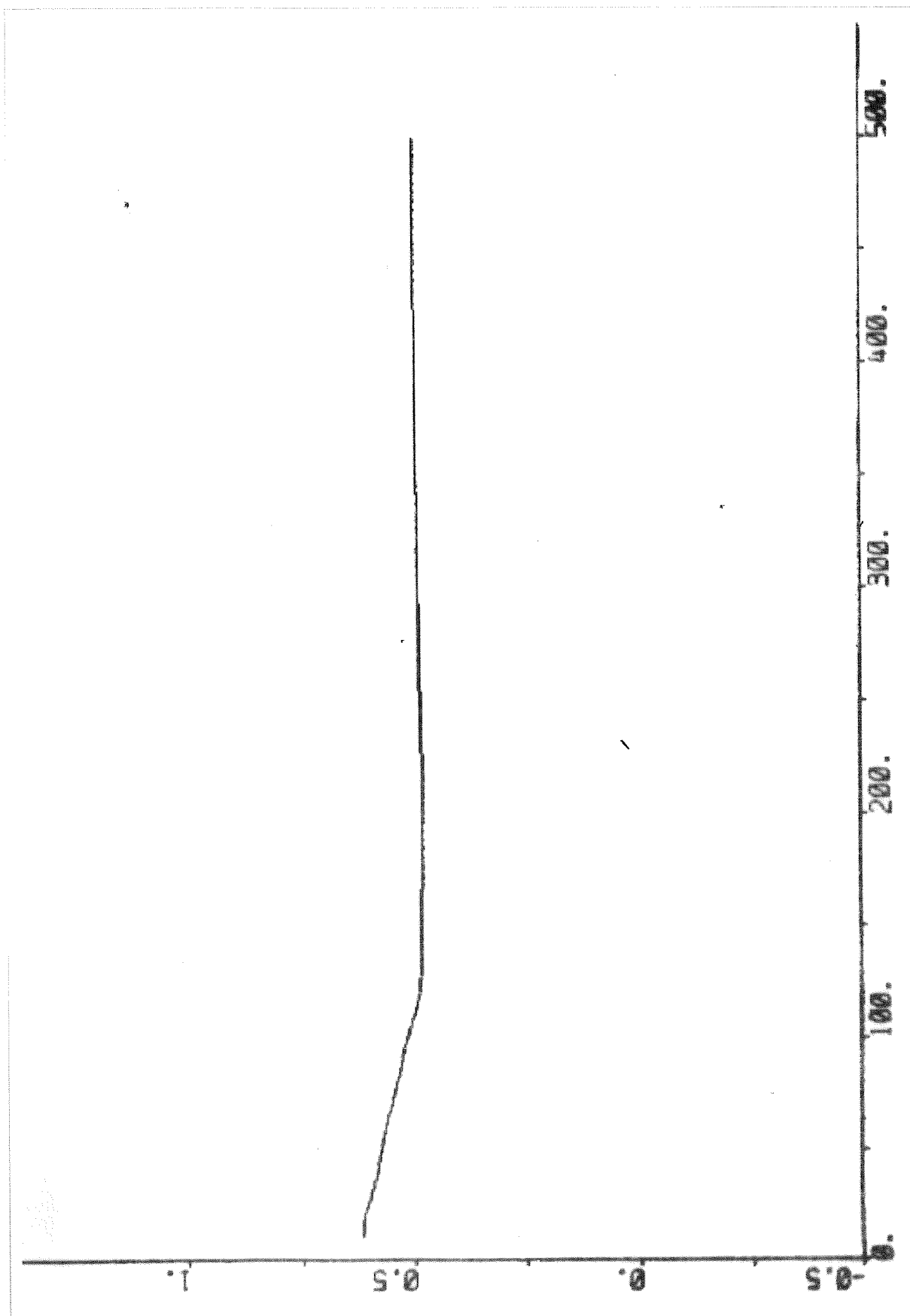


Fig. 13.21 - Response of the stroke of the control valve during transfer from normal to alert mode.

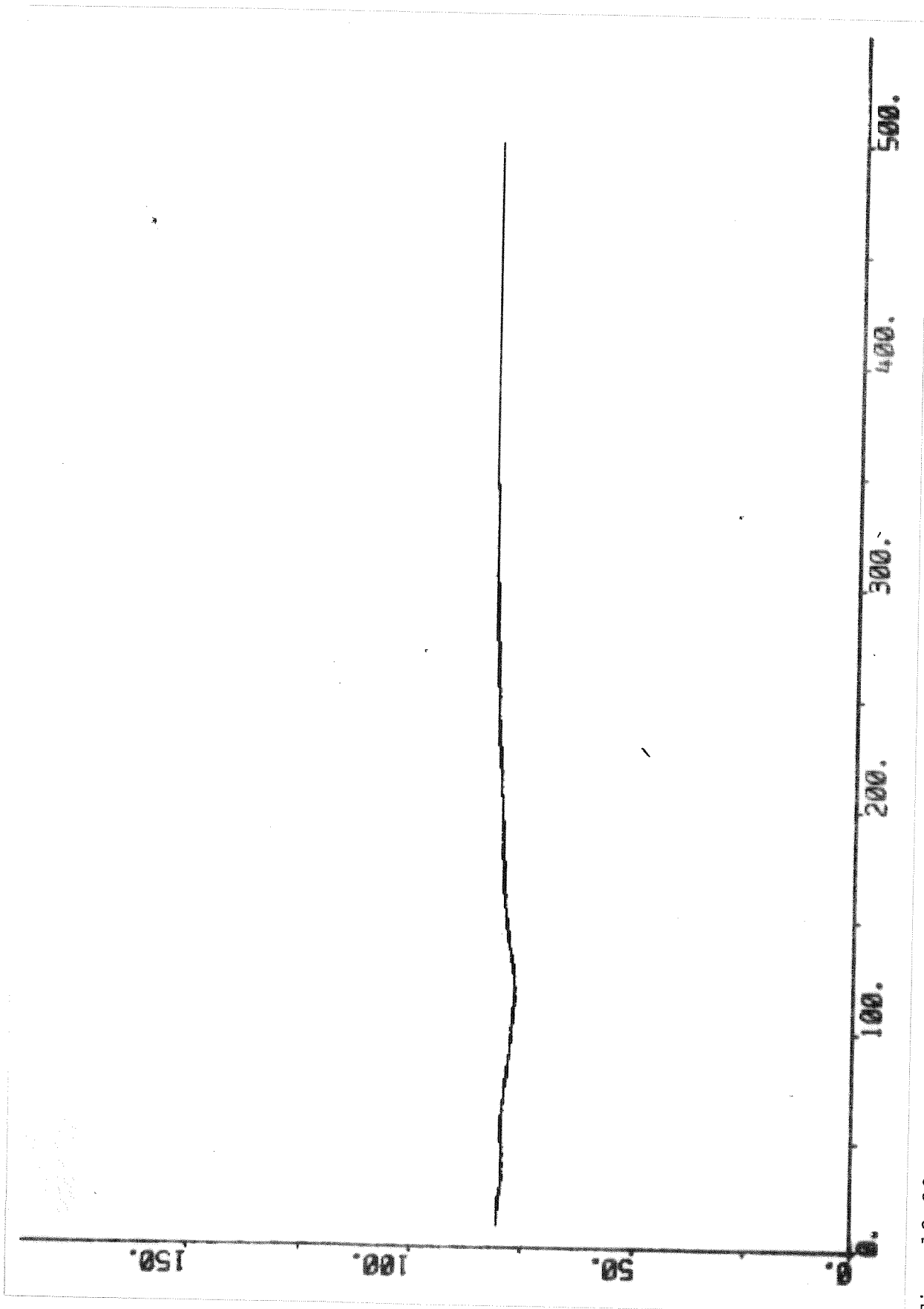


Fig. 13.22 - Response of the steam flow during transfer from normal to alert mode.

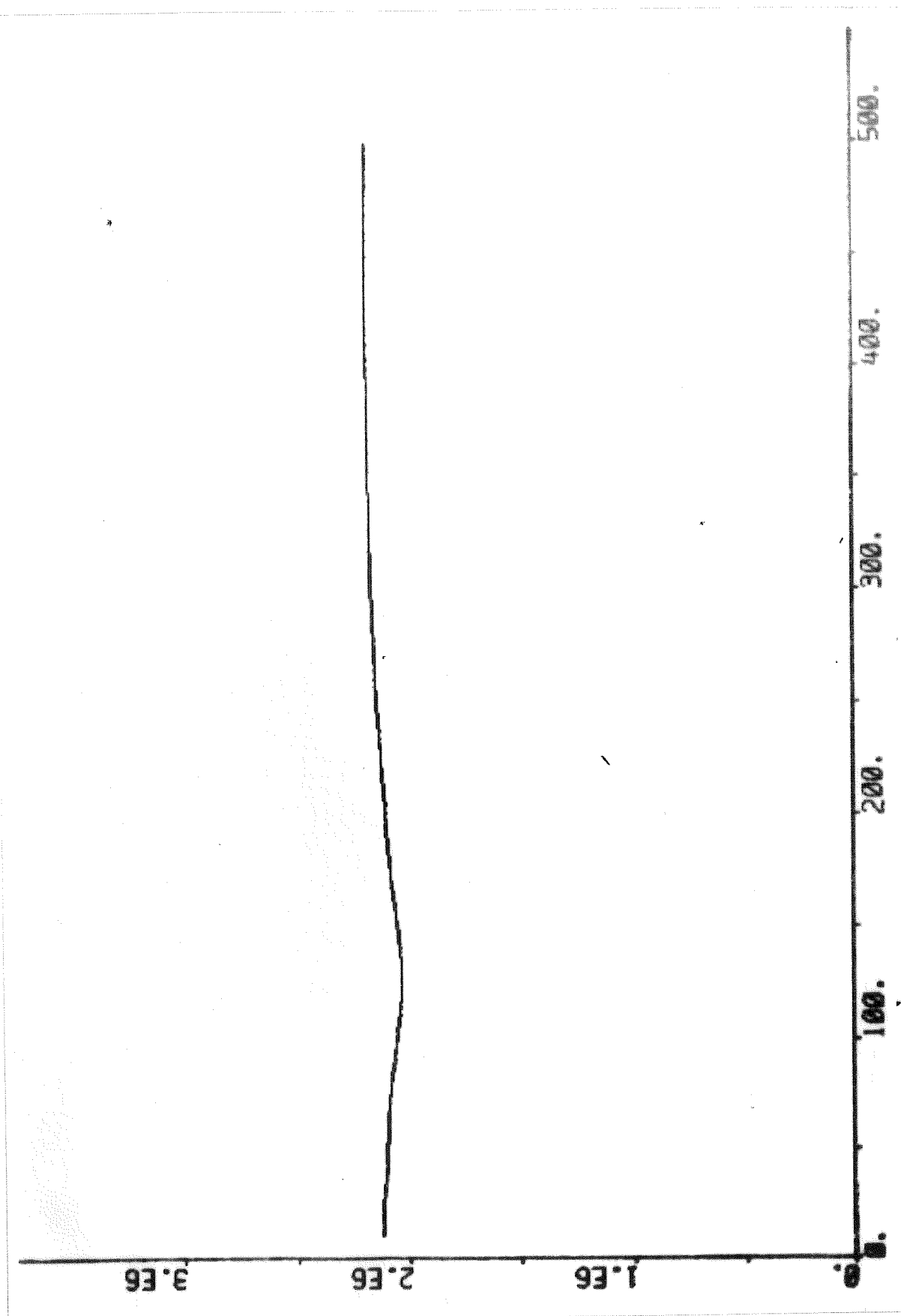


Fig. 13.23 - Response of the reheater steam pressure during transfer from normal to alert mode.

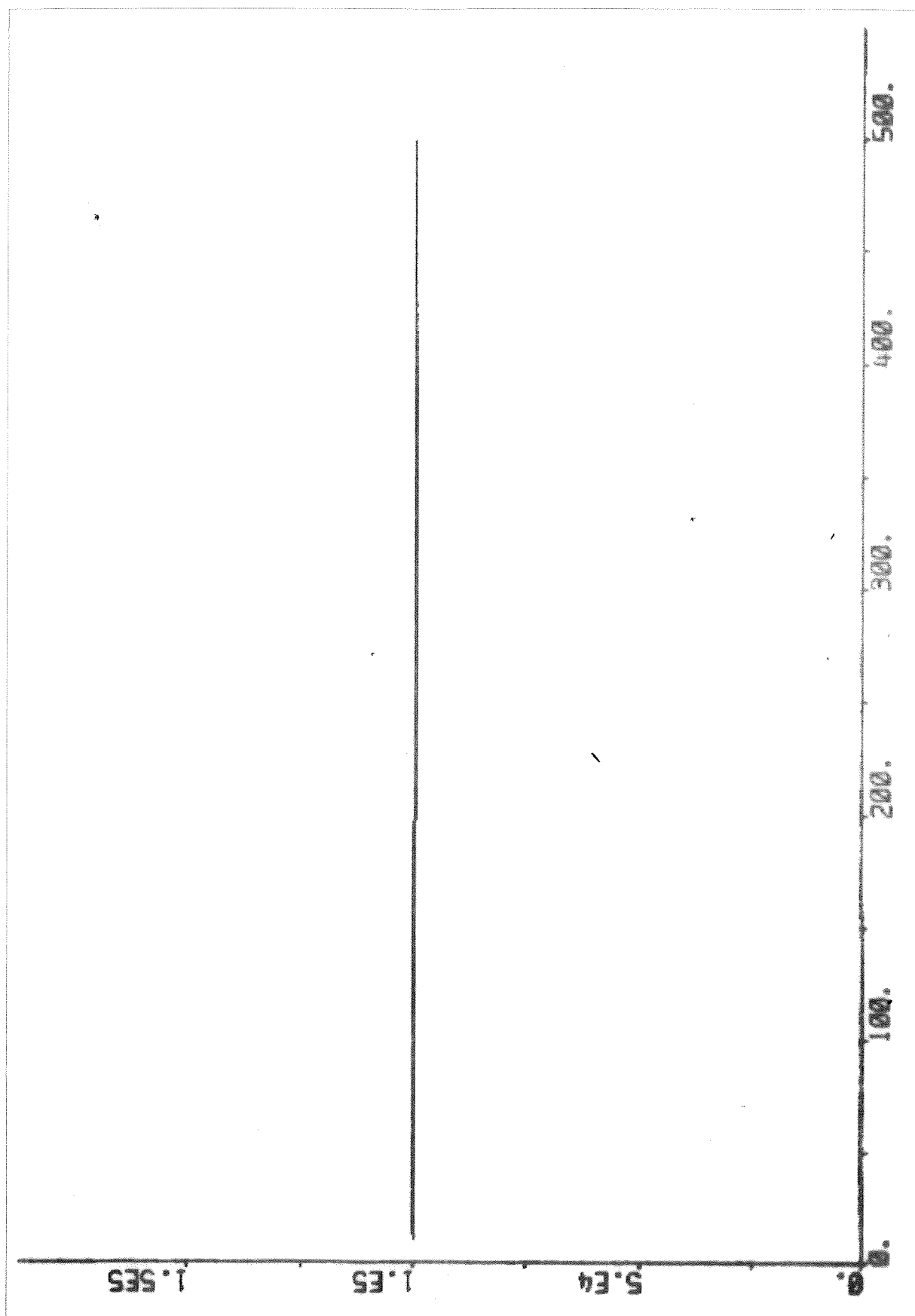


Fig. 13.24 - Response of the output power during transfer from normal to alert mode.

#### 14. INCREASE OF OUTPUT POWER IN ALERT MODE.

The performance of the control system when the output power is increased in alert mode will be examined in this section. The output power was changed by changing the power demand signal from 100 MW (63%) to 150 MW (94%) at  $t = 10$  s. The power demand signal,  $s_{nslr}$  is input to the power demand setter (PDS), which generates the reference value of the output power. The reference value of the output power,  $N_{gs2r}$  is limited by the jump-and-rate circuit (PDS3) in Fig. 5.3. The numerical value of the jump of  $N_{gs2r}$  is 24 MW (15%) and the numerical value of the rate of  $N_{gs2r}$  is 19.2 MW/min (12%/min) in this case. The performance of the drum pressure loop, the drum level loop, the steam temperature loop and the output power loop will now be examined.

##### The drum pressure loop.

The task of the drum pressure loop is to control the drum pressure by manipulating the fuel flow. The reference value of the drum pressure,  $p_{ds2r}$  is generated by the drum pressure reference setter (DPRS), which was described in Section 6. The reference value of the drum pressure is determined by the reference value of the output power,  $N_{gs2r}$  and by the mode of the control system (normal to alert). In this case  $p_{ds2r}$  is constant and equal to  $145 \cdot 10^5$  Pa (97%). The steam flow (Fig. 14.22), the feedwater flow (Fig. 14.6) and the feedwater temperature after the economizer (Fig. 14.20) disturb the drum pressure loop. The mean density of the steam-water mixture in the riser tubes, the steam temperature after the primary superheater, the heat flows to the superheaters, to the reheater, and to the economizer are disturbed by the fuel flow variations. The fuel flow,  $w_{bol}$  is the output of the fuel flow servo (FFS), which was described in Section 7. The reference value of the fuel flow,  $w_{bolr}$  is determined by the drum pressure controller (DPC), which was described in Section 7. The inputs to the DPC are  $p_{ds2r}$  and its derivative,  $s_{bolt}$ , the drum pressure,  $p_{ds2}$ , and the steam flow,  $w_{ts1}$ . The block diagram of the DPC is given in Fig. 7.1. The rate of change of the fuel flow is limited

in the FFS. The limits are parameters,  $w_{b0lo}$  and  $w_{b0ls}$  of the first nonlinear block in Fig. 7.2. The numerical value of  $w_{b0lo}$  and  $w_{b0ls}$  are both 0.1 kg/s (60%/min).

The response of the fuel flow is shown in Fig. 14.1. The fuel flow increases linearly for  $10 < t < 25$  s due to the limited rate of change of the fuel flow. The fuel flow is at most 1 kg/s (12%) higher than the final value. The fuel flow has reached its final value at  $t = 300$  s.

The response of the drum pressure is shown in Fig. 14.2. The drum pressure decreases for  $10 < t < 25$  s due to the rapid increase of the steam flow. The fuel flow is increased as fast as possible during the decrease of the drum pressure. The maximum drum pressure error is  $3 \cdot 10^5$  Pa (2%). The maximum rate of change of the drum pressure is  $18 \cdot 10^5$  Pa/min (12%/min).

The response of the steam pressure before the control valve is shown in Fig. 14.3. The steam pressure decreases  $6 \cdot 10^5$  Pa (4%) at  $t = 10$  s due to the increased steam flow (Fig. 14.22). The increased steam flow increases the pressure drop in the superheaters due to friction losses. The steam flow is changed by a factor 1.5 and the friction losses by a factor 2.2.

The response of the steam temperature after the primary superheater is shown in Fig. 14.4. The steam temperature variation is about  $3^\circ\text{C}$ . The temperature decreases for  $10 < t < 110$  s due to the increased steam flow (Fig. 14.22) and the decreased steam temperature before the primary superheater without corresponding increase of the heat flow to the primary superheater. The steam temperature before the primary superheater is determined by the drum pressure (Fig. 14.2). The heat flow to the primary superheater is roughly proportional to the fuel flow (Fig. 14.1).

Properties: The steam flow is the most severe disturbance of the drum pressure loop. The steam flow and the derivative of the reference value of the drum pressure influence the fuel flow through

the feedforward terms. The effects of the other disturbances are reduced by feedback. The limited rate of change of the fuel flow deteriorates the performance of the drum pressure loop for  $10 < t < 25$  s. This must, however, be accepted because of the restrictions of the burner equipment. The maximum drum pressure error is  $3 \cdot 10^5$  Pa (2%).

#### The drum level loop.

The task of the drum level loop is to control the drum level,  $z_{dl4}$  by manipulating the feedwater control valve. The reference value of the drum level,  $z_{dl4r}$  is constant. The steam flow (Fig. 14.22) and the fuel flow (Fig. 14.1) disturb the drum level loop. The drum level loop disturbs the feedwater temperature. If the drum level is too high there is a danger that water will reach the turbine. If the drum level is too low there is a danger that the riser tubes will be damaged due to insufficient cooling. The reference value of the feedwater flow,  $w_{fw5r}$  is determined by the drum level controller (DLC), which was described in Section 8. The inputs to the DLC are  $z_{dl4r}$  and  $z_{dl4}$ , and the steam flow,  $w_{ts1}$ . The block diagram of the DLC is given in Fig. 8.1. The rate of change of the stroke of the feedwater valve is limited in the feedwater servo (FWS). The limits are parameters,  $s_{ww2o}$  and  $s_{ww2s}$  of the first nonlinear block in Fig. 8.2. The numerical values of  $s_{ww2o}$  and  $s_{ww2s}$  are both 5%/s.

The response of the stroke of the feedwater valve is shown in Fig. 14.5. The valve opening has to be increased in order to increase the feedwater flow. The valve is opening for  $10 < t < 15$  s due to the feedforward from the steam flow (Fig. 14.22). The valve is closing for  $15 < t < 30$  s due to the feedback from the drum level. The valve is finally opening for  $30 < t$  s due to the feedforward from the steam flow and the feedback from the drum level.

The response of the feedwater flow is shown in Fig. 14.6. The



response of the feedwater flow is similar to the response of the stroke of the feedwater valve. The response of the feedwater flow is also similar to the response of the steam flow (Fig. 14.22). The effect of the changing mean density of the steam-water mixture in the drum system is visible for  $10 < t < 120$  s. The feedwater flow is at most 15 kg/s (10%) lower than the steam flow.

The response of the drum level is shown in Fig. 14.7. The swell phenomenon increases the drum level 5 cm at  $t = 30$  s. The drum level has returned to its reference value at  $t = 60$  s.

The response of the drum water temperature is shown in Fig. 14.8. The rate of change of drum water temperature determines the thermal stresses of the drum material. The decrease in temperature is less than  $2^{\circ}\text{C}$  and the rate of change is less than  $2^{\circ}\text{C}/\text{min}$ . This is less than can be predicted from the rate of change of drum pressure.

Properties: The steam flow is the most severe disturbance of the drum level loop in this case. The control of the drum level is difficult due to the shrink-and-swell phenomenon. The steam flow influences the feedwater flow through the feedforward term. The effects of the other disturbances are reduced by feedback. The maximum drum level error is 5 cm.

#### The steam temperature loop.

The task of the steam temperature loop is to control the steam temperature after the tertiary superheater,  $T_{ts2}$  by manipulating the first and the second attemperators spray flow valves. The reference value of the steam temperature after the tertiary superheater,  $T_{ts2r}$  is constant. The heat flows to the secondary and tertiary superheaters, the steam temperature after the primary superheater (Fig. 14.4), and the steam flow (Fig. 14.22) disturb the steam temperature loop. The heat flows to the secondary and

tertiary superheaters are both approximately proportional to the fuel flow (Fig. 14.1). The specific fuel consumption is reduced if the steam temperature after the tertiary superheater is increased. The steam temperature is limited by the properties of the superheater material. The steam temperature before the secondary superheater,  $T_{ss1}$  is the output of the secondary superheater steam temperature servo (SSSTS), which was described in Section 9. The steam temperature before the tertiary superheater,  $T_{ts1}$  is the output of the tertiary superheater steam temperature servo (TSSTS), which was described in Section 9. The reference value of the steam temperature before the tertiary superheater,  $T_{ts1r}$  is determined by the tertiary superheater steam temperature controller (TSSTC), which was described in Section 9. The inputs to the TSSTC are  $T_{ts2r}$ ,  $T_{ts2}$ , the steam flow,  $w_{ts1}$ , and the fuel flow,  $w_{bol}$ . The block diagram of the TSSTC is given in Fig. 9.1. The reference value of the steam temperature before the secondary superheater,  $T_{ss1r}$  is determined by the secondary superheater steam temperature controller (SSSTC), which was described in Section 9. The inputs to the SSSTC are  $T_{ss2r}$ ,  $T_{ss2}$ ,  $w_{ts1}$ , and  $w_{bol}$ . The rate of change of the stroke of the second attemperator spray flow valve is limited in the TSSTS. The limits are parameters,  $s_{tw2o}$  and  $s_{tw2s}$  of the first nonlinear block in Fig. 9.3. The numerical values of  $s_{tw2o}$  and  $s_{tw2s}$  are both 4%/s. The rate of change of the stroke of the first attemperator spray flow valve is limited in the SSSTS. The limits are parameters,  $s_{sw2o}$  and  $s_{sw2s}$  of the first nonlinear block in Fig. 9.4. The numerical values of  $s_{sw2o}$  and  $s_{sw2s}$  are both 4%/s. The difference between  $T_{ss2r}$  and  $T_{ts1r}$  is a parameter,  $g_{sw2b}$  of the SSSTC. The numerical value of  $g_{sw2b}$  is 30°C and is chosen so that the second attemperator spray flow valve is approximately halfopen. This means that the steam temperature before the tertiary superheater can be changed rapidly in both directions.

The response of the stroke of the first attemperator spray flow valve is shown in Fig. 14.9. The valve closes for  $10 < t < 25$  s due to the increasing steam flow through the secondary superheater without corresponding increase of the heat flow. The valve

opens for  $25 < t < 140$  s due to the increasing heat flow to the secondary superheater. The valve closes again for  $140 < t$  s due to the decreasing heat flow to the secondary superheater.

The response of the spray flow of the first attemperator is shown in Fig. 14.10. The spray flow follows the stroke of the valve fairly well. The final value of the spray flow is about 60% higher than the initial value but the final value of the stroke is only about 2% higher than the initial value. This increase of spray flow is due to the increased pressure drop in the economizer and the primary superheater.

The response of the steam temperature before the secondary superheater is shown in Fig. 14.11. The steam temperature is increased for  $10 < t < 25$  s in order to compensate for the increased steam flow. The steam temperature is decreased for  $25 < t < 140$  s in order to compensate for the increased heat flow. The steam temperature is finally increased for  $140 < t$  s in order to compensate for the decreased heat flow.

The response of the steam temperature after the secondary superheater is shown in Fig. 14.12. The steam temperature decreases about  $3^{\circ}\text{C}$  for  $10 < t < 20$  s due to the increasing steam flow. The steam temperature then increases for  $20 < t < 60$  s due to the increasing heat flow and the increasing steam temperature before the secondary superheater.

The response of the stroke of the second attemperator spray flow valve is shown in Fig. 14.13. The valve is closing for  $10 < t < 20$  s due to the increasing steam flow. The valve is opening for  $20 < t < 60$  s due to the increasing fuel flow. The valve is finally closing for  $t > 60$  s due to the increasing steam flow.

The response of the spray flow of the second attemperator is shown in Fig. 14.14. The spray flow follows the stroke of the valve fairly well. The final value of the spray flow is about 60% higher than the initial value but the final value of the

stroke is only about 2% higher than the initial value. The increase of the spray flow is due to the increased pressure drop in the economizer, the primary and the secondary superheater. The peak of the spray flow at  $t = 10$  s is due to the very rapid increase of the steam flow at  $t = 10$  s.

The response of the steam temperature before the tertiary superheater is shown in Fig. 14.15. The steam temperature is increased about  $10^{\circ}\text{C}$  for  $10 < t < 20$  s in order to compensate for the increasing steam flow. The steam temperature is then decreased for  $t > 20$  s in order to compensate for the increasing heat flow.

The response of the steam temperature after the tertiary superheater is shown in Fig. 14.16. The maximum steam temperature error is less than  $3^{\circ}\text{C}$ .

Properties: The steam flow and the fuel flow are the most severe disturbances of the steam temperature loop. The steam flow and the fuel flow influence the spray flows by feedforward terms. The effects of the other disturbances are reduced by feedback. The maximum steam temperature error is  $3^{\circ}\text{C}$ . The spray flows are extracted after the feedwater valve, which means that the spray flows increase with the steam flow. This increase of gain counteracts the decrease of gain in the attemperators with the steam flow, which is an advantage.

#### The output power loop.

The task of the output power loop is to control the output power,  $N_{gs2}$  by manipulating the steam control valve and the extraction steam valves. The reference value of the output power,  $N_{gs2r}$  is generated by the power demand setter (PDS), which was described in Section 5. A preliminary reference value of the output power,  $s_{nsl}$  is determined from the setpoint of the output power,  $s_{nslr}$  in the first part of the power demand setter (PDS1). The block diagram of the PDS1 is given in Fig. 5.1. The  $s_{nslr}$  is modified

with respect to the network-frequency in the second part of the power demand setter (PDS2). The block diagram of the PDS2 is given in Fig. 5.2. The  $N_{gs2r}$  is obtained from the third part of the power demand setter (PDS3), which limits the jump and the rate of  $N_{gs2r}$ . The block diagram of the PDS3 is given in Fig. 5.3. The steam pressure before the control valve,  $P_{ts2}$  (Fig. 14.3) and the steam temperature before the control valve,  $T_{ts2}$  (Fig. 14.16) disturb the output power loop. The superheated steam flow,  $w_{ts1}$  (Fig. 14.22), the reheated steam flow,  $w_{rs2}$  and the extraction steam flows,  $w_{hs2}$ ,  $w_{is2}$ ,  $w_{is4}$ ,  $w_{is6}$ ,  $w_{is8}$ ,  $w_{ls2}$  and  $w_{ls4}$  are disturbed by the output power loop. The stroke of the control valve is the output of the control valve servo (CVS), which was described in Section 10. The strokes of the high-pressure preheater extraction valves are the outputs of the high-pressure preheater servo (HPPS), which was described in Section 10. The reference value of the stroke of the control valve,  $s_{vs2r}$  is determined by the turbine power controller (TPC), which was described in Section 10. The inputs to the TPC are  $N_{gs2r}$  and  $N_{gs2}$ . The block diagram of the TPC is given in Fig. 10.1. The reference value of the strokes of the high-pressure preheater extraction valves,  $s_{fs2r}$  are determined by the high-pressure preheater controller (HPPC), which was described in Section 10. The input to the HPPC is  $N_{gs2r}$ . The block diagram of the HPPC is given in Fig. 10.3. The reference value of the strokes of the low-pressure extraction valves,  $s_{fs7r}$  are determined by the low-pressure preheater controller (LPPC), which was described in Section 10. The inputs of the LPPC are  $N_{gs2r}$ , the reference value of the deaerator steam pressure,  $p_{as2r}$  and the deaerator steam pressure,  $p_{as2}$ . The rate of change of the stroke of the control valve is limited in the CVS. The limits are parameters,  $s_{vs2o}$  and  $s_{vs2s}$  of the first nonlinear block in Fig. 10.2. The numerical values of  $s_{vs2o}$  and  $s_{vs2s}$  are 20%/s and 200%/s respectively. The rates of change of the strokes of the high-pressure extraction steam flow valves are limited in the HPPS. The limits are parameters,  $s_{fs2o}$  and  $s_{fs2s}$  of the first nonlinear block in Fig. 10.4. The numerical values of  $s_{fs2o}$  and  $s_{fs2s}$  are both 100%/s. The rates of change of the strokes of the low-pressure extraction steam flow valves are li-

mitted in the LPPS. The limits are parameters,  $s_{fs7o}$  and  $s_{fs7s}$  of the first nonlinear block in Fig. 10.6. The numerical values of  $s_{fs7o}$  and  $s_{fs7s}$  are both 100%/s.

The responses of the strokes of the LP-preheater extraction valves are shown in Fig. 14.17. The valves start to close at  $t = 10$  s and are fully closed at  $t = 12$  s. The valves are then closed for  $12 < t < 30$  s. The effect of the high-pass filtering of  $N_{gs2r}$  is clearly visible at  $t = 90$  s.

The response of the strokes of the HP-preheater extraction valves are shown in Fig. 14.18. The valves close for  $10 < t < 15$  s and opens again for  $t > 15$  s. The high-pass filtering of  $N_{gs2r}$  is clearly visible at  $t = 90$  s.

The response of the feedwater temperature after the HP-preheater is shown in Fig. 14.19. The temperature increases about  $20^{\circ}\text{C}$  due to the final increase of extraction steam flows. The closing of the extraction valves do not affect the feedwater temperature seriously. The low-pass filtering effect of the seven preheater stages are pronounced.

The response of the feedwater temperature after the economizer is shown in Fig. 14.20. The temperature increases due to the increasing fuel flow and to the increasing feedwater temperature after the HP-preheater. The final feedwater temperature after the economizer increases about  $20^{\circ}\text{C}$ .

The response of the stroke of the control valve is shown in Fig. 14.21. The valve is opened rapidly for  $10 < t < 13$  s in order to increase the output power rapidly. The valve is then opened with a lower rate in order to increase the output power like a ramp. The control valve is completely open for  $100 < t < 120$  s. The output power loop has been tuned for fast response. This explains the peak in the response of the stroke of the control valve at  $t = 13$  s. This type of response may lead to unacceptable wear of the control valve and its servo. The wear can, however, be reduced by reducing the response rate. The fast response was chosen

to demonstrate that it does not lead to severe interaction between the control loops.

The response of the steam flow is shown in Fig. 14.22. The response of the steam flow is similar to the response of the stroke of the control valve. The nonlinearity of the control valve is clearly visible for  $50 < t < 150$  s.

The response of the reheater steam pressure is shown in Fig. 14.23. The pressure is approximately proportional to the steam flow. The pressure responds, however, more slowly due to the mass storage in the reheater.

The response of the output power is shown in Fig. 14.24. The output power has an almost perfect jump-and-rate response. The settling-time is about 3 s. The output power has reached its final value within 130 s.

Properties: There are no severe disturbances of the output power loop in this case. The output power error is 1 MW for  $t > 15$  s. The response of the stroke of the control valve may lead to unacceptable wear of the control valve and its servo. The wear can be reduced by reducing the response rate of the output power loop. The high response rate has been chosen to demonstrate the performance that can be obtained using the proposed control system.

### Conclusions.

The performance of the control system when the output power is increased from 100 MW (63%) to 150 MW (94%) in alert mode has been investigated by simulation. In order to increase the output power it is necessary to increase both the steam flow and the fuel flow. The steam flow is the most severe disturbance of the drum pressure loop, the drum level loop, and the steam temperature loop. The fuel flow is a severe disturbance of the

steam temperature loop. The fuel flow is a severe disturbance of the steam temperature loop. The influences of the steam flow and the fuel flow have been reduced by feedforward. The limited rate of change of the fuel flow deteriorates the performance of the drum pressure loop. The maximum drum pressure error is  $3 \cdot 10^5$  Pa (2%). The control of the drum level is difficult due to the shrink-and-swell phenomenon. The maximum drum level error is 5 cm. The limited capacity of the attemperators do not introduce any errors of the steam temperature. The maximum steam temperature error is  $3^{\circ}\text{C}$ . The load dependent pressure drops in the economizer and the superheaters have been exploited in order to obtain load independent gains of the steam temperature servos. There are no severe disturbances of the output power loop in this case. The output power error is less than 1 MW for  $t > 15$  s. The output power loop has been tuned for fast response, which may cause unacceptable wear of the control valve and its servo. The simulations show that even with such a tight loop there are no difficulties due to interaction with other loops.



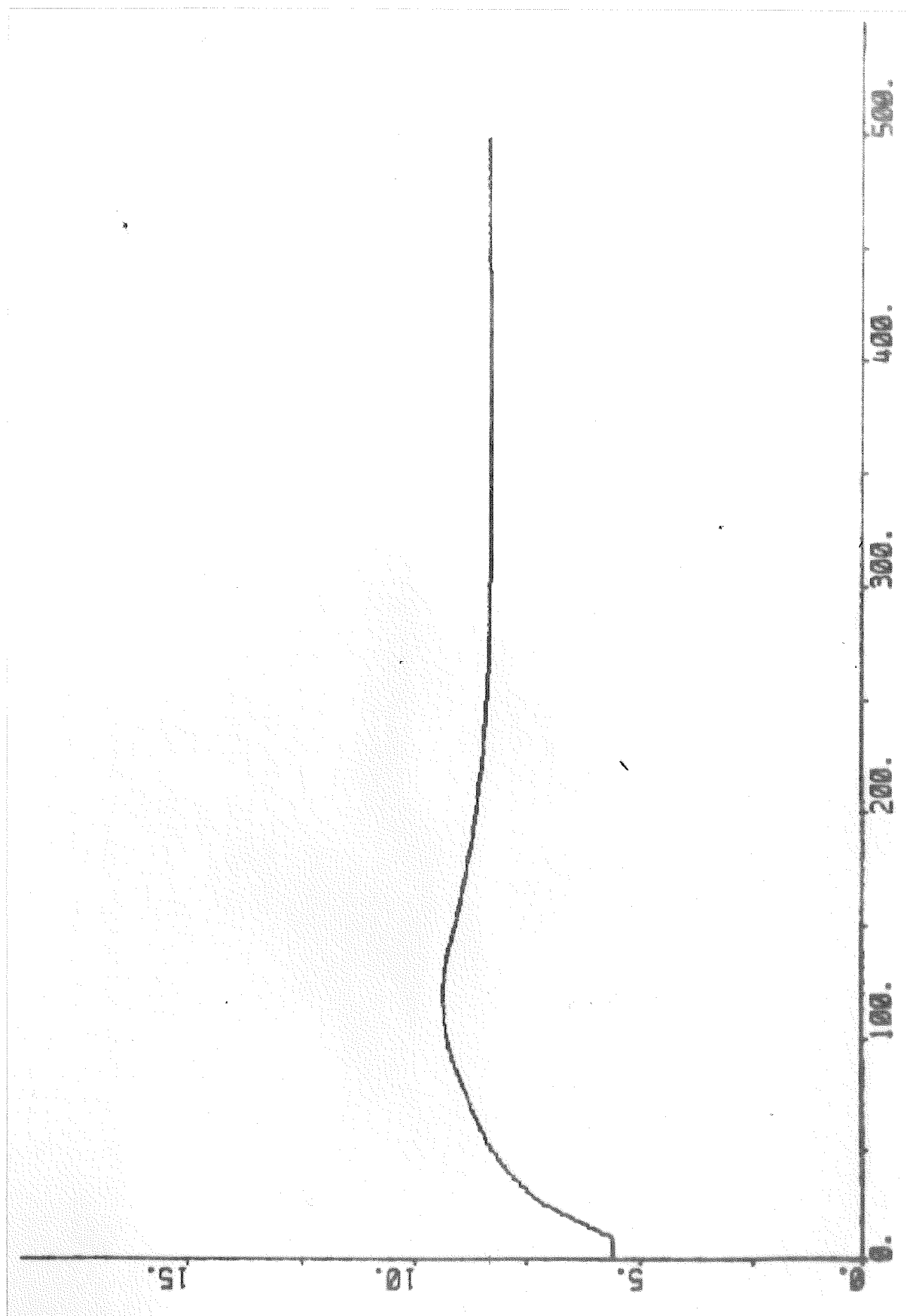


Fig. 14.1 - Response of the fuel flow due to increase of output power in alert mode.

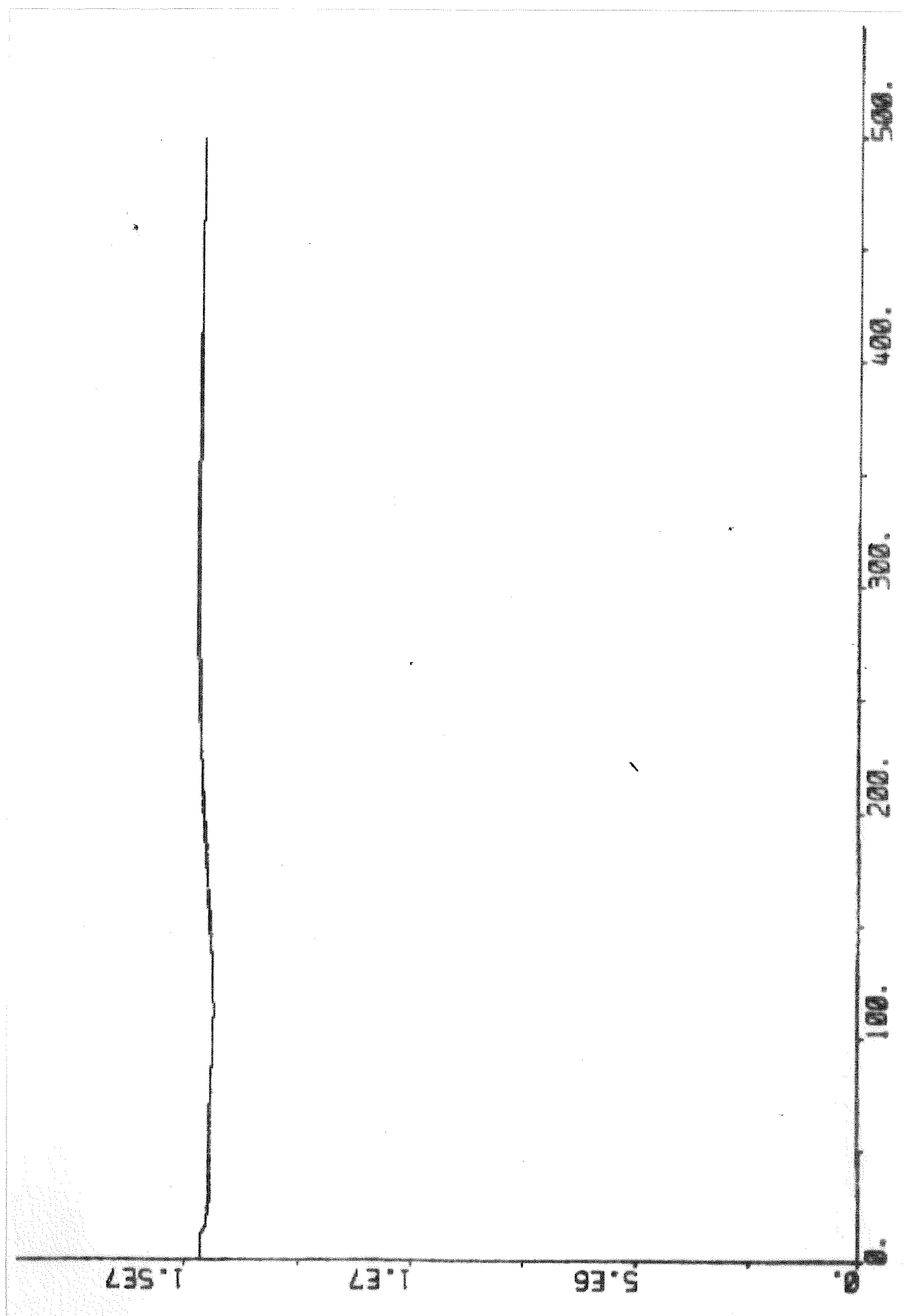


Fig. 14.2 - Response of the drum pressure due to increase of output power in alert mode.

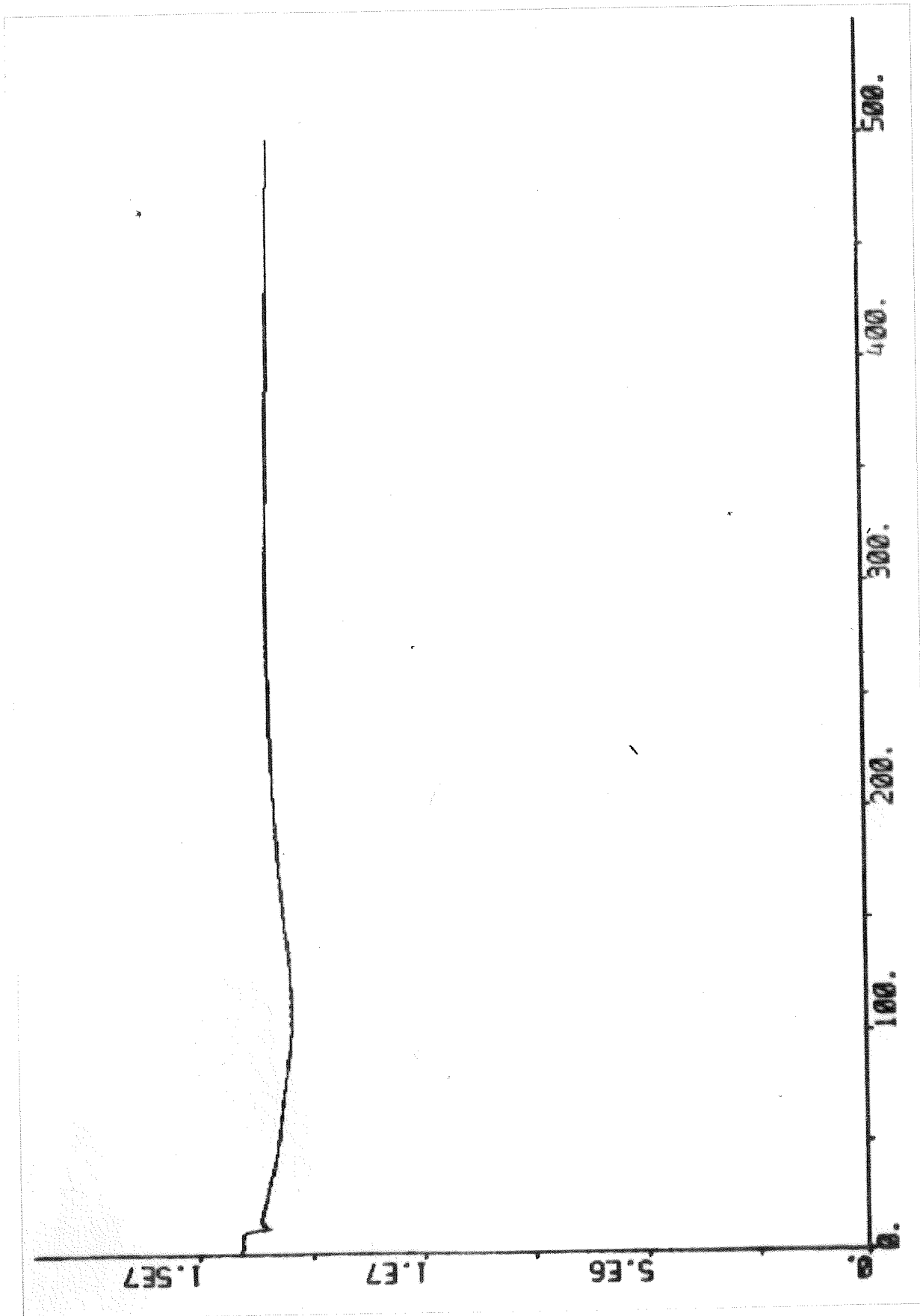


Fig. 14.3 - Response of the steam pressure before the control valve due to increase of output power in alert mode.

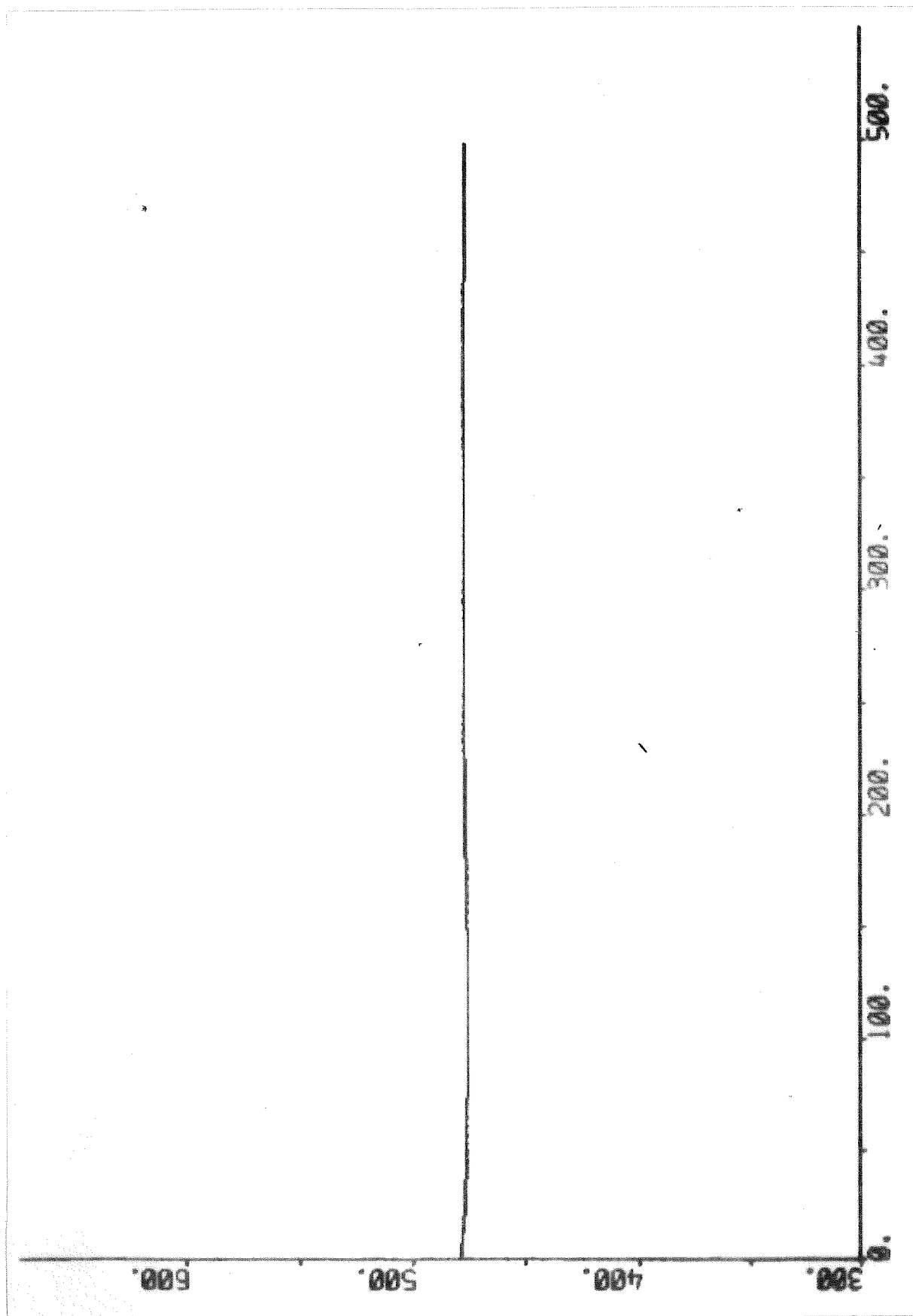


Fig. 14.4 - Response of the steam temperature after the primary superheater due to increase of output power in alert mode.

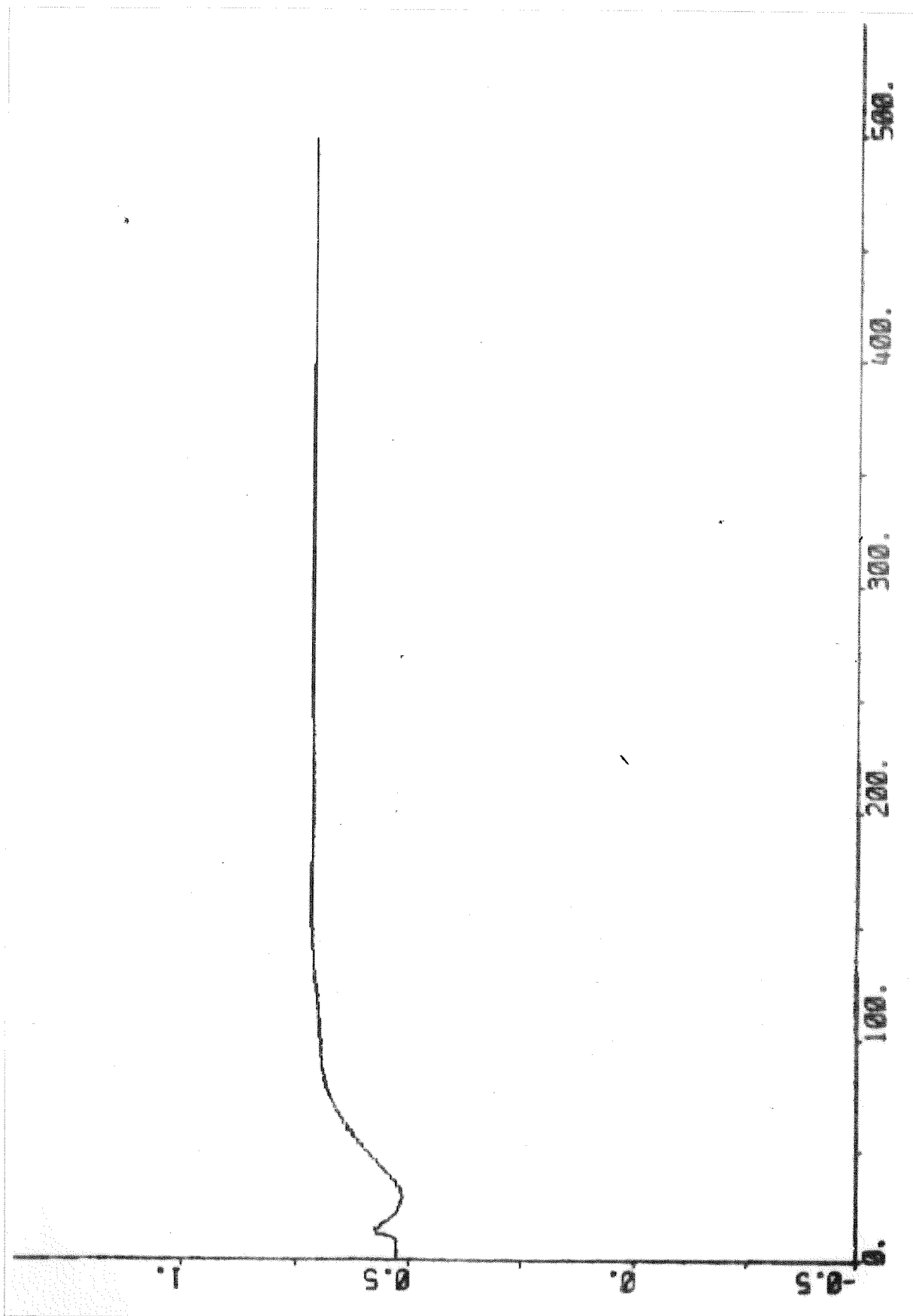


Fig. 14.5 - Response of the stroke of the feedwater valve due to increase of output power in alert mode.

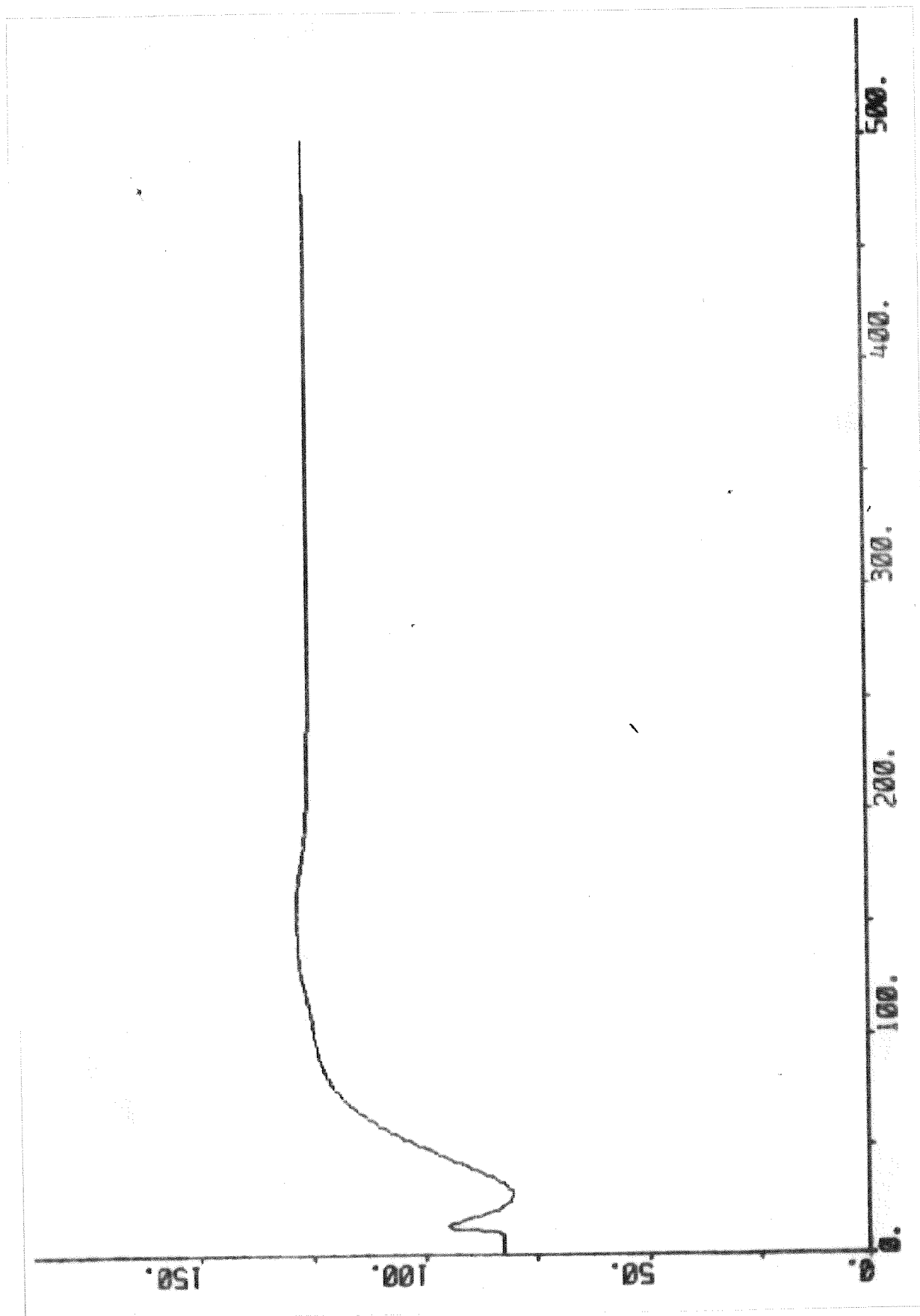


Fig. 14.6 - Response of the feedwater flow due to increase of output power in alert mode.

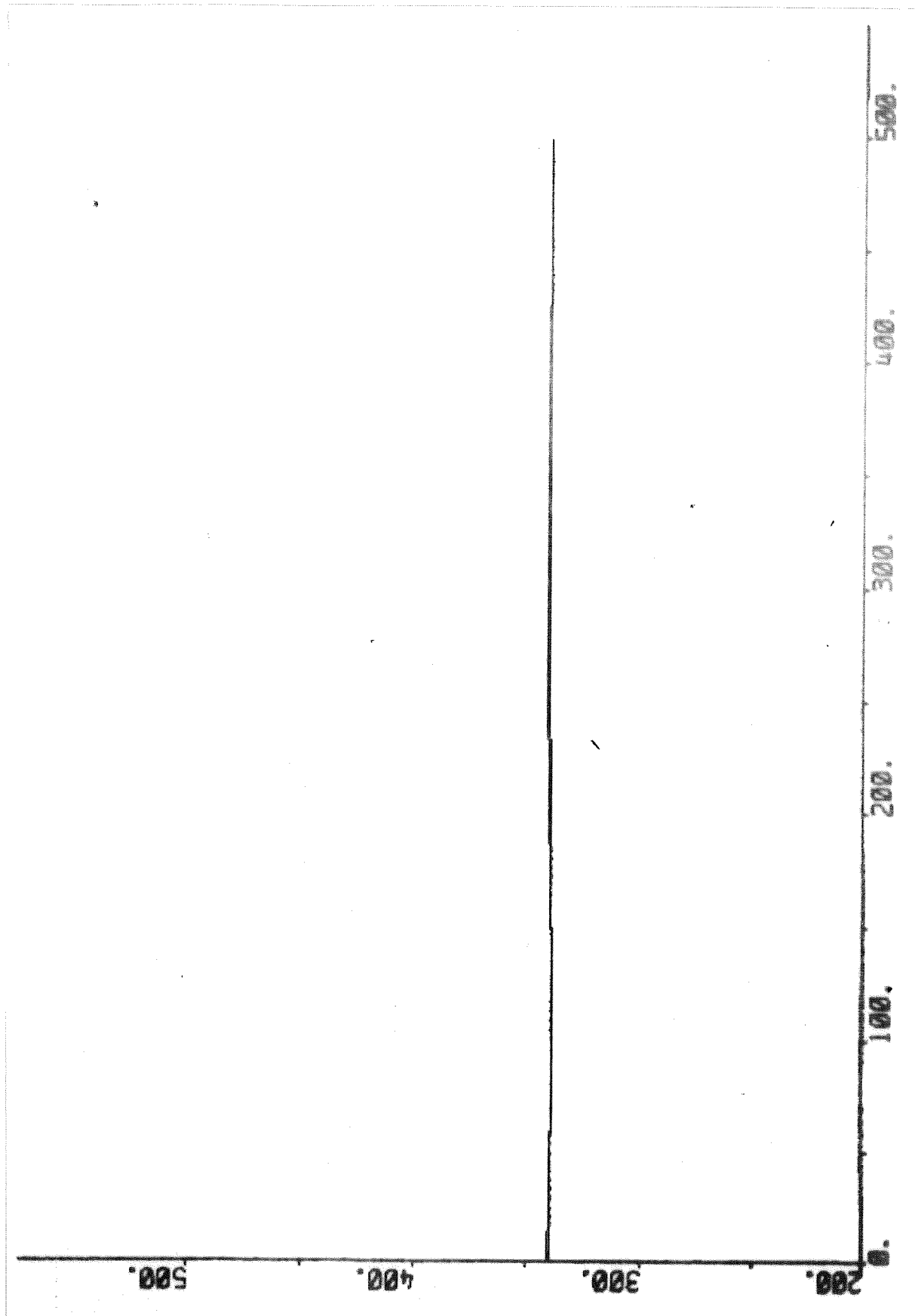


Fig. 14.8 - Response of the drum water temperature due to increase of output power in alert mode.

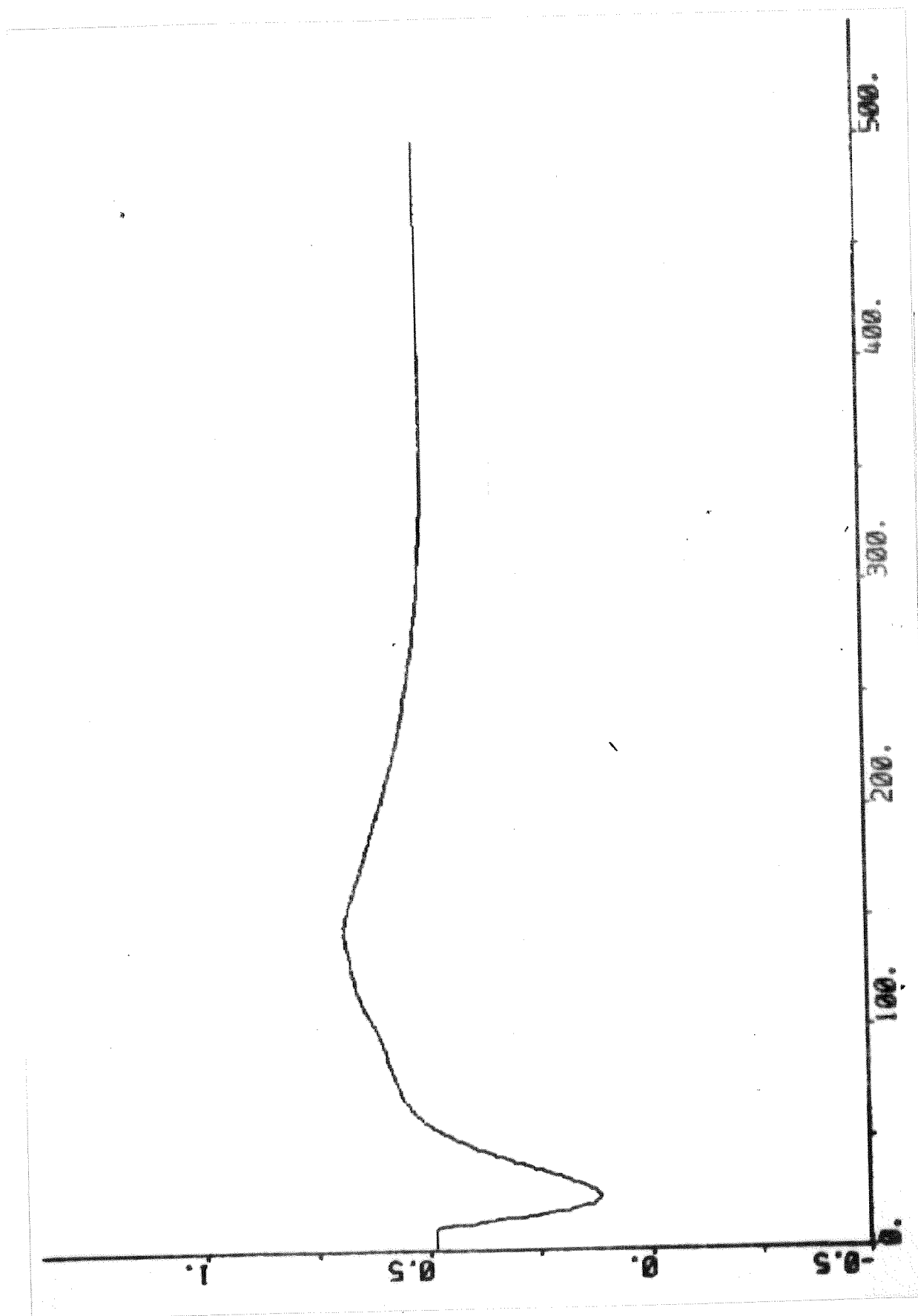


Fig. 14.9 - Response of the stroke of the first attenuator spray flow valve due to increase of output power in alert mode.



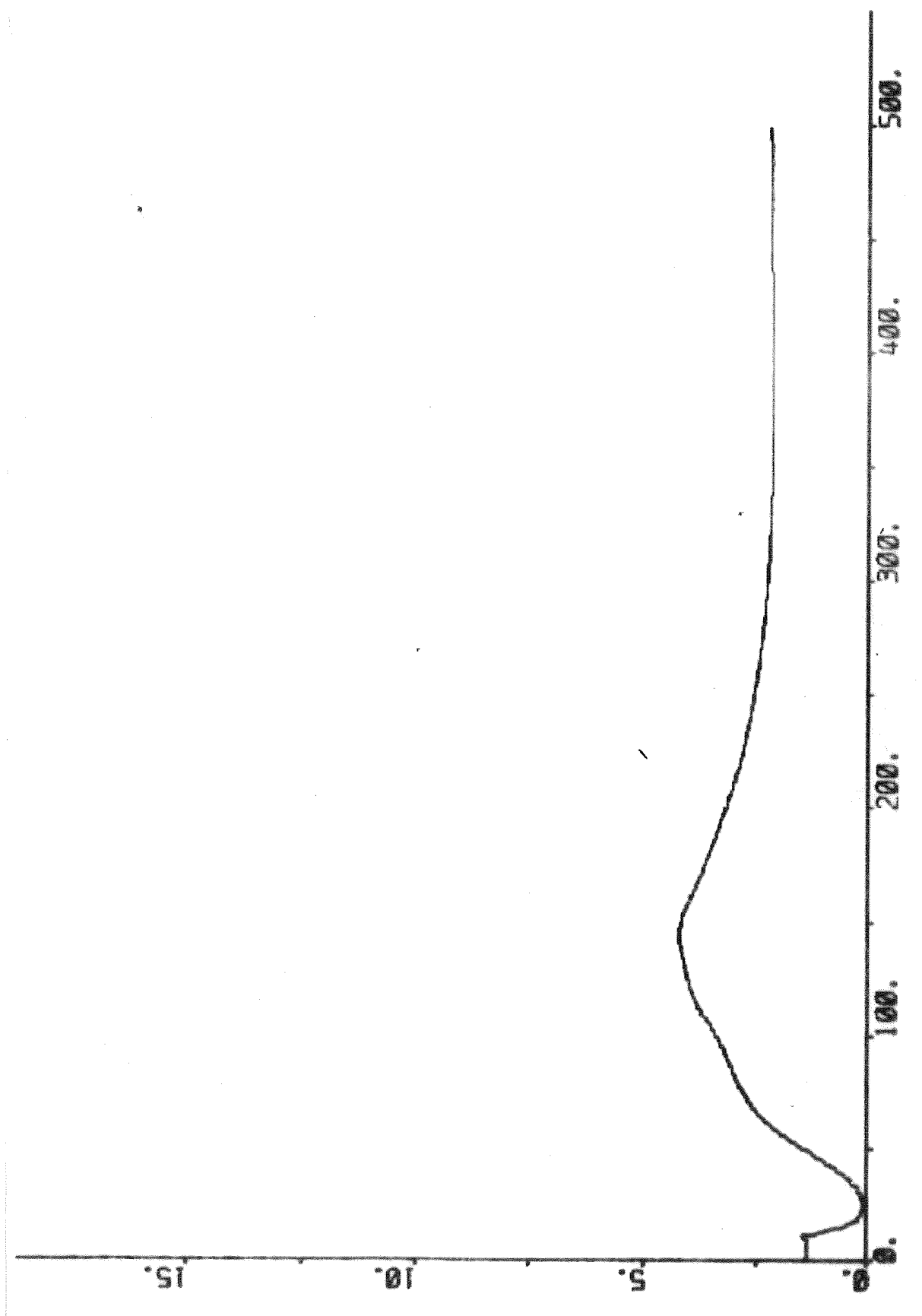


Fig. 14.10 - Response of the spray flow of the first attenuator due to increase of output power in alert mode.

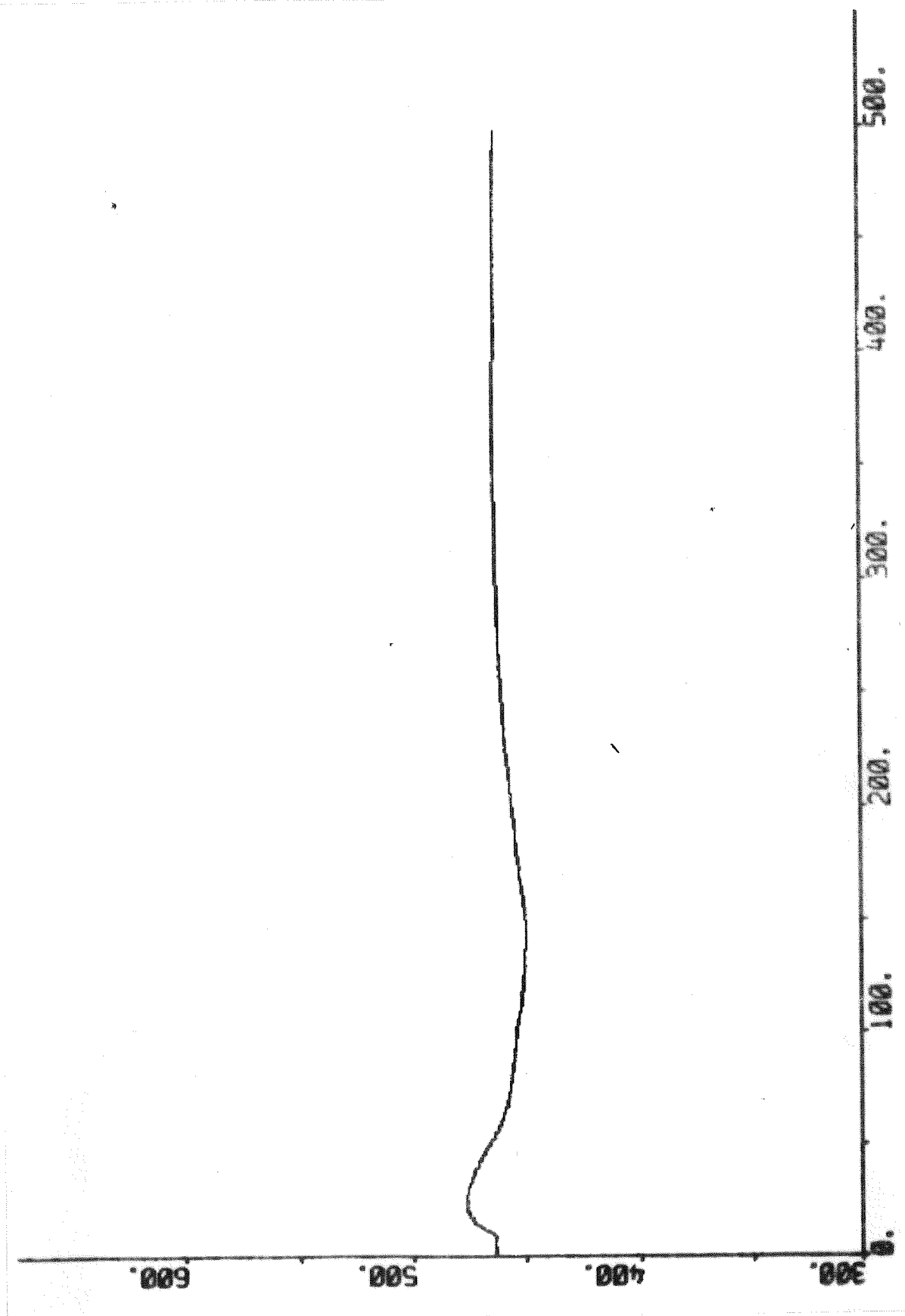


Fig. 14.11 - Response of the steam temperature before the secondary superheater due to increase of output power in alert mode.

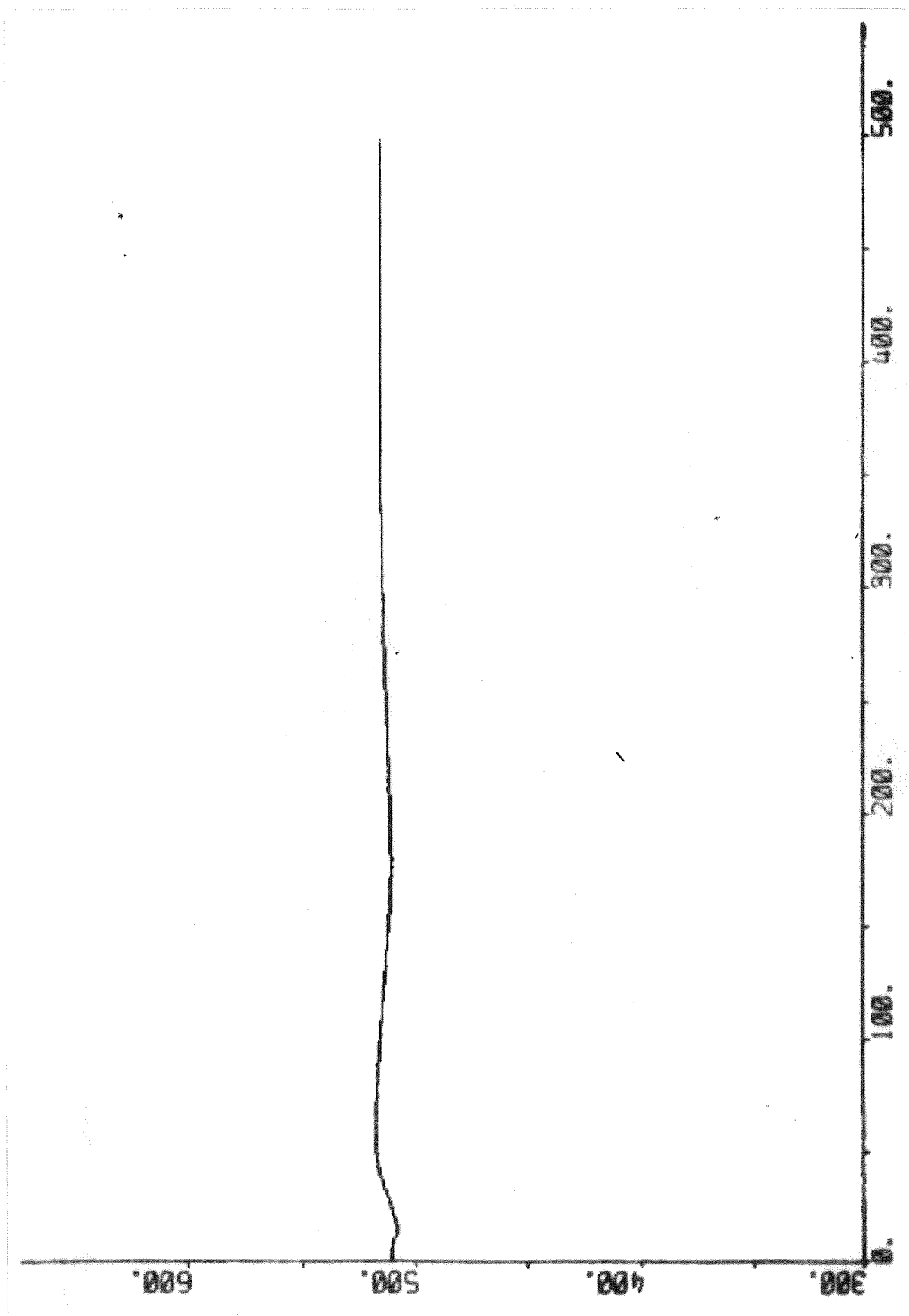


Fig. 14.12 - Response of the steam temperature after the secondary superheater due to increase of output power in alert mode.

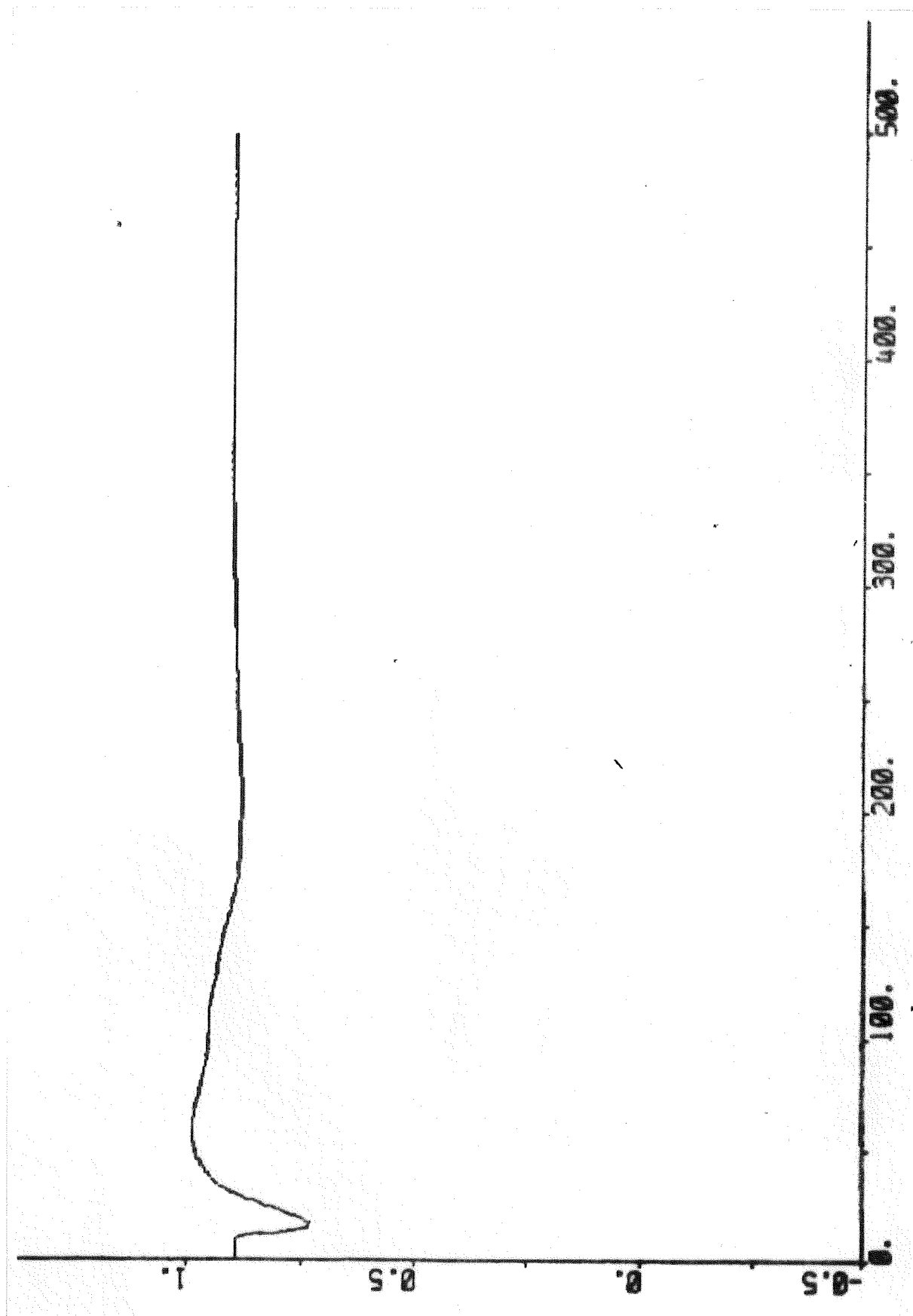


Fig. 14.13 - Response of the second attenuator spray flow valve due to increase of output power in alert mode.

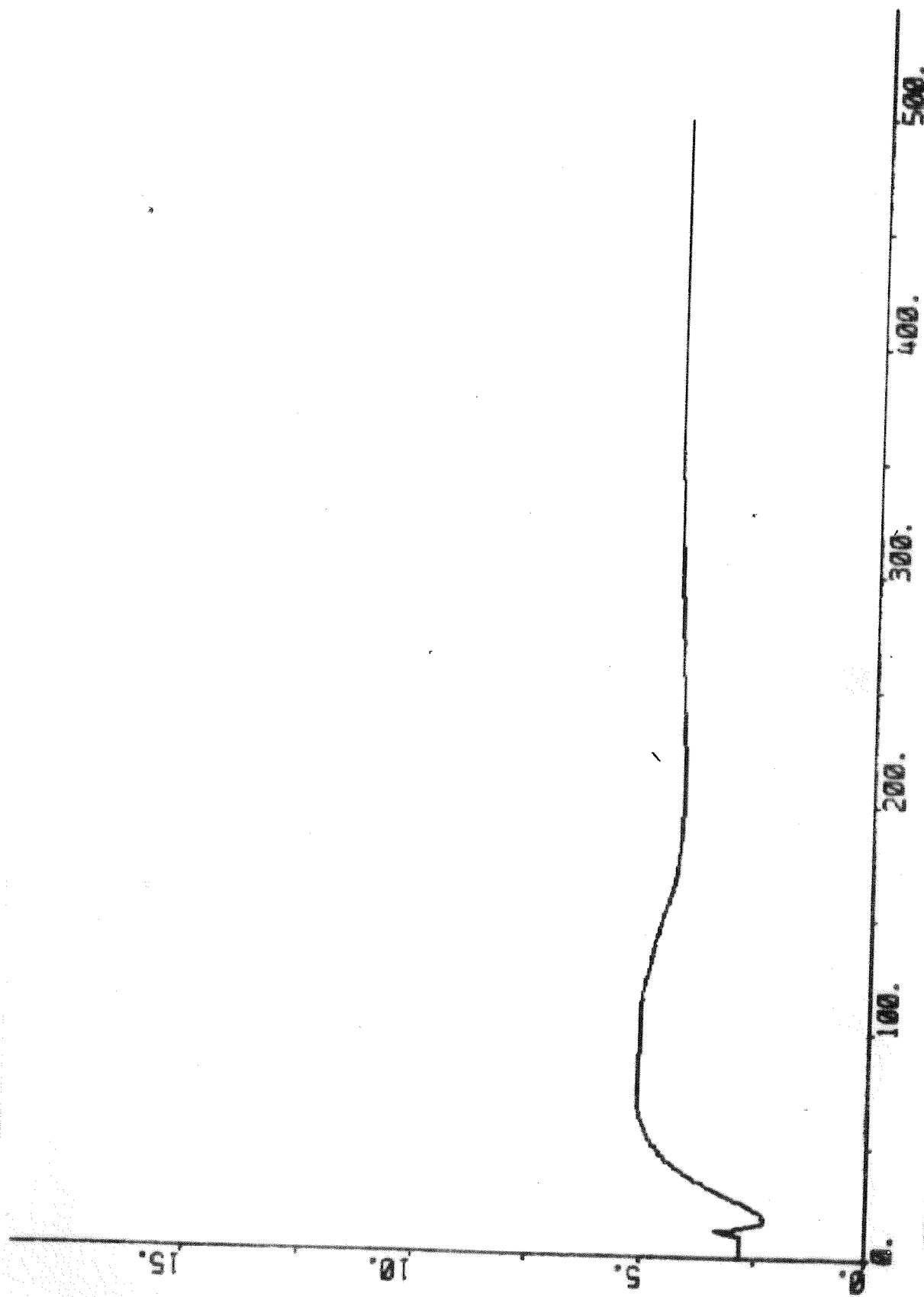


Fig. 14.14 - Response of the spray flow of the second attenuator due to increase of output power in alert mode.

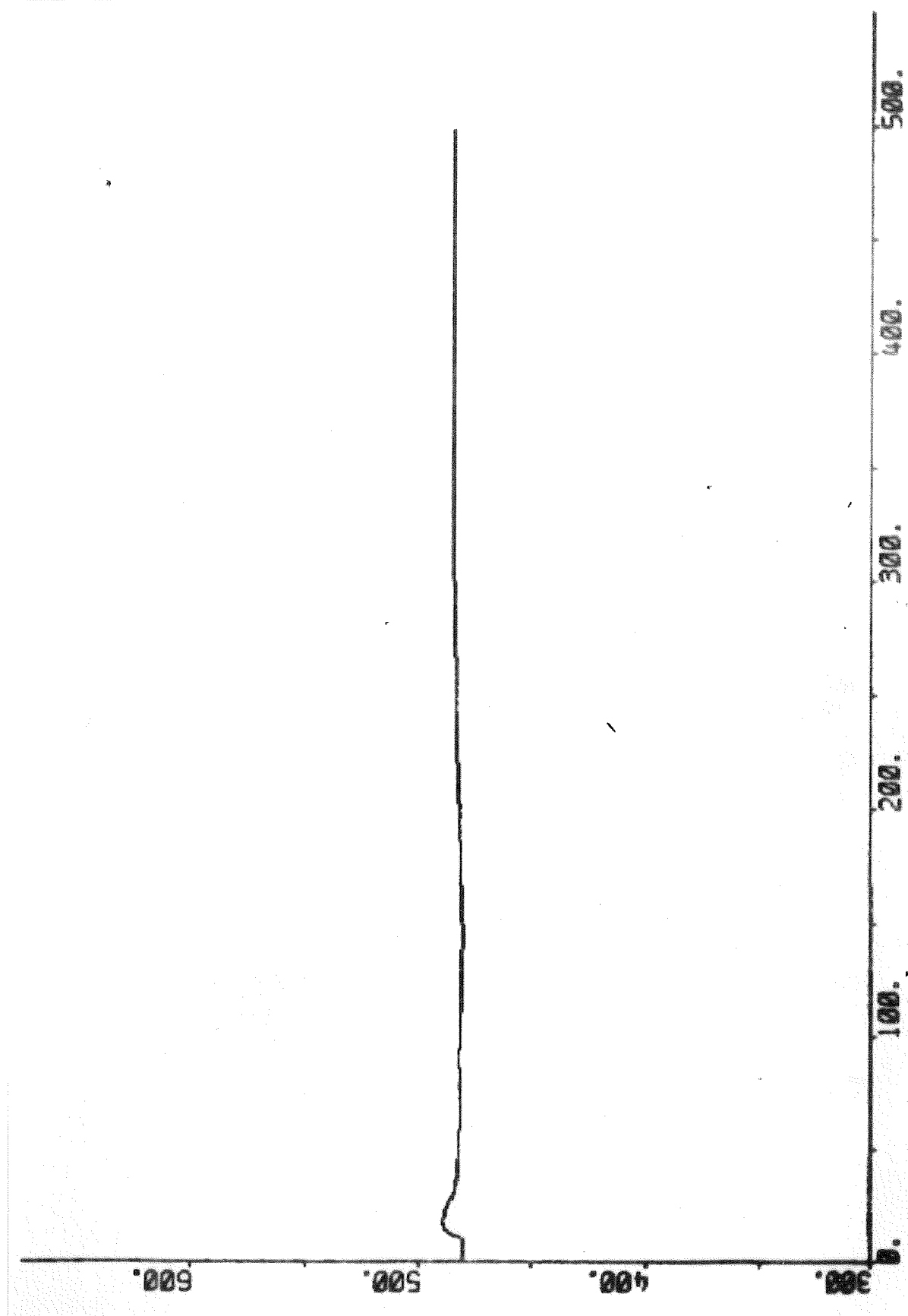


Fig. 14.15 - Response of the steam temperature before the tertiary superheater due to increase of output power in alert mode.

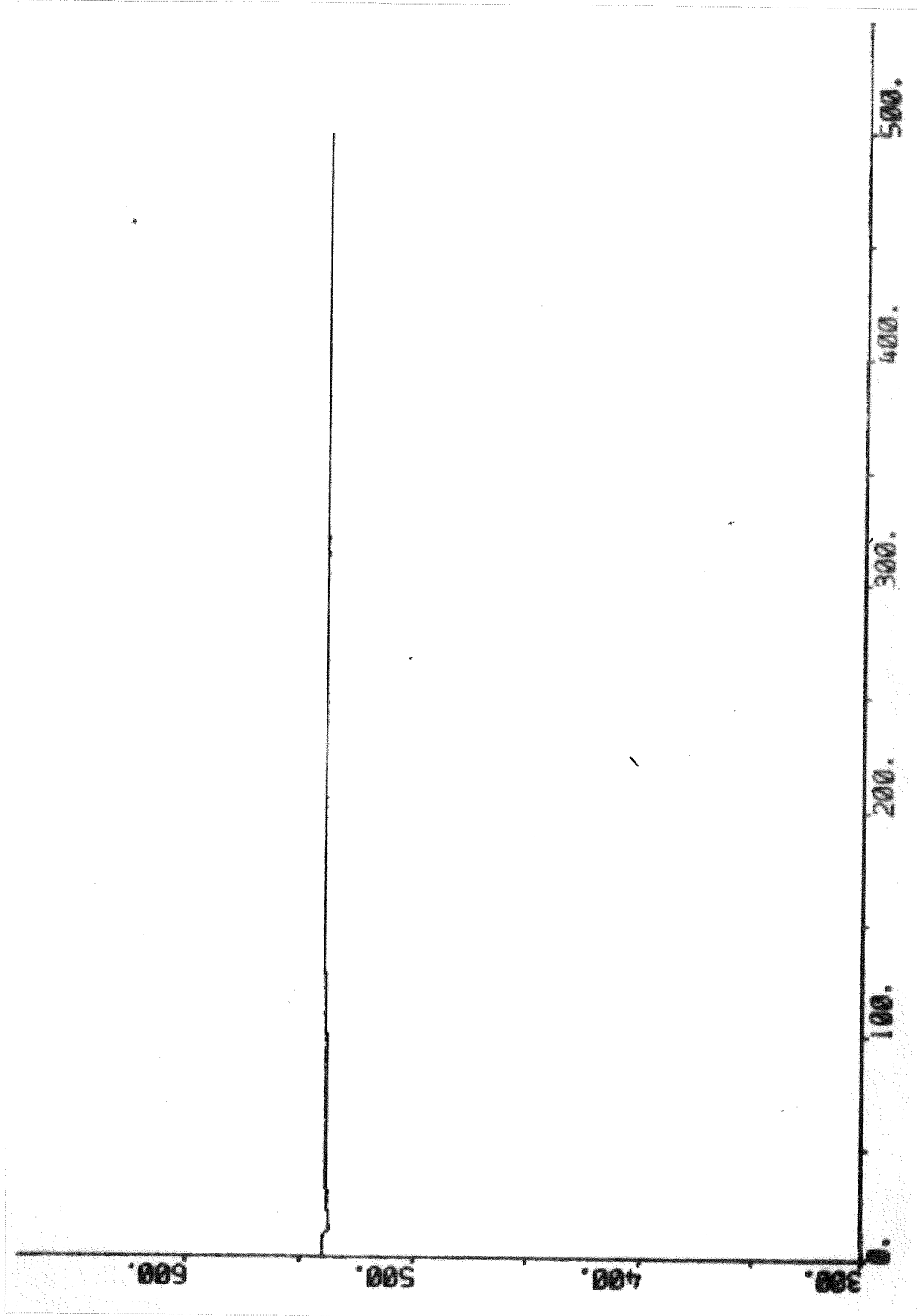


Fig. 14.16 - Response of the steam temperature after the tertiary superheater due to increase of output power in alert mode.

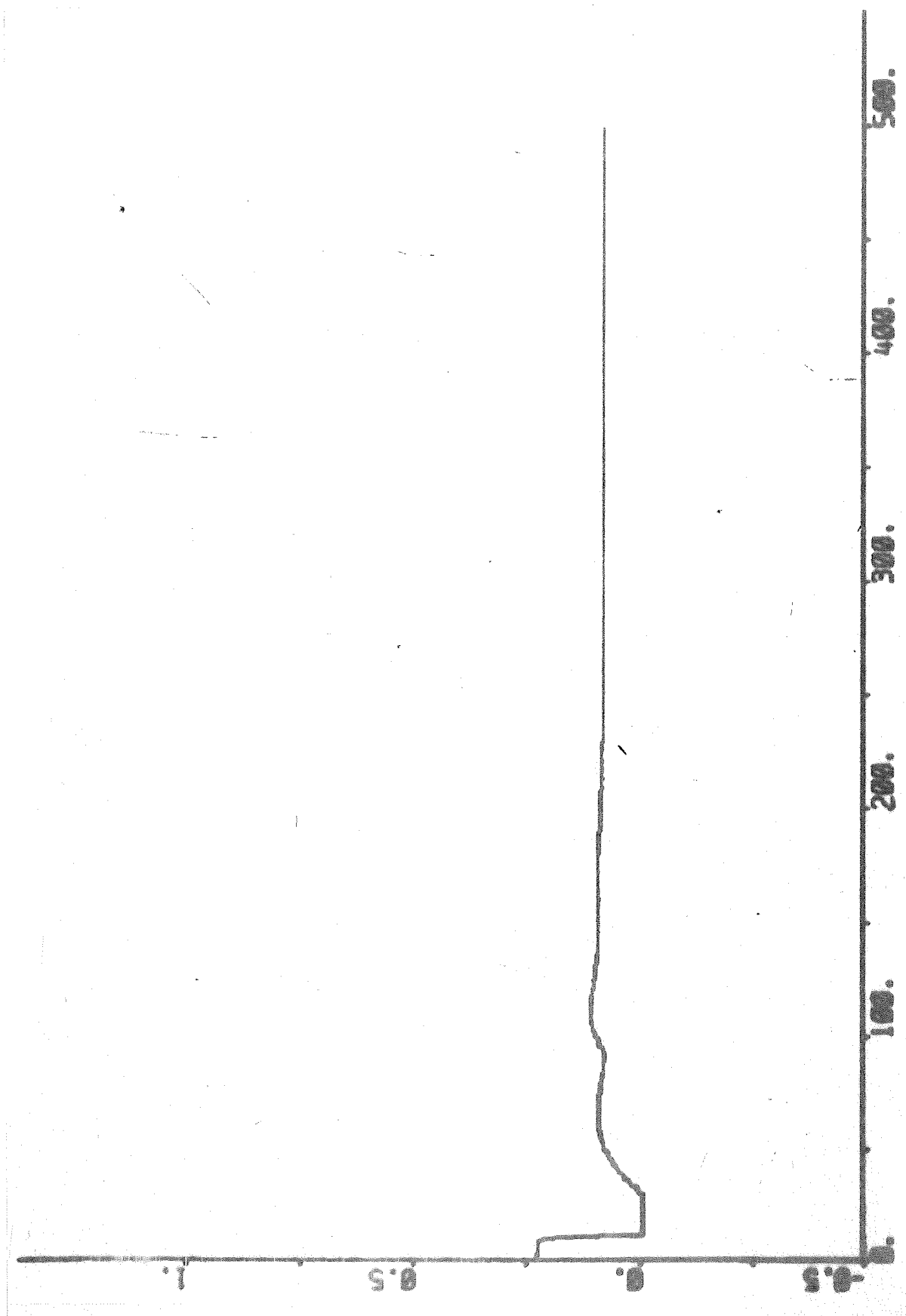


Fig. 14.17 - Responses of the strokes of the low-pressure preheater extraction valve due to increase of output power in alert mode.



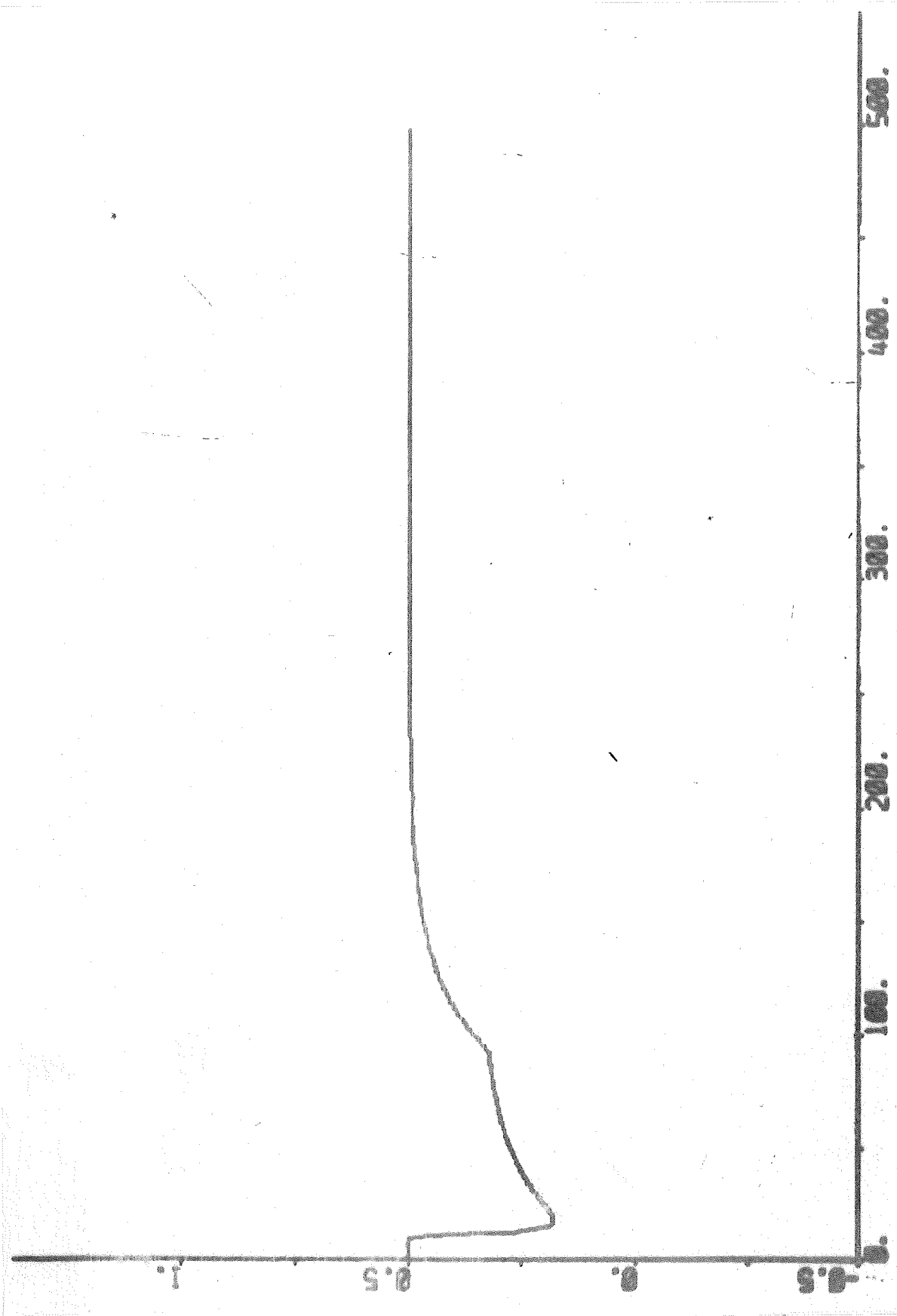


Fig. 14.18 - Response of the stroke of the high-pressure preheater extraction valve due to increase of output power in alert mode.

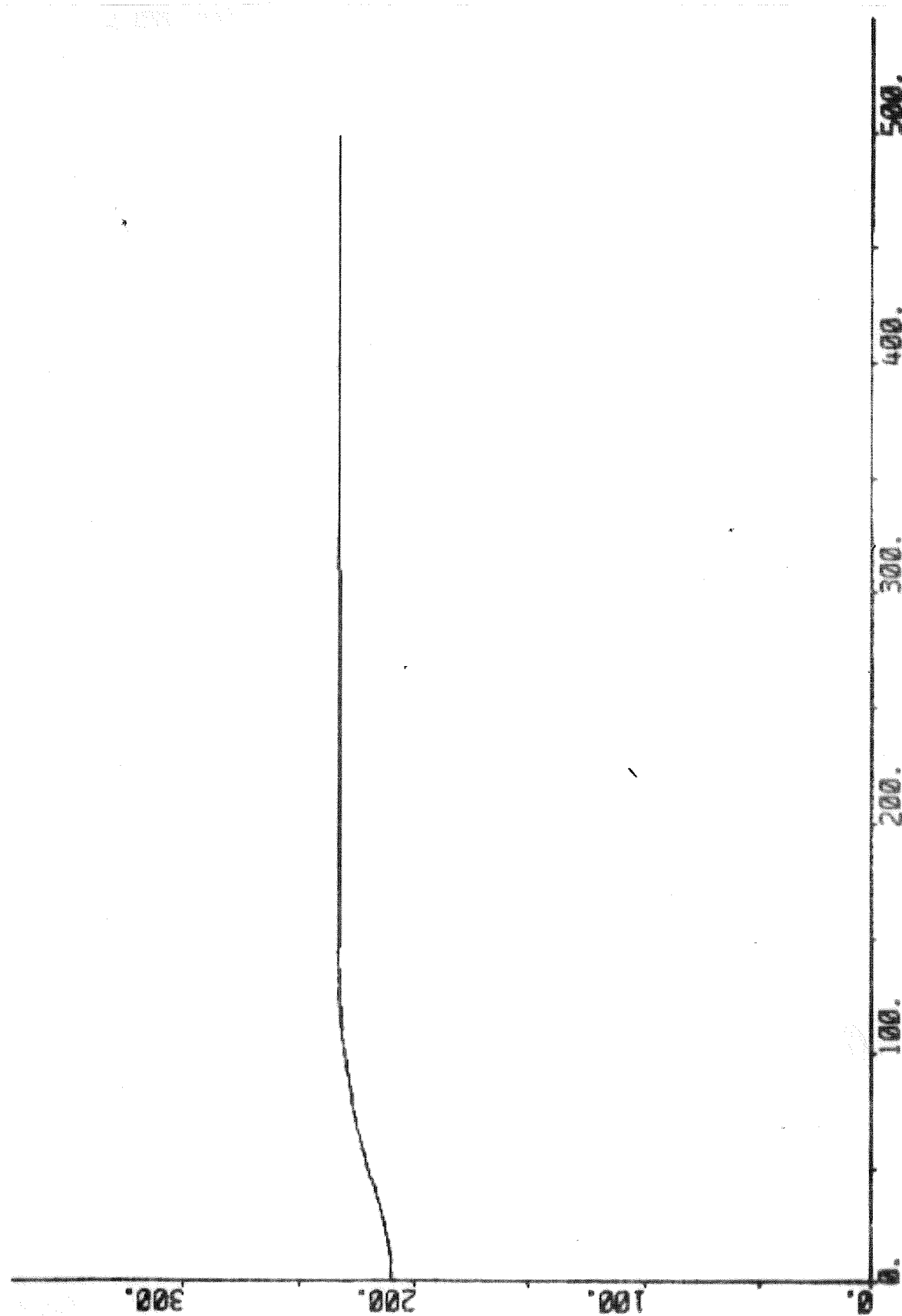


Fig. 14.19 - Response of the feedwater temperature after the high-pressure preheater due to increase of output power in alert mode.

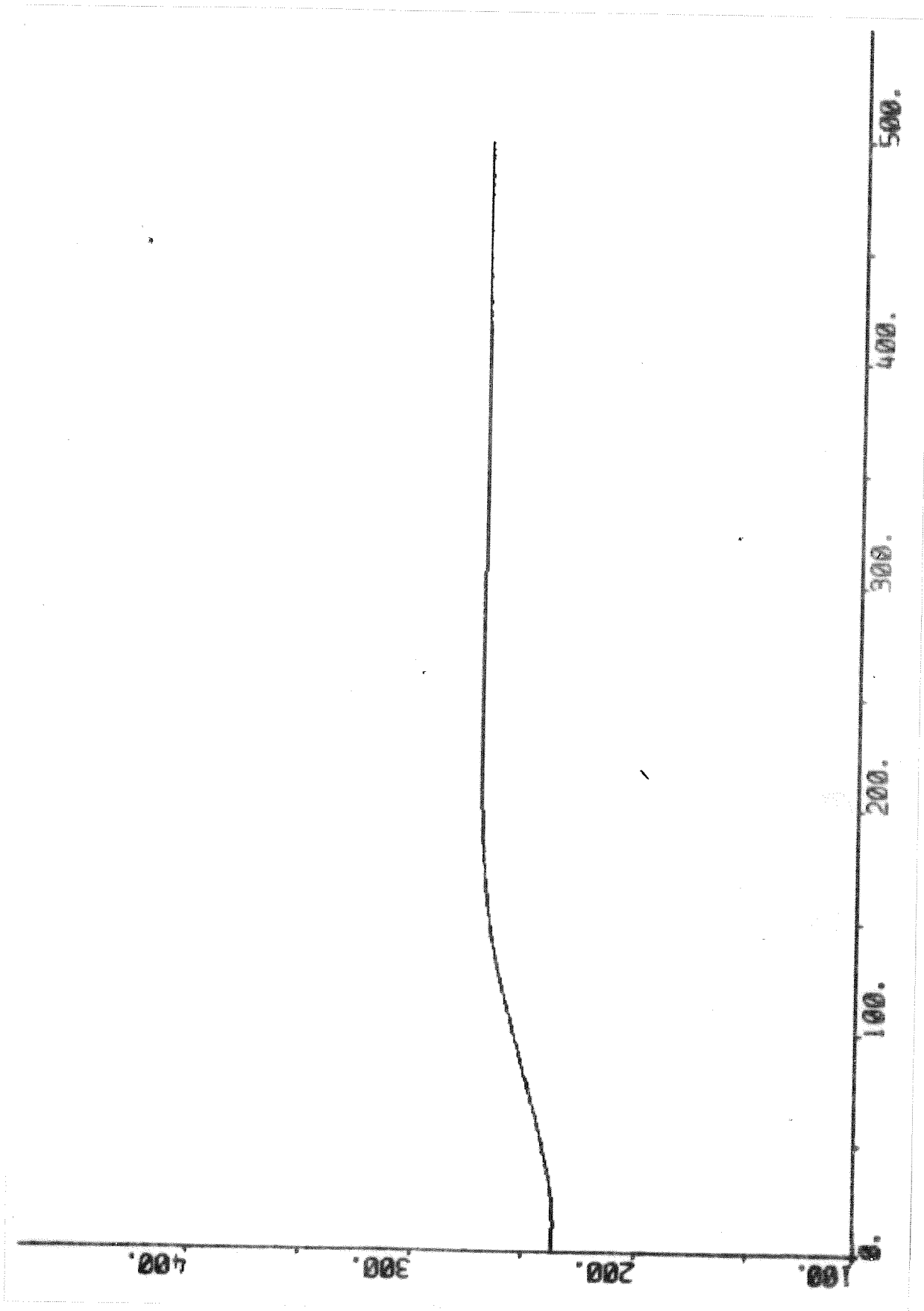


Fig. 14.20 - Response of the feedwater temperature after the economizer due to increase of output power in alert mode.

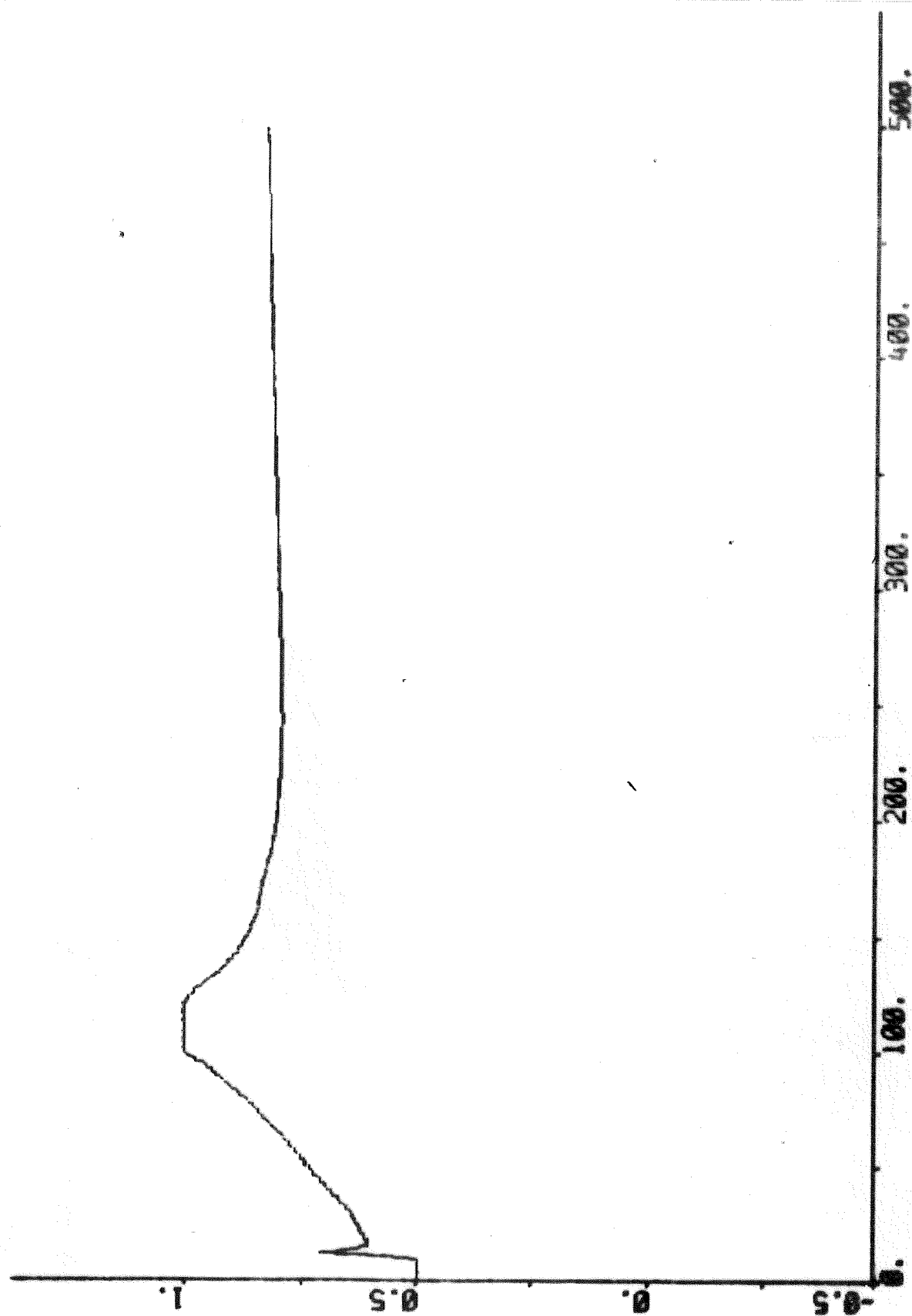


Fig. 14.21 - Response of the stroke of the control valve due to increase of output power in alert mode.

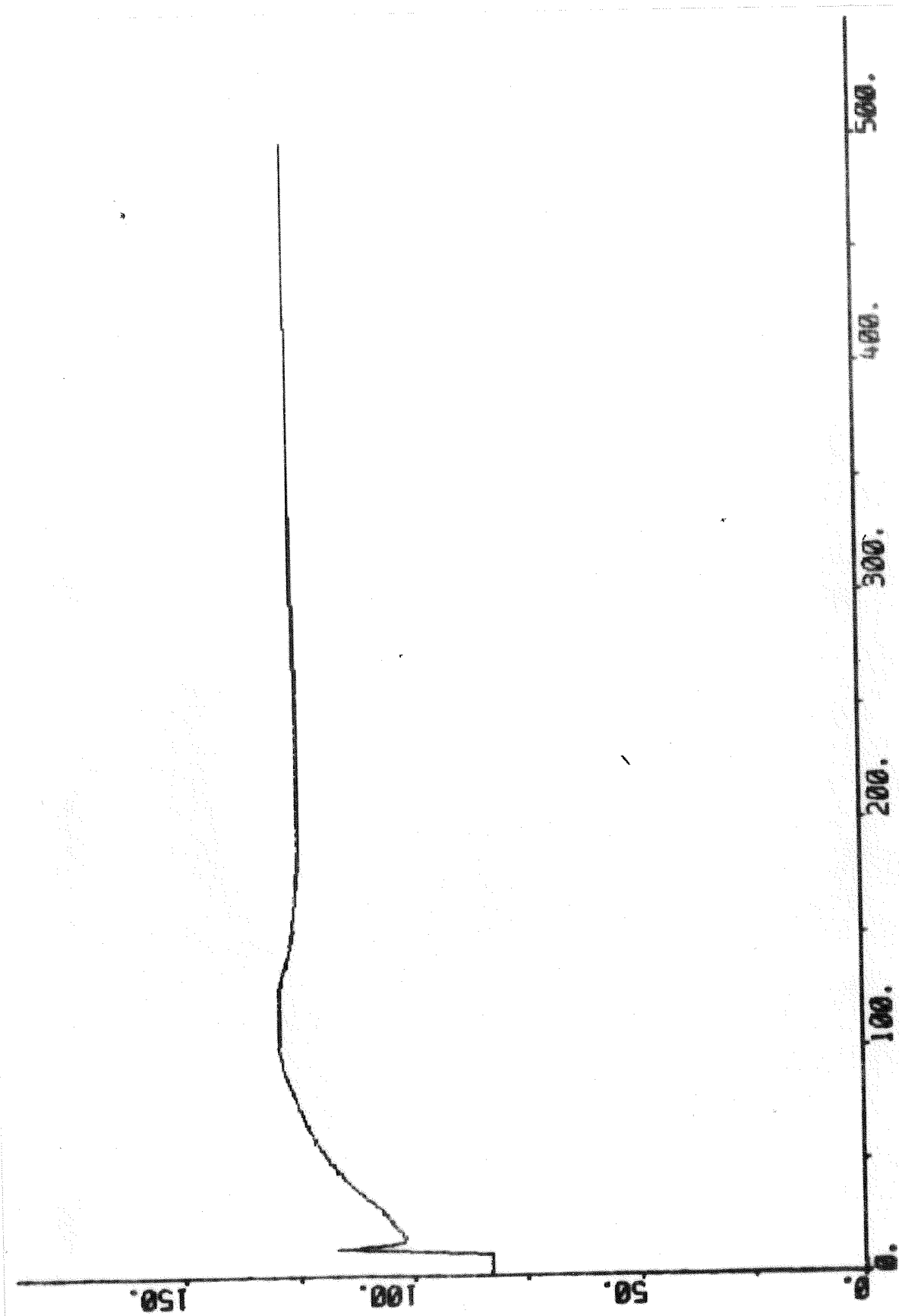


Fig. 14.22 - Response of the steam flow due to increase of output power in alert mode.

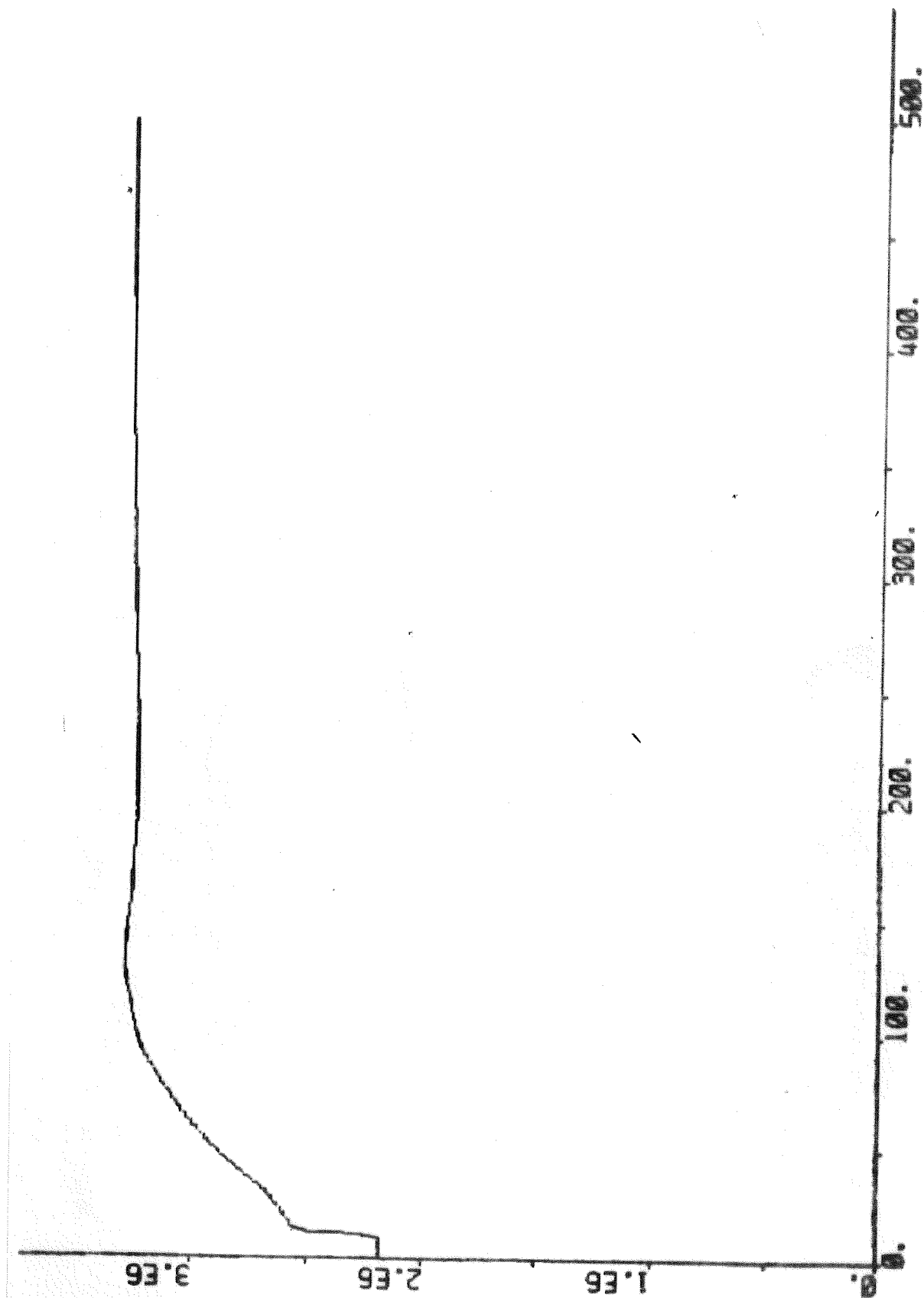


Fig. 14.23 - Response of the reheater steam pressure due to increase of output power in alert mode.

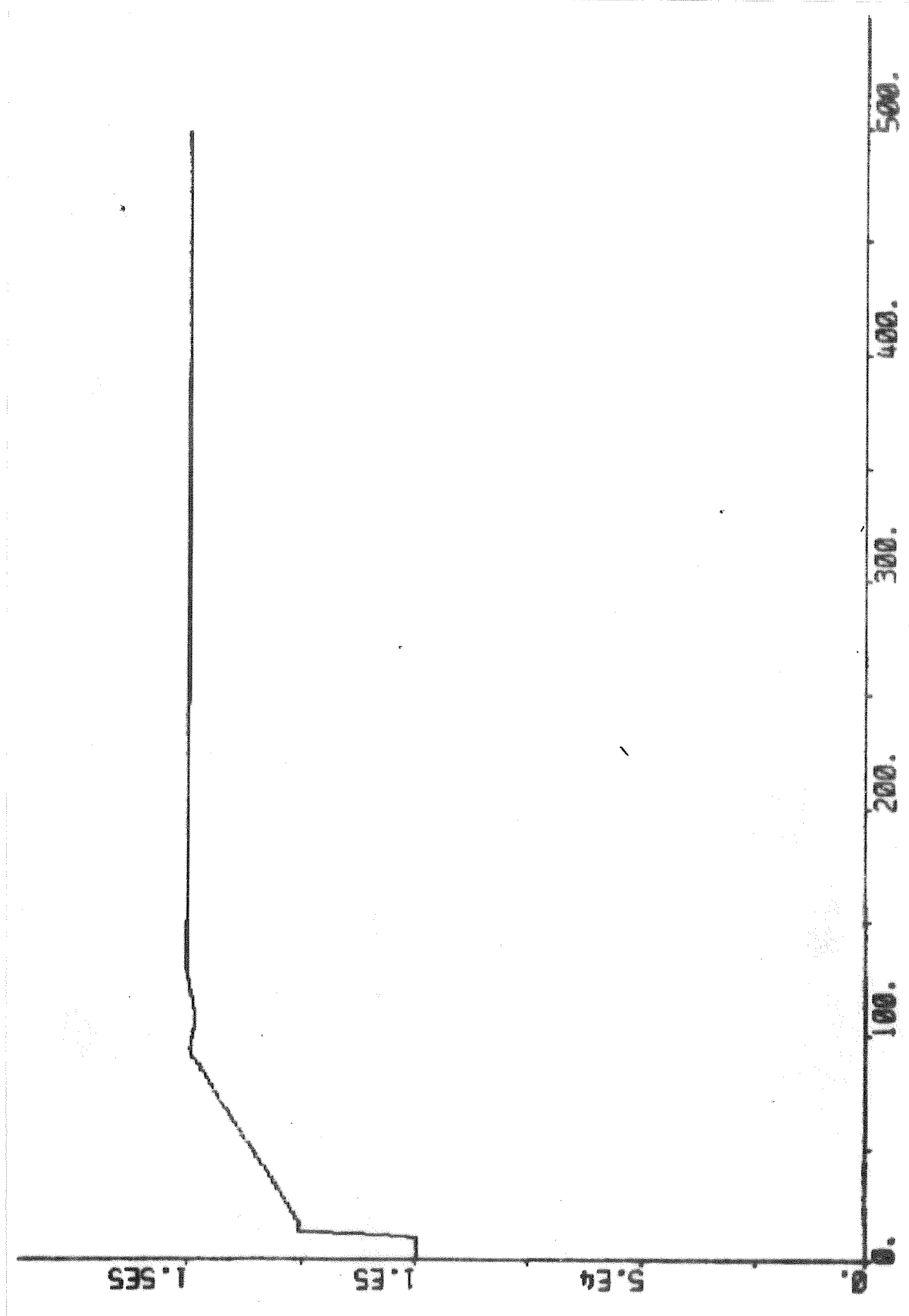


Fig. 14.24 - Response of the output power in alert mode.

## 15. DECREASE OF OUTPUT POWER IN ALERT MODE.

The performance of the control system when the output power is decreased in alert mode will be examined in this section. The output power was changed by changing the power demand signal from 150 MW (94%) to 100 MW (63%) at  $t = 10$  s. The power demand signal,  $s_{nslr}$  is input to the power demand setter (PDS), which generates the reference value of the output power. The reference value of the output power,  $N_{gs2r}$  is limited by the jump-and-rate circuit (PDS3) in Fig. 5.3. The numerical value of the jump of  $N_{gs2r}$  is 24 MW (15%) and the numerical value of the rate of  $N_{gs2r}$  is 19.2 MW/min (12%/min) in this case. The performance of the drum pressure loop, the drum level loop, the steam temperature loop and the output power loop will now be examined.

### The drum pressure loop.

The task of the drum pressure loop is to control the drum pressure by manipulating the fuel flow. The reference value of the drum pressure,  $p_{ds2r}$  is generated by the drum pressure reference setter (DPRS), which was described in Section 6. The reference value of the drum pressure is determined by the reference value of the output power,  $N_{gs2r}$  and by the mode (normal or alert) of the control system. In this case  $p_{ds2r}$  is constant and equal to  $145 \cdot 10^5$  Pa (97%). The steam flow (Fig. 15.22), the feedwater flow (Fig. 15.6) and the feedwater temperature after the economizer (Fig. 15.20) disturb the drum pressure loop. The mean density of the steam-water mixture in the riser tubes, the steam temperature after the primary superheater, the heat flows to the superheaters, to the reheater, and to the economizer are disturbed by the fuel flow variations. The fuel flow,  $w_{bol}$  is the output of the fuel flow servo (FFS), which was described in Section 7. The reference value of the fuel flow,  $w_{bolr}$  is determined by the drum pressure controller (DPC), which was described in Section 7. The inputs to the DPC are  $p_{ds2r}$  and its derivative,  $s_{bolt}$ , the drum pressure,  $p_{ds2}$ , and the steam flow,  $w_{ts1}$ . The block diagram of the DPC is



given in Fig. 7.1. The rate-of-change of the fuel flow is limited in the FFS. The limits are parameters,  $w_{bolo}$  and  $w_{bols}$  of the first nonlinear block in Fig. 7.2. The numerical value of  $w_{bolo}$  and  $w_{bols}$  are both  $0.1 \text{ kg/s}^2$  (60%/min).

The response of the fuel flow is shown in Fig. 15.1. The fuel flow decreases linearly for  $10 < t < 35 \text{ s}$  due to the limited rate of change of the fuel flow. The fuel flow is at most  $1 \text{ kg/s}$  (12%) lower than the final value. The fuel flow has reached its final value at  $t = 450 \text{ s}$ . The effect of the feedforward term from the steam flow is clearly visible for  $50 < t < 150 \text{ s}$ . (Compare Fig. 15.22 which shows the steam flow.)

The response of the drum pressure is shown in Fig. 15.2. The drum pressure increases for  $10 < t < 35 \text{ s}$  due to the rapid decrease of the steam flow. The fuel flow is decreased as fast as possible during the increase of the drum pressure. The maximum drum pressure error is  $3 \cdot 10^5 \text{ Pa}$  (2%). The maximum rate of change of the drum pressure is  $6 \cdot 10^5 \text{ Pa/min}$  (4%/min). The drum pressure reaches the final value at  $t = 350 \text{ s}$  without any undershoot.

The response of the steam pressure before the control valve is shown in Fig. 15.3. The steam pressure increases  $8 \cdot 10^5 \text{ Pa}$  (5%) at  $t = 10 \text{ s}$  due to the decreased steam flow (Fig. 15.22). The decreased steam flow decreases the pressure drop in the superheaters due to friction losses. The steam flow is changed by a factor 0.64 and the friction losses by a factor 0.41.

The response of the steam temperature after the primary superheater is shown in Fig. 15.4. The steam temperature variation is about  $3^\circ\text{C}$ . The steam temperature increases for  $10 < t < 40 \text{ s}$  due to the decreased steam flow (Fig. 15.22) and the increased steam temperature before the primary superheater with no corresponding decrease of the heat flow to the primary superheater. The steam temperature before the primary superheater is determined by the drum pressure (Fig. 15.2). The heat flow to the primary superheater is roughly proportional to the fuel flow (Fig. 15.1).

Properties: The steam flow is the most severe disturbance of the drum pressure loop. The steam flow and the derivative of the reference value of the drum pressure influence the fuel flow through the feedforward terms. The effects of the other disturbances are reduced by feedback. The limited rate of change of the fuel flow deteriorates the performance of the drum pressure loop for  $10 < t < 35$  s. This must, however, be accepted because of the restrictions of the burner equipment. The maximum drum pressure error is  $3 \cdot 10^5$  Pa (2%).

### The drum level loop.

The task of the drum level loop is to control the drum level,  $z_{dl4}$  by manipulating the feedwater control valve. The reference value of the drum level,  $z_{dl4r}$  is constant. The steam flow (Fig. 15.22) and the fuel flow (Fig. 15.1) disturb the drum level loop. The drum level loop disturbs the feedwater temperature. If the drum level is too high there is a danger that water will reach the turbine. If the drum level is too low there is a danger that the riser tubes will be damaged due to insufficient cooling. The feedwater flow,  $w_{fw5}$  is the output of the feedwater servo (FWS), which was described in Section 8. The reference value of the feedwater flow,  $w_{fw5r}$  is determined by the drum level controller (DLC), which was described in Section 8. The inputs to the DLC are  $z_{dl4r}$ ,  $z_{dl4}$  and the steam flow,  $w_{ts1}$ . The block diagram of the DLC is given in Fig. 8.1. The rate of change of the stroke of the feedwater valve is limited in the feedwater servo (FWS). The limits are parameters,  $s_{ww2o}$  and  $s_{ww2s}$  of the first nonlinear block in Fig. 8.2. The numerical values of  $s_{ww2o}$  and  $s_{ww2s}$  are both 5%/s.

The response of the stroke of the feedwater valve is shown in Fig. 15.5. The valve opening has to be decreased in order to decrease the feedwater flow. The valve is closing for  $10 < t < 20$  s due to the feedforward from the steam flow (Fig. 14.22). The valve is opening for  $20 < t < 35$  s due to the feedback from the

drum level. The valve is finally closing for  $t > 35$  s due to the feedforward from the steam flow and the feedback from the drum level.

The response of the feedwater flow is shown in Fig. 15.6. The response of the feedwater flow is similar to the response of the stroke of the feedwater valve. The response of the feedwater flow is also similar to the response of the steam flow (Fig. 15.22). The effect of the changing mean density of the steam-water mixture in the drum system is visible for  $10 < t < 120$  s. The feedwater flow is at most 15 kg/s (10%) higher than the steam flow.

The response of the drum level is shown in Fig. 15.7. The shrink phenomenon decreases the drum level 6 cm at  $t = 30$  s. The drum level response looks oscillatory but the variations are mainly due to the disturbances from the steam flow (Fig. 15.22). The drum level has returned to its reference value at  $t = 160$  s.

The response of the drum water temperature is shown in Fig. 15.8. The rate of change of drum water temperature determines the thermal stresses of the drum material. The variation of drum water temperature is less than  $2^{\circ}\text{C}$  and the rate of change is less than  $2^{\circ}\text{C}/\text{min}$ . This is less than can be predicted from the rate of change of drum pressure.

Properties: The steam flow is the most severe disturbance of the drum level loop in this case. The control of the drum level is difficult due to the shrink-and-swell phenomenon. The steam flow influences the feedwater flow through the feedforward term. The effects of the other disturbances are reduced by feedback. The maximum drum level error is 6 cm.

### The steam temperature loop.

The task of the steam temperature loop is to control the steam temperature after the tertiary superheater,  $T_{ts2}$  by manipulating the first and the second attemperator spray flow valves. The reference value of the steam temperature after the tertiary superheater,  $T_{ts2r}$  is constant. The heat flows to the secondary and tertiary superheaters, the steam temperature after the primary superheater (Fig. 15.4), and the steam flow (Fig. 15.22) disturb the steam temperature loop. The heat flows to the secondary and tertiary superheaters are both approximately proportional to the fuel flow (Fig. 15.1). The specific fuel consumption is reduced if the steam temperature after the tertiary superheater is increased. The steam temperature is limited by the properties of the superheater material. The steam temperature before the secondary superheater,  $T_{ss1}$  is the output of the secondary superheater steam temperature servo (SSSTS), which was described in Section 9. The steam temperature before the tertiary superheater,  $T_{ts1}$  is the output of the tertiary superheater steam temperature servo (TSSTS), which was described in Section 9. The reference value of the steam temperature before the tertiary superheater,  $T_{ts1r}$  is determined by the tertiary superheater steam temperature controller (TSSTC), which was described in Section 9. The inputs to the TSSTC are  $T_{ts2r}$ ,  $T_{ts2}$ , the steam flow,  $w_{ts1}$ , and the fuel flow,  $w_{bol}$ . The block diagram of the TSSTC is given in Fig. 9.1. The reference value of the steam temperature before the secondary superheater,  $T_{ss1r}$  is determined by the secondary superheater steam temperature controller (SSSTC), which was described in Section 9. The inputs to the SSSTC are  $T_{ss2r}$ ,  $T_{ss2}$ ,  $w_{ts1}$ , and  $w_{bol}$ . The rate of change of the stroke of the second attemperator spray flow valve is limited in the TSSTS. The limits are parameters,  $s_{tw2o}$  and  $s_{tw2s}$  are both 4%/s. The rate of change of the stroke of the first attemperator spray flow valve is limited in the SSSTS. The limits are parameters,  $s_{sw2o}$  and  $s_{sw2s}$  of the first nonlinear block in Fig. 9.4. The numerical values of  $s_{sw2o}$  and  $s_{sw2s}$  are both 4%/s. The difference between  $T_{ss2r}$  and  $T_{ts1r}$  is a parameter,  $g_{sw2b}$  of the SSSTC. The numerical value of  $g_{sw2b}$

is  $30^{\circ}\text{C}$  and is chosen so that the second attemperator spray flow valve is approximately halfopen. This means that the steam temperature before the tertiary superheater can be changed rapidly in both directions.

The response of the stroke of the first attemperator spray flow valve is shown in Fig. 15.9. The valve opens for  $10 < t < 25$  s due to the decreasing steam flow through the secondary superheater without corresponding decrease of the heat flow. The valve closes for  $25 < t < 110$  s due to the decreasing heat flow to the secondary superheater. The valve opens again for  $t > 110$  s due to the increasing heat flow to the secondary superheater.

The response of the spray flow of the first attemperator is shown in Fig. 15.10. The spray flow follows the stroke of the valve fairly well. The final value of the spray flow is 68% of the initial value but the final value of the stroke is approximately the same as the initial value. The decrease of the spray flow is due to the reduced pressure drop in the economizer and the primary superheater.

The response of the steam temperature before the secondary superheater is shown in Fig. 15.11. The steam temperature is decreased for  $10 < t < 25$  s in order to compensate for the decreased steam flow. The steam temperature is increased for  $25 < t < 110$  s in order to compensate for the decreasing heat flow. The steam temperature is finally increased for  $t > 110$  s in order to compensate for the increased heat flow.

The response of the steam temperature after the secondary superheater is shown in Fig. 15.12. The steam temperature increases about  $2^{\circ}\text{C}$  for  $10 < t < 20$  s due to the decreasing steam flow. The steam temperature then decreases for  $20 < t < 45$  s due to the decreasing steam temperature before the secondary superheater and the decreasing heat flow to the secondary superheater.

The response of the stroke of the second attemperator spray flow valve is shown in Fig. 15.13. The valve is opening for  $10 < t < 20$  s due to the decreasing steam flow. The valve is closing for  $20 < t < 50$  s in order to compensate for the decreasing heat flow to the tertiary superheater and the decreasing steam temperature after the secondary superheater. The valve is finally opening for  $t > 50$  s in order to compensate for the decreasing steam flow (Fig. 15.22).

The response of the spray flow of the second attemperator is shown in Fig. 15.14. The spray follows the stroke of the valve fairly well. The first peak of the spray flow at  $t = 10$  s is due to the rapid decrease of the steam flow at  $t = 10$  s (Fig. 15.22). The final value of the spray flow is about 61% of the initial value but the final value of the stroke of the valve is about 98% of the initial value. The decrease of the spray flow is due to the decreased pressure drop in the economizer, the primary and the secondary superheater.

The response of the steam temperature before the tertiary superheater is shown in Fig. 15.15. The steam temperature is decreased about  $10^{\circ}\text{C}$  for  $10 < t < 30$  s in order to compensate for the decreasing steam flow. The steam temperature is then increased for  $t > 30$  s in order to compensate for the decreasing heat flow.

The response of the steam temperature after the tertiary superheater is shown in Fig. 15.16. The maximum steam temperature error is less than  $3^{\circ}\text{C}$ .

Properties: The steam flow and the fuel flow are the most severe disturbances of the steam temperature loop. The steam flow and the fuel flow influence the spray flows by feedforward terms. The effects of the other disturbances are reduced by feedback. The maximum steam temperature error is less than  $3^{\circ}\text{C}$ . The spray flows are extracted after the feedwater valve, which means that the spray flows increase with the steam flow. This increase of

gain counteracts the decrease of gain in the attenuators with the steam flow, which is an advantage.

### The output power loop.

The task of the output power loop is to control the output power,  $N_{gs2}$  by manipulating the steam control valve and the extraction steam valves. The reference value of the output power,  $N_{gs2r}$  is generated by the power demand setter (PDS), which was described in Section 5. A preliminary reference value of the output power,  $s_{nsl}$  is determined from the power demand signal,  $s_{nslr}$  in the first part of the power demand setter (PDS1). The block diagram of the PDS1 is given in Fig. 5.1. The  $s_{nslr}$  is modified with respect to the network-frequency in the second part of the power demand setter (PDS2). The block diagram of the PDS2 is given in Fig. 5.2. The  $N_{gs2r}$  is obtained from the third part of the power demand setter (PDS3); which limits the jump and the rate of  $N_{gs2r}$ . The block diagram of the PDS3 is given in Fig. 5.3. The steam pressure before the control valve,  $p_{ts2}$  (Fig. 15.3) and the steam temperature before the control valve,  $T_{ts2}$  (Fig. 15.16) disturb the output power loop. The superheated steam flow,  $w_{ts1}$  (Fig. 14.22), the reheated steam flow,  $w_{rs2}$ , and the extraction steam flows,  $w_{hs2}$ ,  $w_{is2}$ ,  $w_{is4}$ ,  $w_{is6}$ ,  $w_{is8}$ ,  $w_{ls2}$ , and  $w_{ls4}$  are disturbed by the output power loop. The stroke of the control valve is the output of the control valve servo (CVS), which was described in Section 10. The reference value of the stroke of the control valve,  $s_{vs2r}$  is determined by the turbine power controller (TPC), which was described in Section 10. The inputs to the TPC are  $N_{gs2r}$  and  $N_{gs2}$ . The block diagram of the TPC is given in Fig. 10.1. The strokes of the low-pressure preheater extraction valves are the outputs of the low-pressure preheater servo (LPPS), which was described in Section 10. The reference value of the strokes of the low-pressure preheater extraction valves,  $s_{fs7r}$  is determined by the low-pressure preheater controller (LPPC), which was described in Section 10. The input to the LPPC are  $N_{gs2r}$ , the reference value of

the deaerator steam pressure,  $p_{as2r}$ , and the deaerator steam pressure,  $p_{as2}$ . The block diagram of the LPPC is given in Fig. 10.5. The strokes of the high-pressure preheater extraction valves are the outputs of the high-pressure preheater servo (HPPS), which was described in Section 10. The reference value of the strokes of the high-pressure preheater extraction valves,  $s_{fs2r}$  is determined by the high-pressure preheater controller (HPPC), which was described in Section 10. The input to the HPPC is  $N_{gs2r}$ . The block diagram of the HPPC is given in Fig. 10.3. The rate of change of the stroke of the control valve is limited in the CVS. The limits are parameters,  $s_{vs2o}$  and  $s_{vs2s}$  of the first nonlinear block in Fig. 10.2. The numerical values of  $s_{vs2o}$  and  $s_{vs2s}$  are 20%/s and 200%/s respectively. The rates of change of the strokes of the high-pressure extraction steam flow valves are limited in the HPPS. The limits are parameters,  $s_{fs2o}$  and  $s_{fs2s}$  of the first nonlinear block in Fig. 10.4. The numerical values of  $s_{fs2o}$  and  $s_{fs2s}$  are both 100%/s. The rates of change of the strokes of the low-pressure extraction steam flow valves are limited in the LPPS. The limits are parameters,  $s_{fs7o}$  and  $s_{fs7s}$  of the first nonlinear block in Fig. 10.6. The numerical values of  $s_{fs7o}$  and  $s_{fs7s}$  are both 100%/s.

The response of the strokes of the low-pressure preheater extraction valves are shown in Fig. 15.17. The opening of the valves are increased for  $10 < t < 20$  s due to the decreasing reference value of the output power. The opening of the valves are then decreased due to the feedback from the deaerator pressure. The reference value of the output power reaches its final value at  $t = 90$  s, which is clearly visible in the response of the strokes.

The response of the strokes of the high-pressure preheater extraction valves are shown in Fig. 15.18. The opening of the valves are increased for  $10 < t < 15$  s due to the feedforward term from the decreasing reference value of the output power. The opening of the valve is then decreasing with a time constant of about 30 s. The target value is higher than 0.5 and is determined by the rate of the reference value of the output power. The reference value of the output power reaches its final value at  $t = 90$  s, which is



clearly visible in the response of the strokes.

The response of the feedwater temperature after the high-pressure preheater is shown in Fig. 15.19. The temperature decreases about  $20^{\circ}\text{C}$  due to the final decrease of extraction steam flows. The temporary opening of the extraction valves do not affect the feedwater temperature seriously. The low-pass filtering effect of the seven preheater stages are pronounced.

The response of the feedwater temperature after the economizer is shown in Fig. 15.20. The temperature decreases due to the decreasing fuel flow and due to the decreasing feedwater temperature after the high-pressure preheater. The final decrease of the feedwater temperature after the economizer is about  $20^{\circ}\text{C}$ .

The response of the stroke of the control valve is shown in Fig. 15.21. The valve opening is decreased rapidly for  $10 < t < 13$  s in order to decrease the output power rapidly. The valve opening is then decreased with a lower rate for  $20 < t < 90$  s in order to decrease the output power like a ramp. The output power loop has been tuned for fast response. This explains the peak in the response of the stroke of the control valve at  $t = 13$  s. This type of response may lead to unacceptable wear of the control valve and its servo. The wear can, however, be reduced by reducing the response rate. The fast response was chosen to demonstrate that it does not lead to severe interactions between the control loops.

The response of the steam flow is shown in Fig. 15.22. The response of the steam flow is similar to the response of the stroke of the control valve. The final value of the steam flow is about 66% of its initial value but the final value of the stroke of the control valve is about 61% of its initial value.

The response of the reheater steam pressure is shown in Fig. 15.23. The pressure is approximately proportional to the steam flow. The pressure responds, however, more slowly due to the mass storage in the reheater.

The response of the output power is shown in Fig. 15.24. The settling-time of the output power is about 3 s. The output power error is less than 1 MW for  $t > 15$  s. The output power has reached its final value within 90 s.

Properties: There are no severe disturbances of the output power loop in this case. The output power error is less than 1 MW for  $t > 15$  s. The response of the stroke of the control valve may lead to unacceptable wear of the control valve and its servo. The wear can be reduced by reducing the response rate of the output power loop. The high response rate has been chosen to demonstrate the performance of the control system.

### Conclusions.

The performance of the control system when the output power is decreased from 150 MW (94%) to 100 MW (63%) in alert mode has been investigated by simulation. In order to decrease the output power it is necessary to decrease both the steam flow and the fuel flow. The steam flow is the most severe disturbance of the drum pressure loop, the drum level loop, and the steam temperature loop. The fuel flow is a severe disturbance of the steam temperature loop. The influence of the steam flow and the fuel flow have been reduced by feedforward. The limited rate of change of the fuel flow deteriorates the performance of the drum pressure loop. The maximum drum pressure error is  $3 \cdot 10^5$  Pa (2%). The control of the drum level is difficult due to the shrink-and-swell phenomenon. The maximum drum level error is 6 cm. The limited capacity of the attemperators do not deteriorate the performance of the steam temperature loop in this case. The maximum steam temperature error is less than  $3^\circ\text{C}$ . The load dependent pressure drops in the economizer and the superheaters have been exploited in order to obtain load independent gains of the steam temperature servos. There are no severe disturbances of the output power loop in this case. The output power error is less than 1 MW for  $t > 15$  s. The output power loop has been tuned for fast response, which may cause unacceptable wear of the control valve

and its servo. The simulations show that even with such a tight loop there are no difficulties due to interaction with other loops.

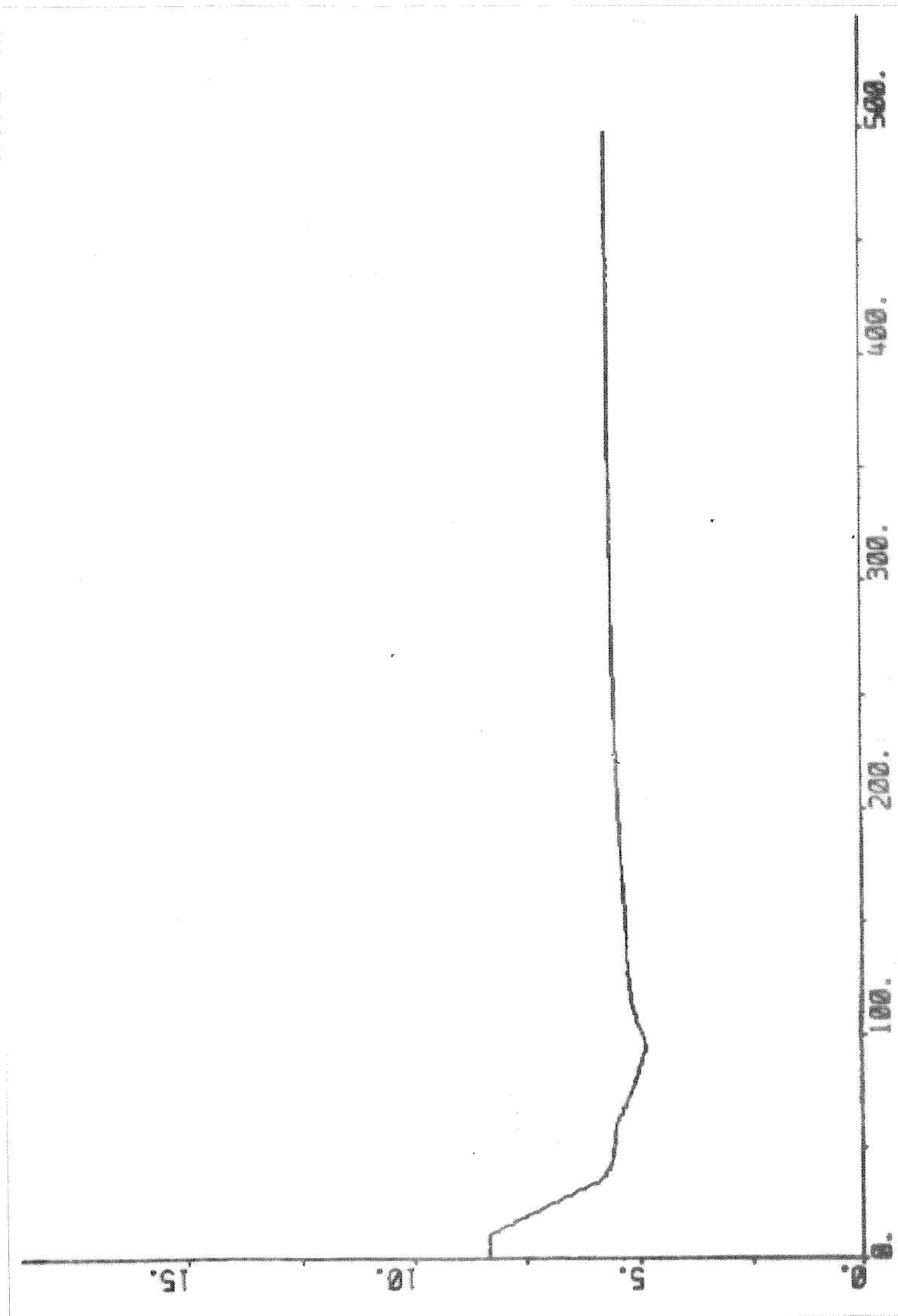


Fig. 15.1 - Response of the fuel flow due to decrease of output power in alert mode.

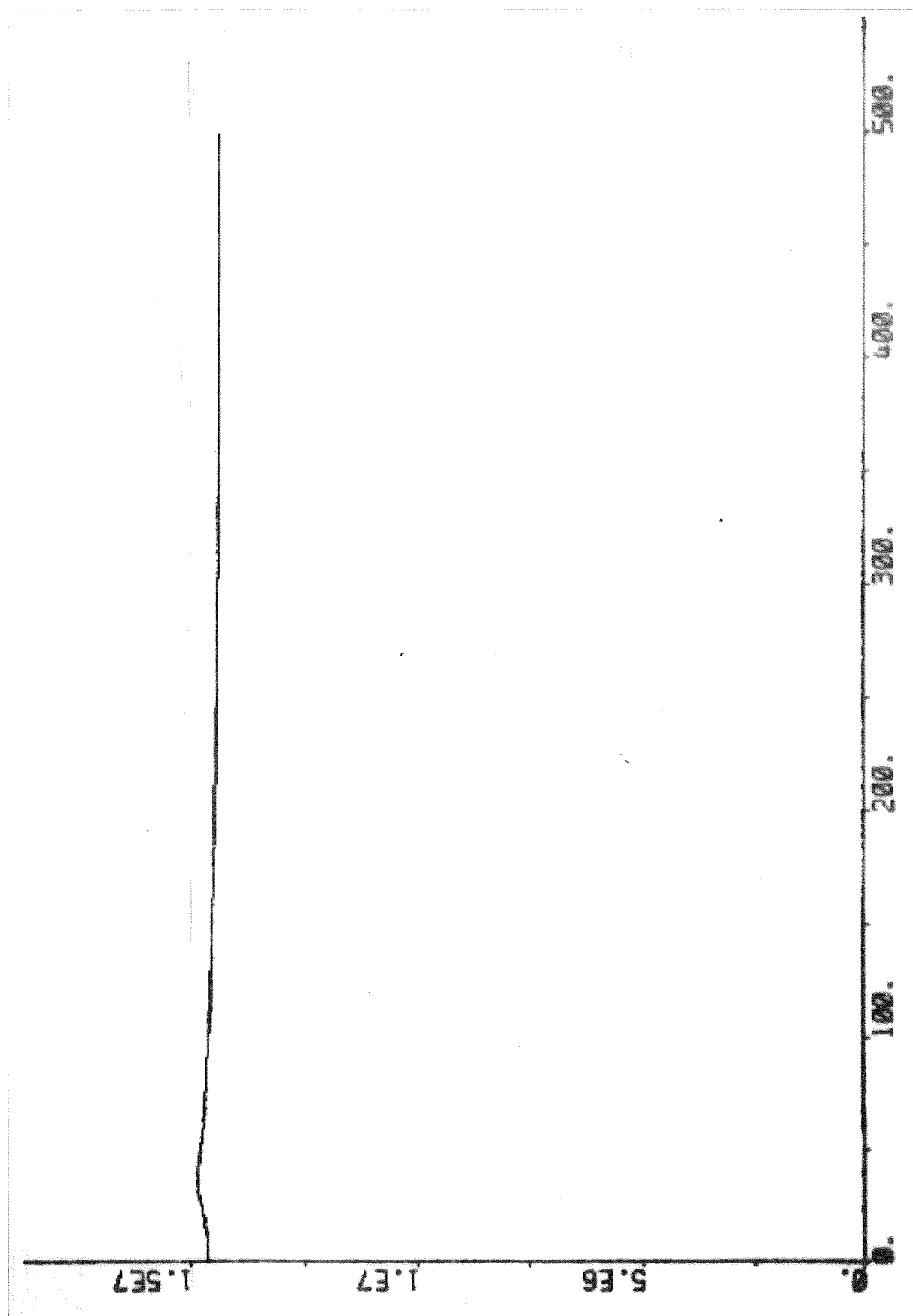


Fig. 15.2 - Response of the drum pressure due to decrease of output power in alert mode.

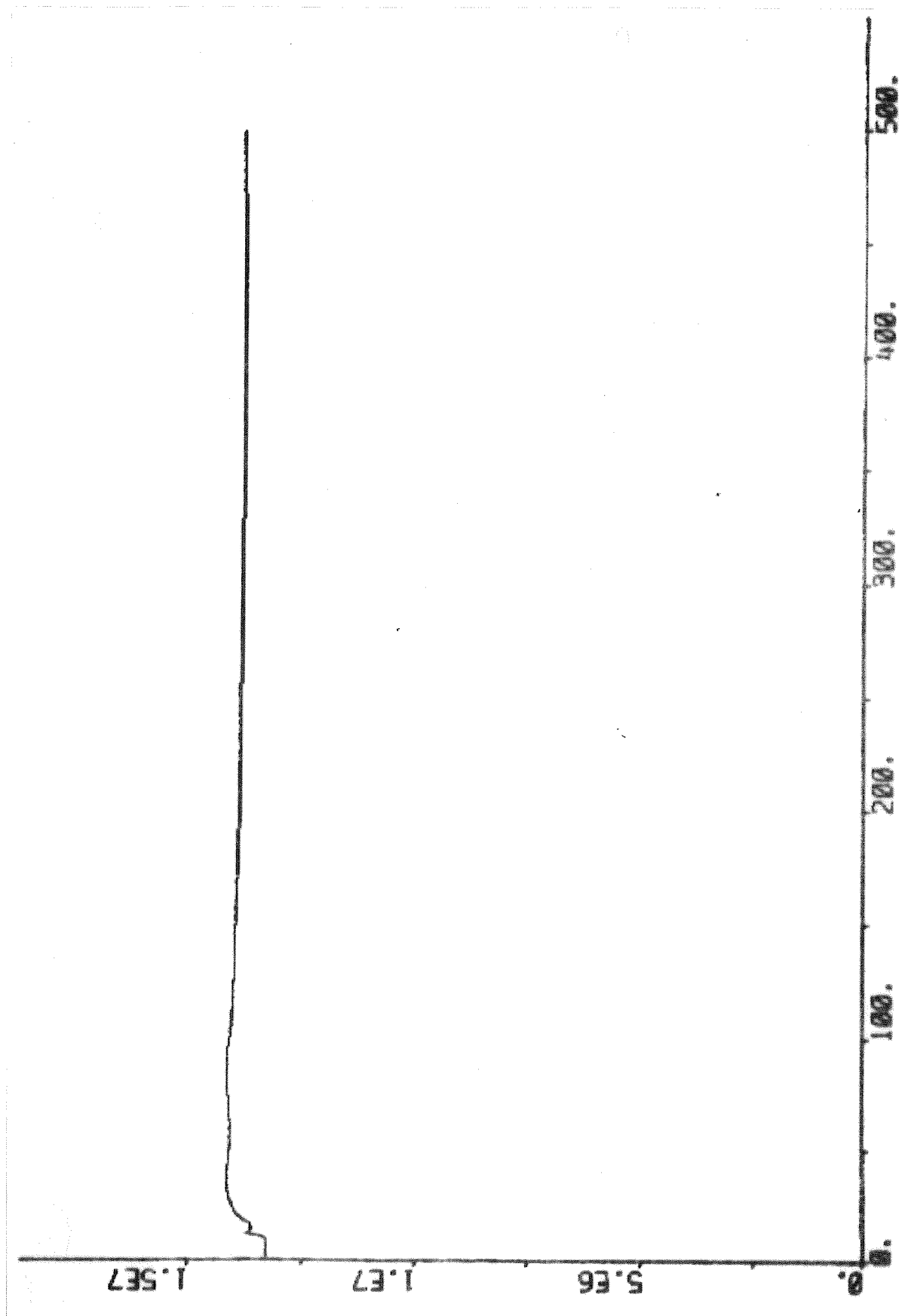


Fig. 15.3 - Response of the steam pressure before the control valve due to decrease of output power in alert mode.

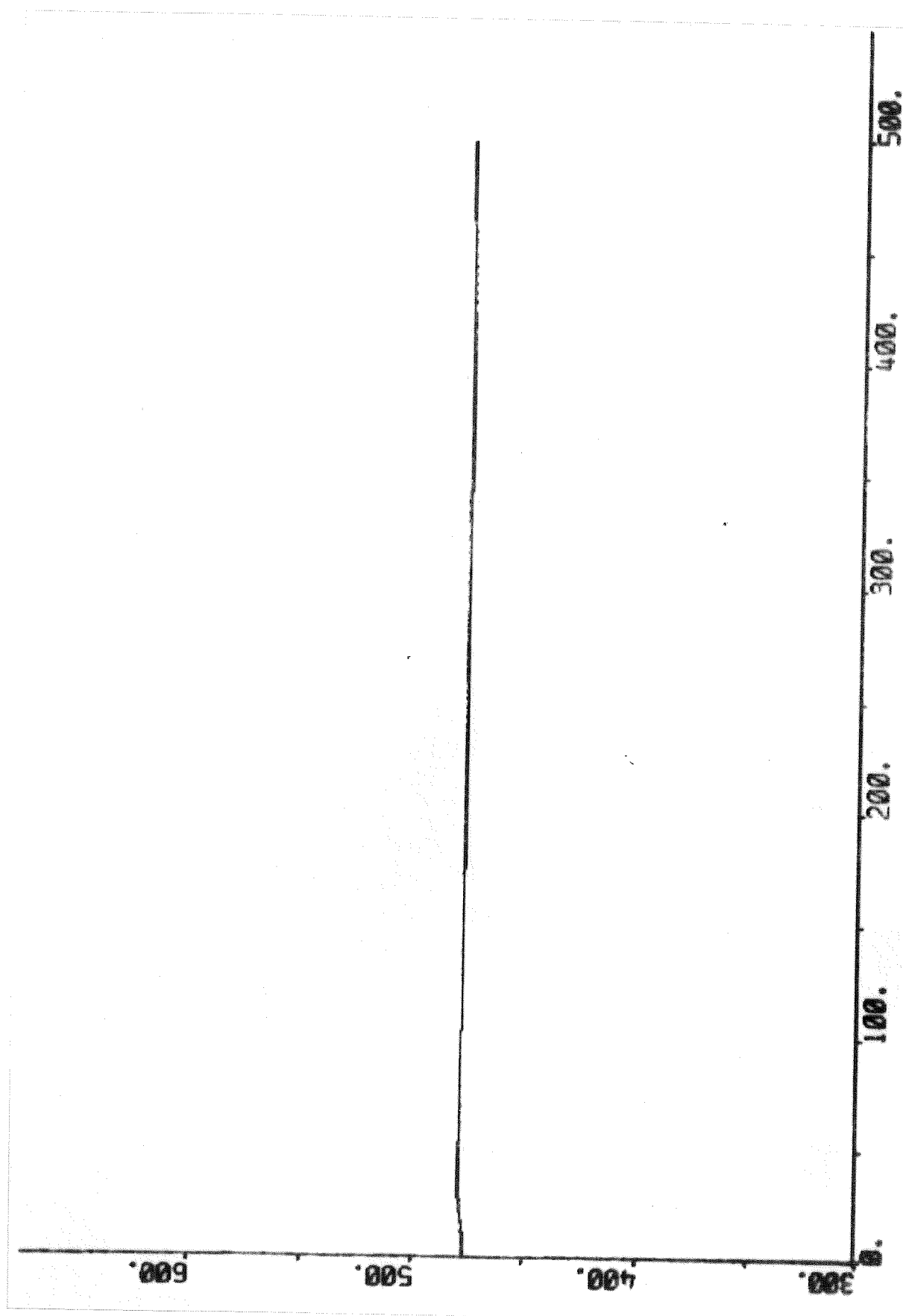


Fig. 15.4 - Response of the steam temperature after the primary superheater due to decrease of output power in alert mode.

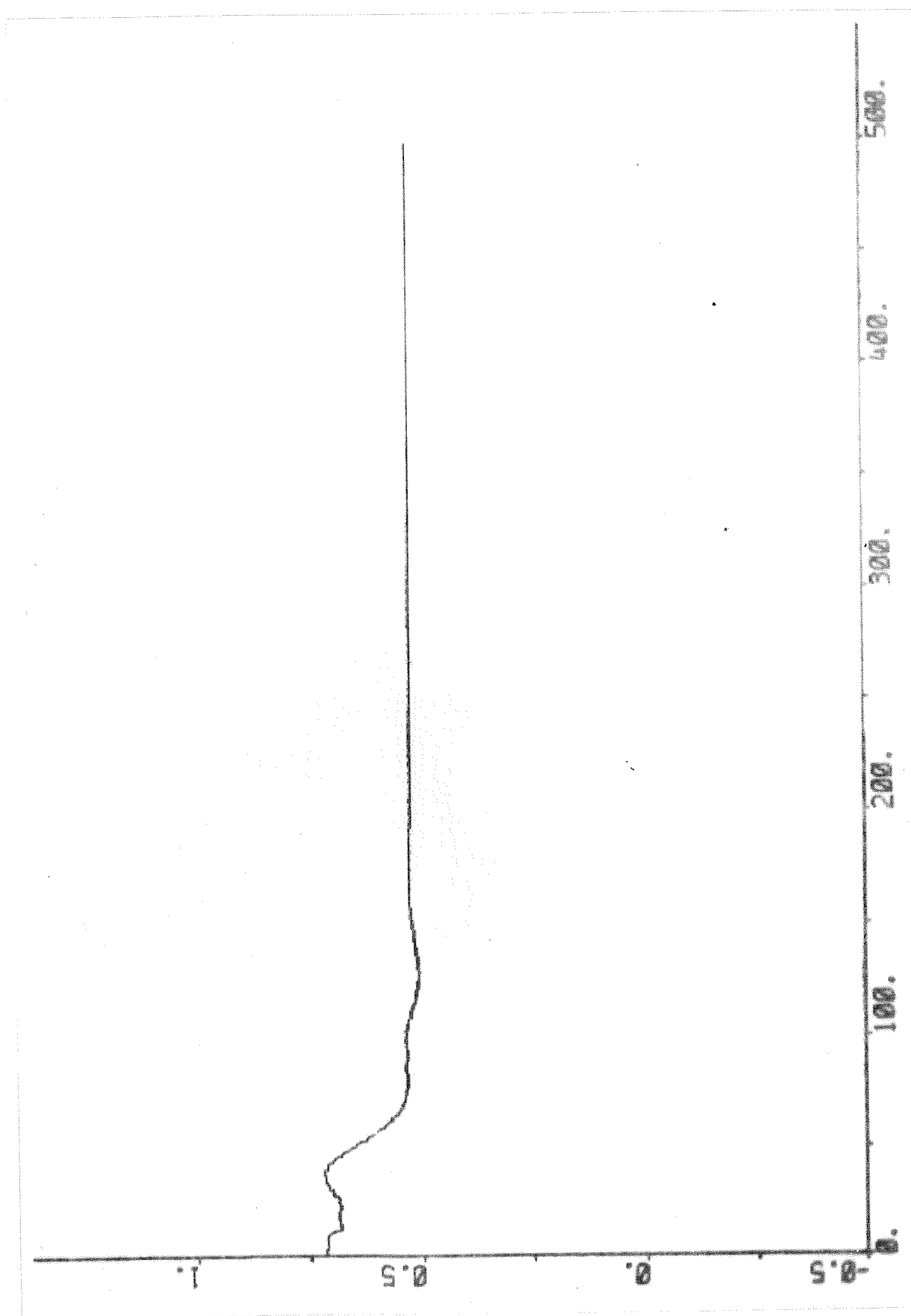


Fig. 15.5 - Response of the stroke of the feedwater valve due to decrease of output power in alert mode.



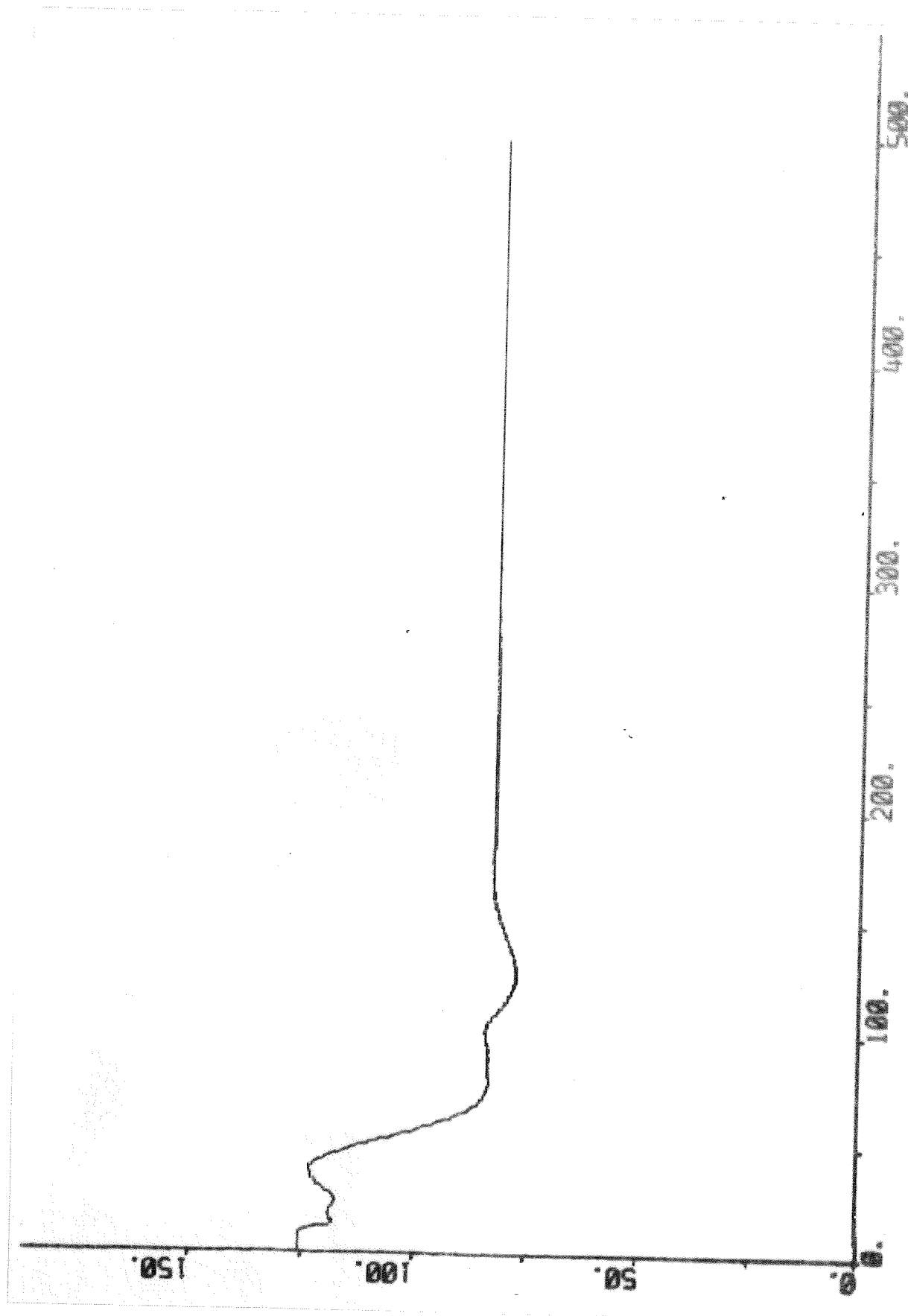


Fig. 15.6 - Response of the feedwater flow due to decrease of output power in alert mode.

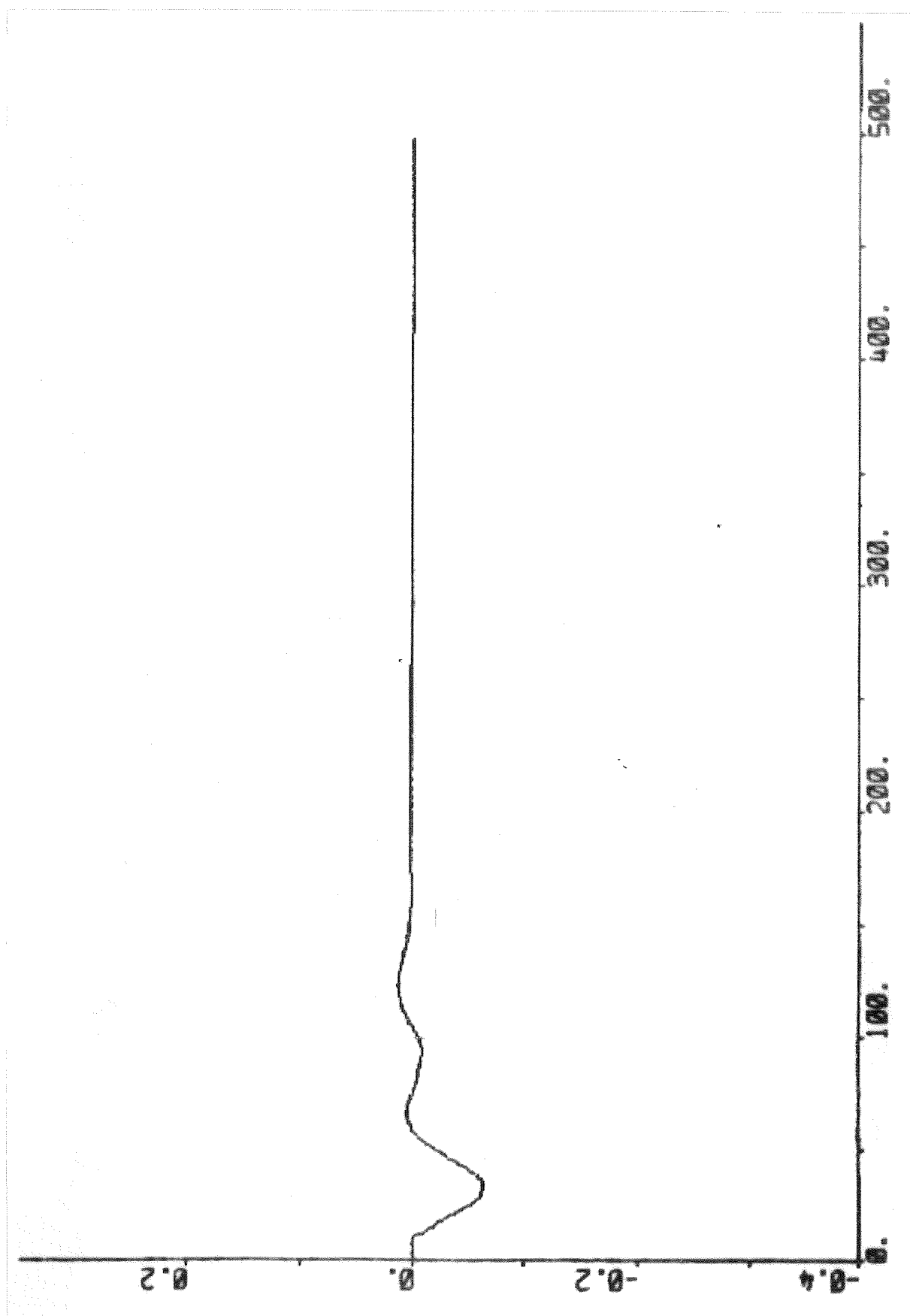


Fig. 15.7 - Response of the drum level due to decrease of output power in alert mode.

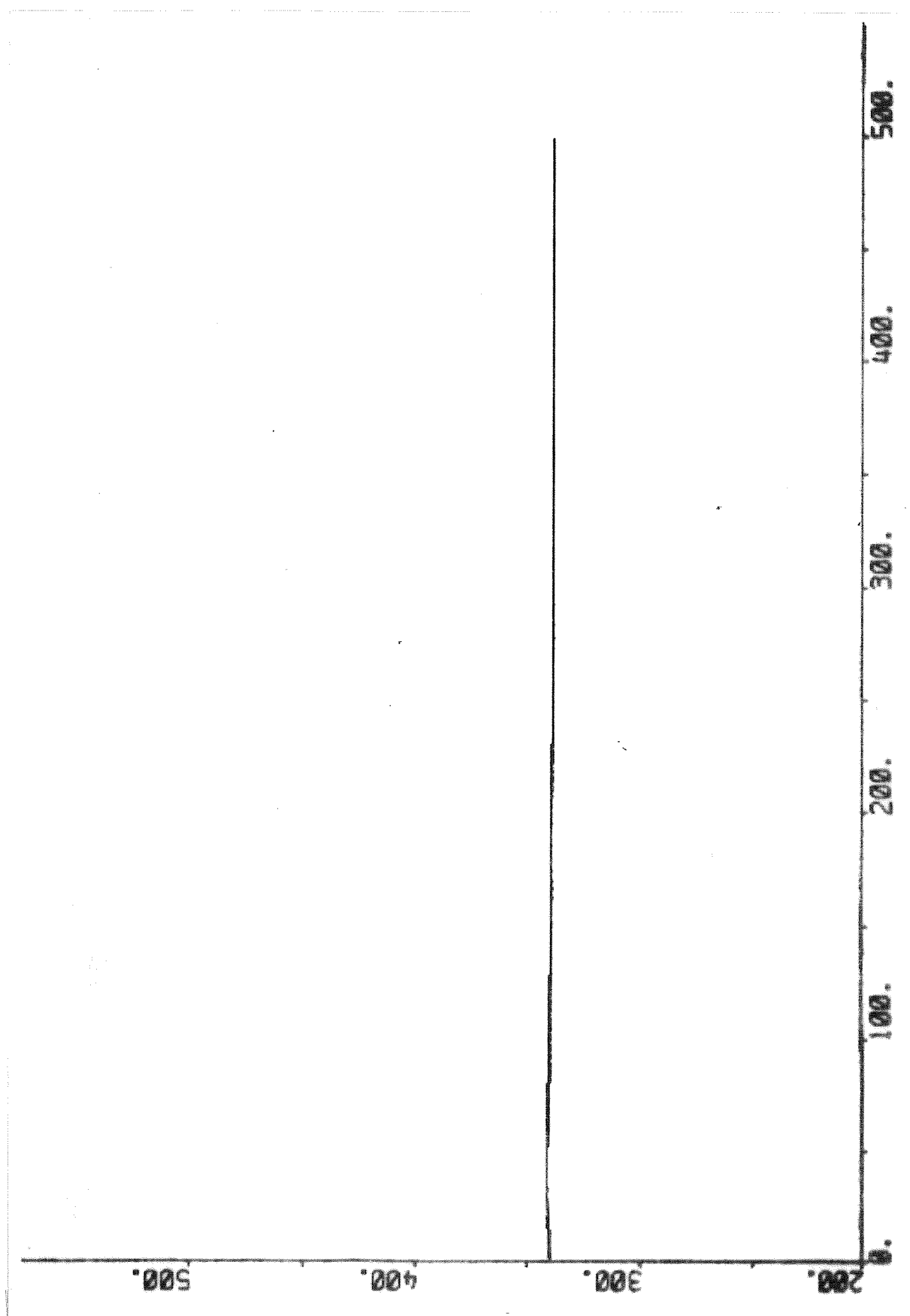


Fig. 15.8 - Response of the drum water temperature due to decrease of output power in alert mode.

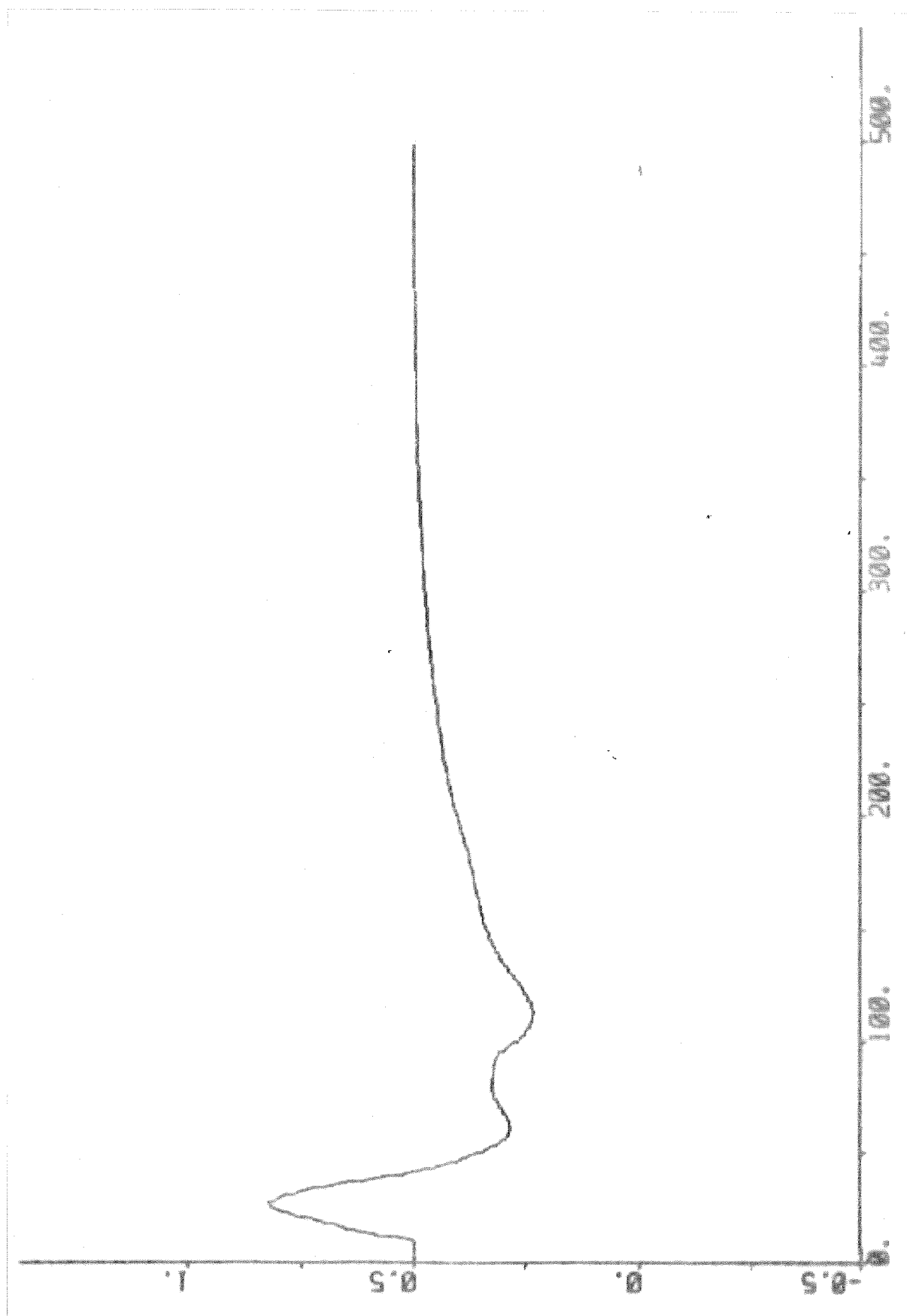


Fig. 15.9 - Response of the first attenuator spray flow valve due to decrease of output power in alert mode.

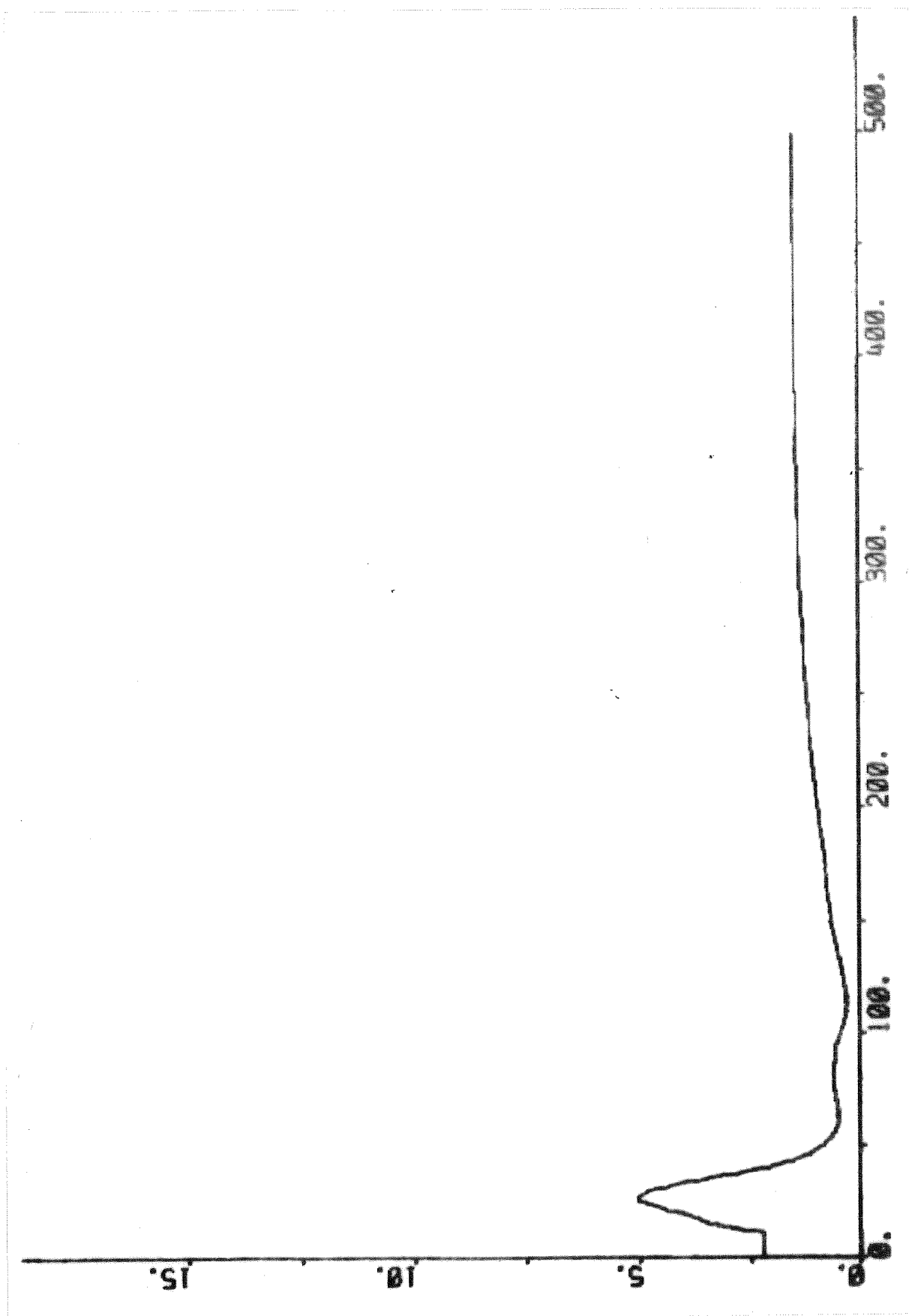


Fig. 15.10 - Response of the spray flow of the first attenuator due to decrease of output power in alert mode.

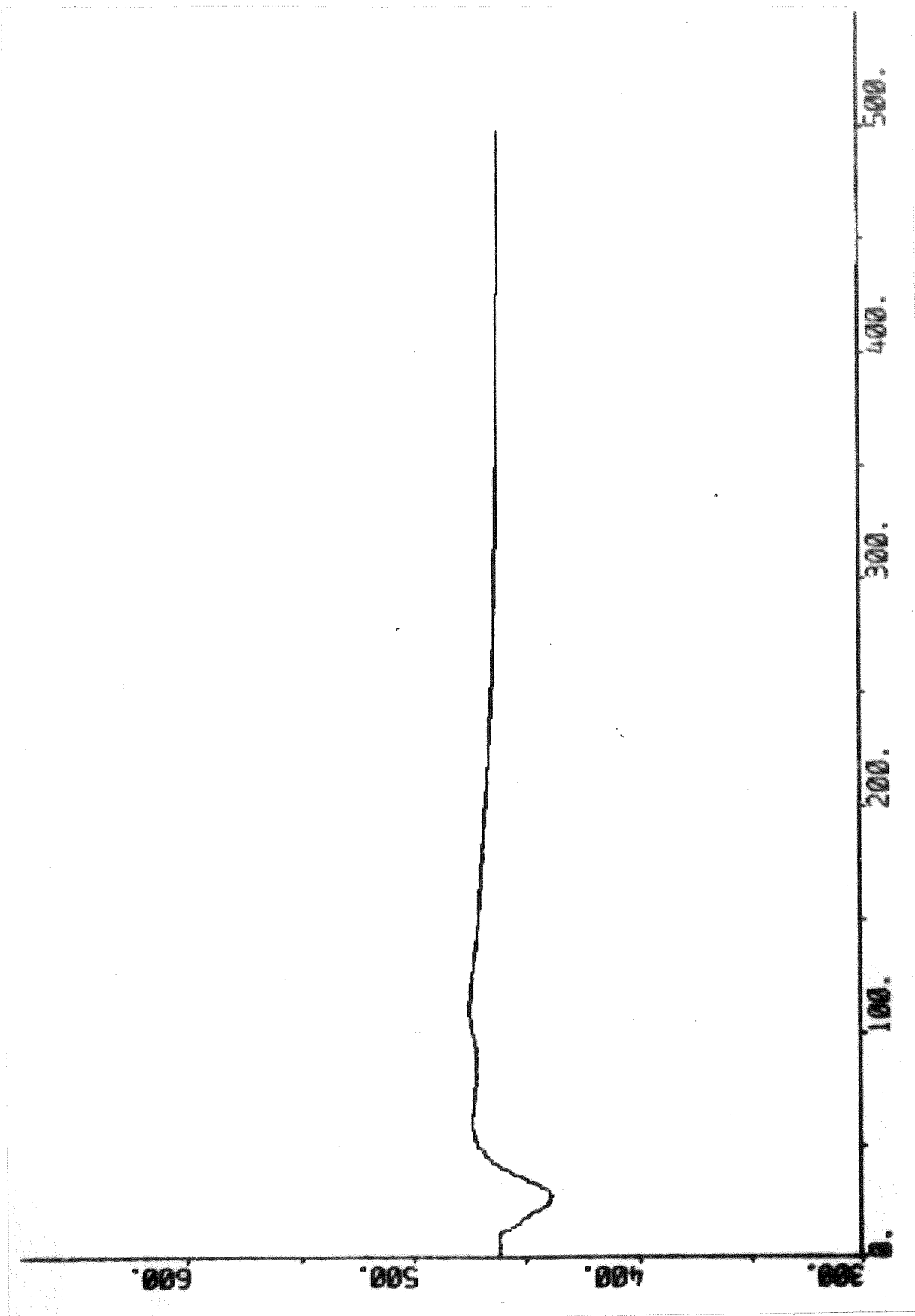


Fig. 15.11 - Response of the steam temperature before the secondary superheater due to decrease of output power in alert mode.

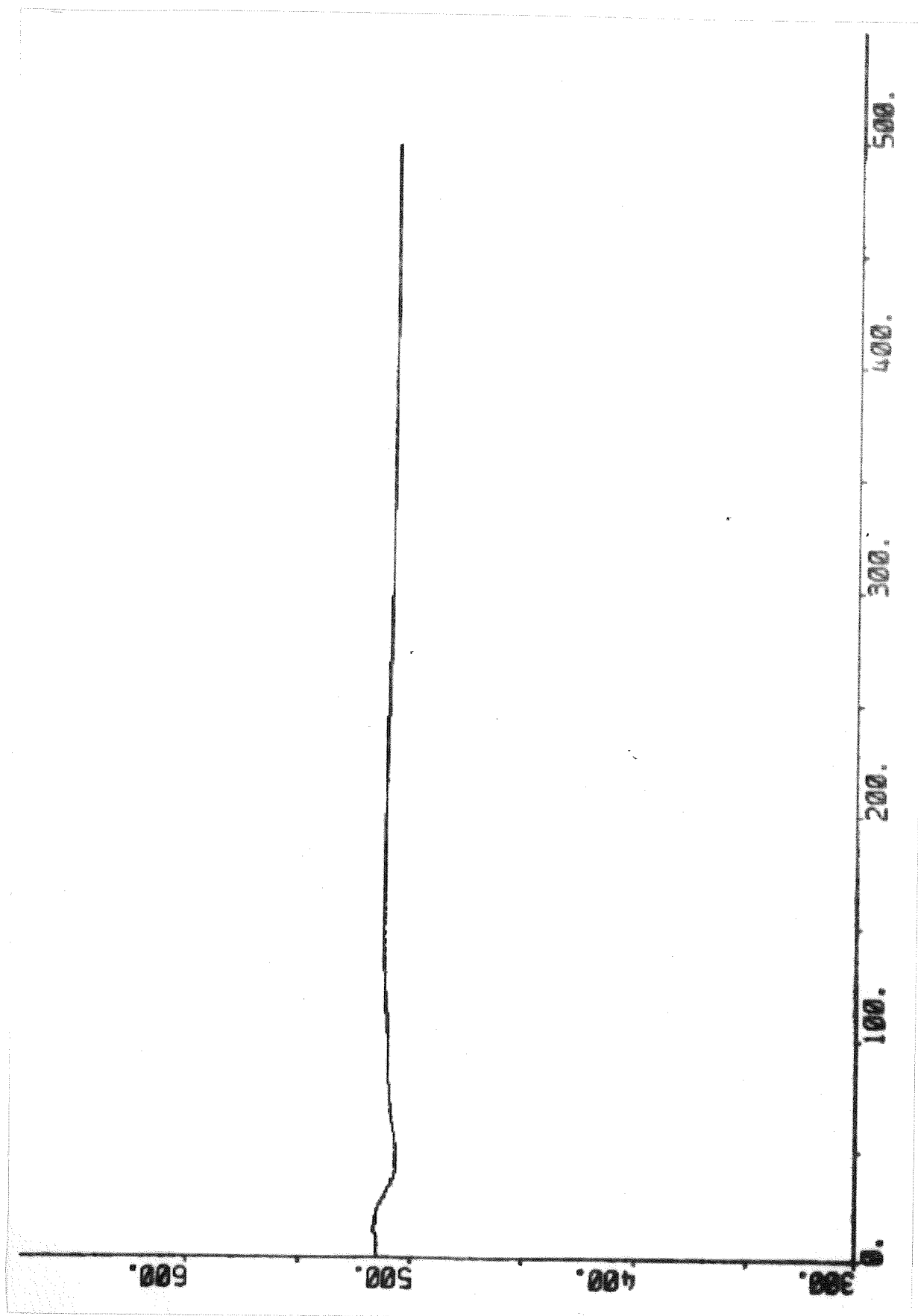


Fig. 15.12 - Response of the steam temperature after the secondary superheater due to decrease of output power in alert mode.

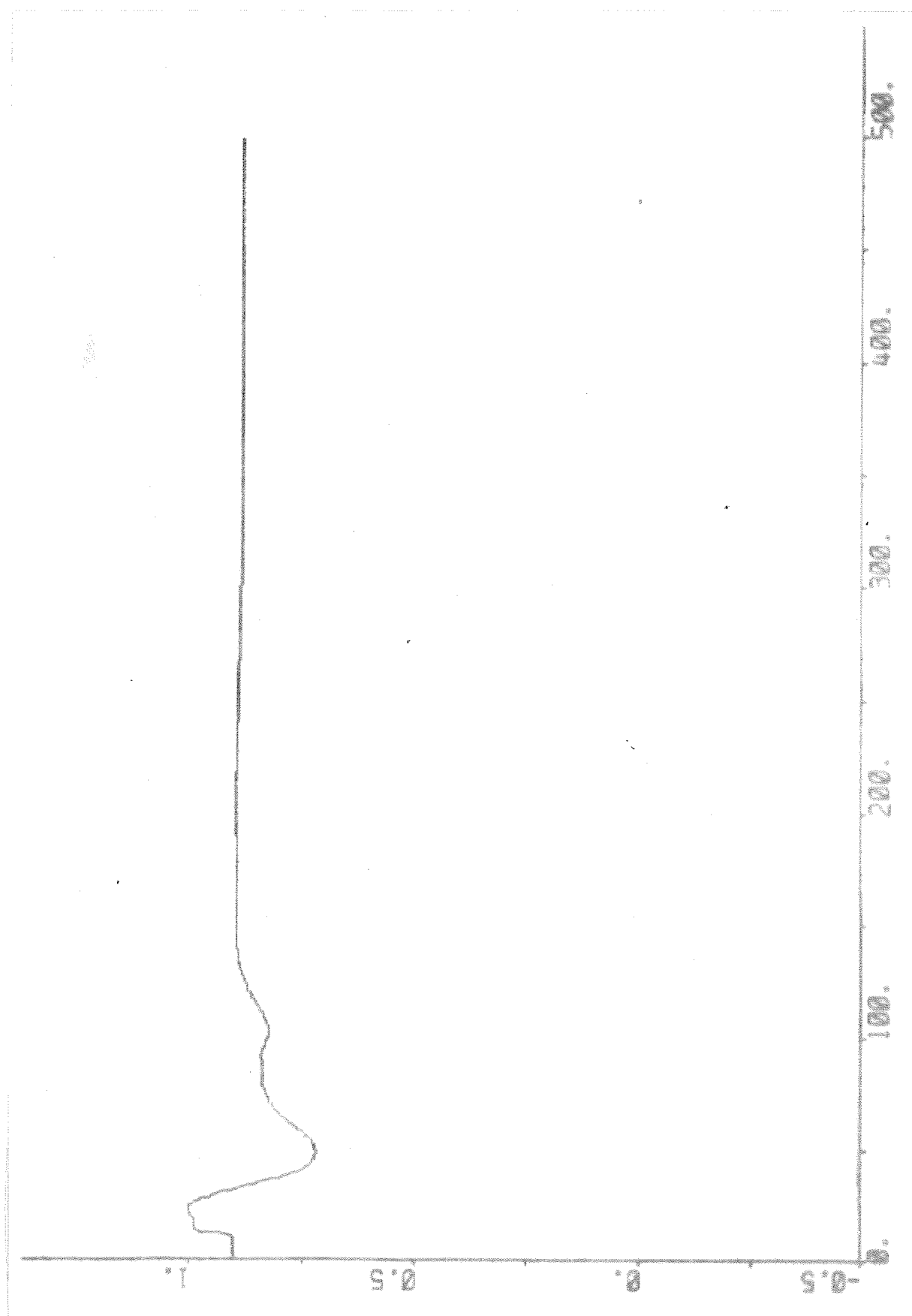


Fig. 15.13 - Response of the stroke of the second attenuator spray flow valve due to decrease of output power in alert mode.



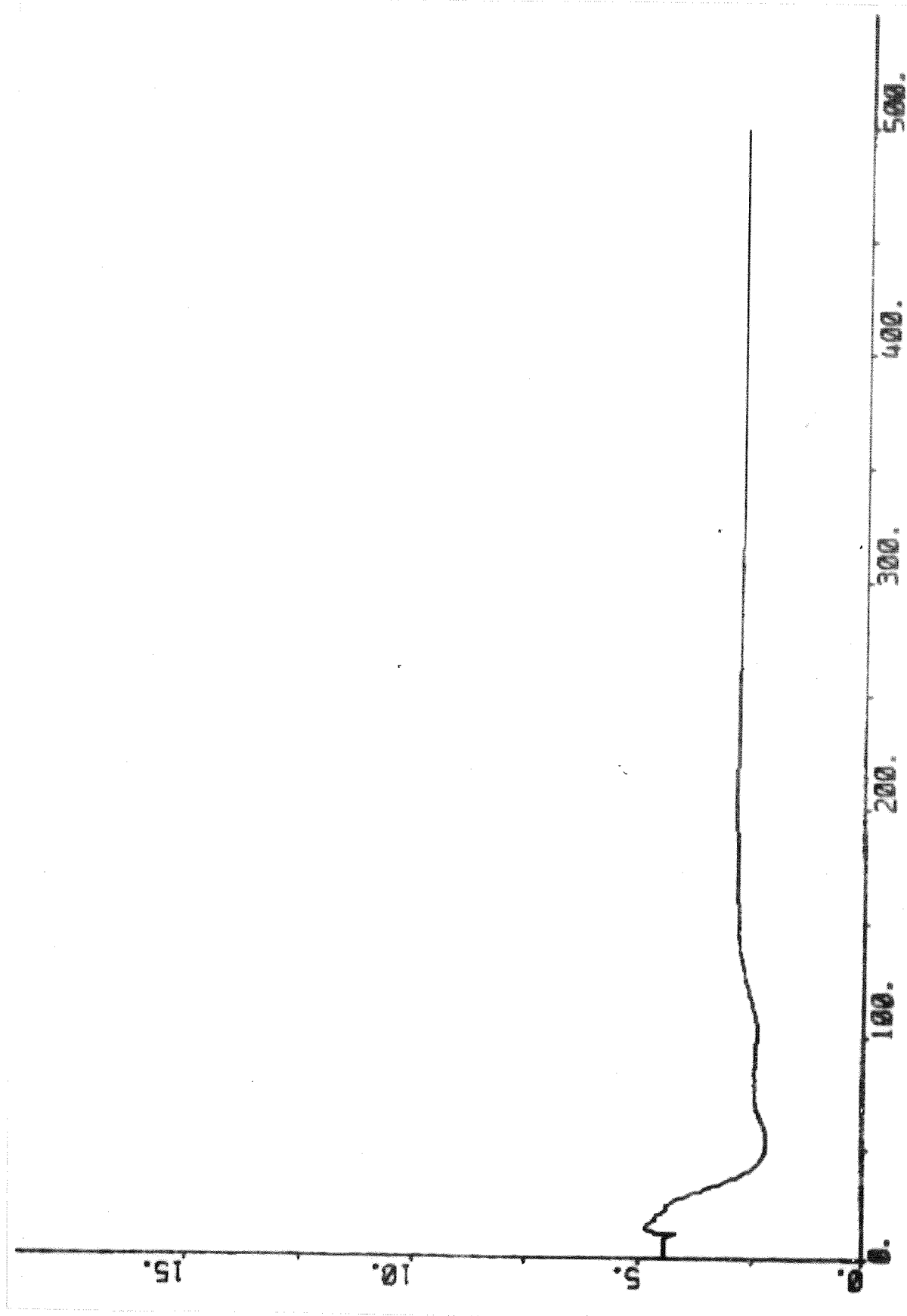


Fig. 15.14 - Response of the spray flow of the second attenuator due to decrease of output power in alert mode.

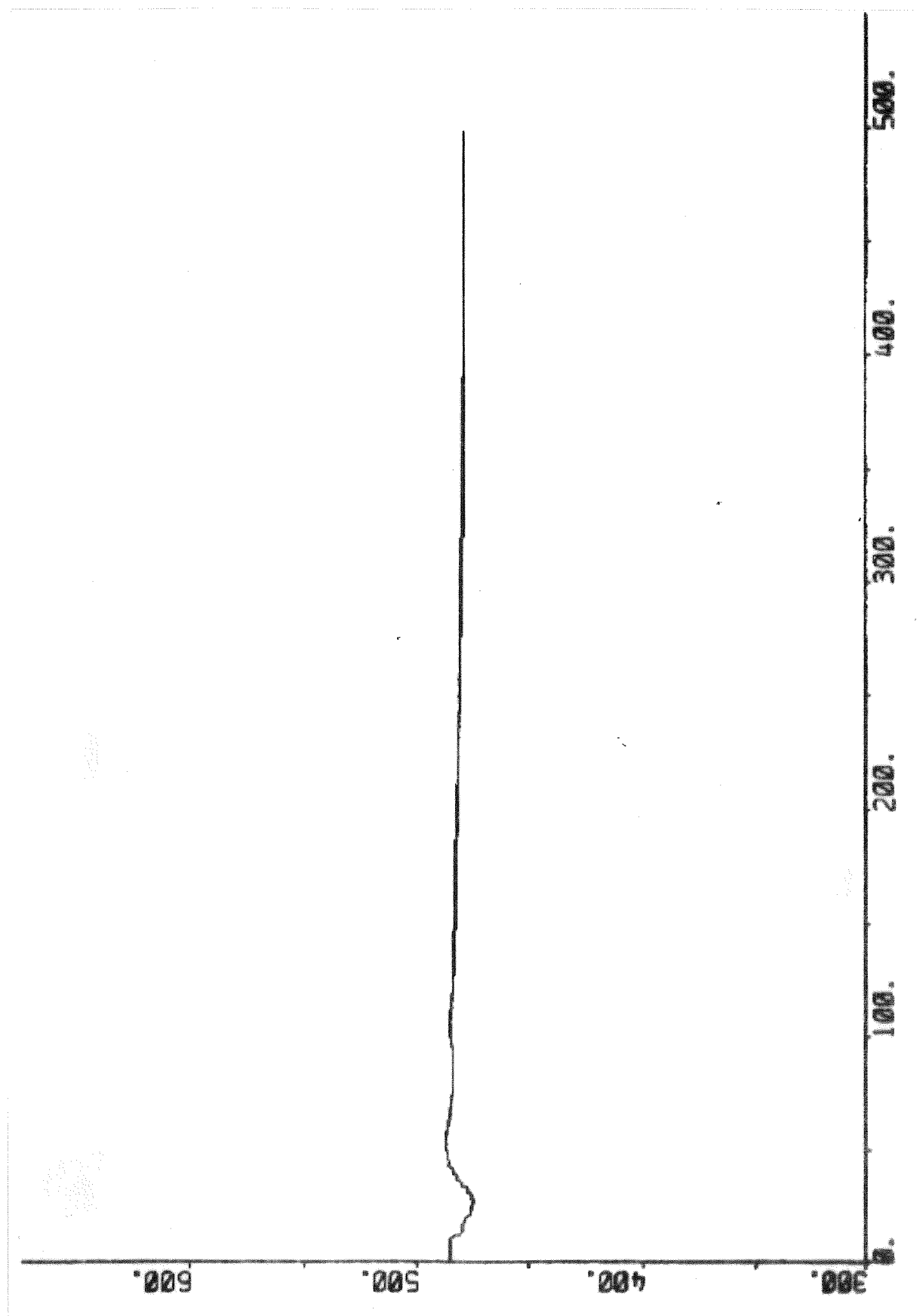


Fig. 15.15 - Response of the steam temperature before the tertiary superheater due to decrease of output power in alert mode.

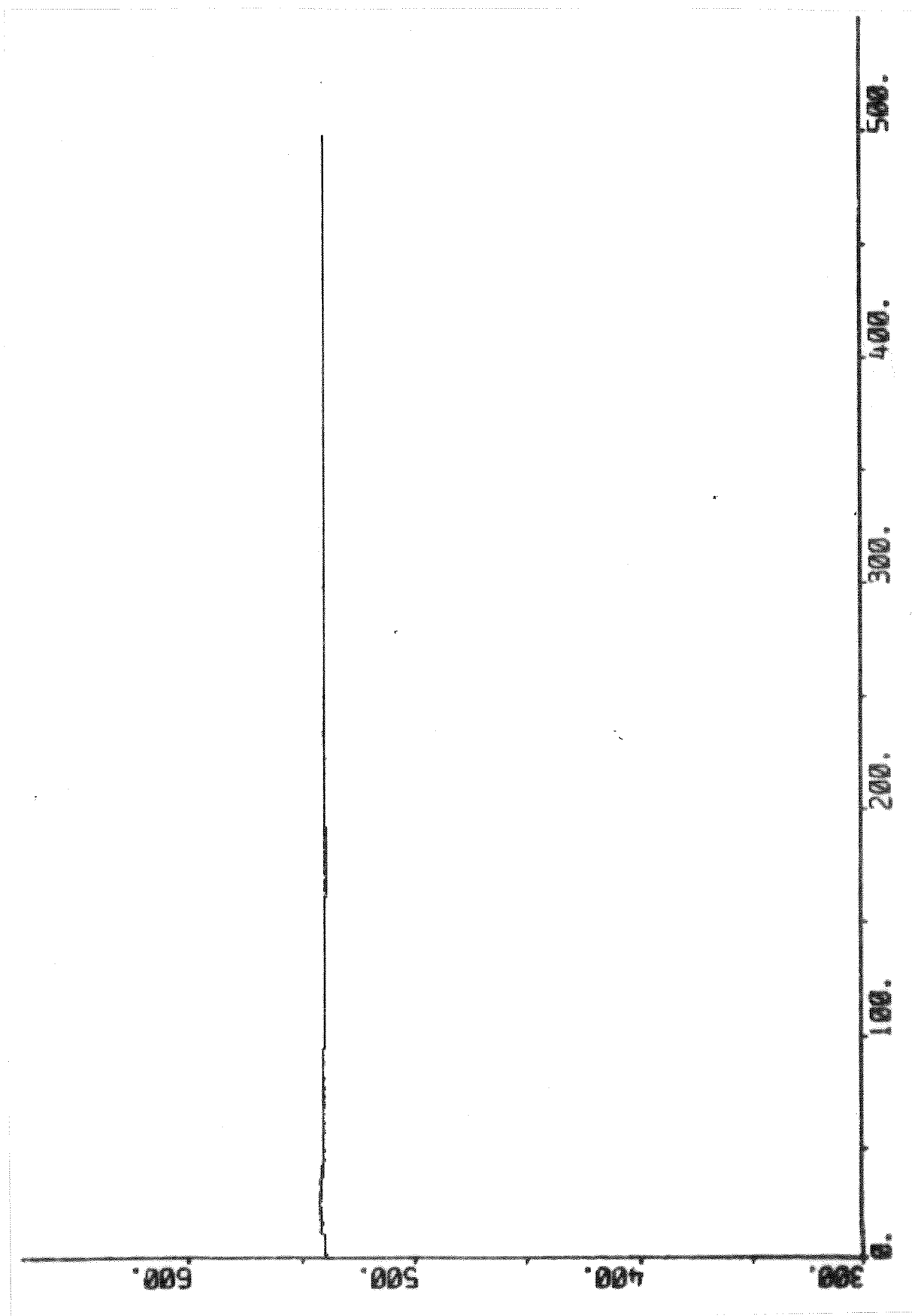


Fig. 15.16 - Response of the steam temperature after the tertiary superheater due to decrease of output power in alert mode.

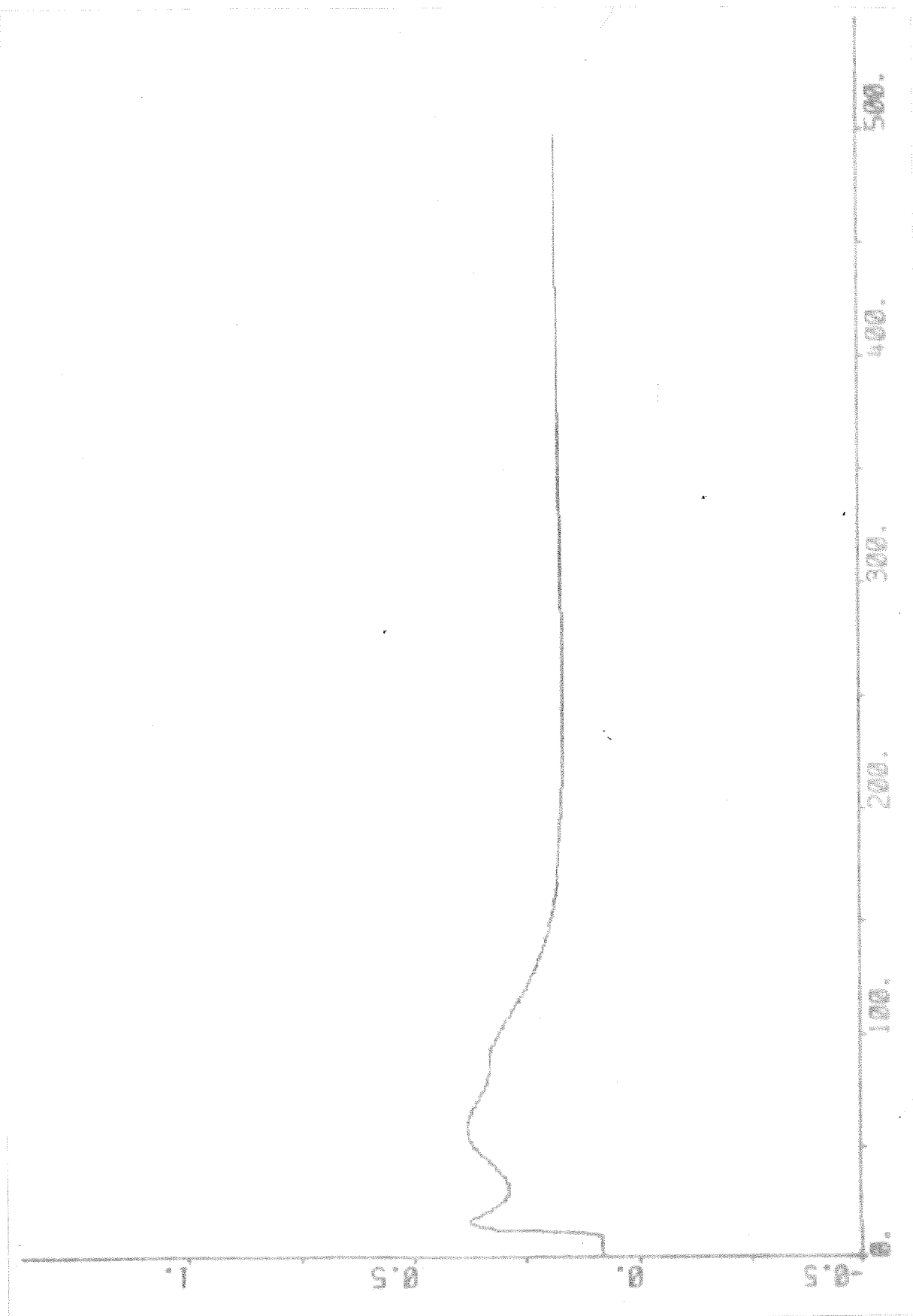


Fig. 15.17 - Response of the strokes of the low-pressure preheater extraction valves due to decrease of output power in alert mode.

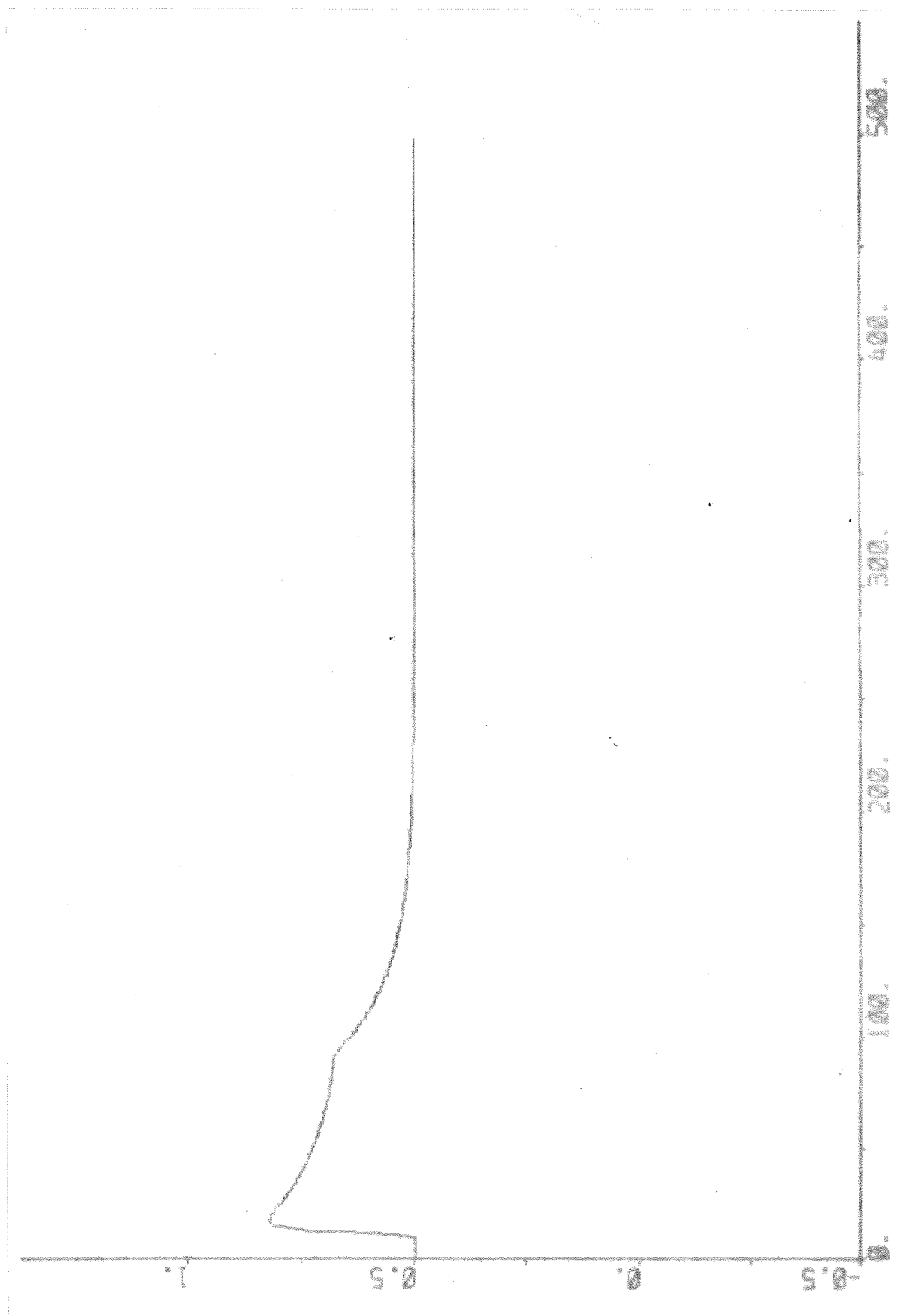


Fig. 15.18 - Response of the strokes of the high-pressure preheater extraction valves due to decrease of output power in alert mode.

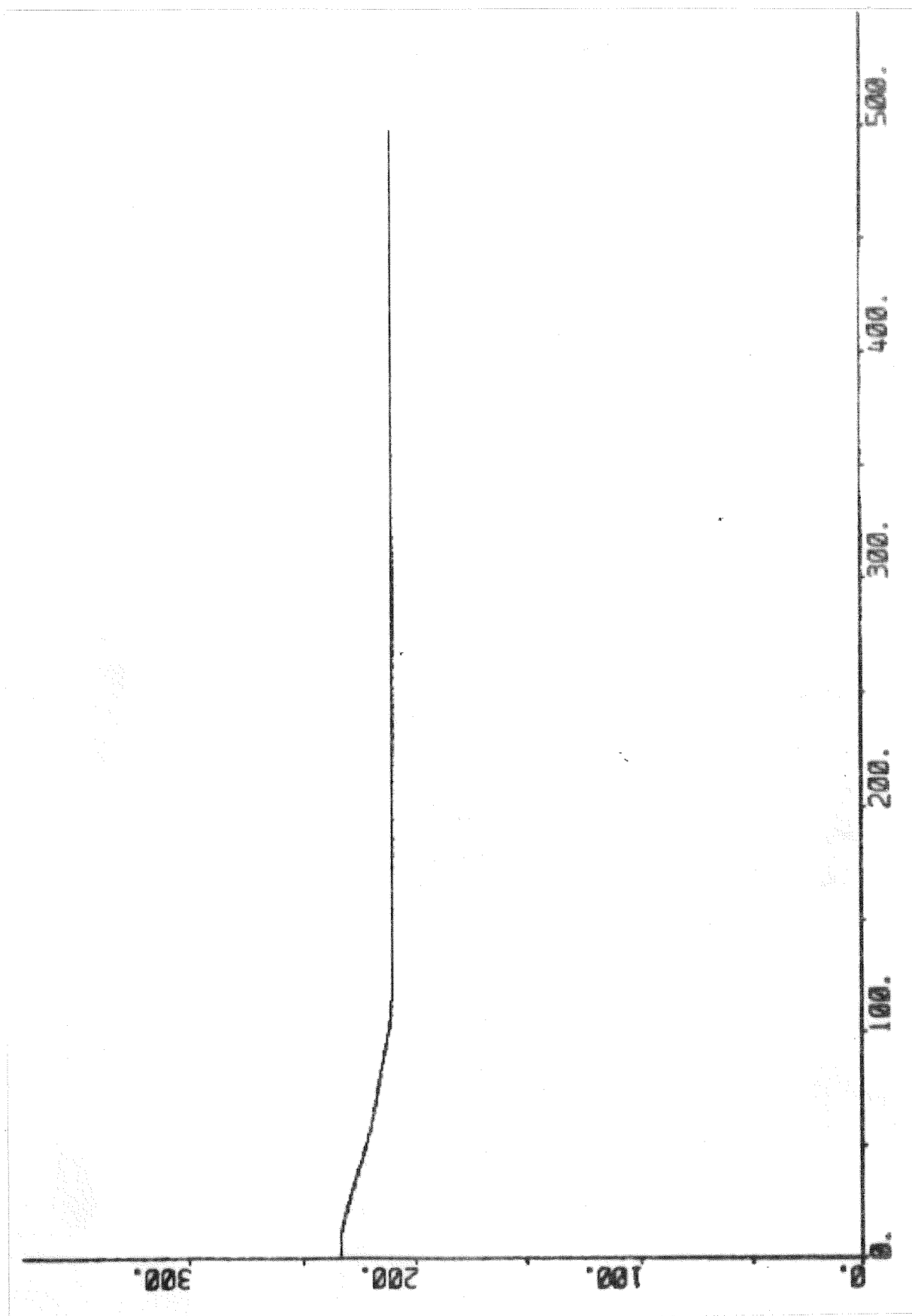


Fig. 15.19 - Response of the feedwater temperature after the HP-preheater due to decrease of output power in alert mode.

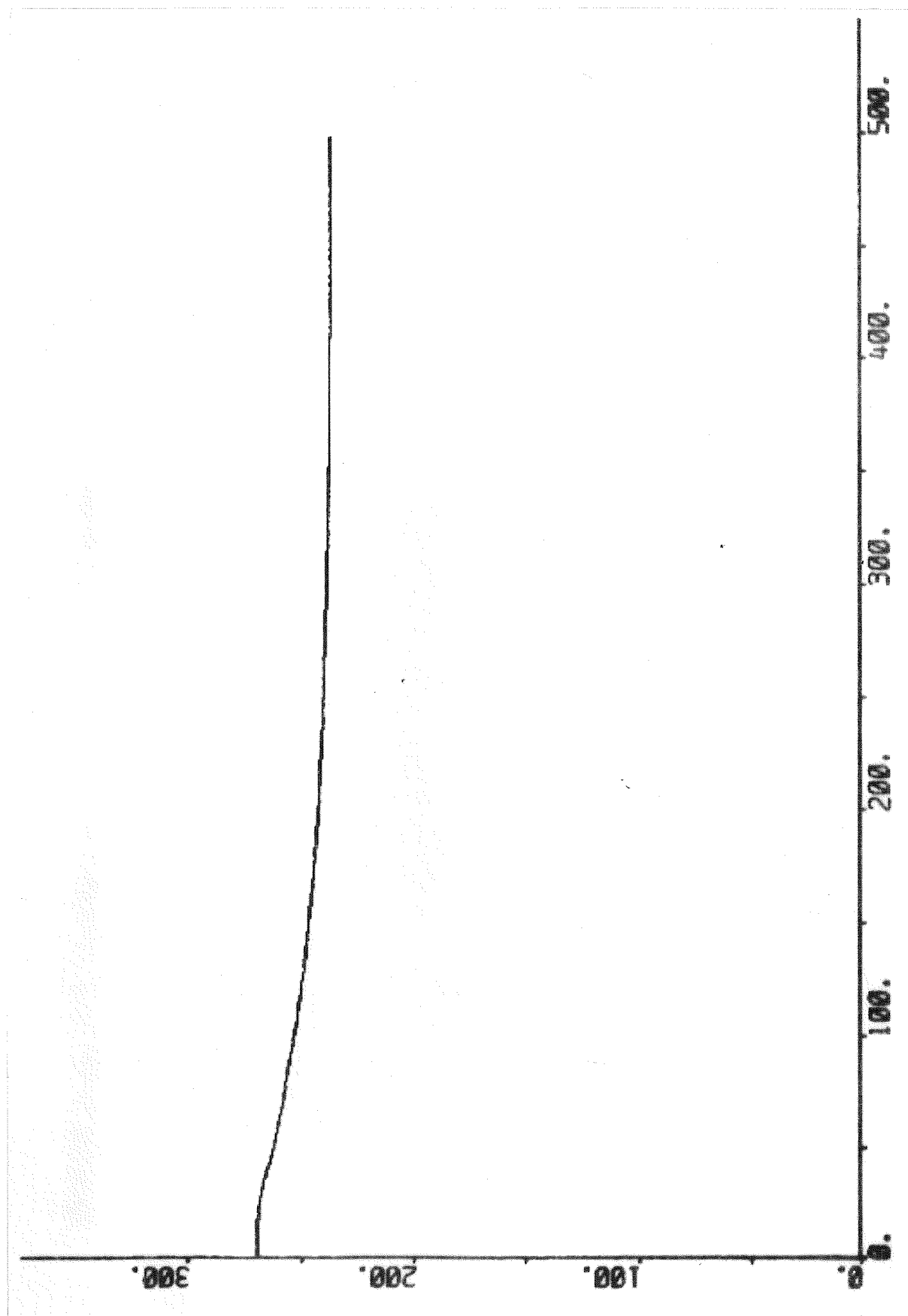


Fig. 15.20 - Response of the feedwater temperature after the economizer due to decrease of output power in alert mode.

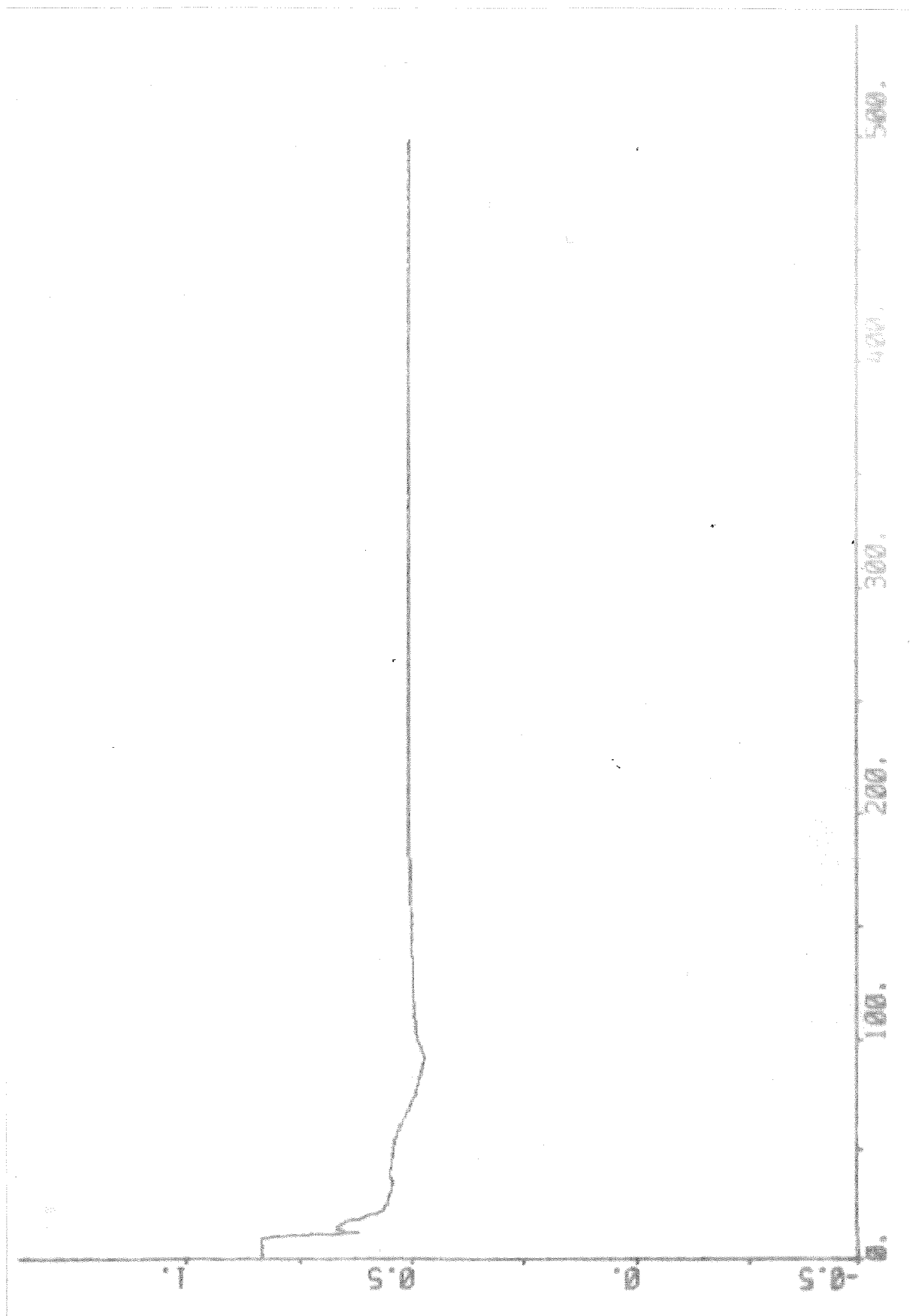


Fig. 15.21 - Response of the stroke of the control valve due to decrease of output power in alert mode.



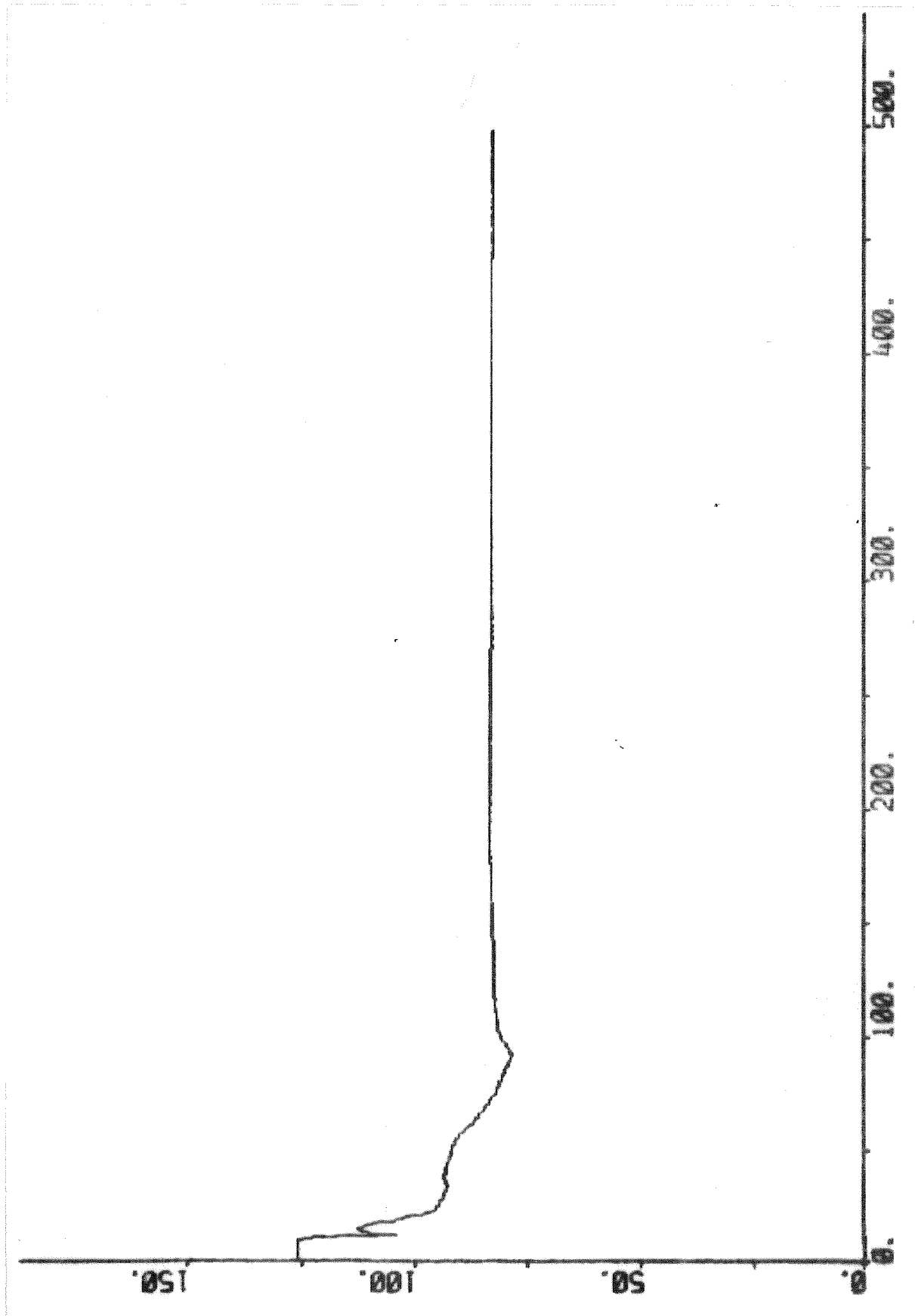


Fig. 15.22 - Response of the steam flow due to decrease of output power in alert mode.

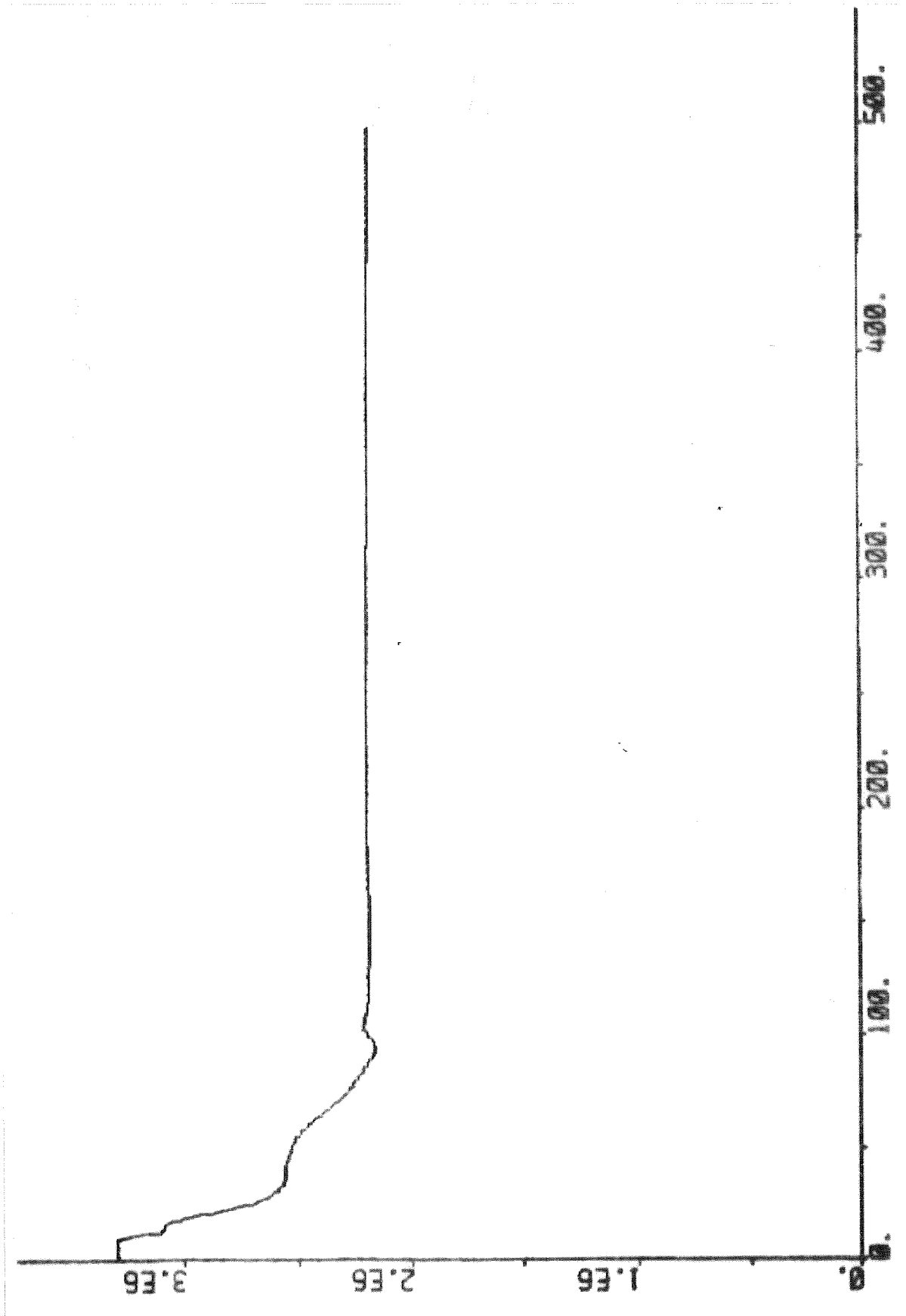


Fig. 15.23 - Response of the reheater steam pressure due to decrease of output power in alert mode.

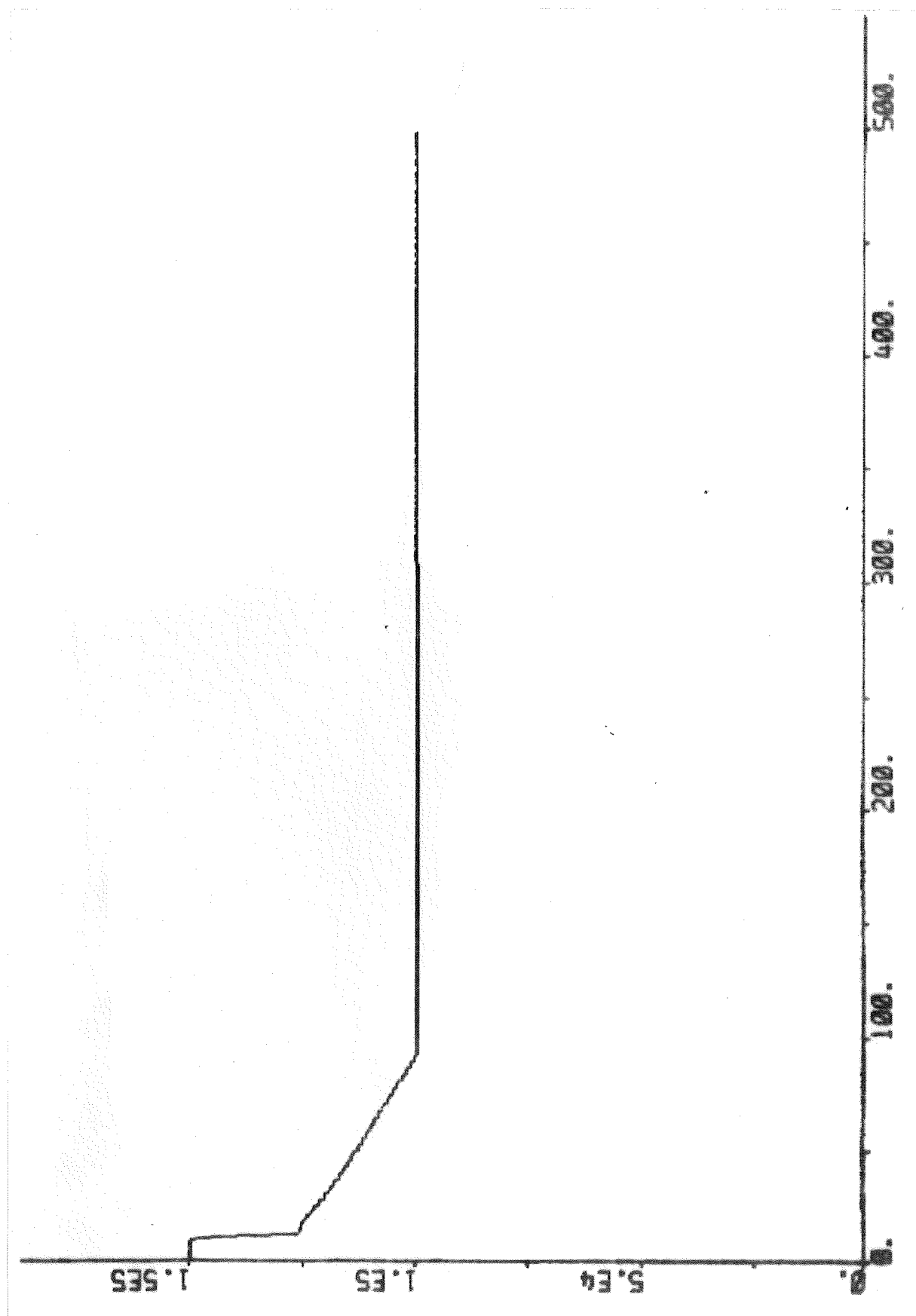


Fig. 15.24 - Response of the output power in alert mode.

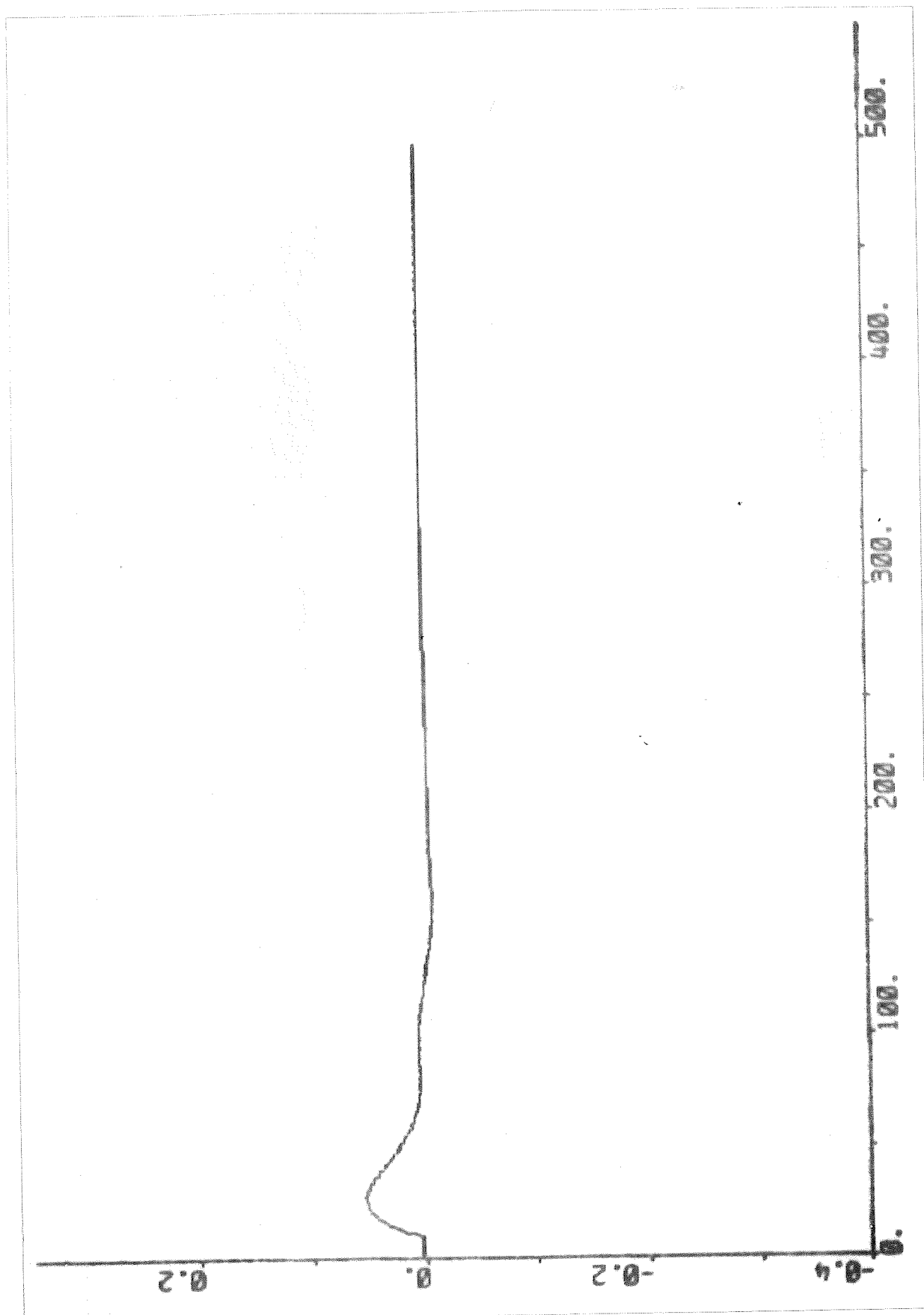


Fig. 14.7 - Response of the drum level due to increase of output power in alert mode.

## 16. TRANSFER FROM ALERT TO NORMAL MODE.

The performance of the control system during transfer from alert to normal mode will be examined in this section. The reference value of the output power,  $N_{gs2r}$  is constant and equal to 100 MW (63%) during the transfer from alert to normal mode. The mode was changed by changing the parameter ALERT from 1 to 0 at  $t = 10$  s. The parameter ALERT determines the magnitude of the jump and the rate of  $N_{gs2r}$ . The parameter ALERT also determines the relation between the reference value of the drum pressure,  $p_{ds2r}$  and  $N_{gs2r}$ . In this case  $p_{ds2r}$  is decreased from  $145 \cdot 10^5$  Pa (97%) to  $113 \cdot 10^5$  Pa (75%) with a limited,  $4.5 \cdot 10^5$  Pa/min (3%/min), rate of change. The performance of the drum pressure loop, the drum level loop, the steam temperature loop, and the output power loop will now be examined.

### The drum pressure loop.

The task of the drum pressure loop is to control the drum pressure,  $p_{ds2}$  by manipulating the fuel flow,  $w_{bol}$ . The reference value of the drum pressure,  $p_{ds2r}$  is generated by the drum pressure reference setter (DPRS), which was described in Section 6. The reference value of the drum pressure is determined by the reference value of the output power,  $N_{gs2r}$  and by the mode of the control system (normal or alert). In this case  $p_{ds2r}$  is decreased from  $145 \cdot 10^5$  Pa (97%) to  $113 \cdot 10^5$  Pa (75%) with a limited,  $4.5 \cdot 10^5$  Pa/min (3%/min), rate of change. The steam flow (Fig. 16.22), the feedwater flow (Fig. 16.23), and the feedwater temperature after the HP-preheater (Fig. 16.19) disturb the drum pressure loop. The mean density of the steam-water mixture in the riser tubes, the steam temperature after the primary superheater, the heat flows to the superheaters, to the reheater, and to the economizer are disturbed by the fuel flow variations. The fuel flow,  $w_{bol}$  is the output of the fuel flow servo (FFS), which was described in Section 7. The inputs to the DPC are  $p_{ds2r}$  and its derivative,  $s_{bolt}$ , the drum pressure,  $p_{ds2}$ , and the steam flow,  $w_{ts1}$ . The block dia-

gram of the DPC is given in Fig. 7.1. The rate of change of the fuel flow is limited in the FFS. The limits are parameters,  $w_{\text{bolo}}$  and  $w_{\text{bols}}$  of the first nonlinear block in Fig. 7.2. The numerical value of  $w_{\text{bolo}}$  and  $w_{\text{bols}}$  are 0.1 kg/s (60%/min).

The response of the fuel flow is shown in Fig. 16.1. The fuel flow is about 0.7 kg/s (7%) lower than normally during the pressure decrease. The effect of the feedforward term from the derivative of the reference value of the drum pressure can be observed at  $t = 430$  s.

The response of the drum pressure is shown in Fig. 16.2. The maximum deviation from the reference value is about  $2 \cdot 10^5$  Pa (1%).

The response of the steam pressure before the control valve is shown in Fig. 16.3. The steam pressure before the control valve follows the drum pressure closely. The increased pressure drop due to lower density is visible.

The response of the steam temperature after the primary superheater is shown in Fig. 16.4. The steam temperature reduction is about  $20^\circ\text{C}$ . The steam temperature decreases slowly for  $10 < t < 450$  s due to the decreased heat flow to the primary superheater and the decreased steam temperature before the primary superheater without corresponding decrease of the steam flow (Fig. 16.22). The steam temperature before the primary superheater is determined by the drum pressure (Fig. 16.2). The heat flow to the primary superheater is approximately proportional to the fuel flow (Fig. 16.1).

Properties: The reference value of the drum pressure decreases slowly in this case. The derivative of the reference value of the drum pressure and the steam flow influence the fuel flow through the feedforward terms. The effects of the other disturbances are reduced by feedback. The maximum drum pressure error is about  $2 \cdot 10^5$  Pa (1%).

### The drum level loop.

The task of the drum level loop is to control the drum level,  $z_{dl4}$  by manipulating the feedwater control valve. The reference value of the drum level,  $z_{dl4r}$  is constant. The fuel flow (Fig. 16.1) and the steam flow (Fig. 16.22) disturb the drum level loop. The drum level loop disturbs the feedwater temperature. If the drum level is too high there is a danger that water will reach the turbine. If the drum level is too low there is a danger that the riser tubes will be damaged due to insufficient cooling. The reference value of the feedwater flow,  $w_{fw5r}$  is determined by the drum level controller (DLC), which was described in Section 8. The inputs to the DLC are  $z_{dl4r}$ ,  $z_{dl4}$  and the steam flow,  $w_{ts1}$ . The block diagram of the DLC is given in Fig. 8.1. The rate of change of the stroke of the feedwater valve is limited in the feedwater servo (FWS). The limits are parameters,  $s_{ww2o}$  and  $s_{ww2s}$  of the first nonlinear block in Fig. 8.2. The numerical values of  $s_{ww2o}$  and  $s_{ww2s}$  are both 5%/s.

The response of the stroke of the feedwater valve is shown in Fig. 16.5. There are two reasons for changing the valve opening. The first is that the pressure drop over the feedwater valve has to be increased due to the decreasing drum pressure. The second is that the feedwater flow has to be decreased due to the decreasing mean density of the steam-water mixture in the riser tubes.

The response of the feedwater flow is shown in Fig. 16.6. The feedwater flow is about 5 kg/s (4%) lower than in steady-state during the decrease of the drum pressure. The decrease of the feedwater flow compensates for the decreasing mean density of the steam-water mixture in the riser tubes.

The response of the drum level is shown in Fig. 16.7. The drum level error is about 1 cm during the decrease of the drum pressure. The settling time of the drum level is about 50 s.

The response of the drum water temperature is shown in Fig. 16.8.

The rate of change of the drum water temperature determines the thermal stresses of the drum material. The temperature variation is about  $20^{\circ}\text{C}$ . The rate of change of the temperature is less than  $3^{\circ}\text{C}/\text{min}$ .

Properties: The heat flow to the riser tubes is the most severe disturbance of the drum level loop in this case. The steam flow influences the feedwater flow through the feedforward term. The effects of the other disturbances are reduced by feedback. The maximum drum level error is 1 cm.

#### The steam temperature loop.

The task of the steam temperature loop is to control the steam temperature after the tertiary superheater,  $T_{ts2}$  by manipulating the first and the second attemperator spray flows valves. The reference value of the steam temperature after the tertiary superheater,  $T_{ts2r}$  is constant. The heat flows to the secondary and tertiary superheaters, the steam temperature after the primary superheater (Fig. 16.4), and the steam flow (Fig. 16.22) disturb the steam temperature loop. The heat flows to the secondary and tertiary superheaters are both approximately proportional to the fuel flow (Fig. 16.1). The specific fuel consumption is reduced if the steam temperature after the tertiary superheater is increased. The steam temperature is limited by the properties of the superheater material. The steam temperature before the secondary superheater,  $T_{ss1}$  is the output of the secondary superheater steam temperature servo (SSSTS), which was described in Section 9. The steam temperature before the tertiary superheater,  $T_{ts1}$  is the output of the tertiary superheater steam temperature servo (TSSTS), which was described in Section 9. The reference value of the steam temperature before the tertiary superheater,  $T_{ts1r}$  is determined by the tertiary superheater steam temperature controller (TSSTC), which was described in Section 9. The inputs to the TSSTC are  $T_{ts2r}$ ,  $T_{ts2}$ , the steam flow,  $w_{ts1}$ , and the fuel flow,  $w_{bol}$ . The block diagram of the TSSTC is given in Fig. 9.1. The reference



value of the steam temperature before the secondary superheater,  $T_{sslr}$  is determined by the secondary superheater steam temperature controller (SSSTC), which was described in Section 9. The inputs to the SSSTC are  $T_{ss2r}$ ,  $T_{ss2}$ ,  $w_{tsl}$  and  $w_{bol}$ . The rate of change of the stroke of the second attemperator spray flow valve is limited in the TSSTS. The limits are parameters,  $s_{tw2o}$  and  $s_{tw2s}$  of the first nonlinear block in Fig. 9.3. The numerical values of  $s_{tw2o}$  and  $s_{tw2s}$  are both 4%/s. The rate of change of the stroke of the first attemperator spray flow valve is limited in the SSSTS. The limits are parameters,  $s_{sw2o}$  and  $s_{sw2s}$  of the first nonlinear block in Fig. 9.4. The numerical values of  $s_{sw2o}$  and  $s_{sw2s}$  are both 4%/s. The difference between  $T_{ss2r}$  and  $T_{tslr}$  is a parameter  $g_{sw2b}$  of the SSSTC. The numerical value of  $g_{sw2b}$  is 30°C and is chosen so that the second attemperator spray flow valve is approximately half-open. This means that the steam temperature before the tertiary superheater can be changed rapidly in both directions.

The response of the stroke of the first attemperator spray flow valve is shown in Fig. 16.9. The stroke of the valve is changed in order to maintain the steam temperature before the secondary superheater at its reference value. The valve closes for  $10 < t < 55$  s due to the decreasing heat flow to the secondary superheater and the decreasing steam temperature after the primary superheater. The valve is completely closed for  $55 < t < 460$  s. This means that the performance of the steam temperature loop is affected by the limited capacity of the first attemperator.

The response of the spray flow of the first attemperator is shown in Fig. 16.10. The spray flow follows the stroke of the valve quite well.

The response of the steam temperature before the secondary superheater is shown in Fig. 16.11. The steam temperature is increased about 15°C for  $10 < t < 50$  s. The consequences of the limited capacity of the first attemperator is clearly visible for  $50 < t < 480$  s.

The response of the steam temperature after the secondary superheater is shown in Fig. 16.12. The difference between the steam temperature after the secondary superheater and the steam temperature before the tertiary superheater (Fig. 16.15) shall be about  $30^{\circ}\text{C}$ . This is also the case in spite of the limited capacity of the first attemperator.

The response of the stroke of the second attemperator spray flow valve is shown in Fig. 16.13. The valve is closed for  $10 < t < 30$  s due to the decreasing heat flow to the tertiary superheater. The heat flow is approximately proportional to the fuel flow (Fig. 16.1). The valve is then opened for  $30 < t < 80$  s in order to compensate for the increasing steam temperature after the secondary superheater. The valve is closed for  $80 < t < 440$  s in order to compensate for the decreasing steam temperature after the secondary superheater.

The response of the spray flow of the second attemperator is shown in Fig. 16.14. The spray flow follows the stroke of the valve quite well.

The response of the steam temperature before the tertiary superheater is shown in Fig. 16.15. The steam temperature increases for  $10 < t < 130$  s due to the decreasing spray flow. The spray flow is decreased in order to compensate for the decreasing heat flow to the tertiary superheater. The heat flow is approximately proportional to the fuel flow (Fig. 16.1).

The response of the steam temperature after the tertiary superheater is shown in Fig. 16.16. The steam temperature error is about  $0.5^{\circ}\text{C}$ .

Properties: The heat flows to the secondary and tertiary superheater and the steam temperature after the primary superheater are the most severe disturbances in this case. The fuel flow and the steam flow influence the steam temperature controllers by feedforward terms. The effects of the other disturbances are reduced by feedback. The maximum steam temperature error is about  $0.5^{\circ}\text{C}$ . The

performance of the steam temperature loop is not deteriorated by the limited capacity of the first attemperator.

### The output power loop.

The task of the output power loop is to control the output power,  $N_{gs2}$  by manipulating the steam control valve and the extraction steam valves. The reference value of the output power,  $N_{gs2r}$  is generated by the power demand setter (PDS), which was described in Section 5. A preliminary reference value of the output power,  $s_{nsl}$  is determined from the setpoint of the output power,  $s_{nslr}$  in the first part of the power demand setter (PDS1). The block diagram of the PDS1 is given in Fig. 5.1. The  $s_{nslr}$  is modified with respect to the network-frequency in the second part of the power demand setter (PDS2). The block diagram of the PDS2 is given in Fig. 5.2. The  $N_{gs2r}$  is obtained from the third part of the power demand setter (PDS3), which limits the jump and the rate of  $N_{gs2r}$ . The block diagram of the PDS3 is given in Fig. 5.3. The steam pressure before the control valve,  $p_{ts2}$  (Fig. 16.3) and the steam temperature before the control valve,  $T_{ts2}$  (Fig. 16.16) disturb the output power loop. The superheated steam flow,  $w_{ts1}$  (Fig. 16.22), the reheated steam flow,  $w_{rs2}$  and the extraction steam flows,  $w_{hs2}$ ,  $w_{is2}$ ,  $w_{is4}$ ,  $w_{is6}$ ,  $w_{is8}$ ,  $w_{ls2}$ , and  $w_{ls4}$  are disturbed by the output power loop. The stroke of the control valve is the output of the control valve servo (CVS), which was described in Section 10. The strokes of the high-pressure preheater extraction valves are the outputs of the high-pressure preheater servo (HPPS), which was described in Section 10. The strokes of the low-pressure preheater extraction valves are the outputs of the low-pressure preheater servo (LPPS), which was described in Section 10. The reference value of the stroke of the control valve,  $s_{vs2r}$  is determined by the turbine power controller (TPC), which was described in Section 10. The inputs to the TPC are  $N_{gs2r}$  and  $N_{gs2}$ . The block diagram of the TPC is given in Fig. 10.1. The reference value of the strokes of the high-pressure preheater extraction valves,  $s_{fs2r}$  is determined by the high-pressure preheater controller (HPPC), which was described in Section 10. The input to

the HPPC is  $N_{gs2r}$ . The block diagram of the HPPC is given in Fig. 10.3. The reference value of the strokes of the low-pressure extraction valves,  $s_{fs7r}$  is determined by the low-pressure preheater controller (LPPC), which was described in Section 10. The inputs of the LPPC are  $N_{gs2r}$ , the reference value of the deaerator steam pressure,  $p_{as2r}$  and the deaerator steam pressure,  $p_{as2}$ . The rate of change of the stroke of the control valve is limited in the CVS. The limits are parameters,  $s_{vs2o}$  and  $s_{vs2s}$  of the first nonlinear block in Fig. 10.2. The numerical values of  $s_{vs2o}$  and  $s_{vs2s}$  are 20%/s and 200%/s respectively. The rates of change of the strokes of the high-pressure extraction steam flow valves are limited in the HPPS. The limits are parameters,  $s_{fs2o}$  and  $s_{fs2s}$  of the first nonlinear block in Fig. 10.4. The numerical values of  $s_{fs2o}$  and  $s_{fs2s}$  are both 100%/s. The rates of change of the strokes of the low-pressure extraction steam flow valves are limited in the LPPS. The limits are parameters,  $s_{fs7o}$  and  $s_{fs7s}$  of the first nonlinear block in Fig. 10.6. The numerical values of  $s_{fs7o}$  and  $s_{fs7s}$  are both 100%/s.

The responses of the strokes of the LP-preheater extraction valves are shown in Fig. 16.17. The reference value of the output power is constant and the reference value of the strokes of the LP-preheater extraction valves are only influenced by the deaerator pressure controller. The decrease of the strokes are due to the decreased feedwater flow without corresponding increase of the steam flow.

The response of the strokes of the HP-preheater extraction valves are shown in Fig. 16.18. The reference value of the output power is constant and the strokes of the HP-preheater extraction valves are constant too.

The response of the feedwater temperature after the HP-preheater is shown in Fig. 16.19. The temperature increases about  $2^{\circ}\text{C}$  due to the decreased feedwater flow.

The response of the feedwater temperature after the economizer

is shown in Fig. 16.20. The feedwater temperature decreases for  $10 < t < 200$  s due to the decreased heat flow to the economizer in spite of the increased temperature before the economizer. The heat flow to the economizer is approximately proportional to the fuel flow (Fig. 16.1). The temperature decrease is about  $4^{\circ}\text{C}$ .

The response of the stroke of the control valve is shown in Fig. 16.21. The control valve opening is increased for  $10 < t < 430$  s in order to compensate for the decreasing drum pressure.

The response of the steam flow is shown in Fig. 16.22. The steam flow variation is less than 0.5 kg/s (0.5%).

The response of the reheater steam pressure is shown in Fig. 16.23. The pressure variations are similar to the steam flow variations.

The response of the output power is shown in Fig. 16.24. The reference value of the output power is constant. The output power error is barely visible.

Properties: The steam temperature and the steam pressure before the control valve disturb the output power loop in this case. The effects of the disturbances are reduced by feedback. The output power error is barely visible.

### Conclusions.

The performance of the control system during transfer from alert to normal mode has been investigated by simulation. In this case the reference value of the drum pressure was decreased from  $145 \cdot 10^5$  Pa (97%) to  $113 \cdot 10^5$  Pa (75%) with a limited,  $4.5 \cdot 10^5$  Pa/min (3%/min), rate of change. The reference value of the output power is constant and equal to 100 MW (63%) during the transfer from alert to normal mode. The fuel flow has to be decreased temporarily in order to decrease the drum pressure. The fuel flow is about 0.7 kg/s (7%) lower than normally during the decrease of the drum pressure. The maximum drum pressure error is  $2 \cdot 10^5$  Pa (1%).

The heat flow to the riser tubes is the most severe disturbance of the drum level loop in this case. The maximum drum level error is 1 cm. The heat flows to the secondary and tertiary superheater and the steam temperature after the primary superheater are the most severe disturbances in this case. The maximum steam temperature error is about  $0.5^{\circ}\text{C}$ . The steam temperature and the steam pressure before the control valve disturb the output power loop. The output power error is, however, barely visible in this case.

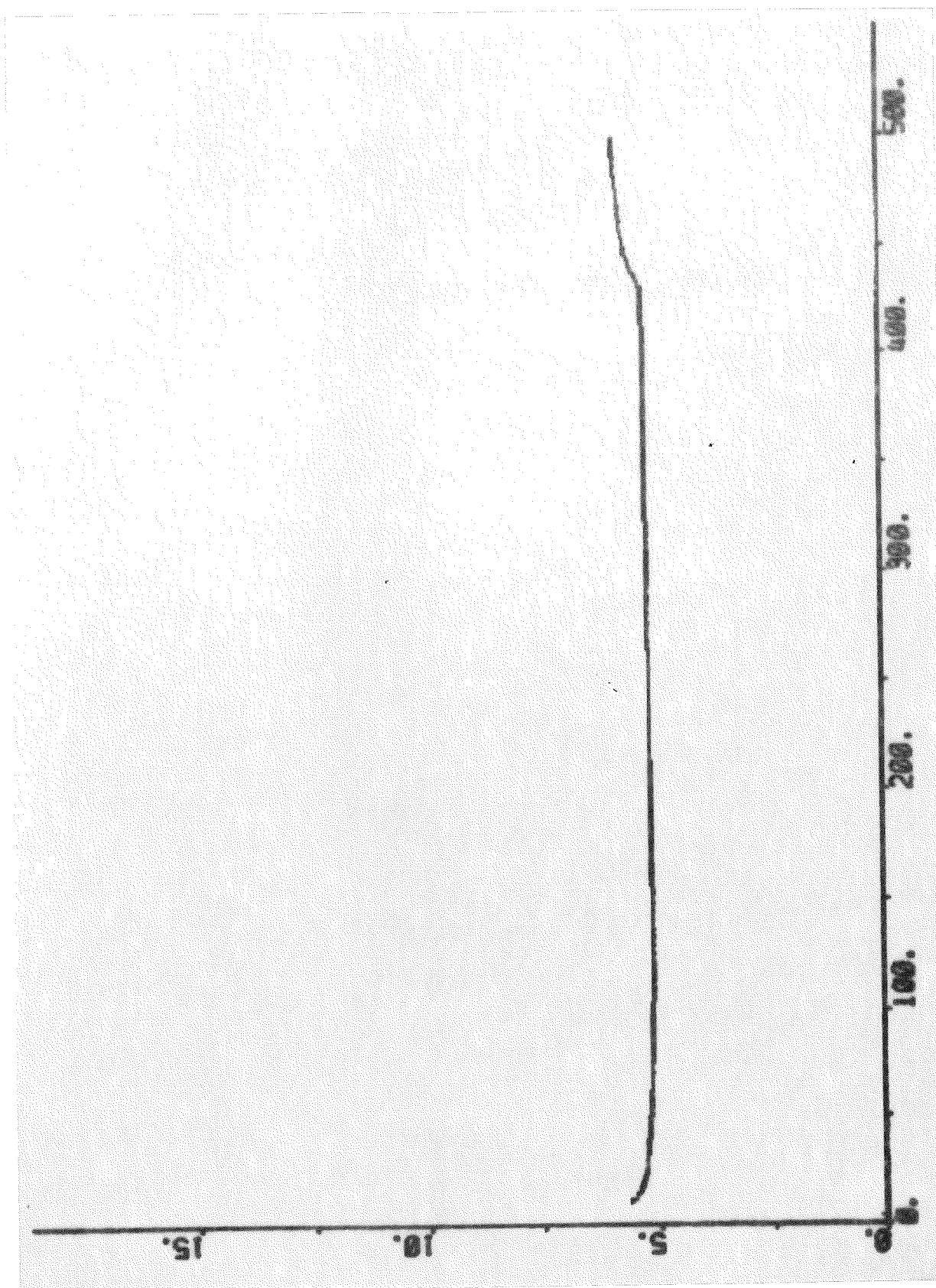


Fig. 16.1 - Response of the fuel flow during transfer from alert to normal mode.

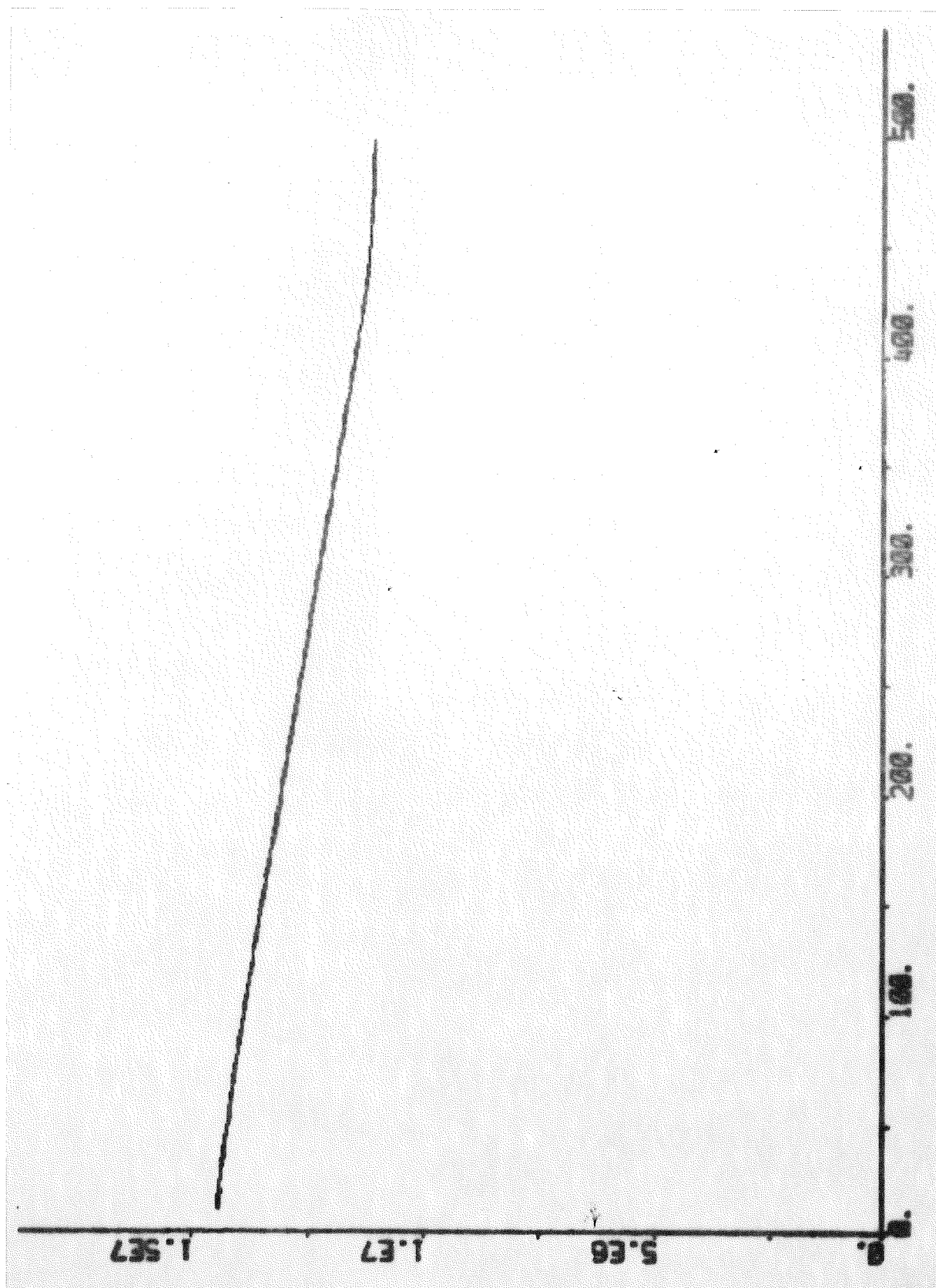


Fig. 16.2 - Response of the drum pressure during transfer from alert to normal mode.



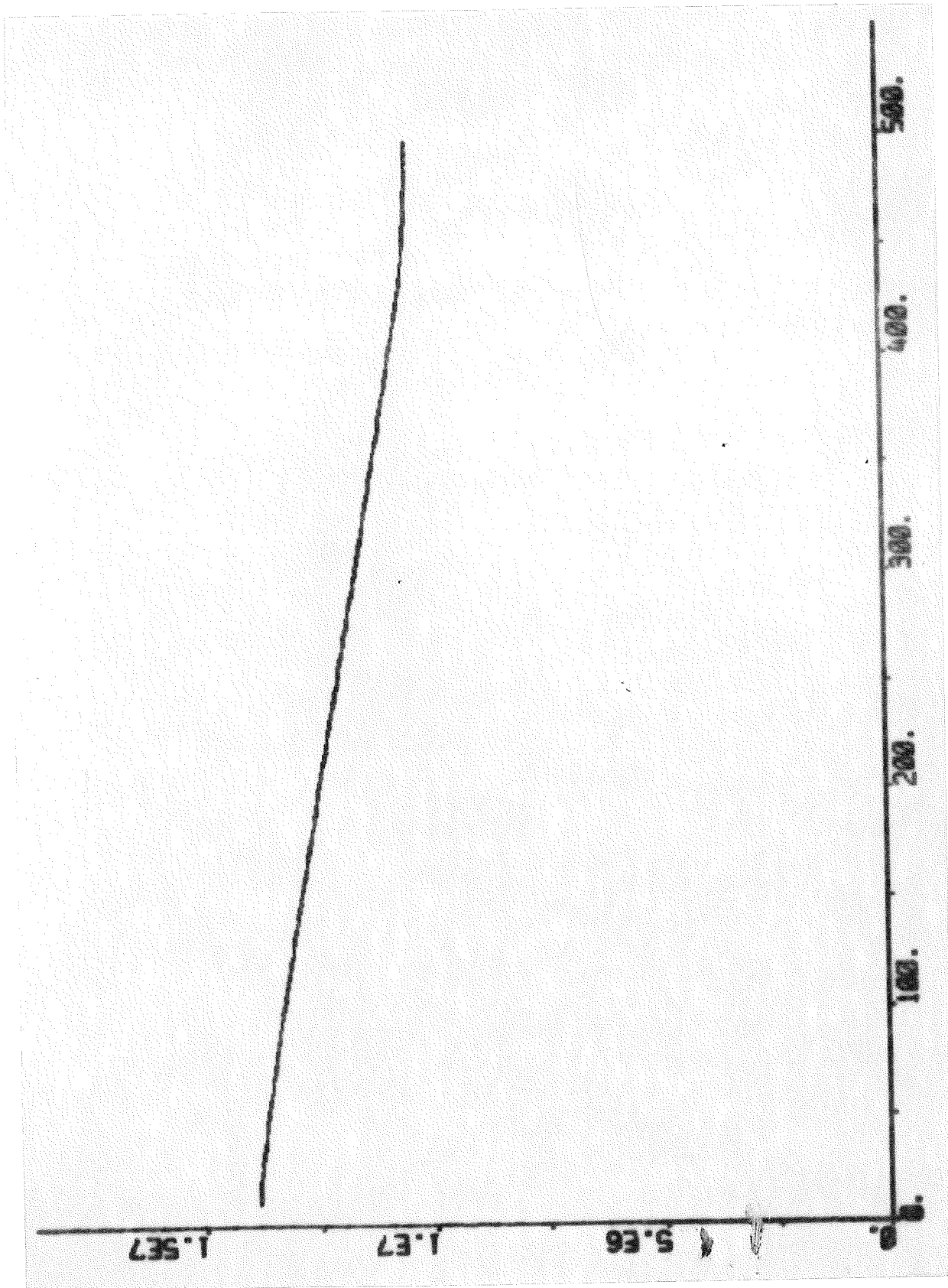


Fig. 16.3 - Response of the steam pressure before the control valve transfer from alert to normal mode.

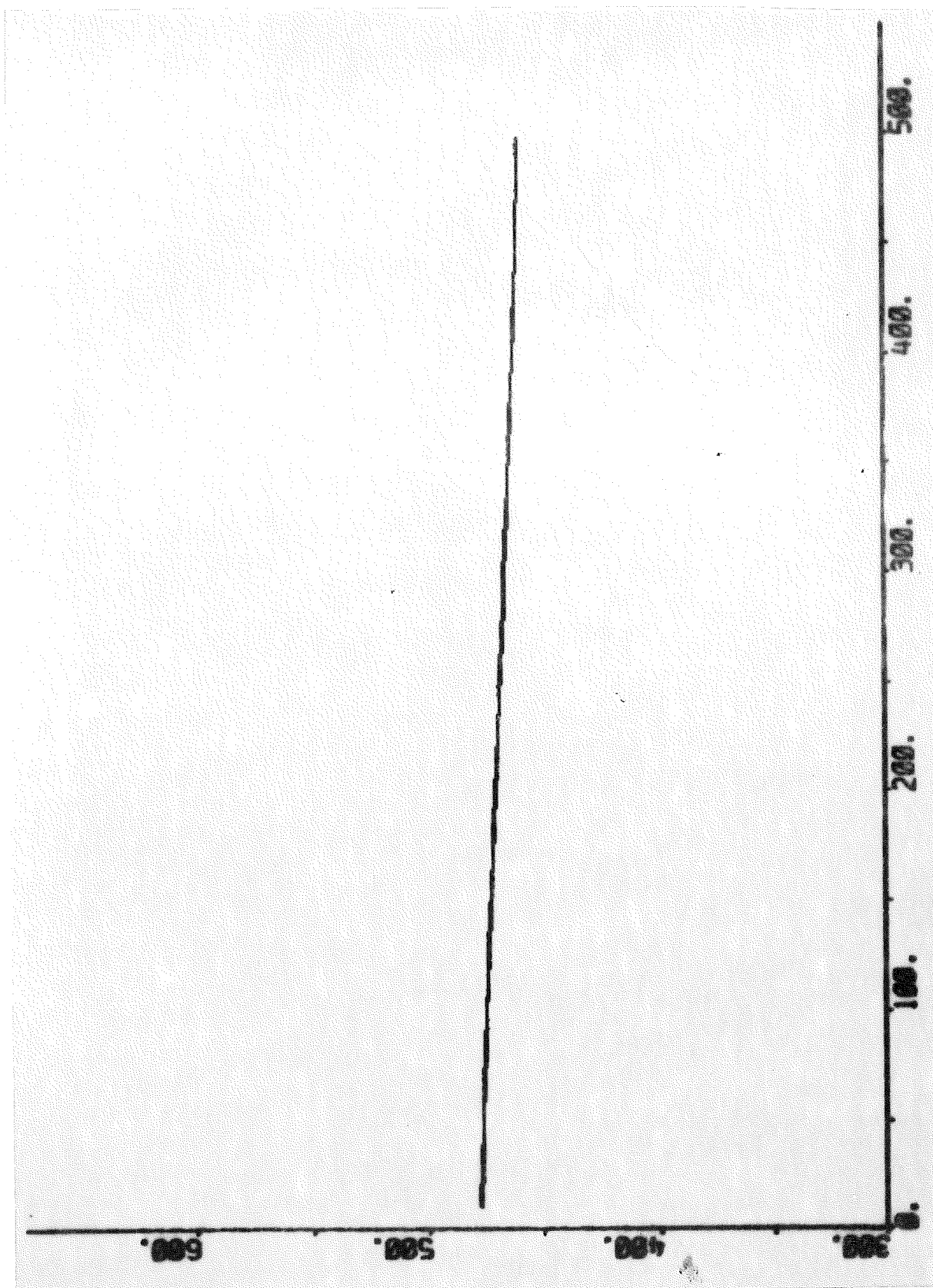


Fig. 16.4 - Response of the steam temperature after the primary superheater during transfer from alert to normal mode.

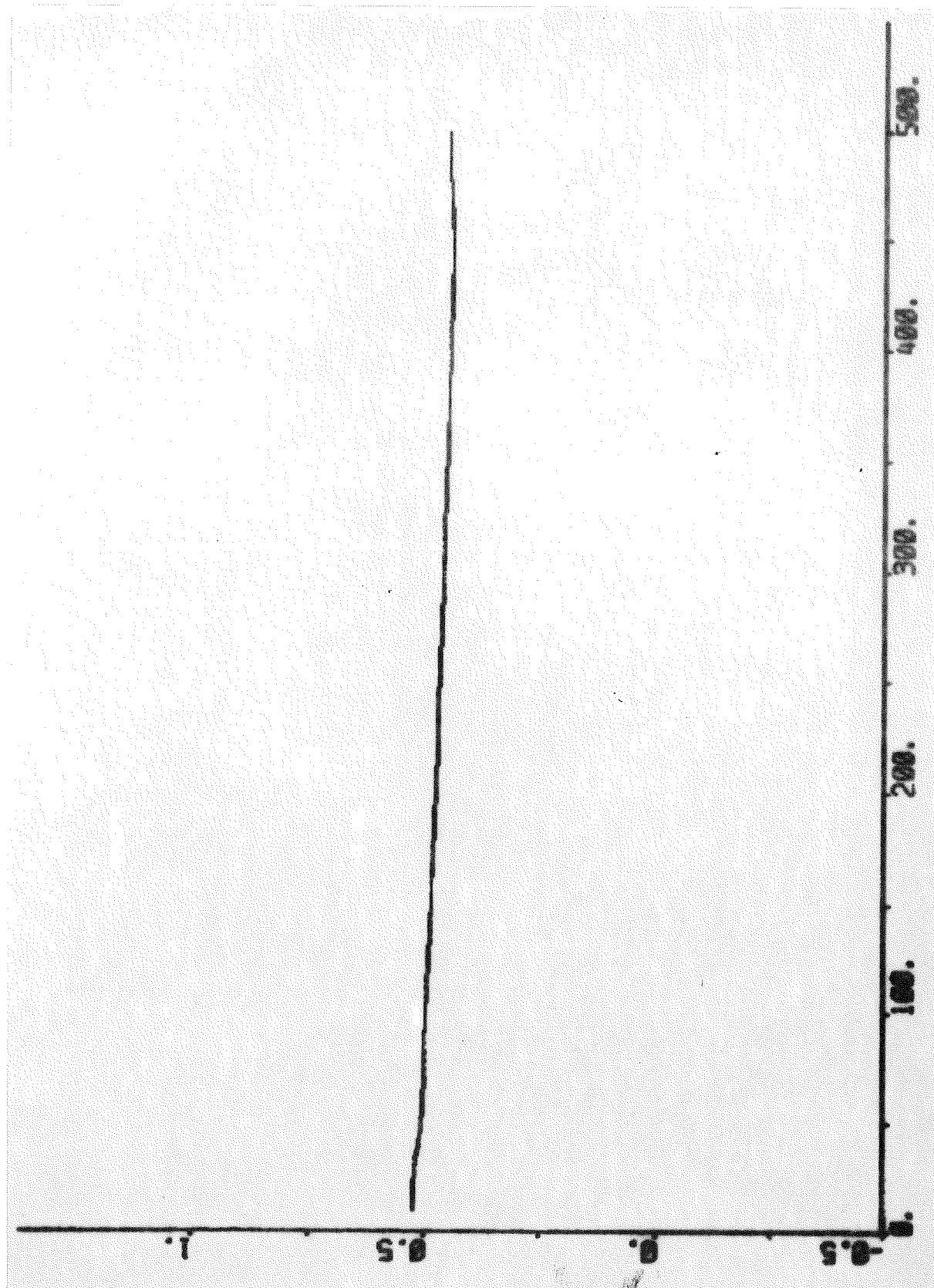


Fig. 16.5 - Response of the stroke of the feedwater valve during transfer from alert to normal mode.

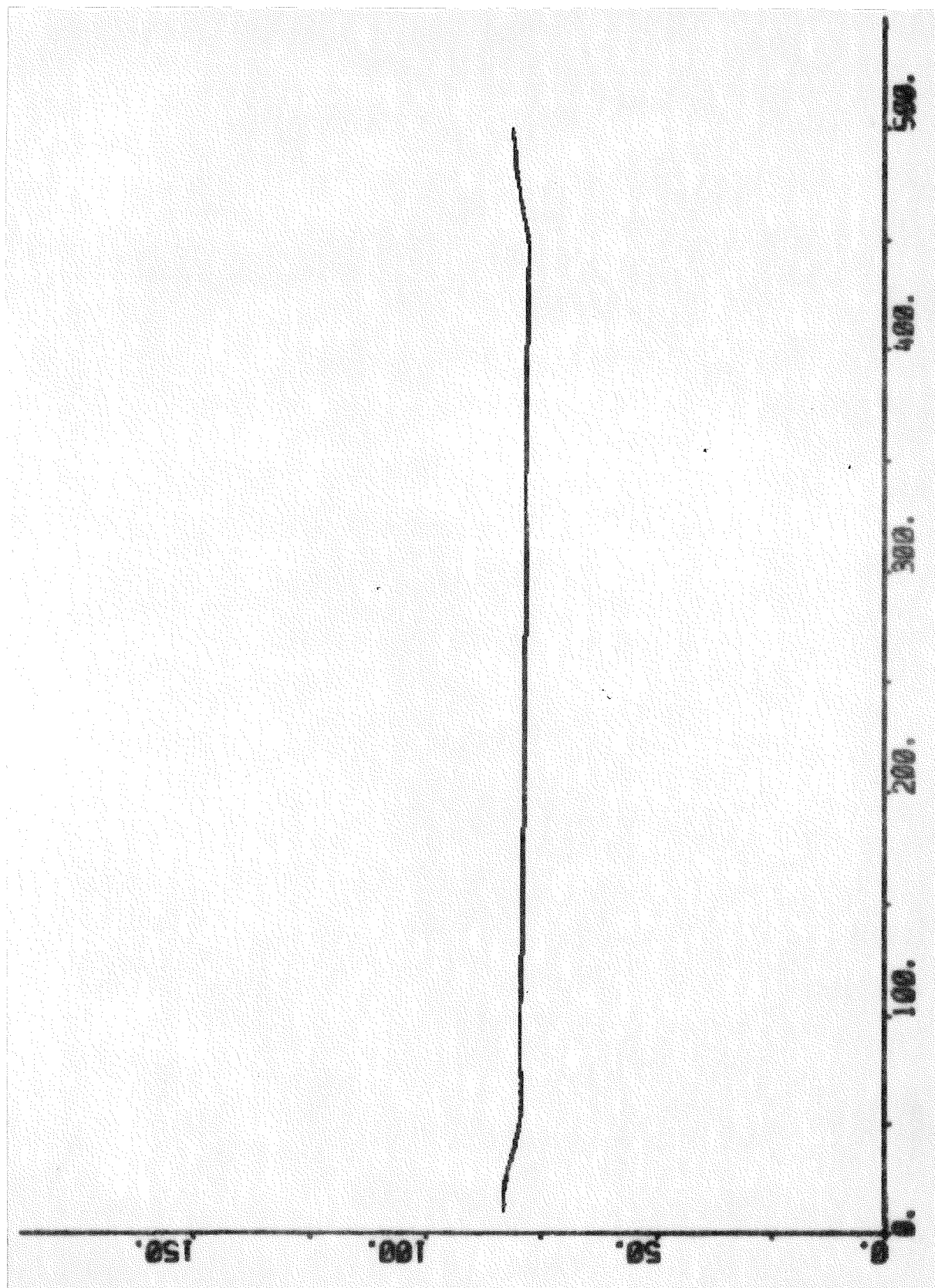


Fig. 16.6 - Response of the feedwater flow during transfer from alert to normal mode.

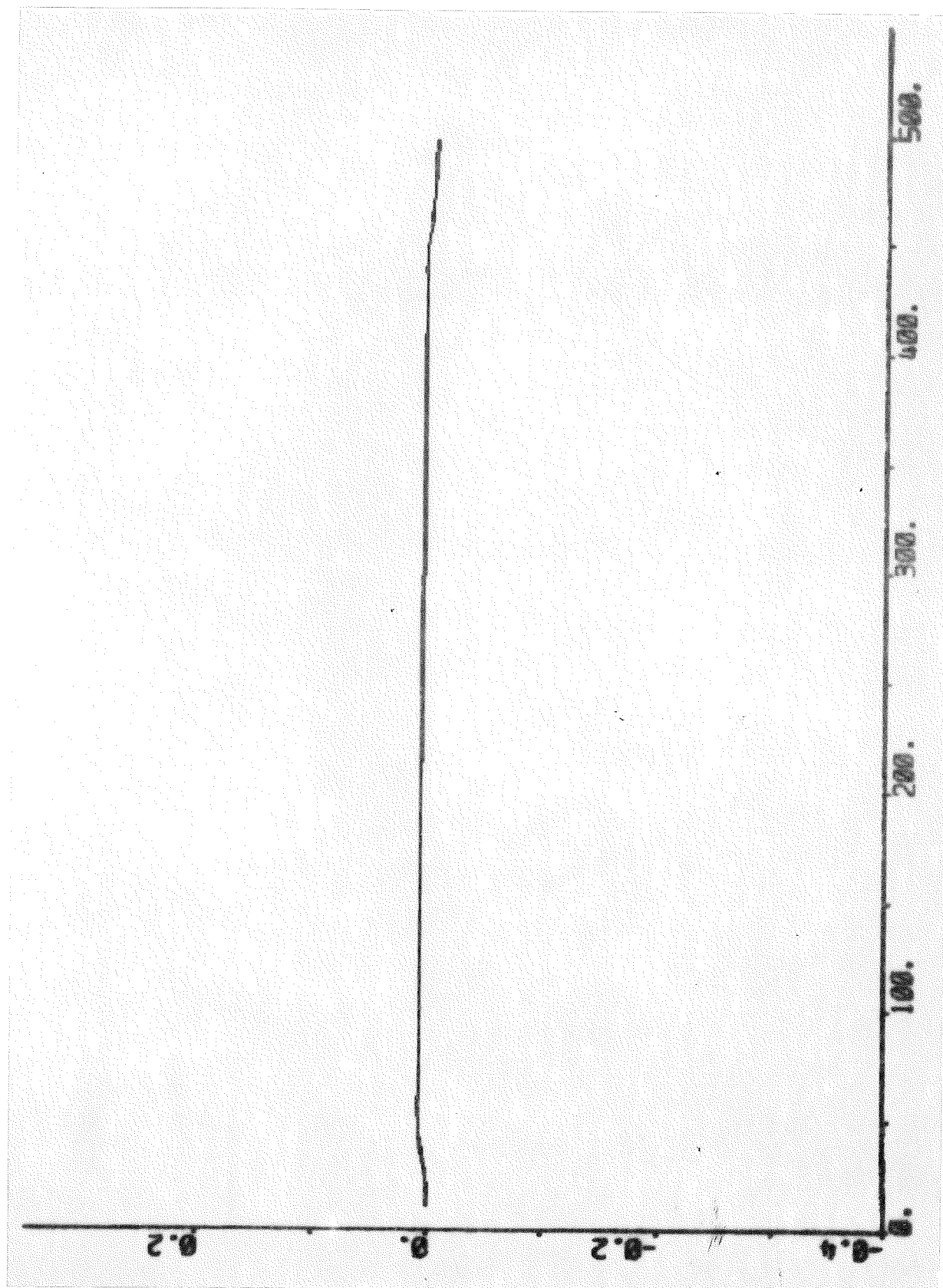


Fig. 16.7 - Response of the drum level during transfer from alert to normal mode.

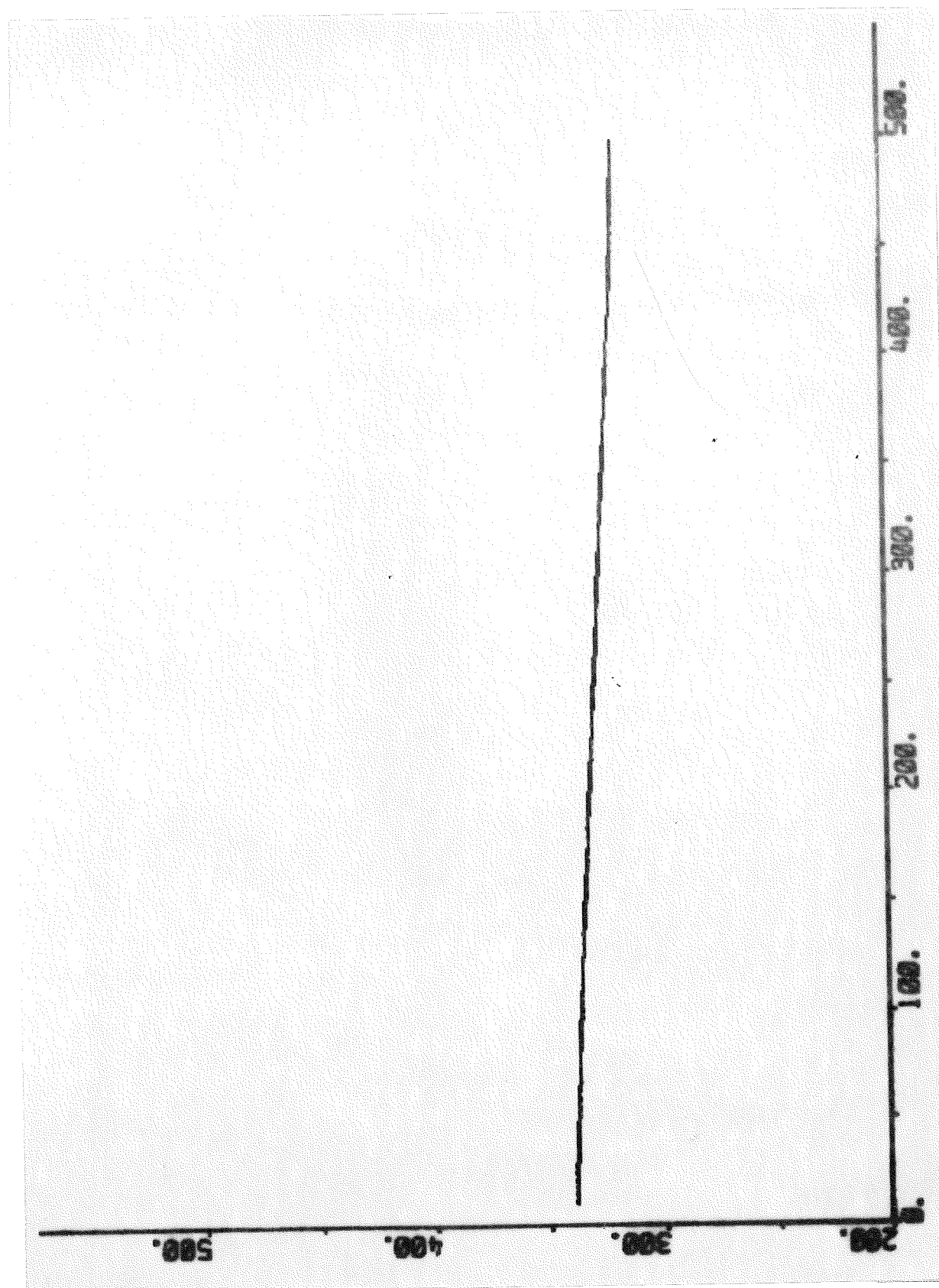


Fig. 16.8 - Response of the drum water temperature during transfer from alert to normal mode.

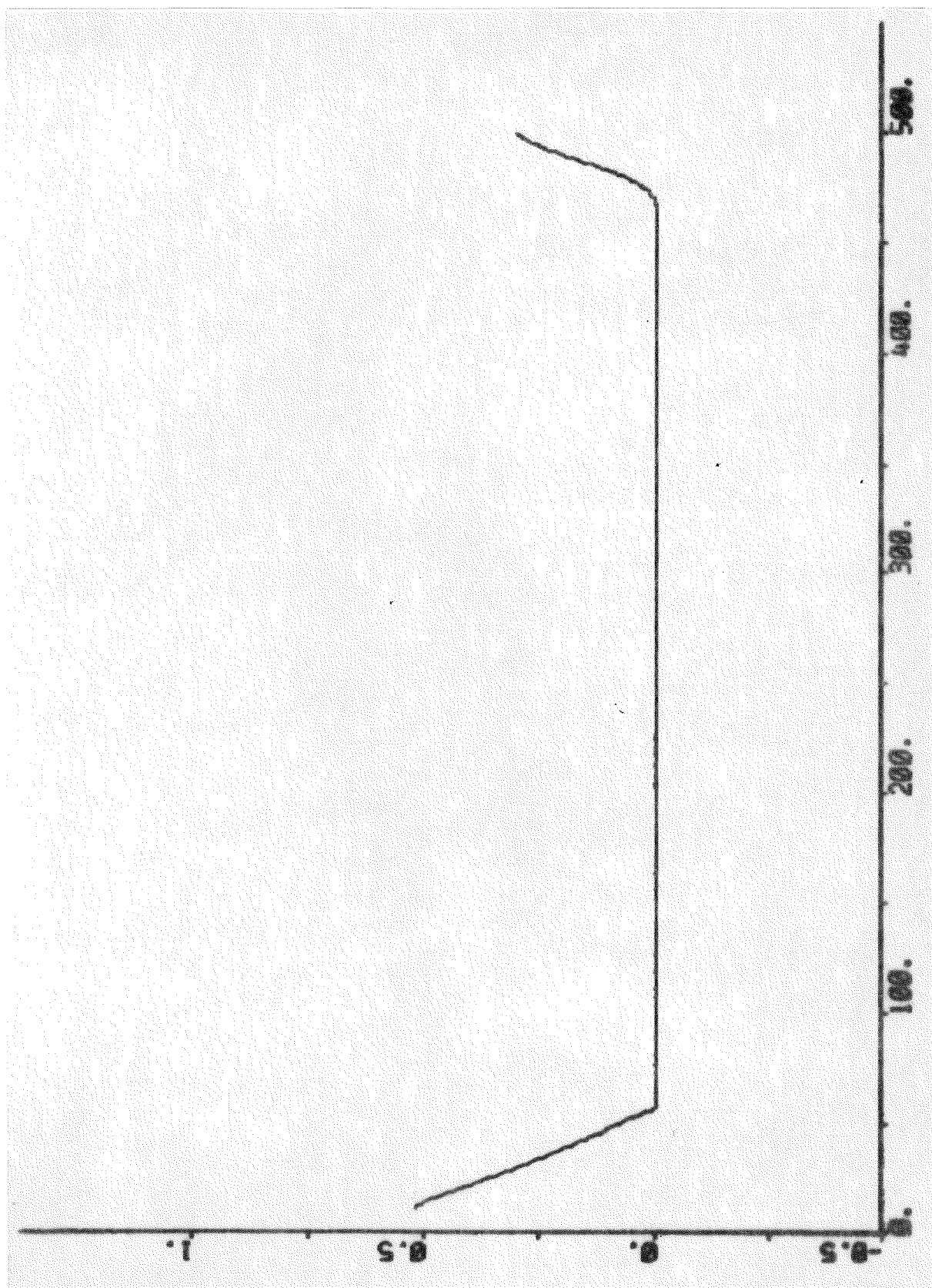


Fig. 16.9 - Response of the stroke of the first attenuator spray flow valve during transfer from alert to normal mode.

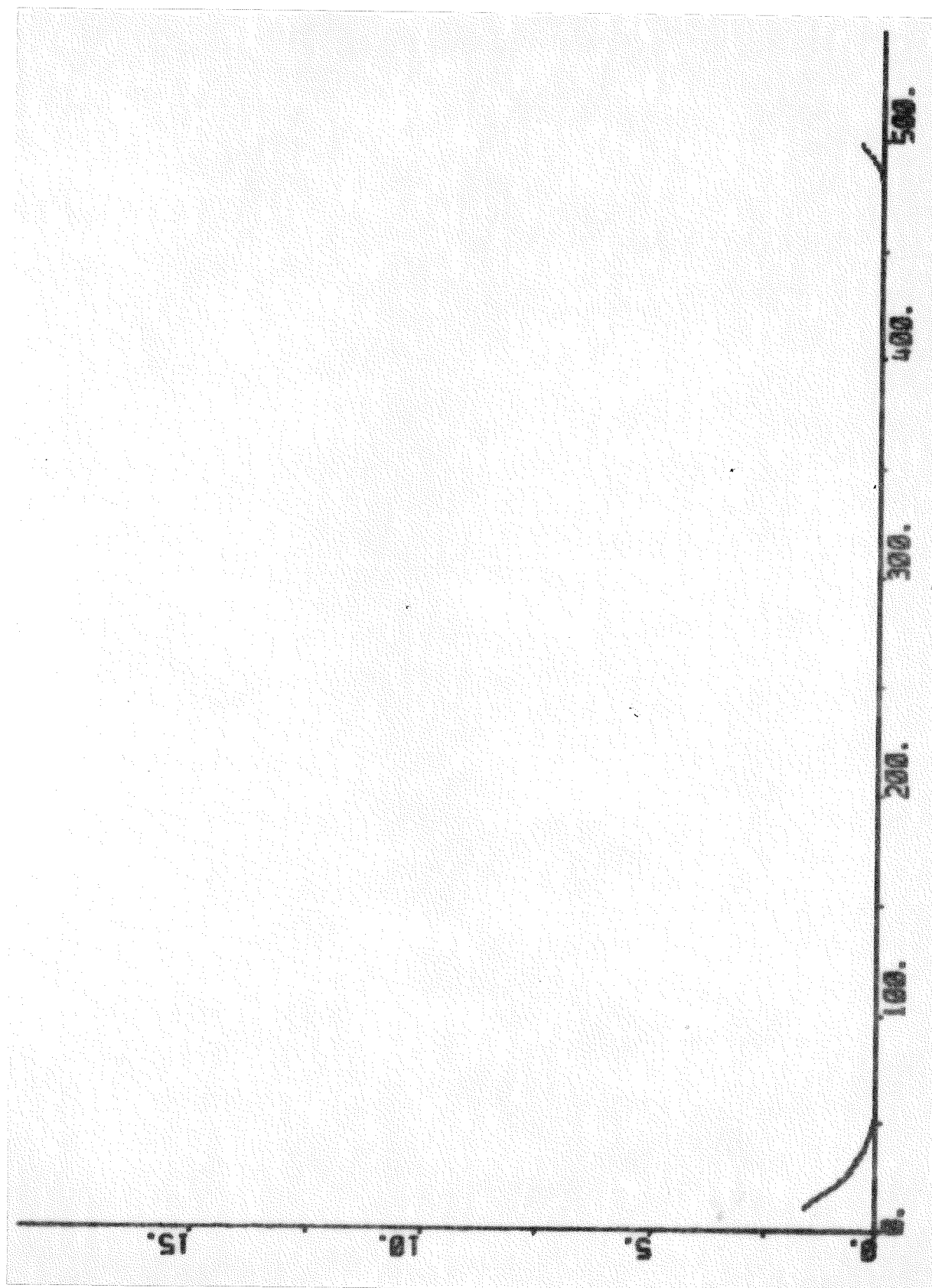


Fig. 16.10 - Response of the spray flow of the first attenuator during transfer from alert to normal mode.



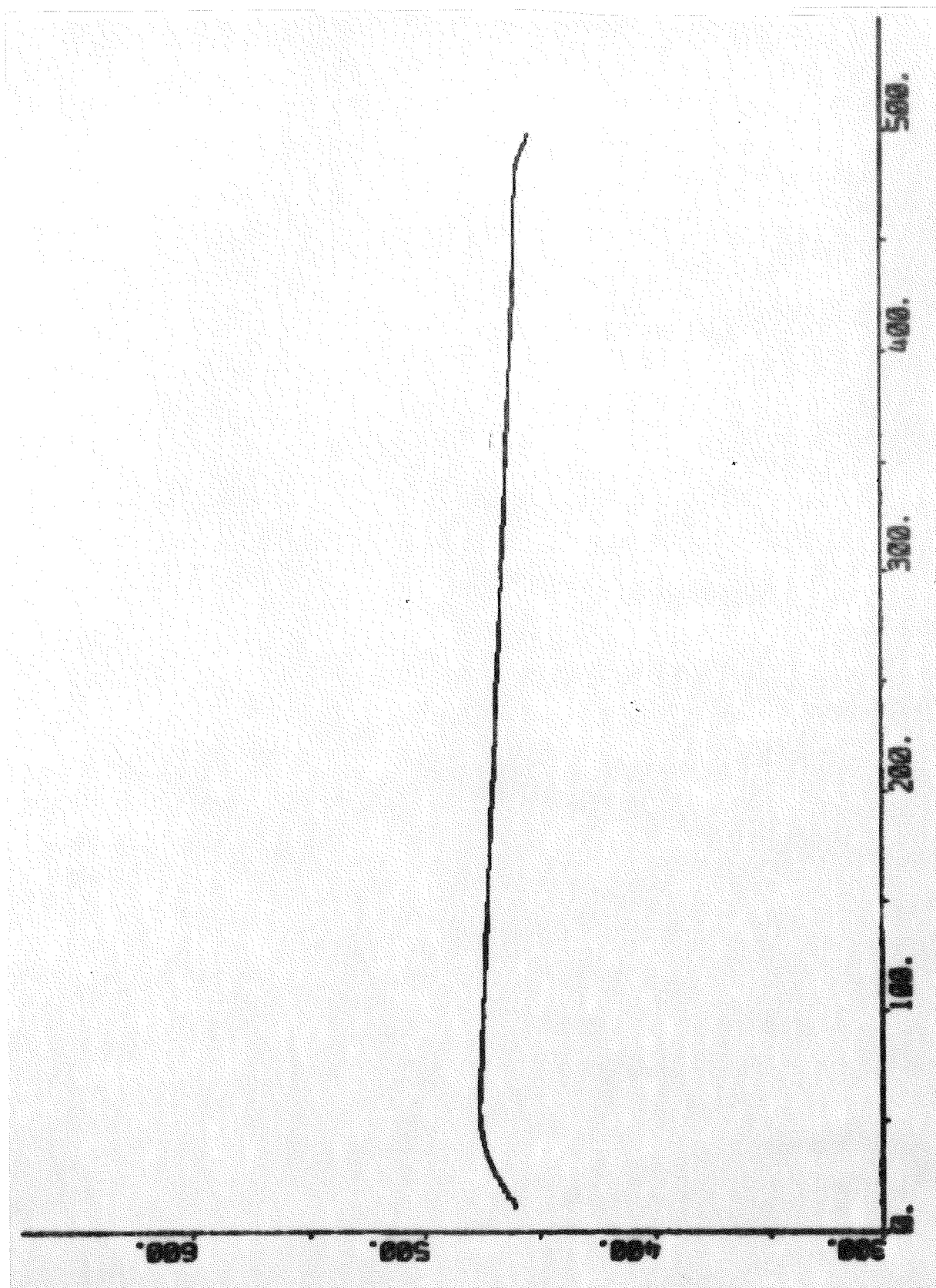


Fig. 16.11 - Response of the steam temperature before the secondary superheater during transfer from alert to normal mode.

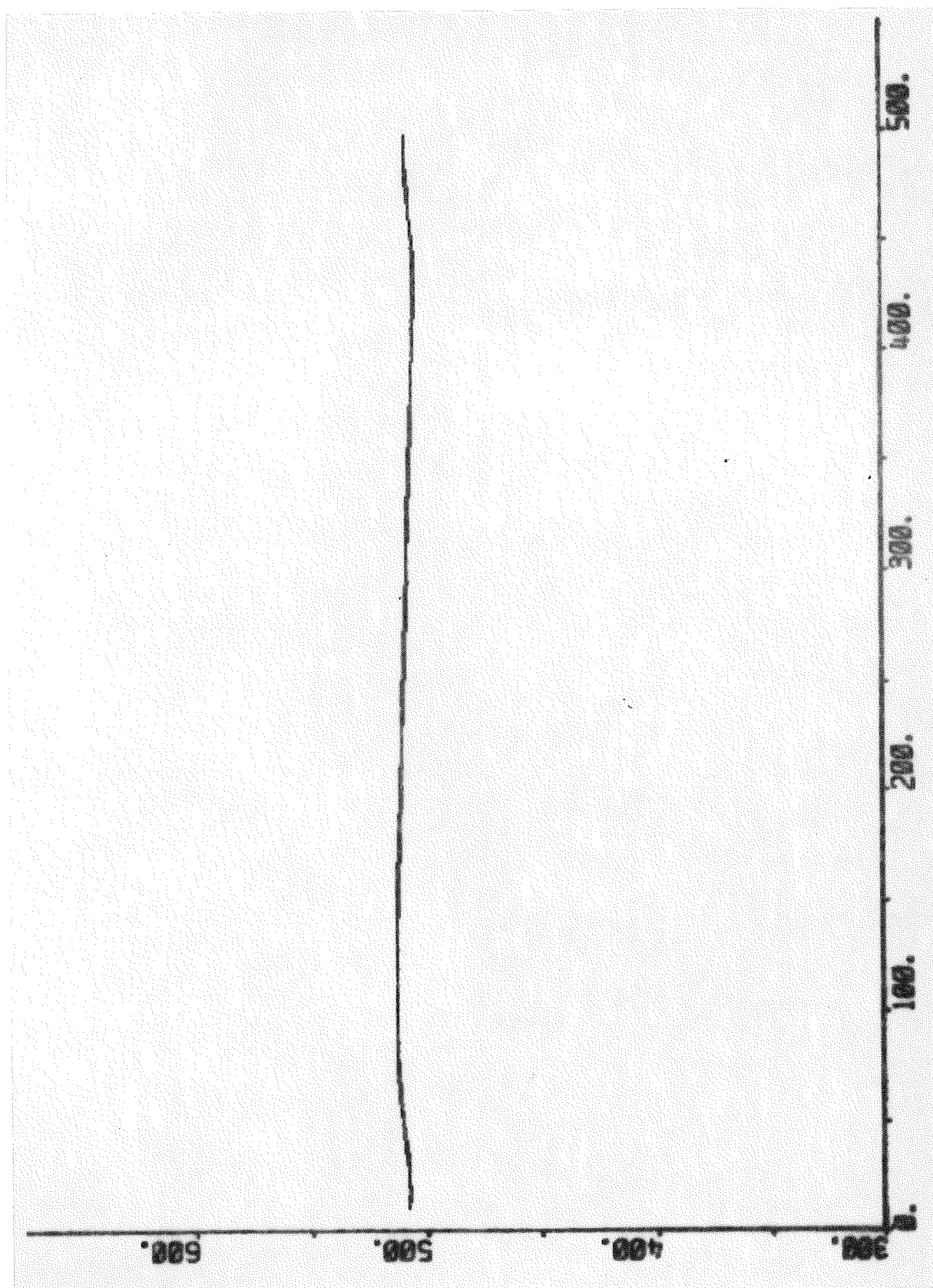


Fig. 16.12 - Response of the steam temperature after the secondary superheater during transfer from alert to normal mode.

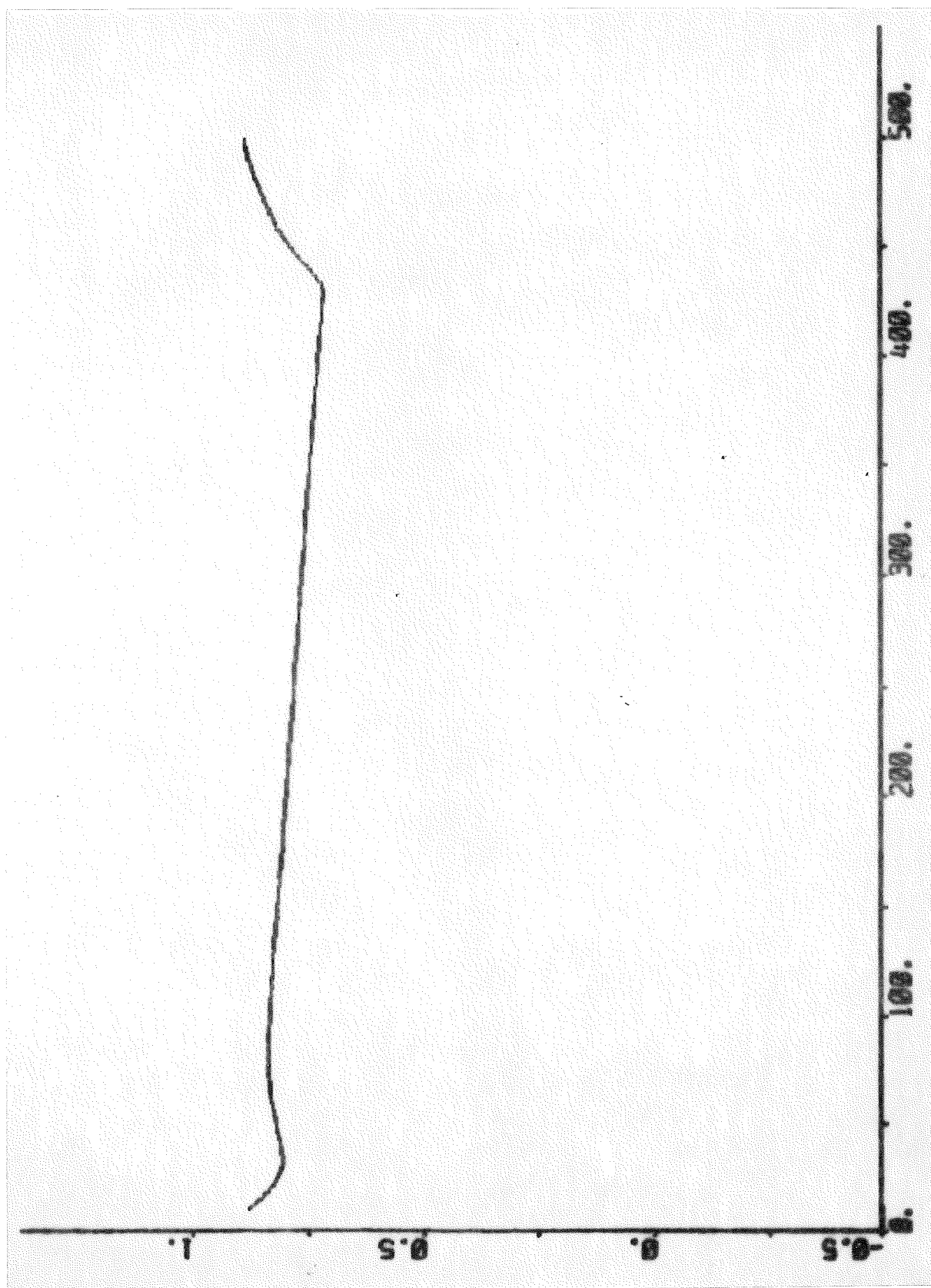


Fig. 16.13 - Response of the stroke of the second attenuator spray flow valve during transfer from alert to normal mode.

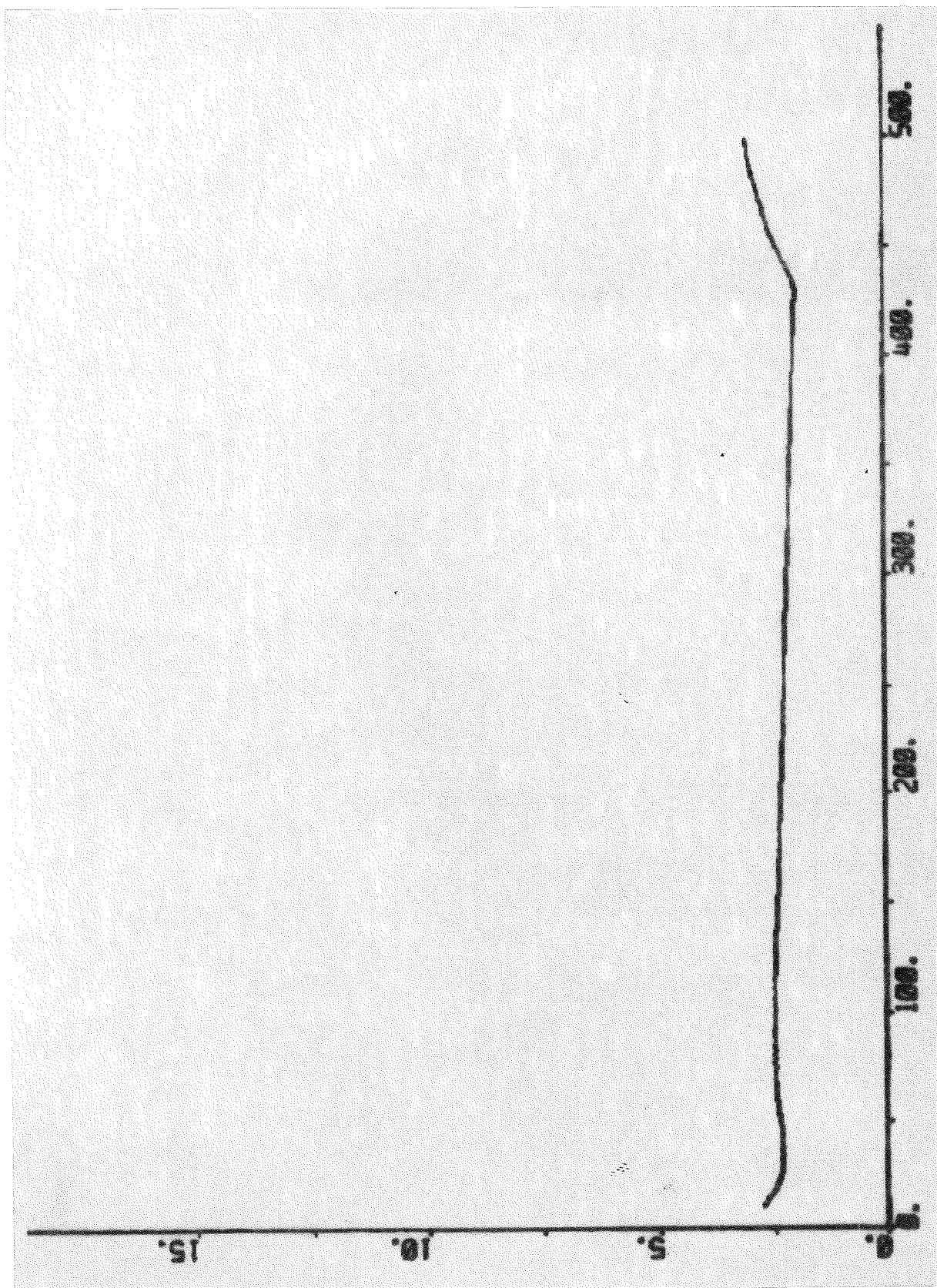


Fig. 16.14 - Response of the spray flow of the second attenuator during transfer from alert to normal mode.

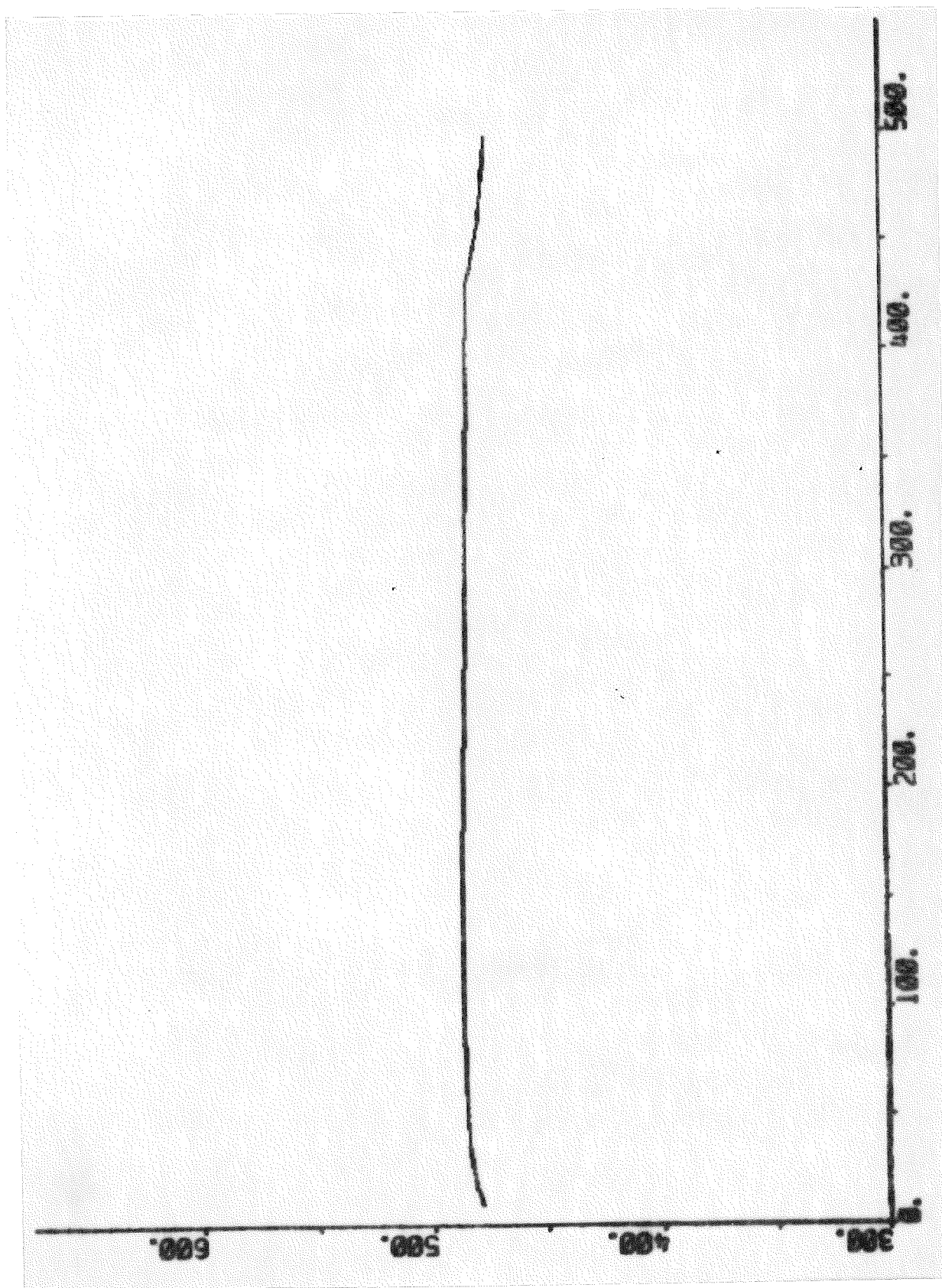


Fig. 16.15 - Response of the steam temperature before the tertiary superheater during transfer from alert to normal mode.

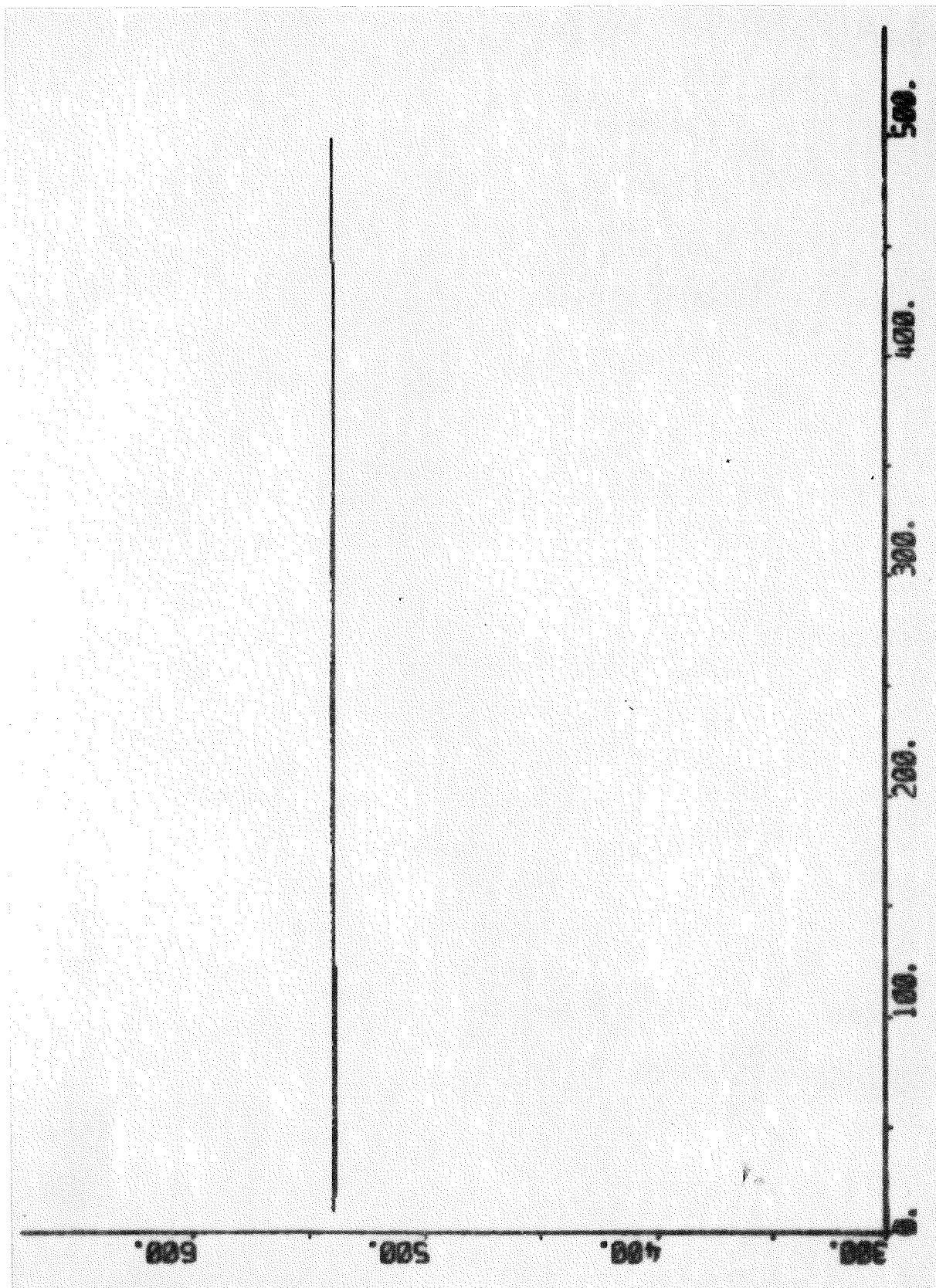


Fig. 16.16 - Response of the steam temperature after the tertiary superheater during transfer from alert to normal mode.

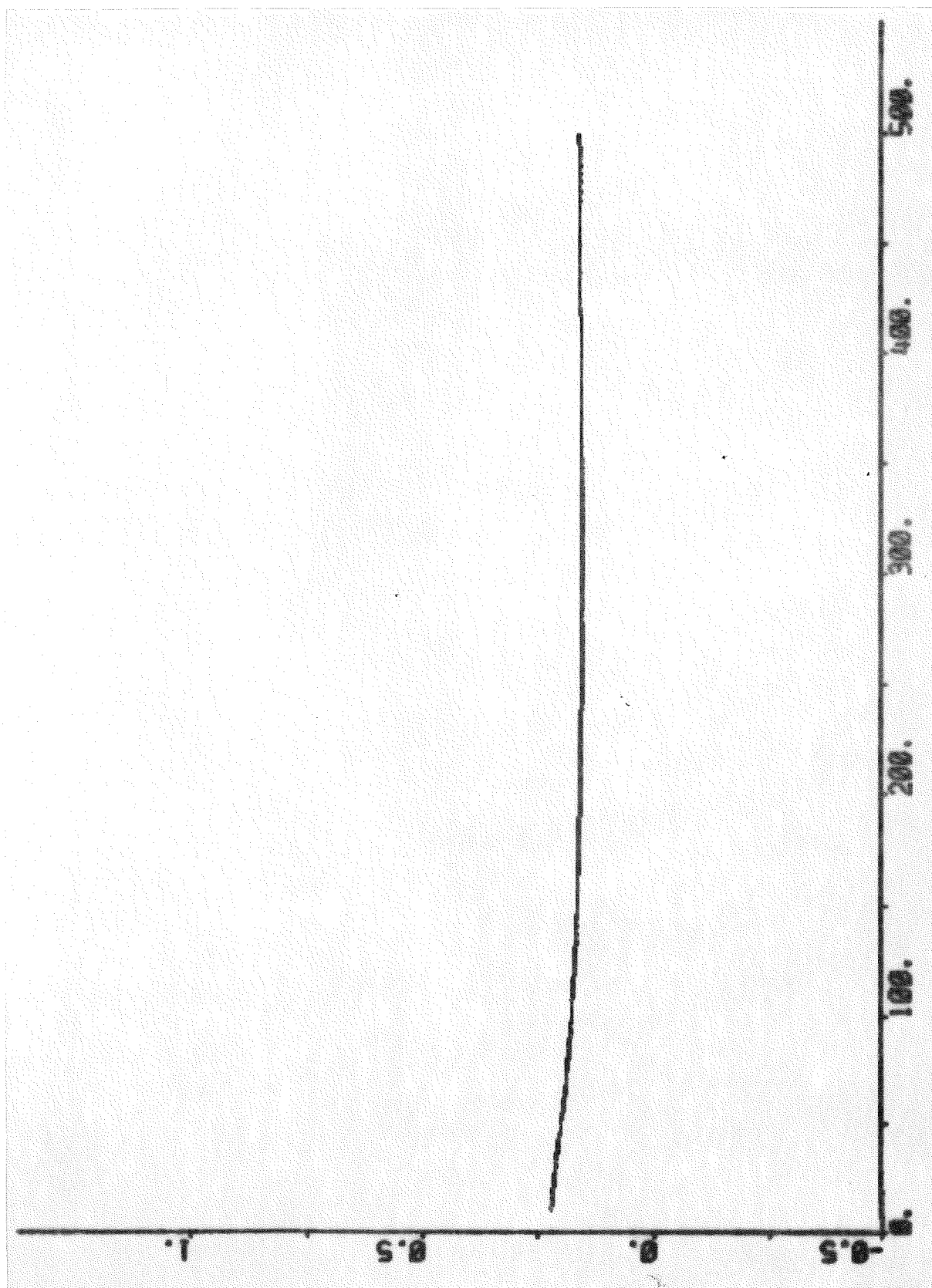


Fig. 16.17 - Responses of the strokes of the LP-preheater extraction valve during transfer from alert to normal mode.



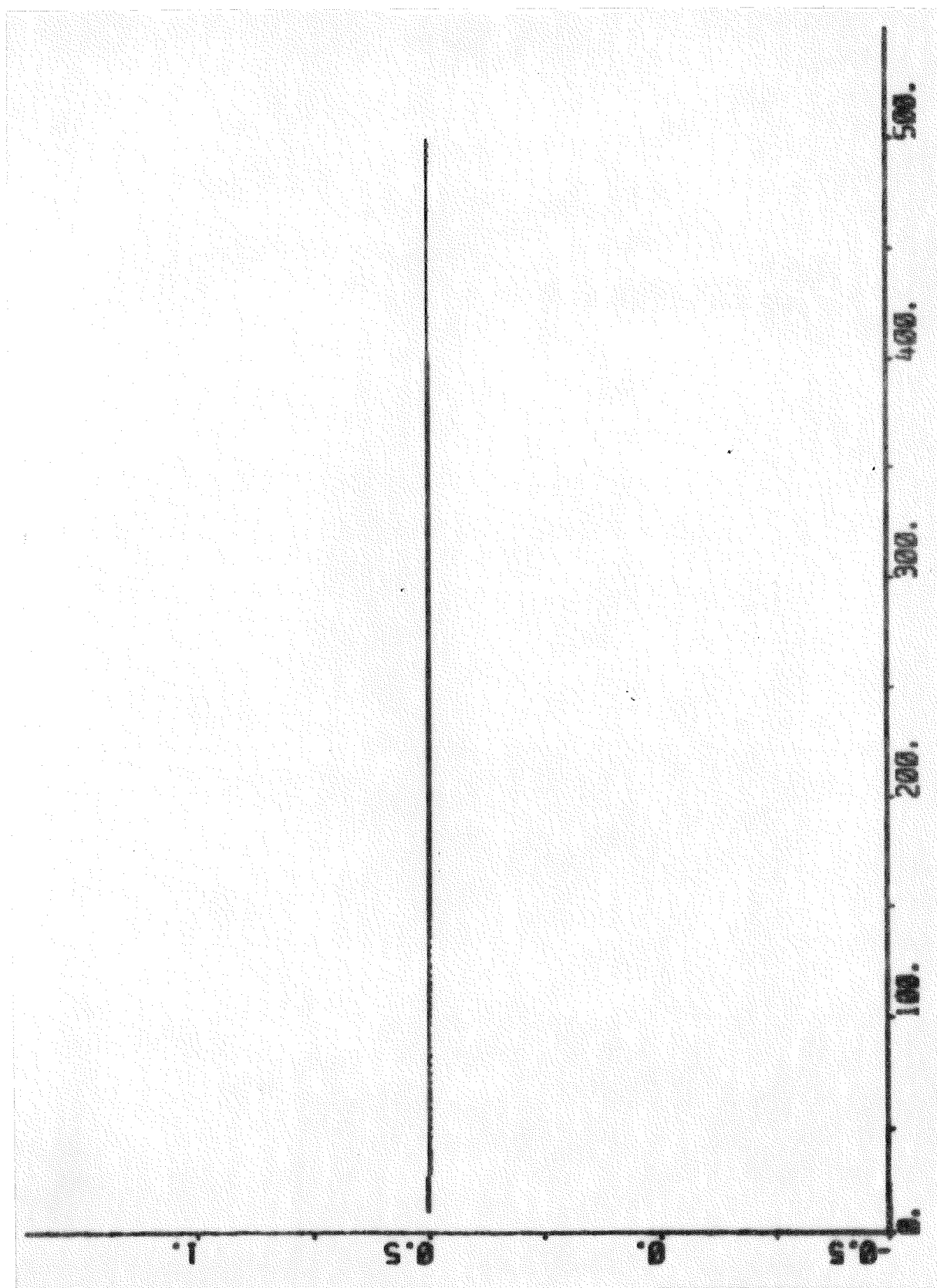


Fig. 16.18 - Response of the stroke of the HP-preheater extraction valve during transfer from alert to normal mode.



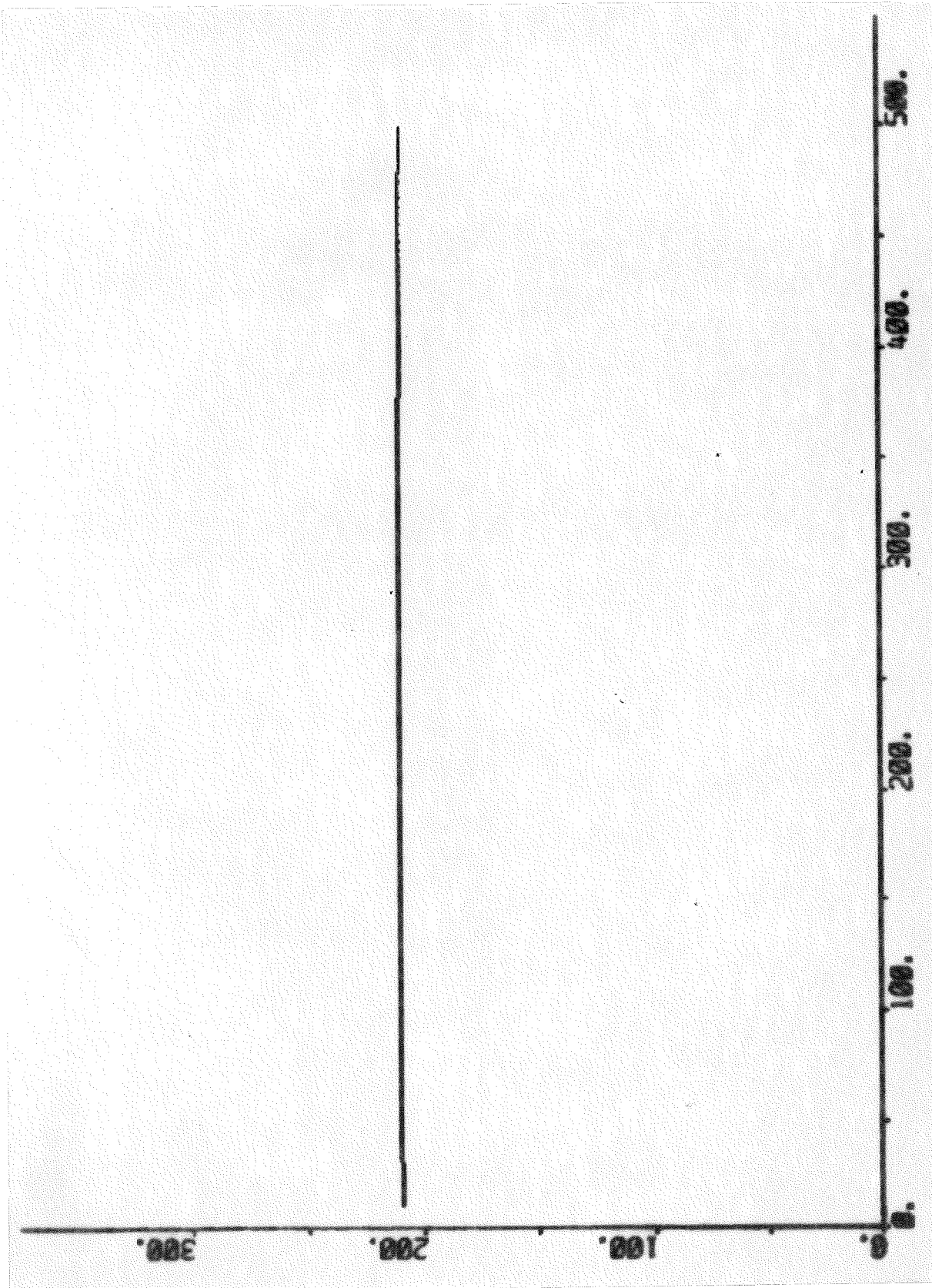


Fig. 16.19 - Response of the feedwater temperature after the HP-preheater during transfer from alert to normal mode.

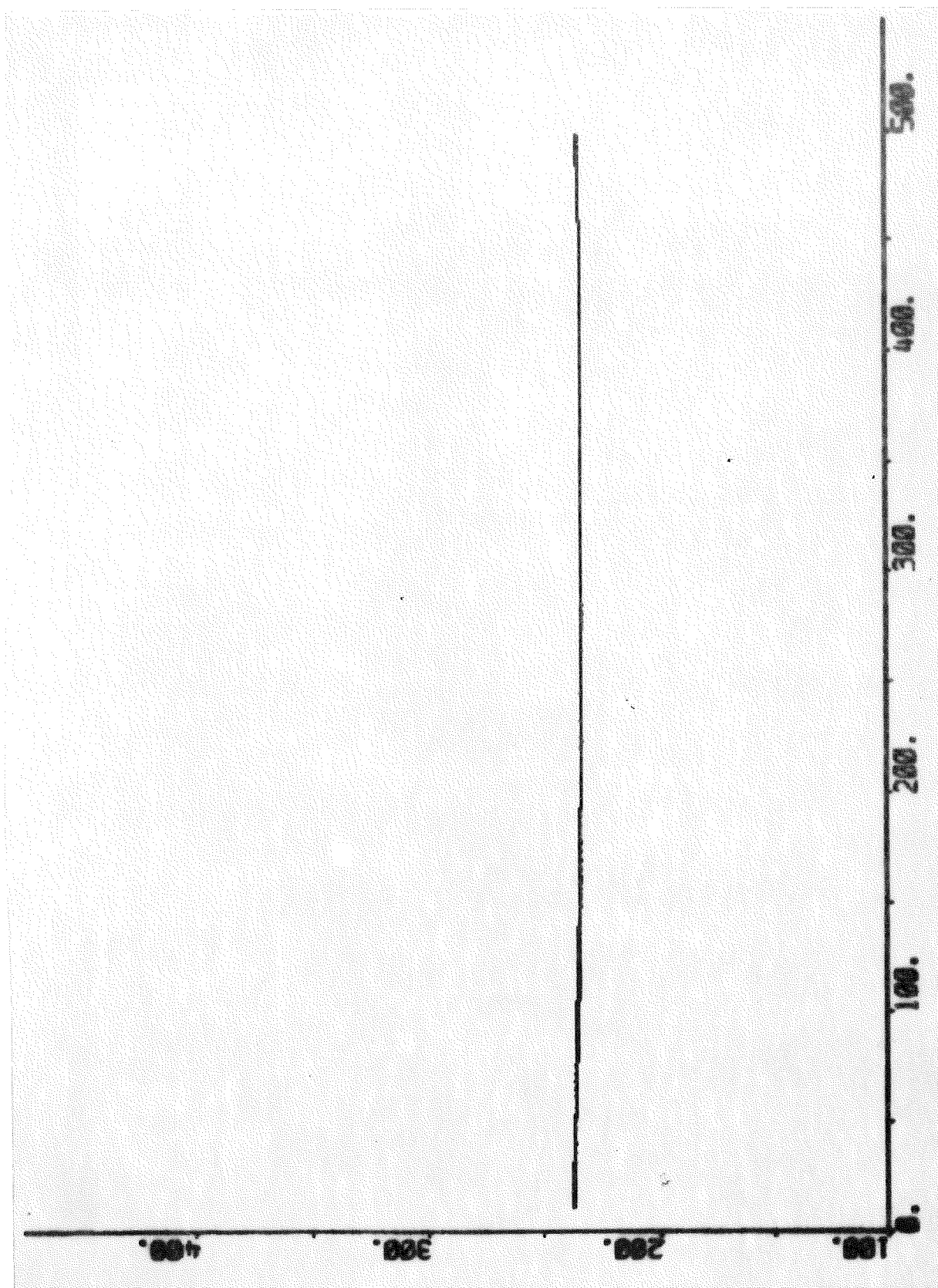


Fig. 16.20 - Response of the feedwater temperature after the economizer during transfer from alert to normal mode.

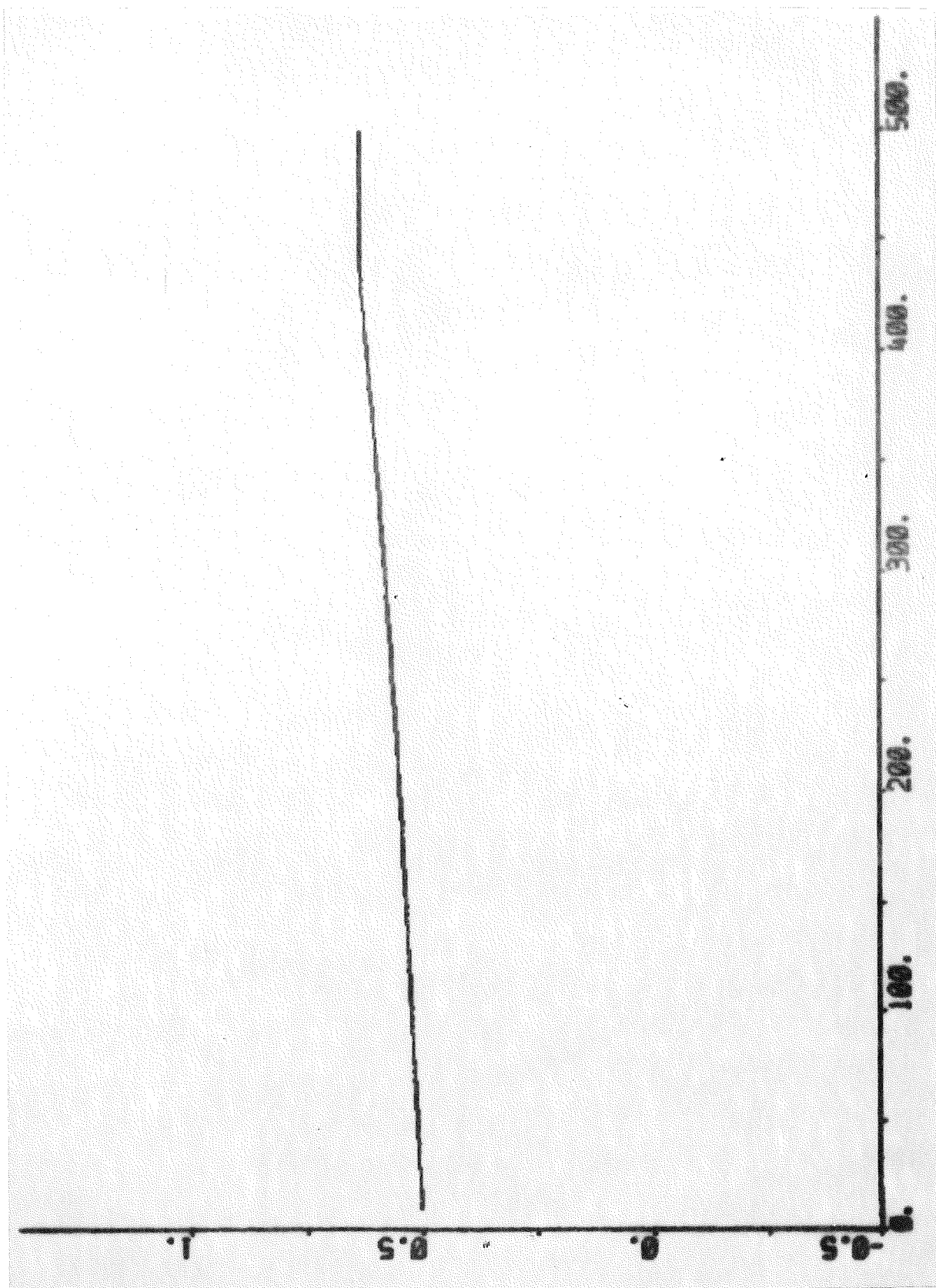


Fig. 16.21 - Response of the stroke of the control valve during transfer from normal to alert mode.

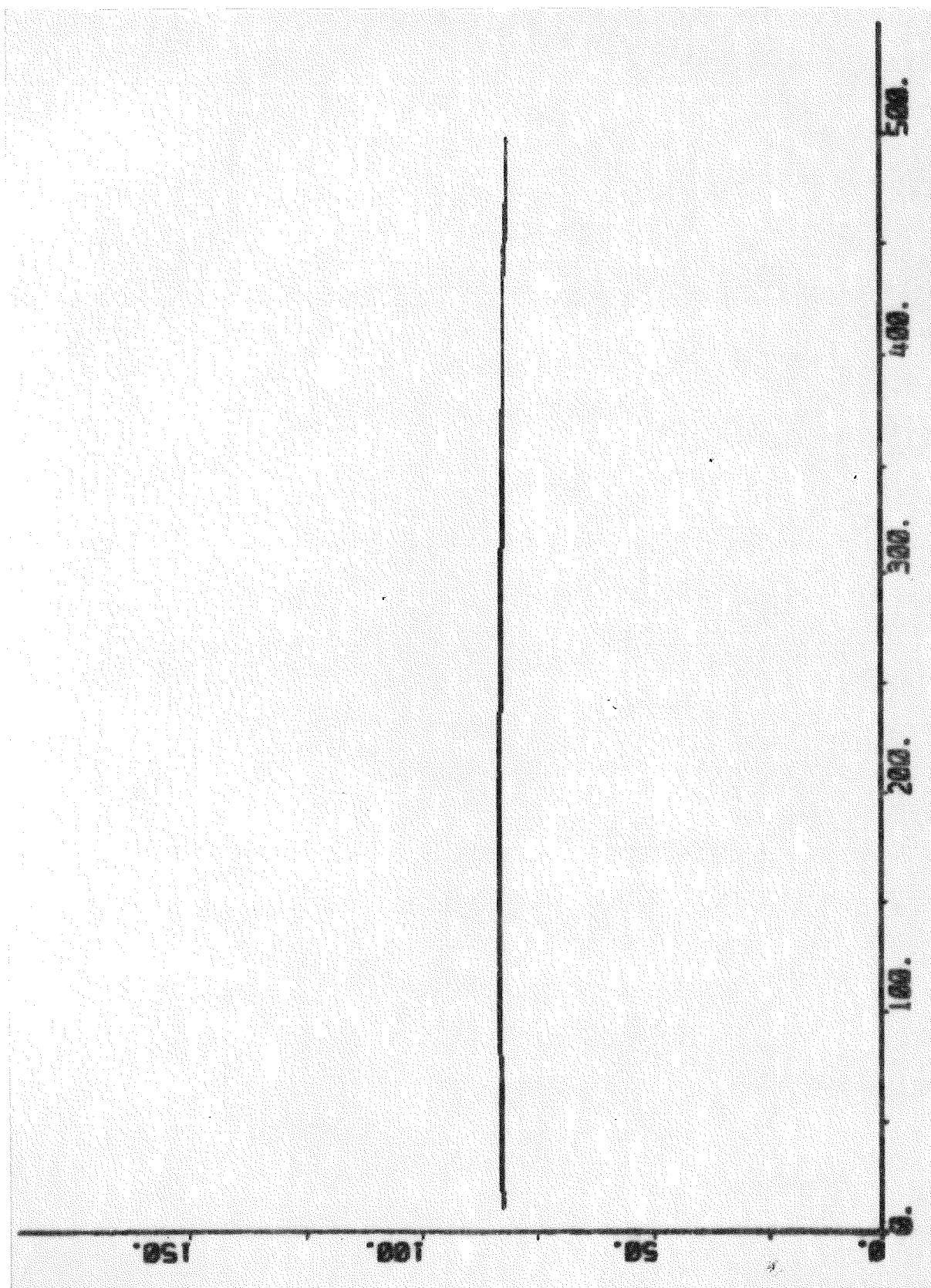


Fig. 16.22 - Response of the steam flow during transfer from alert to normal mode.

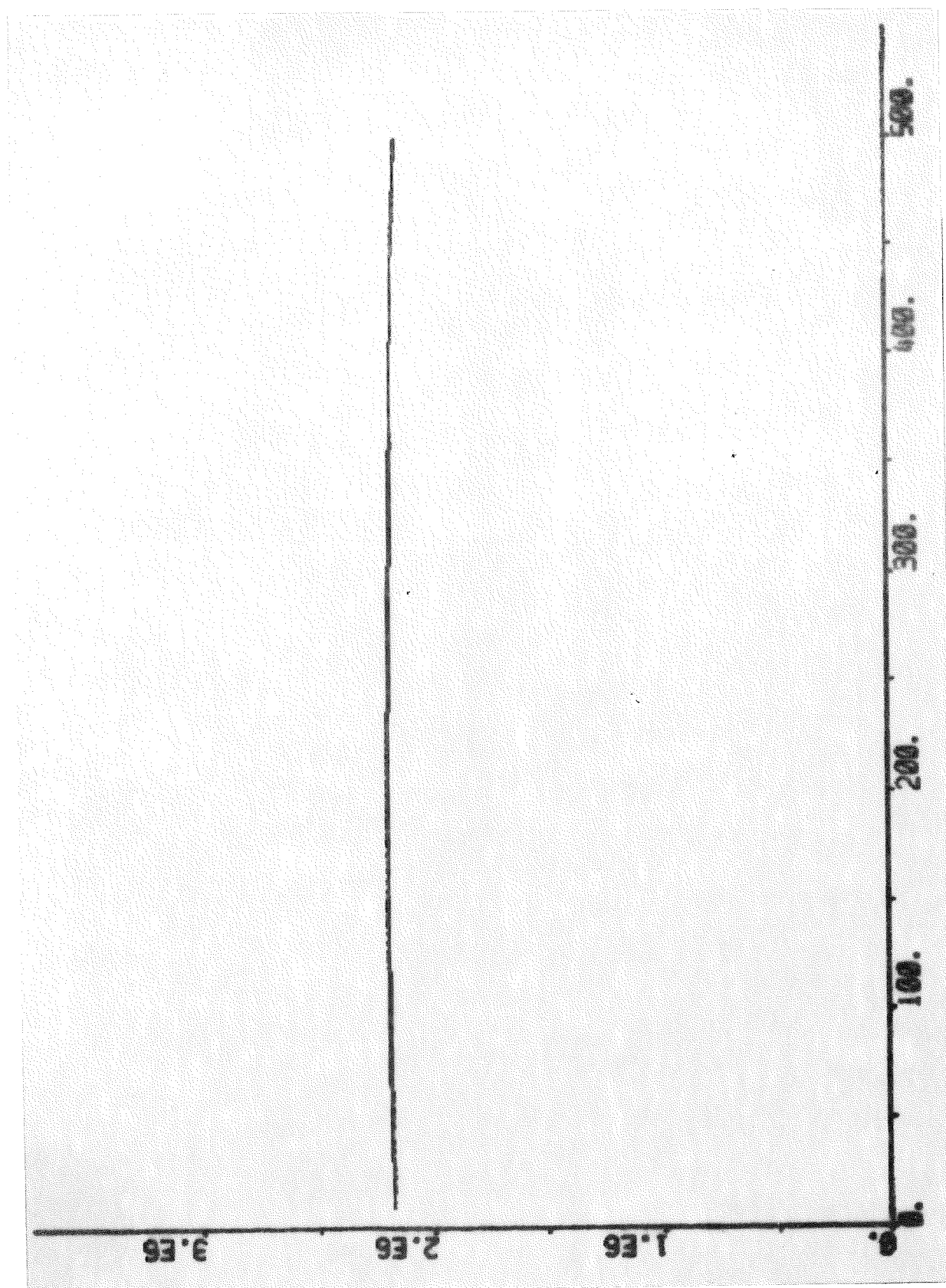


Fig. 16.23 - Response of the reheater steam pressure during transfer from alert to normal mode.

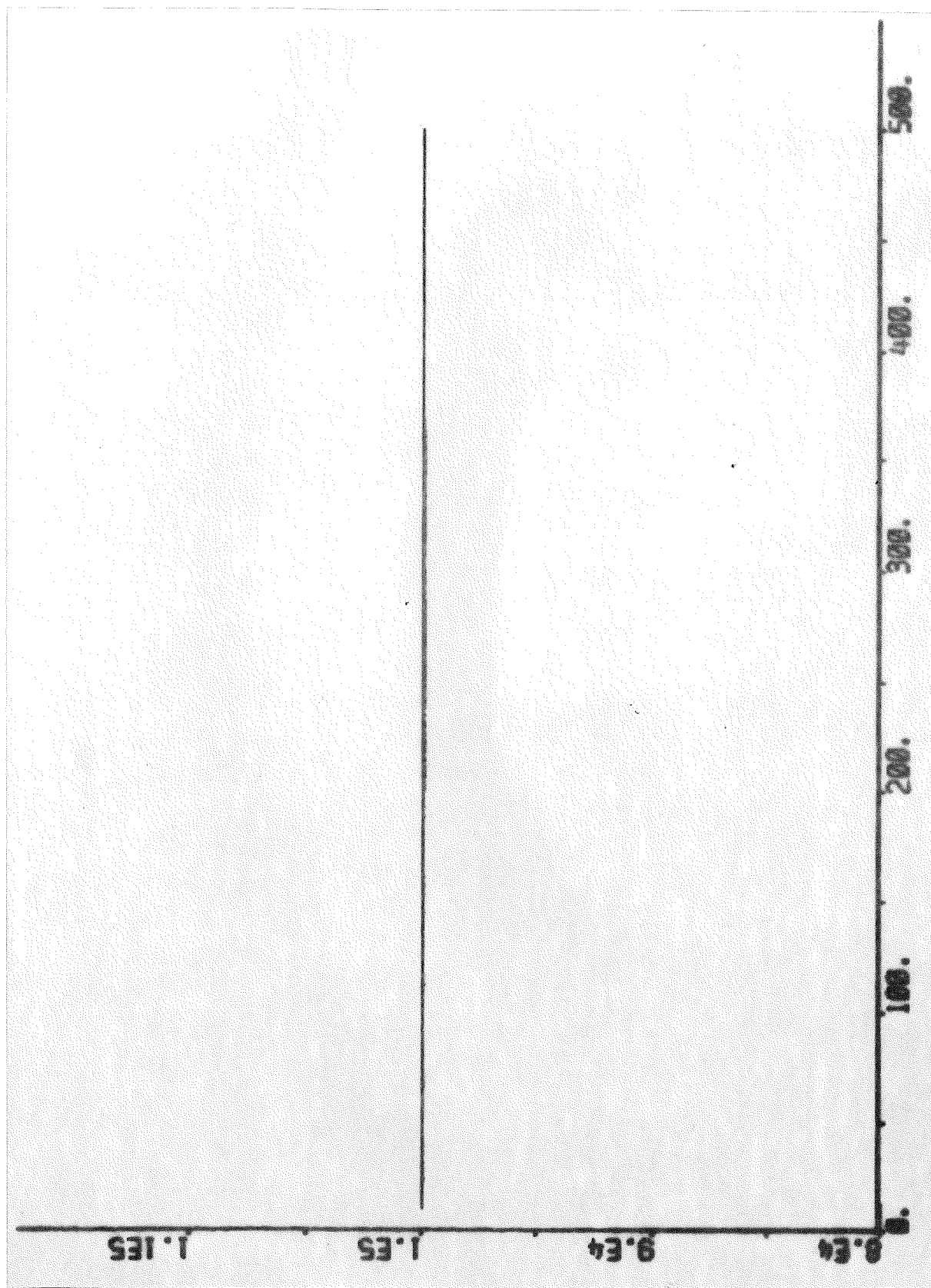


Fig. 16.24 - Response of the output power during transfer from alert to normal mode.

## 17. INCREASE OF OUTPUT POWER IN NORMAL MODE.

The performance of the control system when the output power is increased in normal mode will be examined in this section. The output power was changed by changing the power demand signal from 100 MW (63%) to 160 MW (100%) at  $t = 10$  s. The power demand signal,  $s_{nslr}$  is input to the power demand setter (PDS), which generates the reference value of the output power. The reference value of the output power,  $N_{gs2r}$  is limited by the jump-and-rate circuit (PDS3) in Fig. 5.3. The numerical value of the jump of  $N_{gs2r}$  is 16 MW (10%) and the numerical value of the rate of  $N_{gs2r}$  is 9.6 MW/min (6%/min) in normal mode. The performance of the drum pressure loop, the drum level loop, the steam temperature loop, and the output power loop will now be examined.

### The drum pressure loop.

The task of the drum pressure loop is to control the drum pressure by manipulating the fuel flow. The reference value of the drum pressure,  $p_{ds2r}$  is generated by the drum pressure reference setter (DPRS), which was described in Section 6. The reference value of the drum pressure is determined by the reference value of the output power,  $N_{gs2r}$  and by the mode (normal or alert) of the control system. In this case  $p_{ds2r}$  is increased from  $113 \cdot 10^5$  Pa (75%) to  $145 \cdot 10^5$  Pa (97%) with a limited,  $9 \cdot 10^5$  Pa/min (6%/min) rate-of-change. The steam flow (Fig. 17.22), the feedwater flow (Fig. 17.6), and the feedwater temperature after the HP-preheater (Fig. 17.19) disturb the drum pressure loop. The mean density of the steam-water mixture in the riser tubes, the steam temperature after the primary superheater, the heat flows to the superheaters, to the reheater, and to the economizer are disturbed by the fuel flow variations. The fuel flow,  $w_{bol}$  is the output of the fuel flow servo (FFS), which was described in Section 7. The reference value of the fuel flow,  $w_{bolr}$  is determined by the drum pressure controller (DPC), which was described in Section 7. The inputs to the DPC are  $p_{ds2r}$  and its derivative,  $s_{bolt}$ , the drum pressure,  $p_{ds2}$ , and the steam flow,  $w_{ts1}$ . The block diagram of the DPC is

given in Fig. 7.1. The rate-of-change of the fuel flow is limited in the FFS. The limits are parameters,  $w_{\text{bolo}}$  and  $w_{\text{bols}}$  of the first nonlinear block in Fig. 7.2. The numerical value of  $w_{\text{bolo}}$  and  $w_{\text{bols}}$  are both  $0.1 \text{ kg/s}^2$  (60%/min).

The response of the fuel flow is shown in Fig. 17.1. The fuel flow increases linearly for  $10 < t < 35 \text{ s}$  due to the limited rate-of-change of the fuel flow. The fuel flow is about  $1.2 \text{ kg/s}$  (14%) higher than the final value during the increase of the drum pressure. The effect of the feedforward term from the derivative of the reference value of the drum pressure can be observed at  $t = 220 \text{ s}$ . The fuel flow is reduced rapidly in order to avoid overshoot of the drum pressure.

The response of the drum pressure is shown in Fig. 17.2. The drum pressure decreases somewhat for  $10 < t < 25 \text{ s}$  due to the rapid increase of the steam flow (Fig. 17.22). The increase of the drum pressure starts at  $t = 30 \text{ s}$ , when the rate-of-change of the fuel flow is lower than the maximum value. The drum pressure has an overshoot of  $4 \cdot 10^5 \text{ Pa}$  (3%).

The response of the steam pressure before the control valve is shown in Fig. 17.3. The steam pressure decreases at  $t = 10 \text{ s}$  due to the increased steam flow (Fig. 17.22). The increased steam flow increases the pressure drop in the superheaters due to friction losses. The decrease and the increase of the drum pressure can be observed in the response of the pressure before the control valve too.

The response of the steam temperature after the primary superheater is shown in Fig. 17.4. The total variation of the temperature is about  $20^\circ\text{C}$ . The temperature decreases for  $10 < t < 30 \text{ s}$  due to the increased steam flow (Fig. 17.22) and the decreased steam temperature before the primary superheater with no corresponding increase of the heat flow to the primary superheater. The steam temperature before the primary superheater is determined by the drum pressure (Fig. 17.2). The heat flow to the primary superheater is approximately proportional to the fuel flow (Fig. 17.1).



Properties: The steam flow is the most severe disturbance of the drum pressure loop. The steam flow and the derivative of the reference value of the drum pressure influence the fuel flow through the feedforward. The effects of the other disturbances are reduced by feedback. The limited rate-of-change of the fuel flow deteriorates the performance of the drum pressure loop for  $10 < t < 40$  s. This must, however, be accepted because of the restrictions of the burner equipment. The maximum drum pressure error is  $4 \cdot 10^5$  Pa (3%).

#### The drum level loop.

The task of the drum level loop is to control the drum level,  $z_{dl4}$  by manipulating the feedwater control valve. The reference value of the drum level,  $z_{dl4r}$  is constant. The steam flow (Fig. 17.22) and the fuel flow (Fig. 17.1) disturb the drum level loop. The feedwater temperature is disturbed by the variations of the feedwater flow. If the drum level is too high there is a danger that water will reach the turbine. If the drum level is too low there is a danger that the riser tubes will be damaged due to insufficient cooling. The feedwater flow,  $w_{fw5}$  is the output of the feedwater servo (FWS), which was described in Section 8. The reference value of the feedwater flow,  $w_{fw5r}$  is determined by the drum level controller (DLC), which was described in Section 8. The inputs to the DLC are  $z_{dl4r}$ ,  $z_{dl4}$  and the steam flow,  $w_{ts1}$ . The block diagram of the DLC is given in Fig. 8.1. The rate-of-change of the stroke of the feedwater valve is limited in the feedwater servo (FWS). The limits are parameters,  $s_{ww2o}$  and  $s_{ww2s}$  of the first nonlinear block in Fig. 8.2. The numerical values of  $s_{ww2o}$  and  $s_{ww2s}$  are both 5%/s.

The response of the stroke of the feedwater valve is shown in Fig. 17.5. The valve opening has to be increased in order to increase the feedwater flow and to compensate for the increasing drum pressure. The valve is opening for  $10 < t < 15$  s due to the feedforward from the steam flow (Fig. 17.22). The valve is clos-

ing for  $15 < t < 30$  s due to the feedback from the drum level. The valve is opening again for  $t > 30$  s due to the feedforward from the steam flow and the feedback from the drum level.

The response of the feedwater flow is shown in Fig. 17.6. The response of the feedwater flow is similar to the response of the stroke of the feedwater valve. The response of the feedwater flow is also similar to the response of the steam flow (Fig. 17.22). The effect of the changing mean density of the steam-water mixture in the drum system is visible for  $10 < t < 250$  s. The feedwater flow is lower than the steam flow for  $10 < t < 50$  s. The maximum difference is about 20 kg/s (14%). The feedwater flow is higher than the steam flow for  $60 < t < 250$  s, when the drum pressure is increasing.

The response of the drum level is shown in Fig. 17.7. The swell phenomenon increases the drum level 4 cm at  $t = 25$  s. The drum level is about 0.2 cm low during the increase of the drum pressure.

The response of the drum water temperature is shown in Fig. 17.8. The rate-of-change of drum water temperature determines the thermal stresses of the drum material. The rate-of-change is less than  $6^{\circ}\text{C}/\text{min}$ .

Properties: The steam flow is the main disturbance of the drum level loop. The control of the drum level is difficult due to the shrink-and-swell phenomenon. The steam flow influences the feedwater flow through the feedforward term. The effects of the other disturbances are reduced by feedback. The maximum drum level error is about 4 cm.

### The steam temperature loop.

The task of the steam temperature loop is to control the steam temperature after the tertiary superheater  $T_{ts2}$  by manipulating the first and the second attemperator spray flow valves. The reference value of the steam temperature after the tertiary superheater,  $T_{ts2r}$  is constant. The heat flows to the secondary and tertiary superheaters, the steam temperature after the primary superheater (Fig. 17.4), and the steam flow (Fig. 17.22) disturb the steam temperature loop. The heat flows to the secondary and tertiary superheaters are both approximately proportional to the fuel flow (Fig. 17.1). The specific fuel consumption is reduced if the steam temperature after the tertiary superheater is increased. The steam temperature is limited by the properties of the superheater material. The steam temperature before the secondary superheater,  $T_{ss1}$  is the output of the secondary superheater steam temperature servo (SSSTS), which was described in Section 9. The steam temperature before the tertiary superheater,  $T_{ts1}$  is the output of the tertiary superheater steam temperature servo (TSSTS), which was described in Section 9. The reference value of the steam temperature before the tertiary superheater,  $T_{ts1r}$  is determined by the tertiary superheater steam temperature controller (TSSTC), which was described in Section 9. The inputs to the TSSTC are  $T_{ts2r}$ ,  $T_{ts2}$ , the steam flow,  $w_{ts1}$ , and the fuel flow,  $w_{bol}$ . The block diagram of the TSSTC is given in Fig. 9.1. The reference value of the steam temperature before the secondary superheater,  $T_{ss1r}$  is determined by the secondary superheater steam temperature controller (SSSTC), which was described in Section 9. The inputs to the SSSTC are  $T_{ss2r}$ ,  $T_{ss2}$ ,  $w_{ts1}$ , and  $w_{bol}$ . The rate-of-change of the stroke of the second attemperator spray flow valve is limited in the TSSTS. The limits are parameters,  $s_{tw2o}$  and  $s_{tw2s}$  of the first nonlinear block in Fig. 9.3. The numerical values of  $s_{tw2o}$  and  $s_{tw2s}$  are both 4%/s. The rate-of-change of the stroke of the first attemperator spray flow valve is limited in the SSSTS. The limits are parameters,  $s_{sw2o}$  and  $s_{sw2s}$  of the first nonlinear block in Fig. 9.4. The numerical values of  $s_{sw2o}$  and  $s_{sw2s}$  are both 4%/s. The difference between

$T_{ss2r}$  and  $T_{ts1r}$  is a parameter,  $g_{sw2b}$  of the SSSTC. The numerical value of  $g_{sw2b}$  is  $30^{\circ}\text{C}$  and is chosen so that the second attemperator spray flow valve is approximately halfopen. This means that the steam temperature before the tertiary superheater can be changed rapidly in both directions.

The response of the stroke of the first attemperator spray flow valve is shown in Fig. 17.9. The valve is closing for  $10 < t < 20$  due to the increasing steam flow through the secondary superheater with no corresponding increase of the heat flow. The valve is then opened for  $20 < t < 60$  s due to the increasing heat flow to the secondary superheater. The valve is finally closing for  $t > 220$  s due to the decreasing heat flow.

The response of the spray flow of the first attemperator is shown in Fig. 17.10. The spray flow follows the stroke of the valve fairly well. The increased steam flow gives, however, an increased spray flow in spite of the constant stroke of the valve for  $50 < t < 220$  s. The increase of the spray flow is due to the increased pressure drop in the economizer and the primary superheater.

The response of the steam temperature before the secondary superheater is shown in Fig. 17.11. The steam temperature is increased for  $10 < t < 30$  s in order to compensate for the increased steam flow. The steam temperature is then decreased for  $30 < t < 220$  s in order to compensate for the increasing heat flow. The steam temperature is finally increased for  $t > 220$  s in order to compensate for the decreased heat flow.

The response of the steam temperature after the secondary superheater is shown in Fig. 17.12. The steam temperature decreases for  $10 < t < 15$  s due to the increasing steam flow. The difference between the steam temperature before the tertiary superheater and the steam temperature after the secondary superheater is approximately constant for  $t > 100$  s.

The response of the stroke of the second attemperator spray flow

valve is shown in Fig. 17.13. The valve is closing for  $10 < t < 15$  s due to the increased steam flow. The valve is opening for  $15 < t < 40$  s due to the increased fuel flow. The valve is then closing for  $40 < t < 140$  s in order to compensate for the decreasing steam temperature after the secondary superheater. The valve is finally opening for  $140 < t < 220$  s in order to compensate for the increasing steam temperature after the secondary superheater. The effect of the feedforward term from the fuel flow can be observed at  $t = 220$  s.

The response of the spray flow of the second attemperator is shown in Fig. 17.14. The spray flow follows the stroke of the valve quite well. The first peak of the spray flow at  $t = 10$  s is due to the rapid increase of the steam flow (Fig. 17.22). The final value of the spray flow is about 200% of the initial value but the final value of the stroke of the valve is about 111%. The increase of the gain is due to the increased pressure drop in the economizer, the primary and the secondary superheater.

The response of the steam temperature before the tertiary superheater is shown in Fig. 17.15. The steam temperature is increased for  $10 < t < 15$  s in order to compensate for the increased steam flow. The temperature is then decreased for  $20 < t < 60$  s in order to compensate for the increasing heat flow. The temperature is finally increased for  $220 < t < 350$  s in order to compensate for the decreasing heat flow.

The response of the steam temperature after the tertiary superheater is shown in Fig. 17.16. The maximum steam temperature error is less than  $2^{\circ}\text{C}$ .

Properties: The steam flow and the fuel flow are the most severe disturbances of the steam temperature loop. The steam flow and the fuel flow influence the spray flows through feedforward terms. The effects of the other disturbances are reduced by feedback. The maximum steam temperature error is less than  $3^{\circ}\text{C}$ . The spray flows are extracted after the feedwater valve, which means that the spray

flows increase with the steam flow. The gain in the attenuators decrease with the steam flow. This decrease of gain is hence counteracted, which is an advantage.

### The output power loop.

The task of the output power loop is to control the output power,  $N_{gs2}$  by manipulating the steam control valve and the extraction steam valves. The reference value of the output power,  $N_{gs2r}$  is generated by the power demand setter (PDS), which was described in Section 5. A preliminary reference value of the output power,  $s_{nsl}$  is determined from the power demand signal,  $s_{nslr}$  in the first part of the power demand setter (PDS1). The block diagram of the PDS1 is given in Fig. 5.1. The  $s_{nslr}$  is modified with respect to the network-frequency in the second part of the power demand setter (PDS2). The block diagram of the PDS2 is given in Fig. 5.2. The  $N_{gs2r}$  is obtained from the third part of the power demand setter (PDS3), which limits the jump and the rate-of-change of  $N_{gs2r}$ . The block diagram of the PDS3 is given in Fig. 5.3. The steam pressure before the control valve,  $p_{ts2}$  (Fig. 17.3) and the steam temperature before the control valve,  $T_{ts2}$  (Fig. 17.16) disturb the output power loop. The superheated steam flow,  $w_{ts1}$  (Fig. 17.22), the reheated steam flow,  $w_{rs2}$  and the extraction steam flows,  $w_{hs2}$ ,  $w_{is2}$ ,  $w_{is4}$ ,  $w_{is6}$ ,  $w_{is8}$ ,  $w_{ls2}$ , and  $w_{ls4}$  are disturbed by the output power loop. The stroke of the control valve is the output of the control valve servo (CVS), which was described in Section 10. The reference value of the stroke of the control valve,  $s_{vs2r}$  is determined by the turbine power controller (TPC), which was described in Section 10. The inputs to the TPC are  $N_{gs2r}$  and  $N_{gs2}$ . The block diagram of the TPC is given in Fig. 10.1. The strokes of the low-pressure preheater extraction valves are the outputs of the low-pressure preheater servo (LPPS), which was described in Section 10. The reference value of the strokes of the low-pressure preheater extraction valves,  $s_{fs7r}$  is determined by the low-pressure preheater controller (LPPC), which was described in Section 10. The inputs to the LPPC are  $N_{gs2r}$ , the reference value of the deaerator steam pressure,  $p_{as2r}$ , and the deaerator steam

pressure,  $p_{as2}$ . The block diagram of the LPPC is given in Fig. 10.5. The strokes of the high-pressure preheater extraction valves are the outputs of the high-pressure preheater servo (HPPS), which was described in Section 10. The reference value of the stroke of the high-pressure preheater extraction valves,  $s_{fs2r}$  is determined by the high-pressure preheater controller (HPPC), which was described in Section 10. The input to the HPPC is  $N_{gs2r}$ . The block diagram of the HPPC is given in Fig. 10.3. The rate-of-change of the stroke of the control valve is limited in the CVS. The limits are parameters,  $s_{vs2o}$  and  $s_{vs2s}$  of the first nonlinear block in Fig. 10.2. The numerical values of  $s_{vs2o}$  and  $s_{vs2s}$  are 20%/s and 200%/s respectively. The rate-of-change of the stroke of the high-pressure extraction steam flow valves are limited in the HPPS. The limits are parameters,  $s_{fs2o}$  and  $s_{fs2s}$  of the first nonlinear block in Fig. 10.4. The numerical values of  $s_{fs2o}$  and  $s_{fs2s}$  are both 100%/s. The rate-of-change of the stroke of the low-pressure extraction steam flow valves are limited in the LPPS. The limits are parameters,  $s_{fs7o}$  and  $s_{fs7s}$  of the first nonlinear block in Fig. 10.6. The numerical values of  $s_{fs7o}$  and  $s_{fs7s}$  are both 100%/s.

The response of the stroke of the low-pressure preheater extraction valves are shown in Fig. 17.17. The opening of the valves are decreased for  $10 < t < 15$  s due to the feedforward term from the increasing reference value of the output power. The opening of the valves are then increased with a time constant of about 30 s. The reference value of the output power reaches its final value at  $t = 280$  s, which is clearly visible in the response of the strokes.

The response of the stroke of the high-pressure preheater extraction valves are shown in Fig. 17.18. The opening of the valves are decreased for  $10 < t < 15$  s due to the feedforward term from the increasing reference value of the output power. The opening of the valve is then increasing with a time constant of about 30 s. The target value is lower than 0.5 and is determined by the derivative of the reference value of the output power. The reference value of the output power reaches its final value at  $t = 280$  s, which is clearly visible in the response of the strokes.

The response of the feedwater temperature after the high-pressure preheater is shown in Fig. 17.19. The temperature increases about  $25^{\circ}\text{C}$  due to the final increase of extraction steam flows. The temporary closing of the extraction valves do not affect the feedwater temperature seriously. The low-pass filtering effect of the seven preheater stages are pronounced. The feedwater temperature starts to increase when the pressures before the extraction valves increase.

The response of the feedwater temperature after the economizer is shown in Fig. 17.20. The temperature increases about  $40^{\circ}\text{C}$  due to the increasing temperature before the economizer and the increasing heat flow to the economizer.

The response of the stroke of the control valve is shown in Fig. 17.21. The valve opening is increased with maximum rate for  $10 < t < 13$  s in order to increase the output power rapidly. The control valve is almost completely open for  $t > 300$  s. The output power loop has been tuned for fast responses. This explains the peak in the response of the stroke of the control valve at  $t = 13$  s. This type of response may lead to unacceptable wear of the control valve and its servo. However, the wear can be reduced by reducing the bandwidth of the output power loop. The high bandwidth was chosen to demonstrate that it does not lead to severe interactions between the control loops.

The response of the steam flow is shown in Fig. 17.22. The steam flow starts to increase rapidly for  $10 < t < 13$  s. The rate-of-change is almost constant for  $20 < t < 280$  s. The steam flow is almost constant for  $t > 300$  s.

The response of the reheater steam pressure is shown in Fig. 17.23. The pressure is approximately proportional to the steam flow. The pressure responds, however, more slowly due to the mass storage in the reheater.



The response of the output power is shown in Fig. 17.24. The settling-time is limited to about 4 s because of the servo. The output power has reached its final value at  $t = 300$  s. The output power error is less than 1 MW for  $t > 15$  s.

Properties: The steam pressure before the control valve is the only disturbance of any importance of the output power loop in this case. The variations of the steam pressure before the control valve does not, however, introduce any difficulties. The effects of the disturbances are reduced by feedback. The response of the stroke of the control valve may lead to unacceptable wear of the control valve and its servo. The wear can, however, be reduced by reducing the bandwidth of the output power loop. The high bandwidth has been retained here in order to demonstrate the performance of the control system.

### Conclusions

The performance of the control system when the output power is increased from 100 MW (63%) to 160 MW (100%) in normal mode has been investigated by simulation. In order to increase the output power it is necessary to increase both the steam flow and the fuel flow. The steam flow is the most severe disturbance of the drum pressure loop, the drum level loop, and the steam temperature loop. The fuel flow is a severe disturbance of the steam temperature loop. The influence of the steam flow and the fuel flow has been reduced by feedforward. The limited rate of change of the fuel flow deteriorates the performance of the drum pressure loop. The maximum drum pressure error is  $4 \cdot 10^5$  Pa (3%). The control of the drum level is difficult due to the shrink-and-swell phenomenon. The maximum drum level error is about 4 cm. The limited capacity of the attemperators does not deteriorate the performance of the steam temperature loop in this case. The maximum steam temperature error is less than  $2^\circ\text{C}$ . The load dependent pressure drop in the economizer and the superheaters has been exploited in order to obtain load independent gains of the steam temperature servos. There are no severe disturbances of the out-

put power loop in this case. The output power error is less than 1 MW for  $t > 15$  s. The output power loop has been tuned for fast response, which may cause unacceptable wear of the control valve and its servo. The simulations show that even with such a tight loop there are no difficulties due to interaction with other loops.

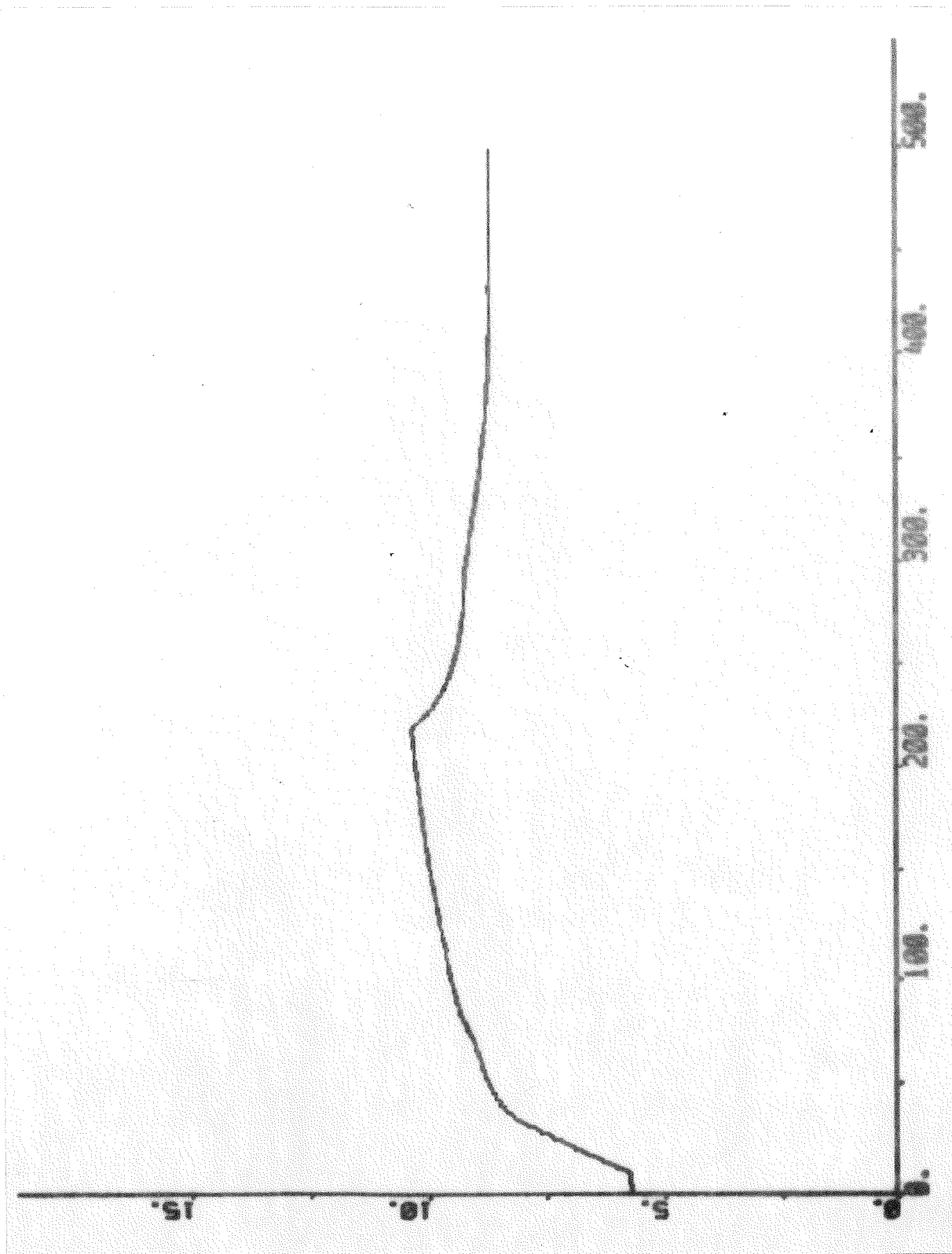


Fig. 17.1 - Response of the fuel flow due to increase of output power in normal mode.

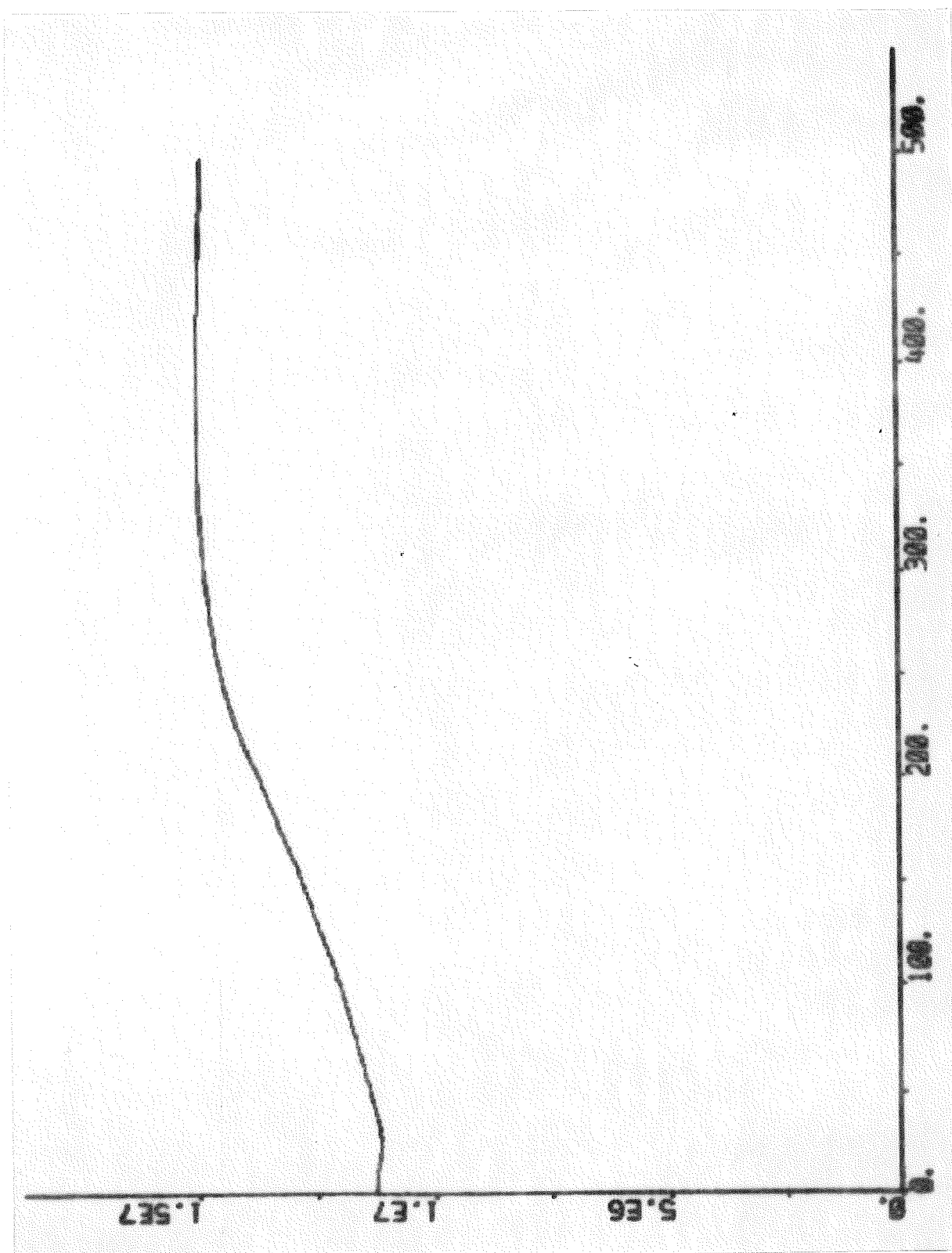


Fig. 17.2 - Response of the drum pressure due to increase of output power in normal mode.

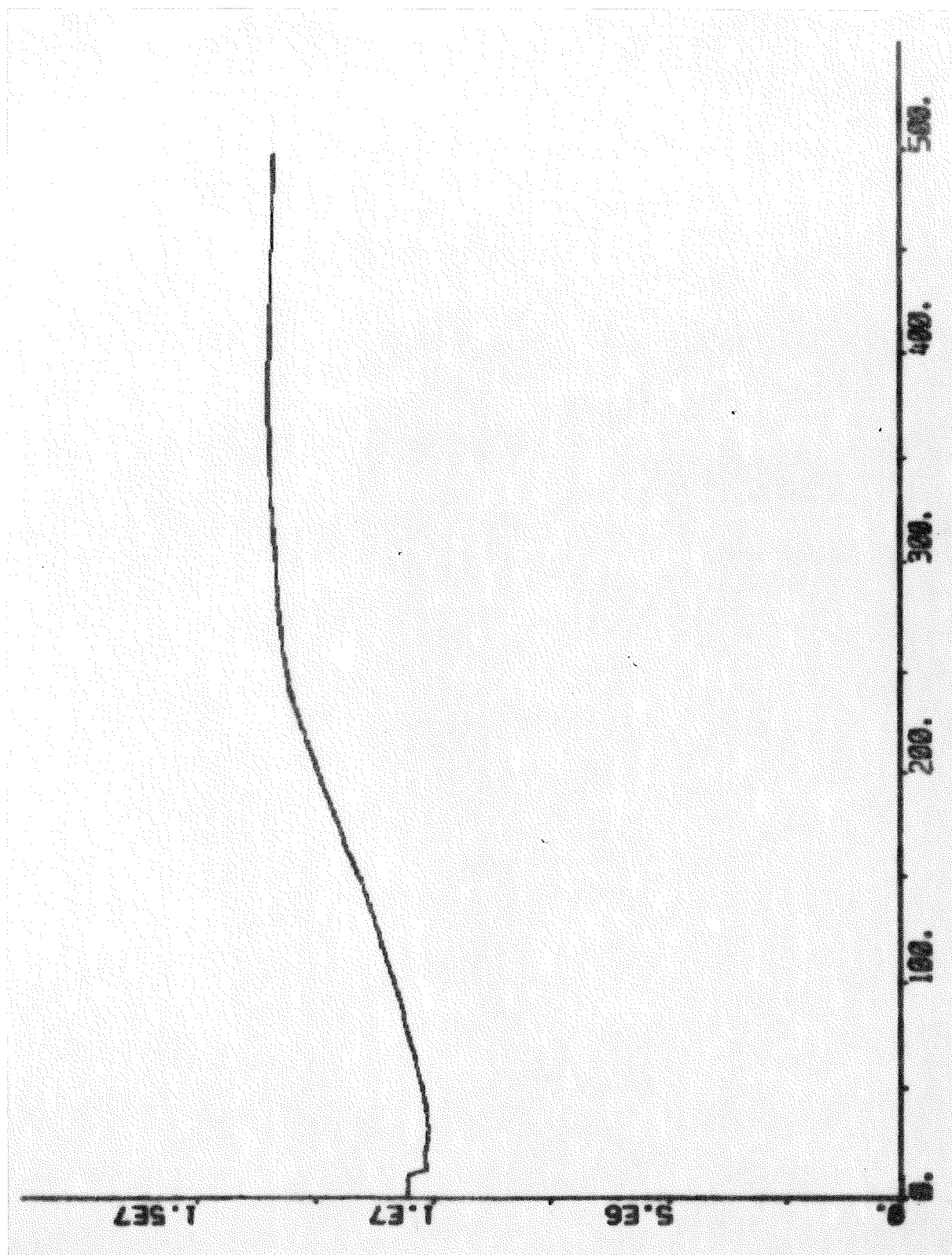


Fig. 17.3 - Response of the steam pressure before the control valve due to increase of output power in normal mode.

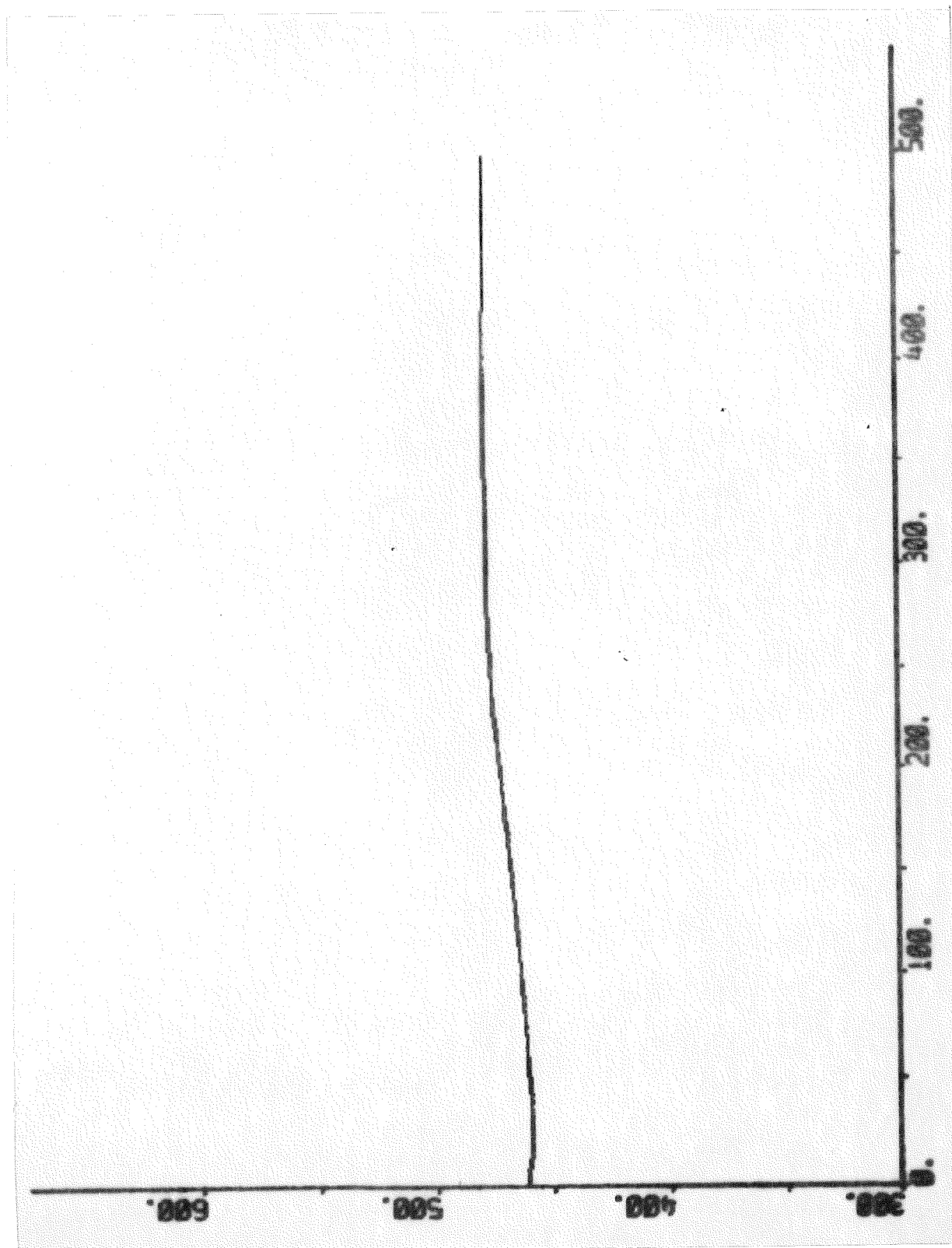


Fig. 17.4 - Response of the steam temperature after the primary superheater due to increase of output power in normal mode.

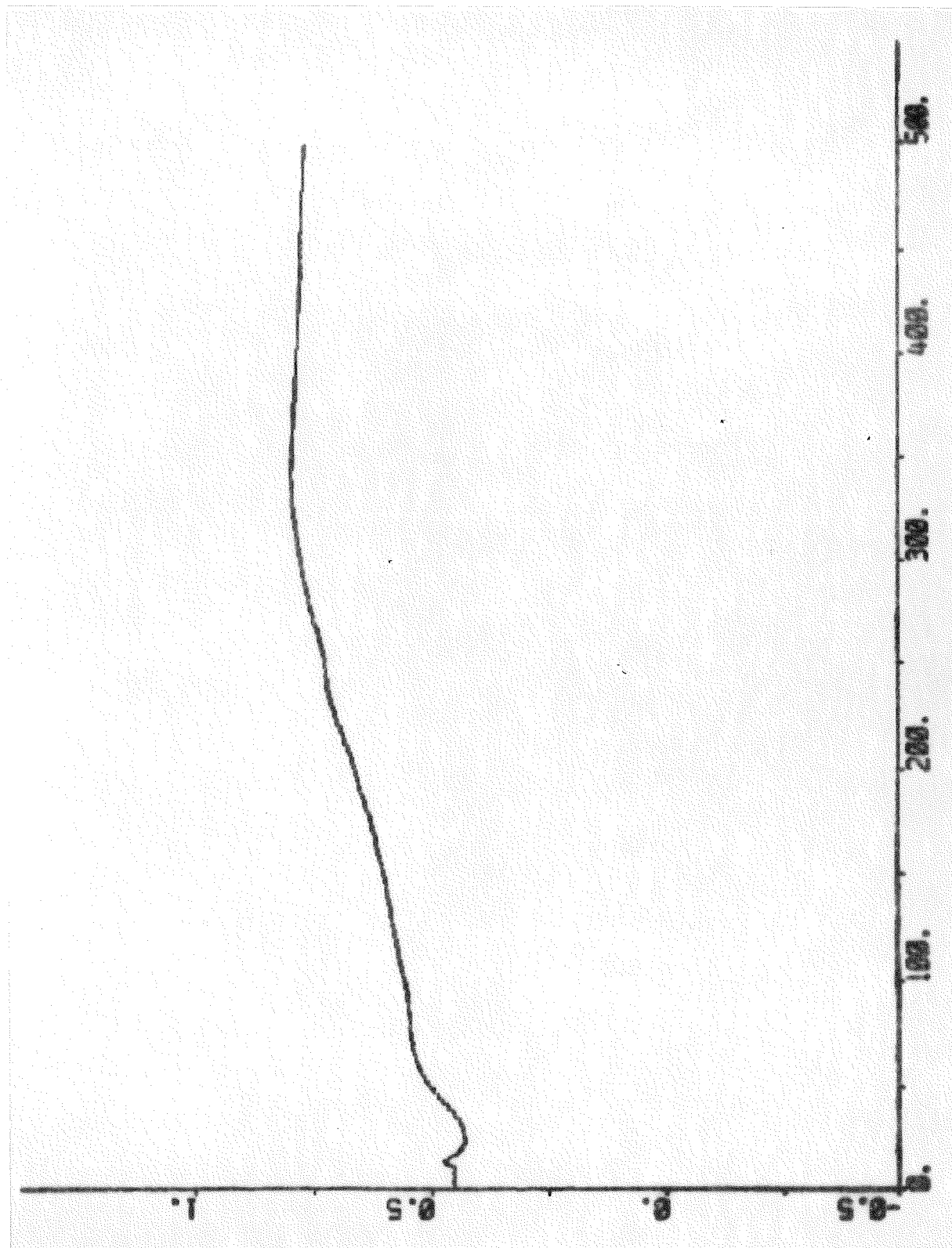


Fig. 17.5 - Response of the stroke of the feedwater valve due to increase of output power in normal mode.

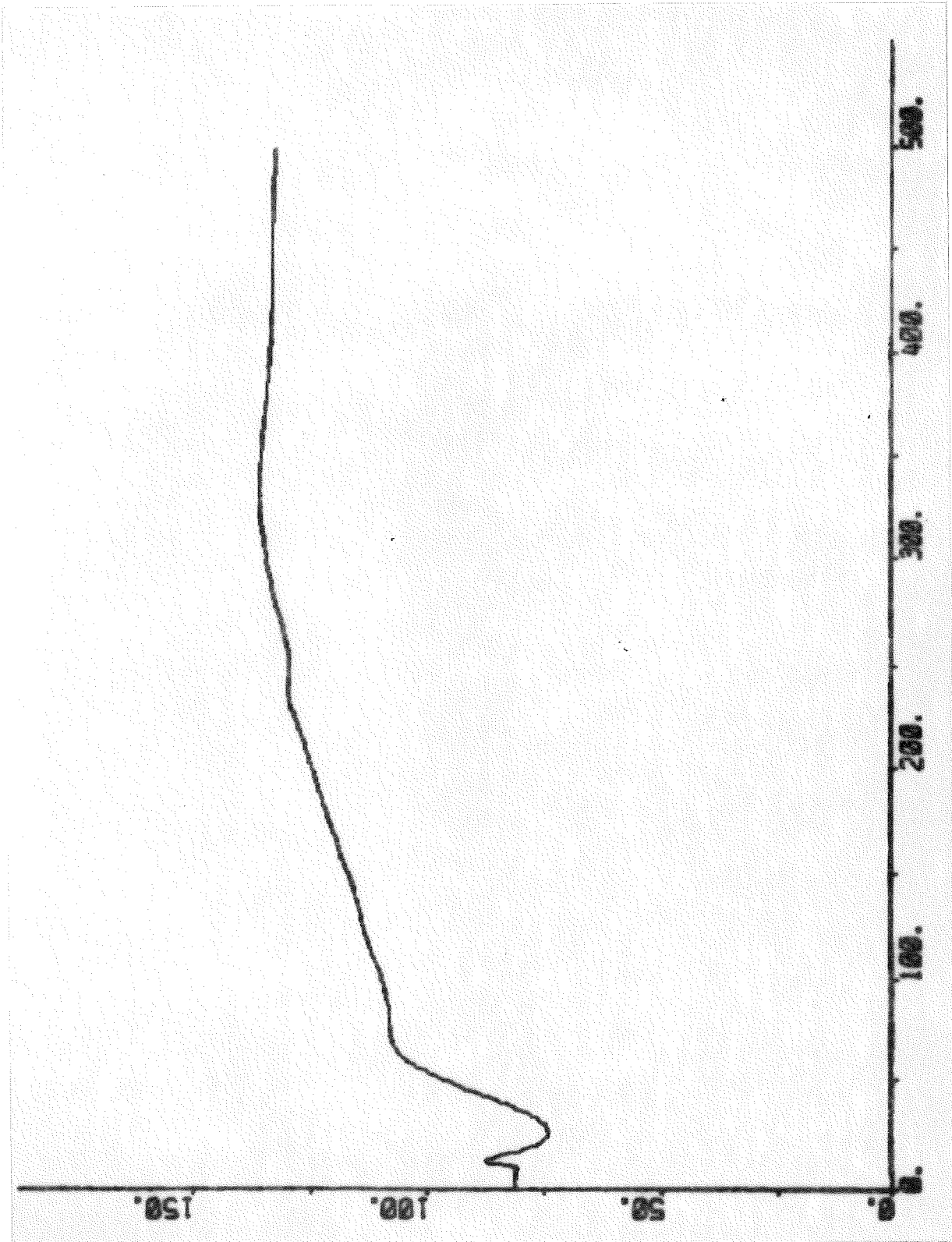


Fig. 17.6 - Response of the feedwater flow due to increase of output power in normal mode.



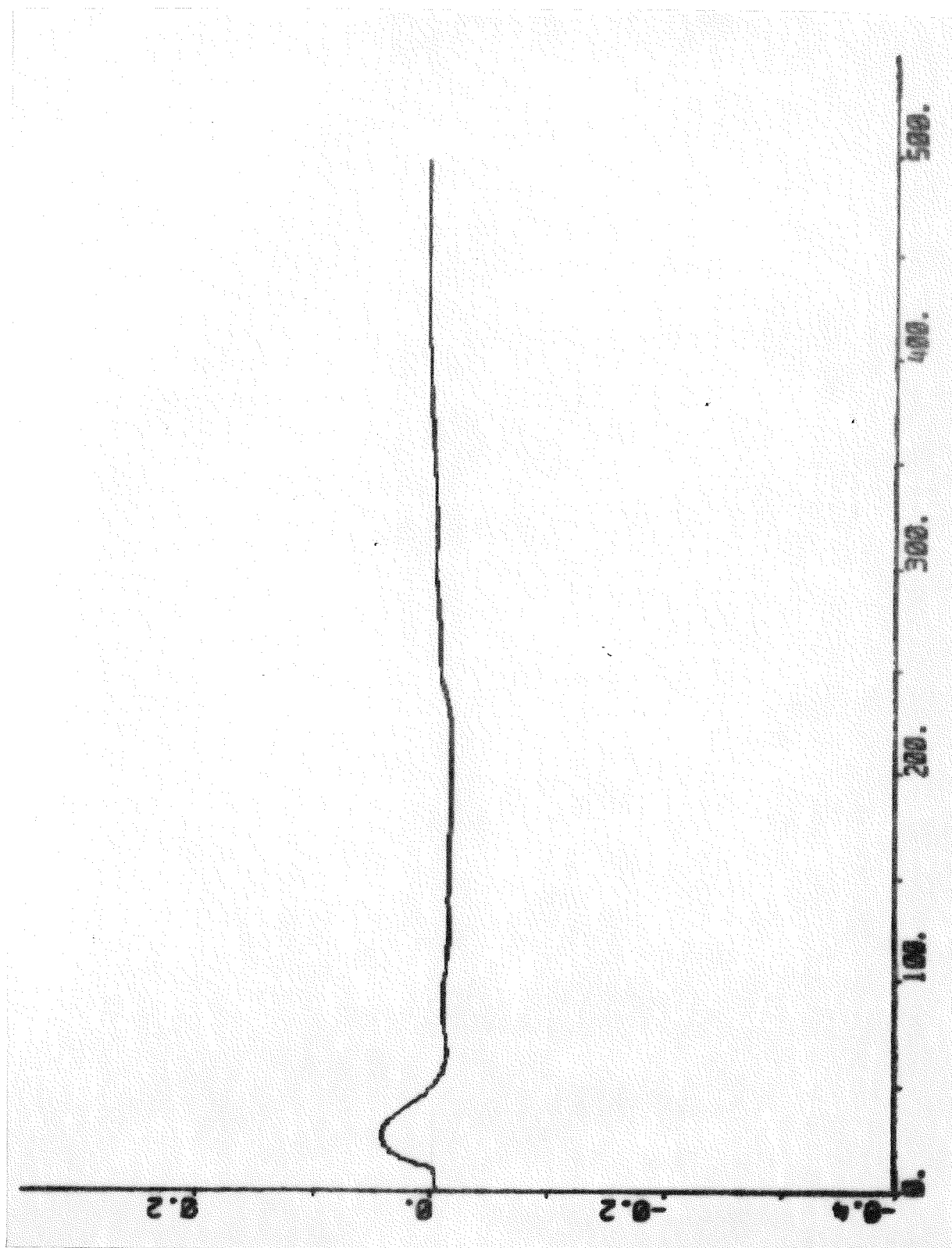


Fig. 17.7 - Response of the drum level due to increase of output power in normal mode.

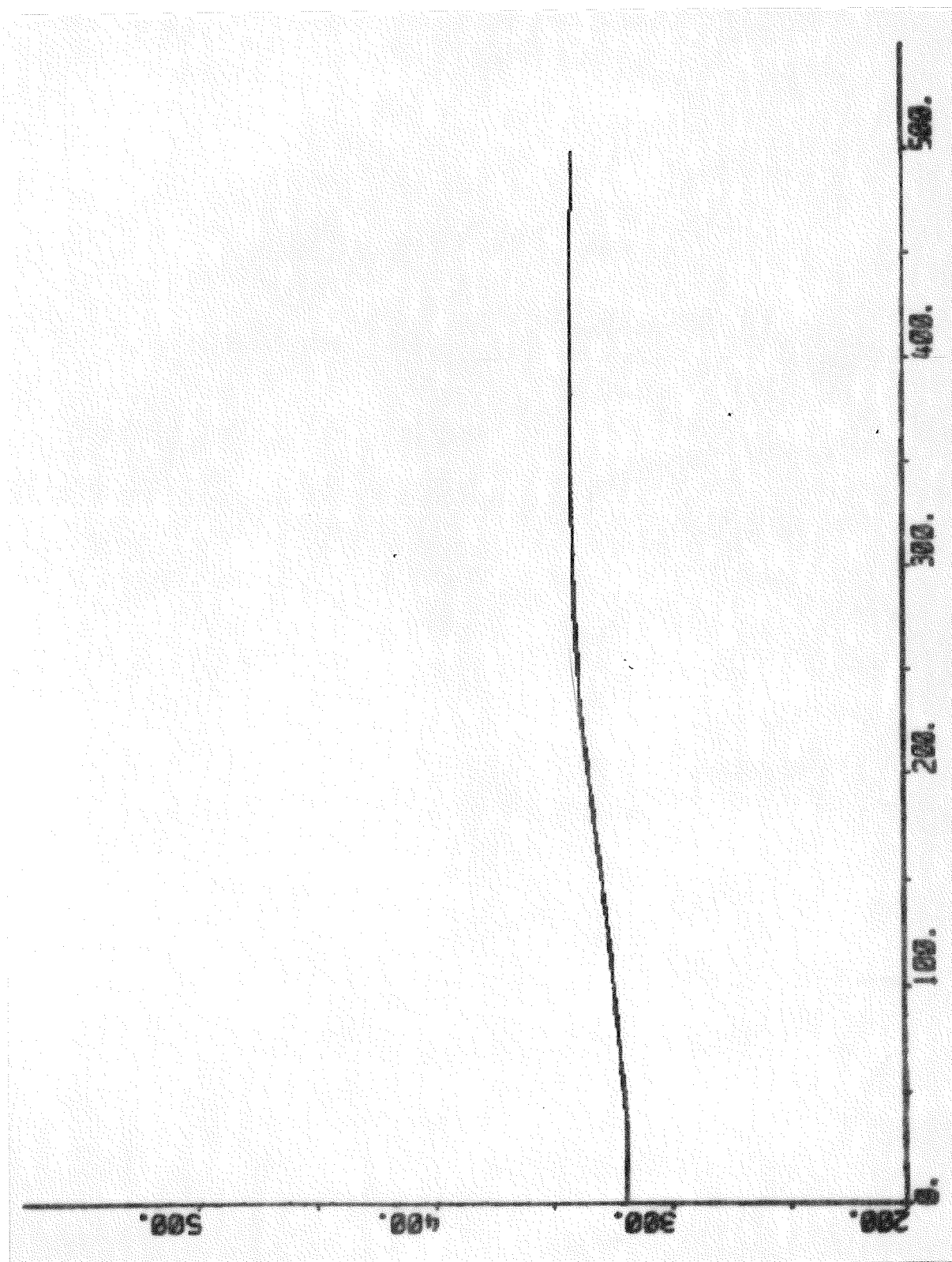


Fig. 17.8 - Response of the drum water temperature due to increase of output power in normal mode.

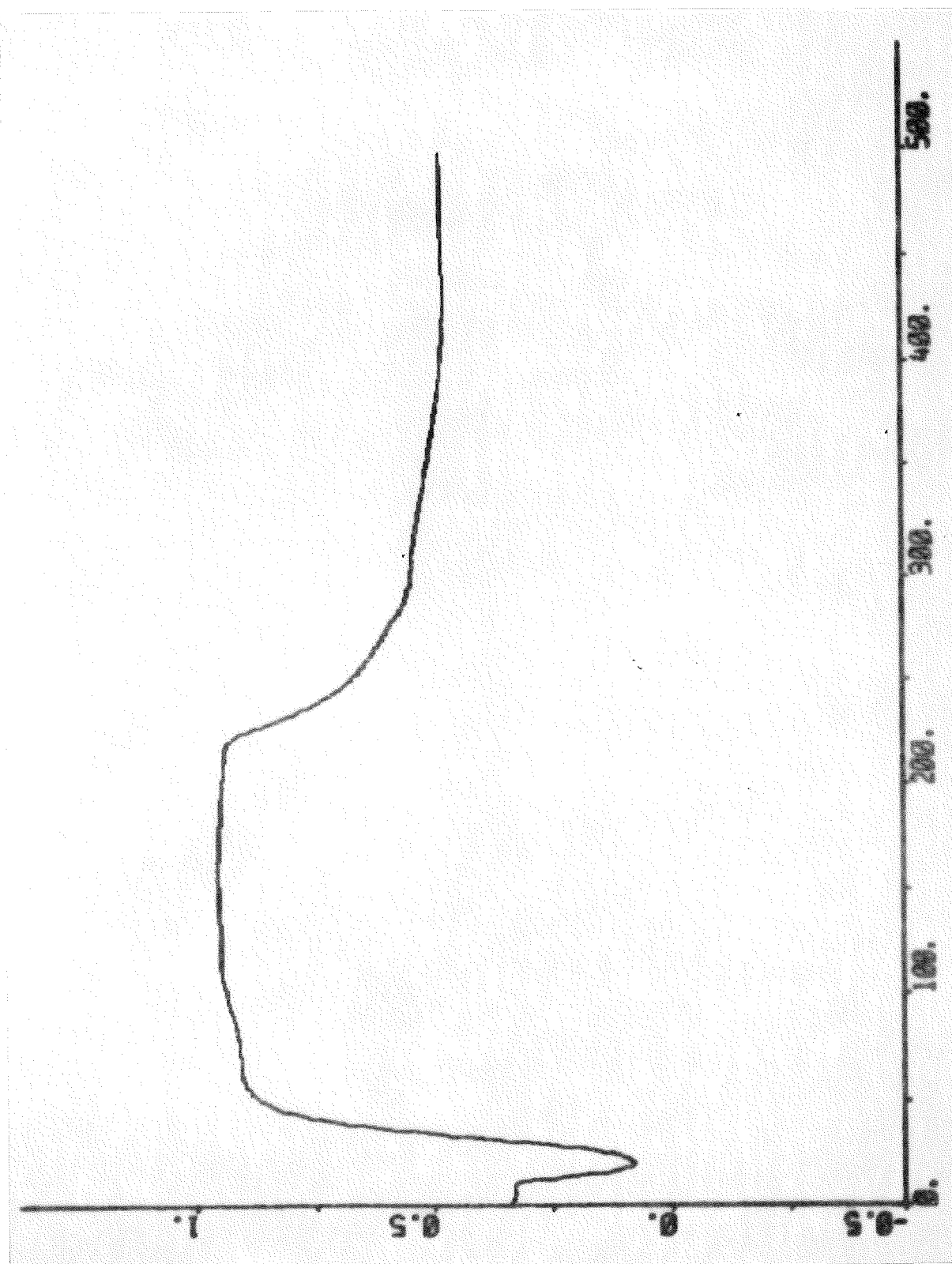


Fig. 17.9 - Response of the stroke of the first attenuator spray flow valve due to increase of output power in normal mode.



Fig. 17.10 - Response of the spray flow of the first attenuator due to increase of output power in normal mode.

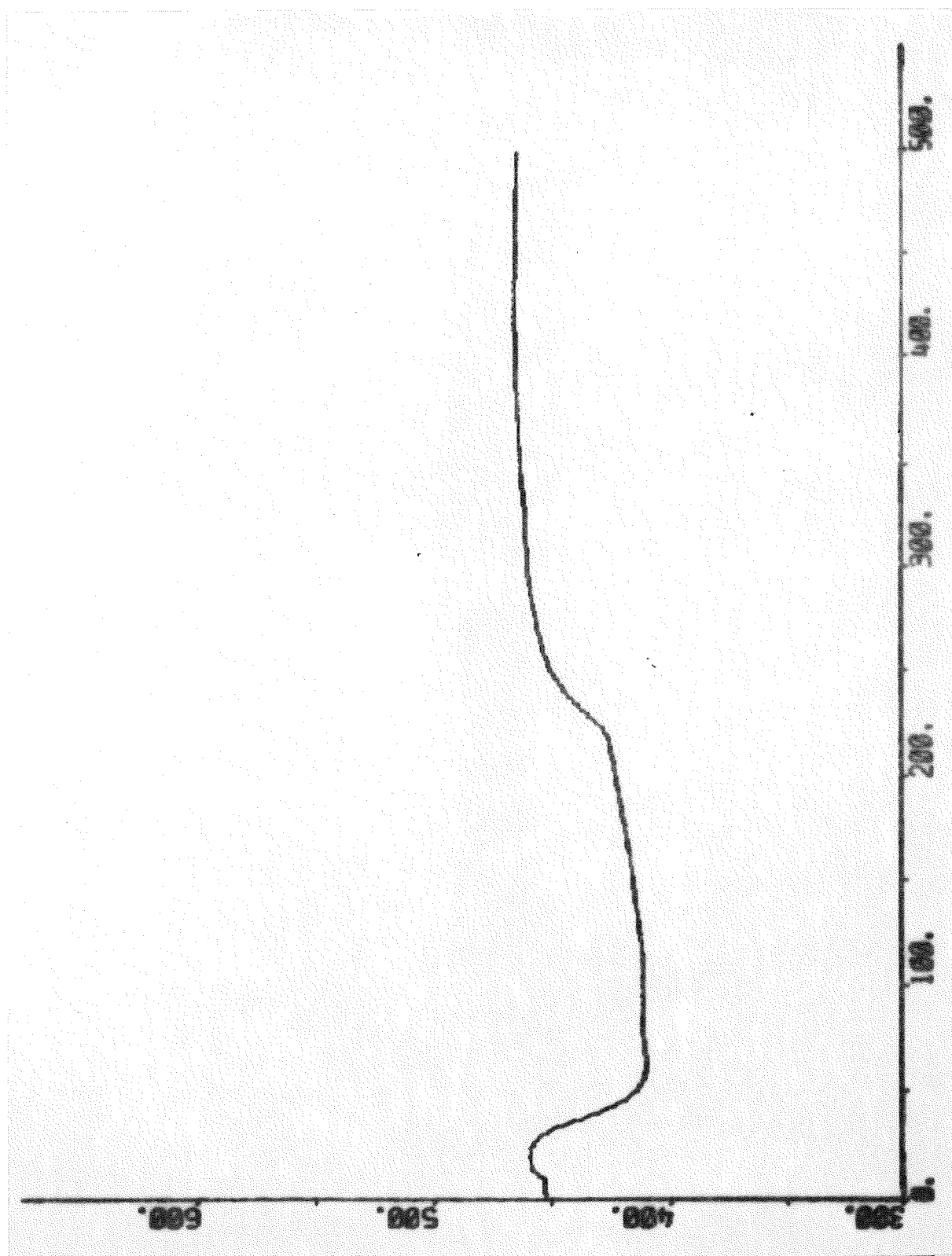


Fig. 17.11 - Response of the steam temperature before the secondary superheater due to increase of output power in normal mode.

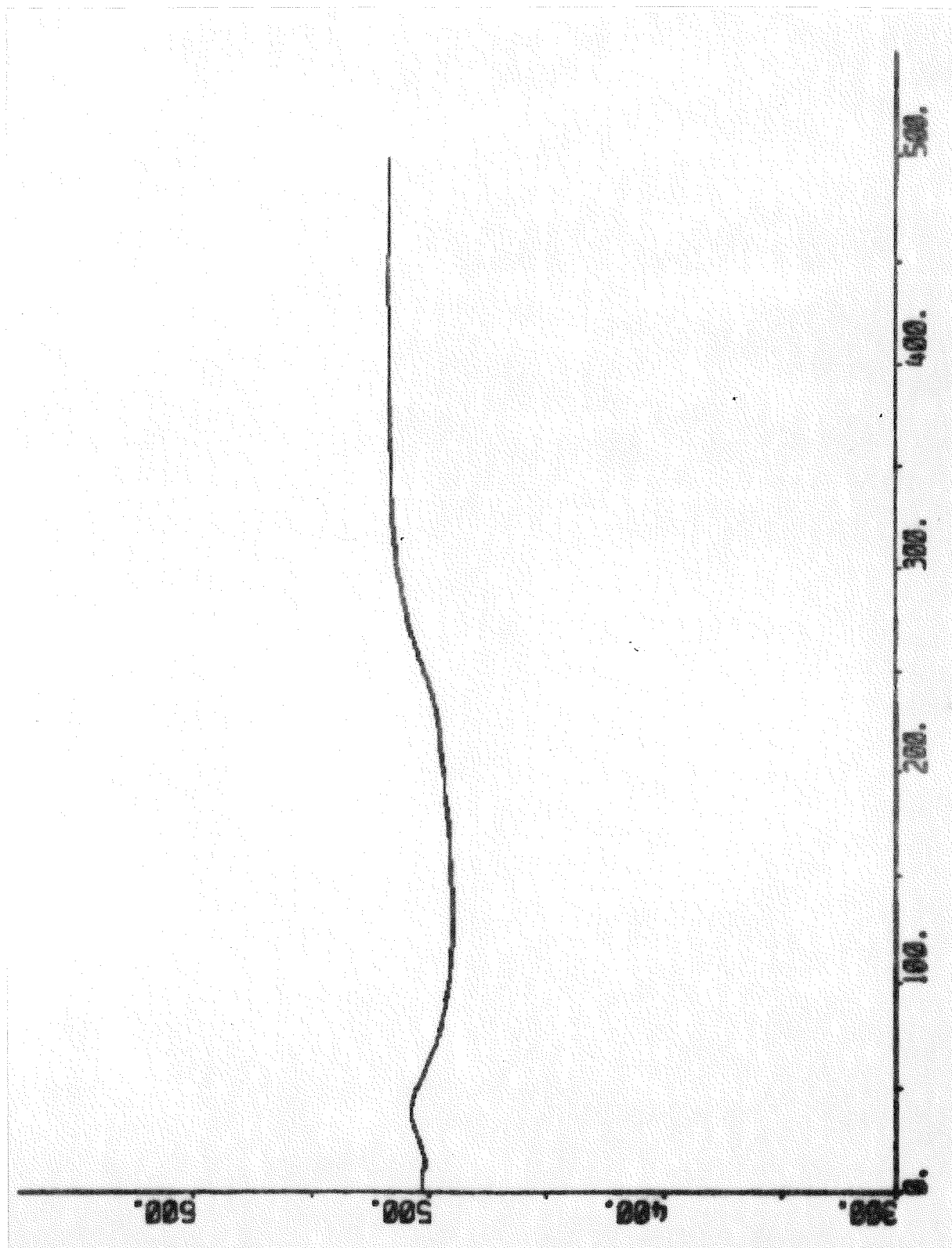


Fig. 17.12 - Response of the steam temperature after the secondary superheater due to increase of output power in normal mode.

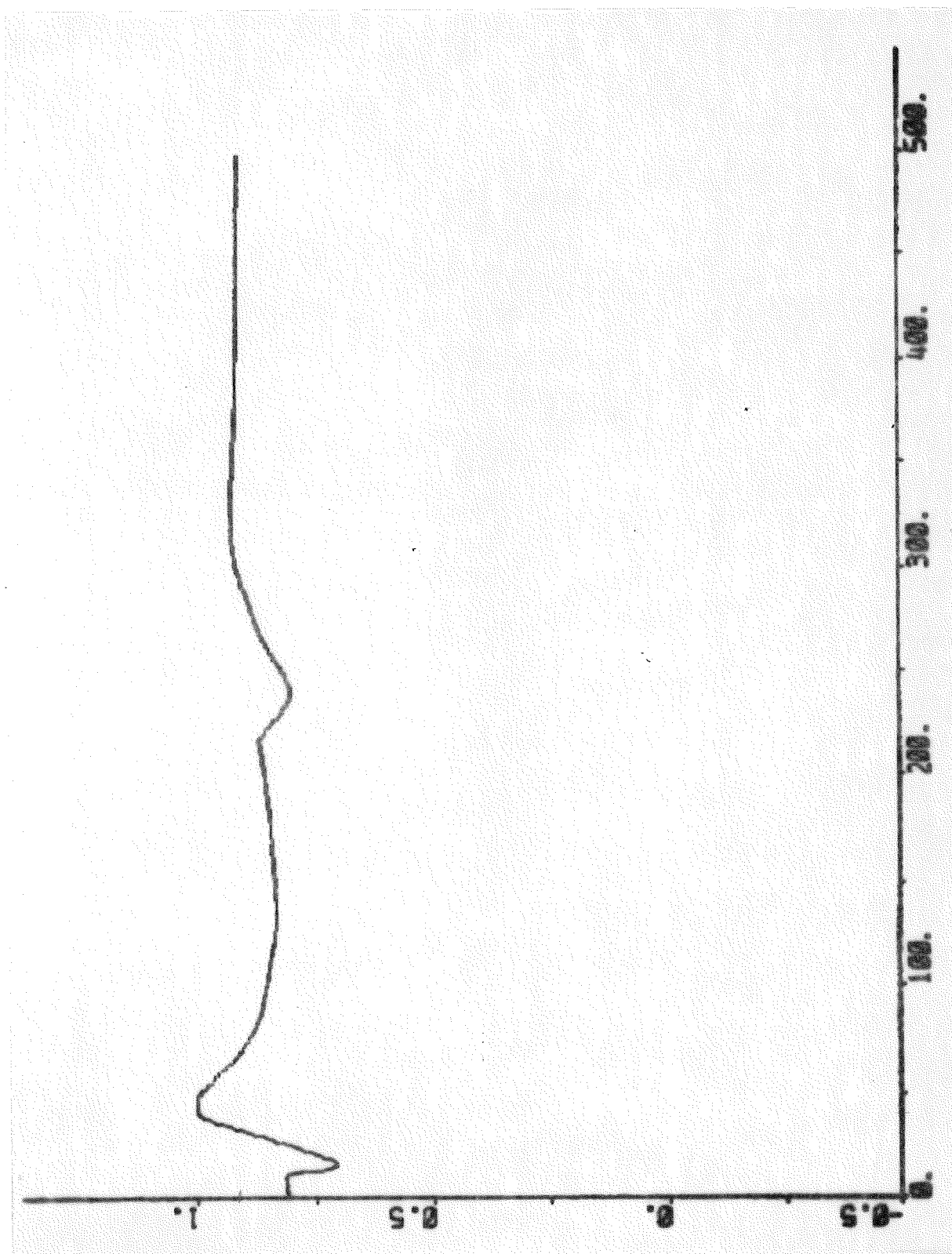


Fig. 17.13 - Response of the stroke of the second attenuator spray flow valve due to increase of output power in normal mode.

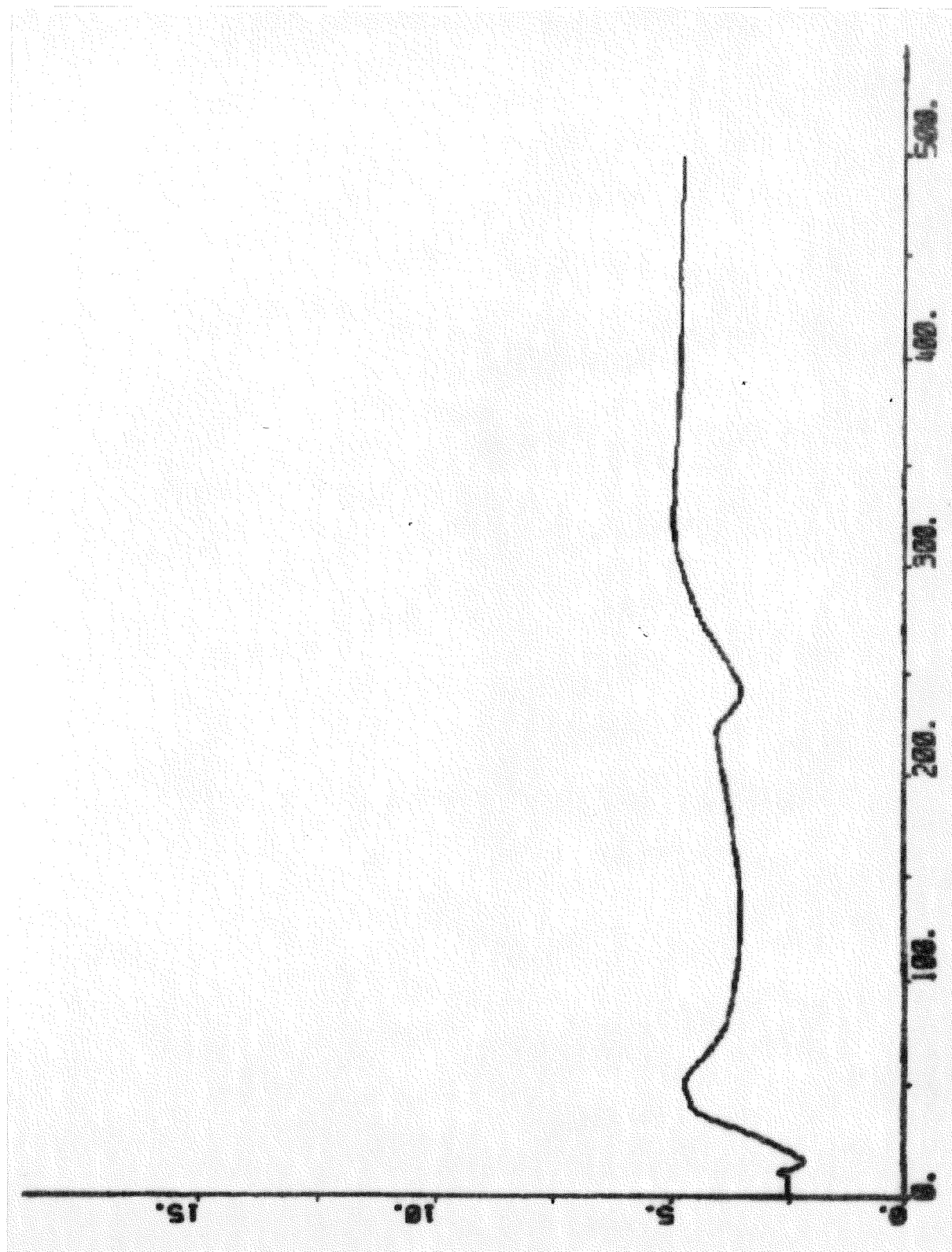


Fig. 17.14 - Response of the spray flow of the second attenuator due to increase of output power in normal mode.



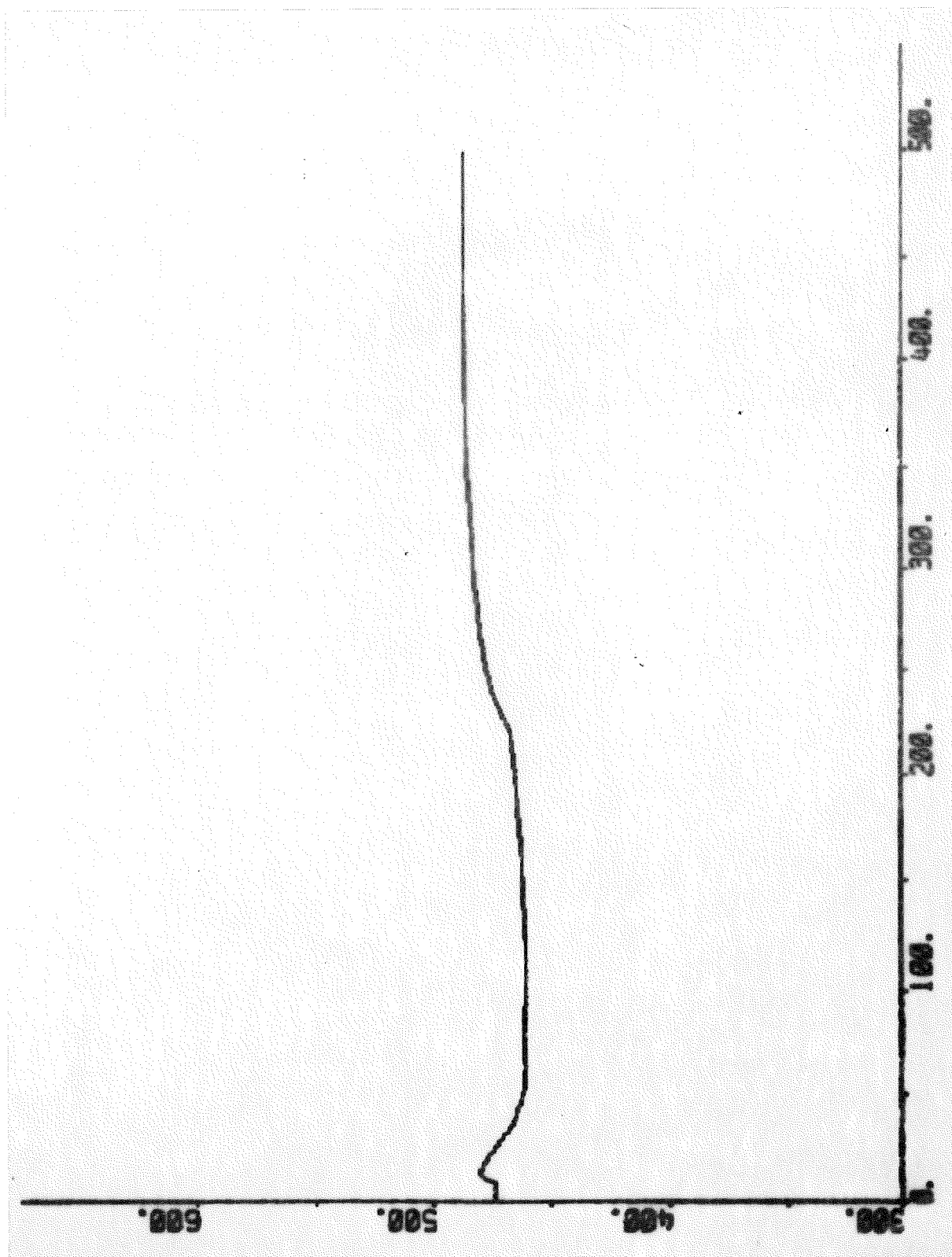


Fig. 17.15 - Response of the steam temperature before the tertiary superheater due to increase of output power in normal mode.

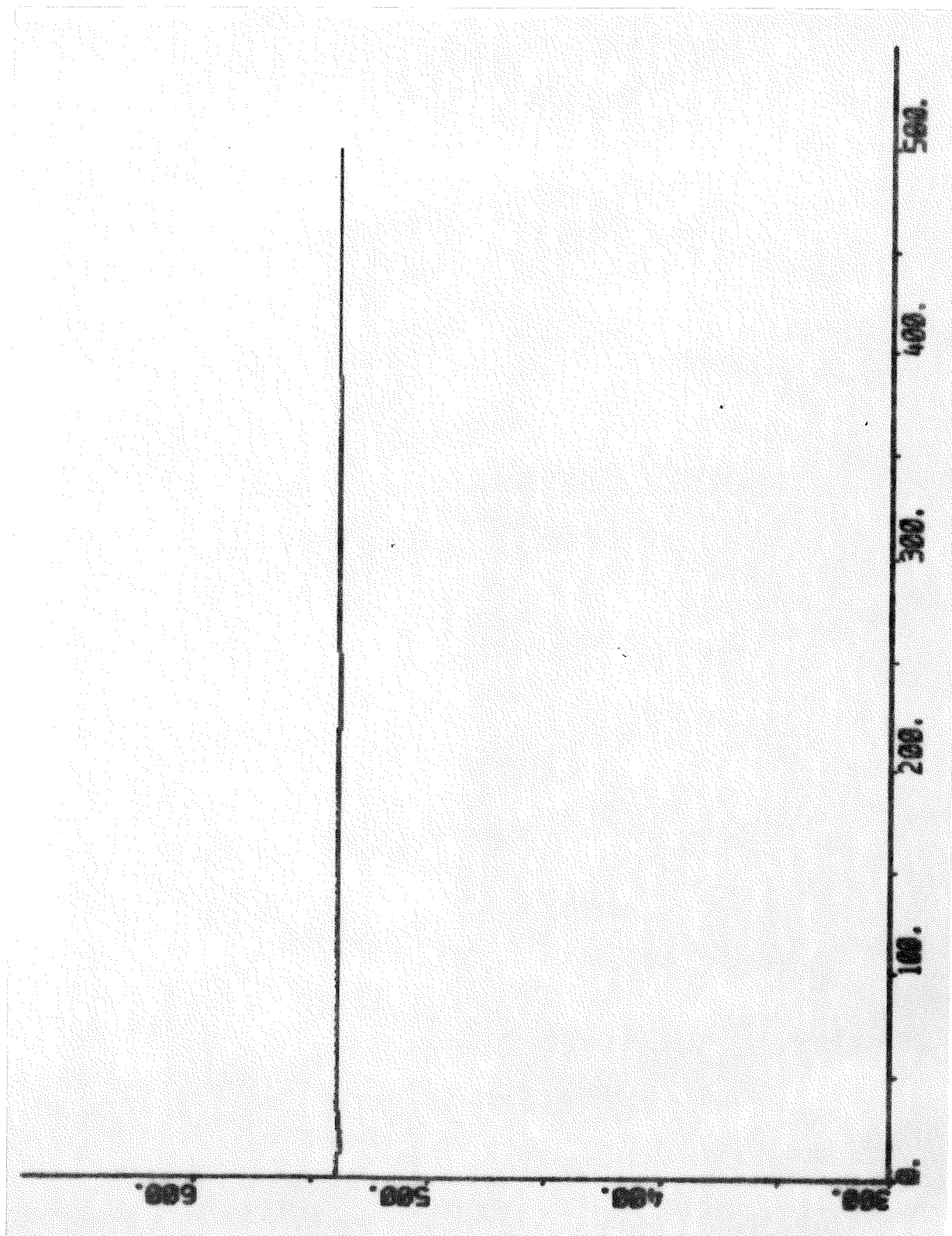


Fig. 17.16 - Response of the steam temperature after the tertiary superheater due to increase of output power in normal mode.

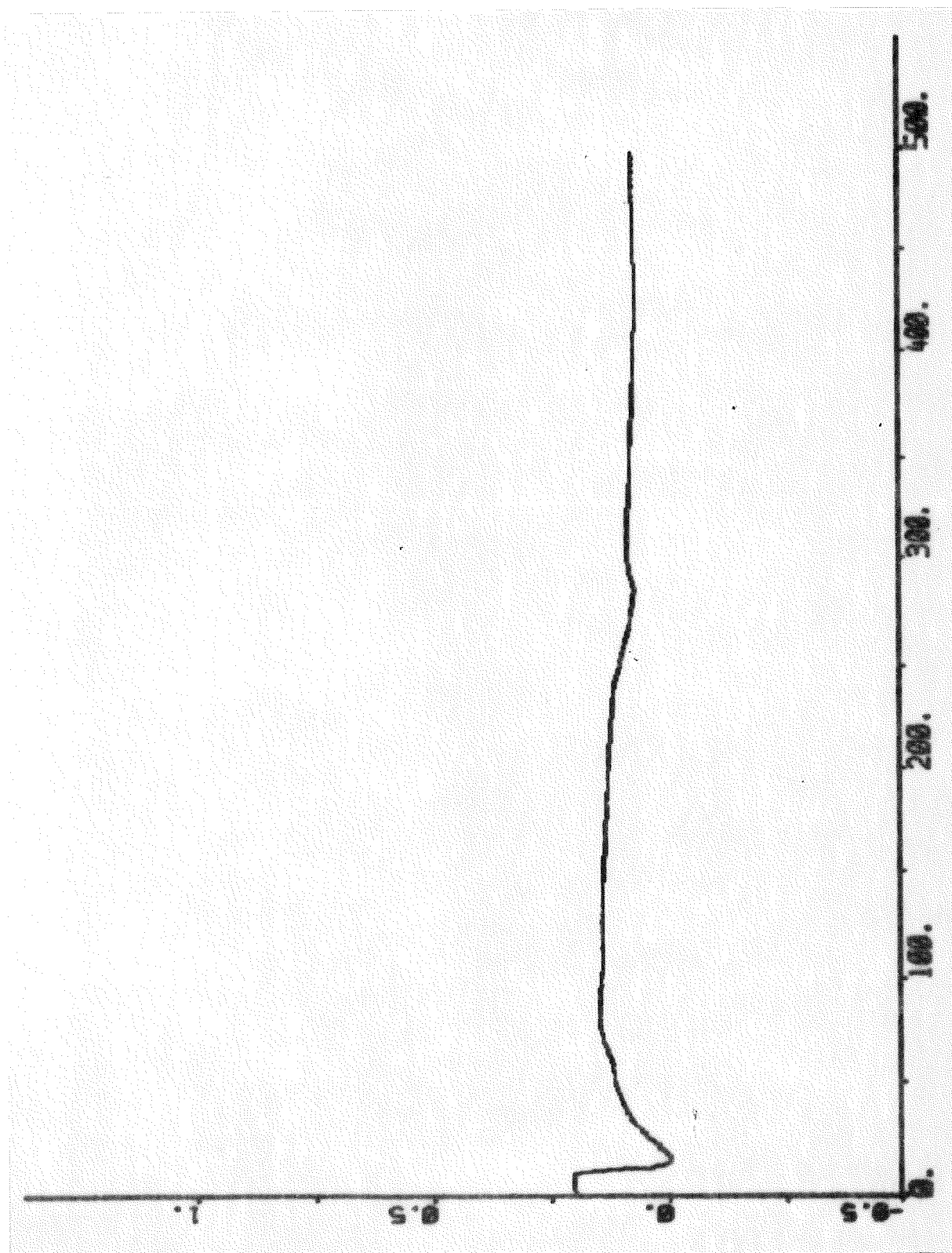


Fig. 17.17 - Response of the stroke of the low-pressure preheater extraction valves due to increase of output power in normal mode.

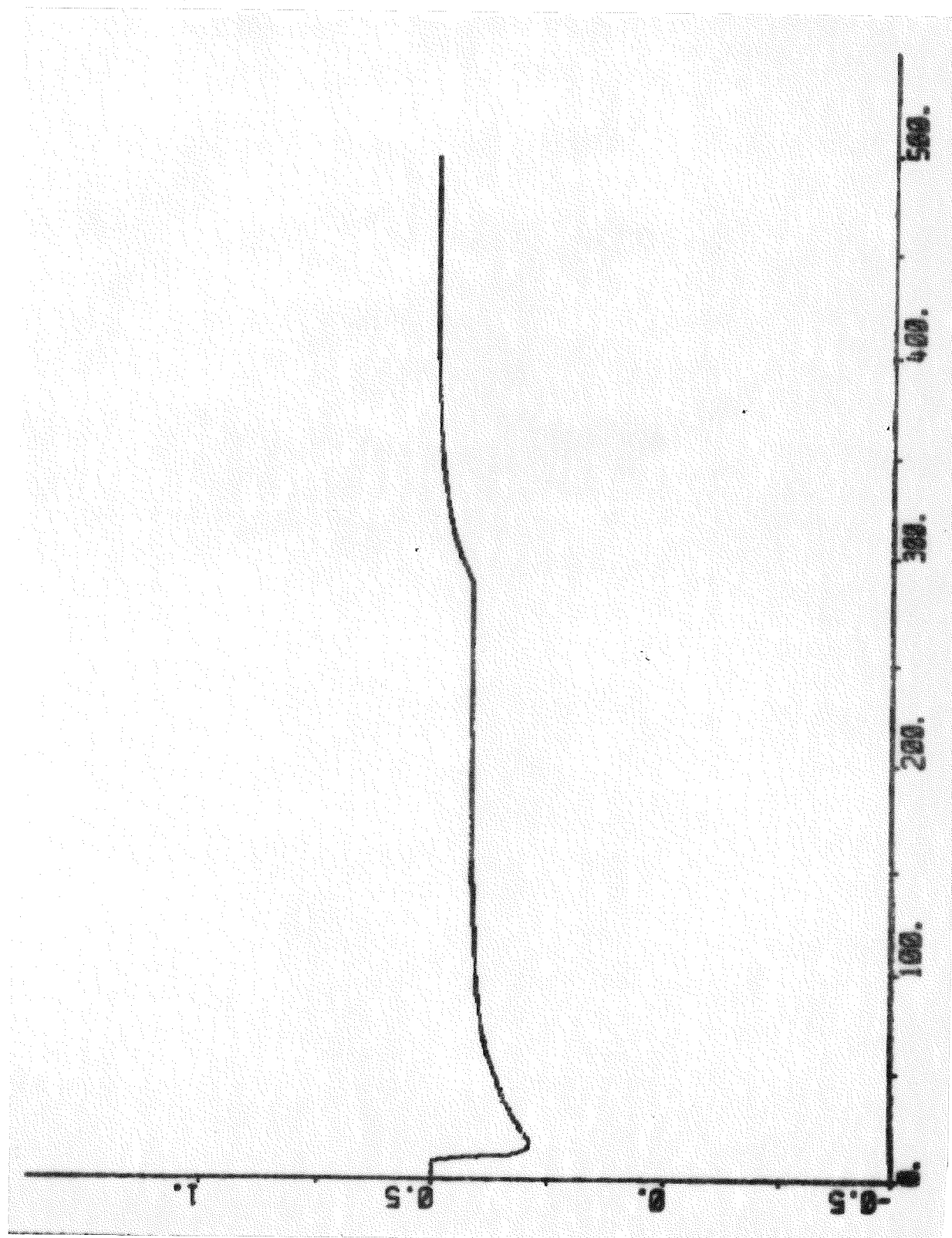


Fig. 17.18 - Response of the stroke of the high-pressure preheater extraction valves due to increase of output power in normal mode.

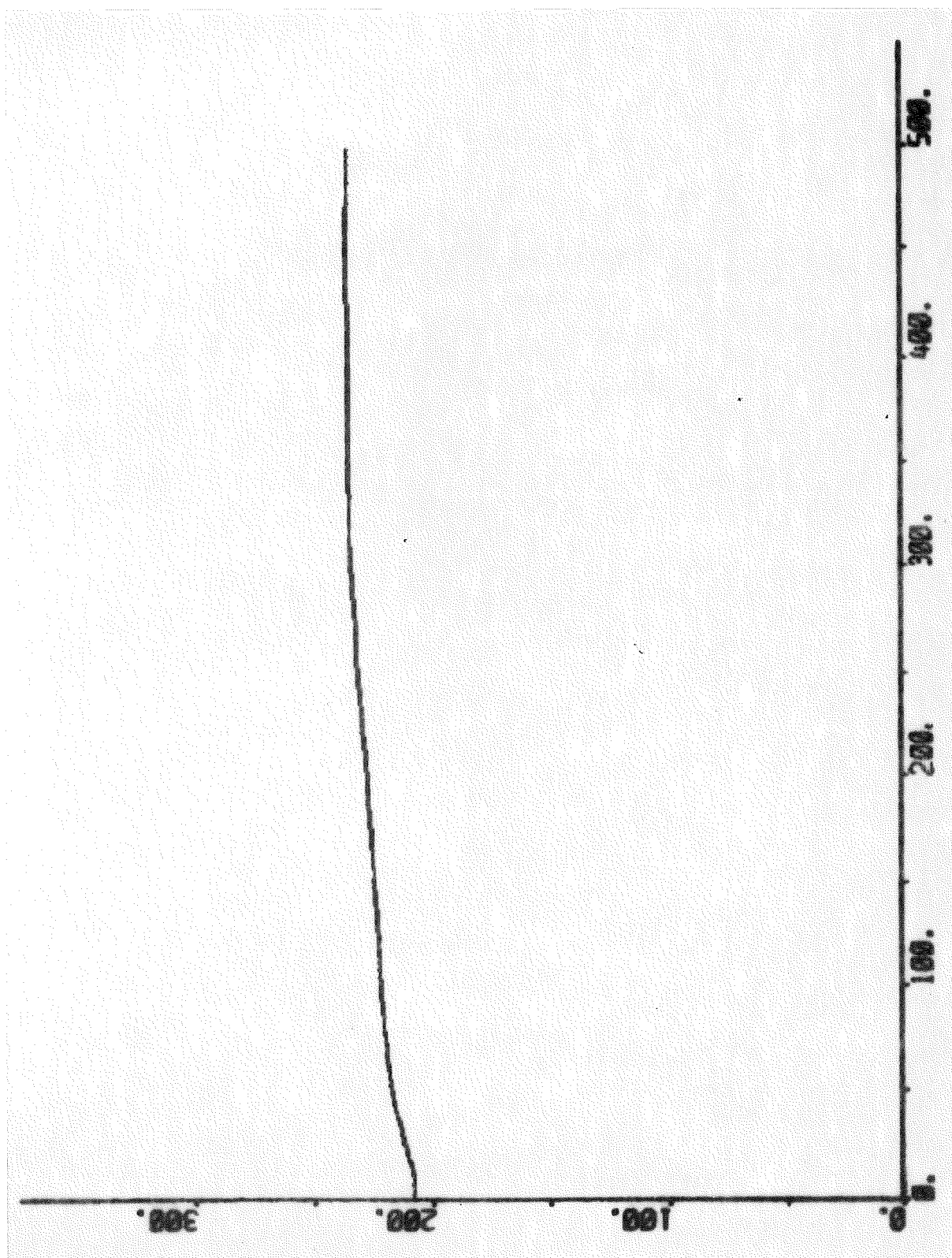


Fig. 17.19 - Response of the feedwater temperature after the high-pressure preheater due to increase of output power in normal mode.

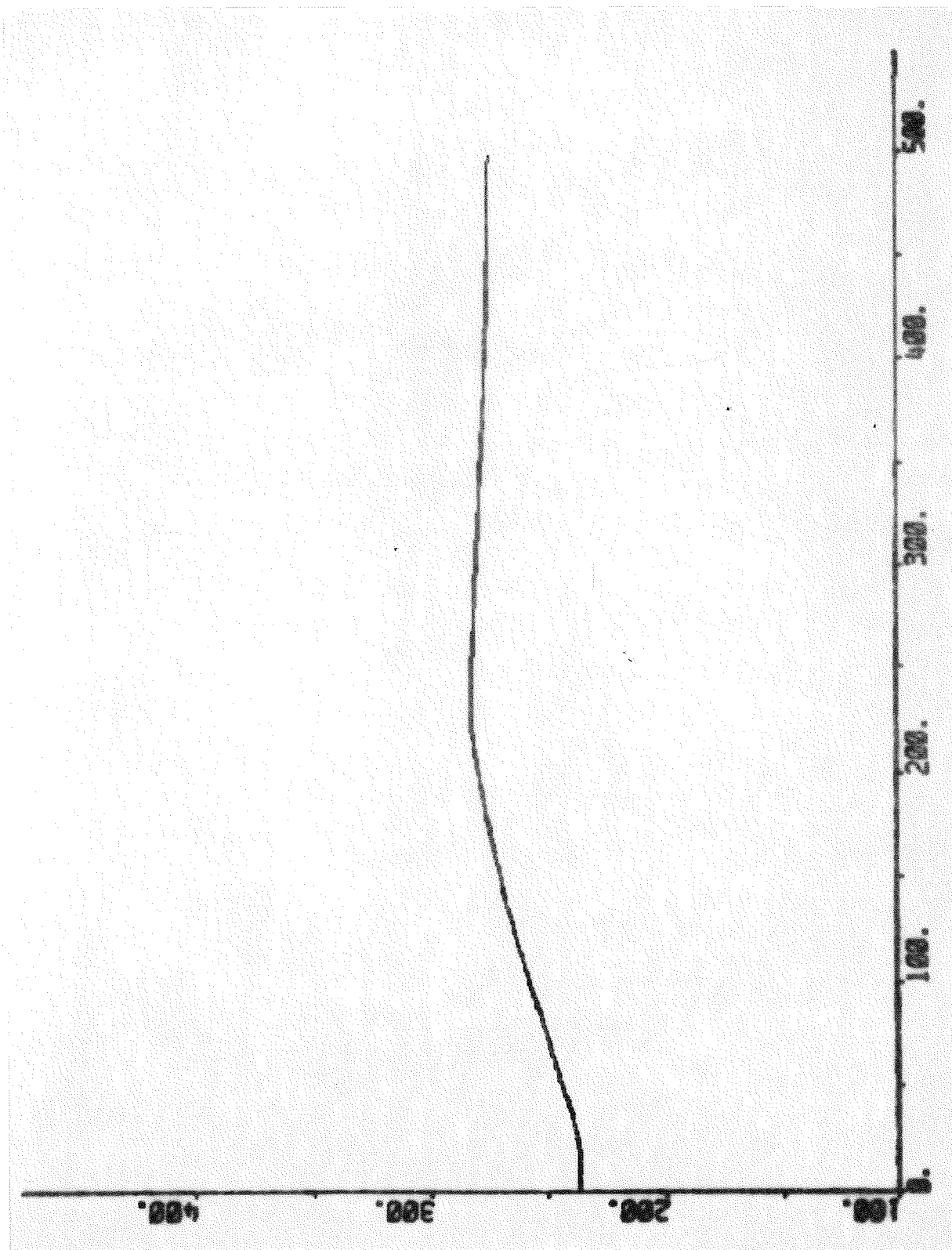


Fig. 17.20 - Response of the feedwater temperature after the economizer due to increase of output power in normal mode.

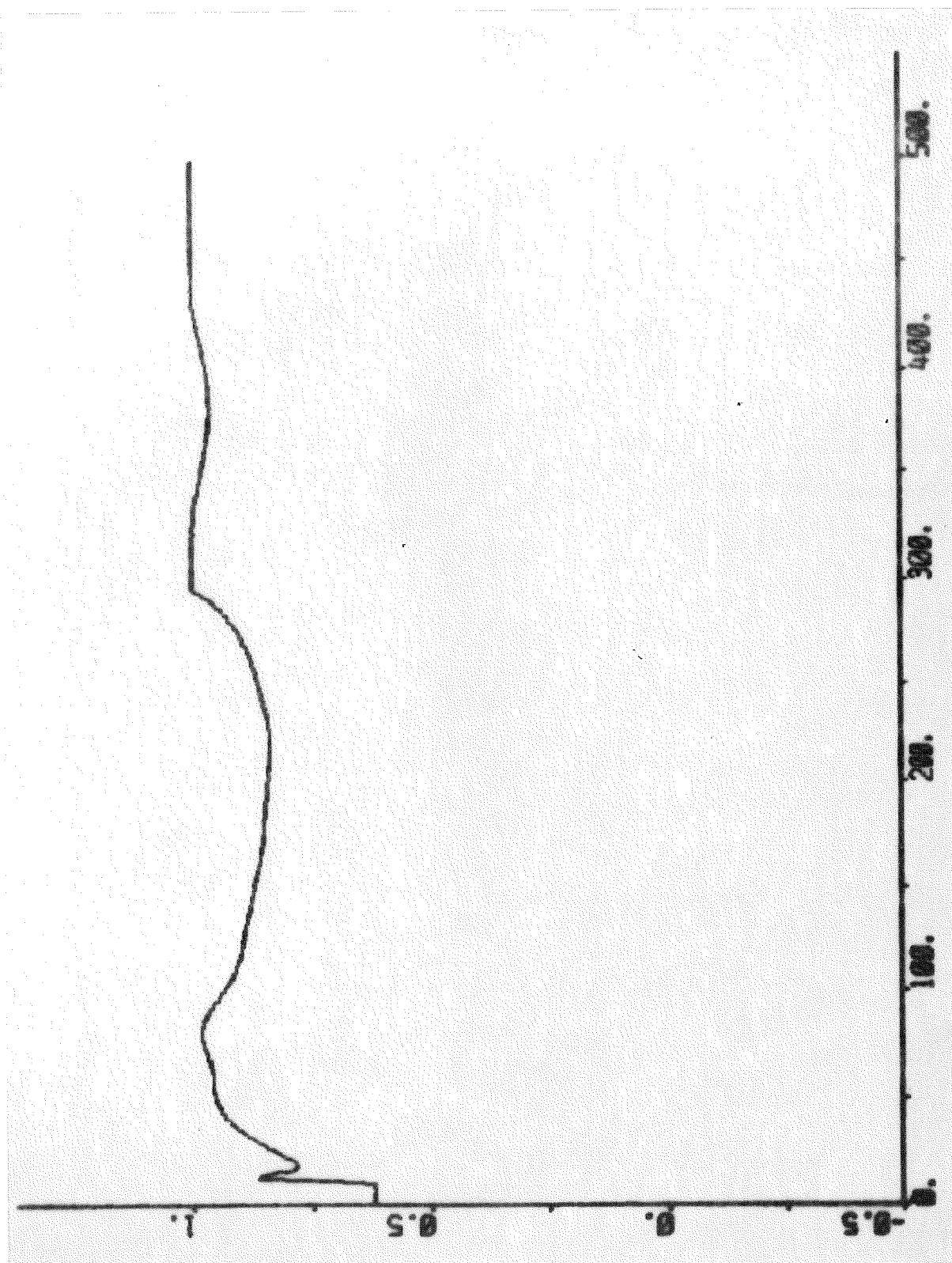


Fig. 17.21 - Response of the stroke of the control valve due to increase of output power in normal mode.

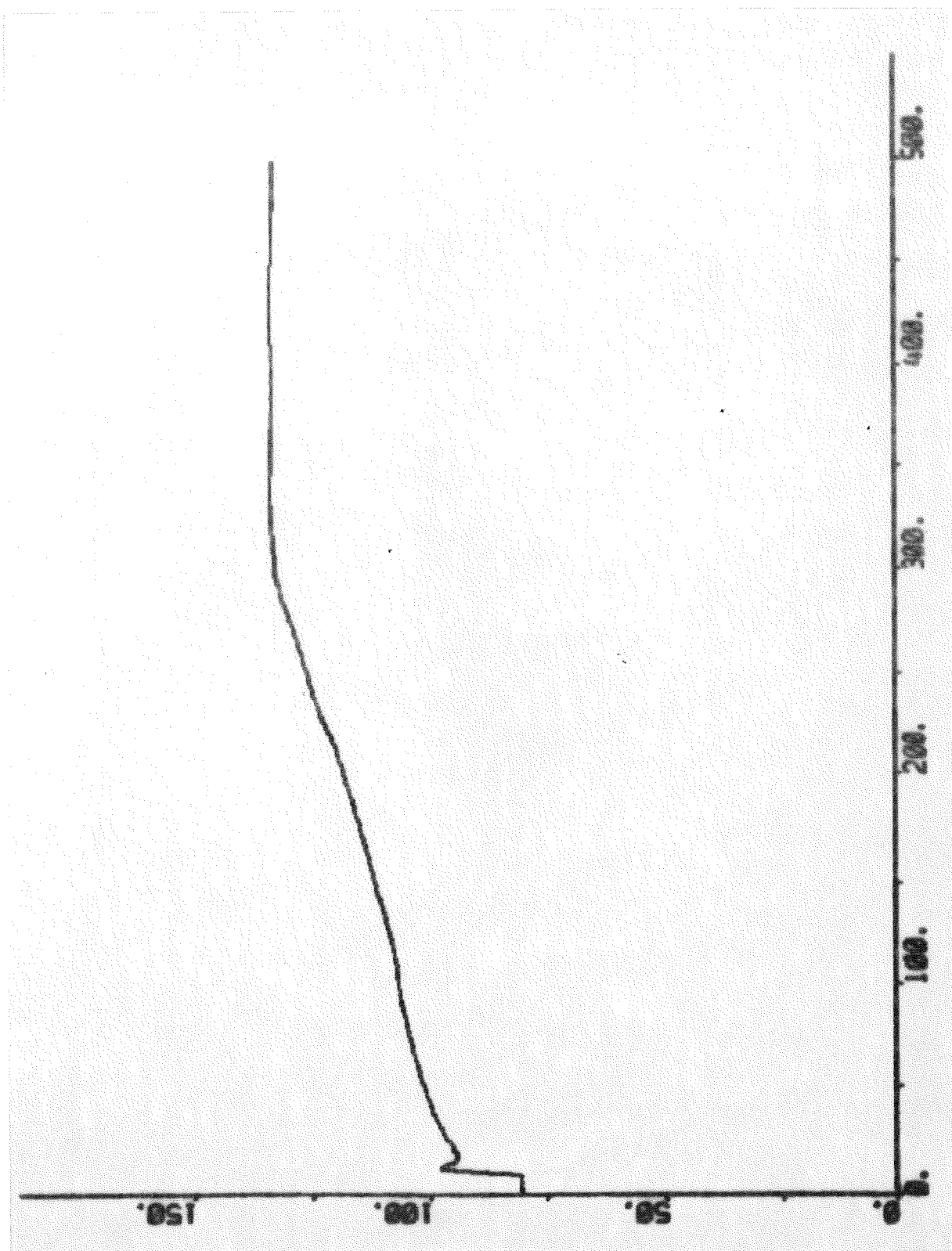


Fig. 17.22 - Response of the steam flow due to increase of output power in normal mode.



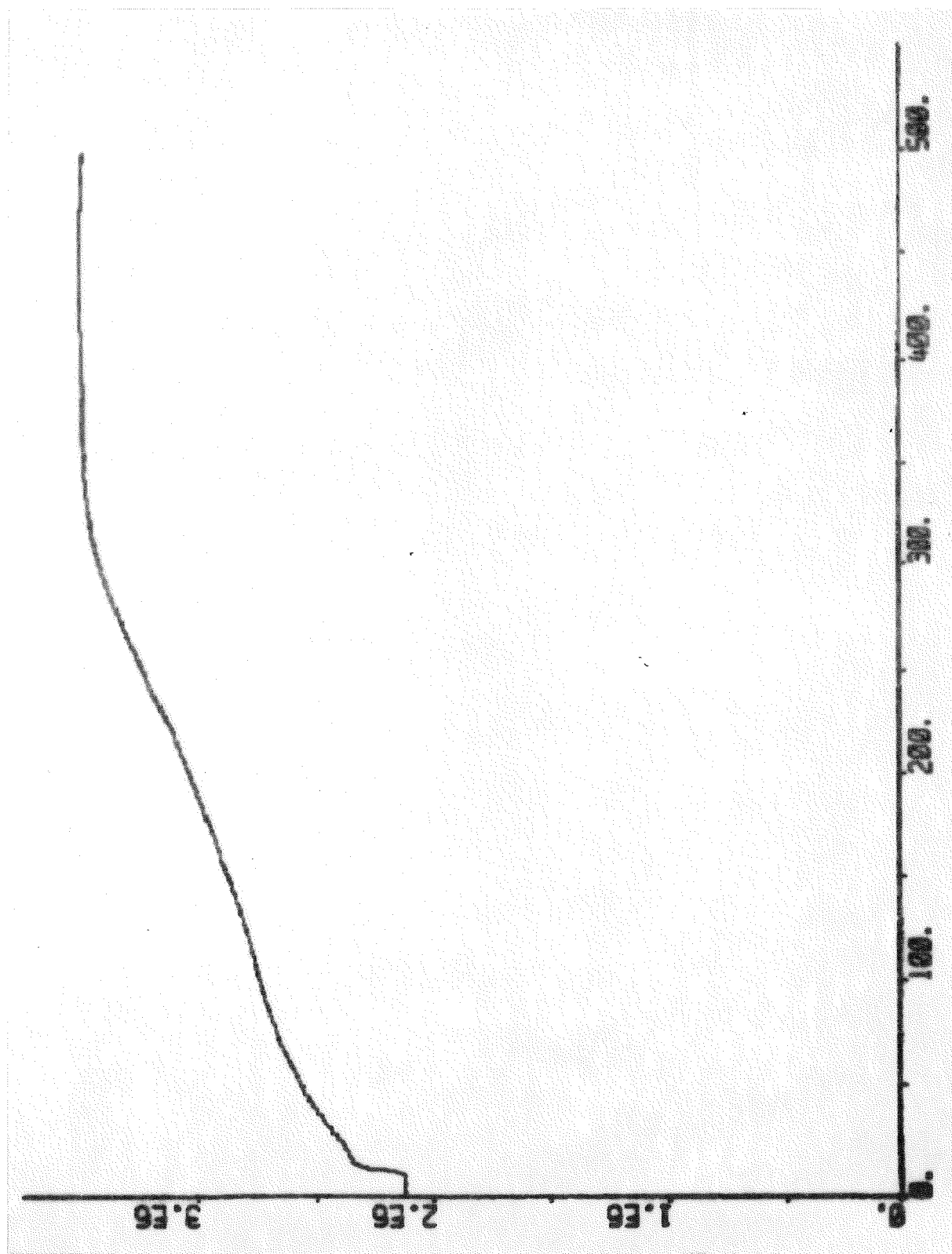


Fig. 17.23 - Response of the reheater steam pressure due to increase of output power in normal mode.

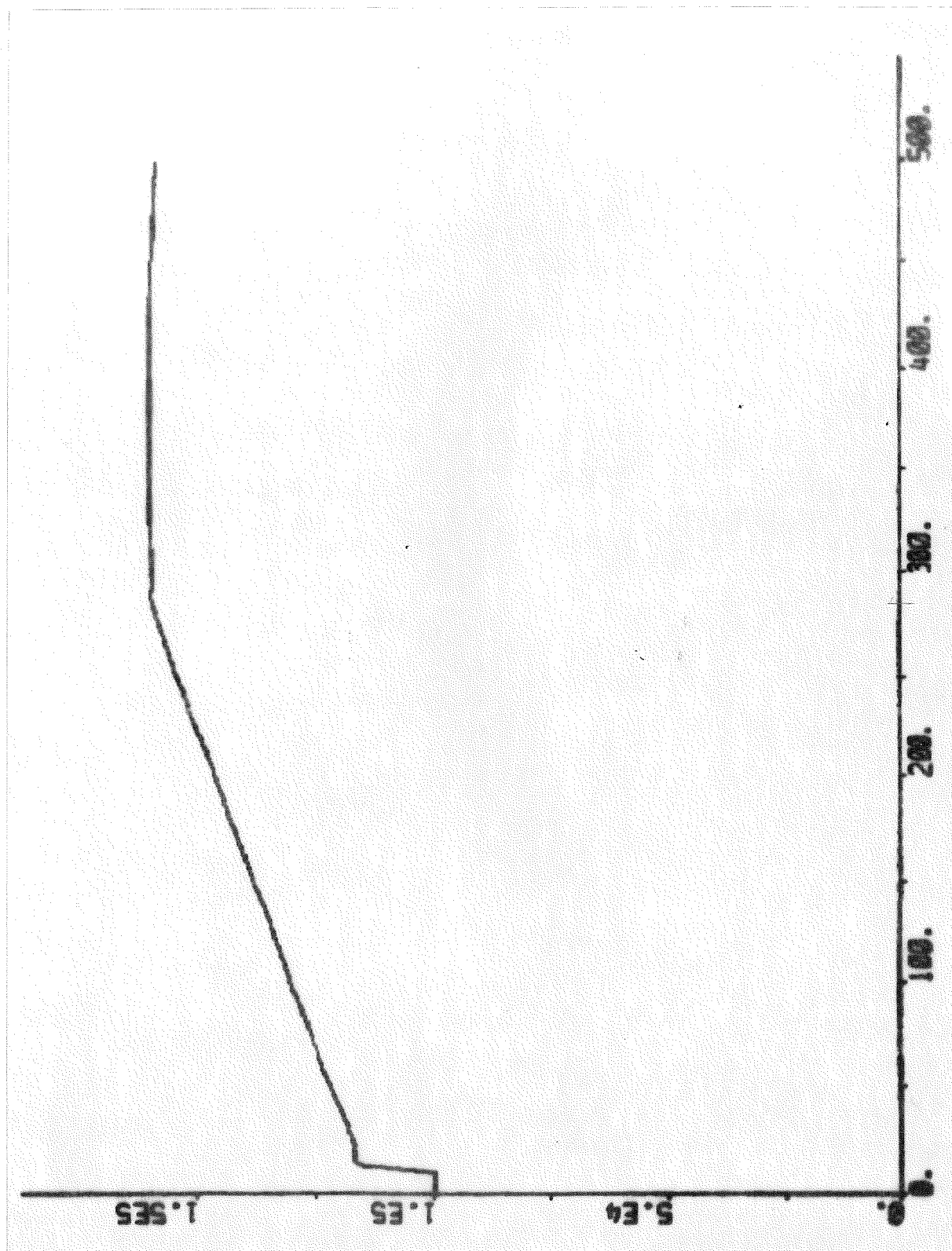


Fig. 17.24 - Response of the output power in normal mode.

## 18. CONCLUSIONS

The interest in the dynamics of thermal power plants has grown in Sweden due to the changing structure of the power system [5, 14, 15]. An increasing share of the electric energy will be produced in nuclear power units. New hydro power units will be installed mainly to cover load peaks. New fossile power units will mainly be back-pressure units.

The nuclear power units will be larger (700-1000 MW) than the existing hydro power units (<250 MW) as well as the existing fossile power units (<340 MW). The newer and larger nuclear units will, due to their complexity, be disconnected from the network more frequently than the units in service today. Many disconnections will happen automatically, rapidly, and without any advance warning. This means that a larger spinning reserve, partly in fossile power units, has to be activated more frequently than today.

The alternating-current interconnection tie-lines between the nordic countries; Denmark (Sjælland), Finland, Norway and Sweden are economically beneficial. The tie-lines have made it possible to exploit the different structure of the production systems as well as the different compositions of the power demands. The transmission capacity of the tie-lines may, however, be reduced by power oscillations. This means that all possible methods for reducing the oscillations should be considered.

The total power demand has to be divided among the available production units so that the total production cost is minimized. This economic dispatch may sometimes indicate that most of the hydro power units should be taken out of service. In such cases the fossile units have to cover the difference between the total power demand and the (constant) output power of the nuclear power units. This means that the fossile power units must participate in the automatic generation control, which is not the case in Sweden today [14].

The changing structure of the power system give rise to more complicated control tasks both during disturbances and during normal operation. This study is motivated by the fact that the total output power of fossile power units equipped with drum-boilers accounts for more than 90% of the total installed power of all fossile power units ( $\sim 6$  GW) in Sweden.

### Control objectives.

The dynamic properties of thermal power units, in terms of power jumps and power rates, have been specified in [5]. In order to make full use of the thermal power units they have to be equipped with automatic control systems. The primary task of such a unit control system is to control the output power, at least from the point of view of supplying the power demand. The control of the drum pressure, the drum level, and the steam temperatures are also crucial for the safe operation of the thermal power unit.

The primary task of the control system is to:

- 1) increase the output power during disturbances (as much as possible within 30 s),
- 2) increase the damping of tie-line oscillations (frequency 0.25 - 1.0 Hz),
- 3) adjust the output power according to the power demand (rate 2 - 4%/min),
- 4) receive a set-point signal from the unit's control room or from a remote dispatch centre,
- 5) modify the set-point of the output power with respect to the network frequency in order to form the reference value of the output power,
- 6) limit the power response rate to adjustable values, one set to be used during normal operation, and another set to be used during disturbances, and

- 7) use the power response rate selected manually from the unit's control room, automatically based on network frequency, or from a remote dispatch centre.

The specifications given above are essentially the ones given in [5, 14].

The secondary task of the control system is to control:

- 1) the drum pressure,
- 2) the drum level, and
- 3) the steam temperatures.

The reference value of the drum pressure is not given a priori. Constant pressure control will result in the most rapid response of the output power. Sliding pressure control will result in the lowest specific fuel consumption. In [5] it was concluded that modified sliding pressure control with opening reserve is a reasonable compromise. Allowable drum pressure errors have not been specified. Allowable drum level errors vary from unit to unit with typical values  $\pm 0.1 - 0.2$  m. Allowable steam temperature errors are  $5 - 10^{\circ}\text{C}$ .

#### Design method

The following aspects of the design have been considered:

- 1) generation of reference values,
- 2) preservation of margins,
- 3) treatment of non-linearities,
- 4) generation of control signals,
- 5) start up and shut down, and
- 6) on-line tuning.

The non-constant reference values were generated by a jump-and-rate circuit for the output power and by a rate-circuit for the drum pressure. This circuit can be implemented using an integrator having limiting circuits at the input and at the output. These intentional non-linearities are pure feedforward elements and do not introduce any extra stability problems in the design of the control system of the thermal power unit.

The preservation of margins is achieved by limiting the jump and the rate of the variable reference values. The non-linearities are the same as mentioned above and the remark on the stability is also valid.

The influences of inherent non-linearities have been reduced by having closed feedback loops around them. The inherent non-linearities of the spray flow valves have been used to obtain suitable gain-scheduling of minor temperature control loops.

The control signals are generated by feedforward as well as by feedback. The feedbacks are simple PI controls. The feedforwards are more unconventional and may contain non-linearities. The control system is designed loop by loop. The final performance is investigated by simulation. There are four variables to be controlled and seven variables to be manipulated. This means that there is a certain arbitrariness in the choice of manipulated variables of the control loops. Some arbitrariness was removed by the decision to use modified sliding pressure control with opening reserve. It is also reasonable to use the extraction valves in order to improve the power response rate. The main control loops; output power, drum pressure, drum level and steam temperature are subdivided into minor control loops. There is also a certain arbitrariness in the choice of these minor control loops. They were chosen in order to reduce the influence of inherent non-linearities and by considering the possibilities to measure certain process variables. The non-linear feedforward compensation in the output power loop and the drum pressure loop are pure feedforwards, which cannot give any stability problems in the design of the control sys-

tem of the fossile power unit. The non-linear feedforward compensation in the steam temperature loop is based on measured signals in other loops. This could potentially give a stability problem. This has, however, not been found in the simulations. The only intentional nonlinearities in the feedback paths are limitation of the integrals of the control errors when the manipulated variables have reached their limits. This means that the control errors are not necessarily reduced to zero for large disturbances.

Some attention has been given to the problem of smooth and safe transfer (bumpless transfer) from manual to automatic control during start up and from automatic to manual control during shut down of the boiler turbine unit. The control system is thus provided with a number of switches selecting manual or automatic control. This means that the control loops can be switched over to automatic control and back again one-by-one and part-by-part. The performance has proven to be acceptable by simulation. The proposed scheme must, however, be investigated more thoroughly before it can be implemented.

The chosen control scheme makes it possible to tune the control system loop by loop. It is advisable to start with the minor control loops for the feedwater flow and the fuel flow. It is then possible to proceed with the drum level loop, the steam temperature loop, the drum pressure loop, and finally the output power loop. This procedure was tried in the simulations.

#### Control system.

The main components of the control system are:

- 1) the power demand setter,
- 2) the drum pressure reference setter,
- 3) the drum pressure loop,

- 4) the drum level loop,
- 5) the steam temperature loop, and
- 6) the output power loop.

A block diagram of the control system was given in Fig. 4.1. The task of the power demand setter is to generate the reference value of the output power. A preliminary reference value of the output power is generated from the set-point of the output power and from the network-frequency according to an adjustable power-frequency characteristic. The final reference value of the output power is obtained from a jump-and-rate circuit, which modifies the preliminary reference value of the output power. The parameters of the jump-and-rate circuit are adjustable in order to protect the boiler-turbine unit from unacceptably large stresses.

The task of the drum pressure reference setter is to generate the reference value of the drum pressure. A preliminary reference value of the drum pressure is determined from the reference value of the output power according to an adjustable power-pressure characteristic. The final reference value of the drum pressure is obtained from a rate circuit, which modifies the preliminary reference value of the drum pressure. The parameters of the rate circuit are adjustable in order to protect the boiler from unacceptably large stresses.

The task of the drum pressure loop is to control the drum pressure by manipulating the fuel flow. The fuel flow is controlled by the fuel flow servo. The reference value of the fuel flow is determined by the drum pressure controller. The drum pressure controller uses feedforward from the steam flow as well as from the rate of the drum pressure. The drum pressure controller also uses feedback from the error in the drum pressure and its integral.

The task of the drum level loop is to control the drum level by manipulating the feedwater control valve. The feedwater flow is controlled by the feedwater servo. The reference value of the feedwater flow is determined by the drum level controller. The drum level controller uses feedforward from the steam flow. The drum



level controller also uses feedback from the error in drum level and its integral.

The task of the steam temperature loop is to control the steam temperature after the tertiary superheater by manipulating the first and the second attemperator spray flow valves. The steam temperatures before the secondary and tertiary superheaters are controlled by the secondary and by the tertiary superheater steam temperature servos. The reference values of the steam temperatures before the secondary and before the tertiary superheaters are generated by the secondary and by the tertiary superheater steam temperature controllers. The difference between the reference value of the steam temperature after the secondary superheater and the reference value of the steam temperature before the tertiary superheater is an adjustable parameter. The steam temperature controller use feedforward from the reference value of the steam temperature, from the fuel flow, and from the steam flow. The steam temperature controllers also use feedback from the errors of the steam temperatures and their integrals.

The task of the output power loop is to control the output power by manipulating the steam control valve and the extraction steam valves. The stroke of the control valve is controlled by the control valve servo. The strokes of the extraction valves are controlled by the high-pressure and by the low-pressure preheater servos. The reference values of the strokes of the extraction valves are generated by the high-pressure and by the low-pressure preheater controllers. The reference value of the stroke of the steam control valve is generated by the turbine power controller. The preheater controllers use feedforward from the reference value of the output power. The low-pressure preheater controller also uses feedback from the error of the deaerator pressure and its integral. The turbine power controller uses feedback from the error of the output power and its integral.

### Simulations.

The dynamic properties of the boiler-turbine unit cannot be represented by one linear model valid for the whole operating range. The given control objectives cannot be achieved with an entirely linear control system. It is very difficult to predict stability, control errors, settling-times, and sensitivity of non-linear multivariable systems using available theory. Since a flexible, interactive simulation program, SIMNON [8] was available it was therefore decided to investigate the performance of the control system by simulation. The drawback of this approach is that extensive simulations are necessary to ensure that the control system was reliable over the whole operating range. The advantage of the approach is that it is easy to communicate with persons, who are not familiar with control theory using the results of the simulations. The following cases have been investigated in detail by simulation:

- A) decrease of output power in normal mode,
- B) transfer from normal to alert mode,
- C) increase of output power in alert mode,
- D) decrease of output power in alert mode,
- E) transfer from alert to normal mode, and
- F) increase of output power in normal mode.

The set-point of the output power was changed from 150 MW (94%) to 100 MW (63%) in order to decrease the output power in normal mode. The jump and the rate of the reference value of the output power were 16 MW (10%) and 9.6 MW/min (6%/min) respectively. Modified sliding pressure control with opening reserve was used. The reference value of the drum pressure was decreased from  $145 \cdot 10^5$  Pa (97%) to  $113 \cdot 10^5$  Pa (75%). The rate of the reference value of the drum pressure was  $4.5 \cdot 10^5$  Pa/min (3%/min).

The reference value of the output power was 100 MW (63%) during the transfer from normal to alert mode. The reference value of the drum pressure was increased from  $113 \cdot 10^5$  Pa (75%) to  $145 \cdot 10^5$  Pa (97%). The rate of the reference value of the drum pressure was  $18 \cdot 10^5$  Pa/min (12%/min).

The set-point of the output power was changed from 100 MW (63%) to 150 MW (94%) in order to increase the output power in alert mode. The jump and the rate of the reference value of the output power were 24 MW (15%) and 19.2 MW/min (12%/min) respectively. Constant pressure control was used. The reference value of the drum pressure was  $145 \cdot 10^5$  Pa (97%).

The set-point of the output power was changed from 150 MW (94%) to 100 MW (63%) in order to decrease the output power in alert mode. The jump and the rate of the reference value of the output power were 24 MW (15%) and 19.2 MW/min (12%/min) respectively. Constant pressure control was used. The reference value of the drum pressure was  $145 \cdot 10^5$  Pa (97%).

The reference value of the output power was 100 MW (63%) during the transfer from alert to normal mode. The reference value of the drum pressure was decreased from  $145 \cdot 10^5$  Pa (97%) to  $113 \cdot 10^5$  Pa (75%). The rate of the reference value of the drum pressure was  $4.5 \cdot 10^5$  Pa/min (3%/min).

The set-point of the output power was changed from 100 MW (63%) to 160 MW (100%) in order to increase the output power in normal mode. The jump and the rate of the reference value of the output power were 16 MW (10%) and 9.6 MW/min (6%/min) respectively. Modified sliding pressure control with opening reserve was used. The reference value of the drum pressure was increased from  $113 \cdot 10^5$  Pa (75%) to  $145 \cdot 10^5$  Pa (97%). The rate of the reference value of the drum pressure was  $9 \cdot 10^5$  Pa/min (6%/min).

### Performance of the drum pressure loop.

The reference value of the drum pressure is constant in alert mode but it varies in normal mode. The most severe disturbance of the drum pressure loop is the steam flow. Six responses of the drum pressure will now be examined.

The response when the output power is decreased in normal mode is shown in Fig. 18.1. The drum pressure error is increased for  $10 < t < 30$  s, when the rate-of-change of the fuel flow is limited (see Fig. 12.1). The drum pressure error is  $4 \cdot 10^5$  Pa (3%). The drum pressure error is reduced from  $4 \cdot 10^5$  Pa (3%) to zero within 300 s.

The response due to transfer from normal to alert mode is shown in Fig. 18.2. The drum pressure error increases for  $10 < t < 25$  s when the rate-of-change of the fuel flow is limited (see Fig. 13.1). The maximum drum pressure error is  $7 \cdot 10^5$  Pa (5%). The overshoot of the drum pressure is  $3 \cdot 10^5$  Pa (2%). The drum pressure error is reduced with a time constant of about 200 s.

The response when the output power is increased in alert mode is shown in Fig. 18.3. The drum pressure error increases for  $10 < t < 20$  s, when the rate-of-change of the fuel flow is limited (see Fig. 14.1). The maximum drum pressure error is  $3 \cdot 10^5$  Pa (2%). The drum pressure error is reduced with a time constant of about 200 s.

The response when the output power is decreased in alert mode is shown in Fig. 18.4. The drum pressure error increases for  $10 < t < 35$  s, when the rate-of-change of the fuel flow is limited (see Fig. 15.1). The increase of the drum pressure error for  $10 < t < 35$  s is  $3 \cdot 10^5$  Pa (2%).

The response due to transfer from alert to normal mode is shown in Fig. 18.5. The drum pressure error is less than  $2 \cdot 10^5$  Pa (1%).

The response when the output power is increased in normal mode

is shown in Fig. 18.6. The drum pressure error increases for  $10 < t < 35$  s, when the rate-of-change of the fuel flow is limited (see Fig. 17.1). The maximum drum pressure error is  $6 \cdot 10^5$  Pa (4%). The overshoot of the drum pressure error starts to decrease for  $t > 400$  s.

The rate-of-change of the fuel flow is as high as possible when the drum pressure errors are created. A steam flow step, with an amplitude of 20 kg/s (15%) caused a drum pressure error of  $3 \cdot 10^5$  Pa (2%). A reference value ramp, with a rate of  $18 \cdot 10^5$  Pa/min (12%/min) caused a drum pressure error of  $7 \cdot 10^5$  Pa (5%). The high rate-of-change of the reference value was chosen to demonstrate that it does not cause severe interactions between the control loops. The rate-of-change has to be chosen in cooperation with the manufacturer of the boiler. The drum pressure errors are eliminated with a time constant of about 200 s.

#### Performance of the drum level loop.

The reference value of the drum level is constant. The most severe disturbance is the steam flow. The control of the drum level is difficult due to the shrink-and-swell phenomenon. The feedwater flow is disturbed by drum pressure variations. Six responses of the drum level will now be examined.

The response when the output power is decreased in normal mode is shown in Fig. 18.7. The drum level error increases for  $10 < t < 30$  s, to a maximum value of 4 cm.

The response due to transfer from normal to alert mode is shown in Fig. 18.8. The drum level error increases for  $10 < t < 35$  s. The drum level error is less than 3 cm when the drum pressure is increasing. The drum level error is eliminated within 60 s, when the increase of the drum pressure ceases.

The response when the output power is increased in alert mode is

shown in Fig. 18.9. The drum level error increases for  $10 < t < 35$  s, to a maximum value of 6 cm. The drum level error is zero for  $t > 250$  s.

The response when the output power is decreased in alert mode is shown in Fig. 18.10. The drum level error increases for  $10 < t < 30$  s, to a maximum value of 6 cm. The drum level oscillations are mainly caused by the steam flow variations (see Fig. 15.22) and not by a badly tuned drum level controller. Observe that nonlinear effects cause differences between the responses in Fig. 18.9 and 18.10. The drum level error is zero for  $t > 250$  s.

The response due to transfer from alert to normal mode is shown in Fig. 18.11. The drum level error is less than 1 cm.

The response when the output power is increased in normal mode is shown in Fig. 18.12. The drum level error is increased for  $10 < t < 25$  s, to a maximum value of 4 cm. The drum level error is less than 2 cm during the increase of the output power. The major part of the drum level error is eliminated within 20 s, when the increase of the output power ceases. The drum level error is reduced to zero within 120 s.

The largest drum level errors are created by the shrink-and-swell phenomenon. A steam flow step, with an amplitude of 20 kg/s (15%), causes a drum level error of 6 cm. The drum level error is eliminated with a time constant of about 100 s.

#### Performance of the steam temperature loop.

The reference value of the steam temperature after the tertiary superheater is constant. The steam flow and the heat flows to the superheaters are the most severe disturbances of the steam temperature loop. If sliding pressure control is used there are also disturbances due to variations in the saturation temperature of the steam entering the primary superheater. Six responses

of the steam temperature after the tertiary superheater will now be examined.

The response when the output power is decreased in normal mode is shown in Fig. 18.13. The steam temperature error increases for  $10 < t < 13$  s, when the rate of the stroke of the second attemperator is limited (see Fig. 12.13). The maximum steam temperature error is  $2^{\circ}\text{C}$ .

The response due to transfer from normal to alert mode is shown in Fig. 18.14. The steam temperature error increases for  $10 < t < 120$  s. The spray flow valve of the second attemperator is completely open for  $t > 30$  s (see Fig. 13.9). The maximum steam temperature error is  $8^{\circ}\text{C}$ . The steam temperature approaches the reference value without overshoot and with a time constant which is less than 100 s.

The response when the output power is increased in alert mode is shown in Fig. 18.15. The steam temperature error increases for  $10 < t < 15$  s, when the rate of the stroke of the second attemperator is limited (see Fig. 14.13). The maximum steam temperature error is  $3^{\circ}\text{C}$ . The steam temperature error decreases with a time constant which is less than 100 s.

The response when the output power is decreased in alert mode is shown in Fig. 18.16. The steam temperature error increases for  $10 < t < 13$  s, when the rate of the stroke of the second attemperator is limited (see Fig. 15.13). The maximum steam temperature error is  $3^{\circ}\text{C}$ .

The response due to transfer from alert to normal mode is shown in Fig. 18.17. The maximum steam temperature error is  $1^{\circ}\text{C}$ . The steam temperature error is eliminated with a time constant of about 100 s.

The response when the output power is increased in normal mode is shown in Fig. 18.18. The steam temperature error increases

for  $10 < t < 15$  s, when the rate of the stroke of the second attemperator valve is limited. The maximum steam temperature error is  $2^{\circ}\text{C}$ . The steam temperature error starts to decrease for  $t > 250$  s with a time constant of about 100 s.

The limited capacity of the attemperators caused the largest steam temperature error during transfer from normal to alert mode. The fuel flow was increased about 3 kg/s (30%). This caused a steam temperature error of  $8^{\circ}\text{C}$ . The steam flow steps caused the most rapid increase of the steam temperature error. A step in steam flow, with an amplitude of 20 kg/s (15%) caused a steam temperature error of  $3^{\circ}\text{C}$ . The servo of the second attemperator operated with maximum rate in these situations. The steam temperature errors were eliminated without any overshoot and with a time constant of about 100 s.

#### Performance of the output power loop.

The reference value of the output power is changed like a step followed by a ramp, but was kept constant during the transfer from one mode to the other. The disturbances of the output power loop are the pressure and the temperature of the steam before the steam control valve. Six responses of the output power loop will now be examined.

The response when the output power is decreased in normal mode is shown in Fig. 18.19. The rise time is about 3 s. The maximum output error is less than 1 MW (0.7%) for  $t > 15$  s.

The response due to transfer from normal to alert mode is shown in Fig. 18.20. The output power error is barely visible.

The response when the output power is increased in alert mode is shown in Fig. 18.21. The rise time is about 3 s. The maximum output power error is less than 1 MW (0.7%) for  $t > 15$  s.



The response when the output power is decreased in alert mode is shown in Fig. 18.22. The rise time is about 3 s. The maximum output power error is less than 1 MW (0.7%) for  $t > 15$  s.

The response due to transfer from alert to normal mode is shown in Fig. 18.23. The output power error is barely visible.

The response when the output power is increased in normal mode is shown in Fig. 18.24. The rise time is about 3 s. The maximum output power error is less than 1 MW (0.7%) for  $t > 15$  s.

The output power loop has been tuned for fast responses. The responses of the control valve servo (see Figs. 12.21, 14.21, 15.21, and 17.21) may lead to unacceptable wear of the control valve and its servo. The high response rate of the output power loop was chosen in order to demonstrate that it does not lead to severe interaction between the control loops.

#### Concluding remarks.

The performance of the control system in six different cases has been examined in detail. A summary of the performance, in terms of control errors, is given in Tab. 18.1.

The multivariable character of the boiler-turbine unit does not prevent the use of simple-minded controllers, designed and tuned loop by loop. The dynamic properties of the boiler-turbine unit is limited, not by the interaction between control loops, but by limited range and limited rate-of-change of the actuators as well as by the necessity to avoid stresses and wear.

The control system can protect the boiler-turbine unit from unacceptably large stresses. The final choice of power jumps, power rates, and pressure rates has to be discussed with the manufacturers of the boiler and the turbine.

| Case   | Drum pres-<br>sure error | Drum level<br>error | Steam tempe-<br>rature error | Output po-<br>wer error<br>( $t > 15$ s) |
|--|--------------------------|---------------------|------------------------------|--|
|  | $10^5$ Pa                | cm                  | $^{\circ}\text{C}$           | MW                                       |
| Increase of the output power<br>in normal mode | 6                        | 4                   | 2                            | 1*)                                      |
| Transfer from normal to alert<br>mode          | 7                        | 3                   | 8                            | $\sim 0$                                 |
| Increase of the output power<br>in alert mode  | 3                        | 6                   | 3                            | 1*)                                      |
| Decrease of the output power<br>in alert mode  | 3                        | 6                   | 3                            | 1*)                                      |
| Transfer from alert to normal<br>mode          | 2                        | 1                   | 1                            | $\sim 0$                                 |
| Decrease of the output power<br>in normal mode | 4                        | 4                   | 2                            | 1*)                                      |

\*) The initial value of the control error is always equal to the jump of the reference value of the output power.

Table 18.1 - Control errors

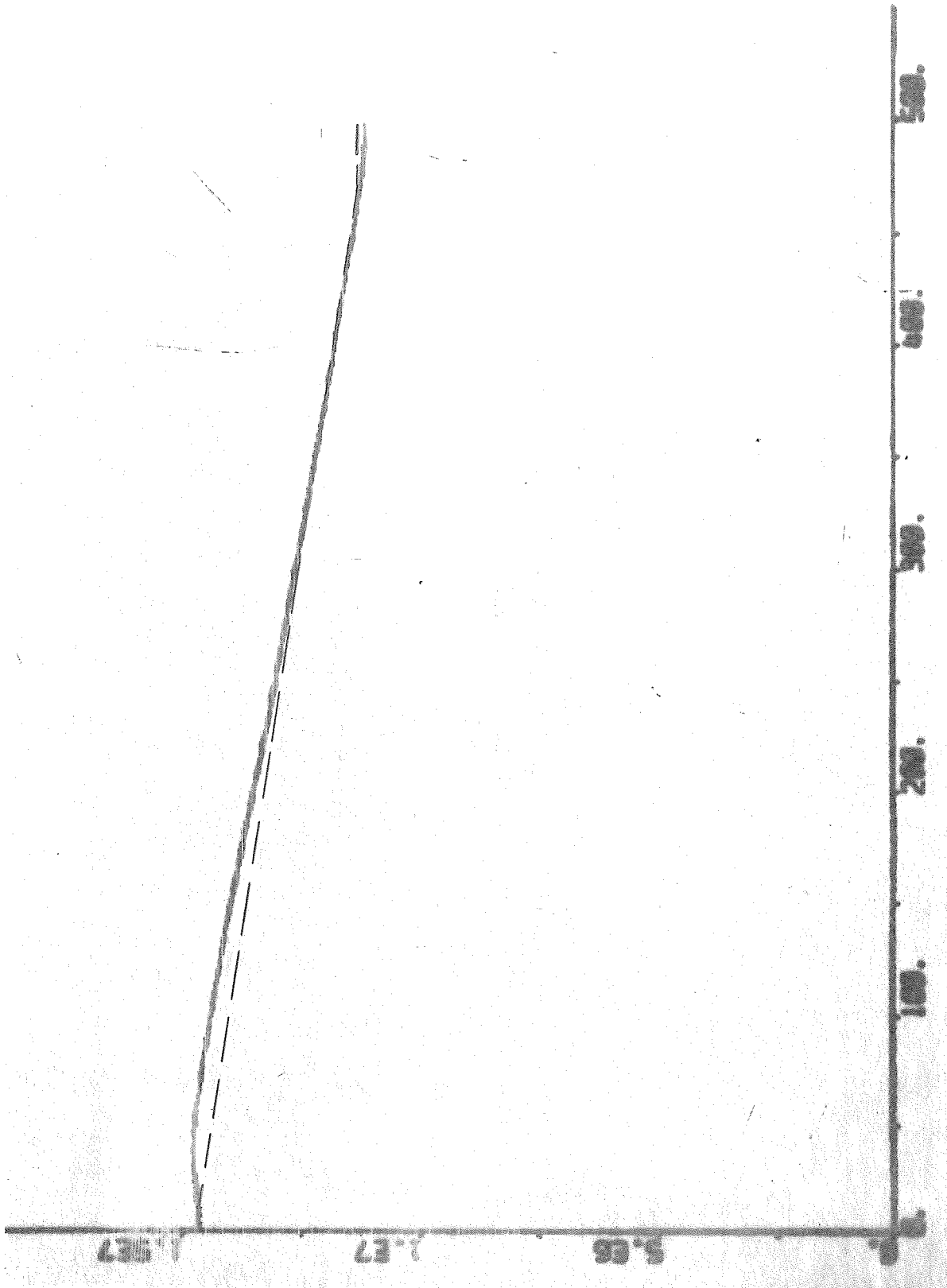


Fig. 18.1 - Response of the drum pressure ( — ) and its reference value ( --- ) due to decrease of the output power in normal mode.

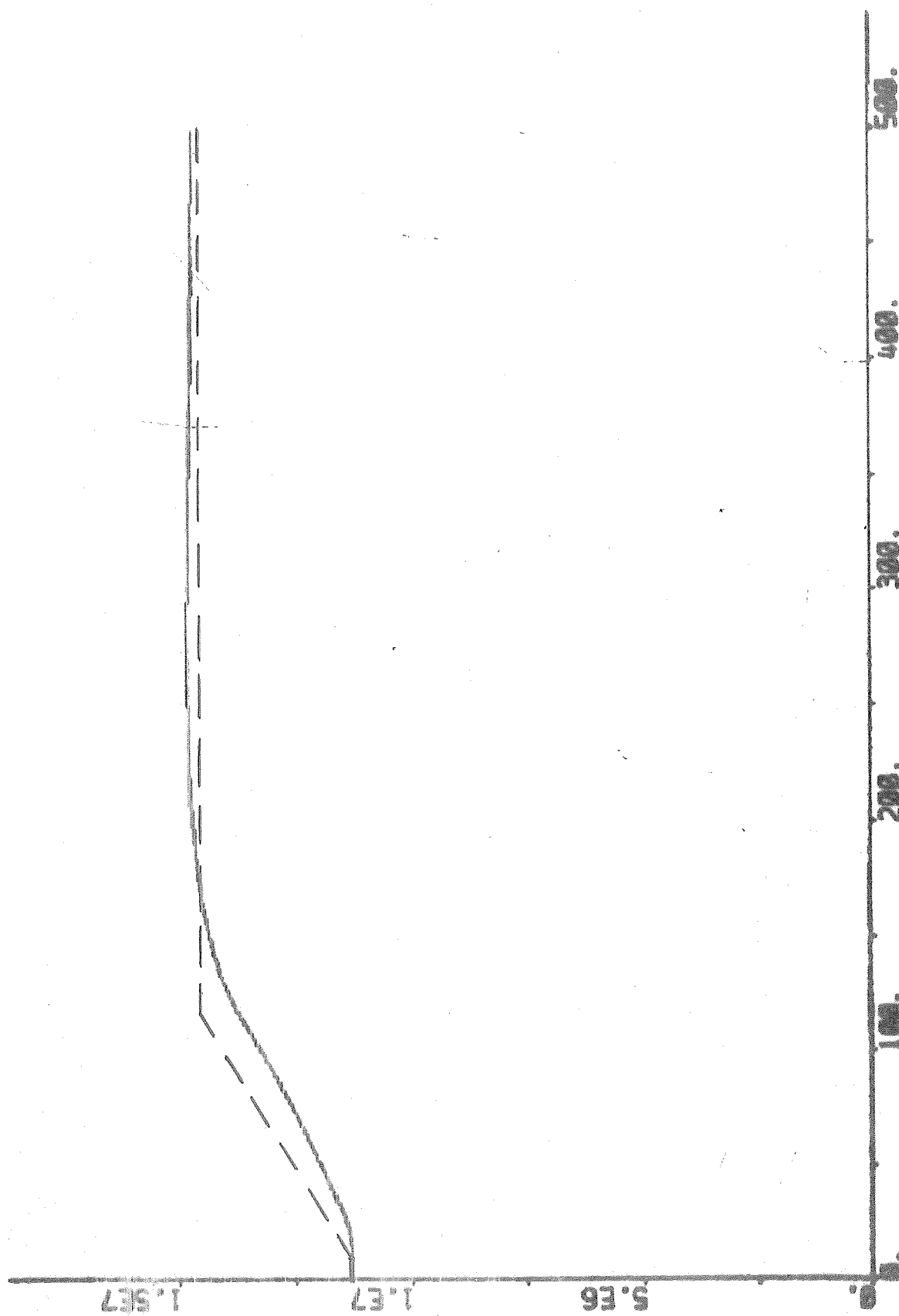


Fig. 18.2 - Response of the drum pressure ( — ) and its reference value ( --- ) due to transfer from normal to alert mode.

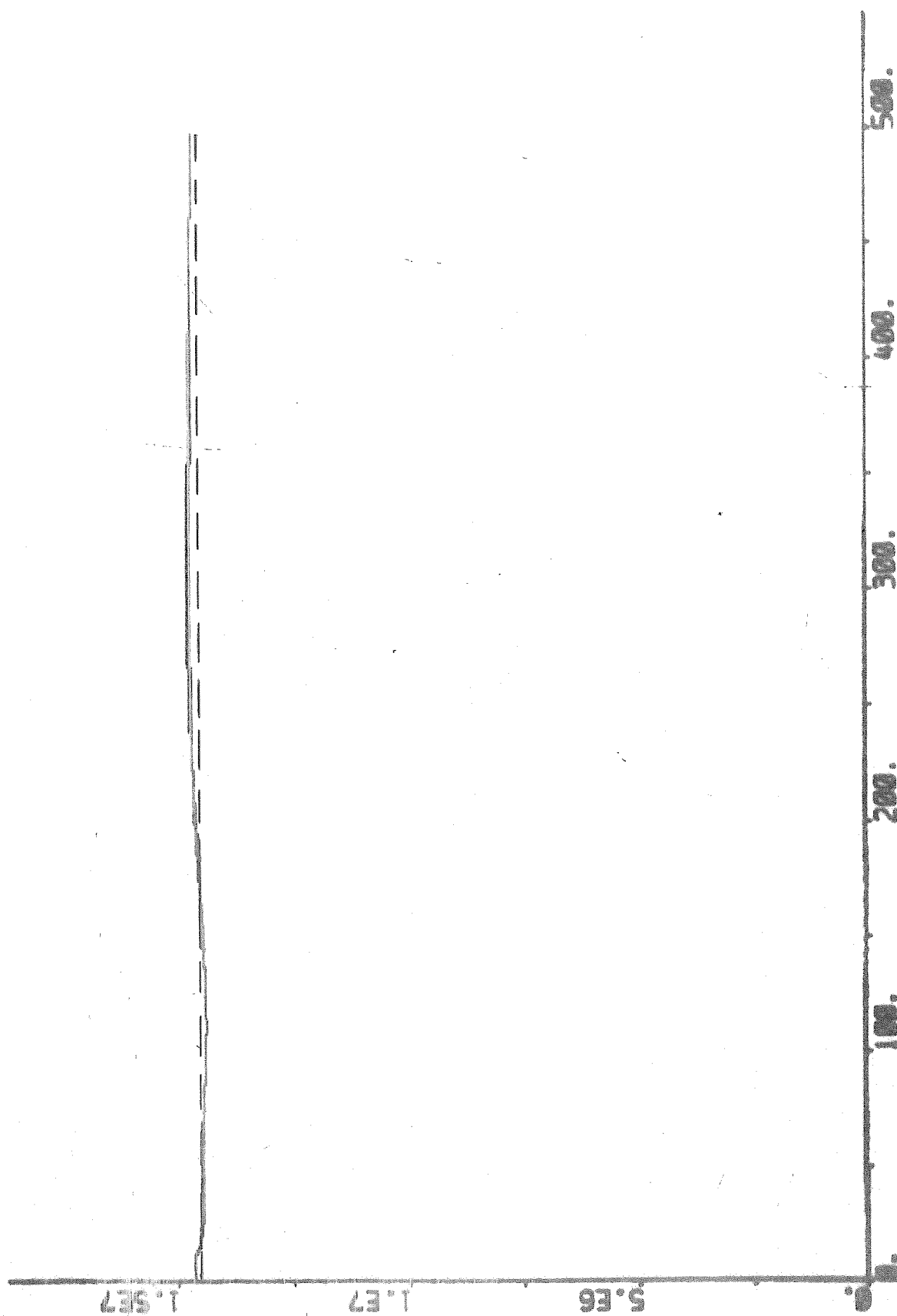


Fig. 18.3 - Response of the drum pressure ( — ) and its reference value ( --- ) due to increase of the output power in alert mode.

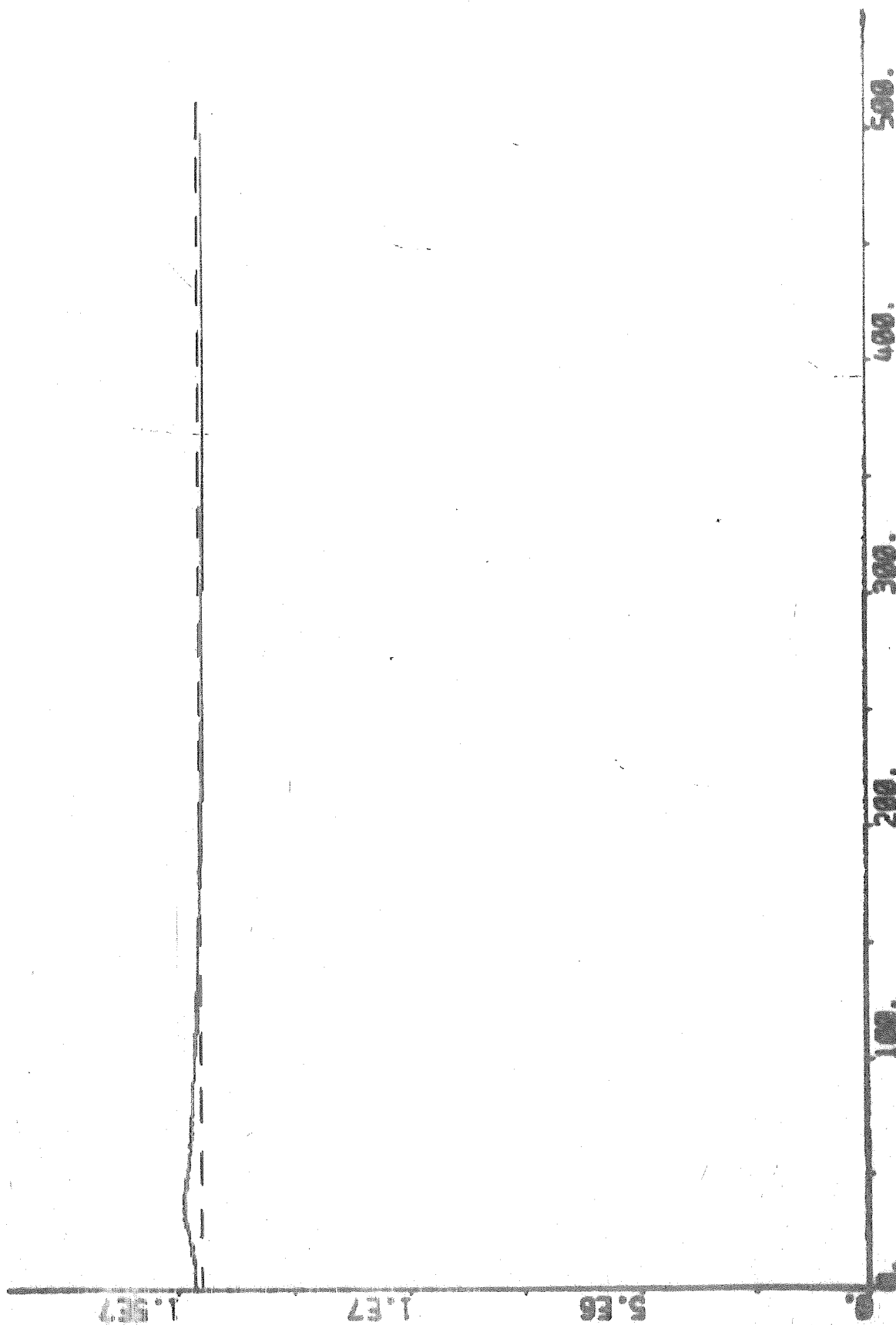


Fig. 18.4 - Response of the drum pressure ( — ) and its reference value ( --- ) due to decrease of the output power in alert mode.

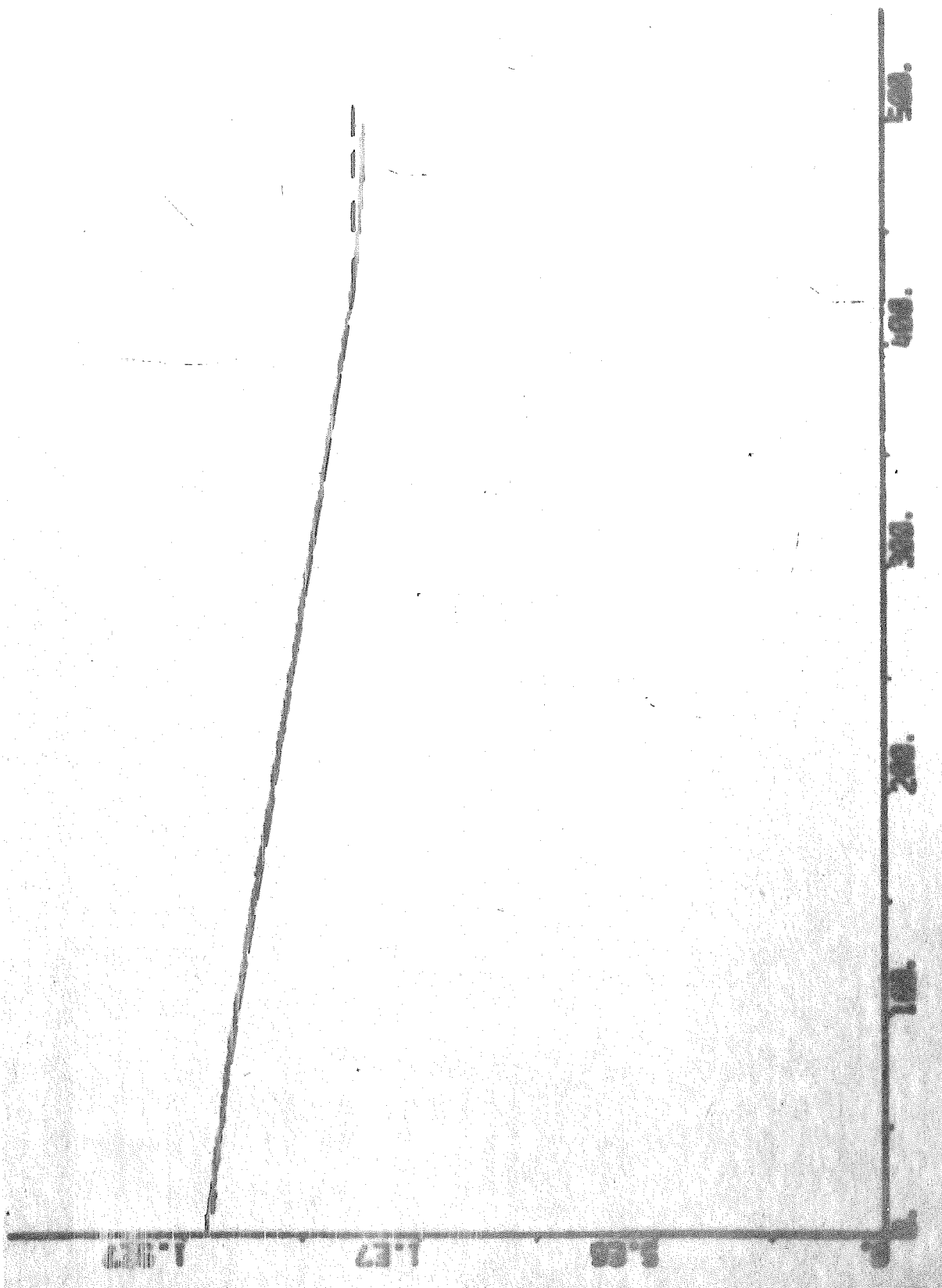


Fig. 18.5 - Response of the drum pressure ( — ) and its reference value ( --- ) due to transfer from alert to normal mode.

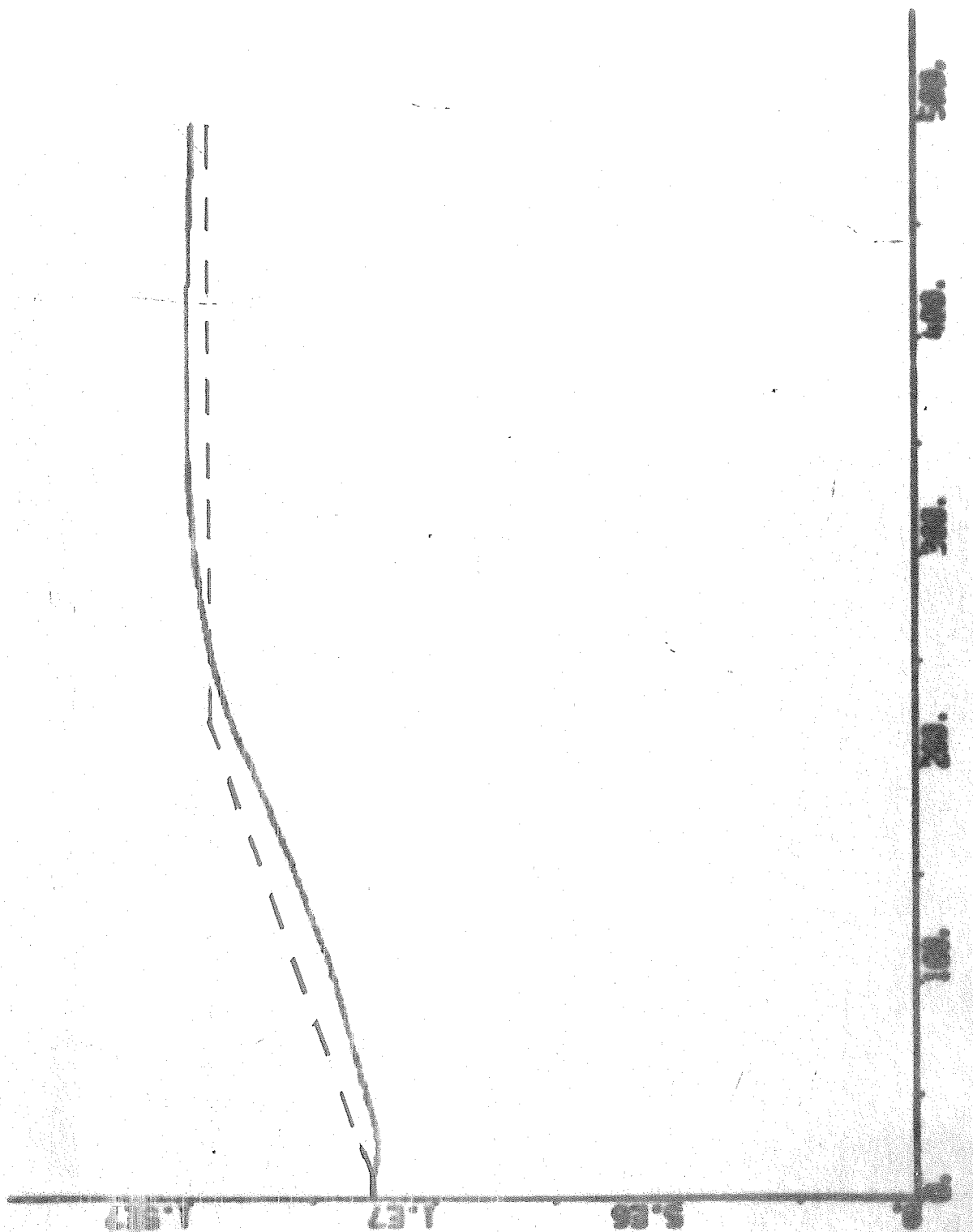


Fig. 18.6 - Response of the drum pressure ( — ) and its reference value ( --- ) due to increase of the output power in normal mode.



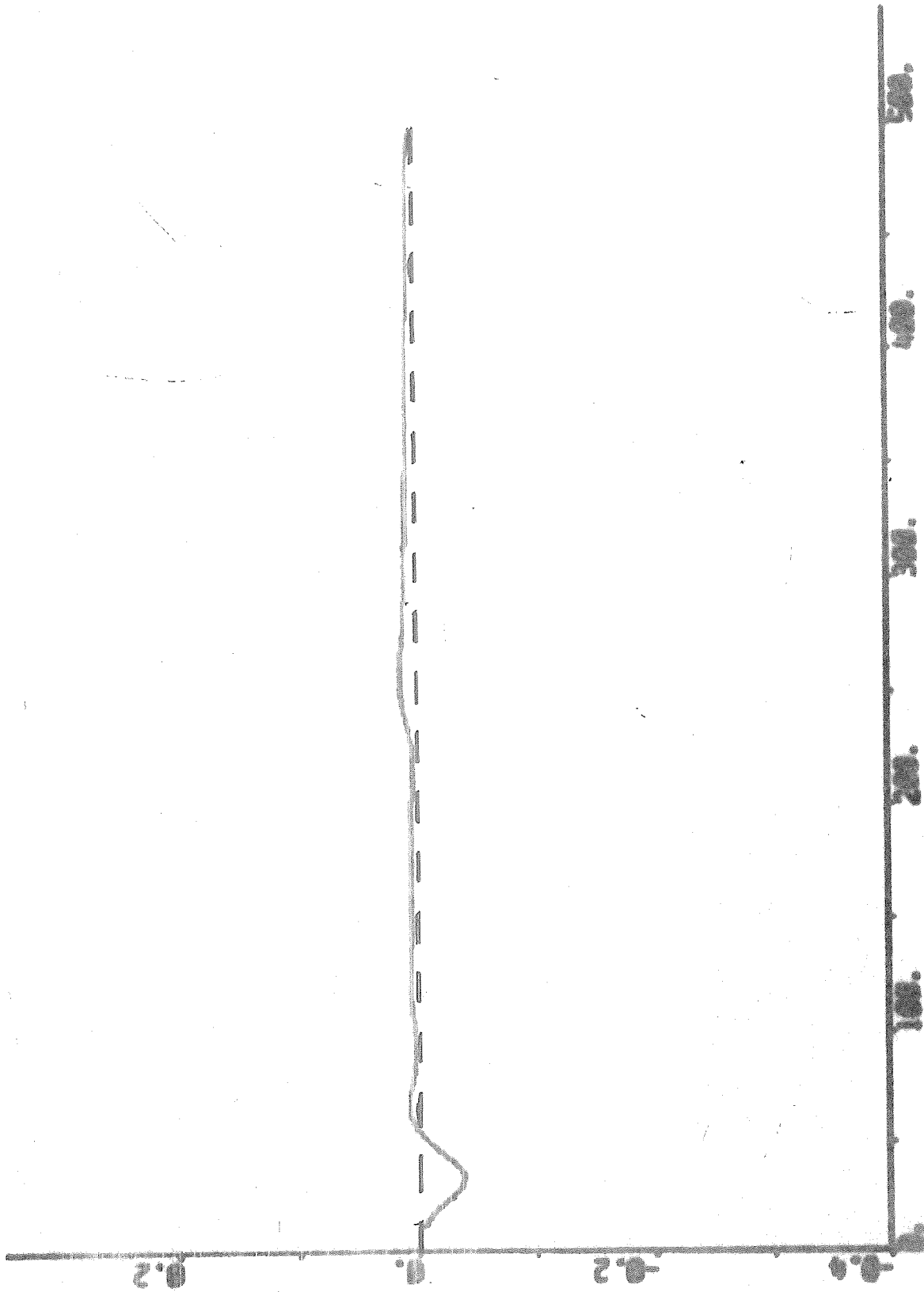


Fig. 18.7 - Response of the drum level ( --- ) and its reference value ( --- ) due to decrease of the output power in normal mode.

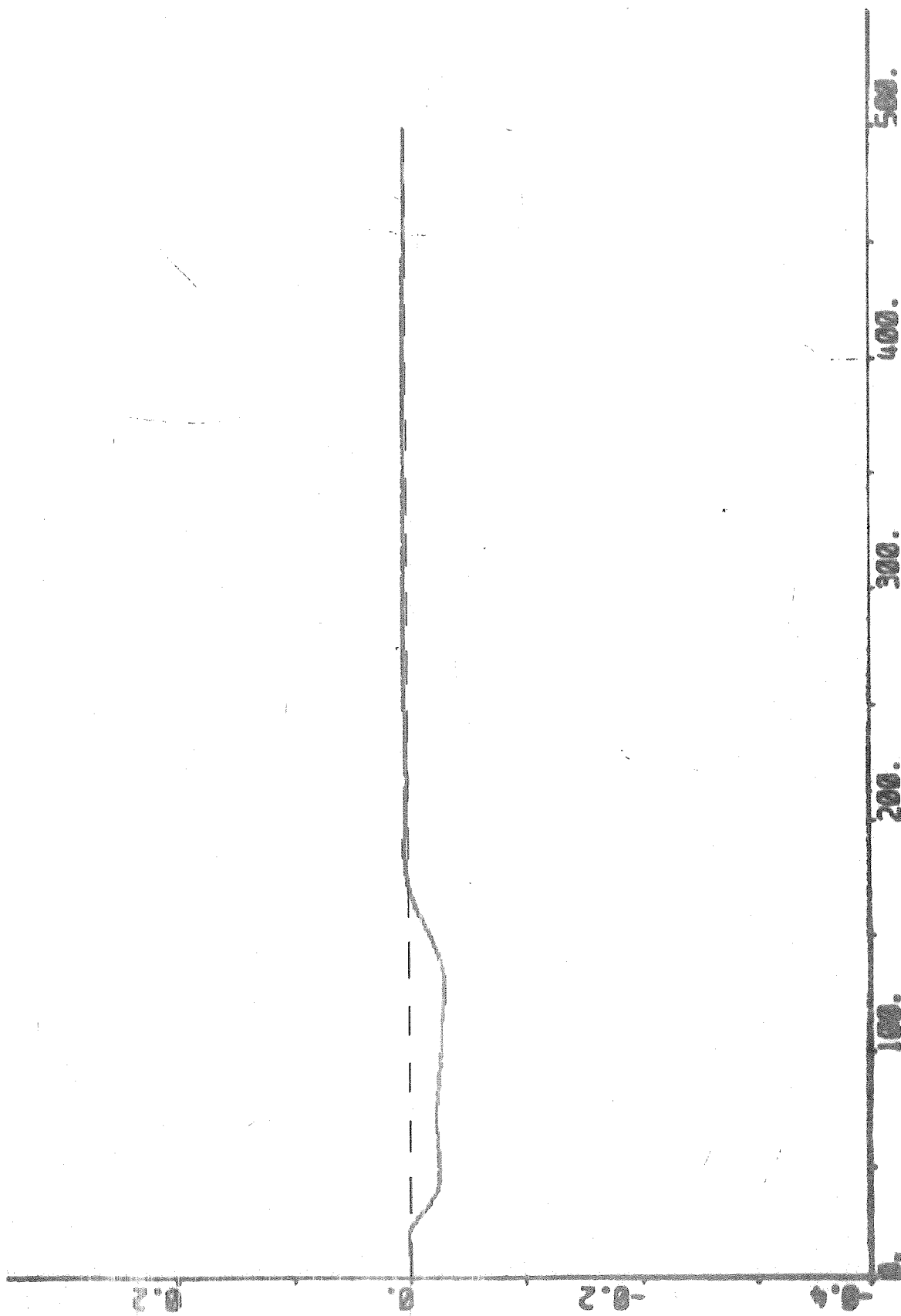


Fig. 18.8 - Response of the drum level ( — ) and its reference value ( --- ) due to transfer from normal to alert mode.

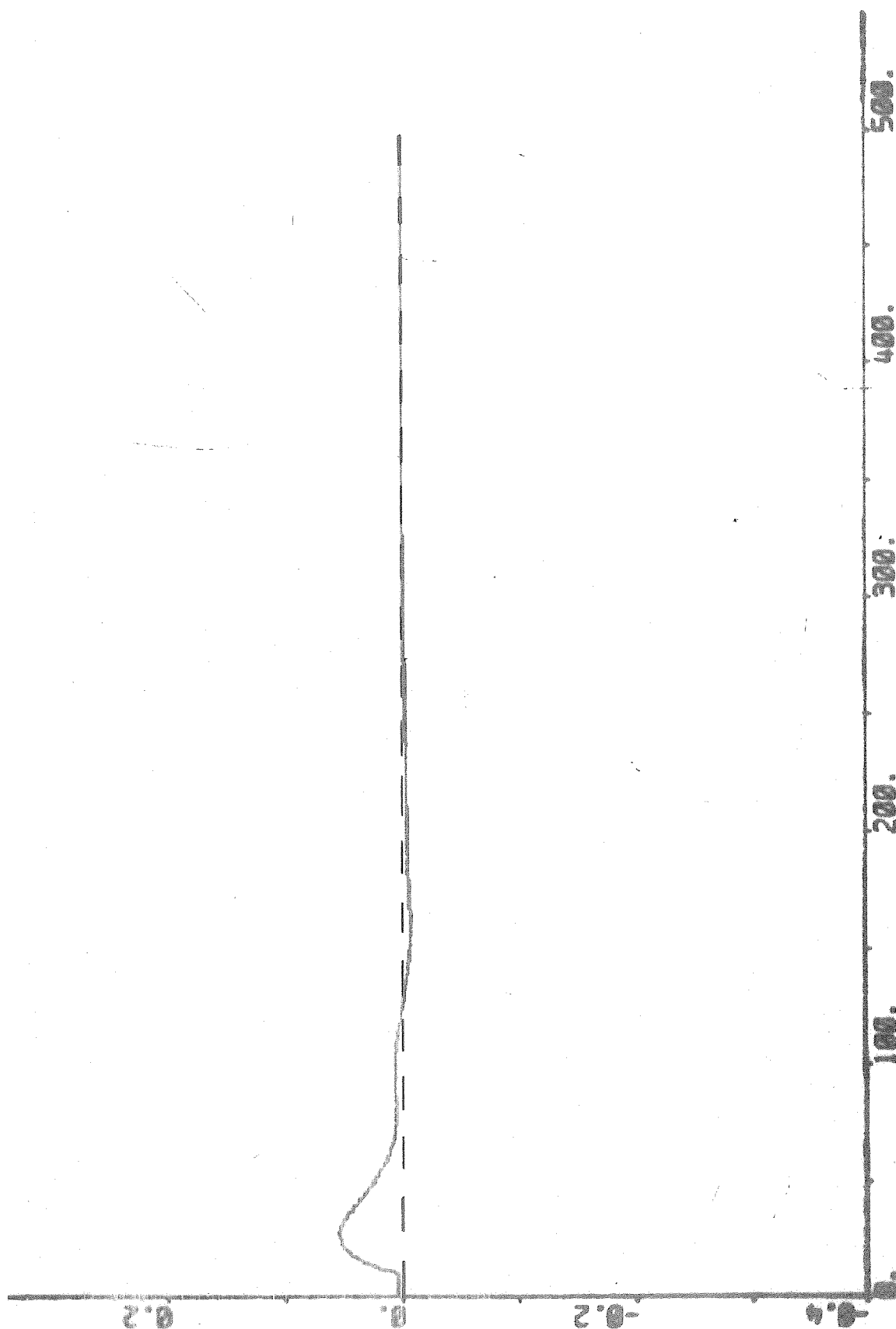


Fig. 18.9 - Response of the drum level ( — ) and its reference value ( --- ) due to increase of the output power in alert mode.

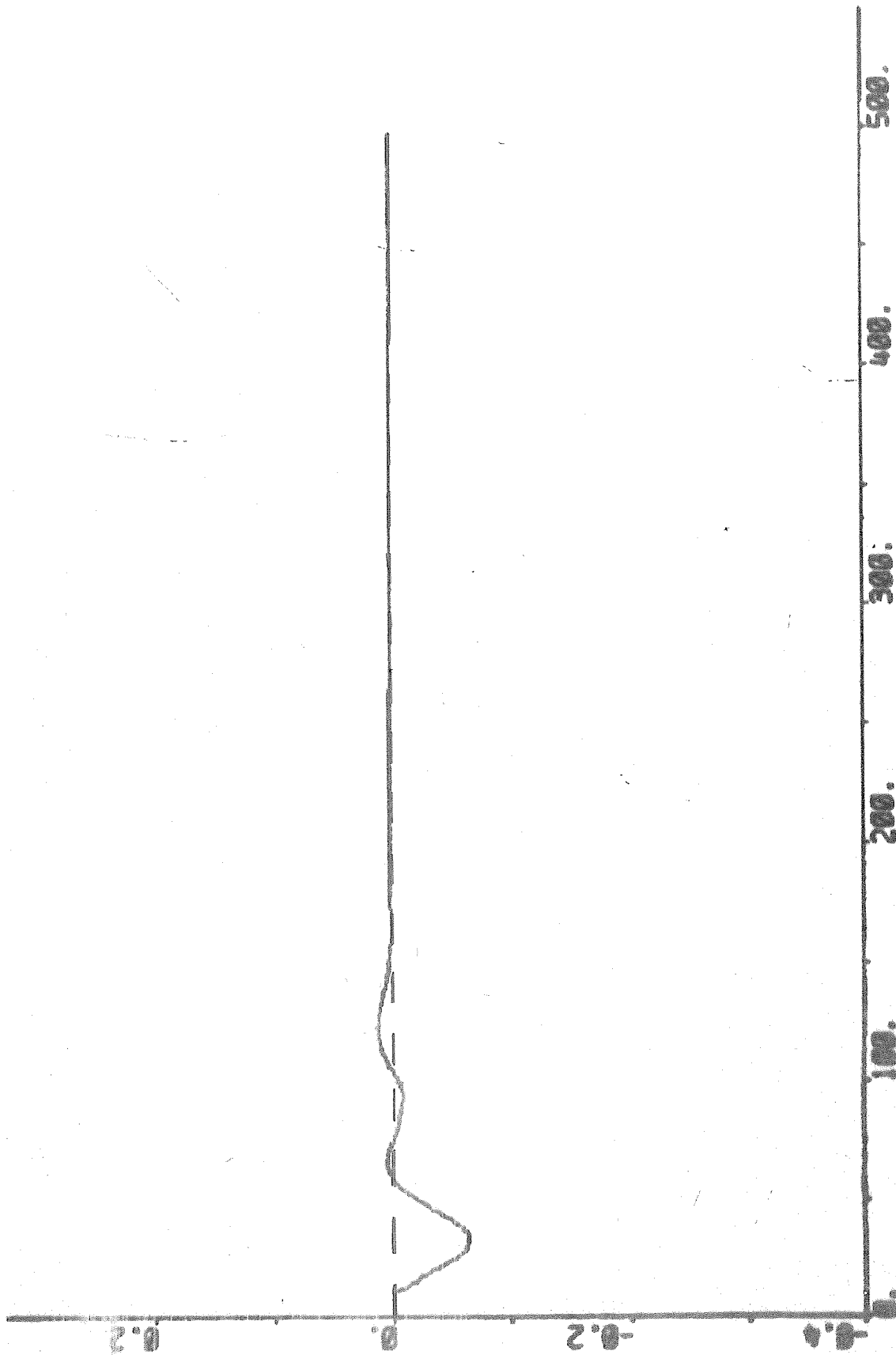


Fig. 18.10 - Response of the drum level ( — ) and its reference value ( ---- ) due to decrease of the output power in alert mode.

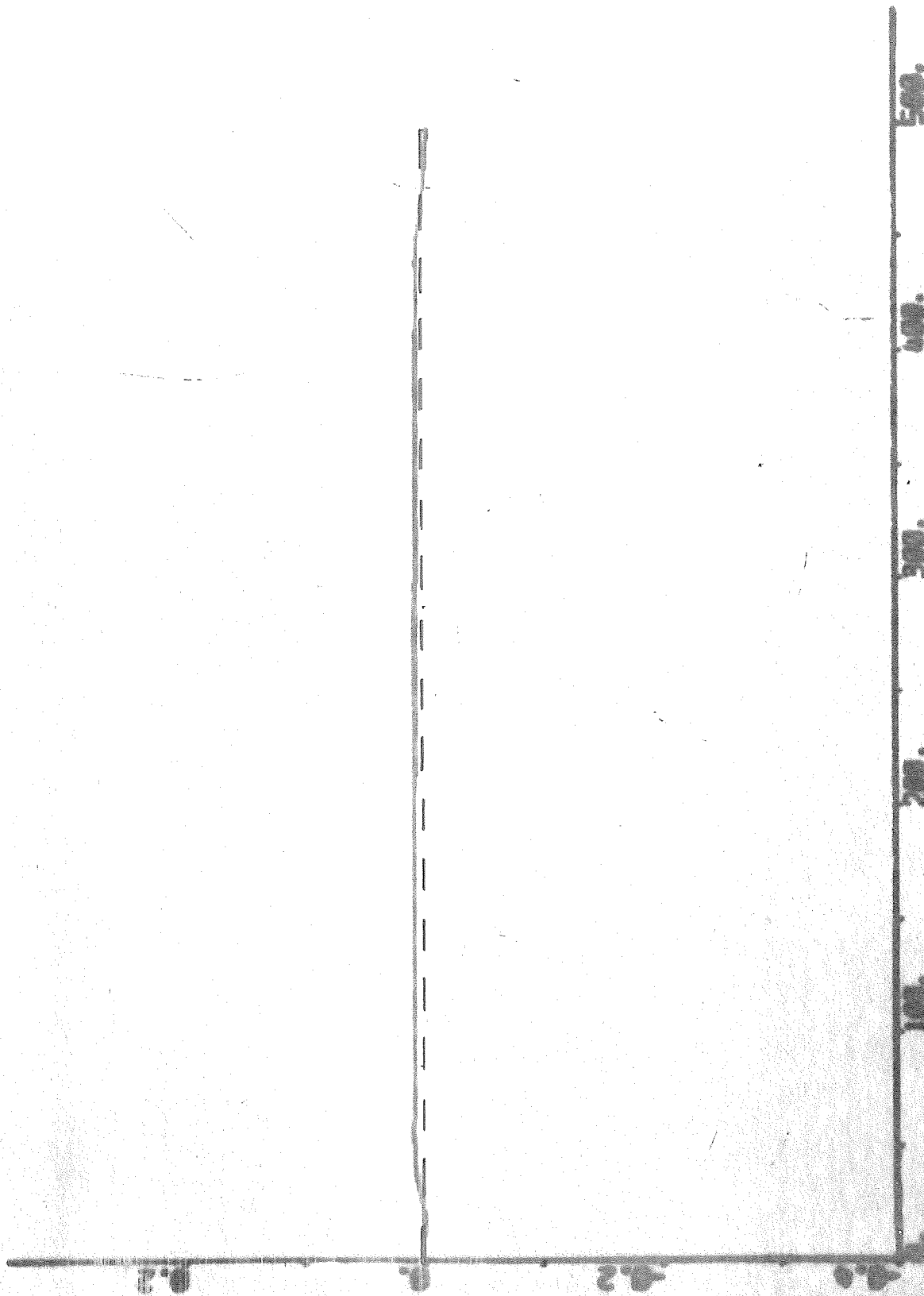


Fig. 18.11 - Response of the drum level ( — ) and its reference value ( --- ) due to transfer from alert to normal mode.

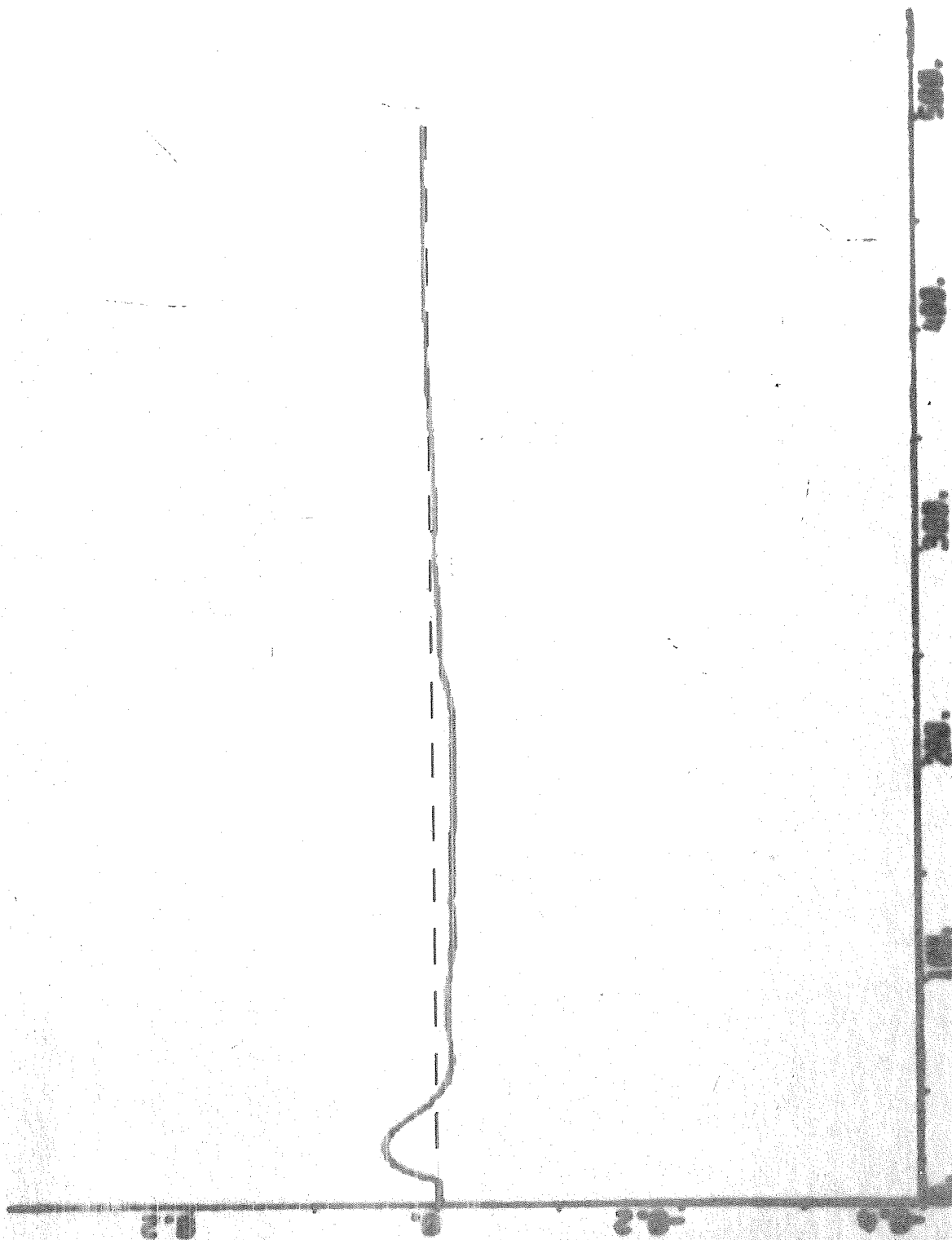


Fig. 18.12 - Response of the drum level ( — ) and its reference value ( --- ) due to increase of the output power in normal mode.

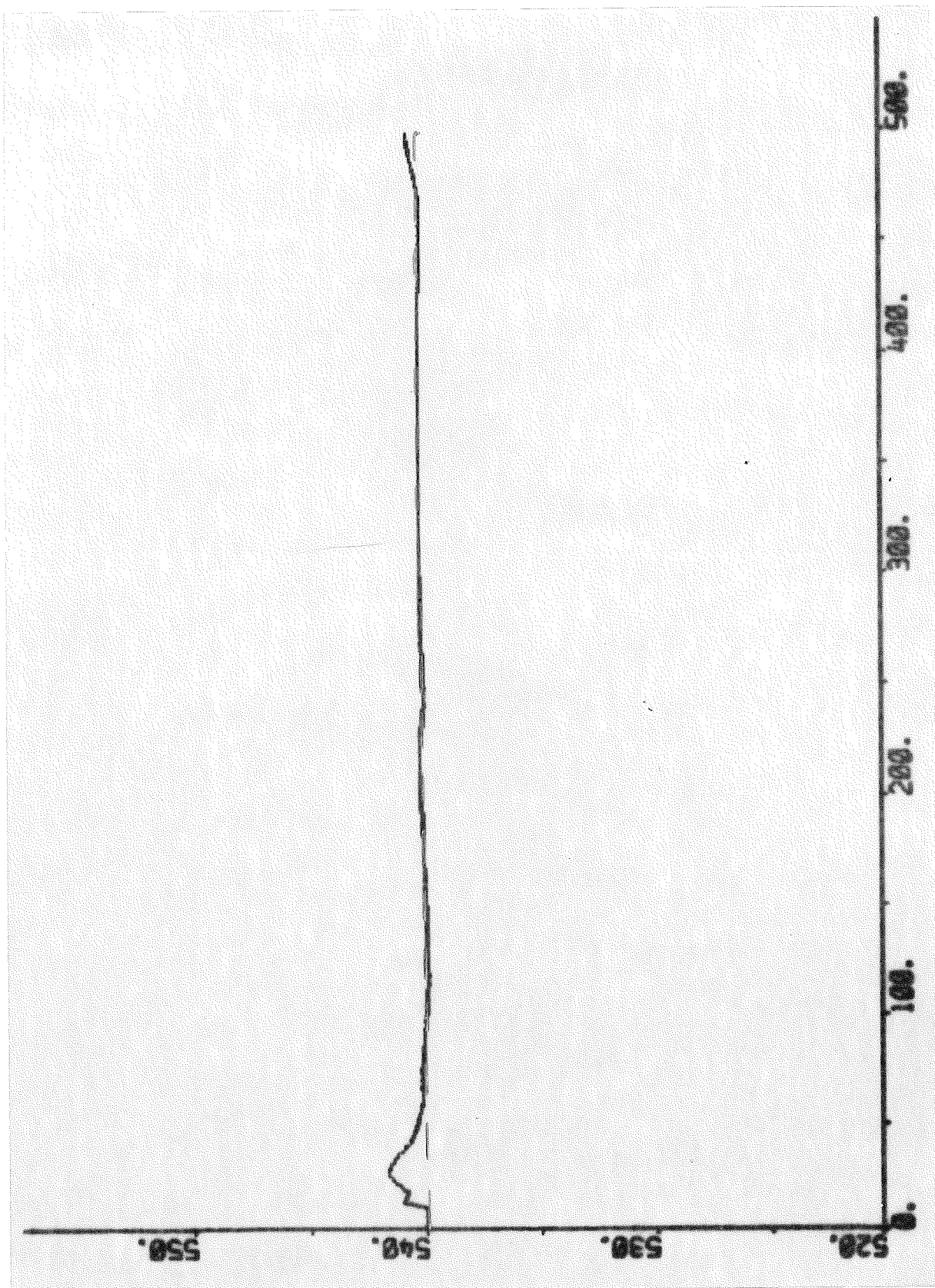


Fig. 18.13 - Response of the steam temperature after the tertiary superheater ( — ) and its reference value ( --- ) due to decrease of the output power in normal mode.

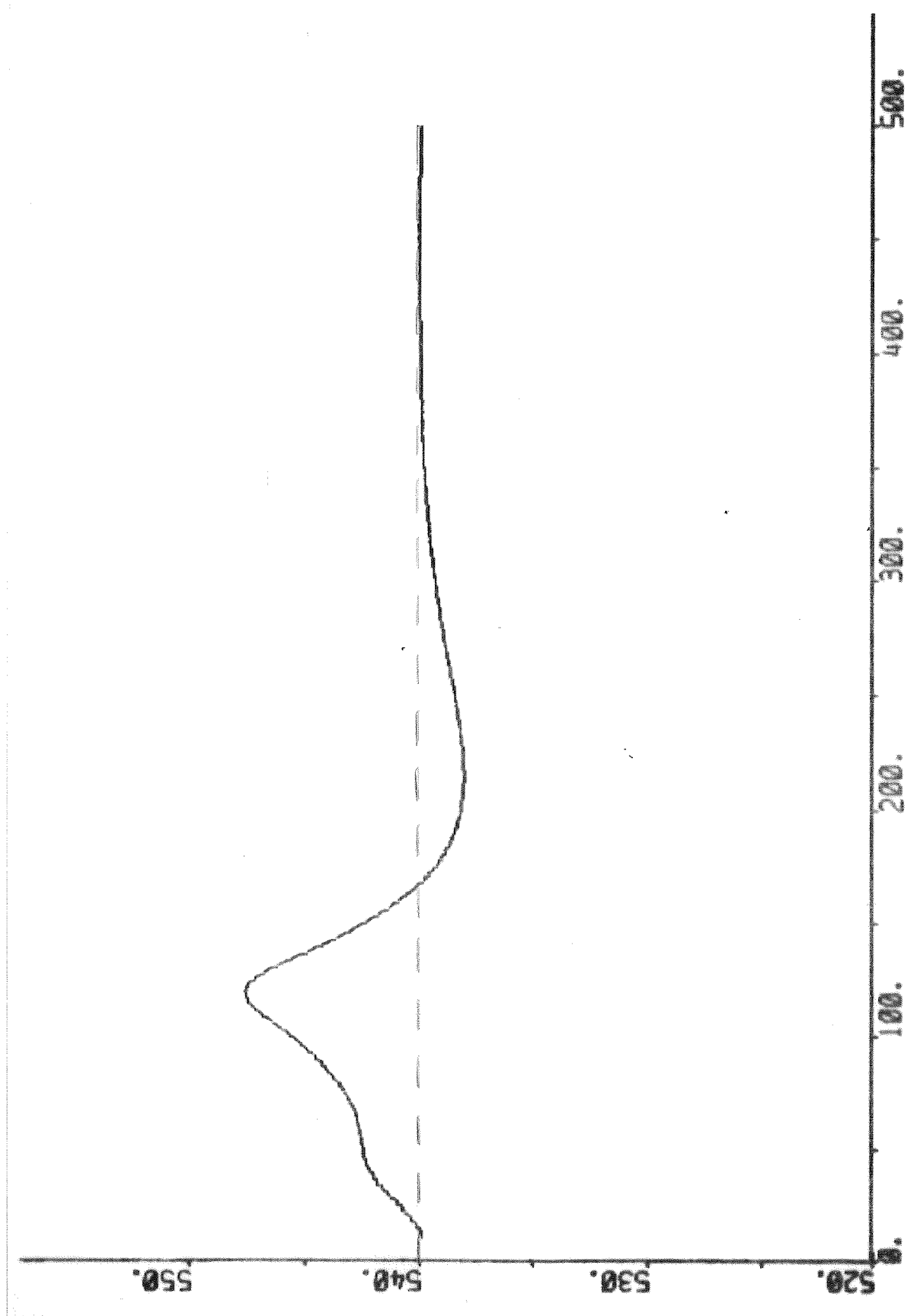


Fig. 18.14 - Response of the steam temperature after the tertiary superheater ( — ) and its reference value ( --- ) due to transfer from normal to alert mode.



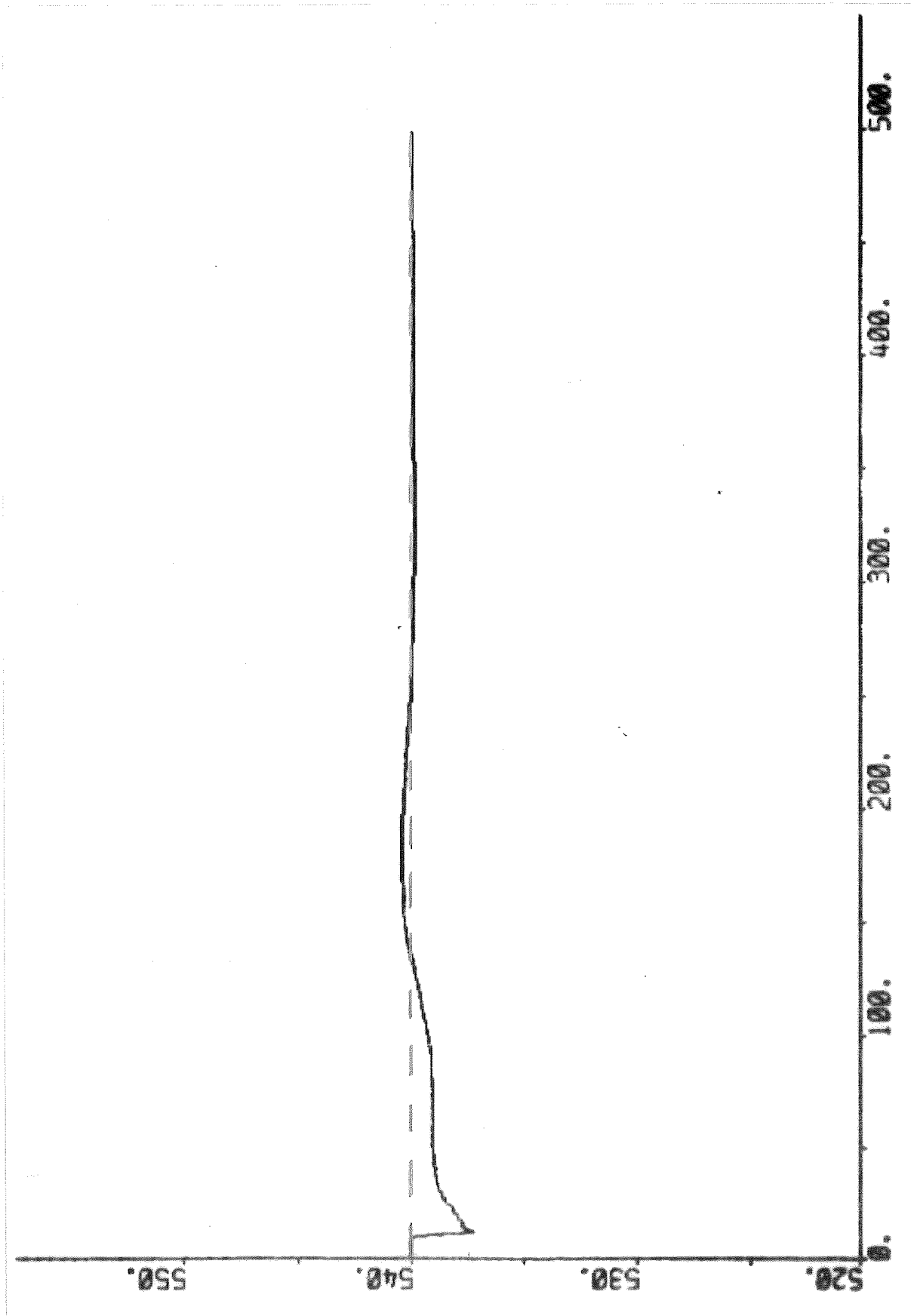


Fig. 18.15 - Response of the steam temperature after the tertiary superheater ( — ) and its reference value ( --- ) due to increase of the output power in alert mode.

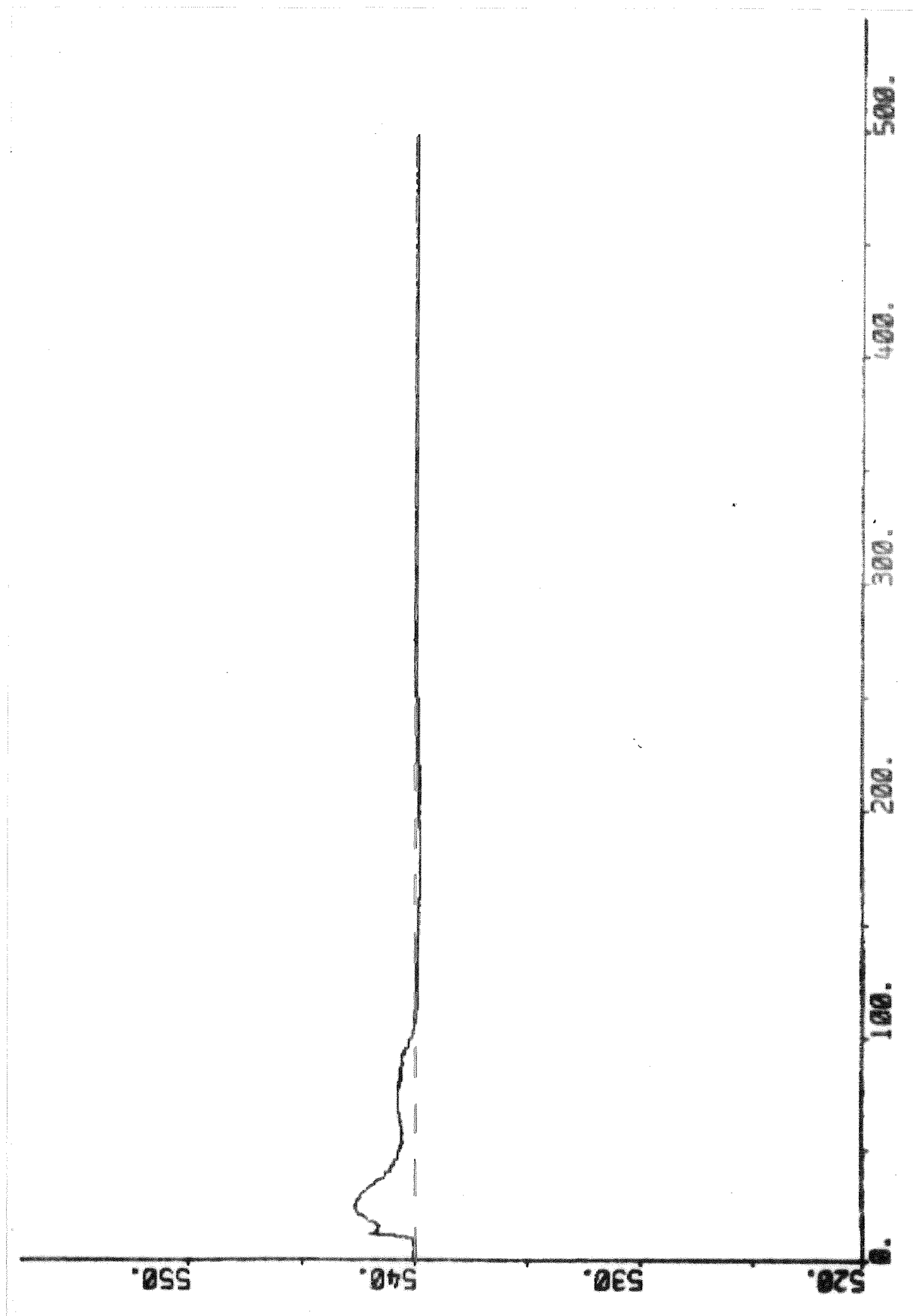


Fig. 18.16 - Response of the steam temperature after the tertiary superheater ( — ) and its reference value ( --- ) due to decrease of the output power in alert mode.

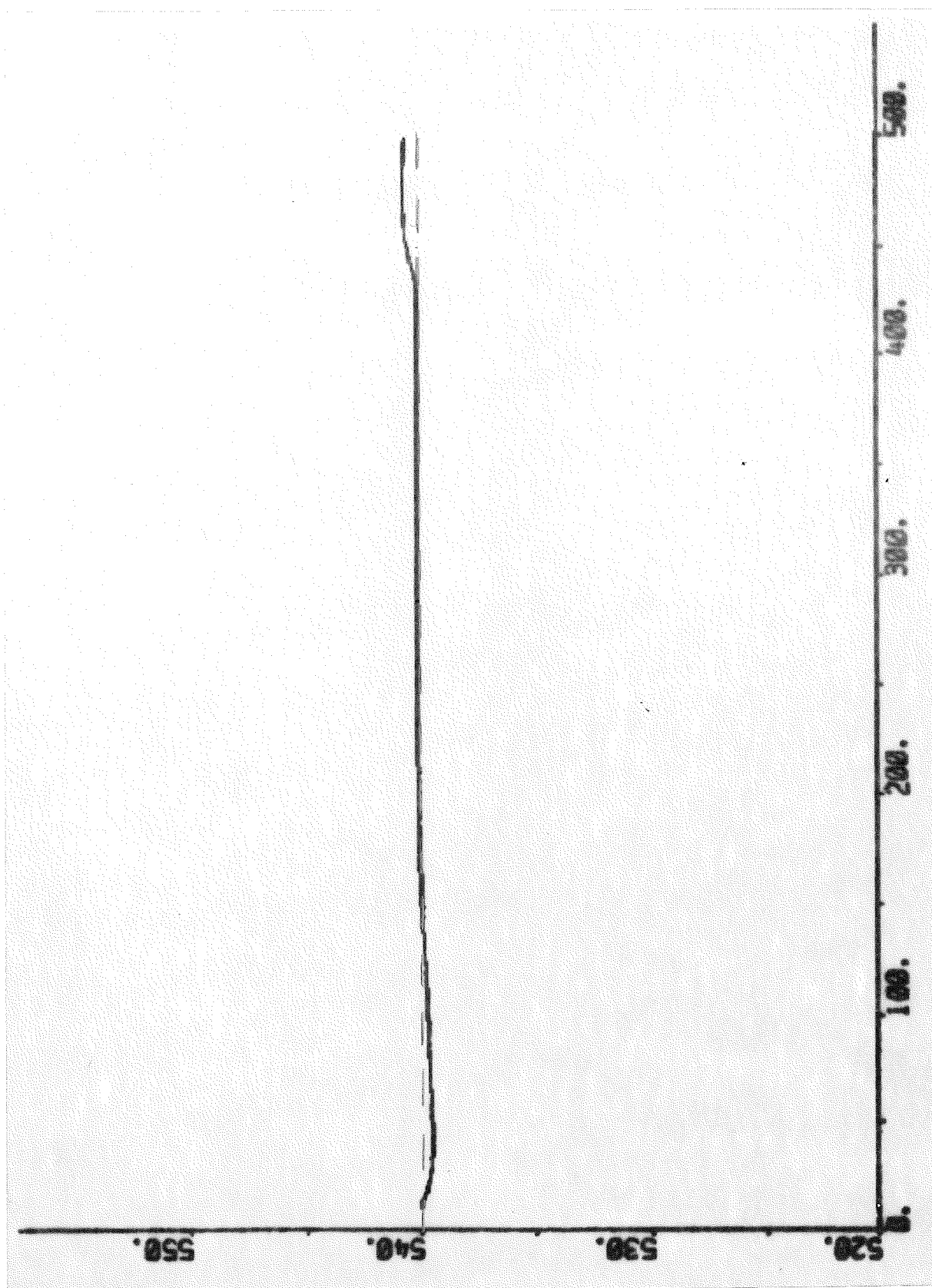


Fig. 18.17 - Response of the steam temperature after the tertiary superheater ( — ) and its reference value ( --- ) due to transfer from alert to normal mode.

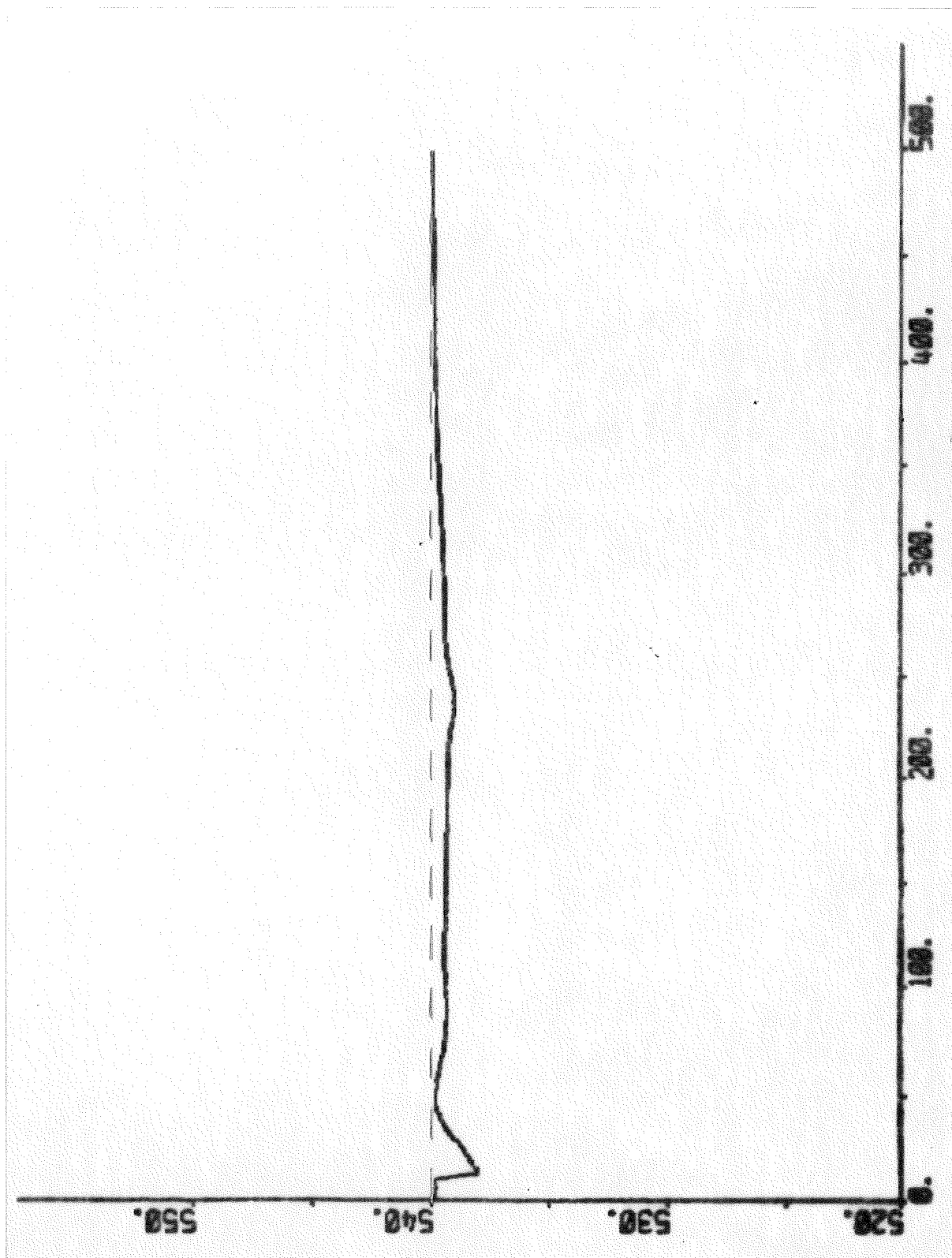


Fig. 18.18 - Response of the steam temperature after the tertiary superheater ( — ) and its reference value ( --- ) due to increase of the output power in normal mode.

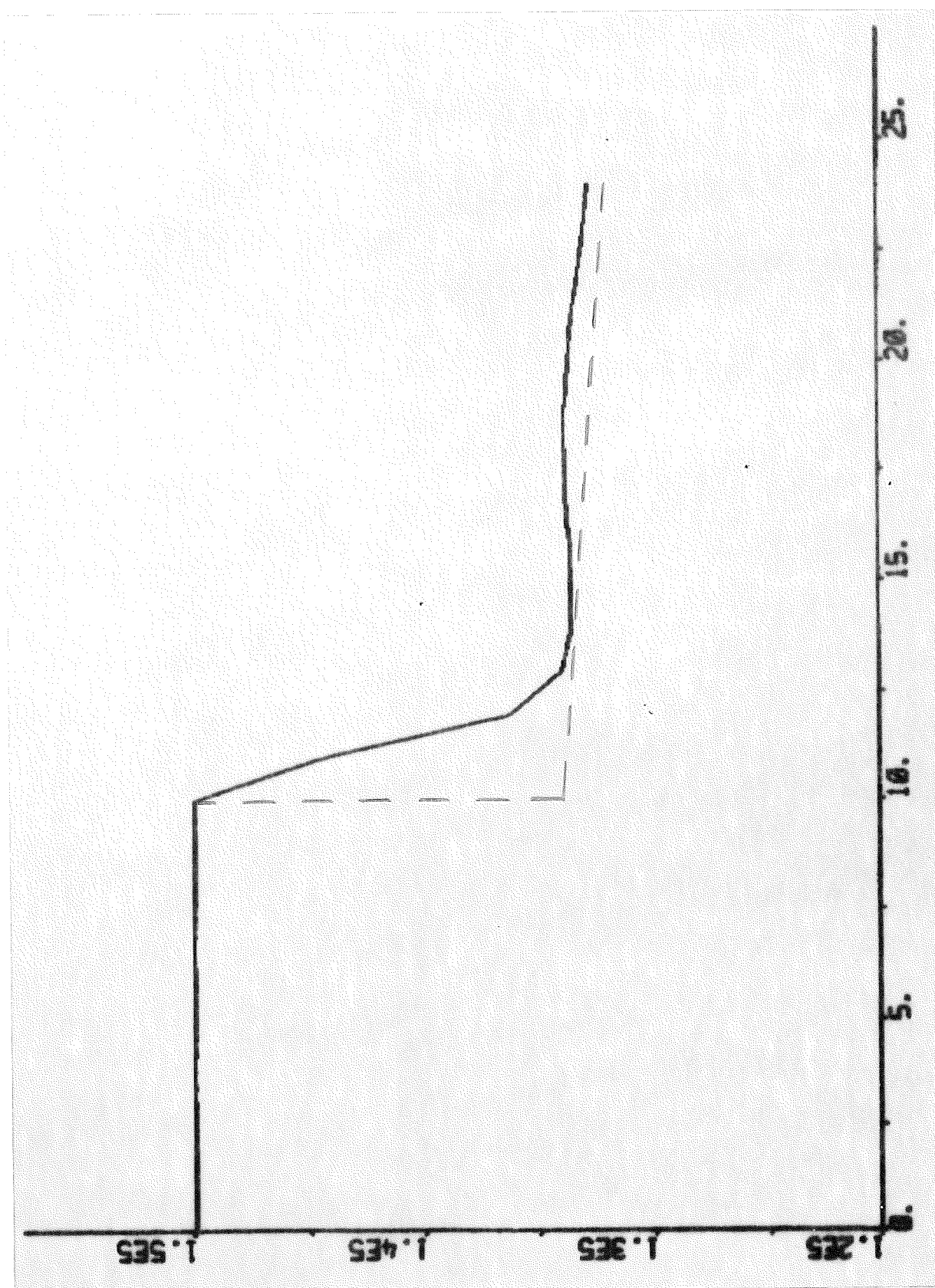


Fig. 18.19 - Response of the output power ( — ) and its reference value ( --- ) due to decrease of the output power in normal mode.

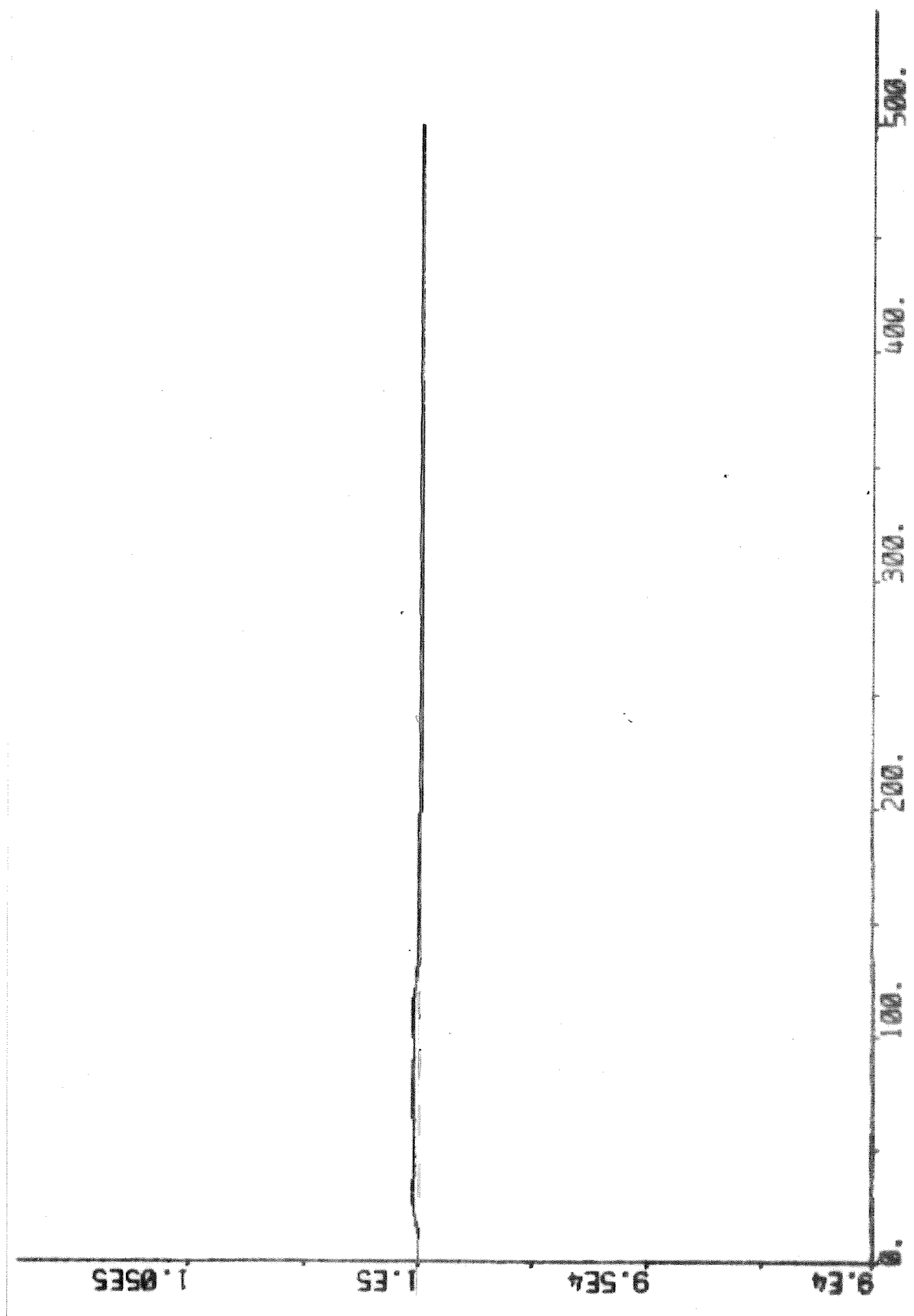


Fig. 18.20 - Response of the output power ( — ) and its reference value ( --- ) due to transfer from normal to alert mode.

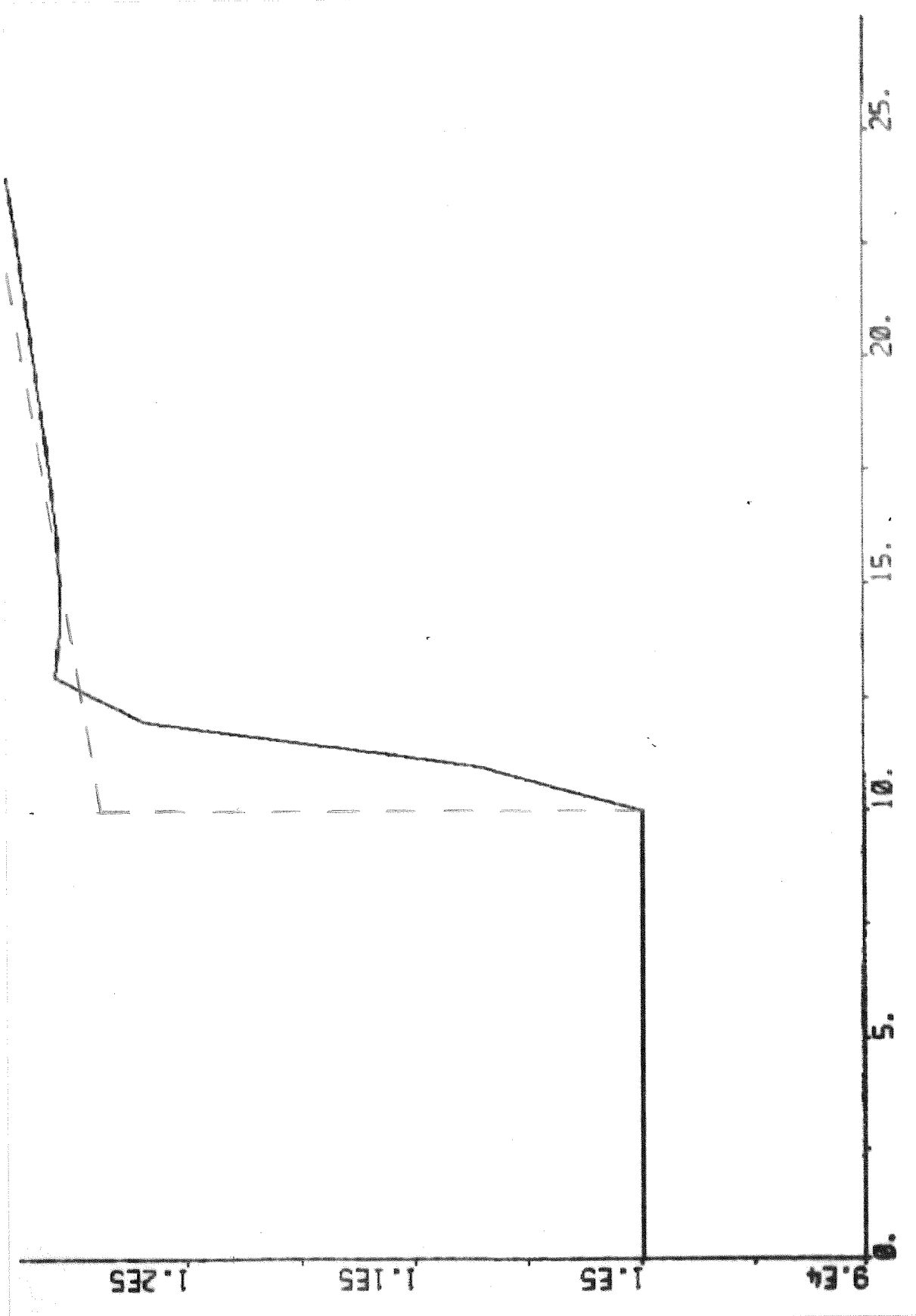


Fig. 18.21 - Response of the output power ( — ) and its reference value ( --- ) due to increase of the output power in alert mode.

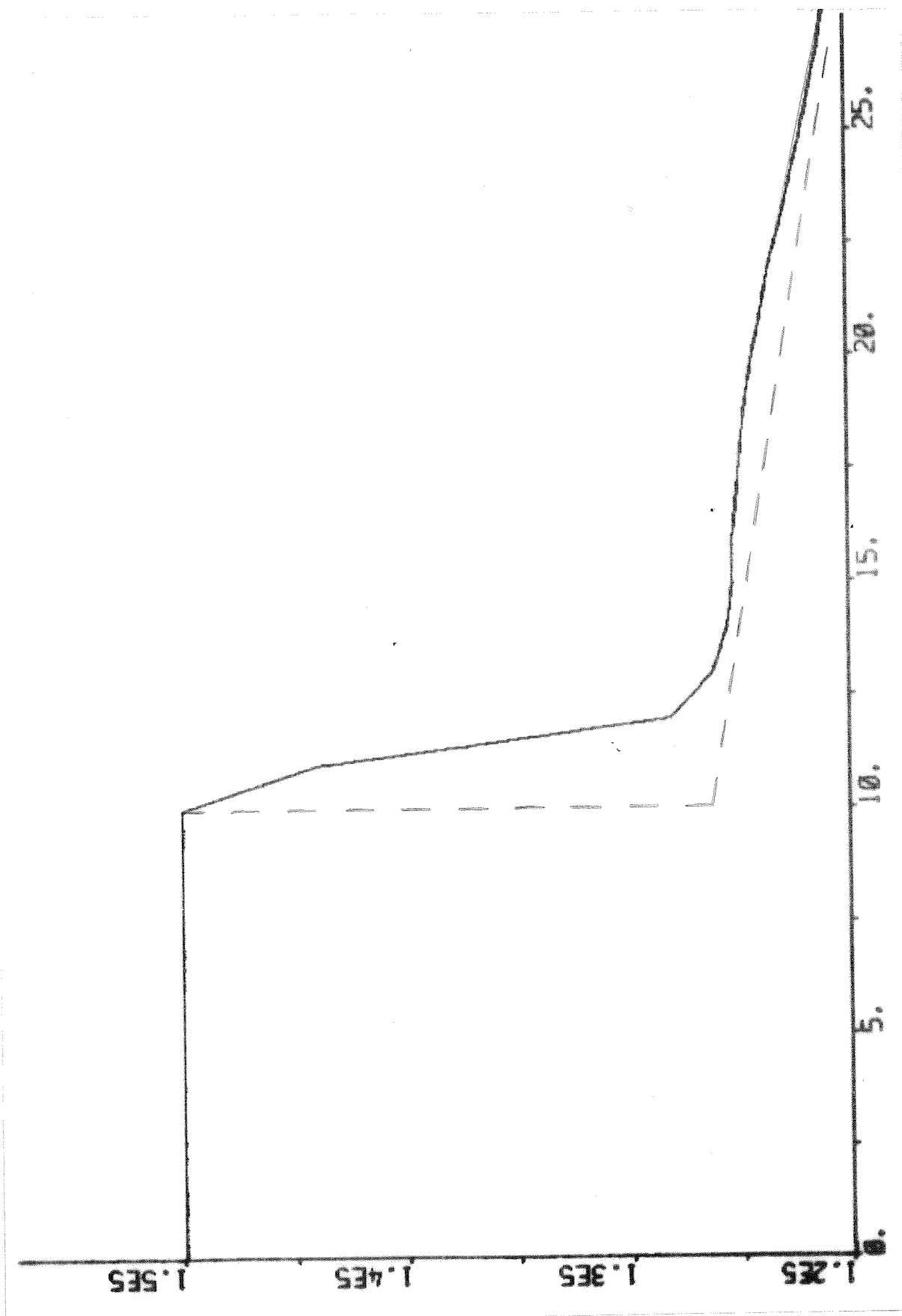


Fig. 18.22 - Response of the output power ( — ) and its reference value ( --- ) due to decrease of the output power in alert mode.



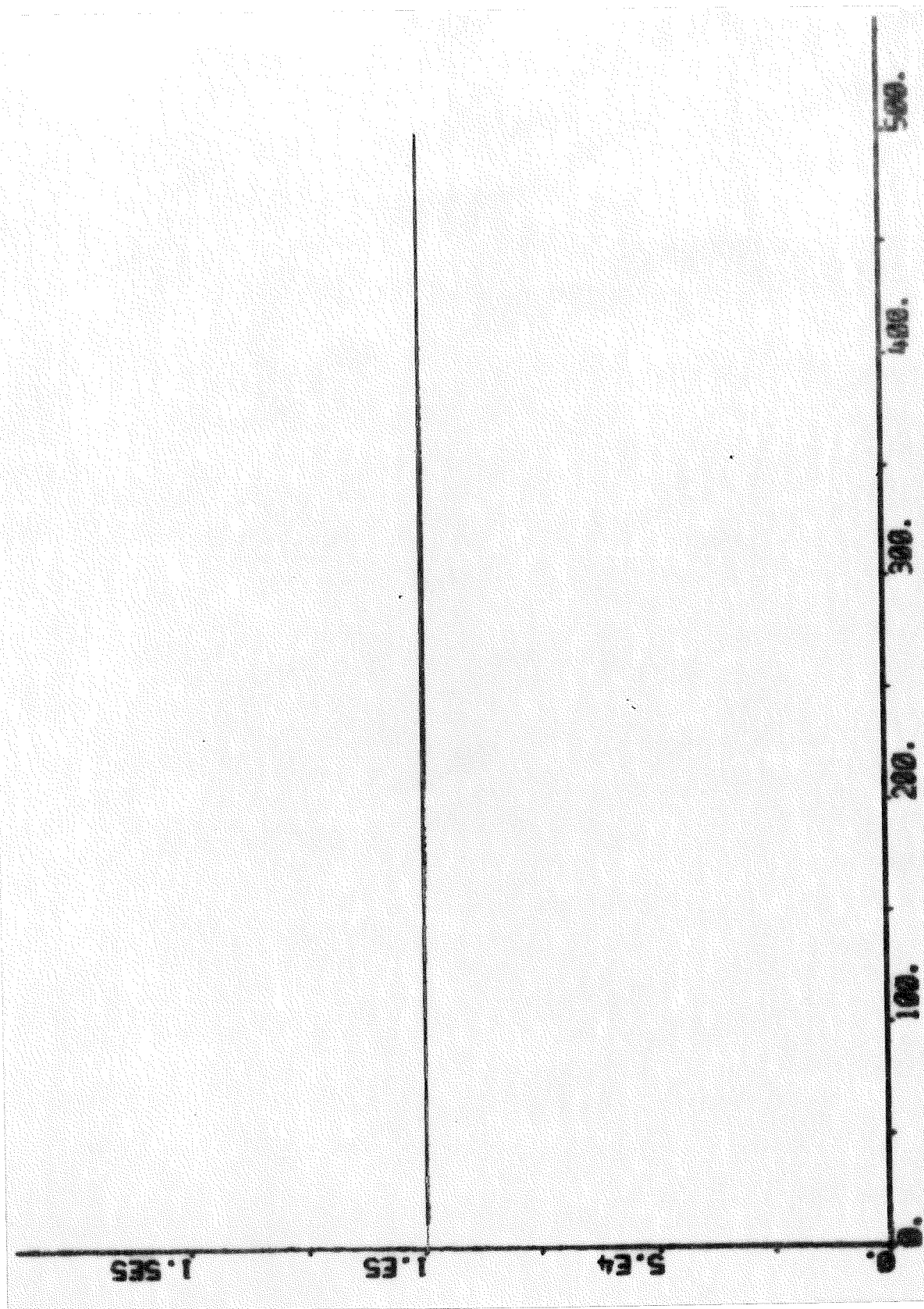


Fig. 18.23 - Response of the output power ( — ) and its reference value ( --- ) due to transfer from alert to normal mode.

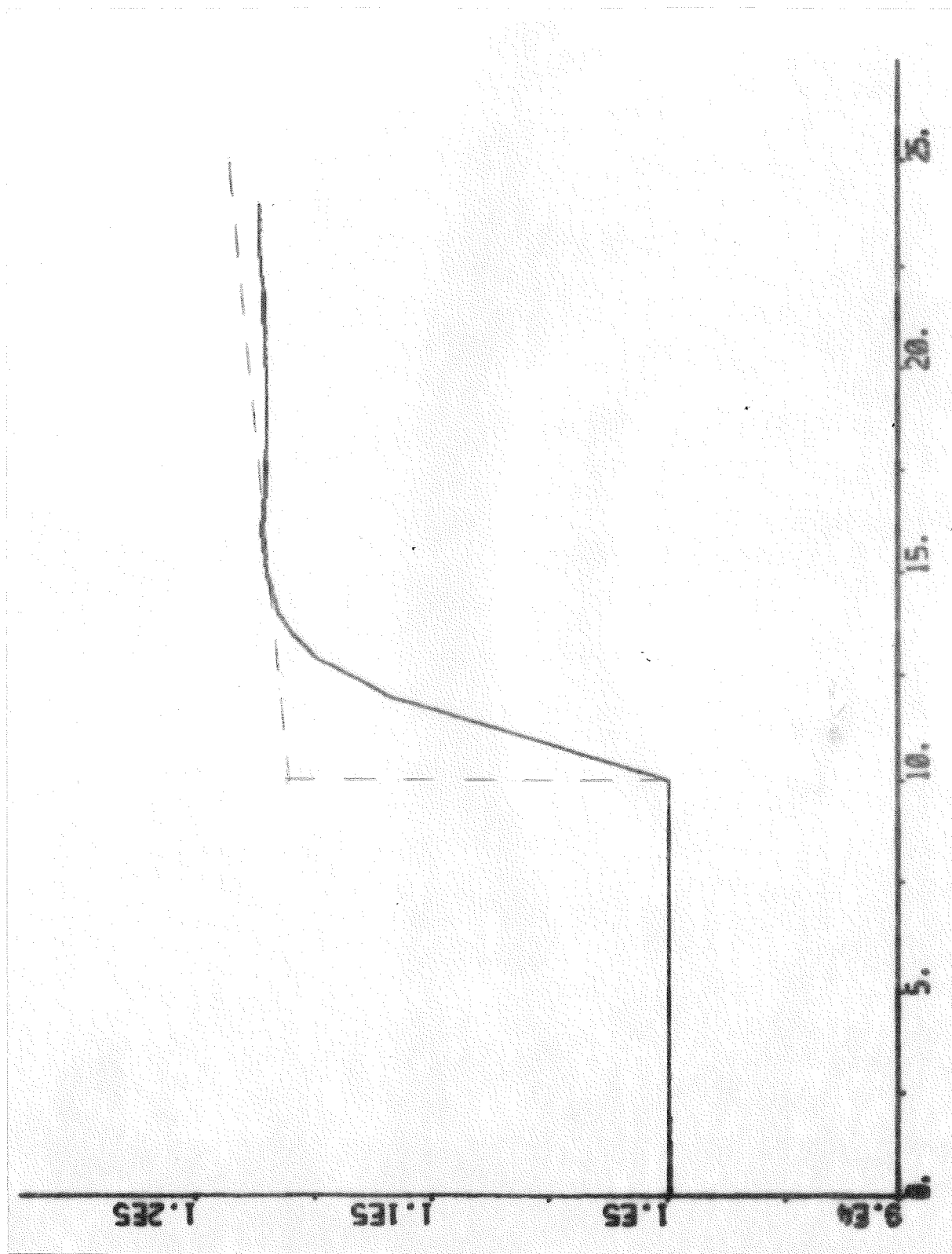


Fig. 18.24 - Response of the output power ( — ) and its reference value ( --- ) due to increase of the output power in normal mode.

## 19. ACKNOWLEDGEMENTS.

This work has been supported by the Swedish Board for Technical Development under Contract No. 733607.

The work has been supervised by Professor Karl Johan Åström, to whom I wish to express my gratitude for his encouraging support and invaluable help.

The dominating part of the model is based on the model developed by Tekn. Dr. Karl Eklund and on the experiments he made in cooperation with Sydsvenska Kraft Ab. Without his solid and foreseeing work it had not been possible to realize this project within the given time.

I am indebted to my colleagues at the Division of Automatic Control for their contributions at different stages of this work. In particular I wish to thank Tekn. Dr. Gunnar Bengtsson for many stimulating discussions on the multivariable control problem, Civ.ing. Göran Andersson for many stimulating discussions on the boiler-turbine control problem, and Civ.ing. Hilding Elmqvist on general simulation problems and for his readiness to modify the SIMNON-program with respect to the experiences of the boiler-turbine simulations. I am also very grateful to Mrs. Gudrun Christensen who typed the manuscript and to Miss Britt-Marie Carlsson who prepared the figures.

## 20. REFERENCES.

- [1] J.H. Anderson: "Dynamic Control of a Power Boiler", Proc. IEE, vol. 116, No. 7, pp. 1257-68, July 1969.
- [2] B.D.O. Anderson & J.B. Moore: "Linear Optimal Control", Prentice-Hall, Englewood Cliffs, New Jersey, 1971.
- [3] K.J. Åström: "Introduction to Stochastic Control Theory", Academic Press, New York, 1970.
- [4] G. Bengtsson: "A Theory for Control of Linear Multivariable Systems", Report 7341, Division of Automatic Control, Lund Institute of Technology, November 1973.
- [5] "Drifttekniska specifikationer för värmekraft" (Operational performance specifications for thermal power units, written in Swedish with a summary in English), Report prepared by a working group appointed by the Operating and Planning Committees of Nordel, NORDEL, July 1975.
- [6] K. Eklund: "Multivariable Control of a Boiler. An Application of Linear Quadratic Control Theory", Report 6901, Division of Automatic Control, Lund Institute of Technology, January 1969.
- [7] K. Eklund: "Linear Drum Boiler-Turbine Models", Report 7117, Division of Automatic Control, Lund Institute of Technology, November 1971.
- [8] H. Elmqvist: "SIMNON - An Interactive Simulation Program for Nonlinear Systems - User's Manual", Report 7502, Division of Automatic Control, Lund Institute of Technology, April 1975.
- [9] J. Falck-Christensen: "Lastspringførsøk på Stigsnaesværket den 25.4.74" (Power step response tests of the Stigsnaes power plant on 25.4.74, written in Danish), Technical Report, NESAS, 1974-05-07.
- [10] G. Klefenz: "Die Regelung von Dampfkraftanlagen", Bibliographisches Institute, Mannheim, 1973.

- [11] C. Larsson & C. Öhbom: "En matematisk modell av ett ångkraftverk" (A Mathematical Model of a Steam Power Plant, written in Swedish), Report RE-55, Division of Automatic Control, Lund Institute of Technology, July 1969.
- [12] S. Lindahl: "A Non-Linear Drum Boiler-Turbine Model", Report 7620(C), Division of Automatic Control, Lund Institute of Technology, March 1976.
- [13] H. Nicholson: "Integrated Control of a Nonlinear Boiler Model", Proc. IEEE, vol. 114, No. 10, pp. 1569-76, October 1967.
- [14] "Produktionsreglering" (Generation Control, written in Swedish), Statens Vattenfallsverk and ASEA, January 1975.
- [15] "Värmekraftens drifttekniska egenskaper" (Operation Conditions of Thermal Power Plants, written in Swedish), Statens Vattenfallsverk, May 1969.

```

001      SUBROUTINE REGU(CTRL)
002      C
003      C      DECLARATIONS
004      C
005      REAL
006      C
007      1MEM2,
008      C
009      2L0L5,MDM8,
010      C
011      3MPM2,
012      C
013      4MSM2,
014      C
015      5MTM2,
016      C
017      6MRM2,
018      C
019      7MCM2,
020      C
021      8MFM1,MFM2,MFM3,MFM4,MFM5,MFM6,MFM7,
022      C
023      9MAM2,
024      C
025      1NHS2,
026      C
027      2NIS2,
028      C
029      3NLS2,
030      C
031      4NGS2,
032      C
033      5NGS2C,
034      C
035      6NGS2E,
036      C
037      7NGS2S,NGS2O,NGS2L,NGS2H,
038      C
039      8NGS2M,
040      C
041      9JUMP1,JUMP2,JUMP3,JUMP4,JUMP5,JUMP6,
042      C
043      1NGS2R,
044      C
045      2NGS2B,
046      C
047      3NGS2D
048      C
049      REAL LIMIT
050      C
051      COMMON /BURNV/   WB01
052      C
053      COMMON /ECONV/   HEW2,QEM2,TEM2,TEW1,TEW2
054      C
055      COMMON /DRUMV/   HDL4,HDS2,HDW8,PDS2,QDM8,TDL4,TDL8,
056      1TDM8,VDS8,WDL5,WDS7,WDS8,WDW1,WDW8,XDS2,ZDL4
057      C
058      COMMON /PSUPV/   HPS2,PPS2,OPM2,TPM2,TPS2,WPS1
059      C
060      COMMON /SSUPV/   ASW1,HSS2,PSS2,QSM2,TSM2,TSS1,TSS2,
061      1WSS1,WSW1
062      C
063      COMMON /TSUPV/   ATW1,HTS2,PTS2,QTM2,TTM2,TTS1,TTS2,

```

|     |   |   |
|-----|---|---|
| 064 |   | 1WTS1,WTW1  |
| 065 | C |   |
| 066 |   | COMMON /SVALV/ AVS1,PVS2,TVS2                       |
| 067 | C |   |
| 068 |   | COMMON /HPTUV/ AHS2,HHS2,NHS2,PHS2,THS2,WHS2        |
| 069 | C |   |
| 070 |   | COMMON /REHEV/ HRS2,PRS1,PRS2,QRM2,TRM2,TRS2,WRS1   |
| 071 | C |   |
| 072 |   | COMMON /IPTUV/ AIS2,AIS4,AIS6,AIS8,HIS2,HIS4,HIS6,  |
| 073 |   | 1HIS8,NIS2,PIS2,PIS4,PIS6,PIS8,TIS2,TIS4,TIS6,TIS8, |
| 074 |   | 2WIS1,WIS2,WIS3,WIS4,WIS5,WIS6,WIS7,WIS8            |
| 075 | C |   |
| 076 |   | COMMON /LPTUV/ ALS2,ALS4,HLS2,HLS4,HLS6,NLS2,PLS2,  |
| 077 |   | 1PLS4,TLS2,TLS4,TLS6,WLS1,WLS2,WLS3,WLS4,WLS5       |
| 078 | C |   |
| 079 |   | COMMON /GENRV/ NGS2                                 |
| 080 | C |   |
| 081 |   | COMMON /CONDV/ HCC2,HCW1,HCW2,PCC2,PCW1,TCC2,TCW1,  |
| 082 |   | 1TCW2,XCC2,WCW1                                     |
| 083 | C |   |
| 084 |   | COMMON /PREHV/ HFC1,HFC4,HFL1,HFL2,HFL3,HFL4,HFL5,  |
| 085 |   | 1HFL6,HFL7,HFW1,HFW2,HFW3,HFW4,HFW5,HFW6,HFW7,PFC1, |
| 086 |   | 2PFC4,PFS1,PFS2,PFS3,PFS4,PFS5,PFS6,PFS7,PFW5,PFW6, |
| 087 |   | 3PFW8,TFC1,TFC4,TFL1,TFL2,TFL3,TFL4,TFL5,TFL6,TFL7, |
| 088 |   | 4TFW1,TFW2,TFW3,TFW4,TFW5,TFW6,TFW7,XFS1,XFS2,XFS3, |
| 089 |   | 5XFS4,XFS5,XFS6,XFS7,WFC1,WFC4,WFL1,WFL2,WFL4,WFL5, |
| 090 |   | 6WFL6,WFW1,WFW5                                     |
| 091 | C |   |
| 092 |   | COMMON /DEARV/ HAW1,HAW2,HAW3,PAS2,TAW2,XAS2,WAW1   |
| 093 | C |   |
| 094 |   | COMMON /WVALV/ AWW1,PWW2                            |
| 095 | C |   |
| 096 |   | COMMON /REGUV/ SNS1,SNS2,SB01,SB02,SB03,SWW1,SWW2,  |
| 097 |   | 1SSW1,SSW2,STW1,STW2,SVS1,SVS2,SFS1,SFS2,SFS5,SFS6, |
| 098 |   | 3SFS7   |
| 099 | C |   |
| 100 |   | COMMON /REGUC/                                      |
| 101 | C |   |
| 102 |   | 1SNS1C,UNS1C,SNS2C,                                 |
| 103 | C |   |
| 104 |   | 2SB01C,PDS2C,WB01C,                                 |
| 105 | C |   |
| 106 |   | 3ZDL4C,WFW5C,                                       |
| 107 | C |   |
| 108 |   | 4TSS1C,TSS2C,                                       |
| 109 | C |   |
| 110 |   | 5TTS1C,TTS2C,                                       |
| 111 | C |   |
| 112 |   | 6NGS2C,SVS2C,                                       |
| 113 | C |   |
| 114 |   | 7SFS2C,   |
| 115 | C |   |
| 116 |   | 8PAS2C,SFS7C  |
| 117 | C |   |
| 118 |   | COMMON /REGUE/                                      |
| 119 | C |   |
| 120 |   | 1SNS2E,   |
| 121 | C |   |
| 122 |   | 2PDS2E,   |
| 123 | C |   |
| 124 |   | 3ZDL4E,   |
| 125 | C |   |
| 126 |   | 4TSS2E,   |
| 127 | C |   |

|     |   |                                 |
|-----|---|---------------------------------|
| 128 |   | 5TTS2E,                         |
| 129 | C |                                 |
| 130 |   | 6NGS2E,                         |
| 131 | C |                                 |
| 132 |   | 7PAS2E                          |
| 133 | C |                                 |
| 134 |   | COMMON /REGUF/                  |
| 135 | C |                                 |
| 136 |   | 1SNS1F,SNS2F,                   |
| 137 | C |                                 |
| 138 |   | 2SB01F,SB02F,SB03F,             |
| 139 | C |                                 |
| 140 |   | 3SWW1F,SWW2F,                   |
| 141 | C |                                 |
| 142 |   | 4SSW1F,SSW2F,                   |
| 143 | C |                                 |
| 144 |   | 5STW1F,STW2F,                   |
| 145 | C |                                 |
| 146 |   | 6SVS1F,SVS2F,                   |
| 147 | C |                                 |
| 148 |   | 7SFS1F,SFS2F,                   |
| 149 | C |                                 |
| 150 |   | 8SFS5F,SFS6F,SFS7F              |
| 151 | C |                                 |
| 152 |   | COMMON /REGUL/                  |
| 153 | C |                                 |
| 154 |   | 1NGS2S,NGS2O,NGS2L,NGS2H,       |
| 155 | C |                                 |
| 156 |   | 2PDS2S,PDS2O,PDS2L,PDS2H,       |
| 157 | C |                                 |
| 158 |   | 3WB01S,WB01O,WB01L,WB01H,       |
| 159 | C |                                 |
| 160 |   | 4SWW2S,SWW2O,SWW2L,SWW2H,       |
| 161 | C |                                 |
| 162 |   | 5SSW2S,SSW2O,SSW2L,SSW2H,       |
| 163 | C |                                 |
| 164 |   | 6STW2S,STW2O,STW2L,STW2H,       |
| 165 | C |                                 |
| 166 |   | 7SVS2S,SVS2O,SVS2L,SVS2H,       |
| 167 | C |                                 |
| 168 |   | 8SFS2S,SFS2O,SFS2L,SFS2H,       |
| 169 | C |                                 |
| 170 |   | 9SFS7S,SFS7O,SFS7L,SFS7H        |
| 171 | C |                                 |
| 172 |   | COMMON /REGUM/                  |
| 173 | C |                                 |
| 174 |   | 1SNS1M,SNS2M,                   |
| 175 | C |                                 |
| 176 |   | 2SB01M,PDS2M,SB03M,WB01M,       |
| 177 | C |                                 |
| 178 |   | 3ZDL4M,WFW5M,AWW1M,             |
| 179 | C |                                 |
| 180 |   | 4TSS1M,TSS2M,ASW1M,             |
| 181 | C |                                 |
| 182 |   | 5TTS1M,TTS2M,ATW1M,             |
| 183 | C |                                 |
| 184 |   | 6NGS2M,SVS2M,AVS1M,             |
| 185 | C |                                 |
| 186 |   | 7SFS2M,AHS2M,AIS2M,AIS4M,AIS6M, |
| 187 | C |                                 |
| 188 |   | 8PAS2M,SFS7M,AIS8M,ALS2M,ALS4M  |
| 189 | C |                                 |
| 190 |   | COMMON /REGUP/                  |
| 191 | C |                                 |



```

192      1GNS1I,GGT1P,GGT1L,GGT1H,GNS2I,GNS2R,
193      C
194      2GB01F,GB01I,GB01S,GB01D,GB01R,GB03F,GB03D,GB03C,
195      3GB02P,GB02I,GB03I,GB03R,GB02R,
196      C
197      4GWW1I,GWW1P,GWW1R,GWW2I,GWW2R,
198      C
199      5GSW1B,GSW1F,GSW1P,GSW1I,GSW1R,GSW2R,GSW2I,
200      C
201      5GTW1F,GTW1P,GTW1I,GTW1R,GTW2I,GTW2R,
202      C
203      7GVS1I,GVS1P,GVS1R,GVS1H,GVS1L,GVS2I,GVS2R,
204      C
205      8GFS1I,GFS1C,GFS2I,
206      C
207      9GFS6C,GFS5I,GFS5P,GFS5R,GFS6I,GFS7I,
208      C
209      9BAND1,BAND2,
210      C
211      1RATE1,RATE2,RATE3,RATE4,
212      C
213      2JUMP1,JUMP2,JUMP3,JUMP4,JUMP5,JUMP6,
214      C
215      3RATE5,RATE6,RATE7,RATE8
216      C
217      COMMON /REGUR/
218      C
219      1SNS1R,UNS1R,SNS2R,UNS2R,
220      C
221      2SB01R,PDS2R,WB01R,
222      C
223      3ZDL4R,WFW5R,
224      C
225      4TSS1R,TSS2R,
226      C
227      5TTS1R,TTS2R,
228      C
229      6NGS2R,SVS2R,
230      C
231      7SFS2R,
232      C
233      8PAS2R,SFS7R
234      C
235      COMMON /REGUT/
236      C
237      1SNS1T,SNS2T,
238      C
239      2SB01T,SB02T,SB03T,
240      C
241      3SWW1T,SWW2T,
242      C
243      4SSW1T,SSW2T,
244      C
245      5STW1T,STW2T,
246      C
247      6SVS1T,SVS2T,
248      C
249      7SFS1T,SFS2T,
250      C
251      8SFS5T,SFS6T,SFS7T
252      C
253      COMMON /REGUX/  DTYPE,TDIST,TRAMP,ALERT
254      C
255      COMMON /BASEV/

```

```

256      C
257      1SNS1B,UNS1B,SNS2B,
258      C
259      2PDS2B,WB01B,
260      C
261      3ZDL4B,WFW5B,AWW1B,
262      C
263      4TSS1B,TSS2B,ASW1B,
264      C
265      5TTS1B,TTS2B,ATW1B,
266      C
267      6NGS2B,SVS2B,
268      C
269      7SFS2B,AHS2B,AIS2B,AIS4B,AIS6B,
270      C
271      8PAS2B,SFS7B,AIS8B,ALS2B,ALS4B,
272      C
273      9HCW1B,PCW1B,WCW1B,
274      C
275      1PFW5B,
276      C
277      2HAW3B
278      C
279      COMMON /DEVIV/
280      C
281      1SNS1D,UNS1D,YGT1D,SNS2D,
282      C
283      2PDS2D,WB01D,
284      C
285      4ZDL4D,WFW5D,AWW1D,
286      C
287      4TSS1D,TSS2D,ASW1D,
288      C
289      5TTS1D,TTS2D,ATW1D,
290      C
291      6NGS2D,SVS2D,
292      C
293      7SFS2D,AHS2D,AIS2D,AIS4D,AIS6D,
294      C
295      8PAS2D,SFS7D,AIS8D,ALS2D,ALS4D,
296      C
297      9HCW1D,PCW1D,WCW1D,
298      C
299      1PFW5D,
300      C
301      2HAW3D
302      C
303      COMMON /TIME/ T
304      C
305      GO TO(100,200),ICTRL
306      C
307      C
308      C
309      100      DIST=0.0
310      IF(DTYPE.GT.2.5) GO TO 130
311      IF(DTYPE.GT.1.5) GO TO 120
312      IF(DTYPE.GT.0.5) GO TO 110
313      GO TO 140
314      110      IF(T.GT.TDIST) DIST=1.0
315      GO TO 140
316      120      IF(T.GT.TDIST) DIST=(T-TDIST)/TRAMP
317      GO TO 140
318      130      DIST=PRBKE(T,TDIST)
319      140      CONTINUE

```

```

320      C
321      C      PROCESS INPUTS
322      C
323      WB01=SWTCH(SB03,WB01B,WB01D,WB01M,DIST)
324      C
325      AWW1=SWTCH(SWW2,AWW1B,AWW1D,AWW1M,DIST)
326      AWW1=AWW1*AWW1
327      C
328      ASW1=SWTCH(SSW2,ASW1B,ASW1D,ASW1M,DIST)
329      ASW1=ASW1*ASW1
330      C
331      ATW1=SWTCH(STW2,ATW1B,ATW1D,ATW1M,DIST)
332      ATW1=ATW1*ATW1
333      C
334      AVS1=VALVE(SWTCH(SVS2,SVS2B,SVS2D,AVS1M,DIST))
335      C
336      HCW1=HCW1B+HCW1D*DIST
337      PCW1=PCW1B+PCW1D*DIST
338      WCW1=WCW1B+WCW1D*DIST
339      C
340      AHS2=SWTCH(SFS2,AHS2B,AHS2D,AHS2M,DIST)
341      AIS2=SWTCH(SFS2,AIS2B,AIS2D,AIS2M,DIST)
342      AIS4=SWTCH(SFS2,AIS4B,AIS4D,AIS4M,DIST)
343      AIS6=SWTCH(SFS2,AIS6B,AIS6D,AIS6M,DIST)
344      C
345      AIS8=SWTCH(SFS7,AIS8B,AIS8D,AIS8M,DIST)
346      ALS2=SWTCH(SFS7,ALS2B,ALS2D,ALS2M,DIST)
347      ALS4=SWTCH(SFS7,ALS4B,ALS4D,ALS4M,DIST)
348      C
349      PFW5=PFW5B+PFW5D*DIST
350      C
351      RETURN
352      C
353      C      INTERFACE TO CENTRAL NETWORK REGULATOR
354      C
355      200      SNS1R=SWTCH(SNS1C,SNS1B,SNS1D,SNS1M,DIST)
356      C
357      UNS1R=SWTCH(UNS1C,UNS1B,UNS1D,SNS1M,DIST)
358      UNS1R=ABS(UNS1R)
359      C
360      SNS1T=LIMIT(GNS1I*(SNS1R-SNS1),-UNS1R,UNS1R)
361      C
362      C      FREQUENCY INFLUENCE
363      C
364      SNS2C=SNS1+GGT1P*DZONE(-YGT1D*DIST,-BAND1,BAND2)
365      C
366      C      JUMP AND GRADIENT LIMITER
367      C
368      SNS2R=SWTCH(SNS2C,SNS2B,SNS2D,SNS2M,DIST)
369      SNS2R=LIMIT(SNS2R,NGS2L,NGS2H)
370      C
371      C      JUMP AND GRADIENT LIMITER
372      C
373      SNS2E=SNS2R-SNS2
374      NGS2S=RATE1+RATE3*ALERT
375      NGS2O=RATE2+RATE4*ALERT
376      SNS2T=GNS2I*SNS2E
377      SNS2T=SERVO(SNS2,SNS2T,NGS2S,NGS2O,NGS2L,NGS2H)
378      C
379      JUMP5=JUMP1+JUMP3*ALERT
380      JUMP6=JUMP2+JUMP4*ALERT
381      NGS2C=LIMIT(SNS2E,-JUMP5,JUMP6)+SNS2
382      NGS2R=SWTCH(NGS2C,NGS2B,NGS2D,NGS2M,DIST)
383      IF(NGS2M.GT.0.5) SNS2T=NGS2R*(NGS2B-NGS2C)

```

```

384      NGS2=NHS2+NIS2+NLS2
385      NGS2E=NGS2R-NGS2
386      C
387      C      DRUM PRESSURE REFERENCE SETTER
388      C
389      SB01C=GB01F*NGS2C*PDS2H/NGS2H
390      SB01R=SWTCH(SB01C,PDS2B,PDS2D,SB01M,DIST)
391      SB01R=SB01R*(1.0-ALERT)+PDS2H*ALERT
392      SB01R=LIMIT(SB01R,PDS2L,PDS2H)
393      PDS2S=RATE5+RATE7*ALERT
394      PDS2O=RATE6+RATE8*ALERT
395      SB01T=GB01I*(SB01R-SB01)
396      SB01T=SERVO(SB01,SB01T,PDS2S,PDS2O,PDS2L,PDS2H)
397      IF(PDS2M.GT.0.5) SB01T=GB01R*(PDS2B-SB01)
398      C
399      C      DRUM PRESSURE CONTROLLER
400      C
401      PDS2C=SB01
402      PDS2R=SWTCH(PDS2C,PDS2B,PDS2D,PDS2M,DIST)
403      PDS2R=LIMIT(PDS2R,PDS2L,PDS2H)
404      PDS2E=PDS2R-PDS2
405      SB02T=CONDI(PDS2E,SB03,WB01L,WB01H)
406      WB01C=GB03C*WTS1+GB03D*SB01T+GB02P*PDS2E+GB02I*SB02
407      C
408      IF(SB03M.GT.0.5) SB02T=GB02R*(WB01B-WB01C)
409      C
410      C      FUEL FLOW SERVO
411      C
412      WB01R=SWTCH(WB01C,WB01B,WB01D,SB03M,DIST)
413      SB03T=GB03I*(WB01R-WB01)
414      SB03T=SERVO(SB03,SB03T,WB01S,WB01O,WB01L,WB01H)
415      C
416      IF(WB01M.GT.0.5) SB03T=GB03R*(WB01B-WB01C)
417      C
418      C      DRUM LEVEL CONTROLLER
419      C
420      ZDL4R=SWTCH(ZDL4C,ZDL4B,ZDL4D,ZDL4M,DIST)
421      ZDL4E=ZDL4R-ZDL4
422      SWW1T=CONDI(ZDL4E,SWW2,SWW2L,SWW2H)
423      C
424      WFW5C=WTS1+GWW1I*SWW1+GWW1P*ZDL4E
425      C
426      IF(WFW5M.GT.0.5) SWW1T=GWW1R*(WFW5B-WFW5C)
427      C
428      C      FEEDWATER SERVO
429      C
430      WFW5R=SWTCH(WFW5C,WFW5B,WFW5D,WFW5M,DIST)
431      SWW2T=GWW2I*(WFW5R-WFW5)
432      SWW2T=SERVO(SWW2,SWW2T,SWW2S,SWW2O,SWW2L,SWW2H)
433      C
434      IF(AWW1M.GT.0.5) SWW2T=GWW2R*(AWW1B-SWW2)
435      C
436      C      TERTIARY SUPERHEATER STEAM TEMPERATURE CONTROLLER
437      C
438      TTS2R=SWTCH(TTS2C,TTS2B,TTS2D,TTS2M,DIST)
439      TTS2E=TTS2-TTS2R
440      STW1T=CONDI(TTS2E,STW2,STW2L,STW2H)
441      TTS1C=TTS2R-GTW1F*WB01/WTS1-GTW1P*TTS2E-GTW1I*STW1
442      IF(TTS1M.GT.0.5) STW1T=GTW1R*(TTS1B-TTS1C)
443      C
444      C      ATTEMPERATOR 2
445      C
446      TTS1R=SWTCH(TTS1C,TTS1B,TTS1D,TTS1M,DIST)
447      STW2T=GTW2I*(TTS1-TTS1R)

```

```

448 STW2T=SERVO(STW2,STW2T,STW2S,STW2O,STW2L,STW2H)
449 IF(ATW1M.GT.0.5) STW2T=GTW2R*(ATW1B-ATW1)
450 C
451 C SECONDARY SUPERHEATER STEAM TEMPERATURE CONTROLLER
452 C
453 TSS2C=TTS1R+GSW1R
454 TSS2R=SWTCH(TSS2C,TSS2B,TSS2D,TSS2M,DIST)
455 TSS2E=TSS2-TSS2R
456 SSW1T=CONDI(TSS2E,SSW2,SSW2L,SSW2H)
457 TSS1C=TSS2R-GSW1F*WB01/WT81-GSW1P*TSS2E-GSW1I*SSW1
458 IF(TSS1M.GT.0.5) SSW1T=GSW1R*(TSS1B-TSS1C)
459 C
460 C ATTEMPERATOR 1
461 C
462 TSS1R=SWTCH(TSS1C,TSS1B,TSS1D,TSS1M,DIST)
463 SSW2T=GSW2I*(TSS1-TSS1R)
464 SSW2T=SERVO(SSW2,SSW2T,SSW2S,SSW2O,SSW2L,SSW2H)
465 IF(ASW1M.GT.0.5) SSW2T=GSW2R*(ASW1B-SSW2)
466 C
467 C TURBINE POWER CONTROLLER
468 C
469 SVS1T=CONDI(NGS2E,SVS2,SVS2L,SVS2H)
470 SVS2C=SVS2B+GVS1I*SVS1+GVS1P*DZONE(NGS2E,GVS1L,GVS1H)
471 IF(SVS2M.GT.0.5) SVS1T=GVS1R*(SVS2B-SVS2C)
472 C
473 C CONTROL VALVE SERVO
474 C
475 SVS2R=SWTCH(SVS2C,SVS2B,SVS2D,SVS2M,DIST)
476 SVS2T=GVS2I*(SVS2R-SVS2)
477 SVS2T=SERVO(SVS2,SVS2T,SVS2S,SVS2O,SVS2L,SVS2H)
478 IF(AVS1M.GT.0.5) SVS2T=GVS2R*(SVS2B-SVS2C)
479 C
480 C HP-PREHEATER CONTROLLER
481 C
482 SFS1E=NGS2R-SFS1
483 SFS1T=GFS1I*SFS1E
484 SFS2C=SFS2B-GFS1C*SFS1E
485 C
486 C HP-PREHEATER SERVO
487 C
488 SFS2R=SWTCH(SFS2C,SFS2B,SFS2D,SFS2M,DIST)
489 SFS2T=GFS2I*(SFS2R-SFS2)
490 SFS2T=SERVO(SFS2,SFS2T,SFS2S,SFS2O,SFS2L,SFS2H)
491 C
492 C LP-PREHEATER CONTROLLER
493 C
494 PAS2R=SWTCH(PAS2C,PAS2B,PAS2D,PAS2M,DIST)
495 PAS2E=PAS2R-PAS2
496 SFS5T=CONDI(PAS2E,SFS7,SFS7L,SFS7H)
497 C
498 SFS6E=NGS2R-SFS6
499 SFS6T=GFS6I*SFS6E
500 C
501 SFS7C=SFS7B-GFS6C*SFS6E+GFS5I*SFS5+GFS5P*PAS2E
502 IF(SFS7M.GT.0.5) SFS5T=GFS5R*(SFS7B-SFS7C)
503 C
504 C LP-PREHEATER SERVO
505 C
506 SFS7R=SWTCH(SFS7C,SFS7B,SFS7D,SFS7M,DIST)
507 SFS7T=GFS7I*(SFS7R-SFS7)
508 SFS7T=SERVO(SFS7,SFS7T,SFS7S,SFS7O,SFS7L,SFS7H)
509 C
510 C SET TIME DERIVATIVES
511 C

```

```
512      SNS1T=SNS1F*SNS1T
513      SNS2T=SNS2F*SNS2T
514      C
515      SB01T=SB01F*SB01T
516      SB02T=SB02F*SB02T
517      SB03T=SB03F*SB03T
518      C
519      SWW1T=SWW1F*SWW1T
520      SWW2T=SWW2F*SWW2T
521      C
522      SSW1T=SSW1F*SSW1T
523      SSW2T=SSW2F*SSW2T
524      C
525      STW1T=STW1F*STW1T
526      STW2T=STW2F*STW2T
527      C
528      SVS1T=SVS1F*SVS1T
529      SVS2T=SVS2F*SVS2T
530      C
531      SFS1T=SFS1F*SFS1T
532      SFS2T=SFS2F*SFS2T
533      C
534      SFS5T=SFS5F*SFS5T
535      SFS6T=SFS6F*SFS6T
536      SFS7T=SFS7F*SFS7T
537      C
538      RETURN
539      END
```

```
001      REAL FUNCTION CONDI(XT,Y,YL,YH)
002      CONDI=XT
003      IF(XT) 10,90,20
004      10      IF(Y.LE.YL) CONDI=0.0
005              GO TO 90
006      20      IF(Y.GE.YH) CONDI=0.0
007      90      RETURN
008      END
```

```
001      REAL FUNCTION DZONE(Y,YL,YH)
002      IF(YL-Y) 10,20,20
003      10    IF(Y-YH) 30,30,40
004      20    DZONE=Y-YL
005      GO TO 90
006      30    DZONE=0.0
007      GO TO 90
008      40    DZONE=Y-YH
009      90    RETURN
010      END
```



```
001      REAL FUNCTION LIMIT(Y,YL,YH)
002      LIMIT=AMAX1(Y,YL)
003      LIMIT=AMIN1(LIMIT,YH)
004      RETURN
005      END
```

```
001      FUNCTION PRBKE(T,TS)
002      DIMENSION A(60)
003      DATA
004      1A(1)/-1.0/,
005      2A(2)/-1.0/,
006      3A(3)/+1.0/,
007      4A(4)/+1.0/,
008      5A(5)/+1.0/,
009      6A(6)/+1.0/,
010      7A(7)/+1.0/,
011      8A(8)/-1.0/,
012      9A(9)/-1.0/
013      DATA A(10)/-1.0/,
014      1A(11)/-1.0/,
015      2A(12)/-1.0/,
016      3A(13)/+1.0/,
017      4A(14)/+1.0/,
018      5A(15)/+1.0/,
019      6A(16)/-1.0/,
020      7A(17)/-1.0/,
021      8A(18)/-1.0/,
022      9A(19)/-1.0/
023      DATA A(20)/+1.0/,
024      1A(21)/-1.0/,
025      2A(22)/-1.0/,
026      3A(23)/-1.0/,
027      4A(24)/+1.0/,
028      5A(25)/+1.0/,
029      6A(26)/+1.0/,
030      7A(27)/+1.0/,
031      8A(28)/+1.0/,
032      9A(29)/-1.0/
033      DATA A(30)/+1.0/,
034      1A(31)/-1.0/,
035      2A(32)/+1.0/,
036      3A(33)/-1.0/,
037      4A(34)/-1.0/,
038      5A(35)/-1.0/,
039      6A(36)/+1.0/,
040      7A(37)/-1.0/,
041      8A(38)/-1.0/,
042      9A(39)/-1.0/
043      DATA A(40)/-1.0/,
044      1A(41)/+1.0/,
045      2A(42)/+1.0/,
046      3A(43)/+1.0/,
047      4A(44)/+1.0/,
048      5A(45)/+1.0/,
049      6A(46)/-1.0/,
050      7A(47)/+1.0/,
051      8A(48)/-1.0/,
052      9A(49)/-1.0/
053      DATA A(50)/+1.0/,
054      1A(51)/-1.0/,
055      2A(52)/-1.0/,
056      3A(53)/-1.0/,
057      4A(54)/-1.0/,
058      5A(55)/+1.0/,
059      6A(56)/+1.0/,
060      7A(57)/+1.0/,
061      8A(58)/+1.0/,
062      9A(59)/+1.0/
063      DATA A(60)/+1.0/
```

```
064      C
065      IT=IFIX((T-IS)/60.0)
066      IF(IT) 10,10,20
067      C
068      C      THE EXPERIMENT HAS NOT STARTED
069      C
070      10      PRBKE=0.0
071      GO TO 90
072      C
073      20      IF(IT-60) 30,30,40
074      C
075      C      THE EXPERIMENT IS RUNNING
076      C
077      30      PRBKE=A(IT)
078      GO TO 90
079      C
080      C      THE EXPERIMENT IS OVER
081      C
082      40      PRBKE=0.0
083      C
084      90      RETURN
085      END
```

```
001      REAL FUNCTION SERVO(X,XT,XS,XO,XL,XH)
002      SERVO=XT
003      IF(XT) 10,90,20
004      10  SERVO=AMAX1(XT,-XS)
005      IF(X,LE,XL) SERVO=0.0
006      GO TO 90
007      20  SERVO=AMIN1(XT,XO)
008      IF(X,GE,XH) SERVO=0.0
009      90  RETURN
010      END
```

```
001      REAL FUNCTION SWITCH(XC,XB,XD,XM,XN)
002      SWITCH=XC*(1.0-XM)+XB*XM+XD*XN
003      RETURN
004      END
```

```

001      FUNCTION VALVE(U)
036      C
037      DIMENSION A(9),B(9)
038      C
039      DATA
040      1A(1)/0.900/,
041      2A(2)/0.232/,
042      3A(3)/0.280/,
043      4A(4)/0.388/,
044      5A(5)/0.488/,
045      6A(6)/0.568/,
046      7A(7)/0.684/,
047      8A(8)/0.740/,
048      9A(9)/0.928/,
049      1B(1)/0.000/,
050      2B(2)/15.00/,
051      3B(3)/15.00/,
052      4B(4)/25.00/,
053      5B(5)/40.00/,
054      6B(6)/50.00/,
055      7B(7)/60.00/,
056      8B(8)/70.00/,
057      9B(9)/80.00/,
058      1SMAX/96.00/,
059      2SFUL/15.00/,
060      3ANUL/1.0E-8/
061      S=SMAX*U
062      STOT=0.0
063      DO 20 I=1,9
064      SDEL=S-B(I)
065      IF(SDEL) 30,10,10
066      10  SDEL=A(I)*SDEL
067      SDEL=AMIN1(SFUL,SDEL)
068      20  STOT=STOT+SDEL
069      30  VALVE=STOT/135.0
070      VALVE=AMAX1(ANUL,VALVE)
071      RETURN
072      END

```